Oral Cancer Detection

Novel Strategies and Clinical Impact

Prashanth Panta
Editor

Springer

Oral Cancer Detection

Prashanth Panta
Editor

Oral Cancer Detection

Novel Strategies and Clinical Impact

Springer

Editor
Prashanth Panta
Depatment of Oral Medicine and
Radiology, MNR Dental College Oral
Medicine and Radiology
Hyderabad
India

ISBN 978-3-319-61254-6 ISBN 978-3-319-61255-3 (eBook)
https://doi.org/10.1007/978-3-319-61255-3

Library of Congress Control Number: 2018955194

This Springer imprint is published by the registered company Springer Nature Switzerland AG
The registered company address is: Gewerbestrasse 11, 6330 Cham, Switzerland

Foreword

In spite of much research efforts, oral cancer still afflicts many people all over the world. Furthermore, little progress has been made in improving treatment and patient's outcome. This book on oral cancer for which Prashanth Panta is responsible, both as Editor and Author of several Chapters contains a most welcome overview on the subject. In view of his track record in Dental Surgery, Dr. Panta is well qualified for this task and the result meets the required standards. All aspects of oral cancer are covered, both the usual ones such as progression of precancer, epidemiology, imaging and histopathology but also new developments are included: colposcopy, spectroscopy, and other modern analytic methods. A Chapter on diagnostic delays in oral cancer emphasizes the benefit that may be obtained by timely diagnosis and treatment and a Chapter on saliva based diagnosis of oral cancer describes an approach that probably will be useful both in screening as well as follow-up, allowing early detection of primary or recurrent tumor.

Both the Editor as well as the contributors are to be complimented with the result of their efforts.

Nijmegen, Netherlands — Pieter Slootweg, MD, DMD, PhD
Nijmegen, June 2017

Preface

Why Oral Cancer Detection Is Challenging?

More than 90% of all oral cancers are oral squamous cell carcinomas (OSCCs) that arise from oral epithelium. Although OSCCs are superficial cancers, highly accessible to clinicians, they are often discovered late (stage III–IV)! Interestingly, OSCCs develop within an established group of conditions referred to as "Oral Potentially Malignant Disorders" (OPMDs), of which "leukoplakia" and "oral submucous fibrosis" are common candidates. OPMDs are particularly noticed in the south Asian countries, due to the extensive, unregulated, use of tobacco and areca nut products. Moreover, OPMDs present as wide lesions, covering a large surface area (several centimeters wide) and exhibit varying degrees of clinical evolution ranging from "dysplasia" to "invasive cancer." This necessitates thorough screening with different chairside strategies. Additionally, OSCC exhibits "field cancerization," which is characterized by a lateral spread to areas distant from the originally affected oral mucosa.

The challenge of early detection revolves around the discovery of accessible and reliable signatures indicative of native tissue. Biomarkers in OSCC include optical features like "loss of fluorescence," characteristic Raman spectra, classic intrapapillary capillary loop (IPCL) feature like "destructive vessel" pattern, or a signature protein or RNA in saliva, which have all shown sufficient accuracy of detection. The ultimate purpose of early detection is immediate referral for treatment initiation, thereby minimizing harm from extensive surgery, radiation, and chemotherapy, the current modalities of treatment.

How Emerging Technology Simplifies Detection?

OSCC is of particular interest because they are epithelial malignancies. They are therefore easily accessible, and application of technology is possible through hand-held contact probes or through point-of-care testing of signature biomarkers within "representative and closely adherent" body fluids like saliva.

Developments in the frontier areas of optical imaging, if harnessed, are capable of uncovering subclinical malignant lesions. Imaging methods like white-light-based fluorescence imaging and narrow band imaging have shown success in numerous preclinical and clinical studies. Advanced optical techniques like "optical coherence tomography" (OCT) are capable of providing excellent visualization of the oral epithelium, comparable to "microtome sectioning" in standard histology. Furthermore, the incorporation of additional functional features like "microcirculation mapping" along with multimodal approaches can make it an even more powerful instrument to probe suspicious oral lesions. Other modern analytical methods like Raman spectroscopy have also shown good results for OSCC detection on saliva and blood, particularly in combination with nanotechnology. Saliva-based biomarker discovery strategies (proteomics, transcriptomics, metabolomics) have identified over one hundred signatures, some relevant even to stage I lesions. Furthermore, with the emergence of nanotechnology these approaches may be simplified. The electrical methods like "bioimpedance test" which works on variations in conductivity and impedance of cancerous tissue, and occult biophysical methods like "sensitive crystallization test" which works on subtler biochemical changes in blood are also interesting approaches, but need a more deeper scientific investigation.

The Future of the Field!

Intense research commitment in the discussed areas can potentiate early detection of oral cancer. In the near future, "clinician's decision making" will become easier pertaining to "selection of representative biopsy site" in large suspicious OPMDs, and in the "accurate determination of margin status" for existing OSCC. In the long run it may be even possible to arrive at a rapid diagnosis of epithelial malignancies, even without the need for tissue biopsy, because biopsy itself expedites metastasis by increasing the scope for entry of tumor cells into systemic circulation. Moreover, with epithelial malignancies like OSCC, there is a great opportunity to explore using different strategies, unlike deep-tissue malignancies (seated beneath the epithelium), which are inaccessible at early stages. Overall, this book will take you through a journey from basic background of oral cancer to methods and technologies available for early detection, with a focus on the future.

Since most of the oral cancers are OSCCs, these terms have been used interchangeably in some contexts.

Hyderabad, India — Prashanth Panta

Contents

1 Introduction to Oral Cancer

Prashanth Panta and Dimitrios Andreadis

Abstract

Oral cancer is the 6th most common type of human cancer with a 5-year survival rate approximately 50%, and its formation occurs in multiple steps. In the majority of cases, a well-established, preventable risk factor is involved. Several potentially malignant disorders precede oral cancer, each of them showing a well-defined clinical presentation. Spotting such precursor lesions should be no challenge to experienced clinicians. The 2017 World Health Organization (WHO) classification system on "oral potentially malignant disorders" is also presented here. Potentially malignant disorders encompass habit associated conditions, immune-mediated and inflammatory disorders, and also conditions that may arise due to solar radiation like actinic cheilitis and also genetic disorders like dyskeratosis congenita. Like in other cancer models, studies have focused on oral cancer stem cell population as the cancer-initiating cells and hidden culprits. Besides tobacco and alcohol, viruses (HPV), nutritional deficiencies, mechanical trauma and galvanic phenomenon, candidal infection, and inherited mutations are now established etiological or synergistic factors that cannot be underestimated in the genesis and progress of oral cancer. This chapter deals with common risk factors and oral potentially malignant disorders.

1.1 Introduction

Oral cancer (OC) is the sixth common malignancy worldwide, but in India, the scenario is much worse, OC figuring as a leading cause of cancer [1]. Nearly 90% of OC cases are oral squamous cell carcinoma (OSCC), and most of them occur in individuals beyond 40 years, although recently trend is slightly different with more cases recorded among younger individuals [2]. The most common sites for OSCC are lateral border of the tongue, buccal mucosa, gingiva, and floor of the mouth. OSCC is often associated with well-defined risk factors. OSCC burdens millions of people worldwide and is mainly associated with tobacco, alcohol and areca nut, human papilloma virus, nutritional deficiency, mechanical trauma, and also infection with *Candida* spp. The majority of cases arise because tobacco and alcohol are complimentary. OC evolves from several precursor conditions and often is associated with a deleterious habit. Oral cancer may also arise from

P. Panta, MDS (✉)
Department of Oral Medicine and Radiology, MNR Dental College and Hospital, Sangareddy, Telangana, India
e-mail: maithreya.prashanth@gmail.com

D. Andreadis, DDS, PhD
Department of Oral Medicine/Pathology, School of Dentistry, Aristotle University of Thessaloniki, Thessaloniki, Greece

P. Panta (ed.), *Oral Cancer Detection*, https://doi.org/10.1007/978-3-319-61255-3_1

preexisting inflammatory conditions (e.g., oral lichen planus) and sometimes in a distinct set of genetic disorders.

1.2 Risk Factors

1.2.1 Tobacco, Alcohol, and Areca Alkaloids

Tobacco is a major environmental risk factor for OC. It contains many powerful carcinogens like N-nitrosamines, polycyclic aromatic hydrocarbons, nitrosoproline, heavy metals—polonium, benzene, and carbon monoxide and hydrogen cyanide in smoke phase and numerous metabolites [3]. There are over 4000 chemical compounds, and each puff contains 10^{15} damaging free radicals [3, 4]. Among the many, 62 compounds have shown sufficient carcinogenicity [3]. Although many OC patients are often smokers, in India and other Asian countries, tobacco in chewable form is equally common. Smokers diagnosed with oral cancer are at risk to develop a secondary tumor if they continue smoking, but if they give up, there will be a marked reduction of the risk of a second cancer. In a Swedish case control study, a dose of 11–20 cigarettes/day was identified as a strong risk factor [5]. The risk factor with marijuana smokers is not yet established. Cigarette smoke contains compounds that contribute to alterations in a spectrum of genes involved in oxidative metabolism, xenobiotic pathways, cell adhesion and the mismatch repair system, etc. [6]. The effects of tobacco are principally mediated through free radicals. In normal cells the mismatch repair (MMR) system contributes largely to the correction of mutations, but in smokers there is a covalent modification (hypermethylation) of their gene promoters resulting in loss of expression, leading to cancer [7]. Smokeless tobacco is often combined with areca nut, and sometimes areca nut is taken separately, both being independent risk factors for oral cancer [8]. Electronic cigarettes are a safe substitute to tobacco cigarettes [4]. In nonsmokers, the most common site is the tongue.

The use of alcohol strengthens the effect of smoking (synergistic effect). Hard liquor, wine, and beer are common liquor forms mediating this effect. Both salivary and circulatory concentrations of alcohol are almost the same [9]. Intake of alcohol increases the effect of carcinogens by: (1) dehydrating the oral mucosa, (2) increasing mucosal permeability through alteration of physicochemical properties of the cell membrane (membrane fluidity and shape), and (3) causing dysfunction of the liver and impairment of mineral metabolism (retinoids, zinc, etc.) [9]. The effect of ethanol on oral tissues is dose dependent with 100 g/day showing a strong relative risk [9]. The mutations caused by smoking and tobacco are fundamentally mediated through reactive oxygen and nitrogen species (ROS, NOS) [2, 10]. Mitochondrial electron transport is a major producer of ROS. Alcohol is acted by alcohol dehydrogenase and converted to acetaldehyde (AcH), a powerful carcinogen. Acetaldehydes are further activated by acetaldehyde dehydrogenase (ADH) and converted to acetate [10]. Mutations in the ADH enzyme family can also result in accumulation of AcH, which can induce point mutations and also gross chromosomal aberrations. Alcohol may also induce epigenetic alterations like histone deacetylation and methylation at different residues making gene promoters active or inactive [10].

The use of areca nut is common to Asia. It contains many alkaloids mainly arecoline (0.2%), guavacoline, and polyphenols (>11%) which increase collagen production leading to fibrosis [11]. Betel nut and pan chewing also cause chronic inflammatory changes. Catechin and tannins in betel nut have synergistic roles making collagen more resistant to break down by collagenase. High levels of copper in betel nut (~13 parts per million) [12] lead to increased salivary copper levels which upregulates lysyl oxidase expression, a collagen cross-linker that decreases its degradation. Lysyl oxidase supports the formation of aldehydes from lysine residues. Copper in the betel nut quid is due to the use of copper sulfate-rich Bordeaux mixture, a fungicide sprayed during cultivation of areca plants. Transforming growth factor beta (TGF-ß) is an important chemical mediator activated by areca products (arecoline) that mediate collagen deposition [11]. Areca nut is rich in polyphenols and their role cannot be neglected. Areca nut use is associated with oral submucous fibrosis.

1.2.2 Age and Nutritional Deficiency

OSCC normally occurs at more advanced age, in fourth to fifth decades. Patients under 40 years with OSCC are usually nonsmokers and nonalcoholics [11, 12]. It takes many years for genetic changes to accumulate. Also with age the immunological surveillance systems and repair mechanisms decline. In younger patients, the tongue is a frequently involved location [13]. Younger patients with tongue squamous cell carcinoma (TSCC) have reported with worse nodal status and significant perineural invasion [14]. In patients who receive bone marrow transplantation or with inherited cancer disorders like xeroderma pigmentosum and Fanconi's anemia, OSCC may also occur at a young age, even less than 20 years.

Minerals and vitamins are essential micronutrients, and their deficiency is an intrinsic factor in cancer development and a preventable cause. Deficiencies in niacin and antioxidants result in DNA breaks, and correction of their levels reduced the incidence of oral cancer [15]. Vitamin C, A, and E may help in tissue integrity, epithelial maturation, and protection from toxic exogenous or endogenous products and exhibit a significant depletion in many OC patients, which could be not only be a cause but also the result of OC [16, 17]. Vitamin C intake in natural and supplemented form was shown to have an inverse association with the overall incidence of head and neck and OC cases [18–20]. References concerning vitamin A and oral cancer are numerous, and a large body of evidence supports the protective role of vitamin A; depletion in retinol is a common finding in OC patients [17]. Vitamin A and beta-carotene dietary enrichment decreased OC risk in animal models. Vitamin A supplementation also leads to regression of oral leukoplakia, a potentially malignant disorder. Other trace elements of relevance in cancer include iron and selenium.

1.2.3 Viruses

Viruses are important players in many malignancies. Although they cannot be referred as direct contributors, as in cervical carcinoma, they definitely are players in the genesis of OSCC. The viral hypothesis was initiated mainly for the following reasons: viruses can transform cells in vitro, viral genome is present in tumor cells, and viruses induce cancer in experimental models.

Human Papilloma Virus (HPV) is a DNA virus and its subtypes: 16, 18, 6, 11, are frequently found in oropharyngeal mucosa. According to a meta-analysis, approximately 26% of head and neck squamous cell carcinoma (HNSCC) contain HPV genome [2, 21]. OSCC and oropharyngeal squamous cell carcinoma (OPSCC) biopsies in patients without a history of smoking and/or alcohol abuse were positive for HPV in many cases indicating their possible role in pathogenesis. The association between oropharyngeal cancer and HPV varies considerably (0-100%), also varying with geographic locations [22]. The prevalence of HPV 16/18 in oral and oropharyngeal dysplasia is 3 times more than in normal biopsies, as pointed out in a recent meta-analysis (1985–2010) [21]. In a meta-analysis (1982–1997) by Miller and Johnstone, HPV prevalence was 22.2% in benign leukoplakia, 26.2% in dysplasia and carcinoma insitu (intra-epithelial neoplasia) and 46.5% (almost 2 fold) in OSCC [23]. HPV was identified in 80.6% of koilocytic dysplasia, a form of oral epithelial dysplasia [24]. In this lesion, the light microscopic features (koilocytes etc) were sufficient to predict HPV with an accuracy of 80%. HPV-16 prevalence is specific to certain oral sites such as base of tongue, tonsillar and laryngeal SCCs. HPV can be broadly divided based on their pathological ability into low-risk and high-risk type. The low risk ones cause oral warts or papillomas, and the high risk ones (HPV 16/18) cause malignancy. It is also suggested that HPV is sexually acquired (oro-genital contact) [25], which may be the reason for the recent rise in OC cases. HPV is a common inhabitant of the cervical mucosa and well-established risk factor for cervical carcinoma. HPV positivity (particularly HPV 16) is frequently seen in married white patients, belonging to high socio-economic order (50000$ annual income), without history of smoking or alcoholism [2, 26]. Also sero-positivity of herpes simplex virus (HSV-1,-2) modifies OC risk associated with tobacco, alcohol and HPV subtypes. The simultaneous presence of HSV-1 and HPV 16 DNA has been reported. HSV-1 may be a cofactor to cigarette smoking and HPV infection. It is believed to 'hit and run' in the early event. Literature is scarce on the link between Epstein barr virus (EBV) and oral cancer, but EBV is more frequently detected in oral lichen planus, an OC precursor. Studies have identified a significant correlation between EBV-DNA and OSCC, but its contribution in carcinogenesis is unsolved. The identification of virus in OSCC specimens is also limited to the technique employed. Standard method for HPV identification is PCR based detection of E6 mRNA in frozen specimens; another surrogate marker is the overexpression of p16INK4A protein, a cyclin dependent kinase (CDK) inhibitor protein [27]. HPV positivity is an important prognostic factor for survival; such patients had a better 3 year survival rates after adjusting for age, race, tumor and nodal status, tobacco exposure and treatment application [28].

HPV oncoproteins (E6 and E7) exhibit interaction with the two most important tumor suppressor genes: tumor protein p53 (*TP53)* and Retinoblastoma *(RB)*, and telomerase, critical tumor suppressors and cause oral epithelial cell immortalization. E6 causes degradation of TP53, and E7 inactivates retinoblastoma pathway [27]. The activation of these genes and the detection of their relevant products are the gold standard for characterization of HPV-driven head and neck cancer, nowadays.

1.2.4 Trauma and Inflammation

Trauma or irritation to oral mucosa is a neglected but common potential risk factor. Denture irritation, irregular teeth, faulty restorations, and chronic cheek biting cause trauma that results in inflammation and tissue regeneration processes. OSCC was also reported in a patient with mental disorder who indulged in injuring himself using a toothpick [29]. Also mechanical trauma and galvanic phenomena arising from close contact of mucosa with prosthesis may implicate in oral carcinogenesis of certain cases [30]. Evidence is missing whether this occurs directly or via lichenoid dysplasia. The contribution of trauma to malignancy is linked through inflammation and may be intensified by smoking and alcohol consumption [31]. Some patients even develop OSCC in the complete absence of alcohol and smoking, simply from mechanical trauma [32, 33]. We have noticed many patients, who admitted themselves with sharp teeth associated with nodular lesions and non-healing ulcers on the tongue, floor of the mouth, and maxillary retromolar area, which proved to be carcinomas. Clinical judgment whether or not to biopsy such lesions is critical and dependent totally on the clinician's experience. As a guideline clinicians usually wait for 2–3 weeks to see if there is healing after removal of the presumed traumatic agent. There is only little evidence on mechanisms involved in OC arising from trauma, and therefore, this represents a potential area for research. Mechanical trauma needs more attention and is a definitive cause for OC [33]. Chronic mucosal trauma is not an entity in itself but showed significant cancerous potential. This entity is a chronic inflammatory condition; a large body of evidence favors it as a cause of oral cancer.

1.2.5 Mouthwash and Toothpaste

The link between mouthwash/toothpaste with oral cancer is not strong, although there is some evidence. Interviews conducted in patients with oral cancer and healthy controls identified mouthwash as a possible culprit [34]. The incidence of alcohol-containing mouthwash was higher among OSCC individuals than healthy individuals. Many authors have shown Viadent products (toothpaste and mouthwash) containing sanguinaria extract to have a strong association with leukoplakia-like lesions of the maxillary vestibule [35, 36]. In the Indian market, similar products are still sold, some even containing tobacco.

1.2.6 Candida

Changes in microbiome as a cause of neoplasia were disregarded by many authors for several years. Later a role for these was shown in many cancers. *Helicobacter pylori* is implicated in gastric carcinoma; in a similar way, there is some evidence on the role of *Candida* spp. in the emergence of malignancy. *Candida albicans* disrupts epithelial cadherin (E-cadherin) adherens junctions between epithelial cells [37]. *Candida* was shown to exhibit some promoter effect during neoplasia [37–39]. *Candida* is normally a commensal and colonization is limited by the host immune system. Both keratinocyte features and *Candida* type happen to influence *Candida* colonization and adherence [40]. The carcinogenic compounds produced by *Candida* include nitrosamines; N-nitrosobenzylmethylamine (NBMA) can induce mutations. Alcohol consumption can increase the carcinogenic potential of *Candida albicans* as *Candida albicans* produces aldehyde from ethanol through alcohol dehydrogenase isoenzyme which may play some role in oral carcinogenesis [41].

1.2.7 Solar Radiation

Solar radiation is a major risk factor for lip squamous cell carcinoma. It is responsible for a group of potentially malignant lip lesion actinic keratosis of the lip (actinic cheilitis), which may progress into squamous cell carcinoma. SCC of the lip is less aggressive and shows a favorable prognosis. The ultraviolet component in solar radiation primarily targets nucleic acids; in this way it is responsible for cancerous transformation of lip mucosa. The passage of ultraviolet radiation to the earth has also increased with time due to growing industry, and the ultraviolent band in particular is to be blamed in lip cancer, especially in the absence of tobacco habit. Outdoor occupation and lacking sunscreen protection in these patients strengthen the role of solar radiation in OSCC.

1.3 Oral Potentially Malignant Disorders (OPMD)

According to the recent (2017) *World Health Organization (WHO) Classification of Head and Neck Tumors*, "OPMDs are clinical presentations that carry a risk of cancer development in the oral cavity, whether in a clinically definable precursor lesion or in clinically normal oral mucosa" [42, 43]. This revised term eliminated confusion as all precancerous lesions and conditions are essentially the same in one sense, being precursors to oral cancer. Oral cancer can arise at these locations. Oral potentially malignant disorders (OPMD) refer to the entire spectrum of epithelial disorders (major category) associated with tobacco (but not limited to it), or connective tissue or general disorders (genetic defects) associated with some potential or susceptibility for OSCC. The word 'potentially' was applied as these disorders as they do not always lead to cancer, but are 'potentially cancerous'. The word 'disorder' refers to a disturbance of tissue in terms of genetics and microscopic modifications leading to clinical altered appearance compared to normal counterparts. The link between OSCC and certain disorders is undisputed. The rate of malignant transformation is higher when potentially cancerous disorders (PMDs) involve the tongue. For PMDs regular follow-up at least at 2–6-month intervals is advisable, but this approach cannot be generalized and depends on the type of lesion [42]. Although transformation in some lesions is still debatable, for many lesions a large body of evidence highlights the risk of transformation. However more recently in 2017, in the fourth edition of the WHO, a large number of modifications were made [43]. Common OPMDs, as in the fourth edition, include leukoplakia, erythroleukoplakia, erythroplakia, oral submucous fibrosis, actinic keratosis of the lip, smokeless tobacco keratosis, palatal lesions associated with reverse smoking, chronic candidiasis, lichen planus and discoid lupus erythematosus, syphilitic glossitis, and dyskeratosis congenita. We have grouped them based on etiology into:

1. Habit associated conditions
2. Inflammatory, immune-mediated lesions
3. Lesions secondary to solar radiation
4. Infections
5. Rare inherited disorders [44, 45]

Habit-associated conditions and inflammatory and immune-mediated lesions are very common in clinical and community settings. DNA damage can occur following exposure to ultraviolet band in solar radiation. Lesions associated with solar radiation and inherited disorders represent a minor group of disorders with small risk of transformation.

1.4 Group I: Habit-Associated conditions (Major Category)

1.4.1 Leukoplakia

Leukoplakia is a clinical term and is a non-scrapable white plaque which cannot be defined as any other lesion or OPMD. In fact tobacco use and alcohol consumption are associated with many cases of leukoplakia. It is an exclusion diagnosis, made after ruling out the presence of similar white lesions of known origin. It is the most common OPMD of the oral cavity, involving any site. Broadly, leukoplakias are homogenous or nonhomogenous including speckled, erythroleukoplakia, verrucous, and proliferative as well. Idiopathic leukoplakia (nontobacco-induced leukoplakia) described in some reports is a rare, less examined, and less recognized entity. Among all subtypes, homogenous leukoplakia is the most common. Although, generally the transformation risk of leukoplakia globally is approximately 1–2%, some meta-analyses indicate a higher risk. The determinants of malignant transformation are nonhomogeneous appearance of leukoplakia, large size of lesion (>200mm^2), presence of dysplasia, involvement of the lateral and ventral tongue, age, and female gender [46]. There are various forms of leukoplakia, each associated with a different rate of malignant transformation. Malignant transformation is also site specific and differs widely, with buccal lesions possessing low risk (3.53%) and tongue lesions possessing a high risk (22.4%) [47]. Leukoplakia involving the buccal mucosa and lip is more benign (Fig. 1.1). The tongue and floor of the mouth are two high-risk locations for leukoplakia (Fig. 1.2), exhibiting highest dysplasia and aneuploidy status [48]. Generally, nonhomogenous type of leukoplakia shows a higher risk of transformation. In speckled leukoplakia, the site with erythematous (red) component needs to be biopsied (Fig. 1.3) [49]. In addition lesions with increased thickness or a verrucous surface may contain epithelial changes including severe dysplasia and need total excision. Leukoplakia with *Candida* (Fig. 1.4) has a more cancerous potential as these organisms produce carcinogenic nitrosamines and related products. *Candidal* strains with high nitrosation potential were isolated from advanced cancerous lesions, and *Candida* was referred as a promoter of oral epithelial neoplasia [41].

Proliferative verrucous leukoplakia (PVL) is a rare, hyperkeratotic, and proliferative variant associated with the highest malignant transformation rate of over 70% (Fig. 1.5) [50]. It is frequently seen among elderly women, common sites being the tongue, alveolar ridge, and buccal mucosa [50]. It occurs both in smokers and nonsmokers. The female to male ratio is 4:1, and at times it occurs bilaterally. Its histological findings can range from hyperkeratosis without dysplasia to conventional squamous cell carcinoma, each of the foci existing at a different grade [50]. It is a multifocal condition and field cancerization is a striking feature [51]. Recently criteria for PVL were set by with a broad coverage of features such as site, verrucous nature, extension, recurrence in a treated site, wide histological variation being the major criteria, and large size (>3 cm) occurrence in a nonsmoking patient and disease duration greater than 5 years being the minor criteria [50]. Three major criteria (two major plus one minor) confirm PVL. In PVL, multiple malignancies can occur at uncommon locations, due to its multifocal nature. Ideally, PVL patients should be followed up at least once in 6 months [51]. PVL can be managed through

Fig. 1.1 Buccal mucosa (**a**, **b**) and labial mucosa (**c**) are the most common locations for leukoplakia

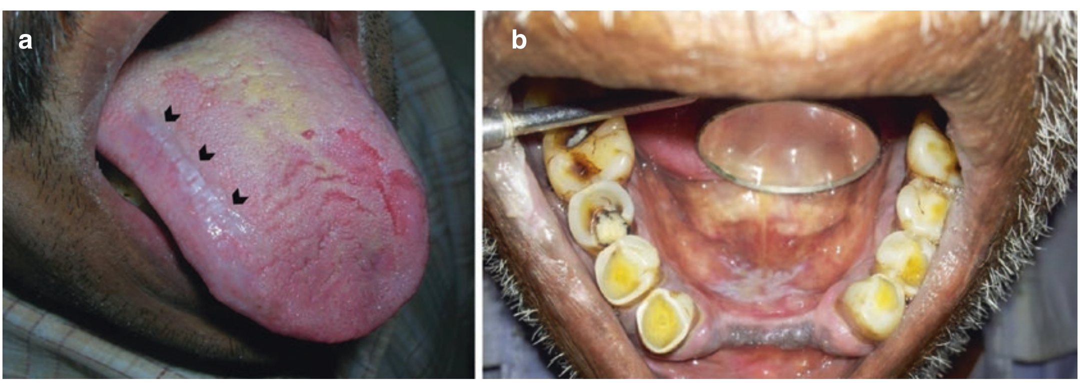

Fig. 1.2 Leukoplakia involving tongue and floor of mouth are high risk variants to be managed with caution

Fig. 1.3 Speckled leukoplakia is a mixed red–white lesion with high malignant potential

Fig. 1.4 Candidal leukoplakia presenting as a non-scrapable white lesion masquerading as speckled leukoplakia (**a**, **b**), responded quickly to local antifungal therapy

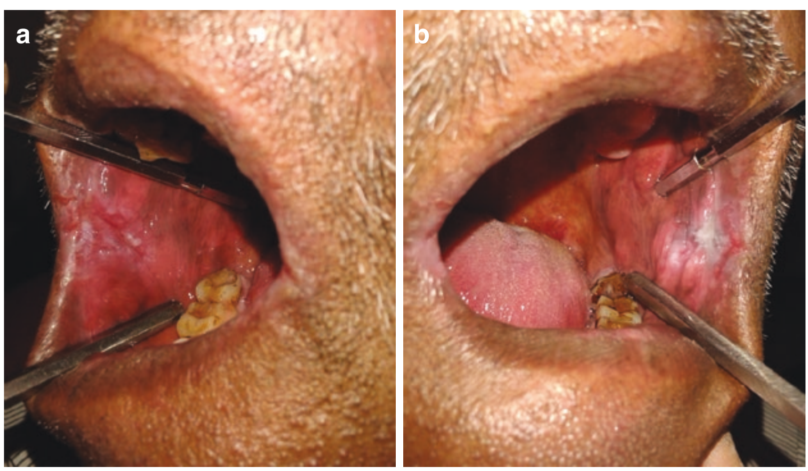

Fig. 1.5 Proliferative verrucous leukoplakia presents as a wide lesion with thick white, and red elements

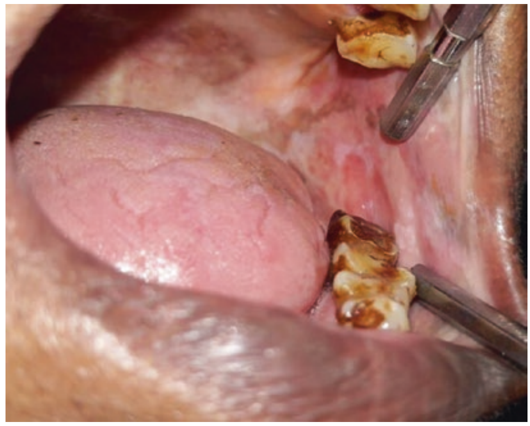

Fig. 1.6 Pale blanched oral mucosa in oral submucous fibrosis

wide excision and carbon dioxide lasers. Leukoplakia may sometimes present as a multi-focal disease, which may reveal multiple areas of malignancy (microscopically) due to the field cancerization phenomenon [52]. Multiple field mapping biopsies are of value in such cases.

1.4.2 Oral Submucous Fibrosis

Oral submucous fibrosis (OSF) is a chronic, insidious, precancerous disorder affecting the oral cavity, pharynx, and esophagus. It is highly prevalent in India and Southeast Asia and also seen among young individuals [53]. This condition presents with fibroelastic changes in the lamina propria and shows epithelial atrophy. Fibroelastic changes lead to stiffness of mucosa and reduced mouth opening. The only risk factor associated with OSF is areca nut (*Areca catechu*), also known as betel nut. OSF is slow, a chronic process developing several years after the initiation of this habit. The risk of developing OSF increases steadily with increasing frequency of the chewing habit and increasing duration (~4 years) [54]. At the initial stage, there is a burning sensation which is aggravated on consumption of spicy foods, and there is mild blanching of oral mucosa. In the advanced stage, there is a burning sensation even in the absence of stimuli (no aggravating factors), moderate to severe blanching, and restricted tongue movements due to fibrotic bands (Fig. 1.6). As time passes, the fibrotic bands become thicker, and ulcers and erosions may appear. Other features of OSF include increased salivation, altered taste sensation, dryness of the mouth, impaired hearing, change in voice, and difficulty in swallowing. Once OSF develops, there is neither regression nor any effective treatment.

An altered collagen deposition and degradation cycle and fibroblast life cycle are central to this pathology. These changes are a direct result of various chemical components in areca nut. Areca nut contains copper as mentioned earlier, which is partly responsible for OSF. Assessment of copper concentration in saliva and histological grade of OSF yielded a significant association, and a threefold increase in saliva copper concentrations was found in OSF individuals [55]. Copper levels were estimated using rhodamine stain, where color intensity and number of copper granules showed marked increase in biopsies obtained from OSF patients [55].

Many studies were conducted evaluating the role of copper and zinc in the pathogenesis of OSF [56]. An elevated copper/zinc ratio is a frequent observation. Hematological investigations in OSF patients usually reveal iron deficiency anemia [55]. Changes in the level of antioxidants, superoxide dismutase, glutathione peroxidase, and vitamin A and E were frequent observations [55]. Histological features of OSF include epithelial atrophy, deep rete pegs, degeneration of basal cells, hyalinization of connective tissue, and inflammatory cell infiltration. Individual susceptibility to OSF varies considerably. This wide variation after the same degree of exposure to areca nut products is most likely due to genetic factors. Six collagen and collagen-connected gene polymorphisms (collagen 1A1, collagen 1A2, collagenase-1, lysyl oxidase, transforming growth factor-1, cystatin C) and polymorphisms in glutathione S-transferases (e.g., glutathione S-transferase theta 1 (GSTT1), glutathione S-transferase mu 1 (GSTM1)), and cytochrome P450 xenobiotic genes increase susceptibility to OSF [57–59].

Follow-up studies have highlighted advanced cases to be associated with malignant transformation. Malignant transformation rate of OSF is approximately 2–8% [60]. Arecoline is a principal etiological factor in this process as it increases oxidative damage to DNA causing double-strand breaks and nitrosation [61]. To further complicate this, local fibrosis restricts oxygenation to oral tissues leading to epithelial hypoxia, another roadway to malignancy. The hypothesis connecting hypoxia and malignant transformation was strengthened by the proportional thickness of fibrosis and dysplasia. Hypoxia induces production of hypoxia-inducible factor 1 alpha (HIF-1α), which was already proven as a cancer marker in malignancies [62, 63]. SCC developed in OSF is more often seen in young individuals, who show better tumor grade and a lower risk for nodal involvement (good prognosis) [64]. Malignancy risk may be higher in individuals who take betel nut, tobacco, and slaked lime (Fig. 1.7).

Fig. 1.7 Oral squamous cell carcinoma arising in a background of oral submucous fibrosis

1.4.3 Erythroplakia

Erythroplakia or "erythroplasia of Queyrat" is a fiery velvety red patch that cannot be characterized as any other lesion. It is a diagnosis of exclusion and considered as the most dangerous oral potentially malignant disorder. Its red appearance is due to atrophic-neoplastic epithelium and reduced keratinization [65]. Thin epithelium and the absence of keratinization allow visibility of underlying microvasculature imparting a red hue. The prevalence rate of erythroplakia is very low (0.02–0.83%). Lesions mostly are less than 1.5 cm in diameter [66]. Preferred sites are the soft palate, the retromolar area, the buccal mucosa, the tongue, and the floor of the mouth. Commonly, elder people are involved in their fifth to seventh decades [67]. Males and females are at equal risk. The exact pathogenesis is not clearly understood, but the two strongest risk factors include smoking and alcoholism [66]. Histologically, the lesions showed severe dysplasia in association with invasive carcinoma in 51% cases [68]. It is recommended to use carbon dioxide laser to excise them, but larger lesions are associated with higher recurrence rate [69].

1.4.4 Palatal Lesions Associated with Reverse Smoking

Reverse smoking is smoking with the burning end of the cigarette kept in the mouth. This habit is commonly seen in females, in the Indian subcontinent, especially in the Coastal Andhra population [70]. Palatal changes occur mainly due to heat, but the role of the smoke itself cannot be disregarded. The palatal changes seen in reverse smokers include hyperpigmentation (smoker's melanosis), depigmentation, excrescences, and ulceration. Temperature is an important regulator of tyrosinase activity and melanin production; therefore hyperpigmentation is the most common finding in reverse smokers [71]. Well-defined potentially malignant disorders like leukoplakia and erythroplakia occur in reverse smokers [72]. Malignancy in reverse smokers was reported to coincide with gland distribution of oral mucosa (middle or posterior half of the hard palate but not in soft palate or anterior halve) [73]. In an interview-based cross-sectional study [74], reverse smoking was identified as a major determinant of palatal cancer with all patients with palatal cancer revealing the habit of reverse smoking, and reverse smoking of chutta (Indianized homemade cigar prepared from folded tobacco leaf) was associated with more lesions than conventional smoking.

1.5 Group II: Inflammatory, Immune-Mediated Lesions

1.5.1 Oral Lichen Planus

Oral lichen planus (OLP) is an immune-mediated disorder. It is common in the general population with an average prevalence rate of 0.5–2% and is seen chiefly among females between the third and sixth decades [75]. Wickham first described the reticulated and striated lesions, and the histological features were elucidated by Darier. Cutaneous lesions are seen in 10–15% of patients with OLP. Oral lesions in lichen planus may occur weeks to months, before they become manifest at other sites [76]. OLP involves the buccal mucosa, lateral border of the tongue, and gingiva often presenting with bilateral lesions. Lichen planus is caused by a cell-mediated immune mechanism leading to basal cell degeneration. Factors to blame in OLP include stress, female hormones, diabetes, hepatitis C infection, etc. [77, 78]. The frequency of certain major histocompatibility complex haplotypes (both higher and lower incidence) was found to show significant association with OLP in different populations [79]. The clinical course includes periods of remissions and acute exacerbations. In general, OLP contains both red and white elements. The major clinical variants include reticular, papular, plaque, bullous, erosive and erythematous, and ulcerative. In the reticular variant, fine white lines in a network pattern referred as "Wickham striae" are seen bilaterally mostly on the buccal mucosa. However, the reticular component is pathognomonic to all forms of LP and is essential to make a tentative diagnosis of lichen planus. The reticular form is the most common, milder form, not associated with malignant transformation, and the erosive form is more painful and precancerous (Fig. 1.8) [76, 77, 80]. In the erosive form, the degree of apoptosis in the epithelium is higher, and in the reticular form, the degree of apoptosis in the subepithelial inflammatory infiltrate is higher [81]. The epithelial thickness in both forms is thinner than in healthy oral mucosa. The clinical manifestations are proportional to the degree of subepithelial inflammation. An increase in inflammatory infiltrate (more lymphocytes) usually results in a higher destruction of basal epithelium making the epithelium erosive and ulcerative. Inflammation also triggers epithelial hyperkeratosis. An inflammatory gradient is observed in and around OLP, and a mild erythematous reaction is noticed at the periphery when there is hyperkeratosis. OLP is histologically characterized by a subepithelial band of inflammatory infiltrate (T lymphocytes and macrophages), liquefaction degeneration of basal cells and saw-toothed rete pegs, and intraepithelial T-cell migration [76]. The mechanism underlying LP is "autoreactivity of T lymphocytes to antigens on basal cells." OLP is chiefly a $CD8^{+}$/$CD4^{+}$ disturbance. Mast cell degranulation and upregulation of matrix metalloproteinases occur adjacent to basal epithelial layers. Mast cell degranulation is a non-specific event, which releases many chemical compounds ranging from inflammatory mediators (tumor necrosis factor alpha (TNF-α)) to proteases (chymase, tryptase) which damage the basal cells and basement membrane [82, 83]. The end result is degeneration of basal cells and apoptosis together with disorganization of the basal membrane zone. Lesions (cutaneous) are pruritic, and both oral and cutaneous lesions heal with pigmentation (post-inflammatory pigmentation). A few patients with LP may have lesions not only in gingiva but also in esophageal [84, 85] and genital region

Fig. 1.8 Erosive lichen planus is a red -white bilateral lesion surrounded by a network of white lines referred as wickham's straie, often associated with burning sensation

(vulvovaginal-gingival syndrome, peno-gingival syndrome) [86, 87]. They present with erosive and erythematous lesions. OLP may be also associated with diabetes and hypertension syndromes and sometimes associated with alopecia and nail changes [82].

It is debatable whether cases of lichen planus proceeding to cancer were genuine LP cases or just lichenoid dysplasia. "Keratotic plaque-like" and "erosive" or the atrophic subtypes of OLP have the highest malignant potential (1.1–6.7%) [88–91]. Hence it is necessary to examine and evaluate and reevaluate OLP cases on a routine basis. The incidence ratio of OSCC arising in OLP was found to be high among patients with hepatitis C virus (HCV) infection, so it is important to screen for HCV and to rule out malignancy; a biopsy may be necessary [78]. OLP responds quickly to systemic and topical corticosteroids, e.g., clobetasol propionate 0.05% or other immunomodulators (tacrolimus) depending on disease severity. All patients need to be informed about its malignant potential. One systematic review reported female gender and old age as two risk factors connected with malignant transformation [92]. Although some studies identified genetic profile of OLP to be similar to benign lesions, ideally we can consider OLP to have some potency for malignancy [93]. The clinical evolution of proliferative verrucous leukoplakia from LP has also been reported [94]. Authors have also hypothesized green tea consumption as a strategy in the prevention of transforming OLP [83].

1.5.2 Discoid Lupus Erythematosus

Discoid oral lesions are part of lupus erythematosus (LE), a well-known connective tissue disorder. LE localized to the skin or mucosa is considered as the discoid form, and when involvement is more generalized, it is considered as systemic LE [95]. The oral discoid lesions range from 0.5 to 2 cm and chiefly involve the labial mucosa, buccal mucosa, gingiva, and vermilion, characteristically among females [96]. The discoid lupus oral lesions present as circumscribed, elevated white lesion surrounded by a red halo. A radiating pattern similar to a lichenoid reaction is seen but in a diverging sunray or brush border form. Sometimes these lesions may also show a leukoplakia-like transformation (leukoplakia-like stage) or mimic lichen planus [97]. Discoid oral lesions are often seen in combination with skin lesions. Histological features include acanthosis, hyperkeratosis and keratin plugging, liquefaction of basal layers, and thickening of the basement membrane.

The pathogenic mechanism underlying LE is defective T-cell-macrophage signaling-killing and autoantibody production. Squamous cell carcinoma arising in oral lesions is uncommon but occasionally reported [98]. The reason for malignancy in these cases is attributed by some authors to the nature of the disorder itself, but some attribute it to drugs like cyclophosphamide taken in LE [99]. Malignancies common with systemic LE are non-Hodgkin lymphoma, squamous cell carcinomas of the sun-exposed skin, and vulvo-vaginal, lung, and hepatobiliary malignancies [100, 101].

1.6 Group III: Lesions Secondary to Solar Radiation

1.6.1 Actinic Keratosis

Actinic keratosis (AK) is a potentially malignant disorder of the lips frequently seen in individuals belonging to geographic locations with heavy exposure to solar radiation [102]. It is seen mainly in males (> 40 years), with a fair complexion, and presents as diffuse erosive keratotic plaques involving the vermilion border [103, 104]. The use of sunscreen and limiting exposure to sunlight are general preventive measures. It is more common among agricultural workers and fishermen (outdoor occupation) who are frequently exposed to ultraviolet (UV) radiation [103]. UV radiation in the range of 100–400 nanometers is pathogenic and filtered by the upper atmospheric layers [103]. In the UV spectrum, the band connected to the genesis of AK is UV-B radiation. UV-B is harmful as it causes covalent bonding of cytosine bases and can lead to P53 depletion, the protein product of an important tumor suppressor gene [102]. Melanin seems to have a protective role in the development of AK, as most of the patients are white complexioned or suffer from albinism. Also, the vermilion border is thin and lacks significant keratin and melanin content thus making it more susceptible for UV-B effects.

AK can present as white non-ulcerated lesion, as erosions or ulcers, or as an admixture of white and erosive pattern and with unclear separation between skin and vermilion border [104]. The keratotic flakes are a hallmark feature and usually progress to thickening, which indurate and ulcerate. Histologically they show keratinization, high mitotic activity, drop-shaped rete pegs, basophilic change in connective tissue, and intact basement membrane together with elastosis of the underlying stroma [104]. Medical management includes the use of topical 5-fluorouracil or imiquimod and other approaches like photodynamic therapy using methyl ester of aminolevulinic acid, vermilionectomy, CO_2 laser, and cryosurgery [105]. Follow up is critical in cases of actinic keratosis.

1.7 Group IV: Infections

1.7.1 Oral Syphilis

Syphilis is a highly infectious condition caused by the organism *Treponema pallidum*. It can be divided into primary, secondary, latent, and tertiary forms, whereas congenital syphilis is a form that occurs as a result of mother-to-child transfer via the placental barrier. In oral mucosa, ulcer named chancre (single or multiple) can be observed, accompanied by lymphadenitis consisting the characteristic feature of primary syphilis, and occur at the site of penetration of organism. Secondary form is characterized by maculopapular areas, mucous patches, or papules called condylomata lata, in the tertiary syphilis, a granulomatous inflammatory lesion known as gumma (nodular or ulcerative destructive lesion) and glossitis as lobulated (interstitial) or atrophic (loss of dorsal tongue papillae). These lesions are abundant with the infective organisms and highly infective but heal spontaneously. In an extensive PubMed survey on oral syphilis cases between 1950 and 2011 by Leuci and colleagues, 23 reports were identified that described 34 patients. Thirty-five were classified as primary, 56% were primary, and 9% were tertiary forms and presented into a variety of forms which include ulcers, mucosal patches, keratosis, pseudomembranous lesions, and rarely gummas [106]. Among the oral manifestations, the characteristic, atrophic, and syphilitic glossitis has been classified as an oral potentially malignant disorder. The manifestations depend on time, site of infection (skin or mucous membranes), and the immune status of the individual. The strength of the delayed hypersensitivity response is also pivotal for defense against syphilis mediated by the $CD4^+$ cell population. And in the immunosuppressed individuals, massive levels of *T. pallidum* may be also found in the internal organs. Major studies on delayed immunity basis of syphilis arise from the study in rabbits [106, 107]. More recently the pathological profiling of secondary syphilis cohort identified intense expression of immune-inflammatory and vascular proteins, namely, intercellular adhesion molecule 1 (ICAM-1), vascular endothelial growth factor (VEGF), and CD34 [108].

In 1994, Michalek et al. identified 350 cases of (OSCC and Kaposi sarcoma) combined in a cohort of 16,420 people diagnosed with syphilis during a 15-year window. Although no conclusions were made, a suspicion was drawn between cancer and syphilis [109]. In the following year, Dickenson et al. identified in a cohort of 63 OSCC patients 5 patients (8%) who reacted positively for syphilis antibodies [109]. Interestingly, syphilitic oral lesions were also misdiagnosed for oral cancer in some patients [107]. Taking into account all the available evidence, OSCC arising in a patient with syphilitic glossitis is extremely rare but possible. Serological screening for syphilis is warranted for all patients with OSCC [110].

1.7.2 Chronic Candidiasis

Oral and esophageal carcinoma was reported in chronic candidal lesions in autoimmune polyendocrinopathy-candidiasis-ectodermal dystrophy (APECED) and primary immunodeficiencies [37, 38]. Chronic mucocutaneous candidiasis is an important feature and may be the first manifestation of APECED with a high predilection for early onset OSCC, even multiple OSCC were noticed in a few cases [37]. The T-lymphocyte defect underlying this syndrome favors the colonization of *Candida* spp., followed by mucositis and malignant transformation [39]. Antifungal therapy and regular surveillance in these patients are valuable. In studies, the degree of dysplasia in OSCC also correlated to the amount of *Candida albicans* in terms of colony-forming units per ml (i.e., oral yeast carriage) [40]. The presence of fungal hyphae may serve as one of the indicators to predict malignant risk in OPMDs.

1.8 Group IV: Rare Inherited Disorders (Minor Category)

Although inherited disorders are rare (<5% of OSCC) and represent only a miscellaneous group of oral potentially cancerous disorders, they contribute heavily to our understanding of the mechanisms in cancer. “Inherited disorders” include both genetic diseases and also inherited disorders associated with cancer syndromes. In conditions like “inherited cancer syndromes,” individuals are born with an inherited defect in one gene copy and develop cancer after the second hit.

1.8.1 Dyskeratosis Congenita (DC)

It was originally described as a form of ectodermal dysplasia involving the skin, nails, and mucous membrane [111]. The main oral change of concern with DC includes oral leukoplakia. Other features include skin hyperpigmentation in lacy networks, dystrophic nails, bone marrow failure, and pancytopenia. Oral leukoplakia, hyperpigmentation, and dystrophic nails form the classic triad of DC. Literature also reports a high incidence of caries, hypodontia, periodontitis, intraoral pigmentation, blunt roots, and taurodontism (decreased tooth root/crown ratio) in this population. Since its identification in 1900, more than 500 DC cases were reported with a cumulative cancer incidence of 40% by the age of 40. Among them OSCC is more common, followed by skin and anorectal cancer [112]. Tongue cancer risk in these patients is increased over 1000-fold. DC patients have short and dysfunctional telomeres, and it is therefore a telomere disorder. In DC the features of bone marrow failure and pancytopenia are attributed to a depletion of stem cells due to shortening to telomeres. DC is the first telomere disorder described in the literature and a powerful model system to understand HNSCC cancer. All patient-derived induced pluripotent stem cells harbor the same telomeric features and biochemical changes; changes also correlated with disease severity [113]. The X-linked form of DC mutations is in dyskerin (*DSK 1*); in the autosomal dominant form, mutations lie in telomerase reverse transcriptase (*TERT*) or telomerase RNA component (*TERC)*, and in the autosomal recessive type, the gene frequently involved is telomerase Cajal body protein 1 (*TCAB1)*. DC is genetically variable, also associated with other mutations including TRF1-interacting nuclear factor 2 (*TINF2*) (severe disease phenotype); nucleolar protein family A, member 3 (*NOP10*); nucleolar protein family A, member 2 (*NHP2*); and regulator of telomere elongation helicase 1 (*RTEL1*) (correlates with severe phenotype and multisystem failure) [114]. Till date, numerous DC-associated mutations have been identified and each gene codes for a component of the telomere. Bleomycin is the line of treatment for oral leukoplakia associated with DC. Inherited disorders like DC are excellent models to explore our understanding of OSCC, as defective telomeres are essential basis to the genesis of both OSCC and DC.

1.9 Oral Squamous Cell Carcinoma

Oral squamous cell carcinoma (OSCC) is generally more prevalent in men than women. The clinical features can range from a completely asymptomatic white patch to a red-white speckled lesion associated with a burning sensation but usually consist of ulcerated lesions with raised margins, solid in palpation or nodular exophytic masses occasionally combined with ulceration. OSCC involves the buccal mucosa, tongue, gingiva and alveolus, soft palate, and retromolar area (Fig. 1.9). Ulcers with induration or mucosal nodularity (rigid to touch) are common clinical presentations and important signs of malignancy. Late lesions can also present as necrotic lesions showing gross destruction. Some patients also demonstrate hemorrhage and oral bleeding. Pain is a feature (30% cases) of advanced lesions located on the tongue and floor of the mouth [115, 116]. Pain is normally a feature of lesions with endophytic growth pattern. Base of tongue lesions is also associated with dysphagia, ear pain, and neck nodes [117]. The 5-year survival rate is 30–60%, and patients are normally at stage III or stage IV at the time of diagnosis [115]. Survival is lowest when the tongue and floor of the mouth are involved; lip lesions show better outcome. The role of trauma in the pathogenesis of OSCC is not fully understood, but 'chronic traumatic ulcer' at the lateral tongue can be considered as a potential OPMD! [33] (Fig. 1.10). Majority of OSCCs are conventional OSCCs or verrucous carcinomas, but other less common entities (15% cases) are also reported [118]. They include acantholytic SCC, spindle-cell carcinoma, adenosquamous carcinoma, basaloid SCC and papillary SCC, and adenosquamous, lymphoepithelial, acantholytic, and carcinoma cuniculatum [119]. However, the most common presentation is conventional squamous cell carcinoma.

Verrucous carcinoma is a warty and verrucous variant of squamous cell carcinoma (Fig. 1.11). It was identified in the 1940s, described by Ackerman as a variant of OSCC (Ackerman's tumor). It is seen in tobacco chewers, smokers, and areca nut users [120]. Verrucous carcinoma

Fig. 1.9 Oral squamous cell carcinoma (OSCC) subsites include tongue, buccal mucosa, floor of mouth, alveolus, retromolar area and soft palate. SCC involving the tongue (panel **a**) is often indurated and associated with restricted tongue movements. Among all the subsites SCC involving the tongue and floor of the mouth (panel **b**) are considered to have significantly poor outcomes. SCC involving the alveolus are associated with tooth mobility (panel **c**) which in some contexts can be the first clinical indicator and complaint of the patient, or at times present localized to the posterior retromolar area presenting with a perforation (panel **d**), which can be missed out during careless examination. SCC involving the soft palate region (panel **e**) is diagnostically (due to poor illumination and shadowing of palate) and therapeutically challenging. Sloughy necrotic presentations (panel **f**) are often associated with significant halitosis concerns

(VC) is pebbly and papillary, painless, and exophytic with a cauliflower morphology [121]. Its surface has many invaginations, growth is slow, and metastasis is not seen by definition. Histologically, it presents with deep epithelial clefts and well-differentiated squamous epithelium with bulbous rete peg organization. There is a low mitotic rate, and "parakeratin plugging" is a hallmark of verrucous carcinoma. The basement membrane is intact, and heavy inflammatory reaction is seen in the adjacent connective tissue. Sometimes minute foci of conventional

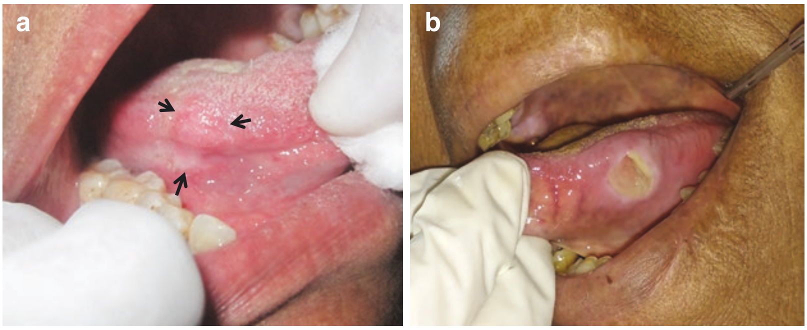

Fig. 1.10 Oral squamous cell carcinoma sequelae arising from trauma is a relatively common but under reported phenomena in the clinical setting, also less understood in terms of biology. Tissue inflammation is the route cause of this and enameloplasty is a mandatory step for sharp molars which often traumatize the lateral borders of tongue. Panel (**a**) shows a painful nodule in a women in the seventh decade with no history of tobacco usage. The lesion showed no surface alterations such as ulceration, but there is a keratotic area at the lesion periphery associated with sharply cusped molars. The patient had histologically proven SCC and survived less than 1 year from diagnosis. Panel (**b**) shows a traumatic ulcer on tongue (with sloppy edges) which has a risk of transformation if there is constant trauma. Trauma to the tongue is far more significant when it comes to malignant transformation compared to trauma in other oral sites like buccal mucosa; the biological attributes of this phenomena is unexplored and a worthy investigation

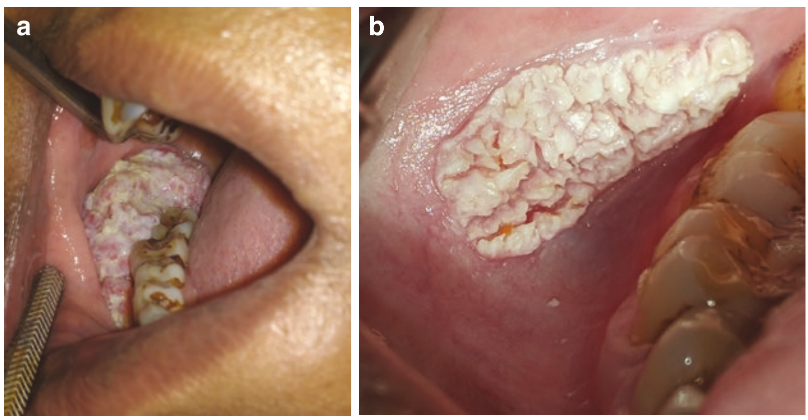

Fig. 1.11 Verrucous carcinoma is characterized by a papillary and warty surface, occurring especially in the gingival mucosa region and tongue. It is a proliferative variant, histologically limited to the epithelium with least potential for metastasis

squamous cell carcinoma may also be found histologically. It is frequently seen in the elderly, in their sixth to seventh decades [121]. A significant male prediction was noted, and the most common sites include the buccal mucosa, gingival-alveolar ridge, palate, and retromolar trigone area. It is predominantly exophytic and often thick and white. The lesions involving the alveolar ridge are sometimes fixed to the periosteum. It is frequently seen in tobacco chewers and bleeding is rare. Verrucous lesions can be multicentric, and each lesion can exist at a different stage [122]. Two biopsies are at times necessary to rule out invasive malignancy. The genomic signature (low mutation rate in *TP53, NOTCH1, CDKN2A*, etc.) and line of treatment also differ considerably from routine OSCC [123, 124]. Variation in antioxidant enzyme levels was found to be more severe in OSCC than VC [125]. It is also important to differentiate a VC from verruciform xanthoma, which is a benign disorder, showing foam cells in the connective tissue [126]. Verrucous hyperplasia (VH) is closely related to VC [125]. It shows male predilection and favors middle-aged individuals, involving the buccal mucosa, tongue, and palate [127, 128]. The local application of tobacco, lime, and areca nut was identified as the etiology [128]. Histologically they may present with moderate dysplasia. The downward displacement of the epithelium into the submucosa rules out VH [127]. The 5-year malignant transformation rate was as high as 10% [128]. Immunostaining with TP53 antibody also did not show a significant demarcation between VC and VH [129]. Clear demarcations between VH and VC cannot be firmly made.

1.9.1 Basic Histological Observations

Dysplasia and carcinoma in situ are two stages that most of OSCCs must transcend during their evolutionary process. Dysplasia is a potentially malignant change, a finding that can be spotted under a microscope, and a marker of cancerous potential. OSCCs emerge in existing dysplasia. Following this event, there is proliferation of dysplastic squamous cells and breach in the basement membrane. Disruption of the basement membrane (invasion) represents an important stage in the evolution of OSCC, and this is responsible for metastasis (Fig. 1.12). The major difference between OSCC and verrucous carcinoma is in their potential for invasion and metastasis; the latter has lower invasive/metastatic ability and better prognosis. The reactive changes in the epithelium of a beginning lesion include hyperkeratosis, benign hyperplasia, and acanthosis.

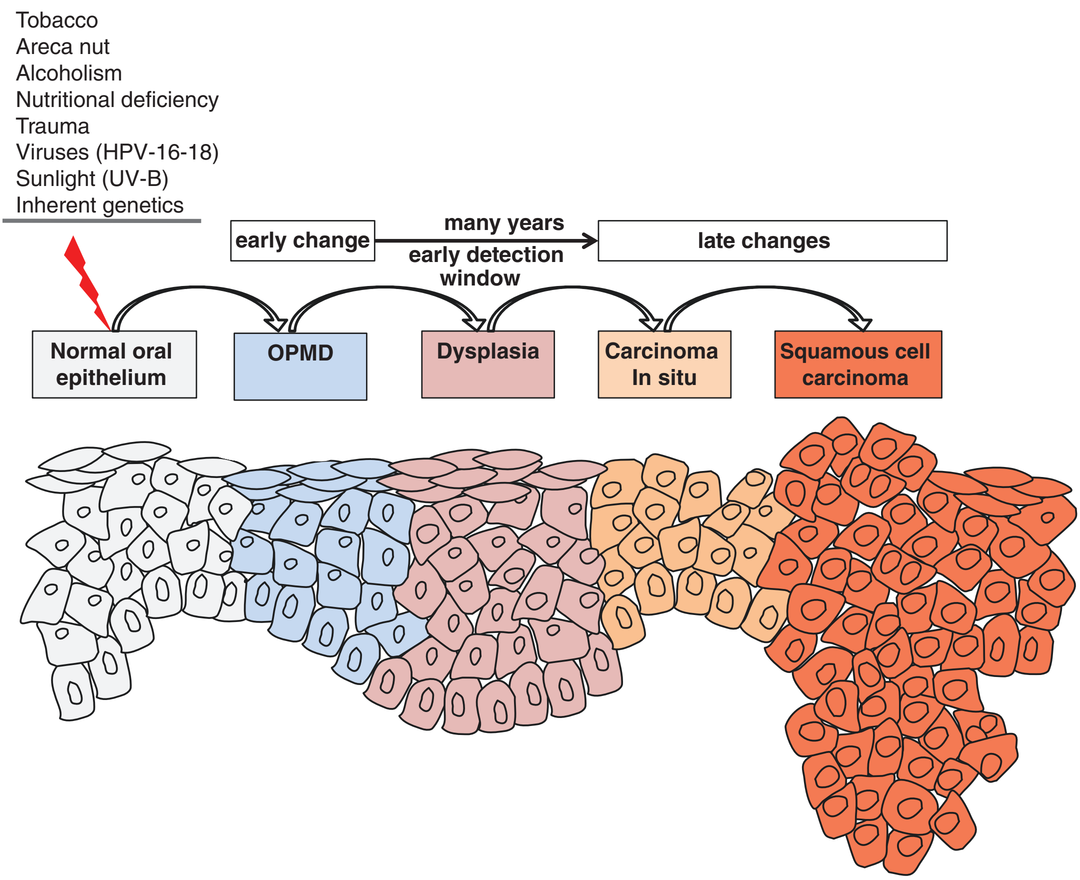

Fig. 1.12 Evolution of oral cancer. The risk factors include: tobacco; viruses like human papilloma virus (HPV-16/-18), fungi like Candida and bacteria like *Treponema pallidum*; mechanical trauma due to sharp tooth, and less recognized triggers like sunlight containing UV-B (which causes actinic keratosis predisposing the lip to squamous cell carcinoma), and inherited telomeric genetic disorders. Nutritional factors have also been proposed in the genesis of oral cancer, and alcohol often acts synergistically with tobacco. It takes several years for the genetic changes to accumulate from the stage of OPMD, and the abnormal architectural changes and cytological features occur only after accumulation of a number of genetic hits

1.9.1.1 Dysplasia

Dysplasia precedes OSCC and can be considered as the first histological stage (change) with an increased risk of progression to malignancy. "Oral dysplasia is a potentially cancerous forerunner of OSCC" found in some cases of leukoplakia and mainly in erythroplakia. Common cellular and architectural changes that constitute dysplasia include abnormal variation in nuclear size/shape, cell size/shape, increased nuclear-cytoplasmic ratio, atypical mitotic figures, increased number/size of nucleoli, nuclear hyperchromatism, irregular stratification of epithelium, loss of basal cells' polarization, drop-shaped rete ridges, frequent and abnormally superficial mitotic figures, premature keratinization in single cells, keratin pearls within rete ridges, and loss of epithelial cohesion [43]. Oral epithelial dysplasia is subdivided into three grades depending on the width of affected epithelium: mild dysplasia refers to changes in basal-parabasal layers, moderate dysplasia corresponds to changes from basal layer to middle layers, and severe dysplasia is dysplasia spanning from basal layer to upper layers. Interestingly, a subset of dysplasias with HPV infection reveal epithelial karyorrhexis and apoptosis [130].

1.9.1.2 Carcinoma In Situ

Carcinoma in situ (CIS) is a histological term. It is a "precancerous intraepithelial carcinoma." At this stage, the lesion is not invasive, but cellular atypia involves the entire thickness of the epithelium. It is an intermediate stage in the evolution of oral carcinoma. As the atypical cells do not yet infiltrate connective tissue, metastasis does not occur. Histologically, it has many variants and the proliferating center is located in the basal layer [131]. In a preliminary study by Waldron and Shafer, the presentations of CIS were variable; many were white (45.1%), some were red, and few were red-white [132]. Based on their study, CIS can present as leukoplakia, erythroplakia, or erythroleukoplakia. The high-risk sites include tongue and floor of mouth. Oral pigmented CIS has also been reported [133]. Such lesions are poorly demarcated and display uneven pigmentation, mimicking malignant melanoma and other melanotic conditions of the oral cavity [134].

1.9.2 Grading and Staging of OSCC

The invasive nature of squamous cell carcinoma can be evaluated both at the histological level using pattern of tumor invasion front and degree of tumor differentiation (poor, moderate, or well differentiated) and using clinical tumor node and metastasis (TNM) staging. Histological grading is prone to subjectivity and is not yet introduced for traditional treatment planning. In the past, Broder, Jackobsson, Anneroth, and Hansen have proposed classifications for squamous cell carcinoma. Anneroth's is a multifactorial classification scoring system with the parameters: degree of keratinization, nuclear polymorphism, and mitosis, which represents cellular features; mode of invasion (pattern), which reflects tumor aggressiveness; and lymphocytic infiltration which reflects host response. Broder's system is a simple descriptive system where tumors are graded as well-differentiated (grade I), moderately differentiated (grade II), and poorly differentiated (grade III) or anaplastic or pleomorphic when it shows >75% undifferentiated cells [134, 135]. All histological features must be visualized in the same microscopic field. The American Joint Committee on Cancer (AJCC) designated staging by the TNM staging system, a clinical method of assessment. Prognostic evaluation for OSCC can be based on TNM staging [135].

1.10 Field Cancerization and Cancer Stem Cell Hypothesis

The entire oral epithelium needs to be considered as one compartment, as mutations even may occur at locations far away from the original site of malignancy. The incidence of multiple primary tumors and recurrent tumors, hinted at the occurrence of large field changes; the entire oral epithelium behaving as one unit. To explain such field changes (cancerization), Slaughter et al., who studied histological changes surrounding OSCC, introduced the "field cancerization model" (Fig 1.13) [136].

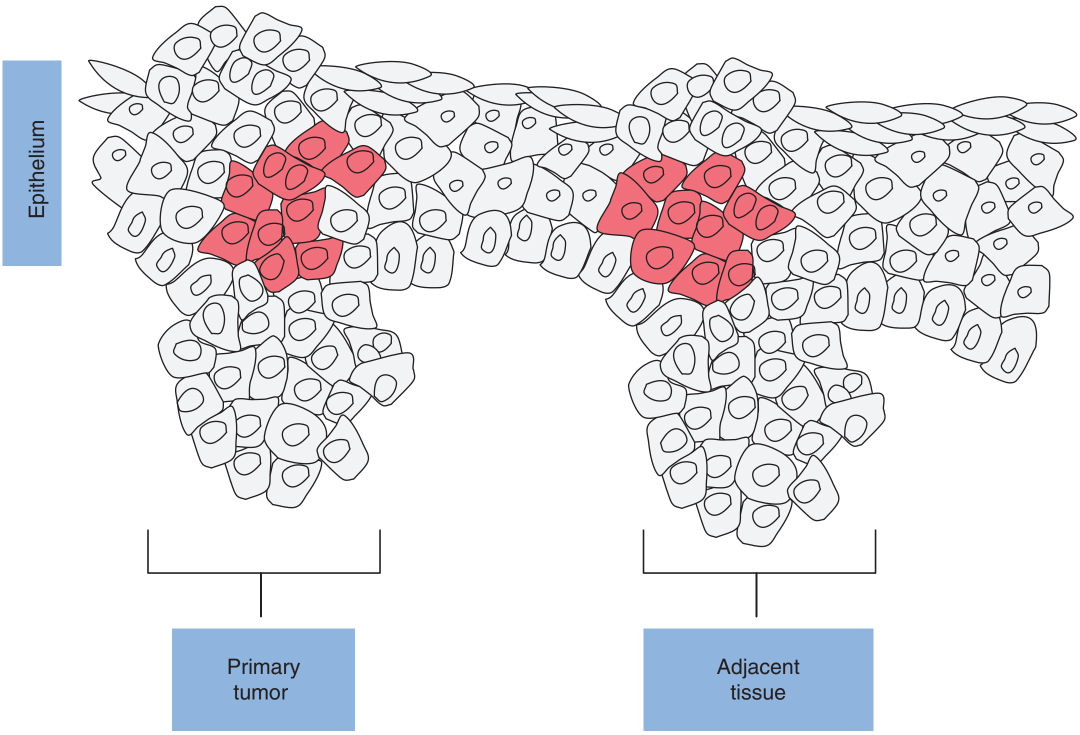

Fig. 1.13 A graphic model of field cancerization. Migration of (micrometastasis) of tumor initiating transformed stem cell progeny through saliva and epithelium has been proposed, but is less probable. The possibility of large field changes in oral cancer is more likely due to the simultaneous exposure of epithelium to the high-risk carcinogens in tobacco, transported in saliva

Although carcinogens in tobacco create severe changes in one area, the surrounding regions may also transform simultaneously. Oral mucosal field cancerization is possible due to the wide exposure of oral mucosa to a range of carcinogens (>5000) in tobacco [137]. Genetic transformation is slow, and early genetic changes cannot be demonstrated using simple histological methods. The first changes to occur in oral cancer are usually positive for *TP53* mutations. Field cancerization is alternatively believed to occur through "micrometastasis" via "saliva" or "intraepithelial migration" of a transformed stem cell progeny. The "micrometastasis model" of field cancerization seems less probable, and cancerization at different locations may occur directly due to carcinogens as independent events [136]. Saliva is more likely a carrier of carcinogens in smoke than a mediator of micrometastasis.

Most tumors are clonal in origin. Therefore only the long-time residents of the epithelium, most likely the stem cells, have the ability to accumulate the number of necessary genetic hits that will result in cancer formation. A tumor should be regarded as an organ with various cell types devoted to play specific roles. A vast body of literature highlighted genetic changes to occur first in stem cells. During the initial phase, a stem cell acquires a genetic alteration (i.e., on p53 locus) that is transferred to its daughter cells forming a patch. The first changes to occur are usually positive for *TP53* mutations. A *clone* is a unit that is genetically homogenous. In the second phase, there is clonal expansion to form a field. As time passes, the stem cells diverge, and alterations occur to form subclones with many genetic alterations. At the next phase (clonal expansion), the patch converts into an expanding field as a result of accumulation of genetic alterations. These fields vary in size and may remain undetected or appear as leukoplakia/erythroplakia. Ultimately, a dominant clone prevails and develops into carcinoma. Unfortunately, this clonal population may appear benign on routine histopathology and thus escape identification.

Early genetic events include loss of heterozygosity (LOH) involving 9p, 3p, and 17p as the most common alterations and late genetic events occurring at 11q, 13q, etc., during progression to OSCC. Unfortunately, this clonal population appears benign on routine histopathology and hence escapes identification. Due to field cancerization, there is 20-fold increased risk of developing a second tumor in a location close to the primary tumor [138]. OC is widespread and even contralateral; mirror image biopsies have shown significant genetic changes [139].

1.10.1 Oral Cancer Stem Cells

Data confirm the existence of a small group of cells, a distinct stem cell population referred as *cancer stem cells* (*CSCs*), which are the hidden culprits in malignancy. This area is well explored in OSCC. Poor prognosis and relapse are believed to be due to these stem cells, capable of self-renewal (Fig. 1.14). As these cells are slowly dividing, they are more resistant to chemo- or radiotherapy (conventional treatment). Poor 5-year survival (<50%) in OC following conventional treatment is attributed to these potential tumor initiating cells [140]. For this reason

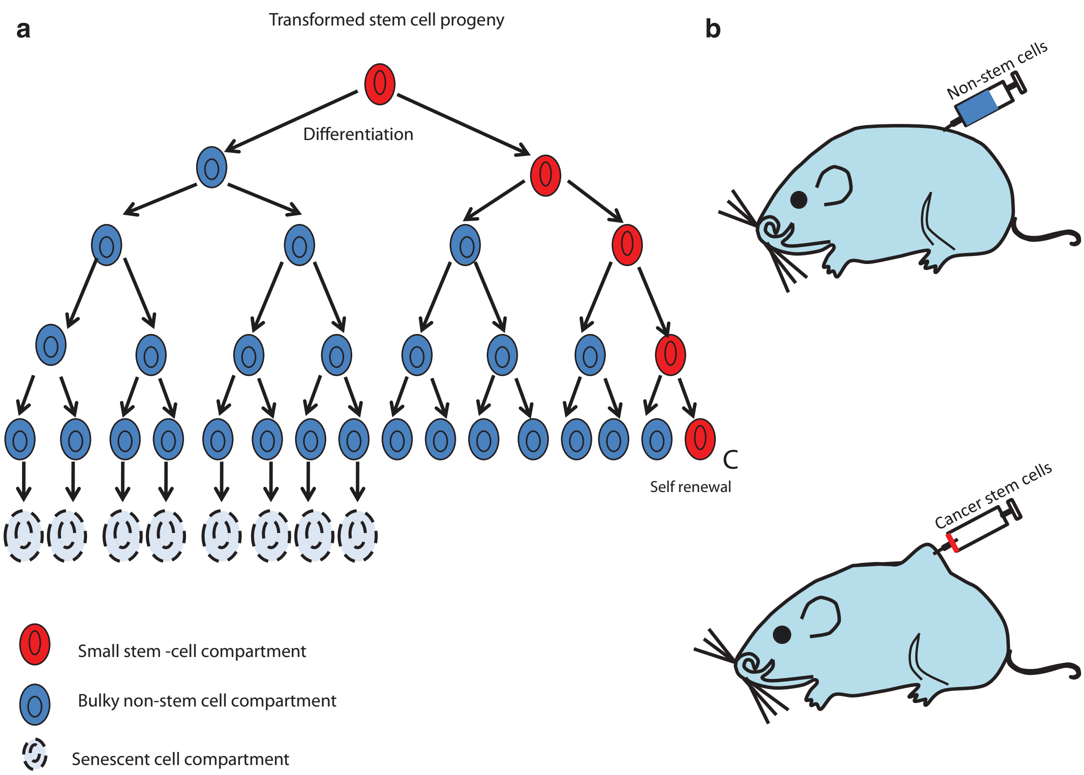

Fig. 1.14 Hierarchy of Oral cancer stem cells (**a**). Oral cancer follows the stem cell cancer hypothesis and only a small group of cells bear the true potential for progression, which have stem cell features (oral cancer stem (OSC) cells). Poor prognosis and relapse are due to these cells capable of self-renewal showing high resistance to chemotherapy and radiotherapy (conventional treatment) (**b**). As each stem cell divides by asymmetric division it forms two cells, non-stem cancer cells (represented in blue), and another stem cell (represented in red color) which is capable of self-renewal; they display high expression of stemness regulators. The stem cells have mechanisms that keep them immortal (immortal cell line), whereas the transit amplifying cells differentiate and after a few generations follow the senescence cascade and do not exhibit resistant to therapy (senescent cell compartment). Introduction of non-stem cancer cells into immunocompromised mice even at high numbers do not induce tumor formation, whereas introduction of only a few hundred cancer stem cells can cause significant tumor formation (**c**)

several nanotechnologists are targeting this cell population to refine cancer management. As stem cell divides, two cells are formed, the tumorigenic cell and non-tumorigenic cell (stem cell). Immunodeficient mice models are used to assess the tumorigenic potential of stem cells. Head and neck CSCs are (CD44) positive cells, constituting approximately 10% of the total tumor cell population [141]. When florescence-assisted cell sorting (FACS) sorted (5×10^3) $CD44^+$ cancer cells and (5×10^5) $CD44^-$ cancer cells were injected, the former initiated tumors, explaining their role in tumor formation [141]. CD44 is a cell surface glycoprotein and its expression indicates tumor progression and metastasis. Other markers of CSCs in OSCC include CD24, CD29, CD133, aldehyde dehydrogenase 1 (ALDH-1), B lymphoma Mo-MLV insertion region 1 homolog (BMI1), octamer-binding transcription factor 4(Oct3/4), and sex-determining region Y-box 2 (Sox2) [142]. Another group of cells positive for both $CD24^+$ and $CD44^+$ was shown to be more representative of the putative oral CSC compartment [142, 143]. The $CD24^+$ and $CD44^+$ cells are more proliferative and invasive both in vitro in collagen gels and in vivo inducing tumors in nude mice models, also displaying high resistance to chemotherapy [142, 143]. Single markers are not strong indicators of stemness, and high expression of metabolic (high ALDH expression) and cell surface markers (CD44, CD24, CD133) can be considered. Mutations in stem cell population may be particularly linked to overall malignant transformation.

Conclusion

Among the OPMDs, leukoplakia, erythroplakia, oral submucous fibrosis, and lichen planus (immediate precursors) are the most prevalent and should alert clinicians. Tobacco (smoke and smokeless form) is the primary risk factor associated with OSCC, as it alters a large field of oral epithelium at the genetic and molecular level. Each region of altered epithelium may represent a different evolutionary stage, and clinicians should consider OPMDs and OSCC as two ends of the same problem. Clinicians must take an active role, screening high-risk oral sites for potential lesions. Patient delay in reporting and clinician's lack of judgment to act on early precursor lesions are the main source of diagnostic delay. Habit discontinuation through proper counseling at the right time is the most powerful method in the prevention of oral cancer.

References

1. India Project Team of the International Cancer Genome Consortium. Mutational landscape of gingivo-buccal oral squamous cell carcinoma reveals new recurrently-mutated genes and molecular subgroups. Nat Commun. 2013;4:2873.
2. Stadler ME, Patel MR, Couch ME, Hayes DN. Molecular biology of head neck Cancer: risks and pathways. Hematol Oncol Clin North Am. 2008;22:1099–124.
3. Chen R-J, Chang LW, Lin P, Wang Y-J. Epigenetic effects and molecular mechanisms of tumorigenesis induced by cigarette smoke: an overview. J Oncol. 2011;2011:654931.
4. Farsalinos KE, Polosa R. Safety evaluation and risk assessment of electronic cigarettes as tobacco cigarette substitutes: a systematic review. Ther Adv Drug Saf. 2014;5:67–86.
5. Rosenquist K. Risk factors in oral and oropharyngeal squamous cell carcinoma: a population-based case-control study in southern Sweden. Swed Dent J Suppl. 2005;179:1–66.
6. Boyle JO, Gümüs ZH, Kacker A, Choksi VL, Bocker JM, Zhou XK, et al. Effects of cigarette smoke on the human oral mucosal transcriptome. Cancer Prev Res (Phila). 2010;3:266–78.
7. Amaral-Silva GK, Martins MD, Pontes HA, Fregnani ER, Lopes MA, Fonseca FP et al. Mismatch repair system proteins in oral benign and malignant lesions. J Oral Pathol Med. 2017;46:241–5.
8. Gupta B, Johnson NW. Systematic review and meta-analysis of association of smokeless tobacco and of betel quid without tobacco with incidence of oral cancer in South Asia and the Pacific. PLoS One. 2014;9:e113385.
9. Liu Y, Chen H, Sun Z, Chen X. Molecular mechanisms of ethanol-associated Oro-esophageal squamous cell carcinoma. Cancer Lett. 2015;361:164–73.
10. Urvalek AM, Osei-Sarfo K, Tang X-H, Zhang T, Scognamiglio T, Gudas LJ. Identification of ethanol and 4-Nitroquinoline-1-oxide induced epigenetic and oxidative stress markers during oral cavity carcinogenesis. Alcohol Clin Exp Res. 2015;39:1360–72.
11. Khan I, Kumar N, Pant I, Narra S, Kondaiah P. Activation of TGF-β pathway by Areca nut constitu-

ents: a possible cause of oral Submucous fibrosis. PLoS One. 2012;7:e51806.
12. Mohammed F, Manohar V, Jose M, Thapasum AF, Mohamed S, Shamaz BH, et al. Estimation of copper in saliva and areca nut products and its correlation with histological grades of oral submucous fibrosis. J Oral Pathol Med. 2015;44:208–13.
13. Bodner L, Manor E, Friger MD, van der Waal I. Oral squamous cell carcinoma in patients twenty years of age or younger—review and analysis of 186 reported cases. Oral Oncol. 2014;50:84–9.
14. Soudry E, Preis M, Hod R, Hamzany Y, Hader T, Bahar G, et al. Squamous cell carcinoma of the oral tongue in patients younger than 30 years: clinicopathologic features and outcome. Clin Otolaryngol. 2010;35:307–12.
15. Ames BN, Wakimoto P. Are vitamin and mineral deficiencies a major cancer risk? Nat Rev Cancer. 2002;2:694–704.
16. Lawal AO, Kolude B, Adeyemi BF, Lawoyin JO, Akang EE. Serum antioxidant vitamins and the risk of oral cancer in patients seen at a tertiary institution in Nigeria. Niger J Clin Pract. 2012;15:30–3.
17. Athirajan V, Razak IA, Thurairajah N, Ghani WM, Ching HN, Yang YH. High serum level of retinol and α-tocopherol affords protection against oral cancer in a multiethnic population. Asian Pac J Cancer Prev. 2014;15:8183–9.
18. de Munter L, Maasland DH, van den Brandt PA, Kremer B, Schouten LJ. Vitamin and carotenoid intake and risk of head-neck cancer subtypes in the Netherlands cohort study. Am J Clin Nutr. 2015;102:420–32.
19. Edefonti V, Hashibe M, Parpinel M, Turati F, Serraino D, Matsuo K, et al. Natural vitamin C intake and the risk of head and neck cancer: a pooled analysis in the international head and neck Cancer epidemiology consortium. Int J Cancer. 2015;137:448–62.
20. Li Q, Chuang SC, Eluf-Neto J, Menezes A, Matos E, Koifman S, et al. Vitamin or mineral supplement intake and the risk of head and neck cancer: pooled analysis in the INHANCE consortium. Int J Cancer. 2012;131:1686–99.
21. Jayaprakash V, Reid M, Hatton E, Merzianu M, Rigual N, Marshall J, Gill S, Frustino J, Wilding G, Loree T, Popat S, Sullivan M. Human papillomavirus types 16 and 18 in epithelial dysplasia of oral cavity and oropharynx: a meta-analysis, 1985–2010. Oral Oncol. 2011;47:1048–54.
22. Gupta K, Metgud R. Evidences suggesting involvement of viruses in oral squamous cell carcinoma. Patholog Res Int. 2013;2013:642496.
23. Miller CS, Johnstone BM. Human papillomavirus as a risk factor for oral squamous cell carcinoma: a meta-analysis, 1982-1997. Oral Surg Oral Med Oral Pathol Oral Radiol Endod. 2001;91:622–35.
24. Fornatora M, Jones AC, Kerpel S, Freedman P. Human papillomavirus-associated oral epithelial dysplasia (koilocytic dysplasia) an entity of unknown biologic potential. Oral Surg Oral Med Oral Pathol Oral Radiol Endod. 1996;82:47–56.
25. D'Souza G, Kreimer AR, Viscidi R, Pawlita M, Fakhry C, Koch WM, Westra WH, Gillison ML. Case-control study of human papillomavirus and oropharyngeal cancer. N Engl J Med. 2007;356:1944–56.
26. Holtzman AL, Medicine HKIC. Human papillomavirus-associated oropharyngeal squamous-cell carcinoma. N Engl J Med. 2016;375:1269.
27. Boscolo-Rizzo P, Del Mistro A, Bussu F, Lupato V, Baboci I, Almadori G, et al. New insights into human papillomavirus-associated head and neck squamous cell carcinoma. Acta Otorhinolaryngol Ital. 2013;33:77–87.
28. Kian Ang K, Harris J, Wheeler R, Weber R, Rosenthal DI, Nguyen-Tân PF, et al. Human papillomavirus and survival of patients with oropharyngeal cancer. N Engl J Med. 2010;363:24–35.
29. Kashyap RR, Kashyap RS. Self-inflicted injury as a potential trigger for carcinoma of lip—a case report. Gerodontology. 2013;30:236–8.
30. Fan H, Yoon K-Y, Kim S-M, Myoung H, Lee J-H, Kim M-J. Relationship between squamous cell carcinoma of the tongue and the position of dental prosthesis. J Adv Prosthodont. 2015;7:129–37.
31. Piemonte ED, Lazos JP, Brunotto M. Relationship between chronic trauma of the oral mucosa, oral potentially malignant disorders and oral cancer. J Oral Pathol Med. 2010;39:513–7.
32. Albuquerque RP, Richards A. Images in clinical medicine. Squamous-cell carcinoma of the tongue. N Engl J Med. 2016;374:e32.
33. Panta P, Sarode SC, Sarode GS, Patil S. 'Chronic traumatic ulcer of lateral tongue'- An underestimated 'oral potentially malignant disorder'? Oral Oncol. 2018;85:101–2.
34. Winn DM, Blot WJ, McLaughlin JK, Austin DF, Greenberg RS, Preston-Martin S, et al. Mouthwash use and oral conditions in the risk of oral and pharyngeal cancer. Cancer Res. 1991;51:3044–7.
35. Damm DD, Curran A, White DK, Drummond JF. Leukoplakia of the maxillary vestibule—an association with Viadent? Oral Surg Oral Med Oral Pathol Oral Radiol Endod. 1999;87:61–6.
36. Mascarenhas AK, Allen CM, Moeschberger ML. The association between Viadent use and oral leukoplakia—results of a matched case-control study. J Public Health Dent. 2002;62:158–62.
37. Shephard MK, Schifter M, Palme CE. Multiple oral squamous cell carcinomas associated with autoimmune polyendocrinopathy-candidiasis-ectodermal dystrophy. Oral Surg Oral Med Oral Pathol Oral Radiol. 2012;114:e36–42.
38. Rosa DD, Pasqualotto AC, Denning DW. Chronic mucocutaneous candidiasis and oesophageal cancer. Med Mycol. 2008;46:85–91.
39. Rautemaa R, Hietanen J, Niissalo S, Pirinen S, Perheentupa J. Oral and oesophageal squamous cell carcinoma—a complication or component

of autoimmune polyendocrinopathy-candidiasis-ectodermal dystrophy (APECED, APS-I). Oral Oncol. 2007;43:607–13.
40. McCullough M, Jaber M, Barrett AW, Bain L, Speight PM, Porter SR. Oral yeast carriage correlates with presence of oral epithelial dysplasia. Oral Oncol. 2002;38:391–3.
41. Bakri MM, Hussaini HM, Holmes AR, Cannon RD, Rich AM. Revisiting the association between candidal infection and carcinoma, particularly oral squamous cell carcinoma. J Oral Microbiol. 2010;2.
42. Van der Waal I. Potentially malignant disorders of the oral and oropharyngeal mucosa; present concepts of management. Oral Oncol. 2010;46:423–5.
43. WHO classification of head and neck tumours/edited by Adel K. El-Naggar, John K.C. Chan, Jennifer R. Grandis, Takashi Takata, Pieter J. Slootweg. 4th edition; Ninth; Lyon: International Agency for Research on Cancer, 2017.
44. Prime SS, Thakker NS, Pring M, Guest PG, Paterson ICA. Review of inherited cancer syndromes and their relevance to oral squamous cell carcinoma. Oral Oncol. 2001;37:1–16.
45. Sarode SC, Sarode GS, Karmarkar S, Tupkari JV. A new classification for potentially malignantdisorders of the oral cavity. Oral Oncol. 2011;47:920–1.
46. Warnakulasuriya S, Ariyawardana A. Malignant transformation of oral leukoplakia: a systematic review of observational studies. J Oral Pathol Med. 2016;45:155–66.
47. Anderson A, Ishak N. Marked variation in malignant transformation rates of oral leukoplakia. Evid Based Dent. 2015;16:102–3.
48. Islam MN, Kornberg L, Veenker E, Cohen DM, Bhattacharyya I. Anatomic site based ploidy analysis of oral premalignant lesions. Head Neck Pathol. 2010;4:10–4.
49. Pagin O, Santos PS d S, Del Neri NB, de Lima HG, Lara VS. The importance of a proper selection area to be biopsied in nodular leukoplakia: a case report. Acta Stomatol Croat. 2014;48:42–7.
50. Cerero-Lapiedra R, Baladé-Martínez D, Moreno-López LA, Esparza-Gómez G, Bagán JV. Proliferative verrucous leukoplakia: a proposal for diagnostic criteria. Med Oral Patol Oral Cir Bucal. 2010;15:e839–45.
51. Bagán JV, Murillo J, Poveda R, Gavaldá C, Jiménez Y, Scully C. Proliferative verrucous leukoplakia: unusual locations of oral squamous cell carcinomas, and field cancerization as shown by the appearance of multiple OSCCs. Oral Oncol. 2004;40:440–3.
52. Thomson PJ, Hamadah O. Cancerisation within the oral cavity: the use of 'field mapping biopsies' in clinical management. Oral Oncol. 2007;43:20–6.
53. Bari S, Metgud R, Vyas Z, Tak A. An update on studies on etiological factors, disease progression, and malignant transformation in oral submucous fibrosis. J Cancer Res Ther. 2017;13:399–405.
54. Bathi RJ, Parveen S, Burde K. The role of gutka chewing in oral submucous fibrosis: a case-control study. Quintessence Int. 2009;40:e19–25.
55. Sharma A, Sahni P, Nayak MT, Singhvi A, Kumar R. Identification of the pattern of copper as an etiological factor in oral submucous fibrosis: a cytological study. J Exp Ther Oncol. 2014;10:317–23.
56. Ray JG, Ghosh R, Mallick D, Swain N, Gandhi P, Ram SS, et al. Correlation of trace elemental profiles in blood samples of Indian patients with leukoplakia and oral submucous fibrosis. Biol Trace Elem Res. 2011;144:295–305.
57. Chiu CJ, Chang ML, Chiang CP, Hahn LJ, Hsieh LL, Chen CJ. Interaction of collagen-related genes and susceptibility to betel quid-induced oral submucous fibrosis. Cancer Epidemiol Biomark Prev. 2002;11:646–53.
58. Agrawal D, Gupta S, Agarwal D, Gupta OP, Agarwal M. Role of GSTM1 and GSTT1 polymorphism: susceptibility to oral submucous fibrosis in the north Indian population. Oncology. 2010;79:181–6.
59. Chaudhuri SR, Mukherjee S, Paul RR, Haldar A, Chaudhuri K. CYP1AI and CYP2E1 gene polymorphisms may increase susceptibility to oral submucous fibrosis among betel quid chewers of eastern India. Gene. 2013;513:268–71.
60. Ray JG, Ranganathan K, Chattopadhyay A. Malignant transformation of oral submucous fibrosis: overview of histopathological aspects. Oral Surg Oral Med Oral Pathol Oral Radiol. 2016;122:200–9.
61. Ekanayaka RP, Tilakaratne WM. Oral submucous fibrosis: review on mechanisms of malignant transformation. Oral Surg Oral Med Oral Pathol Oral Radiol. 2016;122:192–9.
62. Jayasooriya PR, Nadeeka Jayasinghe KA, Mudiyanselage Tilakaratne W. Relationship between thickness of fibrosis and epithelial dysplasia in oral submucous fibrosis. J Investig Clin Dent. 2011;2:171–5.
63. Tilakaratne WM, Iqbal Z, Teh MT, Ariyawardana A, Pitiyage G, Cruchley A, et al. Upregulation of HIF-1alpha in malignant transformation of oral submucous fibrosis. J Oral Pathol Med. 2008;37:372–7.
64. Chaturvedi P, Vaishampayan SS, Nair S, Nair D, Agarwal JP, Kane SV, et al. Oral squamous cell carcinoma arising in background of oral submucous fibrosis: a clinicopathologically distinct disease. Head Neck. 2013;35:1404–9.
65. Shirani S, Kargahi N, Razavi SM, Homayoni S. Epithelial dysplasia in oral cavity. Iran J Med Sci. 2014;39:406–17.
66. Reichart PA, Philipsen HP. Oral erythroplakia—a review. Oral Oncol. 2005;41:551–61.
67. Mortazavi H, Baharvand M, Mehdipour M. Oral potentially malignant disorders: an overview of more than 20 entities. J Dent Res Dent Clin Dent Prospects. 2014;8:6–14.

68. Villa A, Villa C, Abati S. Oral cancer and oral erythroplakia: an update and implication for clinicians. Aust Dent J. 2011;56:253–6.
69. Yang SW, Lee YS, Chang LC, Hsieh TY, Chen TA. Outcome of excision of oral erythroplakia. Br J Oral Maxillofac Surg. 2015;53:142–7.
70. Pindborg JJ, Mehta FS, Gupta PC, Daftary DK, Smith CJ. Reverse smoking in Andhra Pradesh, India: a study of palatal lesions among 10,169 villagers. Br J Cancer. 1971;25:10–20.
71. Kim DS, Park SH, Kwon SB, Joo YH, Youn SW, Sohn UD, et al. Temperature regulates melanin synthesis in melanocytes. Arch Pharm Res. 2003;26:840–5.
72. Sreenivasa Bharath T, Govind Raj N, Kumar AN, Saraswathi TR, Suresh Babu G, Ramanjaneya Raju P. Palatal changes of reverse smokers in a rural coastal Andhra population with review of literature. J Oral Maxillofac Pathol. 2015;19:182–7.
73. Reddy CR, Venkatarathnam G, Kameswari VR. Distribution of glands in the mucosa of the hard palate and its relation to carcinoma. J Oral Surg. 1976;34:232–6.
74. van der Eb MM, Leyten EM, Gavarasana S, Vandenbroucke JP, Kahn PM, Cleton FJ. Reverse smoking as a risk factor for palatal cancer: a cross-sectional study in rural Andhra Pradesh, India. Int J Cancer. 1993;54:754–8.
75. Gupta S, Jawanda MK. Oral lichen planus: an update on etiology, pathogenesis, clinical presentation, diagnosis and management. Indian J Dermatol. 2015;60:222–9.
76. Lauritano D, Arrica M, Lucchese A, Valente M, Pannone G, Lajolo C, et al. Oral lichen planus clinical characteristics in Italian patients: a retrospective analysis. Head Face Med. 2016;12:18.
77. Ingafou M, Leao JC, Porter SR, Scully C. Oral lichen planus: a retrospective study of 690 British patients. Oral Dis. 2006;12:463–8.
78. Alaizari NA, Al-Maweri SA, Al-Shamiri HM, Tarakji B, Shugaa-Addin B. Hepatitis C virus infections in oral lichen planus: a systematic review and meta-analysis. Aust Dent J. 2016;61:282–7.
79. Roitberg-Tambur A, Friedmann A, Korn S, Markitziu A, Pisanti S, Safirman C, et al. Serologic and molecular analysis of the HLA system in Israeli Jewish patients with oral erosive lichen planus. Tissue Antigens. 1994;43:219–23.
80. Rode M, Kogoj-Rode M. Malignant potential of the reticular form of oral lichen planus over a 25-year observation period in 55 patients from Slovenia. J Oral Sci. 2002;44:109–11.
81. Brant JM, Aguiar MC, Grandinetti HA, Rodrigues LV, Vasconcelos AC. A comparative study of apoptosis in reticular and erosive oral lichen planus. Braz Dent J. 2012;23:564–9.
82. Lavanya N, Jayanthi P, Rao UK, Ranganathan K. Oral lichen planus: an update on pathogenesis and treatment. J Oral Maxillofac Pathol. 2011;15: 127–32.
83. Zhang J, Zhou G. Green tea consumption: an alternative approach to managing oral lichen planus. Inflamm Res. 2012;61:535–9.
84. Madhusudhan KS, Sharma R. Esophageal lichen planus: a case report and review of literature. Indian J Dermatol. 2008;53:26–7.
85. Chryssostalis A, Gaudric M, Terris B, Coriat R, Prat F, Chaussade S. Esophageal lichen planus: a series of eight cases including a patient with esophageal verrucous carcinoma. A case series. Endoscopy. 2008;40:764–8.
86. Eisen D. The vulvovaginal-gingival syndrome of lichen planus. The clinical characteristics of 22 patients. Arch Dermatol. 1994;130:1379–82.
87. Rogers RS 3rd, Eisen D. Erosive oral lichen planus with genital lesions: the vulvovaginal-gingival syndrome and the peno-gingival syndrome. Dermatol Clin. 2003;21:91–8. vi-vii
88. Fang M, Zhang W, Chen Y, He Z. Malignant transformation of oral lichen planus: a retrospective study of 23 cases. Quintessence Int. 2009;40:235–42.
89. Markopoulos AK, Antoniades D, Papanayotou P, Trigonidis G. Malignant potential of oral lichen planus; a follow-up study of 326 patients. Oral Oncol. 1997;33:263–9.
90. Eisen D. The clinical features, malignant potential, and systemic associations of oral lichen planus: a study of 723 patients. J Am Acad Dermatol. 2002;46: 207–14.
91. Gandolfo S, Richiardi L, Carrozzo M, Broccoletti R, Carbone M, Pagano M, et al. Risk of oral squamous cell carcinoma in 402 patients with oral lichen planus: a follow-up study in an Italian population. Oral Oncol. 2004;40:77–83.
92. Fitzpatrick SG, Hirsch SA, Gordon SC. The malignant transformation of oral lichen planus and oral lichenoid lesions: a systematic review. J Am Dent Assoc. 2014;145:45–56.
93. Van der Meij EH, Schepman KP, van der Waal I. The possible premalignant character of oral lichen planus and oral lichenoid lesions: a prospective study. Oral Surg Oral Med Oral Pathol Oral Radiol Endod. 2003;96:164–71.
94. Patil S, Rao RS, Sanketh DS, Warnakulasuriya S. Lichenoid dysplasia revisited—evidence from a review of Indian archives. J Oral Pathol Med. 2015;44:507–14.
95. Ranginwala AM, Chalishazar MM, Panja P, Buddhdev KP, Kale HM. Oral discoid lupus erythematosus: a study of twenty-one cases. J Oral Maxillofac Pathol. 2012;16:368–73.
96. Schiödt M, Halberg P, Hentzer B. A clinical study of 32 patients with oral discoid lupus erythematosus. Int J Oral Surg. 1978;7:85–94.
97. Schiødt M, Andersen L, Shear M, Smith CJ. Leukoplakia-like lesions developing in patients with oral discoid lupus erythematosus. Acta Odontol Scand. 1981;39:209–16.
98. Jeffrey David Unsworth, Andrew Baldwin, and Louise Byrd. Systemic lupus erythematosus,

pregnancy and carcinoma of the tongue. BMJ Case Rep. 2013; 2013: bcr2013008864.
99. Grimaldo-Carjevschi M, López-Labady J, Villarroel-Dorrego M. Squamous cell carcinoma on the palate in a patient with systemic lupus erythematosus: case report and review of literature. Lupus. 2011;20:519–22.
100. Bernatsky S, Ramsey-Goldman R, Clarke AE. Malignancy in systemic lupus erythematosus: what have we learned? Best Pract Res Clin Rheumatol. 2009;23:539–47.
101. Bernatsky S, Boivin JF, Joseph L, Rajan R, Zoma A, Manzi S, et al. An international cohort study of cancer in systemic lupus erythematosus. Arthritis Rheum. 2005;52:1481–90.
102. Wood NH, Khammissa R, Meyerov R, Lemmer J, Cheilitis LFA. A case report and a review of the literature. Eur J Dent. 2011;5:101–6.
103. Lopes MLD d S, Júnior FL d S, Lima KC, de Oliveira PT, da Silveira ÉJD. Clinicopathological profile and management of 161 cases of actinic cheilitis. An Bras Dermatol. 2015;90:505–12.
104. Markopoulos A, Albanidou-Farmaki E, Kayavis I. Actinic cheilitis: clinical and pathologic characteristics in 65 cases. Oral Dis. 2004;10:212–6.
105. Rossi R, Assad GB, Buggiani G, Lotti T. Photodynamic therapy: treatment of choice for actinic cheilitis? Dermatol Ther. 2008;21(5):412.
106. Leuci S, Martina S, Adamo D, Ruoppo E, Santarelli A, Sorrentino R. Oral syphilis: a retrospective analysis of 12 cases and a review of the literature. Oral Dis. 2013;19:738–46.
107. Cherniak W, Silverman M. Images in clinical medicine: syphilitic Gumma. N Engl J Med. 2014;371:667.
108. Pires FR, da Silva PJ, Natal RF, Alves FA, Pinto CA, Rumayor A, et al. Clinicopathologic features, microvessel density, and immunohistochemical expression of ICAM-1 and VEGF in 15 cases of secondary syphilis with oral manifestations. Oral Surg Oral Med Oral Pathol Oral Radiol. 2016;121:274–81.
109. Dickenson AJ, Currie WJ, Avery BS. Screening for syphilis in patients with carcinoma of the tongue. Br J Oral Maxillofac Surg. 1995;33:319–20.
110. Rahima S, Riyaz N, Latheef EN, Shyni PM. Squamous cell carcinoma on a syphilitic gumma: a unique presentation. Indian J Sex Transm Dis. 2015;36:89–91.
111. Atkinson JC, Harvey KE, Domingo DL, Trujillo MI, Guadagnini J-P, Gollins S, et al. Oral and dental phenotype of Dyskeratosis Congenita. Oral Dis. 2008;14:419–27.
112. Alter BP, Giri N, Savage SA, Rosenberg PS. Cancer in dyskeratosis congenita. Blood. 2009;113:6549–57.
113. Batista LF, Pech MF, Zhong FL, Nguyen HN, Xie KT, Zaug AJ, et al. Telomere shortening and loss of self-renewal in dyskeratosis congenita induced pluripotent stem cells. Nature. 2011;474:399–402.
114. Walne AJ, Vulliamy T, Beswick R, Kirwan M, Dokal I. TINF2 mutations result in very short telomeres: analysis of a large cohort of patients with dyskeratosis congenita and related bone marrow failure syndromes. Blood. 2008;112:3594–600.
115. Brandizzi D, Gandolfo M, Velazco ML, Cabrini RL, Lanfranchi HE. Clinical features and evolution of oral cancer: a study of 274cases in Buenos Aires, Argentina. Med Oral Patol Oral Cir Bucal. 2008;13:E544–8.
116. Macfarlane TV, Wirth T, Ranasinghe S, Ah-See KW, Renny N, Hurman D, et al. Head and neck Cancer pain: systematic review of prevalence and associated factors. J Oral Maxillofac Res. 2012;e1:3.
117. Gorsky M, Epstein JB, Oakley C, Le ND, Hay J, Stevenson-Moore P. Carcinoma of the tongue: a case series analysis of clinical presentation, risk factors, staging, and outcome. Oral Surg Oral Med Oral Pathol Oral Radiol Endod. 2004;98:546–52.
118. Pathak J, Swain N, Patel S, Poonja LS. Histopathological variants of oral squamous cell carcinoma-institutional case reports. J Oral Maxillofac Pathol. 2014;18:143–5.
119. Pereira MC, Oliveira DT, Landman G, Kowalski LP. Histologic subtypes of oral squamous cell carcinoma: prognostic relevance. J Can Dent Assoc. 2007;73:339–44.
120. Peng Q, Wang Y, Quan H, Li Y, Tang Z. Oral verrucous carcinoma: from multifactorial etiology to diverse treatment regimens (review). Int J Oncol. 2016;49:59–73.
121. Sonalika WG, Anand T. Oral verrucous carcinoma: a retrospective analysis for clinicopathologic features. J Cancer Res Ther. 2016;12:142–5.
122. Terada T. Multiple verrucous carcinomas of the oral cavity. J Maxillofac Oral Surg. 2015;14:393–6.
123. Samman M, Wood HM, Conway C, Stead L, Daly C, Chalkey R, et al. A novel genomic signature reclassifies an oral cancer subtype. Int J Cancer. 2015;137:2364–73.
124. Hosseinpour S, Mashhadiabbas F, Ahsaie MG. Diagnostic biomarkers in oral verrucous carcinoma: a systematic review. Pathol Oncol Res. 2017;23:19–32.
125. Fu TY, Tsai MH, Wang JS, Ger LP. Antioxidant enzymes in oral verrucous carcinoma. J Oral Pathol Med. 2017;46:46–9.
126. Pereira T, Shetty S, Dodal S, Tamgadge A. Verruciform xanthoma of the lip: a rarity. Indian Dermatol Online J. 2016;7:180–2.
127. Patil S, Warnakulasuriya S, Raj T, Sanketh DS, Rao RS. Exophytic oral verrucous hyperplasia: a new entity. J Investig Clin Dent. 2016;7:417–23.
128. Wang YP, Chen HM, Kuo RC, Yu CH, Sun A, Liu BY, et al. Oral verrucous hyperplasia: histologic classification, prognosis, and clinical implications. J Oral Pathol Med. 2009;38:651–6.
129. Sharma P, Wadhwan V, Aggarwal P, Sharma A. Oral verrucous hyperplasia versus oral verrucous carcinoma: a clinicopathologic dilemma revisited using p53 as immunohistochemical marker. J Oral Maxillofac Pathol. 2016;20:362–8.

130. Woo SB, Cashman EC, Lerman MA. Human papillomavirus-associated oral intraepithelial neoplasia. Mod Pathol. 2013;26:1288–97.
131. Kobayashi T, Maruyama S, Cheng J, Ida-Yonemochi H, Yagi M, Takagi R, et al. Histopathological varieties of oral carcinoma in situ: diagnosis aided by immunohistochemistry dealing with the second basal cell layer as the proliferating center of oral mucosal epithelia. Pathol Int. 2010;60:156–66.
132. Waldron CA, Shafer WG. Oral carcinoma in situ. Oral Surg Oral Med Oral Pathol. 1975;39:227–38.
133. Matsumoto N, Kitano T, Oki H, Omagari D, Matsue Y, Okudera M, et al. Pigmented oral carcinoma in situ: a case report and literature review. Oral Surg Oral Med Oral Pathol Oral Radiol. 2014;118:e79–83.
134. Arvanitidis E, Andreadis P, Andreadis D, Belazi M, Epivatianos A. Reviewing the oral carcinogenic process: key genetic events, growth factors and molecular signaling pathways. J Biol Res—Thessaloniki. 2011;16:313–36.
135. Akhter M, Hossain S, Rahman QB, Molla MR. A study on histological grading of oral squamous cell carcinoma and its co-relationship with regional metastasis. J Oral Maxillofac Pathol. 2011;15:168–76.
136. van Oijen MG. Slootweg PJ oral field cancerization: carcinogen-induced independent events or micrometastatic deposits? Cancer Epidemiol Biomark Prev. 2000;9:249–56.
137. Mohan M, Jagannathan N. Oral field cancerization: an update on current concepts. Oncol Rev. 2014;8:244.
138. Martin CL, Reshmi SC, Ried T, Gottberg W, Wilson JW, Reddy JK, et al. Chromosomal imbalances in oral squamous cell carcinoma. Examination of 31 cell lines and review of the literature. Oral Oncol. 2008;44:369–82.
139. Thomson PJ. Field change and oral cancer: new evidence for widespread carcinogenesis? Int J Oral Maxillofac Surg. 2002;31:262–6.
140. Major AG, Pitty LP, Farah CS. Cancer stem cell markers in head and neck squamous cell carcinoma. Stem Cells Int. 2013;2013:319489.
141. Prince ME, Sivanandan R, Kaczorowski A, Wolf GT, Kaplan MJ, Dalerba P, et al. Identification of a subpopulation of cells with cancer stem cell properties in head and neck squamous cell carcinoma. Proc Natl Acad Sci U S A. 2007;104:973–8.
142. Han J, Fujisawa T, Husain SR, Puri RK. Identification and characterization of cancer stem cells in human head and neck squamous cell carcinoma. BMC Cancer. 2014;14:173.
143. Okamoto A, Chikamatsu K, Sakakura K, Hatsushika K, Takahashi G, Masuyama K. Expansion and characterization of cancer stem-like cells in squamous cell carcinoma of the head and neck. Oral Oncol. 2009;45:633–9.

2 Genetics and Molecular Mechanisms in Oral Cancer Progression

Prashanth Panta, Bramanandam Manavathi, and Siddavaram Nagini

Abstract

Exposure to tobacco in smoke or chewable form, in isolation or in association with other risk factors (i.e., alcohol or areca nut), disturbs the balanced expression of numerous genes and leads to loss of coordination of their downstream signaling pathways, finally leading to oral cancer. Initially changes like mild dysplasia and benign hyperplasia are reversible, but continuous exposure to carcinogens leads to accumulation of mutations in multiple genes involved in cell proliferation, differentiation, apoptosis, telomere maintenance, invasion, and angiogenesis, resulting in abnormal cell behavior and cell immortalization. Gains and losses occur on many chromosomal arms, and a well-characterized mutational landscape is associated with oral cancer. This chapter discusses the wide spectrum of genetic and epigenetic events that take place in oncogenes and tumor suppressor genes with special reference to oncogenic miRs (miR-21, miR-31, miR-146a, miR-134, miR-184, miR-7, miR-127, miR-518c-5p), tumor suppressor miRs (miR-200 family, miR-101, miR-26a/b, miR-29a, miR-27b, miR-137, miR-125a, miR-29a, miR-491-5p, miR-124, miR-125, miR-218, miR-99a, miR-375), and long noncoding RNA (HOTAIR, FOXCUT, MALAT1, UCA1, TUG1, CCAT2, FTH1P3, H19, HIFCAR/MIRHG) that influence oncogenic signaling pathways and enable acquisition of cancer hallmarks.

P. Panta, MDS (✉)
Department of Oral Medicine and Radiology, MNR Dental College and Hospital, Sangareddy, Telangana, India
e-mail: maithreya.prashanth@gmail.com

B. Manavathi, PhD
Department of Biochemistry, School of Life Sciences, University of Hyderabad, Hyderabad, India

S. Nagini, PhD
Department of Biochemistry & Biotechnology, Annamalai University, Annāmalai Nagar, Tamil Nadu, India

2.1 Introduction

Oral cancer, the sixth most common malignancy worldwide with an estimated annual incidence of over 300,000 cases and a mortality rate of 48%, presents predominantly as oral squamous cell carcinoma (OSCC) [1, 2]. The aetiology of OSCC is multifactorial with interaction of a number of risk factors and host susceptibility. Tobacco consumption is the single most important risk factor implicated in OSCC development. Additionally, alcohol, viral infection, nutritional deficiency, dental hygiene, and socioeconomic and genetic factors are also recognized to contribute to OSCC development. Despite advances in prevention and treatment, the 5-year survival rate of OSCC remains low due to recurrence, chemoresistance, and lack of suitable markers for early detection [3]. An in-depth understanding of

P. Panta (ed.), *Oral Cancer Detection*, https://doi.org/10.1007/978-3-319-61255-3_2

the molecular pathogenesis is therefore necessary to aid diagnosis and develop preventive and therapeutic strategies.

2.2 Genetic Signature of Oral Cancer

With the advent of genome-wide next-generation sequencing, the mutation profile of OSCC has been extensively elaborated [4–9]. As many as 130 coding mutations per tumor were observed using whole exome sequencing [4]. As compared to other cancers, OSCCs acquire a greater number of mutations, probably due to the wide range of chemical carcinogens in tobacco. Human papillomavirus (HPV)-positive tumors harbor fewer mutations than HPV-negative tumors. In HPV-positive OSCCs, *TP53* inactivation is the most common alteration [4].

Two types of genomic instability underlie the major pathways for oral cancer development and/or progression. The tumor suppressor pathway for aneuploid cancer is characterized by chromosomal instability that activates oncogenes and inactivates tumor suppressor genes (TSGs). In contrast, the mutator pathway for (pseudo)diploid cancer is associated with instability of microsatellites, which are simple, repetitive sequences in DNA. Interaction between the two pathways is recognized to be critical to the development of OSCC.

"Microsatellites" are DNA stretches of 1–5 nucleotides repeated 5–100 times ubiquitously in the genome. Microsatellites are at high risk for slippage by DNA polymerase during replication, a problem that is counteracted by the mismatch repair (MMR) system. Defects in the MMR program occur in oral cancer leading to gain or loss of these repeat units. Microsatellite instability in more than two to three regions may be considered important for cancer progression. This is one mechanism of genomic stability in oral cancer. Chromosomal instability includes gross chromosomal changes such as "loss of heterozygosity" (LOH) or "aneuploidy" (i.e., abnormal chromosomal number). LOH refers to a chromosomal event that includes the loss of an entire gene and surrounding chromosomal elements. LOH is a very common chromosomal aberration seen in oral cancer and usually involves a tumor suppressor gene leading to loss of control over cell proliferation. Several karyotypes were described in oral cancer, ranging from losses (9p, 3p, 17p, 13q, 8p, etc.) to gains (9q, 3q, 7p 5p, 8q 11q, etc.) on chromosomal arms [10] [Table 2.1]. Alterations are more common on chromosomes 9, 3, 8, 13, and 17. Tobacco smoke is also an established aneuploidogen. Remarkably, aneuploidy is known to occur in oral cancer and potentially malignant disorders of the tongue [162].

Multiplex ligation-dependent probe amplification (MLPA) analyses of 133 cancer-related genes on a panel of primary oral tumor samples and its corresponding resection margins (macroscopically tumor-free tissue) identified frequent copy number gains in genes located on chromosomal arms 3q, 6p, 8q, 11q, 16p, 16q, 17p, 17q, and 19q and copy number losses of genes frequently on chromosomal arms 2q, 3p, 4q, 5q, 8p, 9p, 11q, and 18q. Losses included ERBB4, CTNNB1, NFKB1, IL2, IL12B, TUSC3, CDKN2A, and CASP1, while gains of MME, BCL6, VEGF, PTK2, PTP4A3, RNF139, CCND1, FGF3, CTTN, MVP, CDH1, BRCA1, CDKN2D, BAX, as well as exon 4 of TP53 were recorded. Loss of TUSC3 gene may serve as a reliable indicator of malignancy [163].

"Single nucleotide polymorphisms" (SNPs) are genetic alterations that increase the susceptibility to diseases including cancer. SNPs involving many genes in carcinogen detoxification and folate metabolism, DNA repair (ataxia telangiectasia mutated (ATM)), inflammation, cell cycle control and proliferation, immune function, and invasion are known to alter the susceptibility to oral cancer in certain populations [116, 164–166]. In a meta-analysis of SNP research in oral cancer, nine potential SNPs were identified with associated risk of oral cancer [165]. Four SNPs of the fibroblast growth factor receptor 4 (FGFR4) genomic region *FGFR4* (rs2011077, rs351855, rs7708357, and rs1966265) were examined in 955 patients with OSCC and 1191 controls. While the rs351855 GA genotype and a

Table 2.1 Common genetic alterations and their underlying mechanisms in OPMD and oral cancer are listed

Chromosome	Cytogenetic location	Gene Involved	Up-/downregulation	Reported mechanism	Functional role, target genes, and interacting partners	End result	References
1	1p13.3	*GSTM1*	Down	Polymorphism	Metabolism of xenobiotics and carcinogens	Poor tolerance to carcinogen exposure	[11]
	1p21.3	*MIR137*	Down	Promoter methylation	Targets specificity protein (SP1) zinc finger transcription factor participating in proliferation and colony formation	Epithelial-mesenchymal transition (EMT)	[12–16]
	1p31.3	*MIR101*	Down	NA	Correlates inversely with expression of ZEB-1, which is a downstream target of miR-101; ZEB-1 imparts proliferative and invasive capacity to OSCC cells	Lymph node metastasis	[17–20]
					Low expression of miR-101 was shown as marker of poor prognosis, and loss of miR-101 was linked to overexpression of EZH2, a regulator of survival and metastasis through epigenetic silencing		
	1p36.33	*MIR200A*	Down	NA	Regulate E-cadherin repressors: ZEB-1, ZEB-2. A reduction in miR-429 may reduce apoptosis by targeting BCL-2 and SP-1	Epithelial-mesenchymal transition (EMT)	[21, 22]
		MIR200B					
		MIR429					
2	2p23.3	*FTH1P3*	Up	NA	It is a competing endogenous RNA, a sponge for miR-224-5p. Its expression levels correlate with patient survival	Proliferation	[23]
	2q35	*MIR26B*	Down	NA	miR-26b forms a tumor suppressor axis with TMEM184B transmembrane protein necessary for cell migration, invasion, and actin cytoskeleton-pathway genes	Cell migration and Invasion	[24]
		MIR375	Down	NA	Expression is mediated via KLF5 transcription factor	Proliferation, apoptosis, invasion, and migration	[25–29]
					miR-375 regulates MYC expression and forms an axis with SLC7A (Solute carrier family seven number 11) linked to proliferation and invasion		

(continued)

Table 2.1 (continued)

Chromosome	Cytogenetic location	Gene Involved	Up-/downregulation	Reported mechanism	Functional role, target genes, and interacting partners	End result	References
					Downregulation of miR-375 may sensitize cells to HPV infection		
					Some chemotherapeutics (doxorubicin, 5-fluorouracil, trichostatin A, etoposide) were shown to increase expression of *MIR375*		
					Serves as a biomarker in oral cytology specimens		
3	3p14.2	*FHIT*	Down	Mutation Deletion (LOH) Hypermethylation	Genome caretaker and loss induces chromosomal breaks, and genomic instability may further lead to inactivation of p53	Induces chromosomal breaks	[30–32]
	3p22.2	*MIR26A*		Polymorphism	TMEM184B is a known target of MIR26a which regulates genes in 23 pathways. A polymorphism was also linked to oral premalignancy. miR-26a increases expression of MEG3 lncRNA which suppresses expression of DNMT3	Migration and invasion	[24, 33, 34]
	3p25-26	*VHL*	Down	Deletion	"VHL-HIF-1α" complex is necessary for normal cellular response to hypoxia. Its loss stimulates production of VEGF and cyclin D1 and can stimulate EMT through alteration of β-catenin and MMP-2/MMP-9 levels. Loss of VHL also increases glucose uptake	Angiogenesis and EMT	[35, 36]
	3q26	*PI3KCA*	UP	Amplification Mutation	High rate of AKT phosphorylation. Correlation also exists between mutation rate and tumor stage	Lymph node metastasis	[37–39]
4	4p15.31	*MIR218-1*	Down	Methylation	Increases cancer stemness and invasion through BMI1 and also decreases caspase-mediated apoptosis	Cancer stemness, HPV-mediated oncogenesis	[40–45]
					Linked to HPV-mediated OSCC		
					SP1 and mTOR component "Rictor" were shown as targets, resulting in phosphorylation of AKT		
5	5p15.33	*TERT*	Up	Amplification Mutation Hypermethylation Histone deacetylation	NF-κB, β-catenin, and C-MYC regulate TERT expression, and TERT joins with subunit of NF-κB to regulate expression of TNF-α, IL-6, IL-8, and MMP-9	Cell immortalization	[46]

	5q21	*APC*	Down	Deletion (LOH) Mutations Hypermethylation	Loss of APC leads to stabilization of β-catenin, and free β-catenin activates the WNT pathway causing tumor progression. Free β-catenin associates with T-cell factor (TCF) and mediates expression of oncogenes (c-Myc, cyclin D1), causing invasion and metastasis	EMT, invasion, and metastasis	[47–53]
6	6p21.31	*MIR1275*	Up	NA	Significant upregulation was noticed in advanced tumors (stage III–IV and T3–T4). May be linked to the P53 pathway	Lymph node invasion	[54]
	6p25.3	*FOXCUT*	Up	NA	Co-amplified with Fork head box C1 (FOXC1) gene forming a lncRNA-mRNA interaction pair. It is critical for maintenance of MMP-2, MMP-7, MMP-9, and VEGF-A and β-catenin	Proliferation and migration	[55–57]
7	7p11.2	*EGFR*	Up	Amplification Mutation	Mutation and amplification cause autoactivation of EGFR receptor even in absence of ligands, leading to substrate phosphorylation that triggers MAPK pathway, antiapoptotic PI3K/AKT pathway, STAT pathway, KRAS-BRAF-MEK-ERK pathway, phospholipase C gamma protein pathway that inhibits apoptosis, promotes angiogenesis, activates invasion- and metastasis-related cascades and also expression of oncogenes: fos and jun	Proliferation, invasion, and metastasis	[58–64]
					AKT induces NF-κB which has numerous downstream effects		
8	8q24	*MYC*	Up	Amplification	Transcription factor that interacts with numerous oncogenes (RAS, cyclin D1) and tumor suppressors (TP53, APC)	Stemness factor, responsible for tumor-initiating cells, and proliferation	[65–67]
					c-MYC upregulates cyclins, ribosomal RNA, and proteins and downregulates p21 and Bcl-2, leading to cell renewal, immortality, and reduction in apoptosis. Tumor-initiating cells increase by severalfold		

(continued)

Table 2.1 (continued)

Chromosome	Cytogenetic location	Gene Involved	Up-/downregulation	Reported mechanism	Functional role, target genes, and interacting partners	End result	References
		CCAT1	Up	Amplification	It is close to oncogene c-myc. OSCC cases overexpressing CCAT1 had poor therapeutic outcome	Stemness and proliferation	[68]
					Furthermore, CCAT1 overexpression correlated significantly with c-Myc expression through chromatin looping interaction and sponging of miR-155-5p and let7b-5p		
		CCAT2	Up	Polymorphism	Upregulates MYC, miR-17-5p, and miR-20a through TCF7L2-mediated transcriptional regulation	Depleted apoptosis,	[69–74]
					Promotes WNT/β-catenin pathway by regulating β-catenin and glycogen synthase kinase 3 beta (GSK-3β) expression	increased cell proliferation, invasiveness, and metastasis	
9	9p21	*CDKN2A* (p16),	Down	Hypermethylation or deletion (LOH)	Cell cycle proteins that inhibit cyclin-dependent kinase-4 and kinase-6, arresting the cell cycle at G1-S transition	Proliferation	[75–78]
		INK4a/ARF (p14)					
		MIR204	Down	NA	Loss induces stemness through expression of target genes: slug and sox 4	Stemness and lymph node metastasis	[79, 80]
					"miR-204^{low}Slug^{high}Sox4^{high}" is a signature of poor prognosis with lymph node involvement		
					Suppresses CXCR4 expression.		
		MIR31	Up	NA	Targets hypoxia-inducible factor (HIF) and VEGF and stabilizes TERT-mRNA. Functional effects are also mediated through FGF-3 and Rho-A	Immortalization, proliferation, angiogenesis	[81–84]
					Early OSCC-miR saliva signature		
					Inhibits expression of AT-rich interactive domain 1A (ARID1A), which disrupts P53 and/or PTEN pathways and inactivates Nanog/OCT4/Sox2 stemness factors and epithelial cell adhesion molecule (EpCAM)		

		MIR31HG	Up	NA	Genomic locus overlaps MIR31 and is involved with HIF-1α co-activation, regulating HIF-1 transcriptional network, also necessary for oncogene-induced senescence repressing the tumor suppressor gene p16(INK4A)	Oncogene-induced senescence	[85, 86]
					MIR31HG interacts with PRC2 (*polycomb repressive complex 2)* and its levels correlated with prognosis	and cell response to hypoxia	
	9q21.33	*DAPK1*	Down	Hypermethylation	Apoptosis regulator and positive mediator of gamma interferon-induced programmed cell death	Reduced apoptosis	[87]
	9q22.32	*LET-7A1*	Down	NA	Strong downregulation across tumor specimens, with a tendency for co-occurrence. Specifically target numerous genes in P13K/Akt signaling pathway	EMT, stemness	[88–91]
		LET-7D			Let7 family also regulates expression of RAS and stemness-associated genes in tumor-initiating cells		
		LET-7F1					
	9q34.3	*NOTCH1/ NOTCH3*	Up/Down	Mutation	NOTCH-1 encodes a transmembrane protein, and mutation-associated activation leads to expression of NF-κB, c-Myc, Hes family, and IL-7 receptor, leading to cell cycle progression, increased survival through loss of PTEN, and activation of PI3K/Akt pathway	Proliferation, survival, and EMT	[4, 6, 9, 11]
					NOTCH-3 has been identified through deep sequencing		
	9q34.3	*MIR126*	Down	NA	Downregulation induces angiogenesis and lymphangiogenesis via activation of VEGF-A and FGF, the key angiogenic regulators	Angiogenesis and lymphangiogenesis	[92, 93]
10	10q26.3	*MGMT*	Down	Hypermethylation	DNA repair enzyme in cellular defense against mutagenesis. May serve as a biomarker for OSCC prediction	Poor DNA repair	[94]

(continued)

Table 2.1 (continued)

Chromosome	Cytogenetic location	Gene Involved	Up-/downregulation	Reported mechanism	Functional role, target genes, and interacting partners	End result	References
11	11p15.5	*H-RAS*	Up	mutation Amplification	A proto-oncogene and GTPase. Mutational activation promotes oncogenesis by altering gene expression connected to proliferation, survival, and migration	Proliferation, survival, and migration	[95–97]
					RAS signals through Raf/MEK/ERK and PI3K/Akt pathway and is regulated by a wide range of miRNAs		
		H19	Up	Polymorphism	Maintains levels of β-catenin, EZH2, cyclin D1, c-Myc, and mesenchymal genes, N-cadherin and vimentin, while increasing E-cadherin and ZO-1 expression levels	Metastasis and EMT/MET decision	[98–103]
	11q13.1	*MALAT1*	Up	NA	Promotes oncogenesis by interaction with miR-124 and through miR-125b/STAT3 axis, where STAT3 was shown as a binding target of miR-125b. Also linked to inhibition of apoptosis by the modulation of WNT/β-catenin pathway	EMT, invasion, and metastasis and inhibits apoptosis	[104–108]
					Triggers β-catenin and NF-κB pathway		
	11q13.3	*CCND1*	Up	Amplification Polymorphism Chromosomal translocation	CCND1 and pRB exist in a negative equilibrium; synthesis of cyclin D1 causes phosphorylation of RB favoring cell division by shortening the G1 phase	Proliferation	[109–115]
					It was shown to be particularly amplified in aggressive tongue SCC, which correlated with worst survival		
	11q22.3	*ATM*	Down	Polymorphism	A kinase activated by DNA breaks. Certain alleles of this DNA damage response gene increase susceptibility to oral cancer	Poor genome stability	[11, 116]
12	12q13.13	*HOTAIR*	Up	Polymorphism	Causes recruitment of EZH2 and represses E-cadherin by binding with its promoter causing H3K27 trimethylation (gene silencing). This results in increase of β-catenin through the WNT/β-catenin pathway. Expression also correlated with poor patient survival and therapeutic outcomes	EMT, invasion, and metastasis	[117–122]

13	13q14.	*RB1*	Down	Deletion (LOH)	Losses involving *RB1* gene are noted in 66% of tumors and 64% of premalignant lesions	Proliferation, nodal metastasis, and HPV-OSCC	[123–125]
					RB1 is also inactivated by E7 protein of HPV. Phosphorylation of RB by CDKs creates “free E2F.” During entry into the S phase, the cyclin D1/CDK complex to phosphorylate RB(pRB) resulting in dissociation of E2F transcription factor. When E2F is set free, it causes transcription of genes involved in cell cycle progression such as cyclins and proliferating cell nuclear antigen (PCNA)		
	13q14.2	*MIR16-1*	Down	Deletion	Functional pathway analysis yielded 21 oncogenes among its bona fide targets (*BCL2*, *MCL1*, CCND1, WNT3 etc.). It may work through the PI3K/AKT pathway	Cell proliferation and promotes apoptosis	[126]
14	14q32	*MIR127*	Down	Methylation	Stroma-specific miR shows high expression in cancer tissues. Significantly dysregulated in HPV-associated OSCC. miR-127 is intimately linked to cell proliferation and senescence through upregulation of BCL-6	Proliferation and senescence	[127, 128]
		MEG3	Down	NA	DNMT3B negatively regulates MEG3 expression, while miR-26a opposes it by targeting DNMT3B	Apoptosis promotor	[40, 129, 130]
		MIR134	Up	NA	miR-134 is oncogenic in OSCC and works by reversely affecting tumor suppressor protein WW domain-containing oxidoreductase (*WWOX*)	Metastasis	[131–136]
15	15q25.1	*MIR184*	Up	NA	Induces proliferation and apoptosis by targeting *C-MYC* oncogene (MIR184 inhibitors reduce cell proliferation)	Proliferation and inhibits apoptosis	[137–139]
					It also reverses the effect of *WWOX* tumor suppressor		
					Plasma levels of MIR184 reflected the presence of primary tumor. Upregulated by 59-fold		

(continued)

Table 2.1 (continued)

Chromosome	Cytogenetic location	Gene Involved	Up-/downregulation	Reported mechanism	Functional role, target genes, and interacting partners	End result	References
16	16q12.2	*MMP2*	Up	Mutation Polymorphism	MMP-2 is involved in the breakdown of extracellular matrix (type IV collagen), which is a major component of the basement membrane. Snail and miR-29a enhance expression of MMP2	Invasion	[140]
	16q22.1	*CDH1*	Down	Methylation	A calcium-dependent cell-cell adhesion protein. Loss of function is linked to dysregulation of cellular structural organization at several levels (Golgi apparatus to actin cytoskeleton) and cell adhesion molecules (CAMs)	Metastasis	[11, 141]
17	17p13	*TP53*	Down	Mutation Polymorphism	Guardian of genome and a potential transcription factor for 100 genes, including p21 which complexes with CDK2 to act as a stop signal during cell cycle holding the cell at G1/S. It can activate DNA repair proteins when DNA has sustained damage or can initiate apoptosis if DNA damage is irreparable (decision-maker). Also essential for the senescence response to short telomeres	Proliferation, apoptosis	[4, 9, 47, 142–144]
	17q11.2	*MIR144*	Up	NA	Functional pathway analysis revealed tumor suppressor *PTEN* as a major target of miR-144 and bioinformatics predicted miR-144 to inhibit mTOR expression. The paired box gene 4 (PAX4) was shown to drive metastasis by decreasing miR-144 expression, through a disintegrin and metalloproteinase (ADAM) protein family members	Nodal metastasis	[54, 145, 146]
	17q23.1	*MIR21*	Up	NA	Upregulated in tumor stroma myofibroblasts and downregulates tumor suppressors: *PTEN*, *BCL2*, *dickkopf2 (DKK2)*, etc.	Proliferation apoptosis, invasion, and migration	[25, 147–155]
					Stromal expression was linked to poor prognosis, and hypoxic environment stimulates the tumor cells to generate miR-21-rich exosomes which were shown to act as a pro-metastatic signal to normoxic cells. miR-21 enhances snail and vimentin expression and reduced expression of E-cadherin		

					Overexpression was identified in leukoplakias with risk of malignant transformation and higher expression also correlated with perineural invasion and keratinization		
					A strong repression of reversion-inducing cysteine-rich protein with Kazal motifs (RECK), an inhibitor of MMPs, was noticed in miR-21 cell lines		
					miR-21 was also shown as a noninvasive biomarker for TSCC in oral cytology samples and is a potential plasma and saliva diagnosis marker of OSCC		
18	18q21.3	*BCL-2*	Up	Polymorphism Amplification	Apoptosis inhibitor, upstream of caspase pathway. It has been targeted for oral cancer gene therapy	Apoptosis inhibition	[38, 156–158]
19	19p13.12	*UCA1*	Up	Polymorphism	Increases β-catenin expression. lncRNA UCA1-β-catenin-WNT signaling pathway regulatory network	Proliferation, cell migration, invasion, and nodal metastasis	[159]
22	22q11.23	*GSTT1*	down	Polymorphism, deletion	GSTT1 catalyzes conjugation of reduced glutathione to a variety of electrophilic and hydrophobic compounds, engaged in glutathione metabolic process (glutathione peroxidase and transferase activity) and xenobiotic metabolism by cytochrome P450	Impaired glutathione metabolism	[11]
					Polymorphisms in GSTT1 detected in oral cancer and can increase susceptibility to oral leukoplakia and OSF		
	22q12.2	*TUG1*	Up	NA	Maintains mRNA and induces expression of β-catenin, cyclin D1, and c-myc	EMT, metastasis, invasion,	[160, 161]
					Works through the Wnt/β-catenin signaling	proliferation	

A large number of genetic alterations have been reported across the nuclear DNA (i.e., chromosomes 1–23), with mechanisms encompassing single nucleotide polymorphisms (SNPs), mutations, deletions through loss of heterozygosity, amplification, and epigenetic modifications like promoter hypermethylation and histone changes. These mechanisms ultimately lead to loss of balance between the signaling pathways resulting in uncontrolled proliferation of cells, survival, immortalization, invasion, and metastasis which are the components of EMT and also angiogenesis. The genes in oral cancer encompass a large number of oncogenes and tumor suppressor genes and pivotal noncoding RNAs. The microRNA genes are abbreviated as "*miR*" combination of the GA and AA genotypes showed a 1.431-fold and 1.335-fold higher risk of OSCC, *FGFR4* rs351855 polymorphism with a homozygous A/A genotype had a lower risk of advanced stage OSCC. Additionally, patients with the *FGFR4* rs351855/rs1966265 A-A haplotype and betel quid chewers with the A-A haplotype exhibited a higher risk of OSCC. Moreover, an additional integrated in silico analysis proposed that rs351855 G allele variant to the A allele exhibited a relatively low energy of the transmembrane region. The *FGFR4* rs351855 may have a role in susceptibility to OSCC [167].

Several recent studies have revealed the genetic signature for oral cancer susceptibility. Of a total of 264 chromosomal loci found to be associated with oral cancer by candidate gene studies, genome-wide association studies (GWAS), and next-generation sequencing (NGS)-based approaches, 28 loci were validated to be linked to oral cancer. These include 14q32.33 (AKT1), 5q22.2 (APC), 11q22.3 (ATM), 2q33.1 (CASP8), 11q13.3 (CCND1), 16q22.1 (CDH1), 9p21.3 (CDKN2A), 1q31.1 (COX-2), 7p11.2 (EGFR), 22q13.2 (EP300), 4q35.2 (FAT1), 4q31.3 (FBXW7), 4p16.3 (FGFR3), 1p13.3 (GSTM1-GSTT1), 11q13.2 (GSTP1), 11p15.5 (H-RAS), 3p25.3 (hOGG1), 1q32.1 (IL-10), 4q13.3 (IL-8), 12p12.1 (KRAS), 12q15 (MDM2), 12q13.12 (MLL2), 9q34.3 (NOTCH1), 17p13.1 (p53), 3q26.32 (PIK3CA), 10q23.31 (PTEN), 13q14.2 (RB1), and 5q14.2 (XRCC4) [11]. Another GWAS identified two new regions, 2p23.3 (rs6547741, GPN1) and 9q34.12 (rs928674, LAMC3), with susceptibility for oral cancer that was stronger for HPV-positive compared to HPV-negative cases [123]. Genome-wide haplotype association analysis between 112 OSCC patients from the GEO database and 245 normal samples from the HapMap project identified SERPINB9, SERPINE2, GAK, and HSP90B1 as novel risk genes for OSCC [168].

2.3 Molecular Mechanisms of OSCC Development and Progression

The development of OSCC is a multistage process that involves the progressive transition of the normal oral epithelium through dysplastic lesions to invasive carcinomas. These steps are characterized by the sequential accumulation of genetic alterations in proto-oncogenes, tumor suppressor genes (TSGs), and stability genes as well as in genes that influence cellular functions such as cell cycle, DNA repair, apoptosis, cell adhesion, angiogenesis, and signal transduction that eventually lead to the development and progression of OSCC. Gain of function mutations or copy number alterations involving proto-oncogenes and/or loss of function mutations involving TSGs lead to genomic instability tipping the balance toward tumorigenesis (Fig. 2.1). In addition to mutations, epigenetic changes have also been implicated in neoplastic transformation.

2.3.1 Proto-oncogenes

"Proto-oncogenes" are genes that encode proteins involved in cell growth and differentiation. Point mutations, chromosomal translocations, DNA rearrangements, and gene amplification cause proto-oncogene activation and neoplastic transformation. Gain of function or increase in copy number of oncogenes located at 1q, 3q, 5p, 7q, 8q, 9q, 11q, 12p, 14q, and 15q has been documented in OSCC. Overexpression, amplification, and point mutations of several oncogenes have been associated with aggressive tumor behavior and bad prognosis in OSCC. Established proto-oncogenes in OSCC include growth factor receptors (e.g., epidermal growth factor receptor), intracellular messengers (e.g., RAS), transcription factors (c-MYC and cyclin D1), etc. Typical examples of proto-oncogenes are discussed here, while the rest are described in the relevant contextual pathways.

2.3.1.1 Growth Factor Receptors

Epidermal growth factor receptor (EGFR or HER1), one of the intensively studied transmembrane receptors, plays a critical role in differentiation and proliferation [169]. Epidermal growth factor (EGF), a known ligand for this receptor, activates EGFR leading to the phosphorylation of several key substrates that trigger downstream PI3K/Akt, MAPK, JAK/STAT, and

KRAS-BRAF-MEK-ERK signaling pathways [58–60] that promote acquisition of cancer hallmarks [61–63, 169]. "EGFR activation is therefore a primary cell surface signal in several cancers."

Amplification of 7p11.2, the chromosomal locus of EGFR, and mutations are commonly observed in head and neck squamous cell carcinoma (HNSCC) cases [169]. EGFR overexpression is considered a dominant component underlying the malignant phenotype in OSCC (Fig. 2.2a, b). Malignant oral keratinocytes demonstrated nearly 5–50-fold increase in the expression of EGFR, and the levels increase with OSCC progression. In OSCC, mutational inactivation of the EGFR extracellular domain leads to apoptosis evasion, uncontrolled proliferation, and tumor progression [64]. The mutant receptor is active even in the absence of EGF resulting in aberrant activation of PI3K/Akt/mTOR pathway that induces the transcription factor nuclear factor κappaB (NF-κB) which has several downstream affects.

In a long-term prospective randomized trial, high EGFR expression and gene copy number were identified in OSCC developed within oral leukoplakia [61]. EGFR is also a target for cancer therapies (e.g., anti-EGFR antibodies). Recently, curcumin the bioactive polyphenolic component of turmeric was also shown to inhibit

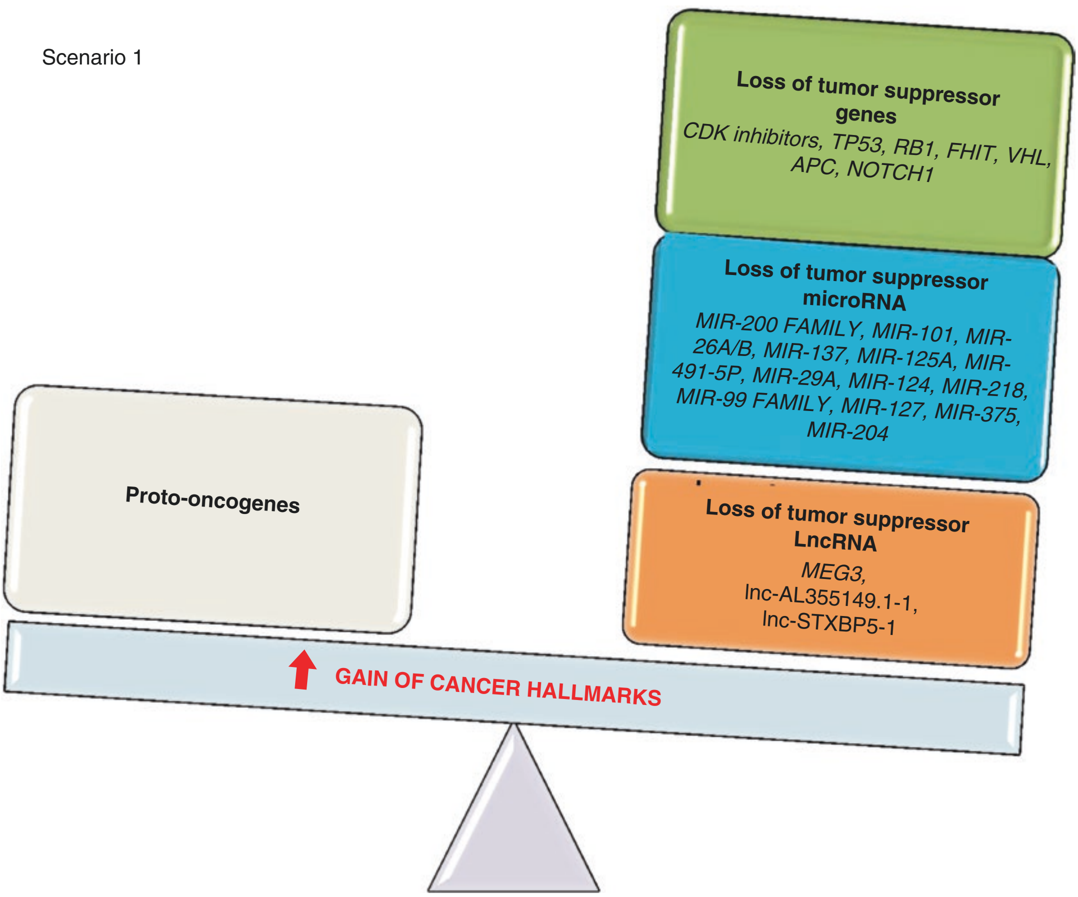

Fig. 2.1 Tumor suppressor and oncogenic molecules constitute a large group of proteins and noncoding RNAs (microRNA, long non-coding RNA, Piwi-interacting RNA and circular RNA) that carefully balance cell cycle, apoptosis, survival and other normal and healthy cell features. In oral cancer scheme, this subtle balance is lost, either through loss of function in tumor suppressors (scenario 1) and/or gain of function in oncogenes (scenario 2), as a result there is tipping in the cell cycle balance and cells tend to hyperproliferative, evade apoptosis, become more motile and invasive, leading to malignant transformation and progression

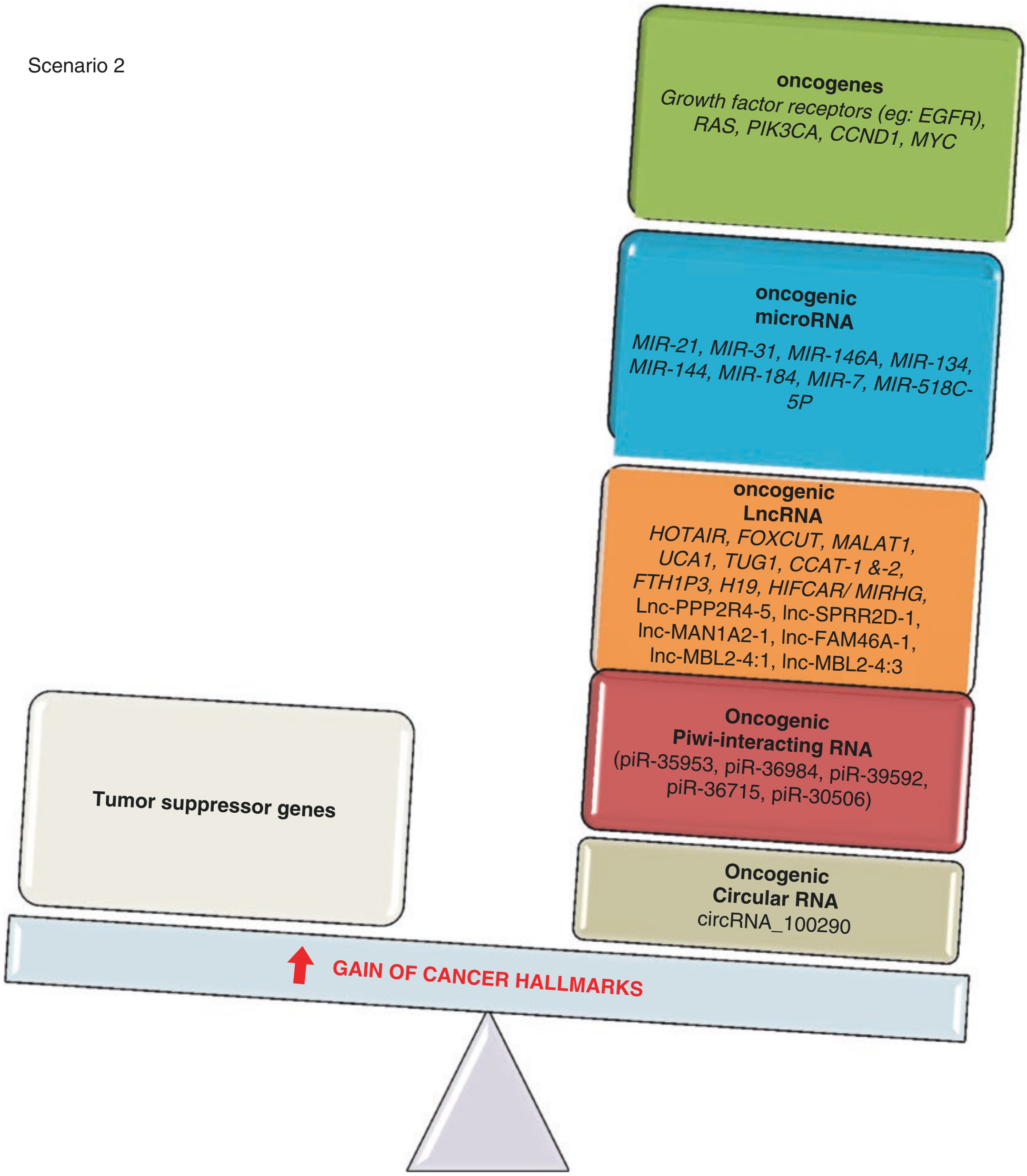

Fig. 2.1 (continued)

proliferation of OSCC by downregulating phosphorylation of EGF-induced phosphorylation of EGFR.

Other receptors significantly upregulated in OSCC include insulin-like growth factor 1 receptor (IGF1R), glucose transporter 1 (GLUT-1), nerve growth factor receptor (NGFR), and fibroblast growth factor receptor (FGFR) and its isoforms (FGFR-1, FGFR-2) [64, 170]. Recently, GLUT 1 expression immunostaining in brush biopsy samples of precancerous lesions was shown as an additional tool in the diagnosis of malignant transformation of the oral mucosa with sufficient overall accuracy [171]. Higher immunostaining scores for GLUT-1 indicated a high-grade stage and poor prognosis. NGFR-positive cells display high tumor growth rate and invasive and metastatic phenotype associated

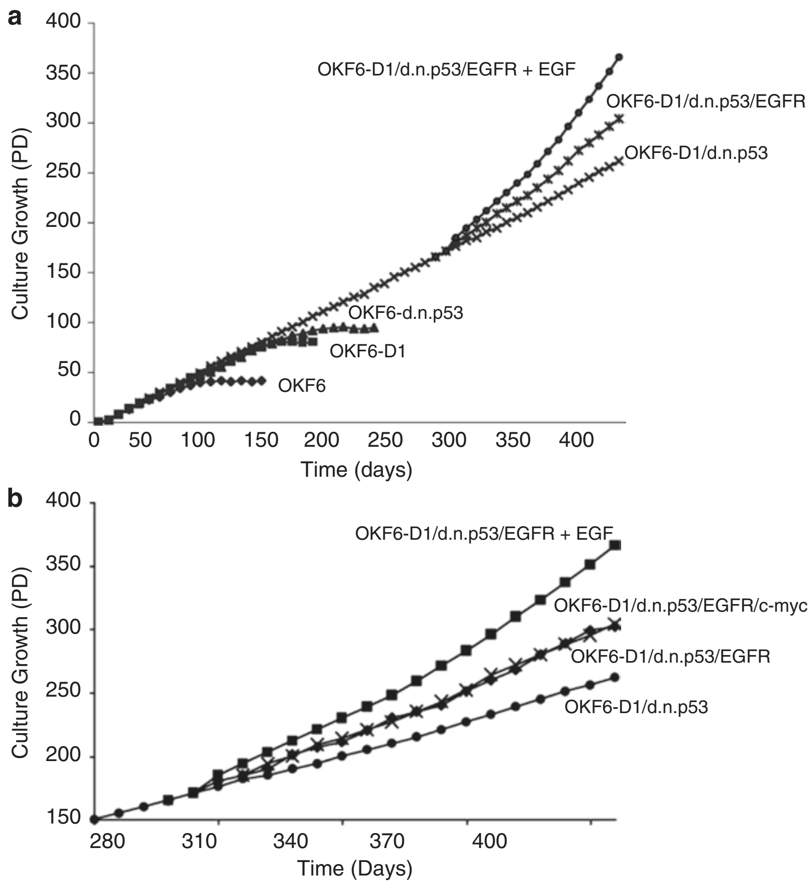

Fig. 2.2 A step-wise genetic model of immortalization and malignant transformation of oral keratinocyte. The growth characteristics of a parental (OKF6) and derived oral keratinocytes (cyclin D1 overexpression (OKF6-D1)), ectopically expressed dominant negative p53 (OKF6-dnp53), combinations of cyclin D1, dnp53 and EGFR (OKF6-D1/dnp53), OKF6-D1/dnp53/EGFR and combination of all OKF6-D1/dnp53/EGFR plus EGF are shown (**a**). Cyclin D1 alone and in combination with dominant negative p53 (dnp53) was ectopically expressed in normal human oral keratinocytes. Cyclin D1 overexpression and p53 inactivation led to immortalization (threefold increase in life-span). The replicative life span was assessed by calculating the PDs of each cell line. Replicative life span of oral keratinocytes additionally overexpressing EGFR and c-myc. Growth characteristics of OKF6-D1/dnp53, OKF6-D1/dnp53/EGFR, OKF6-D1/dnp53/EGFR plus EGF, and OKF6-D1/dnp53/EGFR/c-myc cells (**b**). The replicative life span was assessed by calculating the PD values. Reprinted with permission from Goessel et al. Creating oral squamous cancer cells: a cellular model of oral-esophageal carcinogenesis. Proc Natl Acad Sci U S A. 2005; 102:15599–604."copyright (2005) National Academy of Sciences"

with increased expression of endothelial cell-specific molecule-1 (ESM-1) [172]. Aberrant expression of FGFR-2, FGFR-3, and its growth factor (FGF-2) has been linked to OPMDs transforming into OSCC [173] and serves as a biomarker of malignant transformation. Increased expression of FGFR-2 and FGFR-3 has been reported in oral dysplasia and early invasive carcinoma.

2.3.1.2 Rat Sarcoma Viral Oncogene (RAS)

Abnormalities of the RAS oncogene including mutations, LOH, and amplification have been reported in OSCCs from India and Southeast Asian countries, in contrast to low prevalence of these mutations in Western countries. High-frequency mutations in codons 12 and 61 of H-ras oncogene were detected in Indian OSCC patients, particularly among tobacco chewers [95]. RAS assumes two conformations, *on* when bound to GTP and *off* when bound to GDP, and is controlled by guanine exchange factors. RAS signaling transcriptionally upregulates growth factors (TGF-α), growth factor receptors, and integrins that promote proliferation. RAS proteins not only inhibit the operation of TGF-β by reducing its cognate receptor expression but also upregulate cyclin D1/CDK-4 and CDK-6 leading to phosphorylation of CDKs, release of E2F transcription factor from RB, and cell cycle progression. This can result in replicative stress, genome instability, mutations, and chromosomal aberrations that contribute to tumorigenesis. Gingival carcinoma biopsies exhibited higher expression of H-RAS and a strong correlation between H-Ras expression and COX-2 expression [96]. PI3K/Akt and MAPK are two downstream effector pathways connected to changing RAS levels and may be potential therapeutic targets for oncogenesis driven by RAS [97].

2.3.1.3 MYC

The *MYC* genes encode transcription factors (c-, N-, and L-*MYC*) that frequently heterodimerize with myc-associated factor X (MAX) to form a nucleo-phosphoprotein complex to regulate a large number of genes, participating in global chromatin organization. MYC transcription factors are among the most potent oncoproteins that integrate environmental signals to modulate cell proliferation, growth, apoptosis, and other functions. MYC interacts with a wide range of oncogenes and TSGs and is activated by *WNT* pathway, *SHH*, and EGF. c-MYC upregulates cyclins, ribosomal RNA, and proteins and downregulates p21 and Bcl-2, leading to cell renewal, immortality (Fig. 2.2b), and reduction in apoptosis [65]. Amplification is the main mechanism behind overexpression (80%) of *c-MYC* in OSCC [66]. *c-MYC* expression was also identified in the early stages of oral neoplasia (keratosis and oral potentially malignant disorders (OPMDs)) and advanced lip carcinoma and was associated with poor prognosis in OSCC [67]. c-MYC status resulted in unfavorable therapeutic outcome following chemotherapy with methotrexate [67].

2.3.2 Tumor Suppressor Genes

Loss of function mutations in TSGs is very common in oral cancer, and generally both copies are inactivated, in a two-hit fashion. Frequent loss of TSGs located at 1p, 3p, 4p, 5q, 8p, 10p, 11q, 13q, 17p, and 18q has been documented in OSCC [Table 2.1]. Genetic alterations such as LOH and/or mutations lead to inactivation of TSGs in oral cancers. Loss of heterozygosity (LOH) at chromosomes 3p14, 4q, 5q, 6p, 6q, 7q, 8p, 9p, 9q, 10q, 11q, 13q14.2, 14q, 17q, 18q, 20q, 21q, and 22q has been reported in oral cancer. Certain chromosomal sites are especially susceptible to mutations. These are known as *fragile sites* and their frequency is increased by tobacco chewing and smoking.

The main TSG candidates in OSCC include *TP53*, retinoblastoma (*RB*), CDK inhibitors, fragile histidine triad (*FHIT*), adenomatous polyposis coli (*APC*), von Hippel-Lindau (*VHL*) syndrome, *NOTCH-1*, etc. Accumulation of deleted in oral cancer-1 (*doc-1*) has been proposed as a novel tumor suppressor gene in oral cancer development.

TSGs are inactivated by promoter methylation, point mutations, chromosomal rearrangements, or deletions (LOH). Promoter methylation is an established mechanism of TSG loss of function [64, 87]. Loss of function of TSGs is normally carried by covalent modification such as DNA methylation on their gene promoters.

2.3.2.1 Tumor Protein p53 (TP53)

TP53 codes for a transcription factor "tumor protein p53," which participates in transcription-mediated activation of apoptosis, G1-S cell cycle arrest, inhibition of angiogenesis, DNA repair, and genetic stability. TP53 activates more than 100 downstream genes, including miR-34 and p21. The activated p21 binds to CDK2 and this complex acts as a stop signal arresting cell division. Loss of *TP53* occurs by mutation or LOH encompassing 17p13, its cytogenetic locus. Point mutations lead to structurally altered proteins incapable of their regular functions, and deletion leads to a reduced level or loss of P53 expression.

Mutations in *p53* are the single most frequent genetic alterations in OSCC. Hotspots for p53 mutations are predominantly in codons 141, 175, 179, 205, 220, 237, 245–248, 268, 272, 273, 278–281, and 290. Mutations in p53 are mostly G-A transitions in Japan and Switzerland, G-T transversions in the UK and USA, and transitions in India. Mutations in p53 are rare in developing countries like Sri Lanka, India, and Papua New Guinea but most common in Western countries [142].

TP53 is also shown to be frequently mutated in the presence of HPV in OSCC cell lines [47]. Inverse correlation between P53 and HPV status in HNSCC tissue specimens was observed through genome sequencing [4]. In a recent whole exome analysis by Stransky et al., TP53 mutations were reported in 65% cases of HNSCC which included oral cancers [4]. Disrupted *TP53* is also associated with reduced survival following surgical treatment in HNSCC [143]. Intra-arterial chemotherapy with 5-fluorourcil and carboplatin exerted therapeutic effect by reducing the expression of mutant *P53* (Fig. 2.2a, b) [144].

2.3.2.2 Retinoblastoma (RB1)

Losses involving the retinoblastoma gene (*RB1*) on 13q14 occur in a large fraction of OSCC cases [124]. LOH encompassing this region is also associated with increased nodal metastasis and high recurrence. Deletion of the RB gene has been reported in OSCC with consequent loss in functional Rb pathway and accumulation of mutated TSG p16NK4a. *RB1* that codes for retinoblastoma-associated protein is inactivated by HPV E7 protein [125]. Phosphorylation of RB by CDKs releases E2F that transactivates genes involved in cell cycle progression such as cyclins and proliferating cell nuclear antigen (PCNA) [125].

2.3.2.3 Fragile Histidine Triad *(FHIT)*

The *FHIT* gene located on 3p is a genome caretaker that is highly sensitive to environmental carcinogens like tobacco. While small regional losses occur in mild dysplasia, whole arm losses were noted in high-grade dysplasia and in OSCC [30]. *FHIT* gene expression was reported to be lost in 65% of patients with leukoplakias and erythroplakias [31]. Abnormal transcripts harboring common deletion patterns at exon 5 of FHIT were detected in oral precancerous and cancerous lesions. Loss of FHIT expression is an indicator of poor prognosis, but good susceptibility was shown to postoperative radiotherapy [32].

2.3.2.4 Von Hippel-Lindau (*VHL)* Disease

Von Hippel-Lindau (*VHL*) disease located at 3p plays a central role in the cellular response to hypoxia. During normoxic conditions, hypoxia-inducible factor-1 alpha (HIF-1α) is hydroxylated at specific proline residues followed by binding to and degradation by VHL. However, under hypoxic conditions, VHL is unable to bind to HIF-1α. Consequently, HIF-1α forms a heterodimer with HIF-1α, translocates to the nucleus, and transactivates several hypoxia-sensitive genes such as vascular endothelial growth factor (VEGF). Loss of VHL contributes to epithelial-mesenchymal transition in OSCC and was also associated with poor tumor grade, poor prognosis, and lymph node metastasis [35]. A loss of VHL may also increase glucose uptake by OSCC cells, which is facilitated by GLUT1 transporter [36].

2.3.2.5 Adenomatous Polyposis Coli (*APC*)

The adenomatous polyposis coli (*APC*) gene located on 5q21–22 inhibits the Wingless-type (WNT) signaling pathway, LOH, or mutations in *APC*, stabilizes the transcription factor β-catenin which translocates to the nucleus, and together with T-cell factor (TCF) mediates the transcription of several oncogenes including c-MYC and cyclin D1. Mutations in *APC* although most common in colorectal carcinoma (80%) were also noticed in OPMD and oral cancer (25%) [47–53]. Mutations in *APC* were identified in quid users, oral submucous fibrosis undergoing progression, and OSCC [49, 50]. LOH encompassing *APC* was shown in leukoplakia and OSCC [51].

Mutations were recently identified in several other genes implicated in maintenance of nuclear polarity (spectrin repeat-containing nuclear envelope protein 1(*SYNE1*), spectrin repeat-containing nuclear envelope protein 2(*SYNE2*)), squamous differentiation (regulating synaptic membrane exocytosis 2 (*RIMS2*), piccolo presynaptic cytomatrix protein (*PCLO*)), apoptosis (*caspase 8 (CASP8)*, DEAD-box helicase 3, X-linked (*DDX3X*)), and histone methyltransferases (PR/SET domain 9 with histone methyltransferase activity (*PRDM9*), enhancer of zeste 2 polycomb repressive complex 2 subunit (*EZH2*), and more recently CCAAT/enhancer-binding protein alpha (*CEBPA*) and FES proto-oncogene (*FES*)) [4]. The complete list of tumor suppressor genes is unending, but the mentioned genes constitute a major fraction of TSGs in OSCC.

2.3.3 Epigenetic Alterations in Oral Cancer

The term "epigenetics" refers to heritable changes in gene expression without changes in the DNA sequence [174]. Epigenetic modifications including DNA methylation, histone modifications, and changes in noncoding RNA (ncRNA) play a pivotal role in the development and progression of OSCC [175]. Aberrant promoter hypermethylation can prevent binding of transcription factors to DNA leading to silencing of TSGs involved in regulating cell proliferation. On the other hand, global hypomethylation can activate proto-oncogenes causing genomic instability. Post-translational histone modifications (acetylation, deacetylation, methylation) can either increase or block binding of transcription factors to the promoter by inducing conformational changes in DNA structure. The ncRNA regulates gene expression at the posttranscriptional level by degrading or repressing the mRNA transcript to inhibit translation [94].

DNA methylation, a heritable modification of the DNA, is regulated by DNA methyltransferases (DNMT). Global DNA hypomethylation contributes to OSCC development through multiple mechanisms [94]. While hypomethylation of DNA at repetitive sequences such as LINE-1 and Alu sequences leads to chromosomal instability, promoter hypomethylation of proto-oncogenes results in their reactivation. Additionally, hypomethylation of naturally methylated silent, imprinted bialleles can contribute to loss of imprinting. Hypermethylation on promoter regions of TSGs results in gene silencing and promotes tumor development [176]. In oral cancer, a change in the methylation patterns of DNA was frequently observed [87]. Tobacco and alcohol are two common environmental factors that mediate aberrant methylation. Hypermethylation of TSG promoters is the most frequently characterized epigenetic alteration in OSCC. Genes involved in cell cycle regulation (p16, p15, and p14), cell-cell adhesion (E-cadherin), Wnt signaling pathway (APC, WIF1, RUNX3), DNA repair (MGMT, hMLH1), and apoptosis (apoptosis-associated death-associated protein kinase (DAPK)), as well as p73, PTEN, and Ras association family [RASSF] 1A, are the most commonly hypermethylated genes in OSCC. Hypermethylation of these TSGs causes inactivation and transcriptional gene silencing promoting malignant transformation of oral keratinocytes.

Epigenetic alterations can also occur through histone modifications catalyzed by histone acetyltransferases (HATs) and histone methyltransferases (HMTs) that transcriptionally activate DNA resulting in increased expression of genes that promote tumor development, while histone deacetyltransferases (HDACs) and histone demethylases (HDMs) cause silencing of many TSGs. Overexpression of histone deacetylase-1, a predominant epigenetic reprogramming protein implicated in silencing various growth regulatory pathways and proapoptotic programs, was observed in OSCC.

2.4 Noncoding RNAs: Novel Players in Oral Cancer

For a long time, proteins were considered as the only pivots of tumor evolution. Although unbelievable, less than 3% of the genome codes for proteins, and nearly 75% of the genome is transcribed to RNAs that have no coding potential.

Recent attention has therefore shifted from proteins to these noncoding RNAs (ncRNAs), to microRNAs (miRs), and more recently to long noncoding RNAs (lncRNAs). Based on size and the arbitrary 200 nucleotides cutoff, ncRNAs are classified into small ncRNAs, which include the microRNAs and Piwi-interacting RNAs (piRNAs), and the longer ncRNAs that include long noncoding RNAs (lncRNAs) and circular RNAs (circRNA) [177, 178].

2.4.1 MicroRNAs

MicroRNAs (miRs) are small, 18–25 nucleotides long, noncoding RNAs found ubiquitously in the genome but predominantly in the intergenic and intronic regions [177, 178]. Each miR can act on hundreds of genes or messenger RNAs to maintain key biological processes such as proliferation, apoptosis, and differentiation [88]. It is now accepted that nearly 30% of all genes are regulated by various miRs [179]. As they operate on diverse physiological mechanisms, their dysregulation influences overall cellular functions and forms subtle links in the intricate events in oncogenic transformation.

Alteration in the expression of several miRs was documented in OSCC that correlated with nodal status and metastasis [126]. miRs regulate important signaling pathways involved in tumorigenesis by targeting oncogenes and TSGs. For example, 14 TSGs are targets of miR-21, and 21 oncogenes are targets of miR-16. Many oncogenes (*CCND1, MYC, HRAS, KRAS, CDK-4, CDK-6*, high-mobility group AT-hook 2 (*HMGA2*)) and TSGs (*TP53*, *PTEN*, etc.) are acted upon by multiple miRs [126]. While some miRs regulate P13K/Akt/NF-κB signaling, others are known to inhibit telomerase or induce EMT and angiogenesis. Several studies have revealed that miRs function either as tumor promoters or suppressors in OSCC and play a pivotal role in various cellular processes such as cell growth, differentiation, migration, and cell death. Most importantly, altered expression of miRs correlates with clinicopathological variables and has diagnostic and prognostic value in OSCC [180].

2.4.2 Oncogenic MicroRNAs

Several miRs are significantly upregulated in OSCC. In a study on tongue squamous cell carcinoma (TSCC), among a panel of 156 miRNAs examined, 24 miRs showed a threefold increase in expression [94]. Among them, miR-21, miR-31, miR-146a, miR-134, miR-184, miR-7, miR-127, and miR-518c-5p have been highlighted in the context of OSCC [81].

2.4.2.1 miR-21

miR-21 is one of the most frequently upregulated and researched oncogenic miRs in oral cancer. It downregulates several tumor suppressor genes (e.g., *PTEN*, *BCL-2*, *dickkopf-2 (DKK-2)*, etc.) and has been implicated in migration, invasion, proliferation, and apoptosis [147]. The predominantly high expression of miR-21 in stromal myofibroblasts correlated with poor prognosis in OSCC [147]. Recently, hypoxic environment was shown to stimulate the tumor cells to generate miR-21-rich exosomes which induced a pro-metastatic behavior in the normoxic cells, emphasizing progression of OSCC through exosome interactions [148]. miR-21 was also shown to enhance Snail and vimentin expression and reduced expression of E-cadherin [148]. Inhibiting miR-21 using anti-miR-21 oligonucleotides was shown to induce apoptosis and inhibited invasion and survival in cancer cell lines [149]. Overexpression of miR-21 was also identified among a signature panel of miRs in leukoplakias with risk of malignant transformation [150]. In a study on 60 TSCC specimens, miR-21 overexpression was shown to have a tendency toward poor prognosis [151]. It was also identified among a small panel of upregulated miRs in an integrated analysis and microarray expression profiling [152]. Advanced tumor stage, keratinization state, and high expression of miR-21 were shown as indicators of poor prognosis for oral cancer patients in a study on 17 OSCC tissue specimens [153]. In a study on

100 OSCC specimens, higher expression of miR-21 was related to perineural invasion and worse prognosis [154]. Expression of miR-21 was also shown to be linked to keratinization in tumors [153]. A strong repression of reversion-inducing cysteine-rich protein with Kazal motifs (RECK), an inhibitor of MMPs, was noticed in miR-21 cell lines [153, 155]. Recently, miR-21 was also used as a noninvasive biomarker to discriminate between TSCC and normal controls in oral cytology samples [25].

2.4.2.2 miR-31

The expression of miR-31, a frequently upregulated miR in OPMDs and OSCC, correlated with VEGF expression [81, 82]. miR-31 was shown to facilitate immortalization in OSCC cells in collaboration with *TERT* [81]. The functional effects of miR-31 are mediated via regulation of fibroblast growth factor (FGF-3) and Rho-A leading to proliferation and migration [83]. In a chemically induced carcinogenesis model, miR-31 emerged as the earliest detectable salivary miR [84]. Mechanistic studies also showed that miR-31 inhibited the expression of AT-rich interactive domain 1A (ARID1A), a tumor suppressor that inactivates Nanog/OCT4/Sox2 stemness factors as well as epithelial cell adhesion molecule (EpCAM) [82]. Tumors with high miR-31 and Nanog/OCT4/Sox2/EpCAM expression together with low expression of ARID1A exhibited the worst survival [82]. In a study on 20 saliva samples and 46 OPMD tissue specimens, miR-31 was found to be significantly upregulated. Based on available evidence, miR-31 may be a potential marker for detection of high-risk OPMD [181].

2.4.2.3 miR-146a

Exogenous expression of miR-146a has been shown to increase proliferation in many cell types [88]. In a meta-analysis, a polymorphism (rs2910164) in miR-146a was shown to increase HNSCC risk [182, 183]. miR-146a is upregulated by the NF-κB pathway following activation by Toll-like receptor (TLR), tumor necrosis factor α receptor (TNFR), interleukin 1β receptor (IL1R), and receptor activator of NF-κB (RANK) [88]. The by-product of this pathway NF-κB is critical in the development of OSCC. High expression of TLR4 causes upregulation of AKT phosphorylation and NF-κB activation and therefore increases tumor cell proliferation. The "miR-146a-NF-κB" loop is suspected to link inflammation with oral cancer [88].

2.4.2.4 miR-134

miR-134 is oncogenic in OSCC and works by influencing tumor suppressor protein WW domain-containing oxidoreductase (*WWOX*) that interacts with other binding partners to regulate apoptosis, proliferation, and cell signaling [131]. The cytogenetic locus 16q23.2 of *WWOX* is a fragile chromosomal region lost in a variety of cancers [131]. Reduction in *WWOX*-mRNA was also noticed in OSCC and leukoplakia [131–133]. Tumor induction in *WWOX* knockout mice provides evidence for the putative tumor suppressor role. High expression of miR-134 is an independent predictor of poor survival in OSCC [131]. Polymorphic variants (rs11545028) of WWOX have also been linked to increased susceptibility to oral cancer in a screening of WWOX variants in a large cohort study comprising 761 male patients with oral cancer and 1199 male cancer-free individuals [132]. In 23 leukoplakias, 35% cases demonstrated changes in WWOX including altered mRNA transcription and/or reduced Wwox protein expression [133]. The expression of WWOX also showed significant downregulation in 19 adenoid cystic carcinomas in comparison with 25 mucoepidermoid carcinomas [134]. In another report on salivary gland malignancies, 17 of 28 neoplasms (55%) showed reduction in WWOX RNA [135]. The status of WWOX may be also important for chemotherapeutic resistance to methotrexate. TSCC cell lines with relatively low amount of WWOX have displayed resistance to methotrexate and transiently overexpressed WWOX sensitized SCC cells to apoptosis [136].

2.4.2.5 miR-144

The upregulation of miR-144 was consistently identified among the 46 differentially expressed miR panels in a cohort of 29 OSCC specimens subjected to microarray study, and further validated on 61 OSCC specimens through RT-qPCR. miR-144 was shown to be significantly elevated in nodal invasion positive tumors. Functional pathway analysis identified the tumor suppressor *PTEN* as a target of miR-144 [54]. In a meta-analysis of microarray datasets from 28 tumor studies, miR-144 was identified as a putative oncogene [145]. In a report by Zhang et al., paired box gene 4 (PAX4) was shown as a driver of metastasis in epithelial tumors by decreasing the expression of miR-144, leading to metastasis and invasion through a disintegrin and metalloproteinase (ADAM) protein family members [146].

2.4.2.6 miR-184

miR-184 was identified among the small panel of upregulated microRNAs in a study involving microdissected cells from 4 TSCCs for RT-qPCR analysis and subsequent validation of miR-184 on a set of 20 TSCCs. Suppression of miR-184 by an inhibitor led to inhibition of cell proliferation indicating the potential role of this miR in the genesis of oral cancer. Furthermore, elevated levels of miR-184 before surgical excision of TSCC returned to normal following surgery [137]. More importantly, miR-184 was among a panel of miRs whose decreased expression could be used for predicting assessment of treatment outcome [138]. However, in contrast to several reports demonstrating the oncogenic role of miR-184, in a study by Manikandan et al. on 42 OSCC specimens, miR-184 was found to be downregulated in tumor specimens [139].

2.4.2.7 miR-7

miR-7 was identified as a potential oncogenic miR in many tumor models including OSCC [88]. miR-7 was found to regulate the IGF1R/IRS/PI3K/Akt signaling pathway in a TSCC cell line [89]. miR-7 was significantly upregulated in cancer-associated fibroblasts (CAF) as compared to paired normal fibroblasts. Overexpression of miR-7 in normal fibroblasts increased migration and invasion in cocultured malignant cells, whereas in CAF it led to downregulation of Ras association domain family member 2 (RASSF2) and decreased secretion of prostate apoptosis response-4 (PAR-4) indicating that miR-7 promotes tumor progression via the “miR-7-RASSF2-PAR-4” axis [90]. The elevation of miR-7 was also shown to contribute to regulation of the tumor suppressor RECK. The findings of Jung et al. provided additional evidence that miR-7 is a keratinization-associated miR that shows an inverse correlation with RECK expression [153]. In a study on 18 OSCCs (gingivo-buccal), 12 oral lichen planus (OLP), and 18 leukoplakias, miR-7 was consistently upregulated in OSCC [91]. Pathway analysis revealed the differential expression of genes involved in cell migration, apoptosis, and proliferation, the most disrupted pathways being the proteoglycan and PI3/Akt pathways [91]. Based on available evidence, miR-7 is among the panel of stromal RNAs that play a critical role in OSCC progression.

2.4.2.8 miR-127

miR-127 is another stroma-specific miR that shows increased expression in cancer tissue [127]. In a study on 51 OSCC and pharyngeal SCC specimens (20 OSCCs), it was shown that miR-127-3p was among the most significantly dysregulated miR panels, consisting of 21 miRs, in HPV-associated and normal OSCC [128]. miR-127 is intimately related to cell proliferation and senescence through upregulation of the oncogene *BCL-6* [128].

2.4.2.9 miR-518c-5p

In mice and cell line models of OSCC, miR-518c-5p was shown as a regulator of growth and metastasis [184]. Mice innoculated with miR-518c-5p clones developed tumors with lymph node and lung metastasis. Cell-based assays revealed that miR-518c-5p is a downstream target of the stromal cell-derived factor (SDF)-1/chemokine receptor CXCR4 (CXCR4) axis [184]. This finding assumes significance because cancer stem cells (CSCs) were also shown to express CXCR4, and the “SDF-1/CXCR4” axis is critical for metastasis mediated by oral CSCs [185]. Some groups have also shown an amplification of 19q13.4, the cytogenetic locus encompassing primate-specific microRNA gene cluster (C19MC) and miR-518c-5p, which are in close proximity. Amplification of this genomic locus was observed among salivary adenoid cystic carcinomas and neuro-ectodermal tumors [186, 187]. It is not clear if the same mechanism is involved in the overexpression of miR-518C-5p in oral cancer, and more clinical studies are needed.

2.4.3 MicroRNAs as Tumor Suppressors

MicroRNAs can act as potential tumor suppressors. Some tumor suppressor miRs include miR-200 family, miR-101, miR-26a/b, miR-29a, miR-27b, miR-137, miR-125a, miR-29a, miR-491-5p, miR-124, miR-125, miR-218, miR-99a, miR-375, etc. [88]. These miRs are typically downregulated in tumor tissues through hypermethylation.

2.4.3.1 miR-200 Family

The miR-200 family, miR-200a, miR-200b, miR-200c, miR-141, and miR-429, is found significantly downregulated in cells undergoing EMT. This miR family regulates E-cadherin repressors: zinc finger E-box binding homeobox 1 (ZEB-1) and zinc finger E-box binding homeobox 2 (ZEB-2) [21]. The expression of miR-200 family induces mesenchymal-epithelial transition (MET), highlighting their loss during EMT, and the downregulation of miR-200 family is essential for oral cancer progression. In a study on 66 OSCC, a strong downregulation was identified in OSCC tissues compared to matched controls [21]. Overexpression of miR-429 inhibits apoptosis and suppresses invasion in oral cancer [22].

2.4.3.2 miR-101

miR-101 is underexpressed in OSCC and shows an inverse correlation with ZEB-1 implicated in endowing cancer cells with proliferative and invasive capacity [17]. In a sample of 181 OSCC specimens, low miR-101 expression correlated with high rate of lymph node metastasis, and survival analysis on 40 OSCC patients revealed a poor prognosis in specimens with low miR-101 levels [17]. Bioinformatics analysis indicated that miR-101 is a target of ZEB1 [17]. Through a meta-analysis, loss of miR-101 was linked to worse overall survival in a variety of cancers [18, 19]. Genomic loss of miR-101 was linked to an overexpression of histone methyltransferase EZH2 in cancer, which is a regulator of survival and metastasis through epigenetic silencing [20].

2.4.3.3 miR-26a/b

Loss of miR-26a/b is associated with cancer cell migration and invasion through its target genes: transmembrane protein 184B (*TMEM184B*), E-cadherin, and EGF LAG seven-pass G-type receptor 1 (*CELSR1*) [24]. *TMEM184B* which codes for a transmembrane protein was the most downregulated genes among a panel of 14 gene candidates in miR-26a/b transfects [24]. Data from 36 OSCC specimens suggested overexpression of miR-26a/b in OSCC. The "miR-26a/b-*TMEM184B*" *axis* is a tumor suppressor axis. Silencing *TMEM184B* in cell lines led to reduced invasion and altered expression of genes in 23 pathways, and following pathway analysis significant correlation was identified with actin cytoskeleton genes [24]. In a study on 20 OSCCs, 20 OLP, and 20 oral leukoplakias, the expression of miR-26a was downregulated in leukoplakia and oral cancer tissue and upregulated in lichen planus, compared to 20 normal controls [33]. A polymorphism in miR-26a also correlated with the risk of OPMD. In another report by Jia et al., expression of miR-26a was downregulated in 76 TSCC specimens and was shown to increase the expression of the lncRNA MEG3, through reduction of expression of DNA methyltransferase 3B (DNMT3B) [33, 34].

2.4.3.4 miR-137

Promoter methylation of miR-137 was identified in many studies on OSCC and OPMDs [12, 13]. HNSCC tumors with promoter methylation of miR-137 correlated with poor overall survival (OS) when compared to unmethylated tumors [12]. The target of miR-137 "EZH2" acts as a switch from a proliferation state to a differentiation state [12]. In a study on 20 OLP, 12 OSCCs, and 10 controls, methylation status was highest in OSCC (58.3%), comparatively less in OLP (35%), and completely absent in healthy mucosa [13]. In a report on 99 oral rinse samples derived from HNSCC patients, methylation was identified in 21 oral rinse samples (22.2%) and only 3 (3%) of the 99 healthy controls [14]. Methylation was identified in 14 of 37 OSCC (37.8%) cases, and the odds ratio for miR-137 methylation in OSCC was >12 times than normal subjects [14]. Moreover, tumor tissue miR-137 methylation status was strongly associated with female gender and inversely with body mass index [14]. In a recent report on oral brush biopsy specimens, composed of highly categorized specimens, 11 OSCCs, 11 high-grade squamous intraepithelial lesions (HG-SIL), 9 low-grade SIL (LG-SIL), 9 OLP, and 8 controls, methylation was noticed in 100% OLP and 44.4% OSCC [15]. Ectopic expression of miR-137 results in expression of E-cadherin and inhibits N-cadherin and vimentin and Snail, participating in suppression of EMT [16]. Recently the tumor suppressor function of miR-137 was shown to occur through targeting specificity protein (SP1) zinc finger transcription factor, thereby promoting proliferation and colony formation [16]. In the tumorigenic oral cancer stem cell population, dysregulation of miR-137 was not found [127]. Methylation of miR-137 can serve as a potential signature in OSCC and as a significant prognostic marker [12].

2.4.3.5 miR-125a

miR-125a plays a role in the progression of OSCC by targeting the estrogen-related receptor alpha (*ESRRA*) a member of the nuclear receptor superfamily that regulates cancer cell migration and invasion whose downstream targets encompass genes in cell cycle, metastasis, and metabolism (*WNT11* (wingless-related murine mammary tumor virus integration site 11), *CCNE1* (cyclin E1), *OPN* (osteopontin), and *OPG* (osteoprotegerin)). ESRRA is upregulated in tissues with low miR-125a and high energy requirement. Overexpression of miR-125a in OSCC cells drastically reduced the level of ESRRA, decreased cell proliferation, and increased apoptosis [188]. Downregulation of miR-125a was identified in a study on 20 OSCC patients.

2.4.3.6 miR-491-5p

miR-491-5p participates in OSCC progression through its target G-protein-coupled receptor kinase-interacting protein 1 (GIT1), a scaffold protein associated with paxillin and capable of stimulating lamellipodia formation. The GIT1/paxillin complex regulates focal adhesion formation and cell migration. GIT1 increases expression of MMP-2/MMP-9 via EGFR/ERK1/2 signaling pathway. In a study on 33 OSCC specimens, miR-491-5p underexpression was noticed in 29 (88%) specimens [189]. Survival analysis on 189 patients revealed a correlation between low expression of miR-491-5p with poor survival and lymph node metastasis [189].

2.4.3.7 miR-29a

miR-29a is known to negatively inhibit the expression of matrix metalloproteinase-2 (MMP-2), involved in EMT and invasion [140, 190]. In a study on 50 OSCC specimens, downregulation of miR-29a was observed in 25 (50%) specimens [190]. In a comparative study of 17 nonmetastatic primary OSCCs and 20 metastatic lymph nodes, miR-29a was among a small panel of differentially expressed miRs that displayed a strong positive correlation with their DNA copy numbers [191]. The expression of miR-29a was also downregulated in leukoplakia and upregulated in lichen planus [33]. In a large screening study on genotypic variations in 451 OSCC patients (tobacco stratified analysis), variant allele homozygous genotypes at miR-29a were found to be increased [192]. In a Syrian hamster model of oral cancer, miR-29a was also shown among the panel of downregulated miRs [193]. In a study on 14 carcinomas in situ and 16 OSCC specimens, miR-29a was shown among a panel of 5 miRs with a potential as serum biomarkers [194].

2.4.3.8 miR-124

Reduced miR-124 was shown to upregulate integrin beta-1 (ITGB1) to promote invasion and metastasis [195]. miR-124 was shown to reduce the expression of sphingosine kinase 1 which directs the cell toward an apoptosis program [196]. A 4.59-fold decrease was observed for miR-124 in OSCC specimens than normal controls [196]. In the nasopharyngeal carcinoma model, miR-124 was shown to exert its effects by suppressing the expression of calpain small subunit 1 (Capn4), and the miR-124/capn axis decreased the levels of β-catenin, cyclin D1, and c-Myc [197].

2.4.3.9 miR-218

miR-218, a target of mTOR component Rictor that inhibits AKT phosphorylation, was found to be silenced in OSCC [40–44]. In patients with positive nodal involvement, low expression of miR-218 was shown to increase risk of distant metastasis [44]. In a report on 115 OSCC specimens, low miR-218 level was associated with HPV16/18 (E6)-positive tumors as well as shorter overall survival (OS) and recurrence-free survival (RFS). HPV16/18 infection was negatively associated with miR-218 expression and positively associated with paxillin (PXN) expression. Paxillin, an adaptor protein regulating cell motility through cytoskeleton assembly, was reported to promote tumor progression of OSCC by modifying the levels of miR-218. Survival analysis demonstrated that patients with low-miR-218 tumors or high-PXN tumors exhibited shorter OS and RFS than patients with high-miR-218 tumors or low-PXN tumors. HPV-infected patients with low-miR-218 and high-PXN tumors and both combinations exhibited the worst OS and RFS [43]. Thus miR-218 is an important piece of evidence underlying HPV related OSCC. Methylation was proposed as the basis of miR-218 silencing [44]. A molecular link between miR-218 and PPP2R5A/Wnt signaling pathway has been recently proposed and ectopic expression of miR-218 was shown to induce survival and resistance to cisplatin [45].

2.4.3.10 miR-99 Family

In a meta-analysis of miRNA data in HNSCC, miR-99 family consistently showed downregulation [198]. Its target genes include mTOR, homeobox A1 (HOXA1), CTD small phosphatase-like (CTDSPL), N-myristoyltransferase 1 (NMT1), transmembrane protein 30A (TMEM30A), and SWI/SNF-related matrix-associated actin-dependent regulator of chromatin subfamily A member 5 (SMARCA5) [198–200]. The downregulation of HOX2 decreases expression of *BCL-2* leading to reduced proliferation and cell migration, as well as enhanced apoptosis [199]. miR-99 is also significantly downregulated in OSCC tissues and cell lines [200]. It functions as a tumor metastasis inhibitor, and downregulation was identified in patients demonstrating lympho-vascular invasion. In this study, 28 (70%) of 40 OSCCs demonstrated a >2-fold decrease in miR-99a [200]. In cell lines, miR-99a knockdown resulted in cell proliferation, migration, and invasion [200]. In a study by Yan et al. on 25 OSCC tissue specimens, significant downregulation of miR-99a was identified, and cell line modeling established its role in OSCC development [201].

2.4.3.11 miR-375

miR-375 strongly repressed in OSCC and OLP was shown to act on the Kruppel-like family transcription factor 5 (KLF5) [26, 27]. miR-375 was shown to regulate expression of MYC via repression of cancerous inhibitor of protein phosphatase 2A (CIP2A) coding sequence [27]. This miR-375 may be another piece of evidence linking immune-mediated, inflammatory lesions like OLP with oral cancer [26]. More recently in a study by Yadong et al. on 40 OSCC clinical specimens, miR-375 was strongly downregulated, while its target gene Solute carrier family seven number 11 (SLC7A11) was upregulated [28]. In a report by Jung et al. on TSCC cell lines, the chemotherapeutic drugs doxorubicin, 5-fluorouracil, trichostatin A, and etoposide increased the expression of miR-375 [29]. In a pilot study on 39 oral cytology samples (19 TSCCs vs 20 normal subjects), miR-375 was able to discriminate TSCC and normal controls, serving as a potential noninvasive diagnostic marker [25].

2.4.3.12 miR-204

miR-204 was shown to be frequently downregulated in numerous cancer models [79]. miR-204 binds to Slug and Sox4, suppressing their expression [79]. Downregulation of miR-204 increased oral cancer stemness and lymph node involvement in animal models. Survival analysis using the signature (miR-204^{low}Slug^{high}Sox4^{high}) on a sample of 30 noncancerous tissue and 30 tumor specimens and 30 with lymph node involvement showed poor prognosis, which indicates it as a putative signature for cancer progression [79]. Knockdown of miR-204 resulted in higher incidence of lymph node metastasis in nude mice model [79]. miR-204-5p was also shown to suppress CXCR4 expression [80].

Besides the abovementioned bona fide onco- and tumor suppressor microRNA, there are several others implicated in OSCC. The use of a specific miR or a panel of miRs as diagnostic biomarker signatures of OSCC has been suggested in numerous recent studies. miRs are central players and reliable markers of progression of OPMD and OSCC. The differential expression of miRs seen in saliva of patients with OPMD and OSCC at different stages in progression responded to treatment underscoring their theranostic significance. Thus miRs may function as oncogenes or tumor suppressors and can be used as diagnostic and prognostic markers [41]. Direct targeting of genes through gene therapy may prove challenging, and miRs may be more suitable therapeutic targets.

2.4.4 Piwi-Interacting RNA

Piwi-interacting RNAs (piRNAs) are 26–31 nucleotides long transcribed from repetitive sequences in the genome. The single-stranded piRNA precursors bind to Piwi proteins of the Argonaute family and guide them to endogenous transposable elements, resulting in genetic instability [202].

There are very few studies on piRNAs in oral cancer. Analysis of the expression pattern for a 41-member Piwi panel revealed differences between HPV-positive and HPV-negative HNSCC cases. Of the 11 piRNAs that showed significant overexpression in HPV-positive cases, 5 (piR-35953, piR-36984, piR-39592, piR-36715, and piR-30506) correlated with unfavorable patient survival rates. Recently, a panel of 13 piRNAs was identified in OSCC related to smoking. A positive correlation was observed between the expression of the piRNAs NONHSAT123636 and NONHSAT113708 with tumor stage, whereas NONHSAT067200 was found to be a useful predictor of survival rate. PIWIL1 expression correlated with genomic changes, including in the Tp53 gene [203, 204].

2.4.5 Circular RNAs

Circular RNAs (circRNAs) are circles of ncRNAs whose 5’ and 3’ ends are linked to form a covalently closed loop. They are transcribed similar to mRNAs but differ from them in the processing steps. circRNAs are reported to regulate gene expression by posttranscriptional control, miRNA sponging, or translational repression [16]. The miRNA sponging activity of the circRNAs can be used as a therapeutic strategy to silence overexpressed miRs. Using microarrays, Chen et al. identified many circRNAs that are differentially expressed between OSCC tissue and paired noncancerous matched tissue. In particular, expression of circRNA_100290 that was co-upregulated with CDK6 correlated with proliferation of OSCC cells. Knockdown and luciferase reporter assays revealed that circRNA_100290 regulated CDK6 expression through sponging miR-29b family members [205]

2.4.6 Long Noncoding RNA: Novel and Undisputable Players

Over the last few years, the role of miR in OSCC has been elaborated, but only limited evidence is available on the role of lncRNAs in OSCC. lncRNAs can act as molecular signals, tethers, and decoys to liberate DNA-binding proteins or through antagonism against miRs, as guides recruiting proteins to DNA or through exertion of chromatin looping for transcription enhancement, and as scaffolds to bring proteins into close proximity. They work at all levels of gene modulation, be it epigenetic, transcriptional, or translational, playing critical roles in basic cellular processes like proliferation, differentiation,

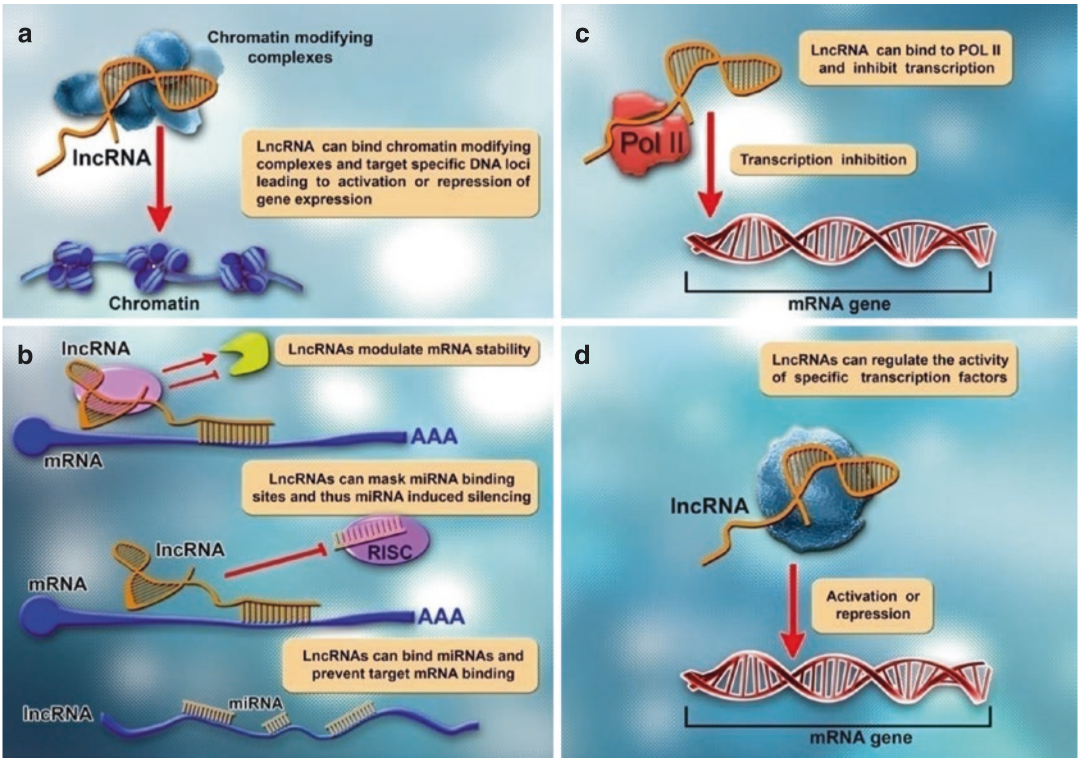

Fig. 2.3 The multi-faceted actions of lncRNAs. (**a**) lncRNAs can bind to chromatin modifying complexes to target specific DNA loci and up/downregulate gene expression. (**b**) lncRNAs can influence translation by (1) modulating mRNA stability, (2) directly binding to the mRNA thereby masking the miR binding site and miR-induced silencing or (3) bind to miRs preventing miR binding to target mRNA (**c**) lncRNAs can inhibit transcription by interacting with RNA pol II; and (**d**) lncRNAs interfere with transcription by interacting with transcription factors. Reprinted with permission from Irimie et al. A Looking-Glass of Non-coding RNAs in oral cancer. Int J Mol Sci. 2017; 18. pii: E2620

apoptosis, and metastasis, which are all pivotal to cancer progression (Fig. 2.3) [206]. In OSCC, the most frequently upregulated lncRNAs include HOTAIR, FOXCUT, MALAT1, UCA1, TUG1, CCAT2, FTH1P3, H19, and HIFCAR/MIRHG, while the downregulated ones include MEG-3. lncRNAs may also act as intermediates in the genesis of HNSCC due to HPV oncoproteins “E5, E6, and E7” and may be potential therapeutic targets for prevention of HPV-HNSCC [117]. About 140 lncRNA transcripts were differentially expressed between HPV-positive and HPV-negative tumors, and 30 lncRNA transcripts were differentially expressed between *TP53*-mutated and *TP53* wild-type tumors [207]. lncRNAs are able to generate lncRNA-binding protein complexes that modulate a large number of genes.

Comparison of the expression levels of 3054 probe sets for lncRNAs between 167 OSCCs and 45 healthy oral mucosae revealed differential expression of 658 lncRNA transcripts with 36 of them (39 probe sets) showing more than a twofold change [208]. Further validation of the top differentially expressed lncRNAs identified three lncRNAs with the highest fold change (LOC441178, HCG22, and C5orf66-AS1). Using the functional annotation algorithm from ncFANs followed by real-time PCR validation, Gao et al. [209] identified eight differentially expressed lncRNAs in TSCCs. While Lnc-PPP2R4-5, lnc-SPRR2D-1, lnc-MAN1A2-1, lnc-FAM46A-1, lnc-MBL2-4:1, and lnc-MBL2-4:3 were upregulated, lnc-AL355149.1-1 and lnc-STXBP5-1 were downregulated in the microdissected TSCC tissues. Furthermore, lncRNAs were associated with T stage and nodal status of TSCC.

2.4.6.1 HOX Antisense Intergenic RNA (HOTAIR)

According to a recent meta-analysis, the HOX transcript antisense RNA (HOTAIR) was suggested as a potential marker for advanced tumor stage and prognosis [118]. In the laryngeal squamous cell carcinoma model, HOTAIR was also shown as a driver of *PTEN* methylation [119]. HOTAIR is expressed from the homeobox C gene (HOXC) locus and is capable of reprogramming chromatin organization and can simultaneously bind with PRC-2 to enhance H3K27 trimethylation and to LSD1-CoREST-REST complex for H3K4 demethylation [120]. The expression profile and functional role of HOTAIR in OSCC were dissected only recently. HOTAIR was among a small panel of lncRNA intermediates to show expression difference in HPV-positive and HPV-negative HNSCC [117]. Wu et al. identified the expression of HOTAIR in 45 of 50 OSCC (90%) specimens [121]. The expression in the para-cancerous tissues was significantly less than cancerous tissue, correlating closely with tumor size and clinical stage. It was suggested as a molecular marker for OSCC diagnosis, and a possible relation to prognosis was hypothesized [121]. Knockdown of HOTAIR in OSCC cells by siRNA interference approach decreased cell proliferation and colony formation, increased cell invasion and migration, and induced apoptosis in vitro. A negative correlation between HOTAIR levels and E-cadherin levels was also found in OSCC tissues and cell lines, and HOTAIR contributed to the regulation of E-cadherin through binding to EZH2 and H3K27me3 with the E-cadherin promoter [121]. HOTAIR acts as a molecular scaffold to link and target the histone modification complexes PRC2 and LSD1 and then reprograms chromatin states by coupling histone H3K27 methylation and H3K4 demethylation for epigenetic gene silencing to promote cancer metastasis. In another study by Wu et al., HOTAIR expression increased in OSCC compared with non-tumor tissue and was also associated with metastasis, stage, and histological differentiation [122]. Overexpression of HOTAIR indicated poor OS and DFS in OSCC patients indicating a poor prognosis.

2.4.6.2 FOXC1 Upstream Transcript, Noncoding (*FOXCUT*)

The Fork head box C1 (FOXC1) gene is overexpressed in numerous malignant tumors and has been functionally correlated with tumor progression [55–57]. FOXC1 upstream transcript (FOXCUT) was overexpressed in 23 OSCC patients, as was the adjacent FOXC1 gene. In OSCC cell lines, downregulation of either FOXC1 or FOXCUT via a siRNA approach could inhibit cell proliferation and cell migration in vitro and was accompanied with a reduction of MMP-2, MMP-7, MMP-9, and VEGF-A [55]. It was concluded that FOXC1 may be co-amplified with FOXCUT in OSCC through the formation of “lncRNA-mRNA pair,” and both together may be functionally involved in tumor progression [55]. This lncRNA-mRNA pair was validated as a nodal point of tumor progression in several closely related cancer models including OSCC.

2.4.6.3 Metastasis-Associated Lung Adenocarcinoma Transcript-1 (*MALAT1*)

The lncRNA metastasis-associated lung adenocarcinoma transcript-1 (MALAT1) has been reported to play an oncogenic role in OSCC, particularly in the event of metastasis. In a report by Chang et al., MALAT1 was upregulated in OSCC cell lines. Bioinformatics screening identified miR-125b as its direct target, and there was a negative correlation between MALAT1 and miR-125b [104]. STAT3 was predicted as the binding target of miR-125b [104]. Overexpression of MALAT1 was able to suppress the tumor inhibitory effect of miR-125b mimics via upregulation of STAT3. Downregulating MALAT1 inhibited OSCC tumor growth, while upregulating MALAT1 promoted OSCC development in vivo, via the miR-125b/STAT3 axis. Mechanistic studies in OSCC have shown that MALAT1 functions as a competing endogenous RNA (ceRNA) to modulate STAT3 expression by absorbing miR-125b [104]. In another study by Zhang et al., MALAT1 was shown to be specifically upregulated in TSCC cell lines, and overexpression promoted TSCC cell growth by targeting miR-124. Knockdown of MALAT1 suppressed growth and invasion of human TSCC cells and inhibited metastasis both in vitro and in vivo. miR-124-dependent jagged1 (JAG1) regulation was required for MALAT1-induced TSCC cell growth [105]. Zhang et al. demonstrated that MALAT1 inhibited TSCC cell growth and metastasis through miR-124-dependent JAG1 regulation [105]. In another recent report by Liang et al. through a relatively simple upregulation-based plasmid transfection study in TSCC, MALAT1 was linked to cell migration, metastasis, and apoptosis through the WNT/β-catenin pathway [106]. In a previous report by Zhou et al. [107], an overexpression of MALAT1 was identified in OSCC tissues as compared to normal oral mucosa. MALAT1 served as a new prognostic factor in OSCC patients through survival analysis, where patients with high expression of MALAT1 were shown to have low survival [107]. MALAT1 knockdown by siRNA approach in OSCC cell lines provided evidence that MALAT1 is essential for the maintenance of EMT-mediated cell migration and invasion. MALAT1 knockdown significantly suppressed N-cadherin and vimentin expression but induced E-cadherin expression in vitro. This was associated with reduced nuclear and cytoplasmic expression levels of β-catenin and NF-κB [107]. Targeting MALAT1 in a xenograft tumor model suppressed TSCCA cell-induced xenograft tumor growth in vivo. These findings have provided mechanistic insights into the role of MALAT1 in regulating OSCC metastasis, suggesting MALAT1 also as an important prognostic factor and therapeutic target [107]. Another group has shown the negative regulation of MALAT1 and small proline-rich proteins (SPRR1B, SPRR2A, and SPRR2E) and also correlated with lymph node metastasis [108].

2.4.6.4 Urothelial Carcinoma-Associated 1 (*UCA 1*)

The lncRNA urothelial carcinoma-associated 1 (UCA1) dysregulated in pancreatic, breast, and lung cancer was found to be aberrantly upregulated in TSCC tissues associated with lymph node metastasis and higher TNM stage. UCA1 silencing suppressed proliferation and metastasis and induced apoptosis of OSCC cell lines both in vitro and in vivo [159]. UCA1 increased β-catenin expression with consequent increased cell proliferation, cell migration, and cell invasion. Their work revealed the importance of lncRNA UCA1-β-catenin-WNT signaling pathway regulatory network in the genesis of OSCC.

2.4.6.5 Taurine Upregulated Gene 1 (*TUG1*)

Taurine upregulated gene 1 (TUG1) has been investigated only recently in OSCC development [160]. Liang et al. have shown that TUG1 was upregulated both in OSCC tissues and cell lines. Higher tissue expression level of TUG1 significantly correlated with TNM stage, lymph node metastasis, and tumor grade in OSCC patients. Knockdown of TUG1 by an siRNA approach suppressed cell growth, cell proliferation, and cell invasion in OSCC cell lines associated with significant downregulation of β-catenin, cyclin D1, and c-MYC. Wnt/β-catenin pathway activator (LiCl) reversed the TUG1 knockdown effect on cell proliferation, cell invasion, and cell apoptosis in the cell lines. TUG1 enhances cell growth, proliferation, and invasion and also reduces apoptosis of OSCC through Wnt/β-catenin pathway targeting [160]. In another recent study by Li et al., TUG1 was concluded as an oncogenic RNA as cell proliferation was significantly inhibited upon its knockdown in cell lines and overexpression was noticed in 27 TSCCs as compared to matched controls [161].

2.4.6.6 Maternally Expressed Gene 3 (MEG3)

In a report by Jia et al., *MEG3* gene expression was strongly downregulated in 76 TSCCs compared to its matched nonmalignant tissues, and low expression levels of both MEG3 and miR-26a combined emerged as an independent prognostic factor for poor clinical outcome in TSCC patients [34]. Survival analysis demonstrated that patients with high expression of MEG3 survived longer than patients with lower expression. The survival rate of patients with low expression of miR-26a and MEG3 combined was shorter than patients with high expression of miR-26a or MEG3 [34]. Furthermore, overexpression of miR-26a or MEG3 in OSCC cell lines inhibited cell proliferation and cell cycle progression and promoted cell apoptosis. MEG3 was also shown as a potential regulator of TGF-β pathway genes by binding to their distal regulatory sequences, through the formation of RNA-DNA triplex structures [129]. Recently, Liu et al. demonstrated that MEG3 can inhibit the growth and metastasis of OSCC by negatively regulating the WNT/β-catenin signaling pathway [130].

2.4.6.7 Long Noncoding RNA Colon Cancer-Associated Transcripts 1 and 2 (CCAT1 and *CCAT2*)

Colon cancer-associated transcript 1 (CCAT1), a lncRNA, mapped to chromosome 8q24 close to the oncogene c-myc, was shown to be differentially expressed in several types of cancers, including colon cancer, gastric cancer, gall bladder cancer, and hepatocellular carcinoma. Recently, Arunkumar et al. [68] analyzed the expression of CCAT1, c-Myc, and the miRNAs miR-155-5p, let7b-5p, miR-490-3p, and miR-218-5p sponged by CCAT1 in 60 oral tumor and 8 normal tissue samples by RT-qPCR. OSCC cases overexpressing CCAT1 had poor therapeutic outcome. Furthermore, CCAT1 overexpression correlated significantly with c-Myc expression and sponging of miR-155-5p and let7b-5p.

CCAT2 was first identified in colon cancer patients, where it was shown as a WNT downstream target. More recently it was identified as a potential oncogenic lncRNA in OSCC [69]. CCAT2 upregulates MYC, miR-17-5p, and miR-20a [69, 70]. Based on a meta-analysis [71, 72], CCAT2 was suggested as a potential marker for lymph node metastasis and distant metastasis, associated with poor clinical outcome [71]. In a study on 86 OSCC specimens, CCAT2 levels strongly correlated with tumor stage, and CCAT2 expression was significantly higher at stage III/IV than stage I/II [73]. CCAT2 expression level was also higher in poorly differentiated relative to highly differentiated OSCC. In another comparatively larger cohort of 102 OSCC patients, CCAT2 was shown as a prognostic biomarker [74]. In a similar recent report by Ma et al. on 62 OSCC specimens, a higher expression also correlated with poor differentiation, higher T stage, and clinical stage, and survival analysis demonstrated CCAT2 as a prognostic biomarker in OSCC [70]. Through pathway analysis, a positive relationship between CCAT2 and WNT/β-catenin pathway activation was identified [70].

2.4.6.8 *H19*: Imprinted Maternally Expressed Transcript

The lncRNA H19 is recognized to alter genome-wide DNA methylation. In a recent meta-analysis, polymorphisms in H19 were shown to be linked to cancer susceptibility, and protective roles for certain alleles were observed [98]. Also, some data is available on the association of H19 in OSCC metastasis and progression [99]. Recently, in a sample of 123 TSCC [99], correlation was found between H19 and EZH2 expression [99, 100]. H19 and EZH2 were upregulated in TSCC tissues compared to matched normal tissues and significantly correlated with WHO grade, lymph node metastasis, and poor prognosis through the survival plots [99]. Through a H19 targeted lentivirus approach, the roles of H19 in cell proliferation, apoptosis, and invasion were deciphered. H19 silencing attenuated cell proliferation, apoptosis, and invasion in vitro. H19 knockdown inhibited activation of β-catenin/GSK-3β/cyclin D1/c-myc, upregulated E-cadherin and zonula occludens-1 (ZO-1), and inhibited N-cadherin, vimentin, Snail1, Twist1, and ZEB1 [99]. Silencing H19 also inhibited tumor progression and lung metastasis in vivo clearly suggesting its role in oral cancer metastasis to the lung [99]. H19 was shown to promote TSCC progression through association with EZH2 and affects downstream β-catenin/GSK3β/EMT signaling, suggesting H19 inhibition as a potential therapeutic target for TSCC [99]. H19 was proposed as a lncRNA in tumor metastasis and in the EMT/MET decision [101]. Downregulation of H19 significantly decreased the expression of β-catenin, EZH2, cyclin D1, c-Myc, and the mesenchymal genes N-cadherin and vimentin, while increasing E-cadherin and ZO-1 expression levels [99]. H19 was shown to act on genome-wide methylation through inhibition of S-adenosylhomocysteine hydrolase (SAHH) that hydrolyses S-adenosylhomocysteine. H19 knockdown activates SAHH which causes DNMT3B-mediated methylation of a gene subset [102]. More recently, the drug metformin was also proposed to act through the H19/SAHH axis and in the future may evolve as a possible epigenetically targeted drug treatment for cancer [103].

2.4.6.9 Ferritin Heavy Chain 1 Pseudogene 3 *(FTH1P3)*

The lncRNA ferritin heavy chain 1 pseudogene 3 (FTH1P3) can act as a ceRNA during tumorigenesis [23]. FTH1P3is overexpressed in OSCC and correlates with low survival rate of OSCC patients [23]. Ectopic expression of FTH1P3 also induced cell proliferation and colony formation in OSCC cell lines. Mechanistic studies have shown that FTH1P3 is a ceRNA, becoming a sponge for miR-224-5p, thereby modulating the expression of frizzled 5. Both FTH1P3 and fizzled 5 were upregulated in OSCC cell lines and tissue specimens, and overexpression of fizzled 5 functions as an oncogene in OSCC scene. Existing data demonstrates that FTH1P3 facilitates OSCC progression by acting as a molecular sponge for miR-224-5p to modulate frizzled 5 expression [23].

2.4.6.10 MIR31 Host Gene (*MIR31HG/HIFCA*R)

MIR31 host gene (MIR31HG/HIFCAR) lncRNA was shown to play a role in myoblast differentiation and senescence though its downstream molecule p16 (INK4A) [210–212]. The expression of LncHIFCAR/MIR31HG was found to be upregulated in a wide range of malignant tumors including OSCC [85]. Clinicopathological data from 42 OSCC specimens indicated substantial upregulation of LncHIFCAR which correlated with age and advanced tumor grade and was significantly associated with poor clinical outcomes underscoring its potential as an independent prognostic predictor. Patients with high LncHIFCAR expression had a significantly worse OS and recurrence-free survival (RES) than those with low LncHIFCAR expression. Higher expression of LncHIFCAR was identified as an independent prognostic factor for RFS. Overexpression and knockdown studies of LncHIFCAR revealed that it induces a pseudo-hypoxic gene signature, and its knockdown impaired hypoxia-induced HIF-1α transactivation, sphere-forming ability, metabolic shift, and metastatic potential in vitro and in vivo. Mechanistically, LncHIFCAR forms a complex with HIF-1α via direct binding and facilitates the recruitment of HIF-1α and p300 cofactor to the target gene promoters [85].

The ncRNAs have emerged as promising biomarkers for diagnosis and prognosis of OSCC and as potential therapeutic targets. Given their small size and stability, they are less susceptible to degradation by RNases compared to mRNAs. Their key roles in OSCC development and in the acquisition of cancer hallmarks have been comprehensively reviewed by Irimie et al. [86].

2.4.7 Oncogenic Signaling Pathways

Successive genetic and epigenetic changes impact a number of cellular signaling pathways that regulate cell growth, differentiation, motility, cell death, and cell fate with loss of homeostatic control eventually leading to the transformation of a normal cell to a malignant tumor. Cellular signaling pathways are complex interconnected networks comprising growth factors, receptors, cytoplasmic proteins, kinases, and transcription factors that transduce signals to regulate a plethora of diverse cellular processes. In particular, altered expression of oncogenic kinases and transcription factors play a significant role in dysregulated signaling in cancer [213].

Changes in the expression of nuclear transcription factors, namely, c-myc, c-fos, c-jun, and ets-1, are common events during the development and progression of OSCC. Amplification and overexpression of c-myc that promotes cell proliferation and inhibits apoptosis has been observed in 10–40% of human OSCC. Upregulation of ets-1 was generally found to significantly correlate with the extent of invasion and metastasis. In contrast to c-myc and ets-1, the expression of c-fos was found to be high in normal oral mucosa and gradually decreased during the advanced stages of OSCC. Constitutive activation of Stat-3, a signaling molecule involved in the Jak/Stat pathway, has been proposed to be an early event in tobacco chewing-mediated oral carcinogenesis [214].

Numerous oncogenic signaling circuits including TGF-β, NF-κB, Wingless-type 1/β-catenin pathway (WNT/β-catenin), PI3K/Akt, and Janus kinase/signal transducer and activator of transcription (JAK/STAT) pathways were found to be dysregulated during OSCC progression (Fig. 2.4). Disruption in TGF-β1-induced Smad signaling due to overexpression of Smad7 and downregulation of TGFβRII, Smad-2, Smad-3, and Smad-4 have been documented in OSCC. Mutations in the runt-related transcription factor 3 (RUNX 3), an important component of TGF-β, have also been detected in OSCC. TGF-β plays a dual role in OSCC progression by functioning as an oncosuppressor during the early stages and as a tumor promoter during the later stages by increasing the affinity of transformed oral epithelial cells toward lymphatic vessels [215].

Aberrant NF-κB signaling due to overexpression of p50 and p65 subunits and IKKβ and reduced IκB expression is a characteristic finding in oral tumors. Overexpression of NF-κB seen in precancerous stages was sustained throughout carcinogenic progression [216]. In a resting cell, NF-κB is present in the cytoplasm sequestered by inhibitor of κB (IκB). Activation of NF-κB occurs via phosphorylation-induced degradation of IκBs. Various stimuli including tobacco and betel nut ingredients cause activation of NF-κB with consequent nuclear translocation and binding to distinct kappa binding sites on DNA. NF-κB is a transcription factor that regulates the expression of a myriad of genes involved in cancer hallmarks including angiogenesis (e.g., VEGF), apoptosis (Bcl-2), cell proliferation (e.g., cyclin D1), inflammation (IL-8), invasion (MMP), etc. Accumulation of NF-κB is an early event in HNSCC even during the epithelial hyperplasia stage, and accumulation swiftly increases with increasing tumor grade [64]. Abnormal expression of this molecule was associated with resistance to radiotherapy and chemotherapy [64]. Downregulation of NF-KappaB-interacting lncRNA (NKILA) significantly correlated with tumor metastasis and poor patient prognosis in TSCC. Overexpression of NKILA inhibited the phosphorylation of IκBα and NF-κB activation as well as EMT, migration, and invasion. Furthermore, NKILA inhibited lung metastasis of NOD/SCID mice with TSCC tumors [217].

Activation of the canonical Wnt/β-catenin signaling pathway has been frequently reported in OSCCs. The components of the canonical Wnt pathway, such as Wnt-3, β-catenin, and cyclin D1, were found to be potentially involved in the progression of dysplasia in oral leukoplakia, a precancerous lesion. Frequent overexpression of Wnt and Fz with mutations of APC, β-catenin, and axin 1 genes and cytoplasmic accumulation of β-catenin have been demonstrated in OSCC. Absence of membrane-bound β-catenin with cytoplasmic localization of the protein has been a consistent finding in oral dysplasia and OSCC [218, 219]. Tsuchiya et al. [220] reported an increase in the expression of cytosolic β-catenin and APC in dysplastic and well-differentiated SCC compared to normal squamous epithelium. Ishida et al. [221] demonstrated that the nuclear localization of β-catenin and activation of its downstream target, cyclin D1, were associated with the malignant transition of oral leukoplakia to dysplasia. Inactivation of glycogen synthase kinase 3β (GSK-β), a component of the Wnt pathway, is an important event in OSCC and can be used as a marker of disease severity [222]. The expression of GSK-3β was significantly higher than GSK-3a. Furthermore, increased expression of the

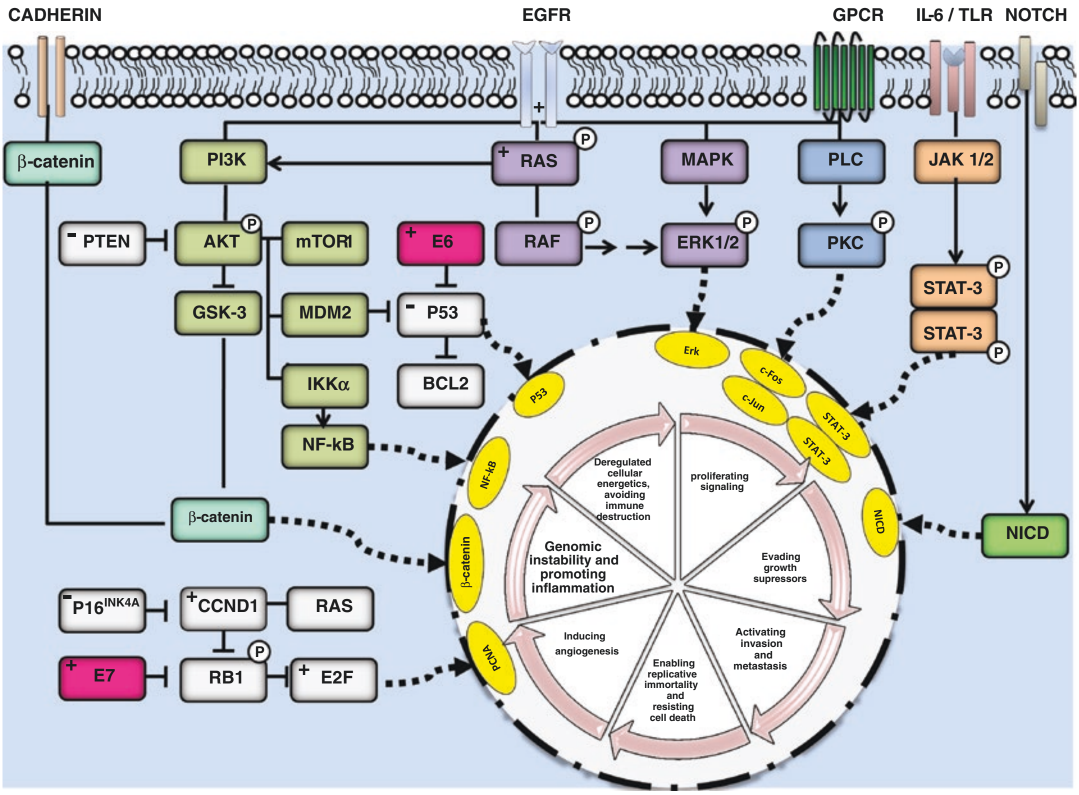

Fig. 2.4 Brief overview of signaling pathways in oral cancer. The tumor suppressor protein P53, referred to as the "guardian of the genome" is among the most frequently mutated genes in oral cancers. Mutational inactivation of P53 disrupts the P53-P21 axis with loss of cell cycle control and consequent enhanced proliferation. Low levels of P53 also leads to inactivation of apoptosis through BCL-2, induction of angiogenesis, impaired DNA repair and genomic instability. HPV protein-E6 is known to inactivate P53. Phosphorylation of retinoblastoma (RB) by CDKs releases E2F transcription factor that can trigger expression of genes (cyclins, proliferating cell nuclear antigen (PCNA)) involved in cell cycle progression. RB1 is also inactivated by HPV protein-E7. In oral cancer, a large number of signals come from the cell surface receptors like EGFR. EGFR activation can occur because of mutation, even in the absence of its ligand, which has several downstream signaling which includes the phosphatidylinositol-3-kinase/protein kinase B (PI3/AKT), Mitogen Activated Protein Kinase (MAPK), phospholipase/protein kinase C (PLC/PKC), and the stimuli from the IL-6 receptors transmit the signals through the Janus kinase/Signal Transducer and Activator of Transcription (JAK/STAT3) signaling. Both EGFR mutations, and mutated PIK3CA which codes for the catalytic subunit of PI3K, lead to phosphorylation of "AKT" which can lead to the activation of NF-kB through the "IKK/IkB" axis. AKT is a master regulator in oral cancer and has profound functions, including phosphorylation and inactivation of glycogen synthase kinase 3β (GSK3β) thereby enabling nuclear translocation of β-catenin and transactivation of cyclin D1 (CCND1), c-MYC, slug, vimentin, fibronectin. STATs phosphorylated by both tyrosine kinases (EGFR) and non-tyrosine kinases target several genes involved in tumor development and progression including CCND1 linked to proliferation and differentiation, BCL-2 linked to apoptosis, and c-MYC linked to oncogenesis. RAS activation at the cell membrane is another important molecule leading to activation of downstream MAPK and P13K/AKT pathways. ERK which is the product of the RAS and MAPK pathway has negative feedback loops. RAS messenger triggers expression of TNF-α and integrins, and inhibits expression of TNF-β. Mutations in adenomatosis polyposis coli (APC) can also result in low protein or truncated APC, impairing down regulation of β-catenin and leading to its stabilization. The free β-catenin accumulates in the cytoplasm and nucleus, associates with T-Cell factor (TCF) forming a potent transcription factor which mediates transcription of oncogenes c-MYC, CCND1, invasion and metastasis. NF-κB and β-Catenin are critical for epithelial mesenchymal transition (EMT) which forms the basis for cell migration, invasion and metastasis. A decrease in E-cadherin, which is considered as "the master switch" in metastasis is regulated by snail family of transcription factors (snail, snail2 or slug) and can lead to an increase in β-Catenin. Together the transcriptional factors propel cancer by contributing to the cancer hallmarks

inactive phosphorylated forms (pS21GSK-3α and pS9GSK3β) showed a positive correlation with cyclin D1 and p53.

Emerging recent data has provided insights into the paradoxical roles of JNKs (c-Jun N-terminal kinases), members of the mitogen-activated protein kinase (MAPK) family in oral cancer [223]. Substantial evidence has demonstrated the onco-suppressive role of JNK in oral cancer mediated by apoptosis induction via negative cross talk with oncogenic signaling pathways such as NF-κB and STAT-3. On the other hand, overwhelming evidence has also indicated the tumor-promoting role of JNK based on activation of invasion and metastasis.

The phosphatidylinositol 3-kinase (PI3K)/AKT signaling pathway is the most deregulated pathway in oral cancer [125]. The oncogenic effect of this pathway is mediated mainly by mTOR which complexes with G protein beta subunit-like (GβL), regulatory-associated protein of mTOR (Raptor), and proline-rich Akt substrate of 40 kDa (PRAS40) proteins to induce cell growth and proliferation. The mTOR inhibitor rapamycin and MEK1/2 inhibitor (PD901) alone or in combination inhibited primary tumor growth in a murine oral cancer model indicating MAPK and/or PI3K/mTOR as core signaling pathways in vivo [224]. Although mutations are commonly found in *PI3KA*, they are absent within *AKT1* and phosphatase and tensin homolog (*PTEN*) [37]. Aberrations in PI3K catalytic subunit alpha (*PIK3CA*) mapped to the cytogenetic location 3q26 are seen in advanced OSCC [38]. Gene amplification and somatic mutations mainly within the helical and kinase domains of PIK3CA seen in OSCC correlated with lymph node metastasis and tumor stage [37–39]. In cell lines showing mutations of *PIK3CA*, AKT was highly phosphorylated [38].

2.4.8 Cancer Hallmarks

Tumor cells are recognized to co-opt cellular signaling pathways and the surrounding microenvironment to effectively evade mechanisms that control proliferation, cell death, and migration. Tumor development is a multistep process and involves the acquisition of eight hallmark capabilities, namely, excessive cell proliferation, self-sufficiency in growth signals, insensitivity to anti-growth signals, resistance to apoptotic cell death, sustained angiogenesis, invasion and metastasis, reprogramming of energy metabolism, and evasion of immune destruction by the incipient cancer cells [225]. Some of the important hallmarks of cancer and key molecules that foster these traits in OSCC are discussed.

2.4.8.1 Dysregulated Cell Cycle

OSCCs display increased cell proliferation as revealed by overexpression of several proteins associated with cell cycle progression that comprises four distinct phases, G1, S, G2, and M. Cell cycle regulation is under the control of cyclins, cyclin-dependent kinases (CDKs), and CDK inhibitors. Perturbation of the cell cycle due to mitotic defects or loss of control at key checkpoints is a hallmark feature of malignant tumors. Overexpression of cyclins and CDKs or loss of CDK inhibitors can result in loss of control of the cell cycle leading to tumorigenesis.

Cyclin D1 (CCND1), a potent cell cycle regulator encoded by the gene CCND1 at 11q3 locus, plays a key role in cell proliferation, growth regulation, DNA repair, modulation of mitochondrial activity, and cell migration [109]. Cyclin D1 and pRB exist in equilibrium, where synthesis of cyclin D1 causes phosphorylation of RB and pRB inhibits cyclin D1 synthesis. Upregulation of cyclin D1 favors cell division by shortening G1 phase [110] and decreasing growth factor dependence. The main mechanism behind overexpression of cyclin D1 in head and neck SCC includes amplification of CCND1, chromosomal translocation, mutations, or polymorphisms (cis-acting regulatory elements) [111, 112]. Cyclin D1 is often overexpressed in OSCC and also verrucous carcinoma [113, 114]. Cyclin D1 upregulation is associated with large tumor size, poor prognosis, lymph node metastasis, and low survival status [115].

p21, a critical downstream mediator of wild-type p53 that regulates several cell cycle proteins including cyclin D1, inhibits CDKs and induces cell cycle arrest. Upregulation of both p21 and cyclin D1 has been reported in OSCCs. The members of the *INK4* family, *p16*^{INK4a}, *p15* ^{INK4b}, *p18*^{INK4c}, *and p19*^{INK4d}, antagonize the action of cyclin D1-CDK4 and cyclin D1-CDK6. CDK inhibition is therefore a potential strategy in cancer management. In oral epithelial dysplasia, the inactivation of *p16 (INK4a)* and *p14 (ARF) (INK4a/ARF)* was as high as 75–80% [75]. *p16* loss mainly occurs through methylation of the gene promoter or LOH [76]. Inactivation of *p16 (INK4a)* may be an early event in stepwise evolution of OSCC [77]. Two genes *p16 (p16*^{INK4A}*/ CDKN2A)* and *p14 (p14ARF)* both mapped to 9p21 have shown LOH and methylation in a majority of OSCC samples [78]. These two genes code for cell cycle proteins that inhibit CDK-4 and CDK-6, thus arresting the cell cycle in G1-S transition.

2.5 Spindle Assembly and Mitotic Defects

Besides structural chromosomal events like translocations, isochromosomes, and dicentrics, changes in chromosomal number are also seen in oral cancer [226]. The spindle assembly checkpoint (SAC) is a highly coordinated system essential for the equal segregation of chromosomes to the daughter cells during mitosis. In OSCC cell lines and primary head and neck tumors, the SAC protein Cdc20 was found to be overexpressed promoting premature anaphase and aneuploidy [227, 228]. In oral cancer, an incorrect number of chromosomes or aneuploidy is noticed in the daughter cells. Accumulation of important mitotic proteins, nuclear spindle-associated protein 1 (NUSAP1) and nuclear mitotic apparatus protein 1 (NuMA), which stabilize and bundle microtubules occurs in OSCC, leading to improper spindle assembly (Fig. 2.5a) [226, 229]. The defects were observed in centrosome number, size, and location. The incidence of centrosome abnormalities was more common in carcinoma than in dysplasia [227]. OSCC cells show lagging chromosomes at both metaphase and anaphase with difficulty to achieve a metaphasic alignment required for proper anaphasic chromosomal separation [226]. The main reason for delay is because of anaphase bridges (seen in tumor or viral-infected cells or in breakage syndromes and rare in healthy mammalian cells). The frequency of micronuclei (20–30%) in oral cancer samples is also high [226]. They may arise either from lagging anaphase chromosomes or anaphase bridges (Fig. 2.5b) [226]. Micronuclei represent a chromosome fragmentation event and may serve as a biomarker of oral cancer and progressing precancer. Key events in oral cancer progression include genetic alterations, centrosome defects, spindle checkpoint errors, and defects in kinetochore microtubule attachment.

2.6 Cell Survival and Apoptosis

Carcinogenesis results from an imbalance between the opposing pathways of cell survival and cell death. In cancer cells, cell survival mechanisms such as telomere maintenance and signaling pathways that promote cell survival such as NF-κB/PI3K, etc. are activated. Additionally, cancer cells evolve mechanisms to evade programmed cell death or apoptosis.

2.6.1 Cell Immortalization and Telomere Maintenance

Oral keratinocyte immortalization is a key event in OSCC mainly due to changes in telomeres found at chromosomal ends. Telomeres contain TTAGGG repeat sequences that are coated with shelterin complex. In the absence of telomerase, the enzyme responsible for telomere maintenance, telomere size reduces by 50–200 bases with every cell division ultimately leading to cell senescence [230, 231]. Malignant tumors frequently show a higher activity of this enzyme.

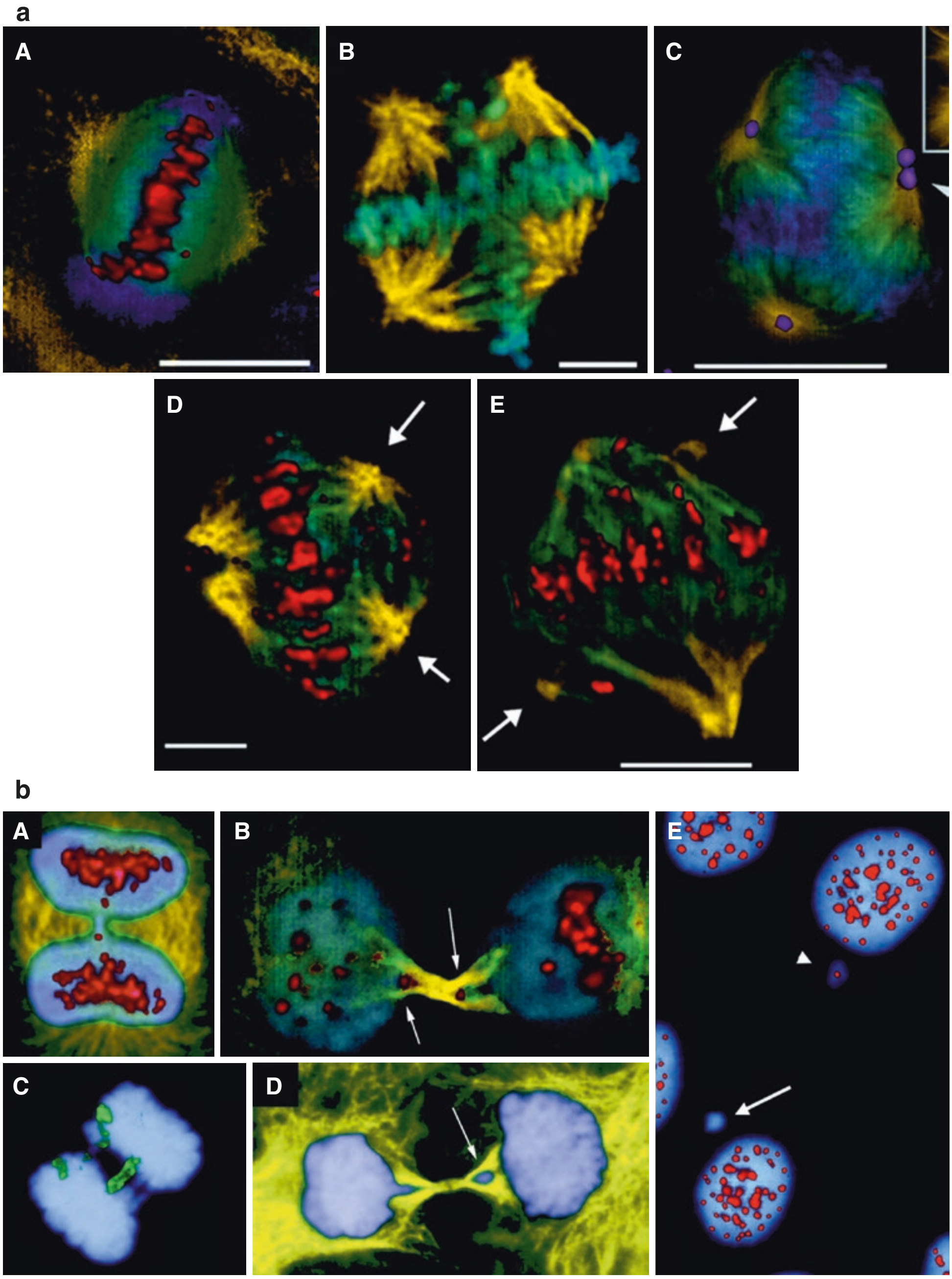

Fig. 2.5 Cytoskeleton defects in oral cancer. (**a**) Oral cancer cells are immunolabeled with Abs to tubulin (yellow), and kinetochores (red in A, D, and E) or NuMA (purple in C) and counterstained with the DNA dye, DAPI (blue). A normal metaphase from this culture is shown in (A), and multipolar metaphase spindles in B–E. (C, Inset). The anti-tubulin image alone of the pole marked with an arrowhead. (D and E) Arrows mark minor spindle poles. (Bars, 5 μm.) (**b**) Anaphase bridges containing centromeres and chromosome 11. Immunolabeling with Abs to tubulin (yellow), centromeres (red), and with DAPI (blue) and FISH with a chromosome 11 paint probe (green). (B) Arrows point to centromeres trapped in the forming midbody as these late telophase cells divide. (D) Arrow points to the trapped lagging chromosome excluded from the reforming nucleus of the cell on the right. (E) Some micronuclei are immunonegative for anti-centromere Abs. Arrow points to negative micronucleus, and arrowhead points to positive (Reprinted with permission from Saunders et al. Chromosomal instability and cytoskeletal defects in oral cancer cells. Proc Natl Acad Sci U S A. 2000; 97: 303–8. "Copyright (2000) National Academy of Sciences, U.S.A.")

Significant elevation in telomerase levels was found in oral cancer specimens, and telomerase activity may be used as an effective prognostic marker as its levels correspond with different grades [232]. Telomere shortening can also be used as a sensor to identify fields with cancerization potential. Telomere shortening recruits more telomerase, necessary for OSCC cell immortalization [233].

Shelterin is a complex of many proteins and the expression of these proteins may also increase in oral cancer [234]. E6 of HPV-16 enhances the catalytic power of telomerase. Other transcription factors (NF-κB, β-catenin, C-MYC) also regulate expression of *TERT* [46]. TERT joins with a subunit of NF-κB to regulate expression of TNF-α, IL-6, IL-8, and MMP-9 which induce epithelial-mesenchymal transition and metastasis [46]. Some studies have also identified mutations in the promoter of *TERT* [46]. Telomerase activation may be the outcome of mutations in a promoter, gene amplification, and epigenetic events [46]. Genetic studies in OSCC have identified amplification of chromosomal arm “5p” common to OSCC, which encompasses the *TERT* gene [46]. Studies have also identified circulating *TERT*-mRNA as biomarker to predict clinical outcome; higher levels correlate with a malignant phenotype showing high rate of metastasis and a low response to treatment. In the future TERT may serve as a potential saliva and blood biomarker for OSCC [46].

2.6.2 Apoptosis

BCL-2 was the first anti-death gene to be discovered [156]. It was first identified in the lymphoid malignancy, Burkitt’s lymphoma. This gene was mapped to the cytogenetic locus 18q21. Members of the BCL-2 protein family regulate cell death programs such as apoptosis, necrosis, and autophagy. The BCL-2 family includes both anti-apoptotic (BCL-2, BCL-X_L, MCL-1, etc.) and proapoptotic (BAX, BAK, BOK) proteins. Oligomerization of these proteins can result in membrane pores or membrane protective complexes. While the proapoptotic members such as BAX and BAK promote mitochondrial permeabilization to activate caspases that execute the cell death program, the antiapoptotic members such as BCL-2 and BCL-xL prevent pore formation [156, 157, 235]. Overexpression of antiapoptotic BCL-2 may protect the cells against endoplasmic reticulum (ER) stress, by reducing basal Ca^{2+} concentrations in the ER. BCL-2 indirectly participates in the lysosomal mechanisms: necrosis and autophagy. BCL-2 and BCL-X_L bind to protein beclin 1 to suppress the autophagy system [156].

Overexpression of the antiapoptotic Bcl-2 proteins (Bcl-2, Bcl-xL, Mcl-1) with downregulation of proapoptotic proteins (Bax and Bid) has been documented in OSCC. An increase in the Bcl-2/Bax ratio, a reliable index of cell survival, is associated with a worse prognosis in patients with OSCC. A large proportion (50–75%) of OSCC cases were shown to overexpress BCL-2 which is undetectable in normal oral epithelium with the exception of cells in the basal layer in some instances [38, 156–158]. Synergy between BCL-2 and MYC has also been reported; BCL-2 inhibits apoptosis induced by MYC [157, 235]. *BCL-2* not only presents as a target gene in survival of oral cancer cells but also showed promise in oral cancer gene therapy [158].

2.7 Invasion and Metastasis

The multistep process of tumor invasion and metastasis involves altered expression of cytoskeletal proteins, proteolytic degradation of the extracellular matrix (ECM), alteration of the cell-cell and cell-ECM interactions, and migration to distant regions.

2.7.1 Cytoskeletal Defects

At the cellular level, oral cancer demonstrates cytoskeletal changes that support the process of invasion and metastasis. Among the various cytoskeletal structures reported to be dysregulated in OSCC, changes in the expression of cytokeratins are most significant [236]. The high molecular weight cytokeratins (CK1, CK5, CK13, CK16, and CK19) were found to be downregulated, whereas the expression of CK8, CK14, and CK18 was upregulated in oral tumors. Cytokeratins 8/18 and 19 have gained particular importance that are known to promote invasion, and movement of cells into microvasculature is associated with poor prognosis [236, 237]. Reduction in cytokeratin 19 may be mediated by EGF as demonstrated in human OSCC cell lines [238]. Cytokeratin profiling by immunohistochemistry and identification of cytokeratins in malignant mucosal smears are valuable in early diagnosis [239, 240].

Besides cytokeratins, proteins that belong to the ERM (ezrin-radixin-moesin) family that facilitate membrane dynamics and signaling are known to contribute to invasion and migration in OSCC [241]. Strong cytoplasmic overexpression of ezrin was linked to lymph node metastasis and aggressive tumor behavior in HNSCC leading to poor prognosis [242]. Ezrin enhances the growth of cancer cells, and its expression correlated well with Ki-67 activity, which is expressed during all stages of the cell cycle except in the G0 resting phase [243, 244]. Both ezrin and moesin are prognostic markers and correlate with poor survival in HNSCC [245].

Epithelial protein lost in neoplasm (EPLIN), a cytoskeletal protein that facilitates actin assembly, is lost in several oral cancer cell lines [243]. EPLIN is preferentially expressed in epithelial cells and is a tumor suppressor. Inactivation of Rho A, a member of the Rho GTPase family in oral cancer, may be mediated by Snail transcription factor. Silencing Snail impaired motility, migration, and invasion of oral cancer cells, and Snail knockdown reduced filopodia formation in OC cell lines [246, 247].

2.7.2 Cell Adhesion Molecules

Disruption in cell-cell interactions contributes to the development and progression of oral cancer. Decreased expression of cadherins and the disruption of cadherin/catenin complex, one of the earliest events in oral transformation, correlate with aggressive tumor behavior and lymph node metastasis.

Cell adhesion molecules (CAMs) present on the cell surface maintain cell-cell contact, act as signaling receptors, and play a role in cell migration and differentiation. Integrins and E-cadherins are the most important CAMs expressed in stratified squamous epithelium, altered in OSCC [248]. Integrin α3 and integrin β4 are valuable genomic biomarkers for assessing the risks of locoregional and hematogenous dissemination of OSCC [249]. Increased expression of alpha (v) beta6 integrin, a consistent finding in OSCC, causes activation of MMPs responsible for tissue invasion [250]. Recently, β1 integrin expression was assessed in oral submucous fibrosis (OSMF) and OSCC relative to control. The percentage staining intensity and stem cells were significantly higher in OSMF and OSCC compared to control. Furthermore, β1 integrin was observed in rete peg region in the control, in basal and suprabasal layers in OSMF, and in central and peripheral cells in OSCC [251].

In a meta-analysis, reduced E-cadherin expression indicated a worse prognosis [252]. OSCC tumor grade, poor survival, and metastasis correlate with downregulation of E-cadherin, the "master switch of EMT" [253]. Loss of E-cadherin can arise from direct mutation or through suppression of E-cadherin gene, *CDH1*. Reduced expression of E-cadherin is most likely due to hypermethylation of *CDH1* promoter [141]. Growth factors (interleukin-6, transforming growth factor β, epidermal growth factor, fibroblast growth factor) may also induce loss of E-cadherin. The Snail family (snail, snail2, or slug) transcription factors regulate E-cadherin by inducing histone deacetylase, preventing transcription of E-cadherin or via the upregulation of ZEB-1. [253, 254]. The loss of E-cadherin leads to cytoplasmic and nuclear translocation of β-catenin with consequent transactivation of oncogenes (*c-MYC*, *CCND1*), transcription factors (slug), and intermediate filaments (vimentin, fibronectin) [253]. During EMT the epithelial markers show underexpression, and mesenchymal markers (e.g., vimentin) show overexpression. Vimentin expression is not noticed in oral mucosal epithelium, but only expressed by transformed oral epithelium during EMT [255]. Cadherin switching (i.e., loss of E-cadherin and gain of N-cadherin) is a critical event in the progression of OSCC [256].

Other CAMs dysregulated in oral cancer include ICAM-1, CD44, and selectins [257]. Higher expression of ICAM-1 (intercellular adhesion molecule) was reported at the invasive front of TSCC [258]. Polymorphisms of ICAM-1 were identified to increase oral cancer susceptibility [259, 260].

2.7.3 Matrix Metalloproteinases

Degradation of the extracellular matrix (ECM) during invasion creates a path for the migration of malignant cells to metastasize to distant organs through the vasculature. Increased activity of the ECM-degrading enzymes matrix metalloproteinases (MMPS) associated with downregulation of the tissue inhibitors of MMPs (TIMPs) as well as RECK, a novel tumor suppressor gene that regulates MMPs, has been documented in OSCC. Recently, Pramanik et al. [261] provided evidence to show that MMP-9 overexpression and activation are important events occurring during OSCC progression/invasion and that this overexpression/activation is regulated by c-Myc, active MMP-2, and inactive GSK-3β mediated pathways. SNPs in MMP gene promoters, particularly MMP-1, MMP-2, MMP-3, and MMP-9, were identified in OSCC [262].

2.7.4 Bone Invasion

The regional bone invasion of alveolar process of maxilla and mandible (Fig. 2.6) is common in OSCC mediated by osteoclasts. Bone involvement associated with OSCC involves a set of genes and pathways and presents with unique erosive, infiltrative, or mixed histological patterns. The infiltrative pattern, presenting with nests and cords of epithelium along an irregular tumor front, is associated with worse prognosis [263]. Expression of interleukins, tumor necrosis factor, and parathyroid hormone-related protein (PTHrP) is higher in the infiltrative pattern. The cytokines upregulate RANKL/RANK signaling (RANKL-RANK binding or through osteoprotegerin suppression) in stromal cells to form osteoclasts [264] (Fig. 2.7). Osteoprotegerin, a decoy receptor for RANK that competes with RANKL PTHrP, was shown as essential to mandibular invasion in OSCC animal models, regulated by multiple signaling pathways converging on the transcription factor, glioma-associated oncogene family zinc finger 2 (Gli2) [265].

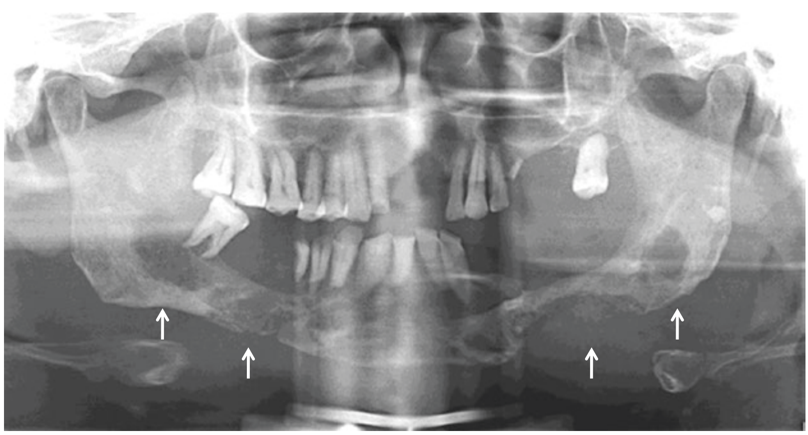

Fig. 2.6 Panoramic view of a highly invasive OSCC in a chronic tobacco chewer which caused gross destruction of mandible (i.e., bone invasion). The white arrows show a generalized radiolucent destructive pattern, mimicking an intraosseous carcinoma

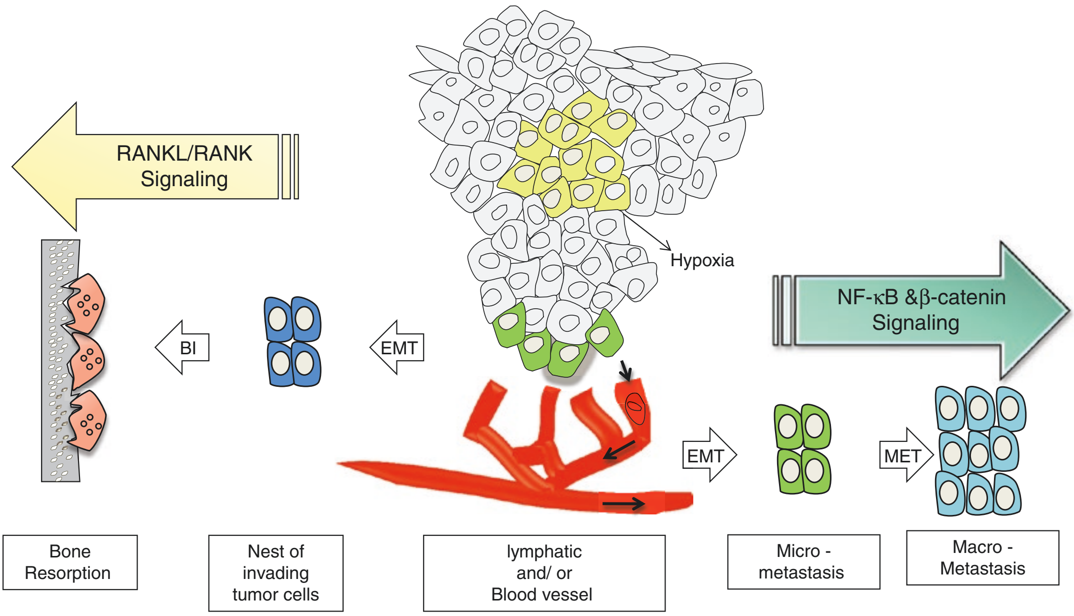

Fig. 2.7 Basic stages of cellular metastasis and bone invasion in OSCC. The key events in OC metastasis includes detachment or shedding of cells from the parent tumor through "epithelial mesenchymal transition" (EMT) that occurs via the master-switch "E-cadherin" through the Wnt/β-catenin, and NF-κB pathways which is mediated by action of miR species: 200 family and miR-21, and through lncRNAs: MALAT1, UCA1, TUG1, H19 etc. Stromal invasion (INV) is mediated by the matrix metallo-proteinases (MMP-2,-9,-10) that are capable to digest the extracellular matrix. At this stage, the tumor cells show a strong expression of mesenchymal markers vimentin and N-cadherin. Simultaneously the in-growth of capillaries occurs in response to vascular endothelial growth factor (VEGF) secreted by tumors in response to cells under hypoxia (represented in yellow), that also expedites the collaborative event of metastasis. Hypoxia is also strongly associated with genomic instability. Following this, there is intravasation of transformed cells into lymphatics and/or blood capillaries through cell membrane extensions. After entry, the circulating tumor cells (CTCs) can form tumor emboli and may be used to monitor tumor activity and treatment response. Through complex homing mechanisms, the CTCs reach a conducive secondary subsite such as the lungs. At this location, there is reversal of EMT referred to as "mesenchymal epithelial transition" (MET), linked to the reacquisition of epithelial markers. The cells are now established at the secondary site forming metastatic tumor deposits. Bone invasion (BI) of maxilla and mandible is very common in OSCC involving alveolar, gingival mucosa, primarily occurs via the RANKL/RANK signaling which forms the bone resorbing osteoclasts

2.7.5 Metastasis

"Dysregulation of cytoskeleton, CAMs, and synthesis of matrix metalloproteinases form the basis for tumor cell migration." Metastasis is a complex process characterized by detachment of cells from parent tumor followed by their dissemination. The cells detach from the primary tumor site, invade the tissue by MMPs, and pass through the lymphatic channels or vascular capillaries to settle at a distant tissue site (Fig. 2.7). Metastasis reflects the advanced stage of disease and increases the chance of mortality.

The organs that are frequent sites for distant metastasis of oral cancer include lungs (~70%), bone, liver and rarely the brain and myocardium, as identified in postmortem dissections [266, 267]. The specific homing mechanisms that dictate the distance metastasis of oral cancer are still unexplored.

In OSCC, metastasis is mediated primarily via lymphatics. Tumor thickness, keratinization, and lymphocytic infiltration are predictors of metastasis, and extracapsular spread of cervical lymph node metastasis is a predictor of spread, treatment failure, and death due to disease [268, 269]. In staging of OC, the tumor size and nodal status can be determined accurately, but distant metastasis (~10%) is largely underestimated, even with state-of-the-art imaging techniques like PET/CT. Podoplanin, a transmembrane glycoprotein seen at the invasive tumor front, is a molecular marker of HNSCC invasion and poor prognosis [270]. Podoplanin specifically expressed in lymph vessel endothelium correlates with lymph vessel density and facilitates lymphatic metastasis [271]. Podoplanin expression levels also correlated with ezrin and Rho-A protein, linking them all in cell movement and tumor invasion [271].

2.8 Angiogenesis

Uncontrolled cell proliferation in OSCC creates hypoxia, a potent stimulus for angiogenesis, a hallmark of cancer. Angiogenesis is also promoted by ECM degradation by MMPs with release of pro-angiogenic factors predominantly vascular endothelial growth factor (VEGF). Activation of the VEGF/VEGF receptor (VEGFR) axis triggers a signaling network that results in the formation of new blood vessels, a prerequisite for metastasis [272].

VEGF is a glycoprotein that increases proliferation and permeability of blood vessels [273]. Six VEGF subtypes, fibroblast growth factors (FGF), and epithelial nitric oxide synthase (eNOS) are known to stimulate tumor angiogenesis in OSCC [274–276]. Vascular density is a marker of metastasis and highly vascular tumors have greater probability for metastasis. In OSCC, mean vessel density (MVD) correlated with tumor grade and lymph node status and was higher in eNOS- or VEGFR-positive tumors [273, 276]. While downregulation of miR-126 induced angiogenesis and lymphangiogenesis by activation of VEGF-A in OSCC, miR-126 overexpression suppressed VEGF and FGF, key angiogenic regulators [92, 93].

The tumor angiogenic process is driven by chemical mediators produced in response to tissue hypoxia characteristic of malignant tumors. HIF-1 regulates several 100 genes primarily *VEGF* critical for angiogenesis [277]. At physiological oxygen tension, HIF-1α is degraded following hydroxylation by prolyl hydrolases, whereas in hypoxia, HIF-1α dimerizes with HIF-1β with consequent nuclear translocation and transactivation of hypoxia-responsive genes such as VEGF and MMPs among several others. Correlation exists between HIF-1 levels and VEGF expression in OSCC [277]. Hypoxia contributes to cancer progression and tumor resistance to therapy and can be a predictor of poor treatment outcome. Hypoxia promotes genetic instability and mutation rate both in oncogenes and tumor suppressors. It can lead to *TP53* upregulation followed by activation of protease-activating factor and caspase-9 or can initiate apoptosis pathways such as *BCL-2* family genes, in a TP53-independent manner [277]. Hypoxia also maintains an inflammatory environment, and both hypoxia through HIF-1 and inflammation through angiogenic cytokines recruit more vessels and facilitate metastatic spread [278].

2.8.1 Cancer-Related Inflammation: A Potential Catalyst

Tissue inflammation, an important hallmark of cancer, predisposes to malignant transformation of the oral epithelium. Moreover, cancer-related inflammation (CRI) can promote tumor progression [279]. It is believed that “genetic imbalance is the match that lights the flame, and inflammation is the fuel that feeds the flames” [279]. In CRI the predominant cells include the tumor-associated macrophages, and the dominant chemical mediators are cytokines (interleukin-1, interleukin-6, TNF-α), chemokines (CXCL2, CCL2), and transcription factors (NF-κB, STAT-3). NF-κB is a key signaling pathway involved in CRI, and its activation requires signal transducer and activator of transcription-3 (STAT-3). Hypoxia also occurs in inflamed tissues. NF-κB activated due to genetic instability or hypoxia increases the expression of inflammatory cytokines, adhesion molecules, angiogenic factors, and enzymes in prostaglandin and nitric oxide pathways [280]. STAT-3 was shown to upregulate oncogenes (*C-MYC* and *CCND1*) and genes involved in cell survival (*BCL-2*). The ECM undergoes changes in inflammation and provides support to growing tumors. CRI alters many aspects of tumor biology, including angiogenesis, metastasis, survival, and proliferation [280, 281]. Chronic inflammation is known to predispose to OSCC. OSCC arises within preexisting inflammatory OPMD like OLP and OSMF which present with characteristic inflammatory infiltration in connective tissue and also in mucosa undergoing prolonged irritation [282–284].

2.8.2 Complex Cannibalism: Adaptation for Survival

Adaptation for Survival Cannibalism is an important mechanism that malignant cells adapt for survival in hypoxia, low pH, and low nutritive conditions. They are particularly resistant to low pH-acidic environment. Moreover, the acidic environment activates the lytic enzymes and ezrin, the actin linker. The malignant cannibal cells feed on adjacent tumor cells and leukocytes to drive their metabolic activities. A large cell engulfs a slightly smaller cell, which is either living or dead. This is mediated by cathepsin B, lysozyme, and other lytic enzymes, mimics phagocytosis, and is a process of nonselective cell eating [285, 286]. In OSCC, this process is much more complex than conventional cannibalism where the tumor cells were shown to engulf more than 2 cells at an instance [287]. Histological specimens of OSCC showing neutrophilic tumor cell cannibalism correlated with poor differentiation and cervical lymph node metastasis [285]. The expression of lysozyme activity correlated with cannibalistic activity in tumor sections [286]. High-grade cannibalism also correlated with positive lymph node metastasis [288]. Cannibalism can be considered as tumor defense against the host immune mechanisms and can be spotted on hematoxylin-/eosin-stained sections of OSCC. Cannibalistic processes may be considered as an important hallmark of oral cancer.

Conclusion

Accumulating evidence over the last decade has provided insights into the complex molecular pathogenesis of oral cancer. Genetic and epigenetic mechanisms that drive oral tumorigenesis have been unraveled. Genome-wide association studies and next-generation sequencing have revealed the genetic signatures that underlie risk for oral cancer. Emerging evidence on the pivotal role of the ncRNAs has opened up new dimensions in understanding the development and progression of OSCC. Further research on biomarkers specific for oral cancer screening, differential diagnosis, prognosis, recurrence, metastasis, drug resistance, and therapy will be valuable in correlation with clinicopathological variables and assessment of therapeutic outcomes. Recent developments in "omics" technologies, especially salivaomics, have immense potential in early diagnosis and prevention of OSCC by population-based screening programs besides disease and therapeutic monitoring to reduce patient morbidity and mortality. Techniques such as LC-MS/MS-based protein expression analysis mass spectrometry, targeted protein measurement, RNA sequencing, electrochemical detection, and liquid biopsy will be useful in the discovery of new molecular targets and novel drugs.

References

1. Vucicevic Boras V, Fucic A, Virag M, Gabric D, Blivajs I, Tomasovic-Loncaric C, et al. Significance of stroma in biology of oral squamous cell carcinoma. Tumori. 2018;104:9–14.
2. Ferlay J, Soerjomataram I, Dikshit R, Eser S, Mathers C, Rebelo M, et al. Cancer incidence and mortality worldwide: sources, methods and major patterns in GLOBOCAN 2012. Int J Cancer. 2015;136:E359–86.
3. Ram H, Sarkar J, Kumar H, Konwar R, Bhatt MLB, Mohammad S. Oral cancer: risk factors and molecular pathogenesis. J Maxillofac Oral Surg. 2011;10:132–7.
4. Stransky N, Egloff AM, Tward AD, Kostic AD, Cibulskis K, Sivachenko A, et al. The mutational landscape of head and neck squamous cell carcinoma. Science. 2011;333:1157–60.

5. Al-Hebshi NN, Li S, Nasher AT, El-Setouhy M, Alsanosi R, Blancato J, et al. Exome sequencing of oral squamous cell carcinoma in users of Arabian snuff reveals novel candidates for driver genes. Int J Cancer. 2016;139:363–72.
6. Yi Y, Tian Z, Ju H, Ren G, Hu J. A novel NOTCH3 mutation identified in patients with oral cancer by whole exome sequencing. Int J Mol Med. 2017;39:1541–7.
7. Tabatabaeifar S, Thomassen M, Larsen MJ, Larsen SR, Kruse TA, Sørensen JA. The subclonal structure and genomic evolution of oral squamous cell carcinoma revealed by ultra-deep sequencing. Oncotarget. 2017;8:16571–80.
8. Vincent-Chong VK, Salahshourifar I, Woo KM, Anwar A, Razali R, Gudimella R, et al. Genome wide profiling in oral squamous cell carcinoma identifies a four genetic marker signature of prognostic significance. PLoS One. 2017;12:e0174865.
9. Cancer Genome Atlas Network. Comprehensive genomic characterization of head and neck squamous cell carcinomas. Nature. 2015;517:576–82.
10. Martin CL, Reshmi SC, Ried T, Gottberg W, Wilson JW, Reddy JK, et al. Chromosomal imbalances in oral squamous cell carcinoma. Examination of 31 cell lines and review of the literature. Oral Oncol. 2008;44:369–82.
11. Sharma V, Nandan A, Sharma AK, Singh H, Bharadwaj M, Sinha DN, et al. Signature of genetic associations in oral cancer. Tumour Biol. 2017;39:1010428317725923.
12. Langevin SM, Stone RA, Bunker CH, Lyons-Weiler MA, LaFramboise WA, Kelly L, et al. MicroRNA-137promotermethylation is associated with poorer overall survival in patients with squamous cell carcinoma of the head and neck. Cancer. 2011;117:1454–62.
13. Dang J, Bian YQ, Sun JY, Chen F, Dong GY, Liu Q, et al. MicroRNA-137 promoter methylation in oral lichen planus and oral squamous cell carcinoma. J Oral Pathol Med. 2013;42:315–21.
14. Langevin SM, Stone RA, Bunker CH, Grandis JR, Sobol RW, Taioli E. MicroRNA-137 promoter methylation in oral rinses from patients with squamous cell carcinoma of the head and neck is associated with gender and body mass index. Carcinogenesis. 2010;31:864–70.
15. Morandi L, Gissi D, Tarsitano A, Asioli S, Monti V, Del Corso G, et al. DNA methylation analysis by bisulfite next-generation sequencing for early detection of oral squamous cell carcinoma and high-grade squamous intraepithelial lesion from oral brushing. J Craniomaxillofac Surg. 2015;43:1494–500.
16. Sun L, Liang J, Wang Q, Li Z, Du Y, Xu X. MicroRNA-137 suppresses tongue squamous carcinoma cell proliferation, migration and invasion. Cell Prolif. 2016;49:628–35.
17. Baolei W, Lei D, Wang L, Yang X, Jia S, Yang Z, et al. MiRNA-101 inhibits oral squamous-cell carcinoma growth and metastasis by targeting zinc finger E-box binding homeobox 1. Am J Cancer Res. 2016;6:1396–407.
18. Jianpei H, Chunyu W, Zhao X, Liu C. The prognostic value of decreased miR-101 in various cancers: a meta-analysis of 12 studies. Onco Targets Ther. 2017;10:3709–18.
19. Ma X, Bai J, Xie G, Liu Y, Shuai X, Tao K. Prognostic significance of microRNA-101 in solid tumor: a meta-analysis. PLoS One. 2017;12:e0180173.
20. Varambally S, Cao Q, Mani RS, Shankar S, Wang X, Ateeq B, et al. Genomic loss of microRNA-101 leads to overexpression of histone methyltransferase EZH2 in cancer. Science. 2008;322:1695–9.
21. Lei W, Liu Y-e, Zheng Y, AG Lin Q. MiR-429 Inhibits Oral Squamous Cell Carcinoma Growth by Targeting ZEB1. Med Sci Monit. 2015;21:383–9.
22. Gregory PA, Bert AG, Paterson EL, Barry SC, Tsykin A, Farshid G, et al. The miR-200 family and miR-205 regulate epithelial to mesenchymal transition by targeting ZEB1 and SIP1. Nat Cell Biol. 2008;10:593–601.
23. Zhang CZ. Long non-coding RNA FTH1P3 facilitates oral squamous cell carcinoma progression by acting as a molecular sponge of miR-224-5p to modulate fizzled 5 expression. Gene. 2017;607:47–55.
24. Fukumoto I, Hanazawa T, Kinoshita T, Kikkawa N, Koshizuka K, Goto Y, et al. MicroRNA expression signature of oral squamous cell carcinoma: functional role of microRNA-26a/b in the modulation of novel cancer pathways. Br J Cancer. 2015;112:891–900.
25. He Q, Chen Z, Cabay RJ, Zhang L, Luan X, Chen D, et al. microRNA-21 and microRNA-375 from oral cytology as biomarkers for oral tongue cancer detection. Oral Oncol. 2016;57:15–20.
26. Shi W, Yang J, Li S, Shan X, Liu X, Hua H, et al. Potential involvement of miR-375 in the premalignant progression of oral squamous cell carcinoma mediated via transcription factor KLF5. Oncotarget. 2015;6:40172–85.
27. Jung HM, Patel RS, Phillips BL, Wang H, Cohen DM, Reinhold WC, et al. Tumor suppressor miR-375 regulates MYC expression via repression of CIP2A coding sequence through multiple miRNA-mRNA interactions. Mol Biol Cell. 2013;24:1638–48. S1–7
28. Yadong W, Sun X, Song B, Qiu X, Zhao J. MiR-375/SLC7A11 axis regulates oral squamous cell carcinoma proliferation and invasion. Cancer Med. 2017;6:1686–97.
29. Jung HM, Benarroch Y, Chan EK. Anti-cancer drugs reactivate tumor suppressor miR-375 expression in tongue cancer cells. J Cell Biochem. 2015;116:836–43.
30. Tsui IFL, Rosin MP, Zhang L, Ng RT, Lam WL. Multiple aberrations of chromosome 3p detected in oral premalignant lesions. Cancer Prev Res (Phila). 2008;1:424–9.
31. Tanimoto K, Hayashi S, Tsuchiya E, Tokuchi Y, Kobayashi Y, Yoshiga K, et al. Abnormalities of

the *FHIT* gene in human oral carcinogenesis. Br J Cancer. 2000;82:838–43.
32. Tai SK, Lee JI, Ang KK, El-Naggar AK, Hassan KA, Liu D, et al. Loss of Fhit expression in head and neck squamous cell carcinoma and its potential clinical implication. Clin Cancer Res. 2004;10:5554–7.
33. Roy R, Singh R, Chattopadhyay E, Ray A, De Sarkar N, Aich R, et al. MicroRNA and target gene expression based clustering of oral cancer, precancer and normal tissues. Gene. 2016;593:58–63.
34. Jia LF, Wei SB, Gan YH, Guo Y, Gong K, Mitchelson K, et al. Expression, regulation and roles of miR-26a and MEG3 in tongue squamous cell carcinoma. Int J Cancer. 2014;135:2282–93.
35. Zhang S, Zhou X, Wang B, Zhang K, Liu S, Yue K, et al. Loss of VHL expression contributes to epithelial-mesenchymal transition in oral squamous cell carcinoma. Oral Oncol. 2014;50:809–17.
36. Fukuzumi M, Hamakawa H, Onishi A, Sumida T, Tanioka H. Gene expression of GLUT isoforms and VHL in oral squamous cell carcinoma. Cancer Lett. 2000;161:133–40.
37. Cohen Y, Goldenberg-Cohen N, Shalmon B, Shani T, Oren S, Amariglio N, et al. Mutational analysis of PTEN/PIK3CA/AKT pathway in oral squamous cell carcinoma. Oral Oncol. 2011;47:946–50.
38. Kozaki K, Imoto I, Pimkhaokham A, Hasegawa S, Tsuda H, Omura K, et al. PIK3CA mutation is an oncogenic aberration at advanced stages of oral squamous cell carcinoma. Cancer Sci. 2006;97:1351–8.
39. Fenic I, Steger K, Gruber C, Arens C, Woenckhaus J. Analysis of PIK3CA and Akt/protein kinase B in head and neck squamous cell carcinoma. Oncol Rep. 2007;18:253–9.
40. Yang PY, Hsieh PL, Wang TH, Yu CC, Lu MY, Liao YW, et al. Andrographolide impedes cancer stemness and enhances radio-sensitivity in oral carcinomas via miR-218 activation. Oncotarget. 2017;8:4196–207.
41. Jamali Z, Asl Aminabadi N, Attaran R, Pournagiazar F, Ghertasi Oskouei S, Ahmadpour F. MicroRNAs as prognostic molecular signatures in human head and neck squamous cell carcinoma: a systematic review and meta-analysis. Oral Oncol. 2015;51:321–31.
42. Peng SC, Liao CT, Peng CH, Cheng AJ, Chen SJ, Huang CG, et al. MicroRNAs MiR-218, MiR-125b, and Let-7g predict prognosis in patients with oral cavity squamous cell carcinoma. PLoS One. 2014;9:e102403.
43. Wu DW, Chuang CY, Lin WL, Sung WW, Cheng YW, Lee H. Paxillin promotes tumor progression and predicts survival and relapse in oral cavity squamous cell carcinoma by microRNA-218 targeting. Carcinogenesis. 2014;35:1823–9.
44. Uesugi A, Kozaki K, Tsuruta T, Furuta M, Morita K, Imoto I, et al. The tumor suppressive microRNA miR-218 targets the mTOR component Rictor and inhibits AKT phosphorylation in oral cancer. Cancer Res. 2011;71:5765–78.
45. Zhuang Z, Hu F, Hu J, Wang C, Hou J, Yu Z, et al. MicroRNA-218 promotes cisplatin resistance in oral cancer via the PPP2R5A/Wnt signaling pathway. Oncol Rep. 2017;38:2051–61.
46. Boscolo-Rizzo P, Da Mosto MC, Rampazzo E, Giunco S, Del Mistro A, Menegaldo A, et al. Telomeres and telomerase in head and neck squamous cell carcinoma: from pathogenesis to clinical implications. Cancer Metastasis Rev. 2016;35:457–74.
47. Min BM, Baek JH, Shin KH, Gujuluva CN, Cherrick HM, Park NH. Inactivation of the p53 gene by either mutation or HPV infection is extremely frequent in human oral squamous cell carcinoma cell lines. Eur J Cancer B Oral Oncol. 1994;30B:338–45.
48. Pérez-Sayáns M, Suárez-Peñaranda JM, Herranz-Carnero M, Gayoso-Diz P, Barros-Angueira F, Gándara-Rey JM, et al. The role of the adenomatous polyposis coli (APC) in oral squamous cell carcinoma. Oral Oncol. 2012;48:56–60.
49. Liao PH, Lee TL, Yang LC, Yang SH, Chen SL, Chou MY. Adenomatous polyposis coli gene mutation and decreased wild-type p53 protein expression in oral submucous fibrosis: a preliminary investigation. Oral Surg Oral Med Oral Pathol Oral Radiol Endod. 2001;92:202–7.
50. Kok SH, Lee JJ, Hsu HC, Chiang CP, Kuo YS, Kuo MY. Mutations of the adenomatous polyposis coli gene in areca quid and tobacco-associated oral squamous cell carcinomas in Taiwan. J Oral Pathol Med. 2002;31:395–401.
51. Sikdar N, Paul RR, Panda CK, Banerjee SK, Roy B. Loss of heterozygosity at APC and MCC genes of oral cancer and leukoplakia tissues from Indian tobacco chewers. J Oral Pathol Med. 2003;32:450–4.
52. Lo Muzio L. A possible role for the WNT-1 pathway in oral carcinogenesis. Crit Rev Oral Biol Med. 2001;12:152–65.
53. Iwai S, Katagiri W, Kong C, Amekawa S, Nakazawa M, Yura Y. Mutations of the APC, beta-catenin, and axin 1 genes and cytoplasmic accumulation of beta-catenin in oral squamous cell carcinoma. J Cancer Res Clin Oncol. 2005;131:773–82.
54. Manikandan M, Deva Magendhra Rao AK, Arunkumar G, Manickavasagam M, Rajkumar KS, Rajaraman R, et al. Oral squamous cell carcinoma: microRNA expression profiling and integrative analyses for elucidation of tumourigenesis mechanism. Mol Cancer. 2016;15:28.
55. Kong XP, Yao J, Luo W, Feng FK, Ma JT, Ren YP, et al. The expression and functional role of a FOXC1 related mRNA-lncRNA pair in oral squamous cell carcinoma. Mol Cell Biochem. 2014;394:177–86.
56. Pan F, Yao J, Chen Y, Zhou C, Geng P, Mao H, et al. A novel long non-coding RNA FOXCUT and mRNA FOXC1 pair promote progression and predict poor prognosis in esophageal squamous cell carcinoma. Int J Clin Exp Pathol. 2014;7:2838–49. eCollection 2014
57. Xu YZ, Chen FF, Zhang Y, Zhao QF, Guan XL, Wang HY, et al. The long noncoding RNA FOXCUT

promotes proliferation and migration by targeting FOXC1 in nasopharyngeal carcinoma. Tumour Biol. 2017;39:1010428317706054.
58. Kowshik J, Baba AB, Giri H, Deepak Reddy G, Dixit M, Nagini S. Astaxanthin inhibits JAK/STAT-3 signaling to abrogate cell proliferation, invasion and angiogenesis in a hamster model of oral cancer. PLoS One. 2014;9:e109114.
59. Concha-Benavente F, Srivastava RM, Trivedi S, Lei Y, Chandran U, Seethala RR, et al. Identification of the cell-intrinsic and -extrinsic pathways downstream of EGFR and IFNγ that induce PD-L1 expression in head and neck cancer. Cancer Res. 2016;76:1031–43.
60. Huang JS, Yao CJ, Chuang SE, Yeh CT, Lee LM, Chen RM, et al. Honokiol inhibits sphere formation and xenograft growth of oral cancer side population cells accompanied with JAK/STAT signaling pathway suppression and apoptosis induction. BMC Cancer. 2016;16:245.
61. Taoudi Benchekroun M, Saintigny P, Thomas SM, El-Naggar AK, Papadimitrakopoulou V, Ren H, et al. Epidermal growth factor receptor expression and gene copy number in the risk of oral cancer. Cancer Prev Res (Phila). 2010;3:800–9.
62. Lin WL, Lin YS, Shi GY, Chang CF, Wu HL. Lewisy promotes migration of oral cancer cells by glycosylation of epidermal growth factor receptor. PLoS One. 2015;10:e0120162.
63. Seshacharyulu P, Ponnusamy MP, Haridas D, Jain M, Ganti AK, Batra SK. Targeting the EGFR signaling pathway in cancer therapy. Expert Opin Ther Targets. 2012;16:15–31.
64. Stadler ME, Patel MR, Couch ME, Hayes DN. Molecular biology of head neck cancer: risks and pathways. Hematol Oncol Clin North Am. 2008;22:1099–124.
65. Dang CV. c-Myc target genes involved in cell growth, apoptosis, and metabolism. Mol Cell Biol. 1999;19:1–11.
66. Pai RB, Pai SB, Lalitha M, Kumaraswamy SV, Lalitha N, Johnston RN, et al. Over-expression of c-Myc oncoprotein in oral squamous cell carcinoma in the South Indian population. Ecancermedicalscience. 2009;3:128.
67. Eversole LR, Sapp JP. c-myc oncoprotein expression in oral precancerous and early cancerous lesions. Eur J Cancer B Oral Oncol. 1993;29B:131–5.
68. Arunkumar G, Murugan AK, Prasanna Srinivasa Rao H, Subbiah S, Rajaraman R, Munirajan AK. Long non-coding RNA CCAT1 is overexpressed in oral squamous cell carcinomas and predicts poor prognosis. Biomed Rep. 2017;6:455–62.
69. Xin Y, Li Z, Zheng H, Chan MTV, Ka Kei Wu W. CCAT2: a novel oncogenic long non-coding RNA in human cancers. Cell Prolif. 2017;50.
70. Ma Y, Hu X, Shang C, Zhong M, Guo Y. Silencing of long non-coding RNA CCAT2 depressed malignancy of oral squamous cell carcinoma via Wnt/β-catenin pathway. Tumour Biol. 2017;39:1010428317717670.
71. Tan J, Hou YC, Fu LN, Wang YQ, Liu QQ, Xiong H, et al. Long noncoding RNA CCAT2 as a potential novel biomarker to predict the clinical outcome of cancer patients: a meta-analysis. J Cancer. 2017;8:1498–506.
72. Jing X, Liang H, Cui X, Han C, Hao C, Huo K. Long noncoding RNA CCAT2 can predict metastasis and a poor prognosis: a meta-analysis. Clin Chim Acta. 2017;468:159–65.
73. Ouyang S, Zhang P, Wang J, Huang Z, Liao L. Expression of long non-coding RNA colon cancer associated transcript 2 and its clinicopathologic significance in oral squamous cell carcinoma. Zhonghua Kou Qiang Yi Xue Za Zhi. 2016;51: 286–91.
74. Zhou N, Liao W, Huang Z, Hu Z, Huang W. Qiutao Wang Overexpression of long non-coding RNA CCAT2 predicts a poor prognosis in patients with oral squamous cell carcinoma. Int J Clin Exp Pathol. 2016;9:110–7.
75. Kresty LA, Mallery SR, Knobloch TJ, Song H, Lloyd M, Casto BC, et al. Alterations of p16(INK4a) and p14(ARF) in patients with severe oral epithelial dysplasia. Cancer Res. 2002;62:5295–300.
76. Koscielny S, Dahse R, Ernst G, von Eggeling F. The prognostic relevance of p16 inactivation in head and neck cancer. ORL J Otorhinolaryngol Relat Spec. 2007;69:30–6.
77. Ruesga MT, Acha-Sagredo A, Rodríguez MJ, Aguirregaviria JI, Videgain J, Rodríguez C, et al. p16(INK4a) promoter hypermethylation in oral scrapings of oral squamous cell carcinoma risk patients. Cancer Lett. 2007;250:140–5.
78. Ohta S, Uemura H, Matsui Y, Ishiguro H, Fujinami K, Kondo K, et al. Alterations of p16 and p14ARF genes and their 9p1 locus in oral squamous cell carcinoma. Oral Surg Oral Med Oral Pathol Oral Radiol Endod. 2009;107:81–91.
79. Yu CC, Chen PN, Peng CY, CH Y, Chou MY. Suppression of miR-204 enables oral squamous cell carcinomas to promote cancer stemness, EMT traits, and lymph node metastasis. Oncotarget. 2016;7:20180–92.
80. Wang X, Li F, Zhou X. miR-204-5p regulates cell proliferation and metastasis through inhibiting CXCR4 expression in OSCC. Biomed Pharmacother. 2016;82:202–7.
81. Hung PS, Tu HF, Kao SY, Yang CC, Liu CJ, Huang TY, et al. miR-31 is upregulated in oral premalignant epithelium and contributes to the immortalization of normal oral keratinocytes. Carcinogenesis. 2014;35:1162–71.
82. Lu WC, Liu CJ, Tu HF, Chung YT, Yang CC, Kao SY, et al. miR-31 targets ARID1A and enhances the oncogenicity and stemness of head and neck squamous cell carcinoma. Oncotarget. 2016;7:57254–67.
83. Chang KW, Kao SY, Wu YH, Tsai MM, Tu HF, Liu CJ, et al. Passenger strand miRNA miR-31* regulates the phenotypes of oral cancer cells by targeting RhoA. Oral Oncol. 2013;49:27–33.

84. Kao YY, Tu HF, Kao SY, Chang KW, Lin SC. The increase of oncogenic miRNA expression in tongue carcinogenesis of a mouse model. Oral Oncol. 2015;51:1103–12.
85. Shih JW, Chiang WF, Wu ATH, Wu MH, Wang LY, Yu YL a. Long noncoding RNA LncHIFCAR/MIR31HG is a HIF-1α co-activator driving oral cancer progression. Nat Commun. 2017;8:15874.
86. Irimie AI, Braicu C, Sonea L, Zimta AA, Cojocneanu-Petric R, Tonchev K, et al. A looking-glass of non-coding RNAs in oral cancer. Int J Mol Sci. 2017;18:E2620.
87. Ha PK, Califano JA. Promoter methylation and inactivation of tumour-suppressor genes in oral squamous-cell carcinoma. Lancet Oncol. 2006;7:77–82.
88. Min A, Zhu C, Peng S, Rajthala S, Costea DE, Sapkota D. MicroRNAs as important players and biomarkers in oral carcinogenesis. Biomed Res Int. 2015;2015:186904.
89. Jiang L, Liu X, Chen Z, Jin Y, Heidbreder CE, Kolokythas A, et al. MicroRNA-7 targets IGF1R (insulin-like growth factor 1 receptor) in tongue squamous cell carcinoma cells. Biochem J. 2010;432:199–205.
90. Shen Z, Qin X, Yan M, Li R, Chen G, Zhang J, et al. Cancer-associated fibroblasts promote cancer cell growth through a miR-7-RASSF2-PAR-4 axis in the tumor microenvironment. Oncotarget. 2017;8:1290–303.
91. De Sarkar N, Roy R, Mitra JK, Ghose S, Chakraborty A, Paul RR, et al. A quest for miRNA bio-marker: a track back approach from gingivo buccal cancer to two different types of precancers. PLoS One. 2014;9:e104839.
92. Sasahira T, Kurihara M, Bhawal UK, Ueda N, Shimomoto T, Yamamoto K, et al. Downregulation of miR-126 induces angiogenesis and lymphangiogenesis by activation of VEGF-A in oral cancer. Br J Cancer. 2012;107:700–6.
93. Yang X, Wu H, Ling T. Suppressive effect of microRNA-126 on oral squamous cell carcinoma in vitro. Mol Med Rep. 2014;10:125–30.
94. Gasche JA, Goel A. Epigenetic mechanisms in oral carcinogenesis. Future Oncol. 2012;8:1407–25.
95. Saranath D, Chang SE, Bhoite LT, Panchal RG, Kerr IB, Mehta AR, et al. High frequency mutation in codons 12 and 61 of H-ras oncogene in chewing tobacco-related human oral carcinoma in India. Br J Cancer. 1991;63:573–8.
96. Moazeni-Roodi A, Allameh A, Harirchi I, Motiee-Langroudi M, Garajei A. Studies on the contribution of Cox-2 expression in the progression of oral squamous cell carcinoma and H-Ras activation. Pathol Oncol Res. 2017;23:355–60.
97. Murugan AK, Munirajan AK, Tsuchida N. Ras oncogenes in oral cancer: the past 20 years. Oral Oncol. 2012;48:383–92.
98. Li XF, Yin XH, Cai JW, Wang MJ, Zeng YQ, Li M, et al. Significant association between lncRNA H19 polymorphisms and cancer susceptibility: a meta-analysis. Oncotarget. 2017;8:45143–53.
99. Zhang DM, Lin ZY, Yang ZH, Wang YY, Wan D, Zhong JL, et al., editors. IncRNA H19 promotes tongue squamous cell carcinoma progression through β-catenin/GSK3β/EMT signaling via association with EZH2. Am J Transl Res. 2017;9:3474–86.
100. Kim KH, Roberts CW. Targeting EZH2 in cancer. Nat Med. 2016;22:128–34.
101. Matouk IJ, Halle D, Raveh E, Gilon M, Sorin V, Hochberg A. The role of the oncofetal H19 lncRNA in tumor metastasis: orchestrating the EMT-MET decision. Oncotarget. 2016;7:3748–65.
102. Zhou J, Yang L, Zhong T, Mueller M, Men Y, Zhang N, et al. H19 lncRNA alters DNA methylation genome wide by regulating S-adenosylhomocysteine hydrolase. Nat Commun. 2015;6:10221.
103. Zhong T, Men Y, Lu L, Geng T, Zhou J, Mitsuhashi A, et al. Metformin alters DNA methylation genome-wide via the H19/SAHH axis. Oncogene. 2017;36:2345–54.
104. Chang SM, Hu WW. Long non-coding RNA MALAT1 promotes oral squamous cell carcinoma development via microRNA-125b/STAT3 axis. J Cell Physiol. 2018;233:3384–96.
105. Zhang TH, Liang LZ, Liu XL, Wu JN, Su K, Chen JY, et al. Long non-coding RNA MALAT1 interacts with miR-124 and modulates tongue cancer growth by targeting JAG1. Oncol Rep. 2017;37:2087–94.
106. Liang J, Liang L, Ouyang K, Li Z, Yi X. MALAT1 induces tongue cancer cells' EMT and inhibits apoptosis through Wnt/β-catenin signaling pathway. J Oral Pathol Med. 2017;46:98–105.
107. Zhou X, Liu S, Cai G, Kong L, Zhang T, Ren Y, et al. Long non coding RNA MALAT1 promotes tumor growth and metastasis by inducing epithelial-mesenchymal transition in oral squamous cell carcinoma. Sci Rep. 2015;5:15972.
108. Fang Z, Zhang S, Wang Y, Shen S, Wang F, Hao Y, et al. Long non-coding RNA MALAT-1 modulates metastatic potential of tongue squamous cell carcinomas partially through the regulation of small proline rich proteins. BMC Cancer. 2016;16:706.
109. Ramos-García P, Gil-Montoya JA, Scully C, Ayén A, González-Ruiz L, Navarro-Triviño FJ, et al. An update on the implications of cyclin D1 in oral carcinogenesis. Oral Dis. 2017;23:897–912.
110. van Kempen PM, Noorlag R, Braunius WW, Moelans CB, Rifi W, Savola S, et al. Clinical relevance of copy number profiling in oral and oropharyngeal squamous cell carcinoma. Cancer Med. 2015;4:1525–35.
111. Akervall J, Borg A, Dictor M, Jin C, Jin Y, Tanner M, et al. Chromosomal translocations involving 11q13 contribute to cyclin D1 overexpression in squamous cell carcinoma of the head and neck. Int J Oncol. 2002;20:45–52.
112. Sathyan KM, Nalinakumari KR, Abraham T, Kannan S. CCND1 polymorphisms (A870G and C1722G) modulate its protein expression and survival in oral carcinoma. Oral Oncol. 2008;44:689–97.

113. Saawarn S, Astekar M, Saawarn N, Dhakar N, Sagari SG. Cyclin D1 expression and its correlation with histopathological differentiation in oral squamous cell carcinoma. Sci World J. 2012;2012:978327.
114. Angadi PV, Krishnapillai R. Cyclin D1 expression in oral squamous cell carcinoma and verrucous carcinoma: correlation with histological differentiation. Oral Surg Oral Med Oral Pathol Oral Radiol Endod. 2007;103:e30–5.
115. Zhao Y, Dedong Y, Li H, Nie P, Zhu Y, Liu S, et al. Cyclin D1 overexpression is associated with poor clinicopathological outcome and survival in oral squamous cell carcinoma in asian populations: insights from a meta-analysis. PLoS One. 2014;9:e93210.
116. Bau DT, Chang CH, Tsai MH, Chiu CF, Tsou YA, Wang RF, et al. Association between DNA repair gene ATM polymorphisms and oral cancer susceptibility. Laryngoscope. 2010;120:2417–22.
117. Ma X, Sheng S, Jingbiao W, Jiang Y, Gao X, Cen X, et al. LncRNAs as an intermediate in HPV16 promoting myeloid-derived suppressor cell recruitment of head and neck squamous cell carcinoma. Oncotarget. 2017;8:42061–75.
118. Min SN, Wei T, Wang XT, Wu LL, Yu GY. Clinicopathological and prognostic significance of homeobox transcript antisense RNA expression in various cancers: a meta-analysis. Medicine (Baltimore). 2017;96:e7084.
119. Li D, Feng J, Wu T, Wang Y, Sun Y, Ren J, et al. Long intergenic noncoding RNA HOTAIR is overexpressed and regulates PTEN methylation in laryngeal squamous cell carcinoma. Am J Pathol. 2013;182:64–70.
120. Li X, Wu Z, Mei Q, Li X, Guo M, Fu X, et al. Long non-coding RNA HOTAIR, a driver of malignancy, predicts negative prognosis and exhibits oncogenic activity in oesophageal squamous cell carcinoma. Br J Cancer. 2013;109:2266–78.
121. Wu J, Xie H. Expression of long noncoding RNA-HOX transcript antisense intergenic RNA in oral squamous cell carcinoma and effect on cell growth. Tumour Biol. 2015;36:8573–8.
122. Wu Y, Zhang L, Zhang L, Wang Y, Li H, Ren X, et al. Long non-coding RNA HOTAIR promotes tumor cell invasion and metastasis by recruiting EZH2 and repressing E-cadherin in oral squamous cell carcinoma. Int J Oncol. 2015;46:2586–94.
123. Lesseur C, Diergaarde B, Olshan AF, Wünsch-Filho V, Ness AR, Liu G, et al. Genome-wide association analyses identify new susceptibility loci for oral cavity and pharyngeal cancer. Nat Genet. 2016;48:1544–50.
124. Williams HK. Molecular pathogenesis of oral squamous cell carcinoma. Mol Pathol. 2000;53:165–72.
125. Efthymios ARVANITIDIS, Pavlos ANDREADIS, Dimitrios ANDREADIS, Maria BELAZI, Apostolos EPIVATIANOS. Reviewing the oral carcinogenic process: key genetic events, growth factors and molecular signaling pathways. J Biol Res-Thessaloniki. 2011;16:313–36.
126. Philipone E, Yoon AJ, Wang S, Shen J, Ko YC, Sink JM, et al. MicroRNAs-208b-3p, 204-5p, 129-2-3p and 3065-5p as predictive markers of oral leukoplakia that progress to cancer. Am J Cancer Res. 2016;6:1537–46.
127. Wiklund ED, Gao S, Hulf T, Sibbritt T, Nair S, Costea DE, et al. MicroRNA Alterations and Associated Aberrant DNA Methylation Patterns across Multiple Sample Types in Oral Squamous Cell Carcinoma. PLoS One. 2011;6:e27840.
128. Lajer CB, Nielsen FC, Friis-Hansen L, Norrild B, Borup R, Garnæs E, et al. Different miRNA signatures of oral and pharyngeal squamous cell carcinomas: a prospective translational study. Br J Cancer. 2011;104:830–40.
129. Mondal T, Subhash S, Vaid R, Enroth S, Uday S, Reinius B, et al. MEG3 long noncoding RNA regulates the TGF-β pathway genes through formation of RNA-DNA triplex structures. Nat Commun. 2015;6:7743.
130. Liu Z, Wu C, Xie N, Wang P. LongnoncodingRNAMEG3inhibits the proliferation and metastasis of oral squamous cell carcinoma by regulating the WNT/β-catenin signaling pathway. Oncol Lett. 2017;14:4053–8.
131. Pimenta FJ, Gomes DA, Perdigão PF, Barbosa AA, Romano-Silva MA, Gomez MV, et al. Characterization of the tumor suppressor gene WWOX in primary human oral squamous cell carcinomas. Int J Cancer. 2006;118:1154–8.
132. Cheng HL, Liu YF, Su CW, Su SC, Chen MK, Yang SF, et al. Functional genetic variant in the Kozak sequence of WW domain-containing oxidoreductase (WWOX) gene is associated with oral cancer risk. Oncotarget. 2016;7:69384–96.
133. Pimenta FJ, Cordeiro GT, Pimenta LG, Viana MB, Lopes J, Gomez MV, et al. Molecular alterations in the tumor suppressor gene WWOX in oral leukoplakias. Oral Oncol. 2008;44:753–8.
134. Dincer N, Tezel GG, Sungur A, Himmetoglu C, Huebner K, Güler G. Study of FHIT and WWOX expression in mucoepidermoid carcinoma and adenoid cystic carcinoma of salivary gland. Oral Oncol. 2010;46:195–9.
135. Gomes CC, Diniz MG, Oliveira CS, Tavassoli M, Odell EW, Gomez RS, et al. Impact of WWOX alterations on p73, ΔNp73, p53, cell proliferation and DNA ploidy in salivary gland neoplasms. Oral Dis. 2011;17:564–71.
136. Tsai CW, Lai FJ, Sheu HM, Lin YS, Chang TH, Jan MS, et al. WWOX suppresses autophagy for inducing apoptosis in methotrexate-treated human squamous cell carcinoma. Cell Death Dis. 2013;4:e792.
137. Wong TS, Liu XB, Wong BY, Ng RW, Yuen AP, Wei WI. Mature miR-184 as Potential Oncogenic microRNA of Squamous Cell Carcinoma of Tongue. Clin Cancer Res. 2008;14:2588–92.

138. Santhi WS, Prathibha R, Charles S, Anurup KG, Reshmi G, Ramachandran S, et al. Oncogenic microRNAs as biomarkers of oral tumorigenesis and minimal residual disease. Oral Oncol. 2013;49:567–75.
139. Manikandan M, Deva Magendhra Rao AK, Rajkumar KS, Rajaraman R, Munirajan AK. Altered levels of miR-21, miR-125b-2*, miR-138, miR-155, miR-184, and miR-205 in oral squamous cell carcinoma and association with clinicopathological characteristics. J Oral Pathol Med. 2015;44:792–800.
140. Lu L, Xue X, Lan J, Gao Y, Xiong Z, Zhang H, et al. MicroRNA-29a upregulates MMP2 in oral squamous cell carcinoma to promote cancer invasion and anti-apoptosis. Biomed Pharmacother. 2014;68:13–9.
141. Pannone G, Santoro A, Feola A, Bufo P, Papagerakis P, Lo Muzio L, et al. The role of E-cadherin downregulation in oral cancer: CDH1 gene expression and epigenetic blockage. Curr Cancer Drug Targets. 2014;14:115–27.
142. Heinzel PA, Balaram P, Bernard HU. Mutations and polymorphisms in the p53, p21 and p16 genes in oral carcinomas of Indian betel quid chewers. Int J Cancer. 1996;68:420–3.
143. Poeta ML, Manola J, Goldwasser MA, Forastiere A, Benoit N, Califano JA, et al. TP53 mutations and survival in squamous-cell carcinoma of the head and neck. N Engl J Med. 2007;357:2552–61.
144. Li Y, Zhang J. Expression of mutant p53 in oral squamous cell carcinoma is correlated with the effectiveness of intra-arterial chemotherapy. Oncol Lett. 2015;10:2883–7.
145. Wang W, Peng B, Wang D, Ma X, Jiang D, Zhao J, et al. Human tumor microRNA signatures derived from large-scale oligonucleotide microarray datasets. Int J Cancer. 2011;129:1624–34.
146. Zhang J, Qin X, Sun Q, Guo H, Wu X, Xie F, et al. Transcriptional control of PAX4-regulated miR-144/451 modulates metastasis by suppressing ADAMs expression. Oncogene. 2015;34:3283–95.
147. Hedbäck N, Jensen DH, Specht L, Fiehn AM, Therkildsen MH, Friis-Hansen L, et al. MiR-21 expression in the tumor stroma of oral squamous cell carcinoma: an independent biomarker of disease free survival. PLoS One. 2014;9:e95193.
148. Li L, Li C, Wang S, Wang Z, Jiang J, Wang W, et al. Exosomes derived from hypoxic oral squamous cell carcinoma cells deliver miR-21 to normoxic cells to elicit a prometastatic phenotype. Cancer Res. 2016;76:1770–80.
149. Zhou X, Ren Y, Moore L, Mei M, You Y, Xu P, et al. Downregulation of miR-21 inhibits EGFR pathway and suppresses the growth of human glioblastoma cells independent of PTEN status. Lab Investig. 2010;90:144–55.
150. Cervigne NK, Reis PP, Machado J, Sadikovic B, Bradley G, Galloni NN, et al. Identification of a microRNA signature associated with progression of leukoplakia to oral carcinoma. Hum Mol Genet. 2009;18:4818–29.
151. Supic G, Zeljic K, Rankov AD, Kozomara R, Nikolic A, Radojkovic D, et al. miR-183 and miR-21 expression as biomarkers of progression and survival in tongue carcinoma patients. Clin Oral Investig. 2018;22:401–9.
152. Yan ZY, Luo ZQ, Zhang LJ, Li J, Liu JQ. Integrated analysis and microRNA expression profiling identified seven miRNAs associated with progression of oral squamous cell carcinoma. J Cell Physiol. 2017;232:2178–85.
153. Jung HM, Phillips BL, Patel RS, Cohen DM, Jakymiw A, Kong WW, et al. Keratinization-associated miR-7 and miR-21 regulate tumor suppressor reversion-inducing cysteine-rich protein with kazal motifs (RECK) in oral cancer. J Biol Chem. 2012;287:29261–72.
154. Yu EH, Tu HF, Wu CH, Yang CC, Chang KW. MicroRNA-21 promotes perineural invasion and impacts survival in patients with oral carcinoma. J Chin Med Assoc. 2017;80:383–8.
155. Kowshik J, Mishra R, Sophia J, Rautray S, Anbarasu K, Reddy GD. Nimbolide upregulates RECK by targeting miR-21 and HIF-1α in cell lines and in a hamster oral carcinogenesis model. Sci Rep. 2017;7:2045.
156. Yip KW, Reed JC. Bcl-2 family proteins and cancer. Oncogene. 2008;27:6398–406.
157. Cory S, Huang DC, Adams JM. The Bcl-2family: roles in cell survival and oncogenesis. Oncogene. 2003;22:8590–607.
158. Gibson SA, Pellenz C, Hutchison RE, Davey FR, Shillitoe EJ. Induction of apoptosis in oral cancer cells by an anti-bcl-2 ribozyme delivered by an adenovirus vector. Clin Cancer Res. 2000;6:213–22.
159. Yang YT, Wang YF, Lai JY, Shen SY, Wang F, Kong J, et al. Long non-coding RNA UCA1 contributes to the progression of oral squamous cell carcinoma by regulating the WNT/β-catenin signaling pathway. Cancer Sci. 2016;107:1581–9.
160. Liang S, Zhang S, Wang P, Yang C, Shang C, Yang J, et al. LncRNA, TUG1 regulates the oral squamous cell carcinoma progression possibly via interacting with Wnt/β-catenin signaling. Gene. 2017;608:49–57.
161. Li ZQ, Zou R, Ouyang KX, Ai WJ. An in vitro study of the long non-coding RNA TUG1 in tongue squamous cell carcinoma. J Oral Pathol Med. 2017;46:956–60.
162. Castagnola P, Malacarne D, Scaruffi P, Maffei M, Donadini A, Di Nallo E, et al. Chromosomal aberrations and aneuploidy in oral potentially malignant lesions: distinctive features for tongue. BMC Cancer. 2011;11:445.
163. Ribeiro IP, Marques F, Caramelo F, Pereira J, Patrício M, Prazeres H, et al. Genetic gains and losses in oral squamous cell carcinoma: impact on clinical management. Cell Oncol (Dordr). 2014;37:29–39.

164. Shridhar K, Aggarwal A, Walia GK, Gulati S, Geetha AV, Prabhakaran D, et al. Single nucleotide polymorphisms as markers of genetic susceptibility for oral potentially malignant disorders risk: review of evidence to date. Oral Oncol. 2016;61:146–51.
165. Multani S, Saranath D. Genotypic distribution of single nucleotide polymorphisms in oral cancer: global scene. Tumour Biol. 2016;37:14501–12. Epub 2016 Sep 20
166. Hsu HJ, Yang YH, Shieh TY, Chen CH, Kao YH, Yang CF, et al. TGF-β1 and IL-10 single nucleotide polymorphisms as risk factors for oral cancer in Taiwanese. Kaohsiung J Med Sci. 2015;31:123–9.
167. Chou CH, Hsieh MJ, Chuang CY, Lin JT, Yeh CM, Tseng PY, et al. Functional FGFR4 Gly388Arg polymorphism contributes to oral squamous cell carcinoma susceptibility. Oncotarget. 2017;8: 96225–38.
168. Sun W, Lv W, Lv H, Zhang R, Jiang Y. Genome-wide haplotype association analysis identifies SERPINB9, SERPINE2, GAK, and HSP90B1 as novel risk genes for oral squamous cell carcinoma. Tumour Biol. 2016;37:1845–51.
169. Hsieh CH, Chang JW, Hsieh JJ, Hsu T, Huang SF, Liao CT, et al. Epidermal growth factor receptor mutations in patients with oral cavity cancer in a betel nut chewing-prevalent area. Head Neck. 2011;33:1758–64.
170. Xie X, Wang Z, Chen F, Yuan Y, Wang J, Liu R, Chen Q. Roles of FGFR in oral carcinogenesis. Cell Prolif. 2016;49:261–9.
171. Brands RC, Köhler O, Rauthe S, Hartmann S, Ebhardt H, Seher A, et al. The prognostic value of GLUT-1 staining in the detection of malignant transformation in oral mucosa. Clin Oral Investig. 2017;21:1631–7.
172. Chen C, Shin JH, Eggold JT, Chung MK, Zhang LH, Lee J. ESM1 mediates NGFR-induced invasion and metastasis in murine oral squamous cell carcinoma. Oncotarget. 2016;7:70738–49.
173. Nayak S, Goel MM, Makker A, Bhatia V, Chandra S, Kumar S, et al. Fibroblast growth factor (FGF-2) and its receptors FGFR-2 and FGFR-3 may be putative biomarkers of malignant transformation of potentially malignant oral lesions into oral squamous cell carcinoma. PLoS One. 2015;10:e0138801.
174. Lin Q, Ma L, Liu Z, Yang Z, Wang J, Liu J, Jiang G. Targeting microRNAs: a new action mechanism of natural compounds. Oncotarget. 2017;8:15961–70.
175. Al-Kaabi A, van Bockel LW, Pothen AJ, Willems SM. $p16^{INK4A}$ and $p14^{ARF}$ gene promoter hypermethylation as prognostic biomarker in oral and oropharyngeal squamous cell carcinoma: a review. Dis Markers. 2014;2014:260549.
176. Edwards JR, Yarychkivska O, Boulard M, Bestor TH. DNA methylation and DNA methyltransferases. Epigenetics Chromatin. 2017;10:23.
177. Soga D, Yoshiba S, Shiogama S, Miyazaki H, Kondo S, Shintani S. microRNA expression profiles in oral squamous cell carcinoma. Oncol Rep. 2013;30:579–83.
178. Gomes CC, de Sousa SF, Calin GA, Gomez RS. The emerging role of long noncoding RNAs in oral cancer. Oral Surg Oral Med Oral Pathol Oral Radiol. 2017;123:235–41.
179. Lewis BP, Burge CB, Bartel DP. Conserved seed pairing, often flanked by adenosines, indicates that thousands of human genes are microRNA targets. Cell. 2005;120:15–20.
180. Manasa VG, Kannan S. Impact of microRNA dynamics on cancer hallmarks: an oral cancer scenario. Tumour Biol. 2017;39:1010428317695920.
181. Hung KF, Liu CJ, Chiu PC, Lin JS, Chang KW, Shih WY, et al. MicroRNA-31 upregulation predicts increased risk of progression of oral potentially malignant disorder. Oral Oncol. 2016;53:42–7.
182. Hung PS, Chang KW, Kao SY, Chu TH, Liu CJ, Lin SC. Association between the rs2910164 polymorphism in pre-mir-146a and oral carcinoma progression. Oral Oncol. 2012;48:404–8.
183. Liu CJ, Shen WG, Peng SY, Cheng HW, Kao SY, Lin SC, et al. miR-134inducesoncogenicity and metastasis in head and neck carcinoma through targeting WWOX gene. Int J Cancer. 2014;134:811–21.
184. Kinouchi M, Uchida D, Kuribayashi N, Tamatani T, Nagai H, Miyamoto Y. Involvement of miR-518c-5p to growth and metastasis in oral cancer. PLoS One. 2014;9:e115936.
185. Gelmini S, Mangoni M, Serio M, Romagnani P, Lazzeri E. The critical role of SDF-1/CXCR4 axis in cancer and cancer stem cells metastasis. J Endocrinol Investig. 2008;31:809–19.
186. Kasamatsu A, Endo Y, Uzawa K, Nakashima D, Koike H, Hashitani S, et al. Identification of candidate genes associated with salivary adenoid cystic carcinomas using combined comparative genomic hybridization and oligonucleotide microarray analyses. Int J Biochem Cell Biol. 2005;37:1869–80.
187. Nobusawa S, Yokoo H, Hirato J, Kakita A, Takahashi H, Sugino T, Tasaki K, et al. Analysis of chromosome 19q13.42 amplification in embryonal brain tumors with ependymoblastic multilayered rosettes. Brain Pathol. 2012;22:689–97.
188. Tiwari A, Shivananda S, Gopinath KS, Kumar A. MicroRNA-125a reduces proliferation and invasion of oral squamous cell carcinoma cells by targeting estrogen-related receptor α. J Biol Chem. 2014;289:32276–90.
189. Huang WC, Chan SH, Jang TH, Chang JW, Ko YC, Yen TC, et al. miRNA-491-5p and GIT1 serve as modulators and biomarkers for oral squamous cell carcinoma invasion and metastasis. Cancer Res. 2014;74:751–64.
190. Coutinho-Camillo CM, Lourenço SV, de Araújo Lima L, Kowalski LP, Soares FA. Expression of apoptosis-regulating miRNAs and target mRNAs in oral squamous cell carcinoma. Cancer Gene Ther. 2015;208:382–9.

191. Serrano NA, Xu C, Liu Y, Wang P, Fan W, Upton MP, Houck JR, et al. Integrative analysis in oral squamous cell carcinoma reveals DNA copy number-associated miRNAs dysregulating target genes. Otolaryngol Head Neck Surg. 2012;147:501–8.
192. Roy R, De Sarkar N, Ghose S, Paul RR, Pal M, Bhattacharya C, et al. Genetic variations at microRNA and processing genes and risk of oral cancer. Tumour Biol. 2014;35:3409–14.
193. Yu T, Wang XY, Gong RG, Li A, Yang S, Cao YT, et al. The expression profile of microRNAs in a model of 7,12-dimethyl-benz[a]anthrance-induced oral carcinogenesis in Syrian hamster. J Exp Clin Cancer Res. 2009;28:64.
194. Maclellan SA, Lawson J, Baik J, Guillaud M, Poh CF, Garnis C. Differential expression of miRNAs in the serum of patients with high-risk oral lesions. Cancer Med. 2012;1:268–74.
195. Hunt S, Jones AV, Hinsley EE, Whawell SA, Lambert DW. MicroRNA-124 suppresses oral squamous cell carcinoma motility by targeting ITGB1. FEBS Lett. 2011;585:187–92.
196. Zhao Y, Ling Z, Hao Y, Pang X, Han X, Califano JA, et al. MiR-124 acts as a tumor suppressor by inhibiting the expression of sphingosine kinase 1 and its downstream signaling in head and neck squamous cell carcinoma. Oncotarget. 2017;8:25005–20.
197. Hu H, Wang G, Li C. miR-124 suppresses proliferation and invasion of nasopharyngeal carcinoma cells through the Wnt/β-catenin signaling pathway by targeting Capn4. Onco Targets Ther. 2017;10: 2711–20.
198. Chen Z, Jin Y, Yu D, Wang A, Mahjabeen I, Wang C, et al. Down-regulation of the microRNA-99 family members in head and neck squamous cell carcinoma. Oral Oncol. 2012;48:686–91.
199. Chen D, Chen Z, Jin Y, Dragas D, Zhang L, Adjei BS, et al. MicroRNA-99 family members suppress Homeobox A1 expression in epithelial cells. PLoS One. 2013;8:e80625.
200. Yen YC, Shiah SG, Chu HC, Hsu YM, Hsiao JR, Chang JY, et al. Reciprocal regulation of microRNA-99a and insulin-like growth factor I receptor signaling in oral squamous cell carcinoma cells. Mol Cancer. 2014;13:6.
201. Yan B, Fu Q, Lai L, Tao X, Fei Y, Shen J, et al. Downregulation of microRNA 99a in oral squamous cell carcinomas contributes to the growth and survival of oral cancer cells. Mol Med Rep. 2012;6:675–81.
202. Bamezai S, Rawat VP, Buske C. Concise review: the Piwi-piRNA axis—pivotal beyond transposon silencing. Stem Cells. 2012;30:2603–11.
203. Krishnan AR, Korrapati A, Zou AE, Qu Y, Wang XQ, Califano JA, et al. Smoking status regulates a novel panel of PIWI-interacting RNAs in head and neck squamous cell carcinoma. Oral Oncol. 2017;65:68–75.
204. Firmino N, Martinez VD, Rowbotham DA, Enfield KSS, Bennewith KL, Lam WL. HPV status is associated with altered PIWI-interacting RNA expression pattern in head and neck cancer. Oral Oncol. 2016;55:43–8.
205. Chen L, Zhang S, Wu J, Cui J, Zhong L, Zeng L, et al. circRNA_100290 plays a role in oral cancer by functioning as a sponge of the miR-29 family. Oncogene. 2017;36:4551–61.
206. Li X, Cao Y, Gong X, Li H. Long noncoding RNAs in head and neck cancer. Oncotarget. 2017;8:10726–40.
207. Nohata N, Abba MC, Gutkind JS. Unraveling the oral cancer lncRNAome: identification of novel lncRNAs associated with malignant progression and HPV infection. Oral Oncol. 2016;59:58–66.
208. Feng L, Houck JR, Lohavanichbutr P, Chen C. Transcriptome analysis reveals differentially expressed lncRNAs between oral squamous cell carcinoma and healthy oral mucosa. Oncotarget. 2017;8:31521–31.
209. Gao W, Chan JY, Wong TS. Long non-coding RNA deregulation in tongue squamous cell carcinoma. Biomed Res Int. 2014;2014:405860.
210. Ballarino M, Cazzella V, D'Andrea D, Grassi L, Bisceglie L, Cipriano A, et al. Novel long noncoding RNAs (lncRNAs) in myogenesis: a miR-31 overlapping lncRNA transcript controls myoblast differentiation. Mol Cell Biol. 2015;35:728–36.
211. Yang H, Liu P, Zhang J, Peng X, Lu Z, Yu S, et al. Long noncoding RNA MIR31HG exhibits oncogenic property in pancreatic ductal adenocarcinoma and is negatively regulated by miR-193b. Oncogene. 2016;35:3647–57.
212. Montes M, Nielsen MM, Maglieri G, Jacobsen A, Højfeldt J, Agrawal-Singh S, et al. The lncRNA MIR31HG regulates p16(INK4A) expression to modulate senescence. Nat Commun. 2015;6: 6967.
213. Pawson T, Warner N. Oncogenic re-wiring of cellular signaling pathways. Oncogene. 2007;26:1268–75.
214. Yedida GR, Nagini S, Mishra R. The importance of oncogenic transcription factors for oral cancer pathogenesis and treatment. Oral Surg Oral Med Oral Pathol Oral Radiol. 2013;116:179–88.
215. Wu F, Weigel KJ, Wang XJ. Paradoxical roles of TGF-β signaling in suppressing and promoting squamous cell carcinoma. Acta Biochim Biophys Sin Shanghai. 2017;50:1–8.
216. Nagini S, Tanagala KKK, Chattopadhyay I. NF-κB inhibitors in head and neck cancer. Lett Drug Des Discov. 2017;14(5):619.
217. Huang W, Cui X, Chen J, Feng Y, Song E, Li J, et al. Long non-coding RNA NKILA inhibits migration and invasion of tongue squamous cell carcinoma cells via suppressing epithelial-mesenchymal transition. Oncotarget. 2016;7:62520–32.
218. Shiah SG, Shieh YS, Chang JY. The role of wnt signaling in squamous cell carcinoma. J Dent Res. 2016;95:129–34.
219. González-Moles MA, Ruiz-Ávila I, Gil-Montoya JA, Plaza-Campillo J, Scully C. β-catenin in oral

cancer: an update on current knowledge. Oral Oncol. 2014;50:818–24.
220. Tsuchiya R, Yamamoto G, Nagoshi Y, Aida T, Irie T, Tachikawa T. Expression of adenomatous polyposis coli (APC) in tumorigenesis of human oral squamous cell carcinoma. Oral Oncol. 2004;40:932–40.
221. Ishida K, Ito S, Wada N, Deguchi H, Hata T, Hosoda M, Nohno T. Nuclear localization of beta-catenin involved in precancerous change in oral leukoplakia. Mol Cancer. 2007;6:62.
222. Mishra R, Nagini S, Rana A. Expression and inactivation of glycogen synthase kinase 3 alpha/ beta and their association with the expression of cyclin D1 and p53 in oral squamous cell carcinoma progression. Mol Cancer. 2015;14:20.
223. Gkouveris I, Nikitakis NG. Role of JNK signaling in oral cancer: a mini review. Tumour Biol. 2017;39:1010428317711659.
224. Cash H, Shah S, Moore E, Caruso A, Uppaluri R, Van Waes C, et al. mTOR and MEK1/2 inhibition differentially modulate tumor growth and the immune microenvironment in syngeneic models of oral cavity cancer. Oncotarget. 2015;6: 36400–17.
225. Aktipis CA, Boddy AM, Jansen G, Hibner U, Hochberg ME, Maley CC, et al. Cancer across the tree of life: cooperation and cheating in multicellularity. Philos Trans R Soc Lond Ser B Biol Sci. 2015;370:20140219.
226. Saunders WS, Shuster M, Huang X, Gharaibeh B, Enyenihi AH, Petersen I, et al. Chromosomal instability and cytoskeletal defects in oral cancer cells. Proc Natl Acad Sci U S A. 2000;97:303–8.
227. Thirthagiri E, Robinson CM, Huntley S, Davies M, Yap LF, Prime SS, et al. Spindle assembly checkpoint and centrosome abnormalities in oral cancer. Cancer Lett. 2007;258:276–85.
228. Mondal G, Sengupta S, Panda CK, Gollin SM, Saunders WS, Roychoudhury S. Overexpression of Cdc20 leads to impairment of the spindle assembly checkpoint and aneuploidization in oral cancer. Carcinogenesis. 2007;28:81–9.
229. Okamoto A, Higo M, Shiiba M, Nakashima D, Koyama T, Miyamoto I, et al. Down-regulation of nucleolar and spindle-associated Protein 1 (NUSAP1) expression suppresses tumor and cell proliferation and enhances anti-tumor effect of paclitaxel in oral squamous cell carcinoma. PLoS One. 2015;10:e0142252.
230. Gramatges MM, Bertuch AA. Short telomeres: from dyskeratosis congenita to sporadic aplastic anemia and malignancy. Transl Res. 2013;162:353–63.
231. Bertuch AA. The molecular genetics of the telomere biology disorders. RNA Biol. 2016;13:696–706.
232. Rai A, Naikmasur VG, Sattur A. Quantification of telomerase activity in normal oral mucosal tissue and oral squamous cell carcinoma. Indian J Med PaediatrOncol. 2016;37:183–8.
233. Raghunandan BN, Sanjai K, Kumaraswamy J, Papaiah L, Pandey B, Jyothi BM. Expression of human telomerase reverse transcriptase protein in oral epithelial dysplasia and oral squamous cell carcinoma: an immunohistochemical study. J Oral MaxillofacPathol. 2016;20:96–101.
234. Benhamou Y, Picco V, Pagès G. The telomere proteins in tumorigenesis and clinical outcomes of oral squamous cell carcinoma. Oral Oncol. 2016;57:46–53.
235. Loro LL, Johannessen AC, Vintermyr OK. Loss of BCL-2 in the progression of oral cancer is not attributable to mutations. J Clin Pathol. 2005;58: 1157–62.
236. Fillies T, Jogschies M, Kleinheinz J, Brandt B, Joos U, Buerger H. Cytokeratin alteration in oral leukoplakia and oral squamous cell carcinoma. Oncol Rep. 2007;18:639–43.
237. Fillies T, Werkmeister R, Packeisen J, Brandt B, Morin P, Weingart D, et al. Cytokeratin 8/18 expression indicates a poor prognosis in squamous cell carcinomas of the oral cavity. BMC Cancer. 2006;6:10.
238. ohnishi Y, watanabe M, yasui H, kakudo K. Effects of epidermal growth factor on the invasive activity and cytoskeleton of oral squamous cell carcinoma cell lines. Oncol Lett. 2014;7:1439–42.
239. Ogden GR, Lane EB, Hopwood DV, Chisholm DM. Evidence for field change in oral cancer based on cytokeratin expression. Br J Cancer. 1993;67:1324–30.
240. Ogden GR, McQueen S, Chisholm DM, Lane EB. Keratin profiles of normal and malignant oral mucosa using exfoliative cytology. J Clin Pathol. 1993;46:352–6.
241. Alblazi KM, Siar CH. Cellular protrusions--lamellipodia, filopodia, invadopodia and podosomes--and their roles in progression of orofacial tumours: current understanding. Asian Pac J Cancer Prev. 2015;16:2187–91.
242. Saito S, Yamamoto H, Mukaisho K-i, Sato S, Higo T, Hattori T, et al. Mechanisms underlying cancer progression caused by ezrin overexpression in tongue squamous cell carcinoma. PLoS One. 2013;8:e54881.
243. Collins RJ, Jiang WG, Hargest R, Mason MD, Sanders AJ. EPLIN: a fundamental actin regulator in cancer metastasis? Cancer Metastasis Rev. 2015;34:753–64.
244. Bretscher A, Edwards K, Fehon RG. ERM proteins and merlin: integrators at the cell cortex. Nat Rev Mol Cell Biol. 2002;3:586–99.
245. Schlecht NF, Brandwein-Gensler M, Smith RV, Kawachi N, Broughel D, Lin J, et al. Cytoplasmic ezrin and moesin correlate with poor survival in head and neck squamous cell carcinoma. Head Neck Pathol. 2012;6:232–43.
246. Wheeler AP, Ridley AJ. Why three Rho proteins? RhoA, RhoB, RhoC, and cell motility. Exp Cell Res. 2004;301:43–9.
247. Li YY, Zhou CX, Gao Y. Snail regulates the motility of oral cancer cells via RhoA/Cdc42/

p-ERM pathway. Biochem Biophys Res Commun. 2014;452:490–6.
248. Thomas GJ, Speight PM. Cell adhesion molecules and oral cancer. Crit Rev Oral Biol Med. 2001;12:479–98.
249. Nagata M, Noman AA, Suzuki K, Kurita H, Ohnishi M, Ohyama T, et al. ITGA3 and ITGB4expressionbiomarkersestimate the risks of locoregional and hematogenous dissemination of oral squamous cell carcinoma. BMC Cancer. 2013;13:410.
250. Bandyopadhyay A, Raghavan S. Defining the Role of Integrin αvβ6 in Cancer. Curr Drug Targets. 2009;10:645–52.
251. Veeravarmal V, Austin RD, Nagini S, MHM N. Expression of β1integrin in normal epithelium, oral submucous fibrosis and oral squamous cell carcinoma. Pathol Res Pract. 2017;214: 273–80.
252. Luo SL, Xie YG, Li Z, Ma JH, Xu X. E-cadherin expression and prognosis of oral cancer: a meta-analysis. Tumour Biol. 2014;35:5533–7.
253. Krisanaprakornkit S, Iamaroon A. Epithelial-mesenchymal transition in oral squamous cell carcinoma. ISRN Oncol. 2012;2012:681469.
254. Qiao B, Johnson NW, Gao J. Epithelial-mesenchymal transition in oral squamous cell carcinoma triggered by transforming growth factor-beta1 is Snail family-dependent and correlates with matrix metalloproteinase-2 and -9 expressions. Int J Oncol. 2010;37:663–8.
255. Zhou J, Tao D, Xu Q, Gao Z, Tang D. Expression of E-cadherin and vimentin in oral squamous cell carcinoma. Int J Clin Exp Pathol. 2015;8:3150–4.
256. Nguyen PT, Kudo Y, Yoshida M, Kamata N, Ogawa I, Takata T. N-cadherin expression is involved in malignant behavior of head and neck cancer in relation to epithelial-mesenchymal transition. Histol Histopathol. 2011;26:147–56.
257. Lyons AJ, Jones J. Cell adhesion molecules, the extracellular matrix and oral squamous carcinoma. Int J Oral Maxillofac Surg. 2007;36:671–9.
258. Usami Y, Ishida K, Sato S, Kishino M, Kiryu M, Ogawa Y, et al. Intercellular adhesion molecule-1 (ICAM-1) expression correlates with oral cancer progression and induces macrophage/cancer cell adhesion. Int J Cancer. 2013;133:568–78.
259. Tang W, Wang Y, Chen Y, Haiyong G, Chen S, Kang M. Polymorphisms in the *intercellular adhesion molecule 1* gene and cancer risk: a meta-analysis. Int J Clin Exp Med. 2015;8:11996–2008.
260. Cheng D, Liang B. Intercellular adhesion molecule-1 (ICAM-1) polymorphisms and cancer risk: a meta-analysis. Iran J Public Health. 2015;44:615–24.
261. Pramanik KK, Nagini S, Singh AK, Mishra P, Kashyap T, Nath N, et al. Glycogen synthase kinase-3β mediated regulation of matrixmetalloproteinase-9 and its involvement in oral squamous cell carcinoma progression and invasion. Cell Oncol (Dordr). 2018;41:47–60.
262. Pereira AC, do Carmo ED, da Silva MAD, Rosa LEB. Matrix metalloproteinase gene polymorphisms and oral cancer. J Clin Exp Dent. 2012;4: e297–301.
263. Wong RJ, Keel SB, Glynn RJ, Varvares MA. Histological pattern of mandibular invasion by oral squamous cell carcinoma. Laryngoscope. 2000;110:65–72.
264. Shin M, Matsuo K, Tada T, Fukushima H, Furuta H, Ozeki S, Kadowaki T, Yamamoto K, Okamoto M, Jimi E. The inhibition of RANKL/RANK signaling by osteoprotegerin suppresses bone invasion by oral squamous cell carcinoma cells. Carcinogenesis. 2011;32:1634–40.
265. Cannonier SA, Gonzales CB, Ely K, Guelcher SA, Sterling JA. Hedgehog and TGFβ signaling converge on Gli2 to control bony invasion and bone destruction in oral squamous cell carcinoma. Oncotarget. 2016;7:76062–75.
266. Takes RP, Rinaldo A, Silver CE, Haigentz M Jr, Woolgar JA, Triantafyllou A et al. Distant metastases from head and neck squamous cell carcinoma. Part I. Basic aspects. Oral Oncol. 2012;48:775–9.
267. Martell K, Simpson R, Skarsgard D. Solitary myocardial metastasis from locoregionally controlled squamous cell carcinoma of the oral cavity. Cureus. 2016;8:e650.
268. Noguti J, De Moura CF, De Jesus GP, Da Silva VH, Hossaka TA, Oshima CT, et al. Metastasis from oral cancer: an overview. Cancer Genomics Proteomics. 2012;9:329–35.
269. Sano D, Myers JN. Metastasis of squamous cell carcinoma of the oral tongue. Cancer Metastasis Rev. 2007;26:645–62.
270. Parhar S, Kaur H, Vashist A, Verma S. Role of podoplanin in potentially malignant disorders and oral squamous cell carcinoma and its correlation with lymphangiogenesis. Indian J Cancer. 2015;52:617–22.
271. Assao A, Nonogaki S, Lauris JR, Carvalho AL, Pinto CA, Soares FA, et al. Podoplanin, ezrin, and Rho-A proteins may have joint participation in tumor invasion of lip cancer. Clin Oral Investig. 2017;21:1647–57.
272. Hanahan D, Weinberg RA. Hallmarks of cancer: the next generation. Cell. 2011;144:646–74.
273. Artese L, Rubini C, Ferrero G, Fioroni M, Santinelli A, Piattelli A. Microvessel density (MVD) and vascular endothelial growth factor expression (VEGF) in human oral squamous cell carcinoma. Anticancer Res. 2001;21:689–95.
274. Koontongkaew S. The tumor microenvironment contribution to development, growth, invasion and metastasis of head and neck squamous cell carcinomas. J Cancer. 2013;4:66–83.
275. Zetter BR. Angiogenesis and tumor metastasis. Annu Rev Med. 1998;49:407–24.
276. Shang ZJ, Li JR. Expression of endothelial nitric oxide synthase and vascular endothelial growth factor in oral squamous cell carcinoma: its correlation

with angiogenesis and disease progression. J Oral Pathol Med. 2005;34:134–9.
277. DE Lima PO, Jorge CC, Oliveira DT, Pereira MC. Hypoxic condition and prognosis in oral squamous cell carcinoma. Anticancer Res. 2014;34:605–12.
278. Fife CM, McCarroll JA, Kavallaris M. Movers and shakers: cell cytoskeleton in cancer metastasis. Br J Pharmacol. 2014;171:5507–23.
279. Balkwill F, Mantovani A. Inflammation and cancer: back to Virchow? Lancet. 2001;357:539–45.
280. Colotta F, Allavena P, Sica A, Garlanda C, Mantovani A. Cancer-related inflammation, the seventh hallmark of cancer: links to genetic instability. Carcinogenesis. 2009;30:1073–81.
281. Mantovani A, Garlanda C, Allavena P. Molecular pathways and targets in cancer-related inflammation. Ann Med. 2010;42:161–70.
282. Bredell MG, Ernst J, El-Kochairi I, Dahlem Y, Ikenberg K, Schumann DM. Current relevance of hypoxia in head and neck cancer. Oncotarget. 2016;7:50781–804.
283. Allavena P, Garlanda C, Borrello MG, Sica A, Mantovani A. Pathways connecting inflammation and cancer. Curr Opin Genet Dev. 2008;18:3–10.
284. Porta C, Larghi P, Rimoldi M, Totaro MG, Allavena P, Mantovani A, et al. Cellular and molecular pathways linking inflammation and cancer. Immunobiology. 2009;214:761–77.
285. Sarode SC, Sarode GS. Neutrophil-tumor cell cannibalism in oral squamous cell carcinoma. J Oral Pathol Med. 2014;43:454–8.
286. Sarode SC, Sarode GS, Chuodhari S, Patil S. Non-cannibalistic tumor cells of oral squamous cell carcinoma can express phagocytic markers. J Oral Pathol Med. 2017;46:327–31.
287. Sarode GS, Sarode SC, Karmarkar S. Complex cannibalism: an unusual finding in oral squamous cell carcinoma. Oral Oncol. 2012;48:e4–6.
288. Jose D, Mane DR, Datar U, Muttagi S, Hallikerimath S, Kale AD. Evaluation of cannibalistic cells: a novel entity in prediction of aggressive nature of oral squamous cell carcinoma. Acta Odontol Scand. 2014;72:418–23.

3 Epidemiology of Oral Cancer

José Manuel García-Martín, Pablo Varela-Centelles, Manuel González, Juan M. Seoane-Romero, Juan Seoane, and María José García-Pola

Abstract

Oral cancer represents a health problem worldwide due to its morbidity and mortality. The prevalence of oral cancer presents some variations around the world. These rates vary by as much as 20-fold among different countries, age groups, gender, races, and ethnic groups. Globally, the emergence of oral cancer is higher in male than female, and the risk increases with age. In 2013, oral cancer incidence ranked eleventh among all sites of cancer. The Indian subcontinent accounts for one-third of the oral cancer burden in the world. Oral cancer is the most common cancer among men in India and the second cancer among Pakistani women. The lowest rates are found in Western Africa and Eastern Asia. North African countries also present low incidences.

Surveillance of oral cavity and pharyngeal cancer at 5 years after diagnosis has estimated survival around 50% and for salivary gland carcinoma up to more than 85%.

Worldwide, the mortality rate of oral cancer was higher in male than in female. Death from oral cancer ranks fifteenth place for men and seventeenth for women in the US population. In Europe, it ranked the seventh and tenth, respectively.

The highest risk for lip cancer is experienced in Spain and in Australia and North America for salivary gland tumors. Globally, salivary gland malignant tumor is an infrequent carcinoma, and it is not considered among the tenth major cancers. Although in some developed countries oral cancer has decreased (the USA or Canada), in another, e.g., certain European countries, it has increased. Many of these differences are undoubtedly caused by differing population habits, life expectancies, preventive education, and the quality of medical records in various countries. These data can be helpful in identifying potential causative factors.

3.1 Introduction

Oral cancer represents a health problem worldwide due to its morbidity and mortality. The relevance of epidemiological knowledge in oral

J. M. García-Martín · M. González
M. J. García-Pola (✉)
Department of Surgery and Medical-Surgical Specialties, School of Medicine and Health Sciences, University of Oviedo, Oviedo, Spain
e-mail: mjgarcia@uniovi.es

P. Varela-Centelles
HULA, EOXI Lugo, Cervo, e Monforte de Lemos, Galician Health Service, Lugo, Spain
e-mail: pabloignacio.varela@usc.es

J. M. Seoane-Romero · J. Seoane
Stomatology Department, School of Medicine and Dentistry, University of Santiago de Compostela, Santiago de Compostela, Spain

P. Panta (ed.), *Oral Cancer Detection*, https://doi.org/10.1007/978-3-319-61255-3_3

cancer is mainly based upon the fact that 5-year survival rates have been reported to be about 50% [1, 2], being most of them diagnosed at an advanced stage (III), especially in developing countries [3].

The interpretation of data from epidemiological studies is sometimes difficult to read into. The term "oral cancer," in some reports, included all malignancies arising from the lips, oral cavity, oropharynx, nasopharynx, and hypopharynx, whereas other descriptions included just intraoral sites and pharynx. Head and neck cancer include cancers of the oral cavity, pharynx, and larynx. It has been documented that oral and pharyngeal cancer together were the sixth most common cancers in the world [4].

Besides, the *Cancer Incidence in Five Continents* (CI5) series published by the International Agency for Research on Cancer (IARC) and the International Association of Cancer Registries (IACR) presented data on oral cancer incidence for different countries around the world in all five continents. The IARC included, under the term oral cancer, malignant tumors localized in lip (COO), tongue, and salivary gland cancer. Tongue locations include the base of the tongue (C01) and other unspecified parts of the tongue (C02). The "mouth" includes the gum (C03), floor (C04), palate (C05), and other unspecified localization (C06)]. Finally, salivary gland cancer gathers parotid (C07) and other salivary gland (C08)]. The last volume of IARC, CI5 Volume X, provides data on cancer incidence in the locations mentioned above, for the period 2003–2007. These data were acquired from 68 countries, 290 registries, and accounting 424 million persons with a proportion of the population of 14% [5].

Another source of information on cancer incidence and mortality is the Surveillance, Epidemiology, and End Results (SEER) Programs with collaborations from the American Cancer Society (ACS), the Centers for Disease Control and Prevention (CDC), the National Cancer Institute (NCI), and the North American Association of Central Cancer Registries (NAACCR) [6]. This database of cancer registries covers approximately 28% of the US population. From other countries the data processing have derived from population-based national cancer registries.

In 2013, oral cancer incidence ranked eleventh among all sites of cancer [7]. At the global level, incidence for oral cancer has decreased slowly between 1990 and 2013, although some countries have experienced increases in this period. In the USA this decreased incidence [8] can be attributed to a substantial decline in smoking prevalence in the general population [9]. These trends of lessening incidence are mirrored in data from the Canadian Cancer Registry between 1992 and 2007, providing a decrease in incidence of oral cancer by 2.1% for men and 0.4% in women [10]. This trend could also be observed in Central America, in Panama, for both genders (−2.2%) [11].

On the other hand, the Indian subcontinent accounts for one-third of the oral cancer burden in the world [12]. Lip and oral cavity rank the first cancer in Bangladesh and the second one in Pakistan, India, and Nepal [7]. The region with the highest recorded incidence was Melanesia: 22 cases per 100,000 among males and 16 cases in female [1].

Furthermore, rates of oral cavity cancer are increasing among both genders in some Eastern and Northern European countries (Czech Republic, Slovak Republic, Slovenia, Denmark, Estonia, Iceland, Ireland, and Finland) and in Japan too [13]. The lowest rates are found in Western Africa and Eastern Asia [14]. North African countries also present low incidences, partly attributed to cultural behavior like prohibition of alcohol consumption [15].

Oral cavity and pharynx tumors most often occur with multiple primary cancers in the lung (and other respiratory organs) and prostate in males and in the lung and breast in females. Among US populations, the oral cavity and pharynx is the second neoplasm with the highest percentage of individuals with multiple primary cancers (15%) [16].

3.2 Demographics Characteristics: Gender, Age, Ethnic, and Race

The IARC has reported that there were 300,400 new cases of oral cancer in 2012, accounting for approximately 2.1% of all new cancer in this year (IARC) [14], although the prevalence of oral cancer presents some variations around the world. These rates vary by as much as 20-fold among different countries, age groups, gender, races, and ethnic groups [4]. For example, in the USA the annual incidence rate of new cases is 7.7 per 100,000 [17] and in South America (Uruguay) is 10.29 cases in men and 2.64 for women [18]. In Australia 2500 new cases are diagnosed per year [19], and solely among Indian females, nearly tenfold more new cases (24,375) were diagnosed in 2008 [20].

Globally, the emergence of oral cancer is higher in male than female [21], and incidence seems to be decreasing among the latter [6]. In the USA, data provided by SEER has also documented that incidence of oral and pharyngeal cancer ranked eighth in men and fourteenth in women [6].

Oral cancer is the most common cancer among men in India [22] and the second cancer among Pakistani women [12]. The overall of oral cancer male-to-female ratio in 2008 ratio was 1.8:1 [23], and 1,9:1 in 2012 [1], similar to that in Japan 1.45:1 [24], Iran 1.9:1 [25], and China [26]. In Uruguay the proportion increases up to 3.8:1 [18] and even to 10.5:1 in Taiwan [24]. A reverse gender ratio was observed in Thailand where the male-to-female ratio is 1:1.56 [24].

In France and Italy, oral cancer rates have declined among men [27] and among women in the UK [21]. Conversely, oral cancer among women has increased in France, Italy, and in other Western European countries [27]. For British women, the risk increases when they have previously suffered from blood and ovarian cancer [28].

Worldwide, the risk of intraoral carcinoma increases with age [29], especially for white males in the USA [17]. The average age at diagnosis of the tongue and oral cavity was stable from 1993 to 2003 (62 years), whereas that of lip cancer had increased in 5 years: from 65 to 70 years. The mean age at diagnosis of salivary gland carcinoma for Caucasian race is 63 years, a decade older than Blacks and Hispanics [30].

Nevertheless Australian aboriginal individuals appear to be more likely to present oral cancer at younger ages, most probably because of the minority people of aboriginal subjects with cancer and due to the significantly reduced life expectancy of this ethnic group, which is about 17 years lower than that of other Australians [19]. In Taiwan, with the fourth highest registered incidence of oral cancer among men worldwide, this neoplasm ranks the first in the 40-year-old group of the male population [31].

Oral cancer is more frequent among Black than within Caucasian in both genders [32] and is increasing among the White race in the USA [9, 16, 33]. Ethnicity has also provided epidemiological variations on oral cancer: US Hispanics of both genders have shown lower cancer incidence than non-Hispanic White and Black [9, 34]. Among Hispanics, Puerto Ricans showed higher risk than Cubans and Mexicans from the state of Florida [35].

Cancer incidence rates among American Indians and Alaskan Natives are very similar to that of Caucasians [34]. A study of oral cancers in the Temuco region (1994–2008) in Chile detected a higher prevalence in people descendent from Mapuche aborigens [36].

Globally, oral cancer prevails in developing countries, especially from South Asia [1, 23]. In some regions the incidence rate for oral cancer was higher in urban areas [27], in suburban neighborhoods [37], and in the lower socioeconomic conditions in the early years of childhood [24].

3.3 Topographical Description

The new cases estimated with age-standardized rates for lip and oral cancer are 4.0 per 100,000 inhabitants, recording the highest values in the Southeast Asia with 6.4 per 100,000 people [13]. But at the individual level, there are also great differences in the incidence of oral cancer according to intraoral locations and geographical areas.

3.3.1 Lip Cancer

Squamous cell carcinoma occurs much more frequently on the lower lip than on the upper lip. Together, they account for 20–30% of all oral squamous cell carcinoma [38]. The average annual incidence rate for white males in the USA is 4 per 100,000, but this ratio increases dramatically with age [17].

Among males, the highest incidence rates for cancer of the lip are reported in Spain, Australia, and Portugal (Azores) (Fig. 3.1). In females, major incidences were reported in Australia, followed by Thailand and Brazil [5] (Fig. 3.2). The mean age of lip cancer is increasing, and the gender distribution is leveling due to an increase in its frequency among women [39].

Although White persons had a significantly higher proportion of SCC of the lower lip than Black people [40], lately there has been a considerable decrease in the annual incidence rate of this location in White males in the USA. Hispanics of both genders had higher rates of incidence of lip cancer than did non-Hispanic black men and women [33].

Globally, in the ranking of 10 major cancers, adjusted at age-standardized rate per 100,000 people, lip cancer has only been registered in ninth position in Spain (Cuenca) [5].

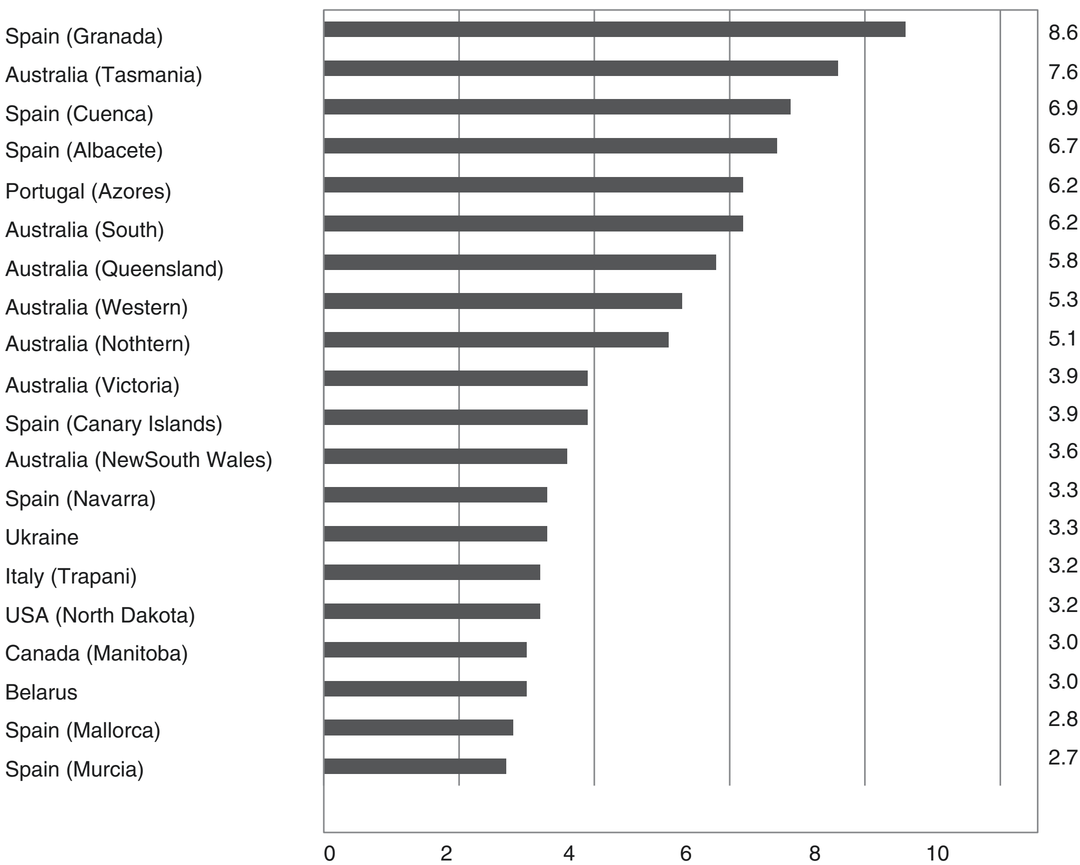

Fig. 3.1 Age-standardized incidence (per 100,000) for lip cancer. Male

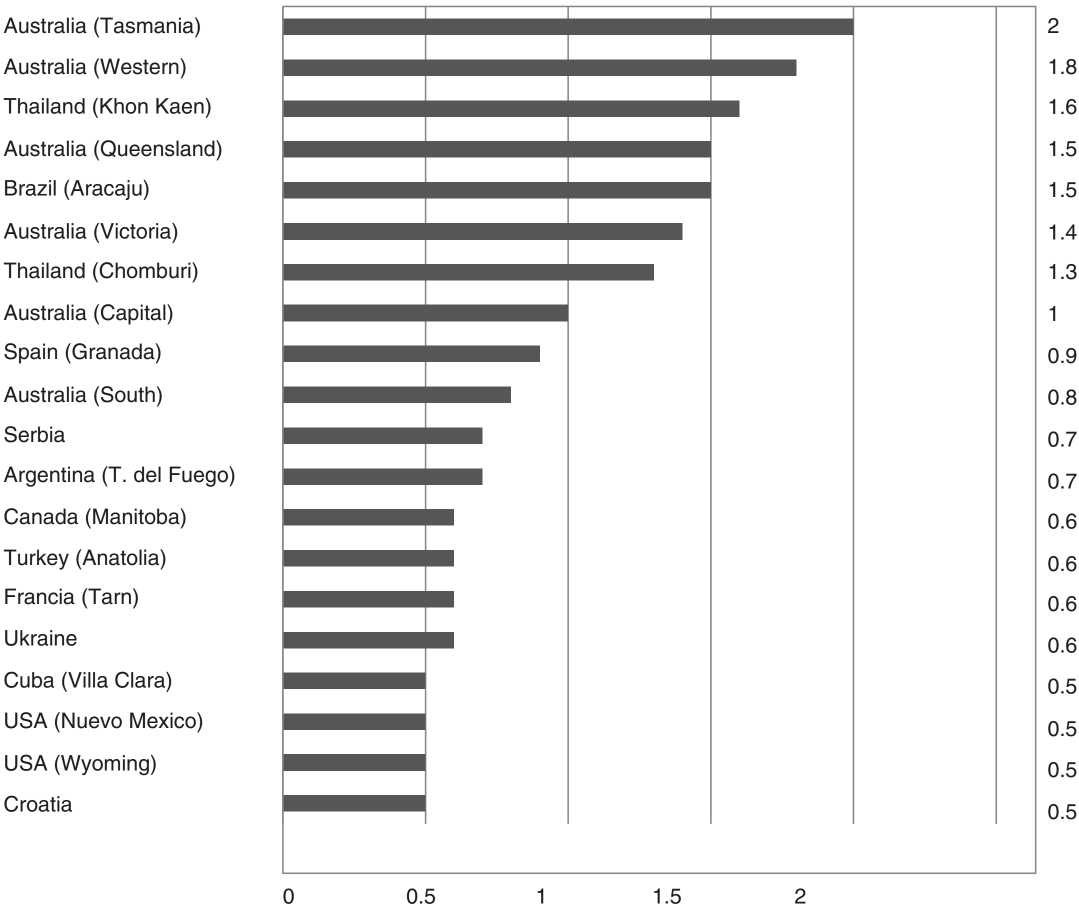

Fig. 3.2 Age-standardized incidence (per 100,000) for lip cancer. Female

3.3.2 Tongue Cancer

Carcinoma of the oral tongue – that includes base of the tongue (pharyngeal tongue) and unspecified tongue – presents different behaviors and prognoses [39]. Carcinoma of the tongue is the most common intraoral malignancy, accounting for 20% to 45% [18, 25, 41]. The next location in frequency is the left lateral border, followed by the right one (61% to 39%), ostensibly because of the greater number of right-handed smokers who aim the smoke stream toward the left side [14].

The highest incidence in both genders was recorded for this location in India (Figs. 3.3 and 3.4). But the highest affectation in women was registered in Australian indigenous territories (5.2 incidence per 100,000 inhabitants) and a comparatively smaller proportion in nonindigenous populations (1.5 incidence per 100,000 people). In women, there were also predilections for Hawaiians with ethnic Chinese or Japanese ancestors [5].

Many countries of Europe present high risk of tongue cancer. Portugal (Azores), Switzerland (Neuchatel), France (Loira, Vendeé), and Slovakia have reported elevated rates.

Around the world, in the ranking of ten major cancers, adjusted at age-standardized rate per 100,000 people, tongue cancer is the third type of cancer among males in Bhopal and the fourth in New Delhi (India).

3.3.3 Carcinoma of the Mouth

India is the country with the highest prevalence of mouth cancer in both genders. Regarding

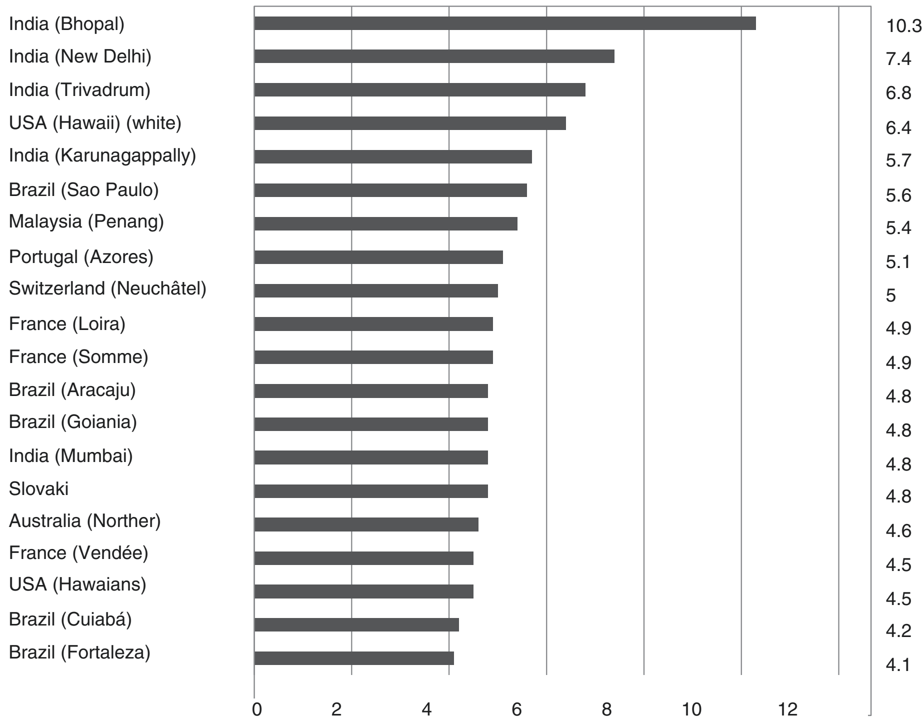

Fig. 3.3 Age-standardized incidence (per 100,000) for tongue cancer. Male

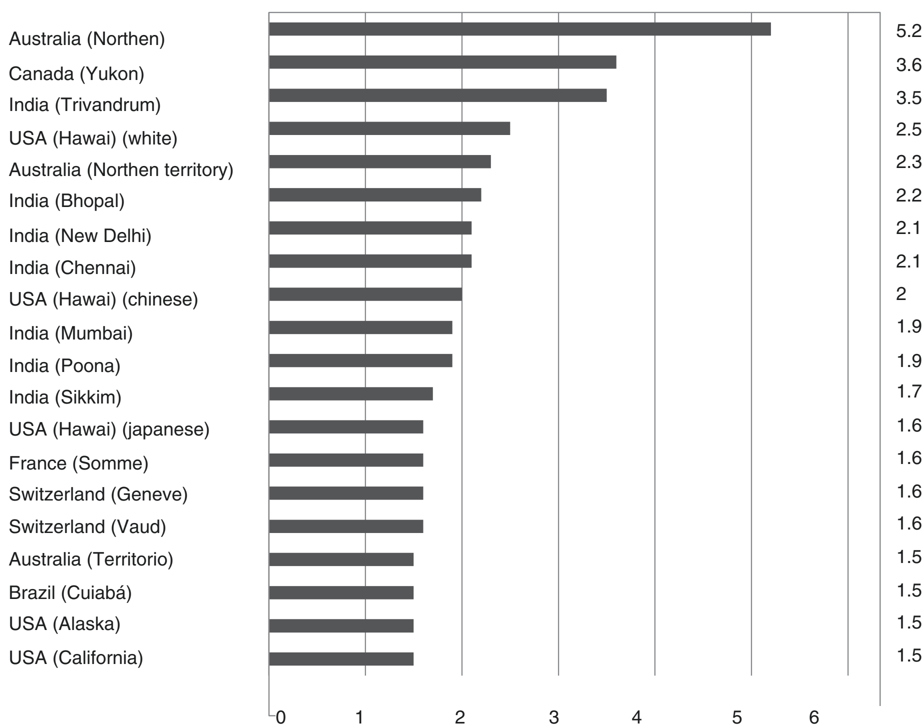

Fig. 3.4 Age-standardized incidence (per 100,000) for tongue cancer. Female

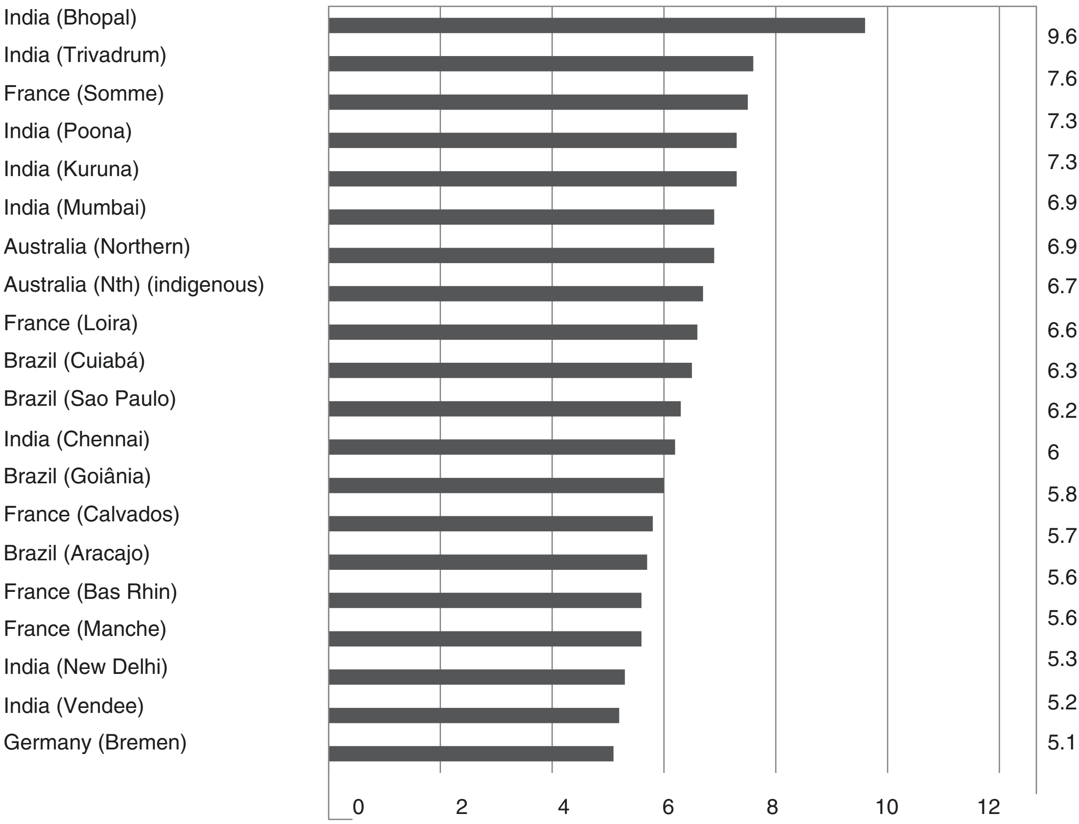

Fig. 3.5 Age-standardized incidence (per 100,000) for mouth cancer. Male

males, a region in France (Somme, Loira) ranks in the second place (Fig. 3.5). Other European countries such as Germany, Slovakia, Portugal, and Spain share a relevant place. In South America, Brazil also shows a high prevalence. In Australian population female mouth cancer is more frequent among indigenous than among nonindigenous population (Fig. 3.6) [5].

Worldwide, when comparing the 10 major cancers after adjusting at age-standardized rate per 100,000, mouth cancer is the first type of cancer in males and fourth in females in Poona (India). Mouth cancer also is the third type of cancer among males in several Indian registers, such as Barshi, Karunagappally, and Mumbai. Apart from Bangalore and Chennai, the trends for mouth cancer show growing incidences, but they do not reach statistical signification [42].

3.3.4 The Salivary Gland

The epidemiology of salivary gland cancer is not very well documented, as they are relatively infrequent and exhibit a marked heterogeneity. The global annual incidence of malignant salivary gland tumors was considered to range from 0.4 to 2.6 cases per 100,000 people [43]. In the USA it was estimated at 0.8 to 1.2 per 100,000 people.

The data on the distribution of salivary gland tumors provided by the IARC do not seem to follow the same pattern as oral cavity cancer. The countries more affected by salivary gland tumors are Australia, Canada, and the USA (Fig. 3.7). In South America, Brazil and Argentina show remarkable incidences. In Europe it is less common, being Mantua and

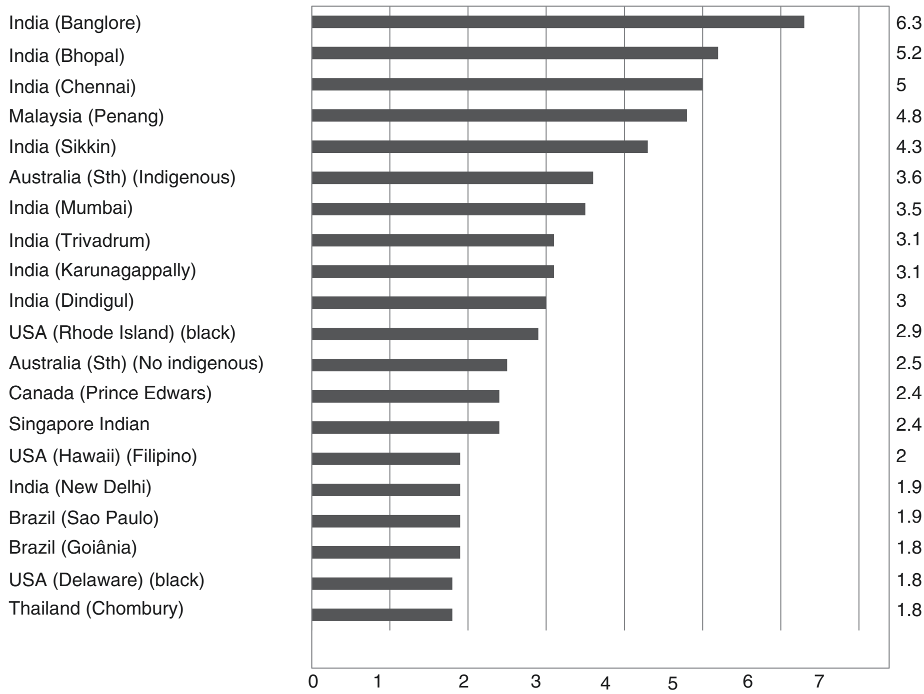

Fig. 3.6 Age-standardized incidence (per 100,000) for mouth cancer. Female

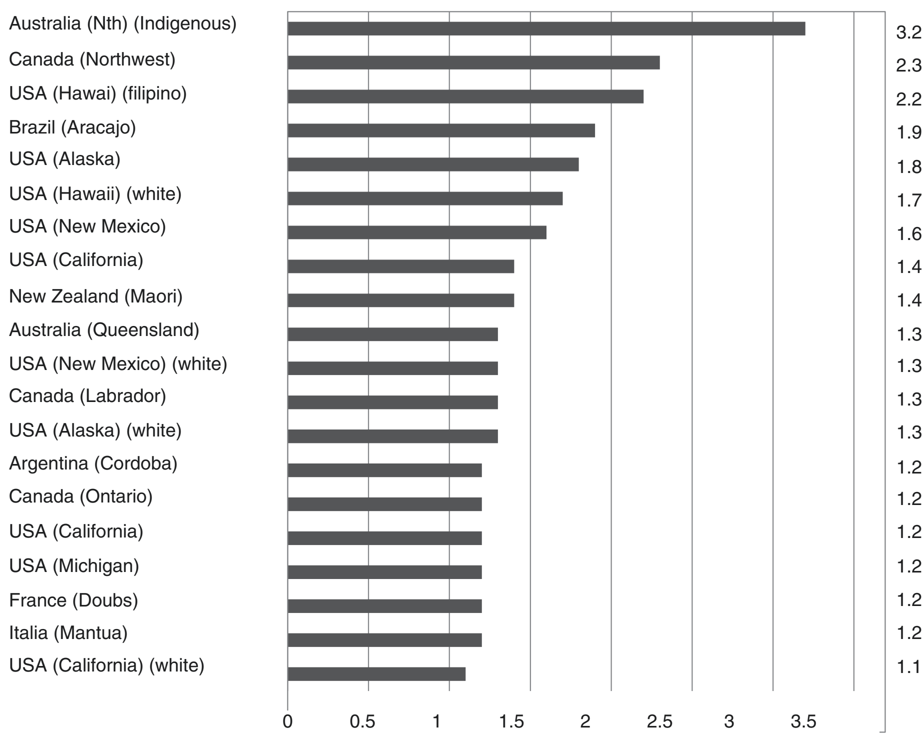

Fig. 3.7 Age-standardized incidence (per 100,000) for salivary glands cancer. Male

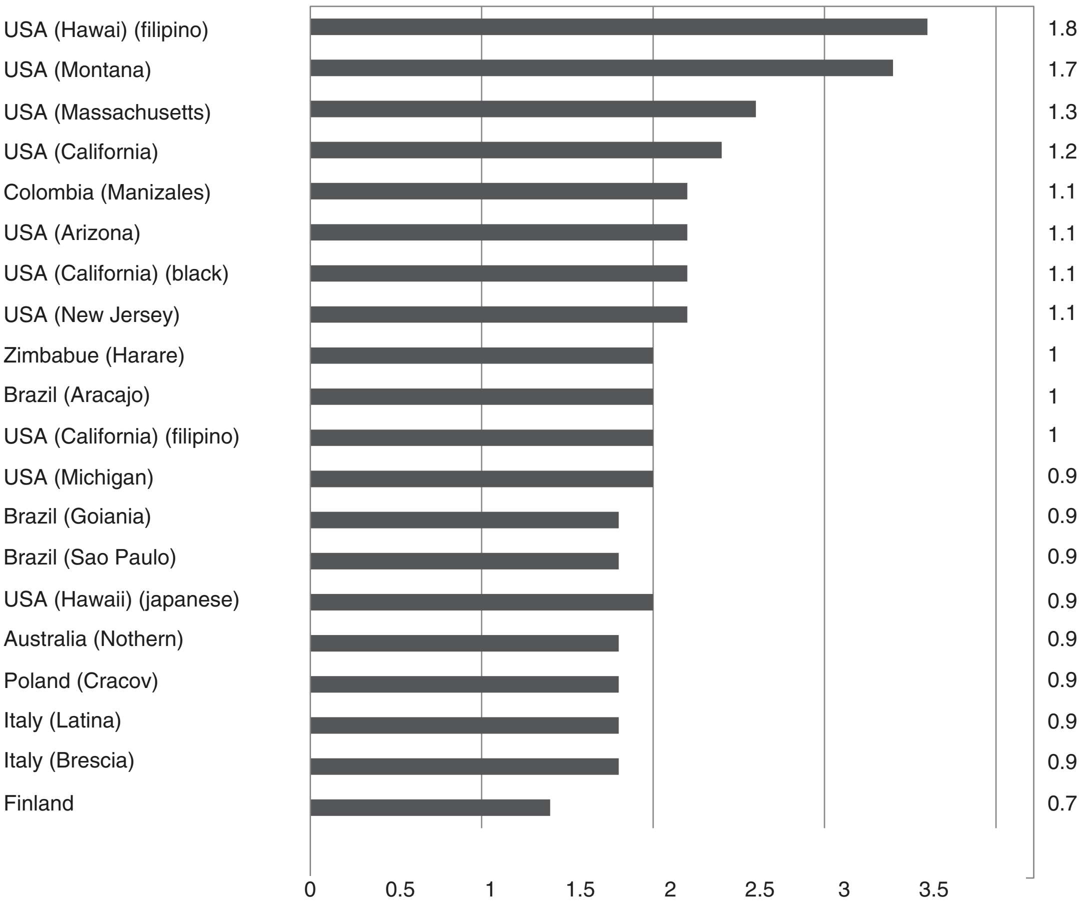

Fig. 3.8 Age-standardized incidence (per 100,000) for salivary glands cancer. Female

Doubs from Italy and France, respectively (Fig. 3.8), the most affected areas. Salivary gland cancer has not been registered in the ranking of 10 major cancers [5].

Among females, the USA shows the highest prevalences. Although in general salivary gland tumors are more frequently in Black persons [44], its prevalence also varies according to the ethnicity. Regarding males, this neoplasm is more common among Filipinos and Whites in the USA and in Hawaii and California than in other ethnic groups from the same countries. There is a predilection for gland carcinomas in female American Indians from different states, such as Montana and Arizona. Other important finding is that Japanese women in Los Angeles suffer from salivary gland carcinoma four times more frequently than do Japanese men, despite that in the actual Japan, this tumor is more prevalent among men than in women. In Asian and Pacific Islander of Georgia, salivary gland carcinoma in females was six times more common than in men. In Cracow (Poland) and in some countries of Africa such as Libya and Zimbabwe, it is also more common in females than among males [5].

3.3.5 Survival

Although oral cancer is a deadly disease, survival has gradually increased in the last two decades. Surveillance of oral cavity and pharyngeal cancer at 5 years after diagnosis has been estimated, survival around 50% [16], and for salivary gland carcinoma up to more than 85% [45]. The 10-year overall survival rate was 30.8% and continued to decline, with only 8.9% of the patients still alive at 25 years post-diagnosis and treatment [41].

The Canadian Cancer Registration Database has shown that survival for oral cavity squamous cell carcinoma is improving with an 8.1% for men [8]. Among women, in other countries of Central Europe, such as Letonia, survival at 5 years posttreatment has increased to 22% in women [46].

Racial and ethnicity factors appear to influence survival to oral cancer. Comparatively, survival among Whites is higher than Blacks in oral cancer (45 vs. 67%) [41], and among Afro-Americans it is better for parotid gland tumors [44]. Hispanic population has a longer median survival time than non-Hispanics after treatment of oral and pharyngeal cancer [34, 44].

On indigenous American populations, First Nations people of Canada diagnosed of oral cancer have significantly decreased survival (33.7%) compared to non-First Nations patients (58.1%) [10]. There is no significant difference in 5-year survival between aboriginal and non-aboriginal subjects of Australian [19].

Lower socioeconomic status was associated with worse survival for oral and pharyngeal cancer, even after adjusting for age, sex, and stage [47].

3.3.6 Mortality

The International Agency for Research on Cancer (IARC) reported that there were 145,353 deaths of oral cancer in 2012, accounting for approximately 1.9% of all cancer deaths in 2012. Although in Bangladesh, the first rank of incidence of cancer is lip and oral, ranking the sixth in mortality [1].

Globally, the mortality rate of oral cancer was higher in male than in female [26]. This trend was observed from 2-year survival right up to 25-year survival [41]. During 2002 to 2011, death rates for oral cancer among women decreased. In males, after having decreased since 1993 to 2003 [8], oral cancer death rates stabilized between 2007 and 2011 [6]. Death from oral cancer ranks fifteenth place for men and seventeenth for women in the US population [33]. In Europe, it ranked the seventh and tenth, respectively [48]. Oral cancer is the third cause of mortality in males in Hungary and Slovakia [1].

In the Netherlands, between 1989 and 2006, the median survival was 3.9 years. After 3 years, 41% of oral cancer patients had died due to their tumors, as did 29% of those suffering from pharynx neoplasms. In that country, oral and pharyngeal cancer patients also experienced high mortality due to esophageal and lung cancer [49].

Black race presents higher mortality from oral cancer than White, American Indian, Alaskan Natives, and Asian/Pacific Islanders. Blacks had a 43% higher hazard of mortality compared with Whites, while those of other racial backgrounds showed a 28% lower risk of mortality [34].

Mortality rates from lip and oral cavity cancers are higher in developing countries for both genders but especially for females [14]. Age is a factor in the prognosis of some tumors [50]. Salivary gland carcinoma patients elder than 60 usually have a poorer prognosis compared to younger patients, which can be explained by more advanced disease stages [51, 52].

In salivary gland cancer, Black race compared to White was also considered a risk factor for poorer prognosis, particularly for mucoepidermoid or squamous cell carcinomas; meanwhile Hispanic ethnicity has no effect on histology-specific survival for any salivary gland carcinoma [18].

Conclusion

In conclusion, there are high-risk countries such as India and Australia for tongue and mouth cancer. The highest risk for lip cancer is experienced in Spain and in Australia and North America for salivary gland tumors. Globally, salivary gland malignant tumor is an infrequent carcinoma, and it is not considered among the ten major cancers. Although in some developed countries oral cancer has decreased (USA or Canada), in another, e.g., certain European countries, it has increased. In developing countries, mortality remains a challenging problem. Many of these differences are undoubtedly caused by differing population habits, life expectancies, preventive education, and the quality of medical records in various countries. These data can be helpful in identifying potential causative factors.

References

1. Ferlay J, Soerjomataram I, Dikshit R, Eser S, Mathers C, Rebelo M, et al. Cancer incidence and mortality worldwide: sources, methods and major patterns in GLOBOCAN 2012. Int J Cancer. 2015;136:E359–86.
2. Leoncini E, Vukovic V, Cadoni G, Pastorino R, Arzani D, Bosetti C, et al. Clinical features and prognostic factors in patients with head and neck cancer: results from a multicentric study. Cancer Epidemiol. 2015;39:367–74.
3. Singh MP, Misra S, Rathanaswamy SP, Gupta S, Tewari BN, Bhatt ML, et al. Clinical profile and epidemiological factors of oral cancer patients from North India. Natl J Maxillofac Surg. 2015;6:21–4.
4. Warnakulasuriya S. Global epidemiology of oral and oropharyngeal cancer. Oral Oncol. 2009;45:309–16.
5. Forman D, Bray F, Brewster DH, Gombe Mbalawa C, Kohler B, Piñeros M, et al., editors Cancer Incidence in Five Continents, Vol. X. IARC Scientific Publication N°. 164. Lyon: International Agency for Research on Cancer. 2014.
6. Kohler BA, Sherman RL, Howlader N, Jemal A, Ryerson AB, Henry KA, et al. Annual Report to the Nation on the Status of Cancer, 1975–2011, Featuring Incidence of Breast Cancer Subtypes by Race/Ethnicity, Poverty, and State. J Natl Cancer Inst. 2015;107:djv048.
7. Global Burden of Disease Cancer Collaboration, Fitzmaurice C, Dicker D, Pain A, Hamavid H, Moradi-Lakeh M, MacIntyre MF et al. The Global Burden of Cancer 2013. JAMA Oncol. 2015;1:505–27.
8. Edwards BK, Brown ML, Wingo PA, Howe HL, Ward E, Ries LA, et al. Annual report to the nation on the status of cancer, 1975-2002, featuring population-based trends in cancer treatment. J Natl Cancer Inst. 2005;97:1407–27.
9. Jemal A, Clegg LX, Ward E, Ries LA, Wu X, Jamison PM, et al. Annual report to the nation on the status of cancer, 1975-2001, with a special feature regarding survival. Cancer. 2004;101:3–27.
10. Erickson B, Biron VL, Zhang H, Seikaly H, Côté DW. Survival outcomes of first nations patients with oral cavity squamous cell carcinoma (Poliquin 2014). J Otolaryngol Head Neck Surg. 2015;44:4.
11. Politis M, Higuera G, Chang LR, Gomez B, Bares J, Motta J. Trend analysis of Cancer mortality and incidence in Panama, using joinpoint regression analysis. Medicine (Baltimore). 2015;94:e970.
12. Khan Z, Muller S, Ahmed S, Tonnies J, Nadir F, Samkange-Zeeb F. Quantitative review of oral Cancer research output from Pakistan. Asian Pac J Cancer Prev. 2015;16:4733–9.
13. Chi AC, Day TA, Neville BW. Oral cavity and oropharyngeal squamous cell carcinoma—an update. CA Cancer J Clin. 2015;65:401–21. https://doi.org/10.3322/caac.21293.
14. Torre LA, Bray F, Siegel RL, Ferlay J, Lortet-Tieulent J, Jemal A. Global cancer statistics, 2012. CA Cancer J Clin. 2015;65:87–108. https://doi.org/10.3322/caac.21262.
15. BenNasir E, El Mistiri M, McGowan R, Katz RV. Oral cancer in Libya and development of regional oral cancer registries: a review. Saudi Dent J. 2015;27:171–9.
16. Hayat MJ, Howlader N, Reichman ME, Edwards BK. Cancer statistics, trends, and multiple primary cancer analyses from the surveillance, epidemiology, and end results (SEER) program. Oncologist. 2007;12:20–37.
17. Neville B, Damm DD, Allen C, Bouquot J. Oral & Maxillofacial Apthology. WB. Saunders Company; 2002.
18. Oliveira ML, Wagner VP, Sant'ana Filho M, Carrard VC, Hugo FN, Martins MD. A 10-year analysis of the oral squamous cell carcinoma profile in patients from public health centers in Uruguay. Braz Oral Res 2015;29. pii: S1806–83242015000100270.
19. Frydrych AM, Slack-Smith LM, Parsons R, Threlfall T. Oral cavity squamous cell carcinoma—characteristics and survival in aboriginal and non-aboriginal western australians. Open Dent J 2014; 8: 168–74.
20. Mishra GA, Dhivar HD, Gupta SD, Kulkarni SV, Shastri SS. A population-based screening program for early detection of common cancers among women in India—methodology and interim results. Indian J Cancer. 2015;52:139–45.
21. Abel GA, Shelton J, Johnson S, Elliss-Brookes L, Lyratzopoulos G. Cancer-specific variation in emergency presentation by sex, age and deprivation across 27 common and rarer cancers. Br J Cancer. 2015;112:S129–36.
22. Bray F, Ren JS, Masuyer E, Ferlay J. Global estimates of cancer prevalence for 27 sites in the adult population in 2008. Int J Cancer. 2013;132:1133–45.
23. Ferlay J, Shin HR, Bray F, Forman D, Mathers C, Parkin DM. Estimates of worldwide burden of cancer in 2008: GLOBOCAN 2008. Int J Cancer. 2010;127:2893–917.

24. Krishna Rao S, Mejia GC, Roberts-Thomson K, Logan RM. Kamath estimating the effect of childhood socioeconomic disadvantage on oral cancer in India using marginal structural models. Epidemiology. 2015;26:509–17.
25. Maleki D, Ghojazadeh M, Mahmoudi SS, Mahmoudi SM, Pournaghi-Azar F, Torab A, et al. Epidemiology of oral Cancer in Iran: a systematic review. Asian Pac J Cancer Prev. 2015;16:5427–32.
26. Zhang S-K, Zheng R, Chen Q, Zhang S, Sun X, Chen W. Oral cancer incidence and mortality in China, 2011. Chin J Cancer Res. 2015;27:44–51.
27. Simard EP, Torre LA, Jemal A. International trends in head and neck cancer incidence rates: differences by country, sex and anatomic site. Oral Oncol 2014;50:387–403.
28. Hippisley-Cox J, Coupland C. Development and validation of risk prediction algorithms to estimate future risk of common cancers in men and women: prospective cohort study. BMJ Open. 2015 Mar 17;5:e007825.
29. Shoaee S, Ghasemian A, Mehrabani K, Naderimagham S, Delavari F, Sheidaei A, et al. Burden of Oral Diseases in Iran, 1990–2010: Findings from the Global Burden of Disease Study 2010. Arch Iran Med 2015;18:486–492.
30. Russell JL, Chen NW, Ortiz SJ, Schrank TP, Kuo YF, Resto VA. Racial and ethnic disparities in salivary gland Cancer survival. JAMA Otolaryngol Head Neck Surg. 2014;140(6):504–12.
31. Kao SY, Lim E. An overview of detection and screening of oral cancer in Taiwan. Chin J Dent Res. 2015;18:7–12.
32. Goodwin WJ, Thomas GR, Parker DF, Joseph D, Levis S, Franzmann E, et al. Unequal burden of head and neck cancer in the United States. Head Neck. 2008;30:358–71.
33. Howe HL, Wu X, Ries LA, Cokkinides V, Ahmed F, Jemal A, et al. Annual report to the nation on the status of cancer, 1975-2003, featuring cancer among U.S. Hispanic/Latino populations. Cancer. 2006;107:1711–42.
34. Espey DK, Wu XC, Swan J, Wiggins C, Jim MA, Ward E, et al. Annual report to the nation on the status of cancer, 1975-2004, featuring cancer in American Indians and Alaska natives. Cancer. 2007;110:2119–52.
35. Pinheiro PS, Sherman RL, Trapido EJ, Fleming LE, Huang Y, Gomez-Marin O, et al. Cancer incidence in first generation U.S. Hispanics: Cubans, Mexicans, Puerto Ricans, and new Latinos. Cancer Epidemiol Biomark Prev. 2009;18:2162–9.
36. Moore SP, Forman D, Piñeros M, Fernández SM, de Oliveira Santos M, Bray F. Cancer in indigenous people in Latin America and the Caribbean: a review. Cancer Med. 2014;3:70–80.
37. Walker BB, Schuurman N, Auluck A, Lear SA, Rosin M. Suburbanisation of oral cavity cancers: evidence from a geographically-explicit observational study of incidence trends in British Columbia, Canada, 1981–2010. BMC Public Health. 2015;15:758.
38. Marx R, Steern D. Oral and maxillofacial pathology. A rationale for diagnosis and treatment Quintessence Publishing Co, Inc Chicago. 2012.
39. Domínguez-Gordillo A, Esparza-Gómez G, García-Jiménez B, Cerero-Lapiedra R, Casado-Gómez I, Romero-Lastra P, et al. The pattern of lip cancer occurrence over the 1990-2011 period in public hospitals in Madrid, Spain. J Oral Pathol Med. 2015;8:202.
40. Khammissa RA, Meer S, Lemmer J, Feller L. Oral squamous cell carcinoma in a South African sample: race/ethnicity, age, gender, and degree of histopathological differentiation. J Cancer Res Ther. 2014;10:908–14.
41. Osazuwa-Peters N, Massa ST, Christopher KM, Walker RJ, Varvares MA. Race and sex disparities in long-term survival of oral and oropharyngeal cancer in the United States. J Cancer Res Clin Oncol. 2016;142:521–8.
42. Badwe RA, Dikshit R, Laversanne M, Bray F. Cancer incidence trends in India. Jpn J Clin Oncol. 2014;44(5):401–7.
43. Barnes L, Eveson J, Reichart P, Sidransky D, editors. World Health Organization classification of tomours. Pathology and genetics of tumours of the head and neck. Lyon: IARC. Press; 2005. WHO.
44. Molina MA, Cheung MC, Perez EA, Byrne MM, Franceschi D, Moffat FL, et al. African American and poor patients have a dramatically worse prognosis for head and neck cancer: an examination of 20,915 patients. Cancer 2008;113:2797–806.
45. Shigeishi H, Ohta K, Okui G, Seino S, Hashikata M, Yamamoto K, et al. Clinicopathological analysis of salivary gland carcinomas and literature review. Mol Clin Oncol. 2015;3:202–6.
46. Innos K, Padrik P, Valvere V, Aareleid T. Sex differences in cancer survival in Estonia: a population-based study. BMC Cancer 2015;15:72.
47. Chu KP, Habbous S, Kuang Q, Boyd K, Mirshams M, Liu FF, et al. Socioeconomic status, human papillomavirus, and overall survival in head and neck squamous cell carcinomas in Toronto, Canada. Cancer Epidemiol. 2016;40:102–12.
48. Ferlay J, Steliarova-Foucher E, Lortet-Tieulent J, Rosso S, Coebergh JW, Comber H, et al. Cancer incidence and mortality patterns in Europe: estimates for 40 countries in 2012. Eur J Cancer. 2013;49:1374–403.
49. van Monsjou HS, Schaapveld M, Hamming-Vrieze O, de Boer JP, van den Brekel MW, Balm AJ. Cause-specific excess mortality in patients treated for cancer of the oral cavity and oropharynx: a population-based study. Oral Oncol. 2016;52:37–44.
50. Olarte LS, Megwalu UC. The impact of demographic and socioeconomic factors on major salivary gland Cancer survival. Otolaryngol Head Neck Surg. 2014;150:991–8.

51. Bjørndal K, Larsen SR, Therkildsen MH, Kristensen CA, Charabi B, Andersen E, et al. Danish head and neck Cancer group (DAHANCA) and academy of geriatric Cancer research (AgeCare). Does age affect prognosis in salivary gland carcinoma patients? A national Danish study. Acta Oncol. 2016;55:19–22.
52. Baddour HM Jr, Fedewa SA, Chen AY. Five- and 10-year cause-specific survival rates in carcinoma of the minor salivary gland. JAMA Otolaryngol Head Neck Surg. 2016;142:67–73.

Diagnostic Delay in Symptomatic Oral Cancer

4

Pablo Varela-Centelles, Juan Seoane,
María José García-Pola, Juan M. Seoane-Romero,
and José Manuel García Martín

Abstract

About half of the oral cancers have already reached an advanced stage (III or IV) when diagnosed, which influences survival rates (5-year survival, 20% to 50% depending upon tumour sites).

Long time intervals since the beginning of symptoms until definitive diagnosis favour advanced disease stages at diagnosis and a worse prognosis in terms of survival. Some agents seem to have responsibilities in the delay in diagnosis of oral symptomatic cancer, namely, patients, healthcare providers, the health system and the actual tumour. In fact, the symptomatic time period related to the patient appears to be the main difficulty for attaining an early diagnosis. However, and in view of the methodological weaknesses of the existing investigations, this information has to be taken with caution.

Recently, a conceptual framework and guidelines for research (Aarhus statement) have been proposed to produce high-quality studies on early diagnosis. Besides, the usage of the term "diagnostic delay" has been discouraged, and the more accurate "time interval to diagnosis and treatment" has been suggested.

P. Varela-Centelles (✉)
CS Praza do Ferrol. EOXI Lugo, Cervo, e Monforte de Lemos, Galician Health Service, Lugo, Spain

Stomatology Department, School of Medicine and Dentistry, University of Santiago de Compostela, A Coruña, Spain
e-mail: pabloignacio.varela@usc.es

J. Seoane · J. M. Seoane-Romero
Stomatology Department, School of Medicine and Dentistry, University of Santiago de Compostela, A Coruña, Spain
e-mail: juanmanuel.seoane@usc.es; jseoaner@hotmail.com

M. J. García-Pola · J. M. García Martín
Department of Surgery and Medical-Surgical Specialties, School of Medicine and Health Sciences, University of Oviedo, Oviedo, Spain
e-mail: mjgarcia@uniovi.es; josemanugarciamartin@gmail.com

4.1 Introduction

Neoplasias of the oral cavity and nearby sites (pharynx) are quite common throughout the world (the sixth most common cancer) [1], although prevalences differ greatly between and within continents up to the point that oropharyngeal cancer (OPC) is the most common malignancy in Malaysia or Sri Lanka [1–5]. These differences may reach 20-fold, and about 66% of OPCs occur in developing countries [2–5].

India and Pakistan, together with Taiwan, also show very high incidences in Asia. In Europe, Hungary, Slovakia and Slovenia have the highest incidence rates. Among the American countries, Brazil, Uruguay, Puerto Rico and Cuba score the highest rates. The most affected countries in Africa are Namibia, Botswana and Mozambique;

P. Panta (ed.), *Oral Cancer Detection*, https://doi.org/10.1007/978-3-319-61255-3_4

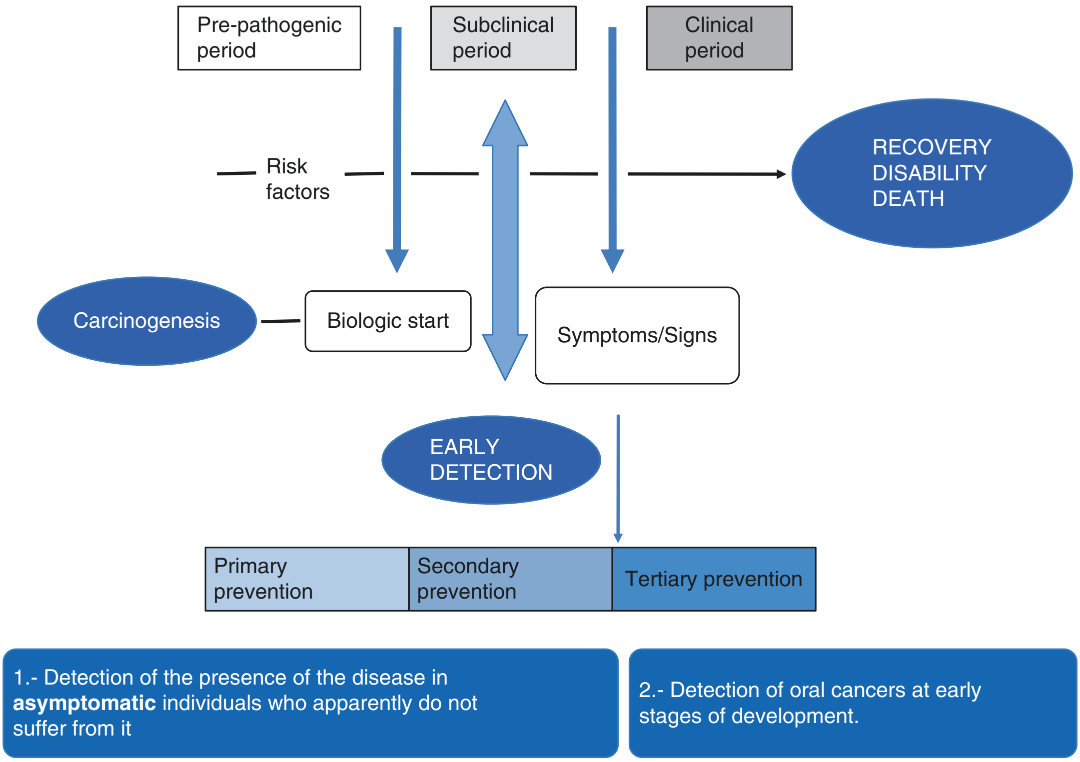

Fig. 4.1 Early detection in oral cancer

and Melanesia and Papua New Guinea rank the highest in Oceania [2–5].

The main problem with these neoplasms is that they are frequently diagnosed (about 50%) when stages III or IV have already been reached. This circumstance undoubtedly influences 5-year survival rates (20–50% depending on tumour sites), and delays in diagnosis may have something to do with it [6–11]. Avoiding diagnostic delays may be a key point for improving survival, as estimations show that if all OPCs were diagnosed and treated at early stages, survival rates would reach 80% [10].

This apparently straightforward assumption is still to be demonstrated [12], and even some research groups wonder whether it would really matter [13]. When dealing with oral cancer, this hypothesis has been proved and the longer the delay in diagnosis, the more advanced the stage [9, 14], mostly due to long time intervals from first cancer symptom to referral to diagnosis. The length of this period of time resulted to be a risk factor for both advanced stage and mortality [14]. This being, studies on early detection and diagnostic delay in oral cancer have to be a research priority in secondary and tertiary prevention [2] if better outcomes are to be achieved (Fig. 4.1) [16, 17].

4.2 Historical Antecedents

Assuming that many cancers are curable if treated early and also that reducing treatment delay is the first step for increasing survival, Pack and Gallo established the basis of the concept of "diagnostic delay" 75 years ago. Their research included 1000 cancer patients, and 90 of these patients had their cancers located in the lip, floor of the mouth and tongue. In this set of patients, the responsibility for the delay was attributed to their physician in 17% of cases. In another 62.3% of the situations, patients and physicians were to blame for delayed diagnoses [18].

This issue has raised the interest of many researchers ever since, who have used a variety of criteria in their investigations [19]. About four decades ago, the prognostic value of the time lapse in diagnosis of oral cancer gained relevance, and two periods were considered: the time since first symptom until professional consultation and the period the patient spends under care until a final diagnosis is made [20, 21]. Currently, diagnostic delay is most frequently defined as "patient delay", the period between the patient first noticing a symptom and their first consultation with a healthcare professional concerning that symptom [9, 22], and "provider/professional delay", the period from the patient's first consultation with a healthcare professional and the definitive pathological diagnosis [9, 22]. Therefore, the "overall or total diagnostic delay" would include the period elapsed since the first symptom or sign until the definitive diagnosis.

When facing the problem of investigating diagnostic delay from the patients' pathway standpoint, it seemed reasonable to divide this path into steps or "stages" for a better understanding of the situation. Thus, several stages have been suggested: a first stage, lasting since the first symptom until the first contact with a clinician; a second stage, since this moment until a referral letter is prepared; a third stage referral letter to appearance at a specialised service; and the fourth stage, since the patient is seen at a specialised service until a final diagnosis is reached [23]. Besides, the time-lapse since diagnosis until treatment is sometimes also assessed [16, 24]. Although interesting, this approach to the problem makes data gathering somehow more difficult in retrospective analyses, but this effort is needed if we are to implement interventions to tackle delays in diagnosis.

Despite an early diagnosis is the cornerstone for improving survival and cure rates, it is very difficult to determine its effect on tumour stage at diagnosis (the main predictor for survival) and to measure the actual effects of interventions for reducing delays in diagnosis [16]. A useful tool in this situation is the guideline "the Aarhus statement" recently developed by an international consensus working group for improving the design and reporting of studies on early cancer diagnosis [16].

4.3 Impact of Diagnostic Delay in Oral Cancer

Although it could be expected that longer delays would always mean worse outcomes in cancer, certain paradoxical and counter-intuitive relationships have been observed in certain cancers [25]. Regarding oral cancer, as mentioned above, tumour stage at diagnosis is still the most important prognostic factor for oral squamous cell carcinoma, with advanced stages linked to high mortality [6, 11]. Unfortunately, the research efforts made for unveiling the role of delays in diagnosis in disease progression have been found to be limited by the usage of different and heterogeneous criteria for defining the concept of "delay" [8]. This limitation has not precluded meta-analytic approaches that have identified diagnostic delay as a risk factor for tumour stage of oropharyngeal carcinomas, being this association stronger when the study is limited to oral cancer, and particularly when the delay is longer than 1 month [9]. Thus, the longer the delay, the more advanced stage at diagnosis [14]. Moreover, longer time intervals from first symptom to referral for diagnosis seem to be a risk factor for mortality, being diagnostic delay a moderate risk factor for mortality from head and neck cancer [26]. Again, and due to the aforementioned limitations of the original studies included in the meta-analyses, these findings should be interpreted with caution.

4.4 Limitations and Biases of Studies on Early Symptomatic Oral Cancer Diagnosis

Studies on diagnostic delay gather an important number of biases, particularly those reporting on patient self-referred data, and this circumstance seriously limits their validity.

Biases are difficult to control in these studies mainly because of methodological restrictions, as randomised trials are impossible due to ethical reasons. Surprisingly, this problem is frequently ignored and rarely discussed in scientific literature on diagnostic delay.

For instance, hospital-based reports [27–35] tend to experience a selection bias, whereas community-based samples [22, 36] would ease generalisation of the obtained results to the entire study population. Another interesting example is the recall bias inherent to retrospective studies [28, 33], which may be diminished by checking patient self-referred data against their relatives [30–32] or their primary care clinicians [19, 32]. This effort is particularly important in this type of studies, as prospective studies on this issue are virtually impossible [22]. Certain research groups have obtained their data for clinical records, either from hospitals [28] or from primary care units [22, 36], being perhaps these ones less prone to bias, as clinicians use to record each visit detailing the reason for attendance, a tentative diagnosis and the treatment established for the patient. Particular attention has to be paid to the circumstance known as "Will Rogers phenomenon" occurring when not all patients are assessed using the same methods that can alter the results of the investigation [35].

Potential confounders have to be controlled for, namely, age [19, 28–34], tumour site, [28, 29, 34] degree of malignancy [36], degree of differentiation [30, 31] and co-morbidity [19, 29]. The aggressiveness of the tumour is a particularly an important factor, as survival is affected more by the proliferative activity of the neoplasm than by the actual delay in diagnosis [30] (less aggressive cancers may show good prognosis despite long delays, and more aggressive ones may have a worse prognosis without any diagnostic delay).

Another relevant issue is the differences in referral protocols, as different prioritisation policies may well imply a "confounding-by-indication" bias in observational studies [34]. Finally, it is worth mentioning that a dichotomised criteria for defining delay in diagnosis (either by arbitrary time points or statistic parameters) may also introduce a bias which could be avoided by analysing time periods as a continuous variable.

4.5 Are there Standardised Definitions for Diagnostic Delay in Oral Cancer?

Even the most widely used intervals, such as "patient delay" [22, 34, 37, 38], and "professional delay" [39–42], are not consistent in the literature because of the different milestones used to define them. These variations are particularly wide when defining the "total delay", as in some groups the end point of their studies is the date of biopsy [43], the date of the pathological diagnosis [7, 27], the first consultation with the treating specialist [34] or the date of treatment [44].

Additional time periods have been identified where delays may exist due to the patient (appraisal, illness, behavioural and scheduling delays) [32], primary care system (referral delay) [43, 44], waiting list (specialised care scheduling interval) [44], specialist delay [32, 45] and pretreatment delay [28, 44]. The final interval of the patients' pathway has been defined as the period between the surgical treatment and the beginning of radiotherapy [46] (Table 4.1).

A marked heterogeneity has also been observed in the way in which the outcomes of diagnostic delay have been presented in the shape of a continuous [37, 47] or a categorical variable [22, 28, 34]: when expressed as a dichotomous variable, the criterion for delay was either arbitrarily established or based upon central trend statistics of the distribution (> 3 weeks [40–48]; > 30 days [32, 46]; > de 45 days [31]; > 6 weeks [49]; > 2 months [50]; > 3 months [51]). Anyhow, there is no consensus on the time point beyond which a diagnosis should be considered delayed [8]. The same difficulties apply to head and neck carcinomas (Table 4.2).

Table 4.1 Summary of the information about diagnostic delay in oral cancer available in scientific literature

Author year	Country	Site	Design	Sample size	Period data collection	Diagnostic delay	Criterion for diagnostic delay	Outcome (prognostic)	Association
Wildt 1995	Denmark	Oral	HB	167	1986–1990	Patient delay Professional delay Total delay	Continuous: Mean Median	Survival	No
Rubright 1996	EEUU	Oral	HB	53	1990–1994	Delay in diagnosis: Discovery tumour to tumour staging	Continuous: Months (descriptive)	TNM (I-II vs III-IV)	No
Kerdpon 2000	Thailand	Oral	HB	161	1996–1998	Patient delay Professional delay Total delay	Categorical: > 1 month 1–3 months >3 months	TNM (I-II vs III-IV)	No
Kantola 2001	Finland	Tongue	CB	75	1974–1994	Referral delay	Dichotomous: Patient referred vs patient not referred (months)	Survival TNM stages (I-II-III vs IV)	Yes
Kumar 2001	India	Oral	CS (HB)	27	N/G	Primary delay Secondary delay Tertiary delay	N/G	Cancer stage: Early vs advanced	Yes
Onizawa 2003	Japan	Oral	HB	152	1991–2000	Step 1 Step 2 Step 3 Step 4	Dichotomous: Beyond the median (2.7 months)	Stage (T category and N category)	No
Scott 2005	UK	Oral	HB	245	1992–2003	Diagnostic delay (first noticed symptoms to diagnosis)	Dichotomous: >3 months	TNM (I-II vs III-IV)	No
Morelatto 2007	Argentina	Oral	HB	70	1992–2004	Patient delay Professional delay Hospital delay	Categorical: >30 days; 30–60 days; 60–120 days >120 days	TNM (I-II vs III-IV)	Yes
Neves 2007	Brazil	Oral	HB	180	1999–2001	ET (first symptoms to hospital) RT (referral to hospital) TT (hospital to start to treatment) TTE total time(ET + TT)	Continuous: Mean (days)	TNM	No
Peacock 2008	EEUU	Oral	HB	50	2003–2007	Time intervals (T1–T6): Aware of symptoms to definitive treatment	Continuous Mean (days)	Reasons for delay	Descriptive NA
Teppo 2008	Finland	Tongue	HB CB	62	1986–1996	Patient delay Professional delay	Dichotomous and categorical <1 month; ≥1, <3 months ≥3 months; ≥ 6 months	Survival	No

(continued)

Table 4.1 (continued)

Author year	Country	Site	Design	Sample size	Period data collection	Diagnostic delay	Criterion for diagnostic delay	Outcome (prognostic)	Association
Gao 2009	UK	Oral	HB	102	2005–2006	Patient delay Professional delay	>1 week	Predictors for delay	NA
Seoane 2010	Spain	Oral	HB	63	1997–2002	Total diagnostic delay	Dichotomous >45 days	Survival	No
Seoane-Romero, 2012	Spain	Oral	HB	88	1998–2003	Total diagnostic delay	Dichotomous >45 days	TNM (I-II vs III-IV)	No
Amar 2014	Brazil	Oral	HB	153	1996–2007	Start treatment – Adjuvant therapy	Categorical: <6w vs 6–8 w vs >8w	Local recurrences	No
Joshi 2014	India	Oral	HB	201	2011–2012	Delay in treatment (primary, secondary, tertiary delay)	Dichotomous ≤3 m vs ≥3 m	Reasons for delay	NA
Panzarella 2014	Italy	Oral	HB	156	2000–2005	Patient delay	Dichotomous and categorical: ≤1 m vs ≥1 m; <1 m vs 1–3 m vs >3 m	Reasons for delay	NA
Tong 2014	China	Oral	HB	77	2009–2011	Total diagnostic delay (symptom-definitive diagnosis)	Dichotomous: 2 months	Survival Recurrence	Yes

HB hospital-based, *HCP* healthcare provider, *CS* case series in a wide regional area, *CB* community-based, *wk.* week, *m* month, *vs* versus, *T* tumour size, *N* node, *M* metastasis, *NA* not available

Table 4.2 Summary of information about diagnostic delay in head and neck cancers

Author Year	Country	Site	Design	Sample size	Period data collection	Diagnostic delay	Type of patient's delay data	Criterion for diagnostic delay	Outcome	Association
Allison 1998	Canada	H&N	HB	76	1995/1997	Patient delay Professional delay Total delay	Categorical <1 month 1–3 months >3 months	> 1 month 1–3 months >3 months	TNM (I-II vs III-IV)	Yes
Amir 1999	UK	H&N	HB	188	1995/1996	Overall delay	Continuous	Weeks	Tumour size	None
Carvalho 2002	Brazil	H&N	CC CB	679	1986/1989	Patient delay Professional delay Total delay	Categorical <1 month 1–3 months >3 months	< 1 month 1–3 months >3 months	TNM (I-II vs III-IV)	Yes
Caudell 2011	EEUU	H&N	HB	427	1995–2007	DT (diagnostic to treatment)	Continuous	Median Mean	Survival	None
Hansen 2005	Denmark	Glottis	HS	544	1965–1997 (conf)	Symptom to diagnosis Diagnosis to treatment	Continuous	Months	TI-TII-TIII-TIV excluded	None
McGurk 2005	UK	H&N	HB	613	1960–1999	Total diagnostic delay	Dichotomous (>3 months)	>3 months	Stage (I-II/ III-IV) Survival	None
Patel 2012	EEUU	H&N	HB	150	2005–2007	DTI (diagnostic to treatment) PTI (otolaryngology visit to treatment)	Continuous	Median (days)	Early /advanced	Yes
Schiff 1990	EEUU	H&N	HB	111	Jan 1975– Dec 1980	Time between surgery and radiation therapy	Categorical	6 weeks	TNM	None
Yu 2008	EEUU	H&N	HB	102	2005–2006	Patient delay Professional delay Total delay	Dichotomous (>median)	> median	Risk indicators	NA

H&N head and neck, *CC* case control, *HB* hospital-based, *CB* community-based

4.6 Theoretical Frameworks, Key Points and Time Intervals on Early Oral Cancer Studies

Bearing in mind that studies on delays in diagnosis of oral cancer do not use any theoretical framework and also that the classical approach (patient and professional delay) is inefficient for monitoring the patients' pathway towards the definitive diagnosis, a consensual research model has been recommended for identifying targets for interventions aimed at an early diagnosis to improve the prognosis of the disease [52].

This model of pathways to treatment [16] describes a series of events, processes, intervals and contributed factors involved in the path to the diagnosis of a symptomatic cancer and allows potential generalisations to different cancer sites and health systems [52, 53]. These events define milestones (detection of bodily changes, perception of reasons to discuss symptoms with a healthcare professional (HCP), first consultation with a HCP, diagnosis and treatment start) which in turn delineate four time intervals (appraisal, help-seeking, diagnostic and pretreatment). The main advantage of this model over the previous ones is that it is dynamic and bidirectional, without a predefined starting point, and also that it permits multiple variations in the course to final diagnosis [52, 53].

This framework (Aarhus statement) discourages the use of the term "delay", due to its evident implications, and recommends the word "interval" as a more accurate one. However, the term "delay" has gained acceptance over the years, and the number of investigations describing intervals or stages without using it is scarce [21, 23, 24].

In an attempt to ease data comparison among reports and to improve the methodology used in this field, the Aarhus guidelines strongly recommend the use of four important dates: date of the first symptoms (bodily sensation or visible alterations), date of first presentation (first consultation with a HCP professional), date of referral (primary care provider to specialist in cancer diagnosis/management) and date of diagnosis [16, 52].

These dates define time intervals named "time to presentation", "time to diagnosis" and "time to treatment" [52] (Fig. 4.2).

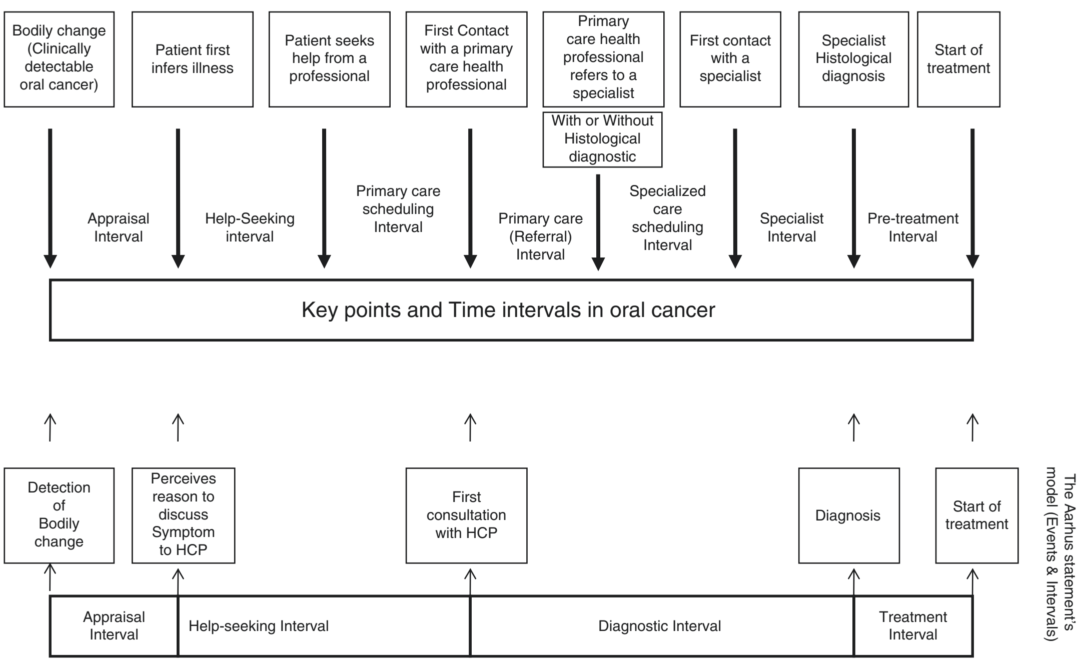

Fig. 4.2 Key points and intervals in oral cancer

4.7 Contributing Factors to a Delayed Diagnosis in Oral Cancer. Who Is to Blame?

Mostly, studies on diagnostic delay in oral cancer or early diagnosis use a biological approach (with no theoretical scaffold) and distribute responsibilities for the delays at each time interval (patient delay [19, 28, 34], provider/professional delay [19, 28, 34], specialist delay [32, 44] and appointment/hospital/system delay [28]. An evident weakness of this conceptualisation is the existence of some overlaps [52], as different agents may act simultaneously at the same interval [54]. The Aarhus statement suggests grouping these agents as contributing factors related to patients, to healthcare providers and health system and to the disease (tumour-depending factors) [16].

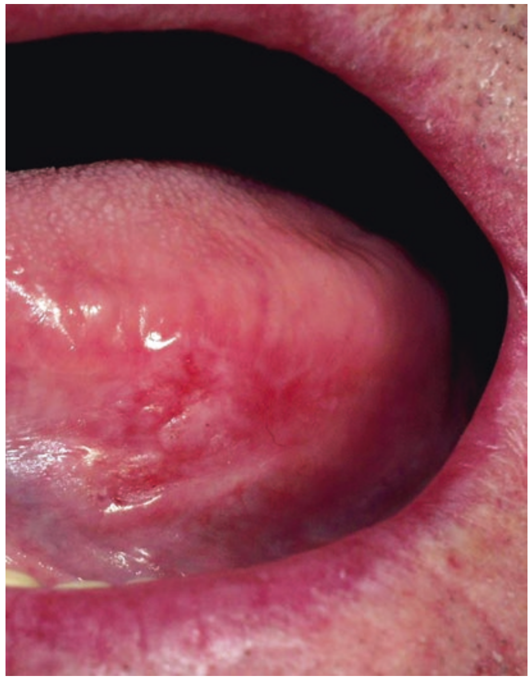

Fig. 4.3 Non-delayed tongue cancer

4.7.1 Patient Interval. Reasons for the Delay

Güneri has recently summarised a limited number of studies to quantify this time interval within a range of 3 to 5.4 months [12], although some authors suggest a patient interval of about 3 weeks as a reasonable one [48]. Thus, the persistence of a bodily change beyond 3 weeks would make the patients seek professional advice [29–52]. This patient interval, also known as symptom interval or time to presentation, accounts for the main component of the overall time to diagnosis and treatment of oral cancer, perhaps due to cognitive and psychosocial factors, such as fate, symptom interpretation, misattribution (to infection or dental problems), belief that the symptom is trivial, stoicism and fear and also because of lack of knowledge about oral cancer [41, 51, 55]. Another factors related to longer patient interval are socioeconomic status [48], alternative medicine [34] and certain health-related behaviours (sexually transmitted disease) [40]. Apart from the difficulties some patients experience to tell symptoms as potentially dangerous (Fig. 4.3) [55], the absence of pathognomonic signs or symptoms of oral cancer may also have a role in the length of this interval. Conversely, a sore, non-healing ulceration and the worsening or persistence of the symptoms seem to be important factors to prompt patient demand for professional help [41].

The duration of the patient interval also has to do with the characteristics of the health system, such as availability [51] and accessibility [12, 54] to care. Any intervention focused at reducing this interval should increase patient awareness of early signs and symptoms of oral cancer and at easing access to the healthcare systems.

4.7.2 Healthcare Providers and System Factors in Diagnostic Delay

The interval attributed to primary care has consistently shown to be shorter than the patient interval [12]. This difference has been estimated in a 2.4 ratio (1.5–4.0) [15]. Both intervals (patient interval and primary care interval) define the pre-referral period [15, 17], which is paramount because a long pre-referral interval has proved to be a risk factor for advanced stage and mortality from oral cancer [14].

The main causes of primary care delays include a low index of suspicion and lack of knowledge about oral cancer [1], together with a lack of familiarity and experience with the disease [8], which has been shown to contribute to delayed referral and treatment [8]. Research has concluded that a standard time interval for a patient to be referred to a specialised service would range between 2 days [56] and 2–3 weeks, according to clinical guidelines [40, 57].

Oral cancer is a particular type of cancer, in the sense that diagnostic biopsies can be taken at the primary care level [70, 79], although this possibility is rarely undertaken, as the number of general dental practitioners performing biopsies ranges from 7% (Turkey [58]), 12% in Northern Ireland [59], or 21% in the UK [2] to 32% in Spain [60]. This circumstance has been put down to a training focused on theoretical aspects rather than on experience or clinical skills. In this situation, the approach "no biopsy and immediate referral" is more common, and a good referral letter and the existence of fast track for these patients become paramount. There are some evidences on the absence of differences in terms of diagnostic, treatment or total delays when the pathological diagnosis was established at the pre-referral period vs patients biopsied at a specialised setting [61].

The diagnostic interval has been defined as the period since first consultation with a HCP until definitive diagnosis [16] (the former concept of "professional delay") [8]. The key points in this interval include the first investigation by the HCP responsible for the patient, first referral to specialised care, first contact with a specialist and definitive diagnosis [16]. This period has been estimated to range between 14 and 21 weeks [12] for oral cancer, although this information comes from studies with a series of methodological weaknesses.

Besides, planning and scheduling a tailored treatment for cancer are complex tasks undertaken during the "pretreatment" interval, which finishes when the treatment is begun. It is somehow surprising that this time period is not usually considered when investigating early diagnosis of oral cancer [19], as reports tend to consider the final pathological diagnosis as the final point of their research [7, 28, 32, 34]. This decision could influence their results particularly when the outcome of the study is patient survival after treatment. Actually, waiting times for surgery and radiotherapy (pretreatment interval) could be an issue in oral cancer, as waiting times prior radiotherapy have an influence on disease progression in head and neck carcinomas [62, 63], although not all studies on this topic support this conclusion. In this situation, and despite that the final event of the Aarhus statement model is "start to treatment" [53], it seems reasonable to consider some other events in the pathway to treatment, such as delays in the pathological processing time of surgical specimens, which may also contribute to delays and to increase the mortality by oral cancer [64].

4.7.3 Disease Factors Influencing the Time to Diagnosis (Tumour Features)

Oral cancer is a relatively proliferative neoplasm with a heterogeneous biological behaviour, being more aggressive those showing HPV negativity, aneuploidy and TP-53 mutations. Other factors to be taken into account are the expression of a series of oncogenic markers, namely, p16, p21, p27, MDM2, MGMT, ERBB2, RARB, MYC, BCR-ABL1, RAS, CCND1, STAT-3 and VGEF, which cause a faster clinical course and reduce the chances for a diagnosis at early disease stages. Some studies on proliferation of head and neck carcinomas have shown these tumours are able to duplicate their size in periods as short as 3 months [65]. Conversely, HPV-positive neoplasms, mostly within the oropharynx, and mainly wild-type TP-53 have elicited a positive prognosis.

Another important idea to keep in mind when investigating diagnostic delay is that tumours of the same type can appear to be similar, but their growth rates may be very different, as well as their aggressiveness [7]. Thus, patients with fast-growing tumours could be diagnosed early but at advanced stages, which may explain why shorter patient and professional delays have been linked to advanced stages in some oral cancer series [22, 26, 27]. We have recently demonstrated in a multivariate study that when the statistical analysis is adjusted for tumour stage at diagnosis (I–II vs III–IV), proliferative activity is an independent factor for survival and diagnostic delay has no influence on the outcome [30]. Therefore, survival to oral cancer may be more affected by the tumour growth rate than by time intervals to diagnosis. Even though some researchers link diagnostic delay to tumour stage [32], it is possible that this link may be veiled by the fact that certain cancers remain silent during their initial stages and cause symptoms only when they reach an advanced phase (silent tumour hypothesis) [7]. In these situations, the tumour growth rate can be considered a confounding factor in the relationship between diagnostic delay and tumour stage, since patients with aggressive tumours and poor prognosis do not usually show a delayed diagnosis, whereas less proliferating tumours demonstrate good prognosis despite long diagnostic delays [66, 67].

Tumour site has been also found to influence the time interval to diagnosis [68], as tumours located on the floor of the mouth, retromolar trigone and gingivae have shown significantly more extension at the moment of diagnosis [31]. When case series include tumours at different locations, a confounding factor is introduced because the patient's self-perception and self-exploration abilities greatly depend on where the lesion is located [37, 45].

Another example of the influence of the site of the tumour is the gingiva: these locations are frequently associated to advanced stages at diagnosis due to the early invasion of neighbouring tissues (T4 primary tumour) rather independently of the time elapsed [38].

The circumstance of tongue cancer (Fig. 4.4) is interesting [22, 36], as shorter delays seem to impair survival. This paradox has been previously described in endometrial, cervix, lung, colon, renal and urethral cancer and highlights the role of the biological aggressiveness of the cancer [8, 13, 25].

Cancer on other sites close to the oral cavity elicit opposing results: patient-related delays longer than 2 months result in higher mortality rates, especially for oropharyngeal and nasopharyngeal carcinomas [26], although a recent investigation failed to establish a link between delay in diagnosis and survival to pharyngeal cancer [22]. For larynx carcinomas, diagnostic delays were found to be an independent prognostic factor for survival, as clinician-related delays exceeding 6 or 12 months were associated to worse survival rates [22], as occurred with the overall delay is considered.

Fig. 4.4 Oral cancer with a long time interval to diagnosis

In any case, the inconsistencies observed in the association between diagnostic delay and outcome in terms of tumour stage and/or survival could well be related to the variability in the biological behaviour of the neoplasms, and differences in tumour aggressiveness would explain tumour's stage at diagnosis and patient survival better than would the mere length of the time interval to diagnosis.

4.8 Practical Implications and Suggestions for Future Research

There seems to be a change in the paradigm of oral symptomatic cancer. The need for quality data, for quantifying time intervals till diagnosis and treatment and for identifying and prioritising targets for future interventions aimed at avoiding delayed diagnoses has favoured the usage and development of theoretical models for monitoring the patients' pathway from the first sign or symptom until the beginning of their treatments. The adherence to the Aarhus guidelines would permit the minimisation of biases and the retrieval of data that are comparable, although some modifications are required to adapt this general framework to the particularities of oral cancer.

Efficient tools have also to be developed if we are to obtain reliable data from self-reported patient experiences, as the reasons for delays at stages involving mainly patients are poorly understood [69].

Apart from patients' or professionals' delays, new agents potentially responsible for diagnostic delays have been incorporated to the initial model, which highlight the role of accessibility, defined as "the ability to obtain services based on patients' health needs" that has to be prioritised in the health systems [70] (Fig. 4.1).

Conclusion

Likewise, strategies for increasing public awareness and knowledge about signs, symptoms and risk factors may decrease the burden of head and neck cancer [71], particularly among high-risk groups. Cancer educational campaigns have demonstrated to significantly increase patients' knowledge of symptoms and risk factors, although it is not known whether this knowledge actually changes patients' behaviour [72]. Moreover, and despite that there is no evidence that educational interventions reduce primary care delay in cancer diagnosis, training on specific skills for physicians and dentists should be facilitated [73]. The efficacy of current community-based oral cancer awareness campaigns seems to be limited [74], so future campaigns should incorporate theoretical models, target high-risk groups and consider the groups towards they are addressed within their socio-cultural context to obtain better results.

Acknowledgements This work has been supported by the research project PI14/01446, belonging to the Spanish National R&D&I Programme 2013–2016 and co-funded by the ISCIII-Subdirección General de Evaluación y Fomento de la Investigación and the European Regional Development Fund (ERDF).

References

1. Warnakulasuriya S. Global epidemiology of oral and oropharyngeal cancer. Oral Oncol. 2009;45:309–16.
2. Johnson NW, Warnakulasuriya S, Gupta PC, Dimba E, Chindia M, Otoh EC, et al. Global oral health inequalities in incidence and outcomes for oral cancer: causes and solutions. Adv Dent Res. 2011;23:237–46.
3. Warnakulasuriya S. Living with oral cancer: epidemiology with particular reference to prevalence and life-style changes that influence survival. Oral Oncol. 2010;46:407–10.
4. Krishna Rao SV, Mejia G, Roberts-Thomson K, Logan R. Epidemiology of oral cancer in Asia in the past decade- an update (2000-2012). Asian Pac J Cancer Prev. 2013;14:5567–77.
5. Warnakulasuriya S. Significant oral cancer risk associated with low socioeconomic status. Evid Based Dent. 2009;10:4–5.
6. Brandizzi D, Chuchurru J, Lanfranchi H, Cabrini R. Analysis of the epidemiological features of oral cancer in the city of Buenos Aires. Acta Odontol Latinoam. 2005;18:31–5.
7. Scott SE, Grunfeld EA, McGurk M. The idiosyncratic relationship between diagnostic delay and stage of oral squamous cell carcinoma. Oral Oncol. 2005;41:396–403.
8. Gómez I, Warnakulasuriya S, Varela-Centelles PI, et al. Is early diagnosis of oral cancer a feasible objective? Who is to blame for diagnostic delay? Oral Dis. 2010;16:333–42.
9. Gómez I, Seoane J, Varela-Centelles P, Diz P, Takkouche B. Is diagnostic delay related to advanced-stage oral cancer? A meta-analysis. Eur J Oral Sci. 2009;117:541–6.
10. Silverman S, Kerr AR, Epstein JB. Oral and pharyngeal cancer control and early detection. J Canc Educ. 2010;25:279–81.
11. McGurk M, Chan C, Jones J, O'regan E, Sherriff M. Delay in diagnosis and its effect on outcome in head and neck cancer. Br J Oral Maxillofac Surg. 2005;43:281–4.
12. Güneri P, Epstein JB. Late stage diagnosis of oral cancer: components and possible solutions. Oral Oncol. 2014;50:1131–6.
13. Neal RD. Do diagnostic delays in cancer matter? Br J Cancer. 2009;101:S9–S12.
14. Seoane J, Alvarez-Novoa P, Gomez I, Takkouche B, Diz P, Warnakulasiruya S, Seoane-Romero JM, Varela-Centelles P. Early oral cancer diagnosis: the Aarhus statement perspective. A systematic review and meta-analysis. Head Neck. 2015;38:E2182.
15. Lyratzopoulos G, Saunders CL, Abel GA, McPhail S, Neal RD, Wardle J, et al. The relative length of the patient and the primary care interval in patients with 28 common and rarer cancers. Br J Cancer. 2015;112:S35–40.
16. Weller D, Vedsted P, Rubin G, Walter FM, Emery J, Scott S, et al. The Aarhus statement: improving design

and reporting of studies on early cancer diagnosis. Br J Cancer. 2012;106:1262–7.
17. Neal RD, Tharmanathan P, France B, Din NU, Cotton S, Fallon-Ferguson J, et al. Is increased time to diagnosis and treatment in symptomatic cancer associated with poorer outcomes? Systematic review. Br J Cancer. 2015;112:S92–107.
18. Pack GT, Gallo JS. The culpability for delay in treatment of cancer. Am J Cancer. 1938;33:443–62.
19. Allison P, Locker D, Feine JS. The role of diagnostic delays in the prognosis of oral cancer: a review of the literature. Oral Oncol. 1998;34:161–70.
20. Shafer WG. Initial mismanagement and delay in diagnosis of oral cancer. J Am Dent Assoc. 1975;90:1262–4.
21. Bruun JP. Time lapse by diagnosis of oral cancer. Oral Surg Oral Med Oral Pathol. 1976;42:139–49.
22. Teppo H, Alho OP. Relative importance of diagnostic delays in different head and neck cancers. Clin Otolaryngol. 2008;33:325–30.
23. Onizawa K, Nishihara K, Yamagata K, Yusa H, Yanagawa T, Yoshide H. Factors associated with diagnostic delay of oral squamous cell carcinoma. Oral Oncol. 2003;39:781–8.
24. Peacock ZS, Pogrel MA, Schmidt DC. Exploring the reasons for delay in treatment of oral cancer. J Amer Dent Assoc. 2008;139:1346–52.
25. Crawford SC, Davis JA, Siddiqui NA, Caestecker L, Ch G, Hole D, et al. The waiting time paradox: population based retrospective study of treatment delay and survival of women with endometrial cancer in Scotland. BMJ. 2002;325:196.
26. Seoane J, Takkouche B, Varela-Centelles P, Tomás I, Seoane-Romero JM. Impact of delay in diagnosis on survival to head and neck carcinomas: a systematic review with meta-analysis. Clin Otolaryngol. 2012;37:99–106.
27. Jovanovic A, Kostense PJ, Schulten EAJM, Snow GB, van der Waal I. Delay in diagnosis of oral squamous cell carcinoma; a report from the Netherlands. Oral Oncol. 1992;28B:37–8.
28. Morelatto RA, Herrera MC, Fernandez EN, Corball AG, Lopez de blanc SA Diagnostic delay in oral squamous cell carcinoma in two diagnostic centres in Cordobe Argentina. J Oral Pathol Med 2007;36: 405–408.
29. Scott SE, Grunfeld EA, Auyeung V, McGurk M. Barriers and triggers to seeking help for potentially malignant symptoms: implications and interventions. J Public Health Dent. 2009;69:34–40.
30. Seoane J, Pita S, Gómez I, Vazquez I, et al. P. Proliferative activity and diagnostic delay in oral cancer. Head Neck. 2010;32:1377–84.
31. Seoane-Romero JM, Vázquez-Mahía I, Seoane J, Varela-Centelles P, Tomás I, López-Cedrún JL. Factors related to late stage diagnosis of oral squamous cell carcinoma. Med Oral Patol Oral Cir Bucal. 2012;17:e35–40.
32. Brouha XD, Tromp DM, Hordijk GJ, Winnubst JA, de Leeuw JR. Oral and pharyngeal cancer: analysis of patient delay at different tumor stages. Head Neck. 2005;27:939–45.
33. Sandoval M, Font R, Mañós M, Dicenta M, Quintana MJ, Bosch FX, et al. The role of vegetable and fruit consumption and other habits on survival following the diagnosis of oral cancer: a prospective study in Spain. Int J Oral Maxillofac Surg. 2009;38:31–9.
34. Kerdpon D, Sriplung H. Factors related to advanced stage oral squamous cell carcinoma in southern Thailand. Oral Oncol. 2001;37:216–21.
35. Rubright WC, Hoffman HT, Lynch CF, Kohout FJ, Robinson RA, Graham S, et al. Risk factors for advanced-stage oral cavity cancer. Arch Otolaryngol Head Neck Surg. 1996;122:621–6.
36. Kantola S, Jokinen K, Hyrynkangas K, Mäntyselkä P, Alho OP. Detection of tongue cancer in primary care. Br J Gen Pract. 2001;51:106–11.
37. Wildt J, Bundgaard T, Bentzen SM. Delay in the diagnosis of oral squamous cell carcinoma. Clin Otolaryngol. 1995;20:21–5.
38. Gao W, Guo CB. Factors related to delay in diagnosis of oral squamous cell carcinoma. J Oral Maxillofac Surg. 2009;67:1015–20.
39. Guggenheimer J, Verbin RS, Johnson JT, Horkowitz CA, Myers EN. Factors delaying the diagnosis of oral and oropharyngeal carcinomas. Cancer. 1989;64:932–5.
40. Pitiphat W, Diehl SR, Laskaris G, Cartsos V, Douglass CW, Zavras AI. Factors associated with delay in the diagnosis of oral cancer. J Dent Res. 2002;81:192–7.
41. Rogers SN, Vedpathak SV, Lowe D. Reasons for delayed presentation in oral and oropharyngeal cancer: the patients' perspective. Br J Oral Maxillofac Surg. 2010;49:349–53.
42. Esmaelbeigi F, Hadji M, Harirchi I, Omranipour R, van Rajabpour M, Zendehdel K. Factors affecting professional delay in diagnosis and treatment of oral cancer in Iran. Arch Iran Med 2014;17:253–7.
43. Holmes JD, Dierks EJ, Homer LD, Potter BE. Is detection of oral and oropharyngeal squamous cancer by a dental health care provider associated with a lower stage at diagnosis? J Oral Maxillofac Surg. 2003;61:285–91.
44. McLeod NM, Saeed NR, Ali EA. Oral cancer: delays in referral and diagnosis persist. Br Dent J. 2005;198:681–4.
45. Tromp DM, Brouha XD, De Leeuw JR, Hordijk GJ, Winnubst JA. Psychological factors and patient delay in patients with head and neck cancer. Eur J Cancer. 2004;40:1509–16.
46. Bastit L, Blot E, Debourdeau P, Menard J, Bastit P, Le Fur R. Influence of the delay of adjuvant postoperative radiation therapy on relapse and survival in oropharyngeal and hypopharyngeal cancers. Int J Radiat Oncol Biol Phys. 2001;49:139–46.
47. Cooke BE, Tapper-Jones L. Recognition of oral cancer. Causes of delay. Br Dent J. 1977;142:96–8.
48. Llewellyn CD, Johnson NW, Warnakulasuriya KA. Risk factors for oral in newly diagnosed patients aged 45 years and younger: a case-control

study in southern England. J Oral Pathol Med. 2004;33:525–332.
49. Pitchers M, Martin C. Delay in referral of oropharyngeal squamous cell carcinoma to secondary care correlates with a more advanced stage at presentation, and is associated with poorer survival. Br J Cancer. 2006;94:955–8.
50. Tong XJ, Shan ZF, Tang ZG, Guo XC. The impact of clinical prognostic factors on the survival of patients with oral squamous cell carcinoma. J Oral Maxillofac Surg 2014;72:2497.e1–10.
51. Kumar S, Heller RF, Pandey U, Tewari V, Bala N, Oanh KTH. Delay in presentation of oral cancer: a multifactor analytical study. Natl Med J India. 2001;14:13–7.
52. Scott SE, Walter FM, Webster A, Sutton S, Emery J. The model of pathways to treatment: conceptualization and integration with existing theory. Br J Health Psychol. 2013;18:45–65.
53. Walter F, Webster A, Scott S, Emery J. The Andersen model of Total patient delay: a systematic review of its application in cancer diagnosis. J Health Serv Res Policy. 2012;17:110–8.
54. Diz Dios P, Padrón González N, Seoane Lestón J, Tomás Carmona I, Limeres Posse J, Varela-Centelles P. Scheduling delay in oral cancer diagnosis: a new protagonist. Oral Oncol. 2005;41:142–6.
55. Panzarella V, Pizzo G, Calvino F, Compilato D, Colella G, Campisi G. Diagnostic delay in oral squamous cell carcinoma: the role of cognitive and psychological variables. Int J Oral Sci. 2014;6:39–45.
56. Schnelter JFC. Oral cancer diagnosis and delays in referral. Br J Oral Maxillofac Surg. 1992;30:210–3.
57. National Institute for Health and Clinical Excellence. (2005). Referral guidelines for suspected cancers. Clinical guideline 27; London; NICE (www.nice.org.uk).
58. Ergun S, Ozel S, Koray M, Kürklü G, AK G, Tanyeri H. Dentist's knowledge and opinions about oral mucosa lesions. Int J Oral Maxillofac Surg. 2009;38:1283–8.
59. Cowan CG, Gregg TA, Kee F. Prevention and detection of oral cancer: the views of primary care dentist in Northern Ireland. Br Dent J. 1995;5:338–42.
60. López-Jornet P, Camacho-Alonso F. New barriers in oral cancer. Patient accessibility to dental examination. A pilot study. Oral Oncol. 2006;42:1022–5.
61. Kaing L, Manchella S, Love C, Nastri A, Wiesenfeld D. Referral patterns for oral squamous cell carcinoma in Australia: 20 years progress. Aust Dent J. 2015;61:29.
62. Jensen AR, Nellemann HM, Overgaard J. Tumor progression in waiting time for radiotherapy in head and neck cancer. Radiother Oncol. 2007;84:5–10.
63. van Harten MC, Hoebers FJ, Kross KW, van Werkhoven ED, van den Brekel MW, van Dijk BA. Determinants of treatment waiting times for head and neck cancer in the Netherlands and their relation to survival. Oral Oncol. 2015;51:272–8.
64. Jerjes W, Upile T, Radhi H, Petrie A, Adams A, Callear J, et al. Delay in pathological tissue processing time vs. mortality in oral cancer: short communication. Head Neck Oncol. 2012;26:14.
65. Seoane Lestón J, Diz Dios P. Diagnostic clinical aids in oral cancer. Oral Oncol. 2010;46:418–22.
66. Evans SJW, Langdon JD, Rapidis AD, Johnson NW. Prognostic significance of STNMP and velocity of tumour growth in oral cancer. Cancer. 1982;49:7773–6.
67. Kaufman S, Grabau JC, Lore JH. Symptomatology in head and neck cancer; a quantitative review of 385 cases. Am J Public Health. 1980;70:520–2.
68. Kowalski LP, Franco EL, Torloni H, Fava AS, Sobrinho JA, Ramos G, et al. Lateness of diagnosis of oral and oropharyngeal carcinoma: factors related to the tumour, the patient and health professionals. Oral Oncol. 1994;30B:167–73.
69. Richards D. Patient delay in reporting oral cancer is poorly understood. Evid Based Dent. 2007;8:21.
70. Guay AH. Access to dental care: solving the problem for underserved populations. J Am Dent Assoc. 2004;135:1599–605.
71. Luryi AL, Yarbrough WG, Niccolai LM, Roser S, Reed SG, Nathan CA, et al. Public awareness of head and neck cancers: a cross-sectional survey. JAMA Otolaryngol Head Neck Surg. 2014;140:639–46.
72. Sommer L, Sommer DD, Goldstein DP, Irish JC. Patient perception of risk factors in head and neck cancer. Head Neck. 2009;31:355–60.
73. Mansell G, Shapley M, Jordan JL, Jordan K. Interventions to reduce primary care delay in cancer referral: a systematic review. Br J Gen Pract. 2011;61:e821–35.
74. Papas RK, Logan HL, Tomar SL. Effectiveness of a community-based oral cancer awareness campaign (United States). Cancer Causes Control. 2004;15:121–31.

5 Imaging of Oral Cancer

Peter Paul, Nilesh Sable, and Supreeta Arya

Abstract

Imaging in oral cavity cancers has received much attention in oncological practice in recent years as clinical examination fails to assess the deeper extent and spread of disease. The death rate of these cancers has been relatively high, particularity owing to presentation at a late stage in the course of disease. Clinical examination has paramount role in early detection as it allows direct visualization of subtle lesions, which cannot be perceived by imaging modalities. In established cases of oral cancer, imaging is needed to accurately evaluate the locoregional extent. Imaging provides guidance in deciding appropriate management strategy (single or multimodality), assessing resectability, and estimating precise extent of resection. The various imaging modalities and their role in the workup of oral cancers are discussed in this chapter, with emphasis on cross-sectional methods as these are routinely employed in staging and follow-up.

P. Paul, MD · N. Sable, MD
S. Arya, MD, DNB, DMRD (✉)
Department of Radiodiagnosis, Tata Memorial Hospital, Mumbai, Maharashtra, India
e-mail: supreeta.arya@gmail.com

5.1 Introduction

Oral cancer is a major concern in oncology with increasing incidence in recent years. Oral cancer forms nearly 30% of cancers seen in India [1]. The major factors responsible for its late presentation include a lack of awareness of early signs or symptoms and absence of screening. Oral cavity squamous cell cancers (OCSCC) comprise approximately 90% of the cancers arising from the all subsites [2]. The commonest causes are tobacco and alcohol with a diet lacking in antioxidants being a contributing factor. Another cause in the Indian population is chewing Areca nut and bidi smoking [1, 2]. Human papillomavirus is now being implicated in a small percentage although this is more commonly associated with oropharyngeal cancers. Other etiologies include long-standing mechanical irritation by a sharp tooth and genetic susceptibility [2].

5.2 Why Imaging?

Detection of oral cancers is usually by clinical examination, and diagnosis is by biopsy. When trismus is present and clinical examination is restricted, imaging may help in detecting disease and corroborating disease suspected on *examination under anesthesia* (EUA). The primary role of imaging in oral cancers is for staging disease. This involves (a) studying local extent of disease

P. Panta (ed.), *Oral Cancer Detection*, https://doi.org/10.1007/978-3-319-61255-3_5

spread, (b) regional nodal spread, and (c) distant metastases. While in early cancers staging is only locoregional, advanced cancers require distant metastatic workup [3].

Imaging is also used in the follow-up of treated OCSCC to evaluate treatment response and may be employed to confirm clinically suspected recurrence. Imaging can help differentiate posttreatment changes from residual or recurrent disease. Since OCSCC also has propensity for second primary malignancies in the upper aerodigestive tract, imaging is useful as an adjunct tool to screen for metachronous tumors.

Several imaging modalities exist such as computed tomography (CT), magnetic resonance imaging (MRI), ultrasonography (US), positron imaging tomography (PET) replaced now by PET-CT, orthopantomography (OPG)/panoramic radiography (PR), and barium study (barium swallow). Awareness of the role of various imaging methods and their limitations is required, along with familiarity with the normal anatomy of the oral cavity and patterns of disease progression. This helps provide an accurate staging report. In addition, knowledge of treatment principles and the clinical issues in the treatment of OCSCC at different subsites helps optimize the use of imaging method(s) and generate a report of clinical relevance.

This chapter is focused on the pretreatment evaluation of OCSCC. It will briefly elucidate the treatment principles of OCSCC, describe the 8th edition AJCC staging of OCSCC, and discuss the role of various imaging methods in the diagnostic workup/staging of OCSCC. The anatomy of the oral cavity will be discussed. The spread patterns of OCSCC at various sites and their implications on treatment and prognosis will be elaborated.

5.3 Treatment Principles

OCSCC from all subsites not only spread locally but also to the lymphatics of the neck. Therapy involves both treatment of the primary tumor and the neck and preservation of form and function with appropriate reconstruction [2, 3].

The 8th edition American Joint Committee on Cancer (AJCC) clinical staging of oral cavity cancers is clinical *and* radiological with imaging providing information about deep extent of disease not amenable to clinical examination and is shown in Table 5.1 [4]. Based on the combination of T, N, and M stages, OCSCC is divided into stages I, II, III, IVA, IVB, and IVC. Stages I and II (T1-T2, N0, M0) are treated with a single modality, either surgery or radiotherapy (RT). Surgery is favored as RT has complications such as xerostomia, mucositis, and osteoradionecrosis [5]. RT is particularly avoided in lesions close to the bone and in young patients [5]. 40–50% of the OCSCC in India present at an advanced stage (III and IV). These are treated with multiple

Table 5.1 AJCC TNM staging of oral cavity cancers 8th edition, 2018

Tumor	
TX	Primary tumor cannot be assessed
T0	No evidence of primary tumor
Tis	Carcinoma in situ
T1	Tumor size 2 cm or less and ≤5 mm DOI (depth of invasion)
T2	≤2 cm & >5 mm & ≤10 mm DOI OR >2 cm ≤4 cm & ≤10 mm DOI
T3	>4 cm or any tumor >10 mm DOI
T4a	Moderately advanced local disease—Invades through the cortical bone, into maxillary sinus, or skin of the face
T4b	Very advanced local disease—Involves masticator space, pterygoid plates, or skull base or encases internal carotid artery
Lymph node (ENE = extranodal extension into adjacent structures)	
NX	Cannot be assessed
N0	No regional lymph node metastasis
N1	Single ipsilateral lymph node ≤3 cm in greatest dimension and ENE -
N2–N2a	Single ipsilateral lymph node, >3 cm and ≤6 cm in greatest dimension and ENE -
N2b	Multiple ipsilateral lymph nodes, ≤6 cm in greatest dimension and ENE -
N2c	Bilateral or contralateral lymph nodes, ≤6 cm in greatest dimension and ENE -
N3	N3a: Lymph node(s) > 6 cm in greatest dimension and ENE -, **N3b**: Metastasis in any node(s) with clinically overt ENE +
Metastasis	
M0	No metastasis
M1	Metastasis present

modalities, usual practice being surgery followed by postoperative RT [2]. Evidence also indicates that addition of chemotherapy to postoperative RT (called concurrent chemoradiation) improves local control in head and neck cancers [6].

The single most important prognostic factor in OCSCC reducing survival by 50% is neck node metastases [7]. Incidence of neck node metastases depends on the subsite, being least common for the hard palate and commonest in tongue cancers reaching up to 45% [2]. When metastatic nodes are detected on clinical examination or imaging, it is called the N+ neck (N1–N3 of AJCC staging) and requires treatment. N0 neck is the neck when no nodes are detected by clinical examination or imaging [3]. A recent randomized controlled trial has generated evidence for elective treatment even in the N0 neck [8].

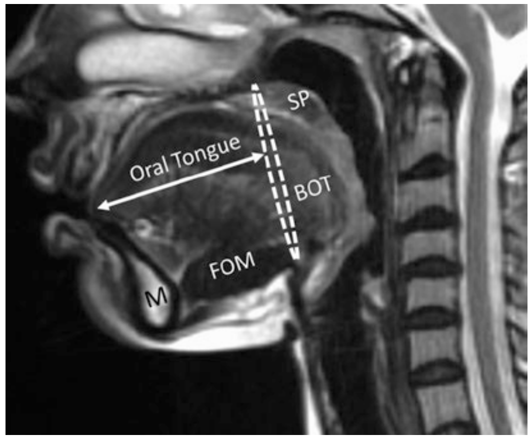

Fig. 5.1 Sagittal T2W MR image showing boundary (circular line) separating oral tongue, a part of oral cavity from base of tongue (BOT), a part of oropharynx. The soft palate (SP) forms superior boundary of oropharynx. The floor of mouth (FOM) at midsagittal plane is predominantly formed by geniohyoid muscle. *M* mandible

5.4 Anatomy

Oral cavity has several subsites which are the buccal mucosa, gingival mucosa covering the upper and lower alveolar ridges, retromolar trigone (RMT), hard palate, oral tongue, and floor of mouth. The lips form the outer boundary of the oral cavity [3]. The detailed anatomy of the oral cavity as seen on imaging is discussed below.

The oral cavity extends from the vermilion border of the lips to a circular region behind, comprising of the circumvallate papillae on the tongue dorsum, anterior tonsillar pillars on either side, reaching up to the junction of hard palate and soft palate superiorly (Fig. 5.1). The papillae are not identified on imaging [9]. The oropharynx is the part of the pharynx located behind the oral cavity and begins just posterior to the circumvallate papillae.

The oral cavity is further divided into the "oral cavity proper" which is located centrally and the "vestibule" located laterally.

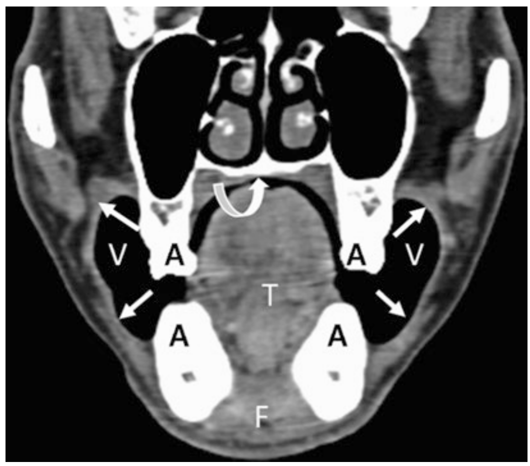

Fig. 5.2 Coronal reformatted CT scan of oral cavity using puffed cheek technique showing the oral cavity proper with tongue (T) at the center, bounded by upper and lower alveolus (A) laterally with hard palate (curved arrow) above and floor of the mouth (F) below. The vestibule (V) is seen on either side, which is laterally bounded by buccal mucosa (straight arrows). The puffed cheek technique distends the vestibule with air separating the gingival and buccal mucosa showing precise origin of tumor

5.4.1 Vestibule and Relations

The vestibule is an air-filled cleft bounded medially by the upper and lower alveolus covered with gingival mucosa and laterally by the buccal mucosa. The vestibule extends from the lips anteriorly to the RMT posteriorly, with the roof and floor being formed by the upper gingivo-buccal sulcus and the lower gingivo-buccal sulcus, respectively (Fig. 5.2).

RMT is a subsite of the oral cavity behind the last molars on either side. It is a triangular mucosal area overlying the vertical ramus of the mandible extending up to the maxillary tuberosity above (Fig. 5.3a and b) [10]. Behind this mucosa lies the pterygomandibular raphe to which are attached the superior pharyngeal constrictor and the buccinator muscles [3]. The pterygomandibular raphe is attached to the pterygoid hamulus superiorly and posterior end of mylohyoid line inferiorly [10]. The RMT is best visualized in its entirety on CT-reformatted images in the oblique sagittal plane (Fig. 5.3). The RMT is a small region but can be a gateway to spread of disease into several areas including the pterygopalatine fossa [3, 10].

The buccal space or buccomasseteric region lies lateral to the vestibule and hence does not form a part of oral cavity. The importance of this space lies in it being a common route of spread of OCSCC (arising in the vestibule) to the posteriorly located masticator space, thereby upstaging disease. The buccal space is bounded medially by the buccinator and laterally by the zygomaticus major (Fig. 5.4). The posterior limit is formed by masseter muscle which is a part of the masticator space. The buccal space contains buccal fat, terminal part of parotid duct, angular branch of facial artery, facial vein, buccal artery, nerves (not seen on imaging), and facial node [9]. The masticator space lies posterior to the buccal space and comprises of the mandible and the four masticator muscles: medial and lateral pterygoids, temporalis, and masseter, as well as the mandibular nerve (Fig. 5.5).

5.4.2 Oral Cavity Proper

The oral cavity proper is bounded on either side by the inner aspect of the gingiva-covered upper and lower alveolus (Fig. 5.2). The roof is formed by the hard palate and floor predominantly by the sling like mylohyoid muscle and the platysma further below. The central part of the oral cavity proper is the oral tongue. It is formed by the anterior two-thirds of the tongue up to the circumvallate papillae, while the posterior one-third of the tongue, also called base tongue, is a part of the oropharynx (Fig. 5.1) [9]. Below the oral tongue and continuous with it is the floor of the mouth. The floor of the mouth (FOM) is formed by muscles and has two spaces contained within, the sublingual and submandibular spaces. These spaces are hidden areas in the oral cavity not amenable to inspection and visualized only on imaging. The anatomy of the FOM is described later in this section.

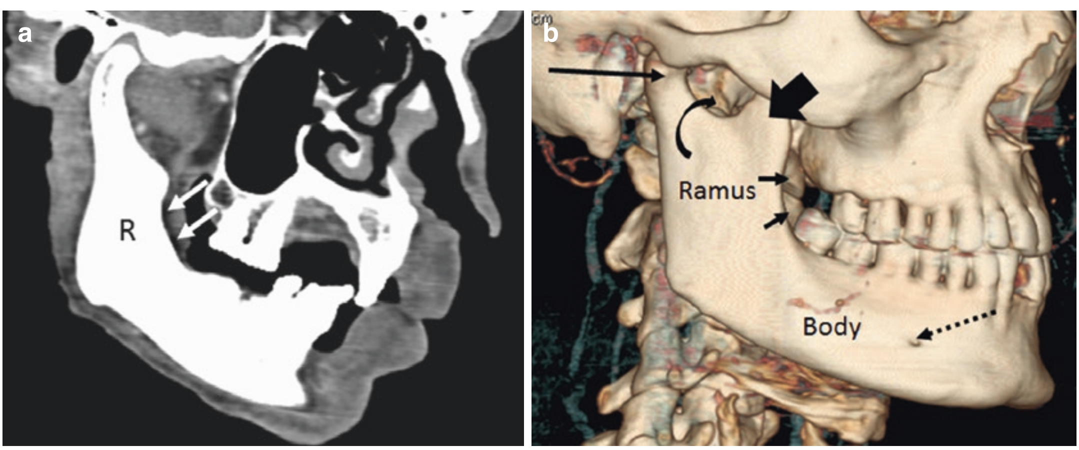

Fig. 5.3 (**a**) Reformatted image (oblique sagittal view) of CT scan of face showing location of retromolar trigone (arrows) anterior to ramus (R) of mandible. (**b**) Volume-rendered oblique sagittal image showing entire right hemimandible and retromolar trigone (short arrows). Sigmoid/mandibular notch (curved arrow) is the notch between the condylar process (long arrow) and coronoid process (block arrow). Dotted arrow shows the mental foramen, where the inferior alveolar nerve enters the inferior alveolar canal of the mandible

The oral tongue is divided into two equal halves by a midline lingual septum and comprises of intrinsic and extrinsic muscles [9]. The anatomy of the oral tongue is best visualized on MR imaging due to its superior soft tissue contrast. The intrinsic muscles of tongue are the superior and inferior longitudinal, transverse, and vertical muscles, which do not have any bony attachment. These muscles interdigitate in the dorsum of the tongue (Fig. 5.6a). The extrinsic muscles of the tongue are the genioglossus, hyoglossus, styloglossus, and palatoglossus, which are attached to the mandible, hyoid bone, and styloid process. All the extrinsic muscles of tongue are supplied by hypoglossal nerve except palatoglossus which is supplied by cranial part of accessory nerve via pharyngeal plexus. The anatomy of tongue muscles are best appreciated on T2W MR images (Fig. 5.6). The important muscles identified consistently on imaging are the genioglossus and hyoglossus [9].

Fig. 5.4 Contrast-enhanced CT scan with puffed cheek showing anatomy of buccal space (area within ellipse) bounded by zygomaticus major (block arrow), masseter (m), medially by buccinator (short arrow). Dashed arrow shows terminal end of parotid duct (content of buccal space) anterior to which is the facial vein (round structure)

The major bulk of the extrinsic muscles is formed by the genioglossus muscle, which can be well seen on axial, coronal, and sagittal T2W images. It is a fan-shaped muscle, which arises from the superior genial tubercle (along the inner aspect of mandible anteriorly in a paramedian position) and sweeps upward to interdigitate with the intrinsic muscles in the tongue dorsum (Fig. 5.6a). The contraction of genioglossus results in protrusion of the tongue. The hyoglossus originates from the greater cornu of the hyoid bone on either side and courses upward lateral to the genioglossus as a thin quadrilateral muscle into the sides of the tongue (Fig. 5.6b and c). It is involved in depression of the tongue. The stylo-

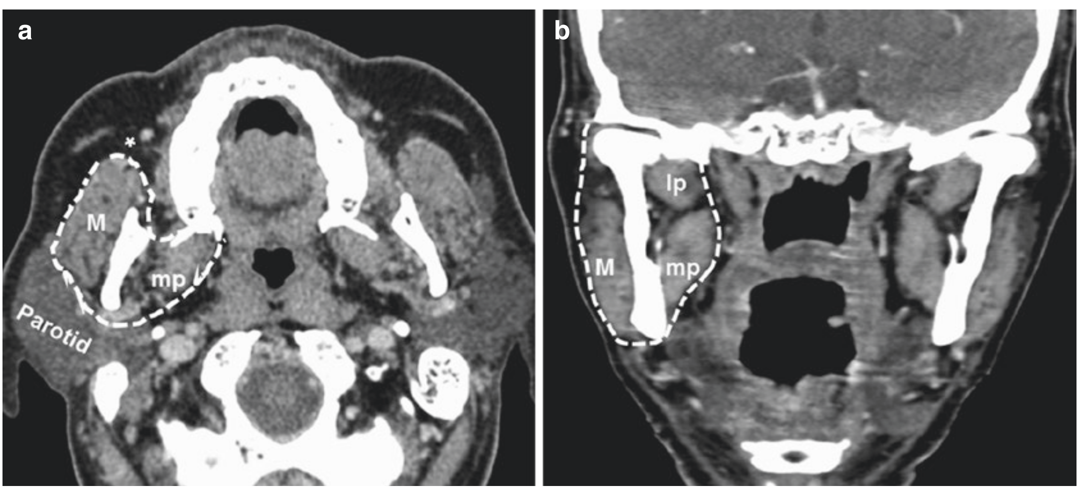

Fig. 5.5 (**a**) Axial and (**b**) coronal contrast-enhanced CT images showing masticator space (bounded by dotted lines) showing muscles of mastication within (m, masseter; mp, medial pterygoid; lp, lateral pterygoid). The buccal space (asterisk) is seen anterior to masticator space, and parotid gland is seen posterior to this space in axial images

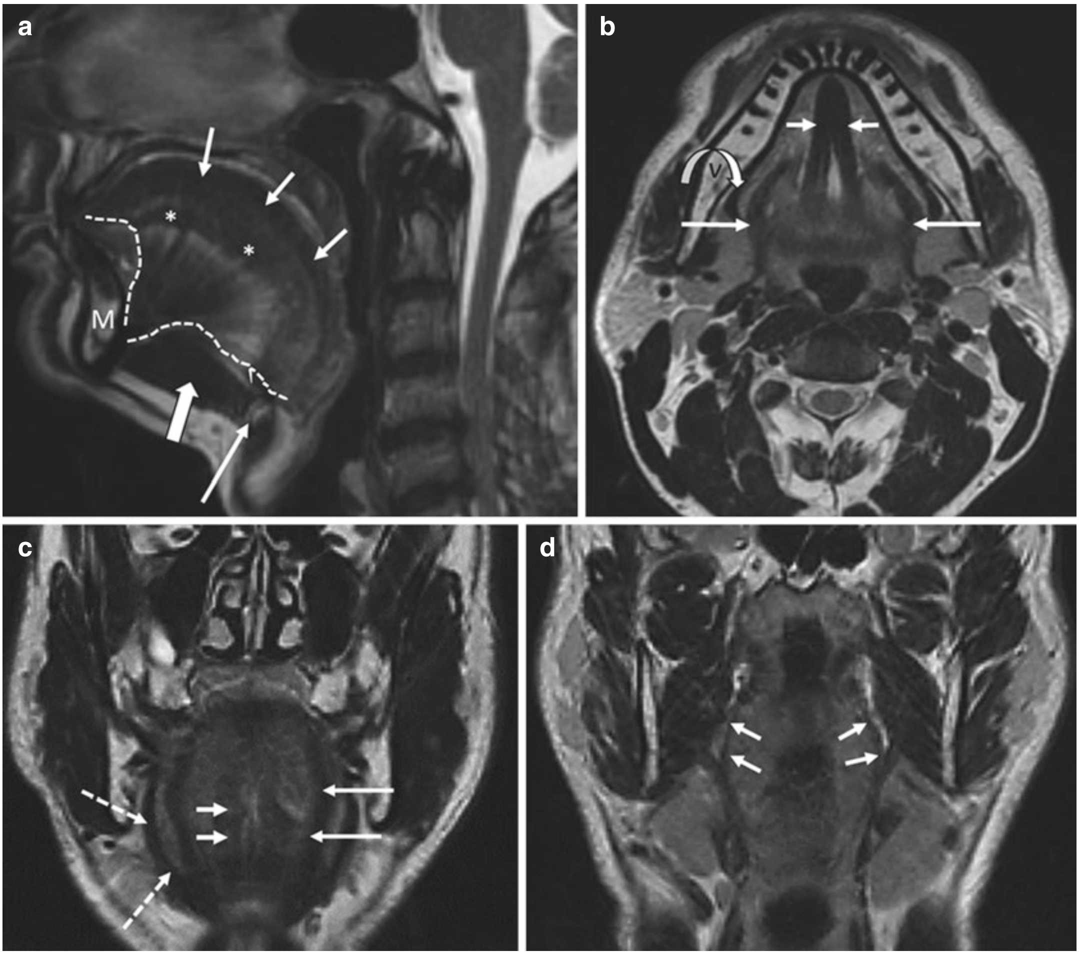

Fig. 5.6 (**a**) Sagittal T2W MR image showing intrinsic muscles of tongue, superior longitudinal muscle (short arrows), and inferior longitudinal muscle (asterisks). The fan-shaped genioglossus is seen (enclosed within dotted lines) extending from superior genial tubercle of mandible (M) interdigitating with the intrinsic muscles above. The midsagittal plane also demonstrates the geniohyoid muscle (block arrow) extending from inferior genial tubercle of mandible to hyoid bone (long arrow). (**b**) Axial T2W MR image and (**c**) sagittal T2W MR image showing genioglossus (short arrows), hyoglossus (long arrows), mylohyoid (curved arrow in b and dashed arrow in c). (**d**) Coronal T2W MR image showing palatoglossus muscle (arrows) within the anterior tonsillar pillar

glossus arises from the tip of the styloid process and stylomandibular ligament and courses anteriorly to interlace with the hyoglossus. Its main function is to elevate and retract the tongue. The palatoglossus arises from the palatine aponeurosis of soft palate and passes downward, forward, and laterally within the anterior tonsillar pillar to insert into the sides of the tongue. It elevates the posterior tongue and aids in initiation of swallowing. It is not always identified clearly on imaging (Fig. 5.6d) [9].

The floor of mouth (FOM) is primarily supported by the mylohyoid muscle. It is a sling-shaped muscle, which arises from the symphysis menti and mylohyoid line in the mandible on both sides extending up to the last molar tooth (Fig. 5.7). It attaches to the midline fibrous raphae as well as hyoid bone and supports the floor of mouth. It separates the deep and superficial lobes of submandibular gland, which ascends along the free posterior edge of mylohyoid. The other muscles that support the FOM are the geniohyoid and anterior belly of digastric muscles. Geniohyoid, as the name indicates, arises from the inferior genial tubercle of mandible and attaches to the hyoid bone. It is seen well on coronal T2W images as darkly hypointense muscle in the paramedian position, lying above the mylohyoid muscle (Figs. 5.6a and 5.7). The anterior belly of digastric lies below the mylohyoid and can be seen on coronal T2W images (Fig. 5.7). All the FOM muscles are well identified on MR imaging [9].

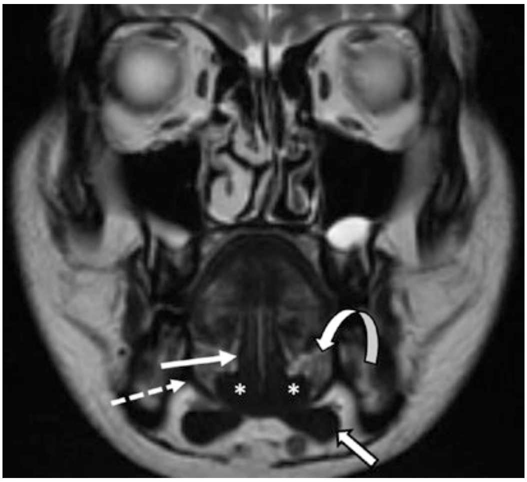

Fig. 5.7 Coronal T2W MR image showing sublingual space (curved arrow) bounded medially by genioglossus muscle (straight arrow) and laterally by mylohyoid muscle (dashed arrow). The geniohyoid muscle (asterisks) and anterior belly of digastric (block arrow) also form floor of mouth in addition to mylohyoid muscle

The sublingual space is located inferolateral to genioglossus muscle and superomedial to mylohyoid muscle. It comprises of sublingual fat, sublingual salivary gland, deep part of submandibular salivary gland, Wharton's duct, lingual artery, lingual vein and lingual nerve, hypoglossal nerve, and anterior fibers of hyoglossus. It appears as hypodense area on CT images and hyperintense on MR images (Fig. 5.7) [9]. The nerves are not visualized on imaging but are located lateral to the flow void of the lingual artery which is seen consistently.

The submandibular space is a horseshoe-shaped space located inferior to the mylohyoid muscle and superior to the platysma. It contains the anterior belly of digastric muscles anteriorly and the bulk of the submandibular glands posteriorly (Fig. 5.8a and b). Posteriorly it communicates with the sublingual space along the free

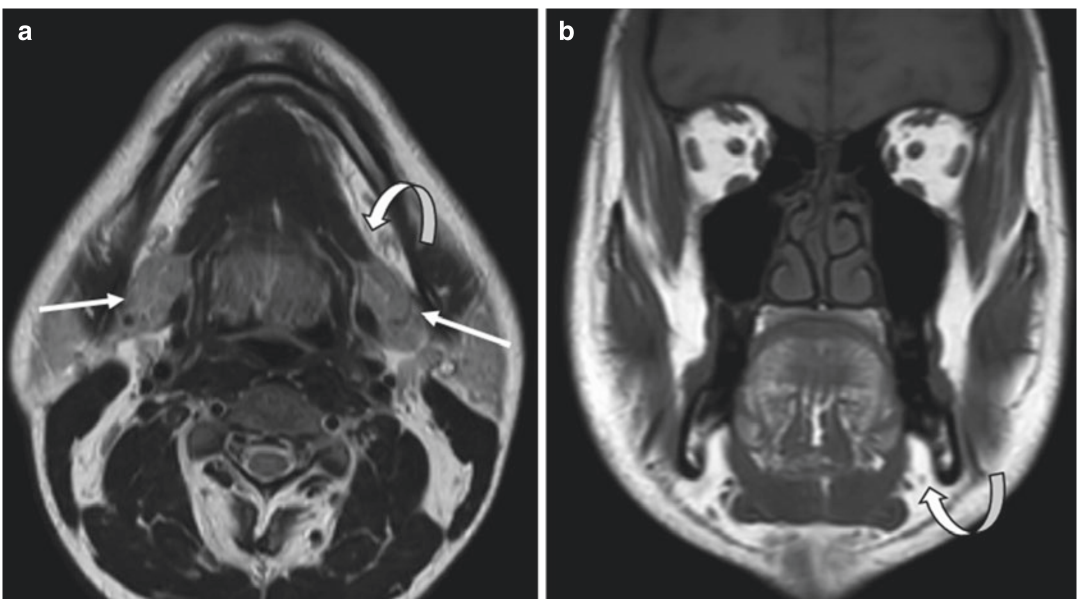

Fig. 5.8 (**a**) Axial T2W and (**b**) coronal T1W MR image showing submandibular space (curved arrow) and submandibular gland (straight arrow)

posterior border of mylohyoid muscle. Posteriorly and superiorly this space communicates with the lower end of the parapharyngeal space [11].

5.5 Imaging Methods

The choice of imaging modality depends on the disease subsite, the issues of clinical relevance, and the stage of disease. In general cross-sectional imaging like CT and MRI is required for locoregional staging, the choice depending on the disease subsite [4]. Advanced disease requires metastatic workup with PET/CT [4]. US is used mainly for evaluating lymphadenopathy in the neck [9]. It has also been used to evaluate tumor thickness in the tongue and buccal mucosa [12–14]. Barium studies best evaluate the mucosa and may be useful to screen for a second aerodigestive tract primary. OPG is most useful for evaluating and planning dental treatment prior to radiotherapy in order to prevent osteoradionecrosis [3].

The role of various imaging methods in the complete workup of OCSCC at various subsites is discussed in this section.

***Primary disease (T staging)*:** Evaluating the primary in OCSCC requires cross-sectional imaging such as *contrast-enhanced CT* or *contrast-enhanced MRI*. Prolonged scanning time, patient claustrophobia, and motion artifacts with swallowing are the problems with MRI, while superior soft tissue resolution, availability of direct multiplanar reformations, and lack of exposure to ionizing radiation are its advantages. CT has the disadvantage of dental amalgam artifacts, but speed of scanning is a great advantage. Advances in CT such as multidetector CT (MDCT) now also permit high resolution indirect reformations, earlier available only with MRI. However optimal imaging requires 16- or higher-row MDCT scanner to generate isotropic coronal, sagittal, and oblique reformations. Both bone and soft tissue algorithms are required. CT is performed with the puffed cheek technique with the patient puffing his cheeks with air to separate the buccal mucosa from the gingival mucosa during quiet breathing [15]. Interactive viewing of the multiplanar images on the workstation helps optimal assessment [10]. The CT and MRI protocols at our institute are discussed in Table 5.2.

Specific issues of clinical relevance at each disease subsite and patient factors also influence the chosen method of imaging. Few studies exist comparing CT and MRI for imaging oral cavity with emphasis on tongue cancers. For oral tongue and FOM SCC, where soft tissue resolution is of

Table 5.2 CT and MRI protocol in OCSCC

Imaging Protocol	CT	MRI
Scanner requirement	16 or more slice MDCT scanner (for high-quality multiplanar reformations)	Minimum 1.0 T, optimum 1.5 T magnet using phased array coil
Volume of coverage	Above base of the skull to root of the neck	Above base of the skull to root of the neck
Slice thickness	2.5–3 mm with 0.625/ 0.75 retro-reconstruction (on 16 slice MDCT scanner)	4 mm thickness with 1 mm intersection gap
Volume of IV contrast	50 ml in adults, 1.5 times body weight in children injected at a rate of 3 ml/sec with scan done at 25–30 seconds of contrast injection	0.1 ml/kg body weight with images acquired after complete contrast administration
Type of IV contrast	Nonionic iodinated contrast medium	Gadolinium-based contrast medium
Imaging sequences	Axial CT images obtained using puffed cheek technique in soft tissue and bone algorithm, multiplanar coronal, and sagittal reformations obtained by reconstruction	Axial and coronal spin echo T1 weighted, axial and sagittal fast spin echo T2-weighted, coronal STIR, post-contrast axial, coronal and sagittal T1W sequences, and diffusion-weighted sequence.(b value of 0 and 1000 s/mm^2)

greatest importance, they favor contrast-enhanced MRI over contrast-enhanced CT for T staging [16–20].

In gingival, buccal, and RMT cancers, bone erosion is far more frequent and ranges from 14 to 72% as compared to tongue cancers (5–10%) [10, 21]. Bone erosion is an important issue in OCSCC. Bone invasion influences management, which can vary from mandible-sparing surgery (when invasion is absent) to the conservative marginal mandibulectomy that preserves function and cosmesis and to the more destructive segmental mandibulectomy (when invasion is extensive) [22]. Bone invasion cannot be predicted by clinical examination alone. Histopathology (HP) can demonstrate bone invasion in the absence of clinically detected bone erosion. Hence imaging assumes vital importance [23, 24]. The point to note is that bone resection margins are difficult to assess by clinical examination or frozen section alone emphasizing the need for accurate preoperative imaging [2, 5]. Contrast-enhanced CT is the method of choice as it has the highest specificity (87–90%) for bone erosion [10, 25, 26]. MRI has high sensitivity and negative predictive value but has lower specificity (54% for cortical invasion) and overestimates both cortical and inferior alveolar canal invasion [26]. OPG has low specificity in detecting mandibular erosion, particularly in poor dental hygiene and quid-chewing populations where periodontitis and odontogenic infections can mimic malignant erosion. Midline erosions are also a pitfall with OPG, and early erosions can be missed as detection requires at least 30% mineral loss [27]. Many modalities have been assessed for evaluating the mandible in OCSCC. Table 5.3 summarizes a review of few

Table 5.3 Review of major studies assessing mandibular invasion in OCSCC

Study	Imaging methods	Conclusion
Weissman et al. 1982	Bone scan	*n* = 40; 43% false-positive cases
Curran et al. 1996	SPECT	*n* = 29; sensitivity = 100%, specificity = 29%
Mukherji et al. 2001	Conventional CT (3 mm sections)	*n* = 49; sensitivity = 96%; specificity = 87%; positive predictive value = 89%; negative predictive value = 95%
Brockenborough et al. 2003	DentaScan (CT software)	*n* = 35; sensitivity = 95%; specificity = 79%; positive predictive value = 87%; and negative predictive value = 92%
Bolzoni et al. 2004	MRI	*n* = 43; sensitivity = 93%; specificity = 93%; accuracy = 93%; NPV = 96% and PPV = 87.5%
Goerres et al. 2005	PET-CT, CT, and SPECT/CT	*n* = 34; accuracy = 88% (SPECT/CT) 94% (PET/CT), 97% (CT) PET component of CT did not add to CT component
Handschel et al. 2012	6-row MDCT	*n* = 107; Sensitivity = 82.6%; specificity = 86.9%; positive predictive value = 82.6%; negative predictive value = 86.9%
Vidiri et al. 2010	MRI and 4-row MDCT	*n* = 36; sensitivity = 93% (MRI), 79% (MDCT); specificity = 82% (MRI), 82% (MDCT); accuracy = 86% (MRI), 81% (MDCT)—In all OCSCC
Imaizumi et al. 2006	CT using DentaScan and MRI	*n* = 51; sensitivity = 96% (MRI), 100% (MDCT); specificity = 54% (MRI), 88% (MDCT) for cortical invasion in all OCSCC
Hendrikx et al. 2010	Panoramic radiography(PR/OPG), cone beam CT (CBCT), and MRI	*n* = 23; sensitivity = 55% (PR), 81% (MRI), 91% (CBCT) Specificity = 92% (PR), 67% (MRI), 100% (CBCT)
Dreiseidler et al. 2011	Cone beam CT (CBCT), MDCT, and SPECT	*n* = 77; sensitivity = 92% (CBCT), 80% (MDCT), 91% (SPECT); specificity = 96.5% (CBCT), 100% (MDCT), 40% (SPECT)
Arya et al. 2013	16-row MDCT	*n* = 37; sensitivity = 94%, specificity = 90%, and accuracy = 91.8% for cortical invasion in RMT SCC

studies analyzing various imaging methods for mandibular invasion in OCSCC [10, 25–36]. Although cone beam CT has shown to have high sensitivity and specificity, it has two particular disadvantages, (a) difficulty in visualizing subtle alveolar crest invasion and (b) lack of contrast and soft tissue information [37].

The other issues while evaluating the local extent in gingival, buccal, and RMT cancers are *posterior soft tissue spread (masticator space invasion)* and *perineural spread*. While MRI has superior soft tissue resolution [38], MDCT is a close alternative for masticator muscle invasion. This is due to the presence of well-defined fat planes seen around these muscles, effacement of which by disease is easily visualized on CT. Perineural spread is best visualized on fat-suppressed contrast-enhanced T1W MRI sequences; the incidence of perineural spread in these cancers is however <10% [39–41]. Contrast-enhanced MRI can be a problem-solving second imaging method in gingival, buccal, and RMT cancers, when perineural spread is suspected.

In hard palate squamous cell cancers (SCC), perineural spread is frequent through the greater palatine canal. Hence hard palate SCC is best imaged with MRI, which also includes fat-suppressed contrast-enhanced T1W sequences (best for perineural spread and soft tissue extent). Bone erosion, best evaluated with CT, is complementary.

Evaluation of the neck (N staging)**:** Low volume tongue or buccal mucosa lesions that present as shallow ulcers are often not imaged for the primary. However, in these early cases, many clinicians may need imaging evaluation of the neck for nodal metastases for planning the extent of neck dissection and evaluating the contralateral neck. US is often ordered by many clinicians in such early cases, due to its wide availability and cost-effectiveness. However US is known to be operator dependent. The incidence of neck node metastases varies from 6 to 45% [7]. Various imaging methods have been evaluated and compared to assess the neck for metastatic adenopathy.

US is widely used in Europe and Asia, although this has not gained popularity in the United States. A meta-analysis comparing US-guided fine-needle aspiration biopsy (US g FNAB), US, CT, MRI, and PETCT has shown US g FNAB with the highest diagnostic odds ratio for detecting metastatic neck nodes [42] with decreasing performance for US alone, MRI with ultra-small particle iron oxide (USPIO), CT, and MRI in that order. However this meta-analysis included both N+ and N0 necks. In the lone study in this meta-analysis, which included only N0 neck, the sensitivity of US g FNAB was only 48% [43].

Contrast-enhanced ultrasound has also been evaluated in a small number of studies for differentiating inflammatory and metastatic nodes with reported high diagnostic accuracy but is not widely used in clinical practice [44]. Retrospective and prospective studies using *CT and MRI* for imaging OCSCC report comparable accuracy for N staging. A meta-analysis analyzing performance of MRI for nodal staging in head and neck SCC found a sensitivity and specificity of 76% and 86%, respectively. Performance of MRI was comparable with PET, CT, and US [45]. Advances in MRI such as diffusion-weighted imaging (DWI) MRI and dynamic contrast-enhanced (DCE) MRI have shown a promising role in differentiating subcentimeter benign and metastatic nodes in initial small studies [46–50]. However a recent study by Lim et al. showed that DWI-MRI does not allow differentiating benign from metastatic cervical lymph nodes in patients with head and neck cancer and non-necrotic, small lymph nodes [51].

Of greater importance is the role of imaging in the N0 or clinically negative neck. There are two meta-analyses in the N0 neck: one involving PETCT reported a detection rate of only 50% [52], and another comparing PET, CT, MRI, and US reported comparable accuracies but inferior to surgical staging [53]. The pooled sensitivity and specificity of CT, MRI, PET, and ultrasound were 52% and 93%, 65% and 81%, 66% and 87%, and 66% and 78%, respectively [53]. Hence the imaging method chosen for the evaluation of the primary is also used for evaluation of the neck in the same patient (no advantage lies in adding a second imaging method).

Sentinel node biopsy (SNB) that requires identification of the sentinel node using PET and subsequent biopsy has also been evaluated to identify metastatic nodes in OCSCC. A diagnostic meta-analysis of SNB in 847 patients of clinically T1/T2 N0 OCSCC and oropharyngeal SCC patients revealed an overall sensitivity of 93% [3, 54]. Another study comparing SNB with USG-guided FNAC in T1/T2 N0 OCSCC found SNB to be clearly superior [55]. However a recent randomized controlled trial in the N0 neck has shown that elective neck dissection is superior to therapeutic neck dissection even in early oral cancers thereby limiting the role of imaging in the ipsilateral neck [8]. If this evidence is accepted, the role of imaging in N staging today is limited to evaluation of the contralateral neck and possibly to plan the extent of neck dissection in the N+ neck.

Metastatic workup (M staging)**:** PET/CT has no additional value over conventional CT or MRI in the evaluation of untreated OCSCC, for evaluating either the primary or the neck [19, 20, 36, 56–58]. Most guidelines recommend the use of PET/CT only in stage III or IV cancers where management may alter due to detection of distant metastases [4]. When PET/CT is not performed, a chest radiograph or contrast-enhanced CT is used to rule out pulmonary metastases, particularly when abnormal level IV nodes are seen in the neck [3]. A CT scan of the abdomen is justified when the clinical index of hepatic metastasis is high [2].

5.6 Spread Patterns of OCSCC and its Implications

Tongue and floor of mouth SCC**:** SCC arising from the oral tongue and the oropharyngeal tongue differ in their management. This chapter will focus on oral tongue squamous cell carcinoma, the vast majority of which arise from the lateral border (85%) with only few seen along the ventral surface. Small tumors along the lateral border can be treated with wide excision glossectomy and negative margins (Fig. 5.9) [3]. Larger tumors are treated with partial to total glossectomy. Reconstruction is planned when approximately one-third volume loss is expected [3]. Further invasion occurs medially into the intrinsic muscles and can extend across the lingual septum into the contralateral side (Fig. 5.10a). This is associated with greater incidence of contralateral nodal metastases. Inferior extension can occur into the sublingual space with encasement of the lingual neurovascular bundle (Fig. 5.10b). Involvement of both neurovascular bundles by contralateral spread requires total glossectomy [3] (Fig. 5.10c). Inferior extension can also invade extrinsic muscles (genioglossus and hyoglossus) (Fig. 5.10d). It is important to note that extrinsic muscles are well seen on T2W MRI but are difficult to visualize intraoperatively or on the histopathology (HP) specimen, hence in the 8th edition AJCC staging, the criteria of extrinsic muscle invasion has been excluded in the T4a staging of oral cancers [3].

Tongue cancers that extend to extrinsic muscles can further invade the FOM muscles (Fig. 5.11a). Tumors that reach the FOM or primary FOM cancers can erode the adjacent mandible (Fig. 5.11b) and even invade the skin. These are resectable but require major reconstruction. Posterior extension in the FOM can reach up to the hyoid and can contraindicate surgery (Fig. 5.11c). Posterior extension from the tongue dorsum may reach into the base tongue and across the anterior tonsillar pillar into the tonsil and lateral pharyngeal wall (Fig. 5.11d). Posterior and inferior spread into the valleculae, pre-epiglottic space, and up to the hyoid bone may also be seen [3, 9]. All the above types of posterior spread may require radical surgery and hence are often treated with chemoradiation instead [3]. Far posterior extension into the masticator space and pterygoid plates constitutes T4b disease, and this is unresectable [4].

Nodal spread from tongue cancers are usually to ipsilateral level I and II nodes (Fig. 5.10a), but skip metastases to levels III and IV and contralateral metastases are known. Midline FOM SCC can spread to bilateral nodes [3].

Prognostic markers: The issues that influence prognosis and therapy in tongue cancers are *depth of invasion (DOI) previously called tumor thickness (TT)*, *T stage*, *posterior soft tissue extent*, and *perineural invasion*, apart from *nodal spread* [3, 4, 7, 39]. TT is the single best prognostic factor

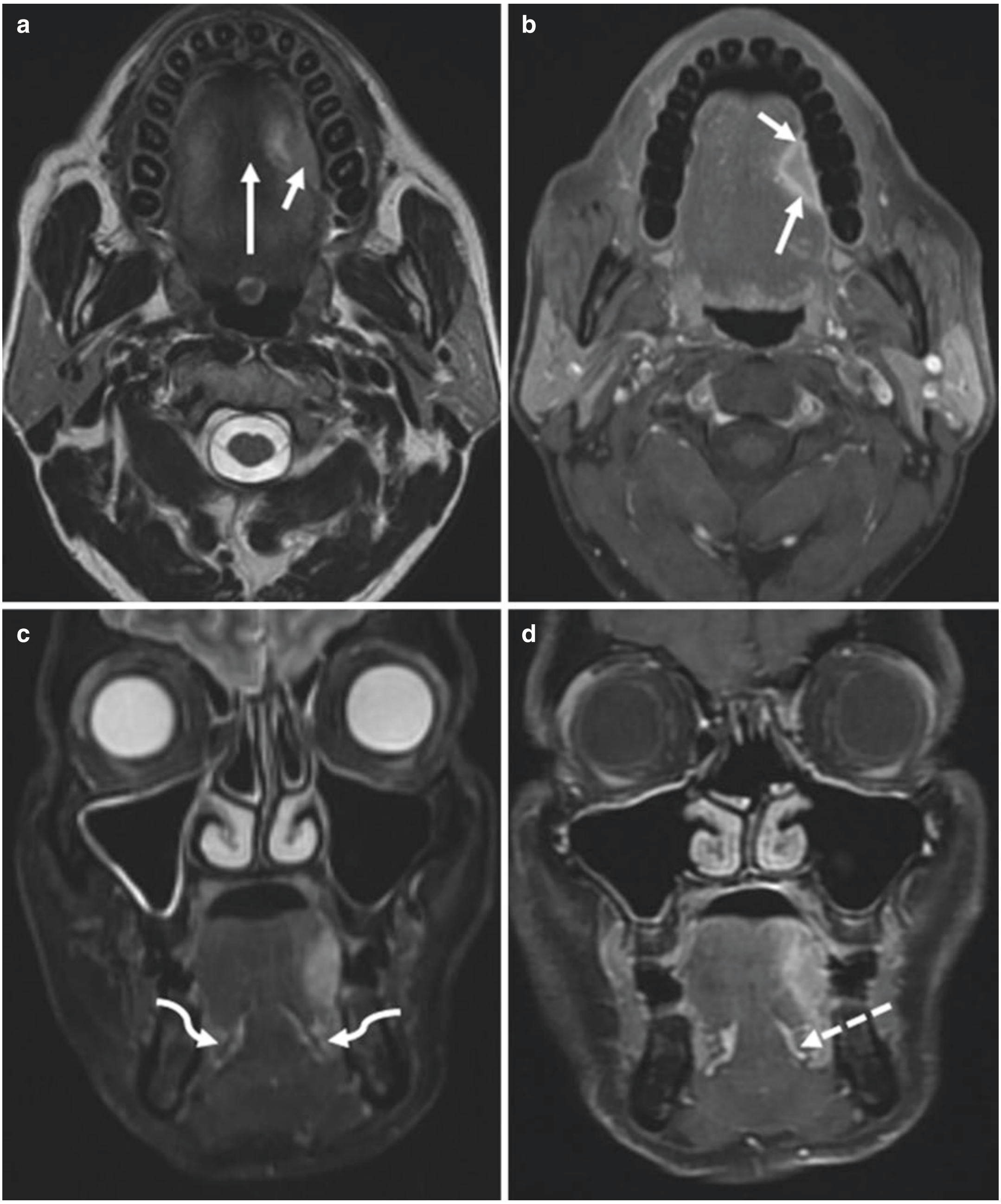

Fig. 5.9 Early carcinoma of tongue. (**a**) Axial T2W and (**b**) contrast-enhanced T1W MR images of tongue showing small enhancing lesion confined to left lateral border of tongue (arrows). There is no extension across midline or involvement of genioglossus (long arrow). (**c**) Coronal STIR and (**d**) post-contrast coronal MR images in same patient show no evidence of extension into sublingual space (curved arrows) or involvement of neurovascular bundle (dashed arrows)

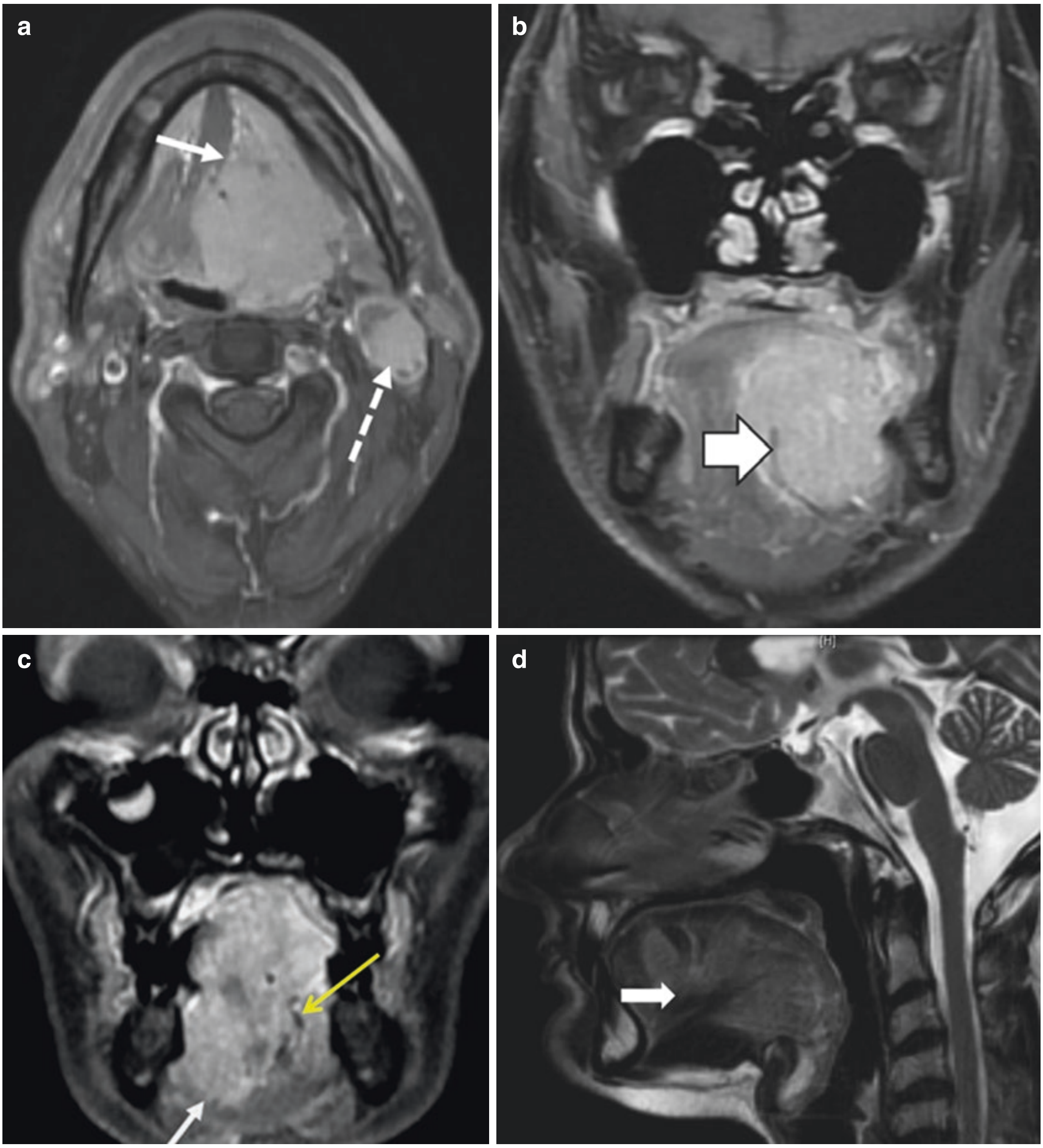

Fig. 5.10 Advanced carcinoma of tongue. (**a**) Axial post-contrast MR image showing enhancing tumor in left lateral aspect of tongue extending across midline with involvement of genioglossus muscle (short arrow). A necrotic metastatic left level II lymph node is seen (dashed arrow). (**b**) Coronal post-contrast MR image showing tumor involving ipsilateral neurovascular bundle (block arrow) and in (**c**) bilateral neurovascular bundles (arrows). (**d**) Sagittal T2W MR image showing extension of tumor into genioglossus and intrinsic muscles of the tongue (block arrow)

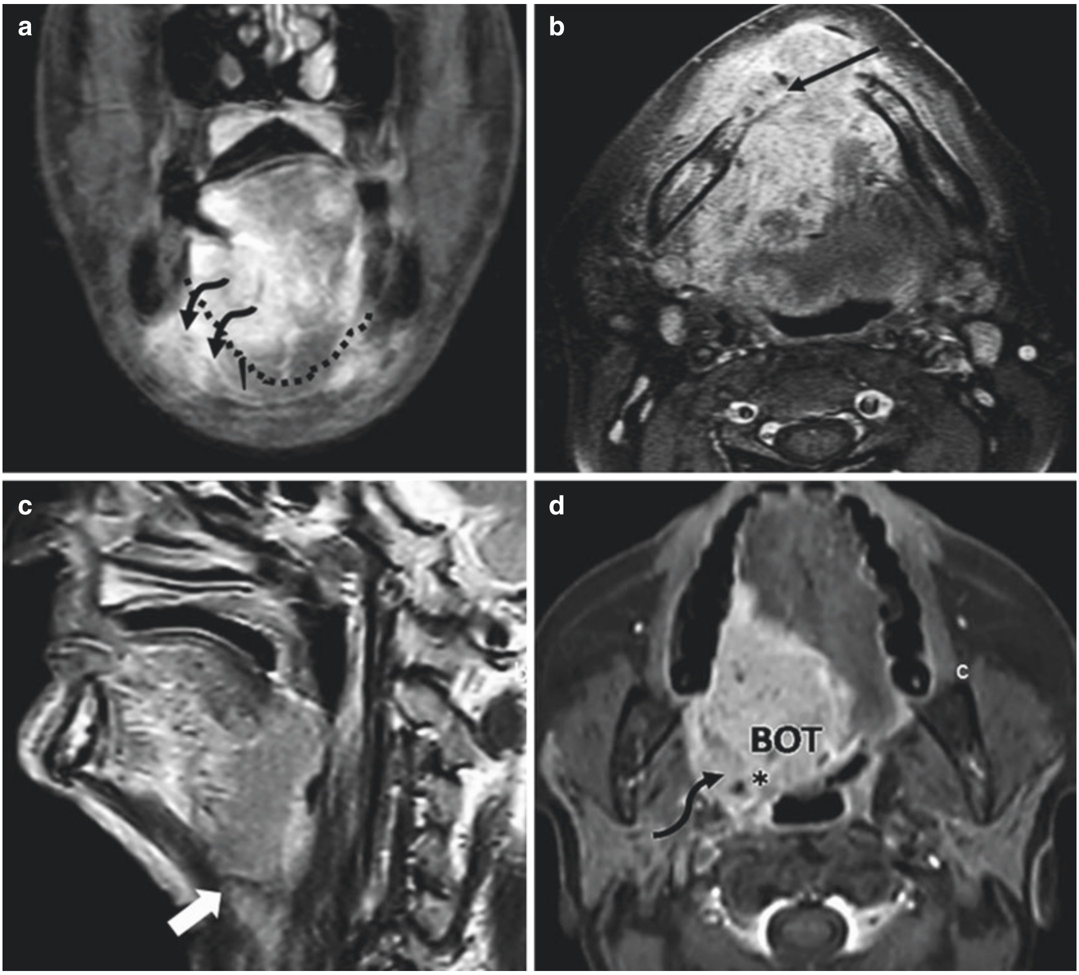

Fig. 5.11 Advanced carcinoma of tongue (**a**) coronal post-contrast MR image showing extension of tumor into submandibular space (curved arrows) across the mylohyoid (dotted lines). (**b**) Axial post-contrast MR image showing tongue SCC invading mandible which shows tumor signal intensity within (arrow) and extending into oral vestibule. (**c**) Sagittal T2W MR image showing tumor of intermediate signal intensity extending into the hyoid bone (block arrow). (**d**) Post-contrast axial image showing tumor extension into base of tongue (BOT), right vallecula (*), and lateral pharyngeal wall (curved arrow)

for predicting survival in *early tongue cancers* in several multivariate analyses [7]. different reports [59], and a meta-analysis by Huang et al. has shown an association of TT greater than 4 mm on histopathology with significant increase in neck node metastases [7]. This has led in the past, to the recommendation of the practice of elective neck dissection when TT exceeds 4 mm [4]. The 8th edition AJCC staging of oral cancer incorporates DOI (earlier referred to as TT) for defining T1-T3 stage (Table 5.1). The DOI measurement depends on the epicenter of the lesion [3]. In those tumors with epicenter along the lateral border of the tongue, the lateral to medial spread within the tongue is the DOI, while for tumors with epicenter along the ventral surface or dorsum of tongue, the cranicaudal spread of tumor (vertical dimension) is the DOI. The method of measuring DOI on imaging has been described [3, 60].

Preoperative and intraoperative US have shown satisfactory accuracy for measurement of TT/DOI in prospective studies [12, 13]. Lam et al. demonstrated the technique of measurement of tumor thickness on MRI (Fig. 5.12). They found contrast-enhanced T1W images had higher concordance (83%) than T2W images (52%) for

TT/DOI measurements as compared to HP [60]. Okura et al. in a prospective study comparing MRI with HP found a TT of >9.7 mm on MRI associated with significant increase in nodal metastases [61]. In practice though, in early tumors (with TT/DOI ≤4 mm), imaging is often not ordered, and hence role of imaging in measuring DOI becomes limited.

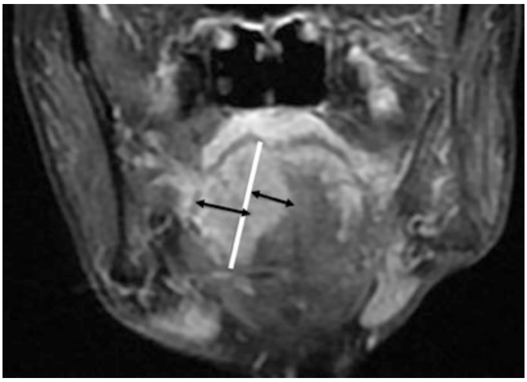

Fig. 5.12 Coronal post-contrast MR image showing measurement of tumor thickness (now called depth of invasion) in carcinoma tongue. The vertical white line is the reference line drawn between two tumor-mucosa junctions. Perpendicular measurements on either side of this reference line (double-ended black arrows) to maximum points of tumor projection are added to obtain depth of invasion

MRI has an established role in accurately defining the p*osterior extent and T stage* that influences therapy and prognosis in advanced cancers [62, 63]. *Perineural invasion* is a prognostic factor, but refers to microscopic invasion of small nerves, not seen on imaging [40, 41]. Perineural spread in contrast refers to macroscopic spread inferred from imaging [41], is best seen on contrast enhanced MRI and is described further later in this chapter. In oral tongue and FOM SCC, perineural spread can occur along the lingual nerve to reach the mandibular nerve in the masticator space. Involvement of mandibular nerve can cause denervation changes and atrophy in the masticator muscles (indirect sign of perineural spread) [40, 41]. The other factors that influence prognosis are *nodal metastases and extranodal spread*. CT and MRI are comparable for assessment of nodal metastases and extranodal spread (Figs. 5.10a and 5.13) [64].

Contribution of various MRI sequences: Optimal MR imaging requires multiplanar sequences including post-gadolinium T1W sequences and preferably diffusion-weighted imaging. The tumor-tongue contrast is maximum on contrast-enhanced T1W sequences [62]. Extrinsic muscle involvement is best appreciated on axial and coronal T2W sequences [62, 63].

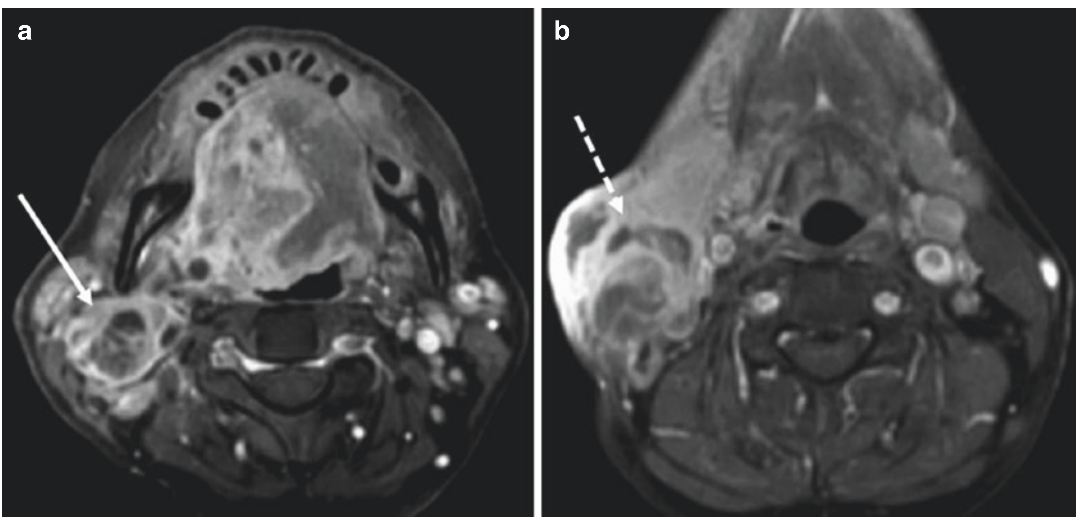

Fig. 5.13 Features of metastatic nodes. (**a**) Post-contrast axial MR images showing enlarged peripherally enhancing right level II lymph node with central necrosis and (**b**) enlarged right level II lymph node with extracapsular spread (shown by ill-defined margins and invasion of surrounding structures)

Cortical bone erosion is well depicted on non-contrast T1W sequences, while marrow involvement is studied on unenhanced T1W, STIR, and post-gadolinium T1W sequences [26]. We evaluate nodes on axial T2W, coronal STIR, and post-contrast T1W sequences.

***Lips*, *gingiva*, *buccal mucosa, and RMT*:** SCC of the *lips* can spread posteriorly into the buccal mucosa and medially across the gingivo-buccal sulci to abut or erode the mandible. Perineural spread through mental foramen is seen as a widened foramen on CT and enhancement around the foramen on contrast-enhanced MRI [3, 39].

Lower gingival/alveolar ridge SCC frequently erodes the mandible and can spread medially into the tongue muscles. The most common OCSCC in the Indian subcontinent is that of the lower gingivo-buccal complex due to tobacco chewing and has been described as the "Indian oral cancer" (Fig. 5.14) [65]. SCC arising or reaching the *upper gingival/alveolar ridge* can erode the maxillary alveolus and invade the maxillary sinus (Fig. 5.15).

Buccal SCC can also extend across the upper and lower gingivo-buccal sulci to the mandible/maxilla. The route of tumor entry in the dentate mandible is the point of abutment of tumor to the

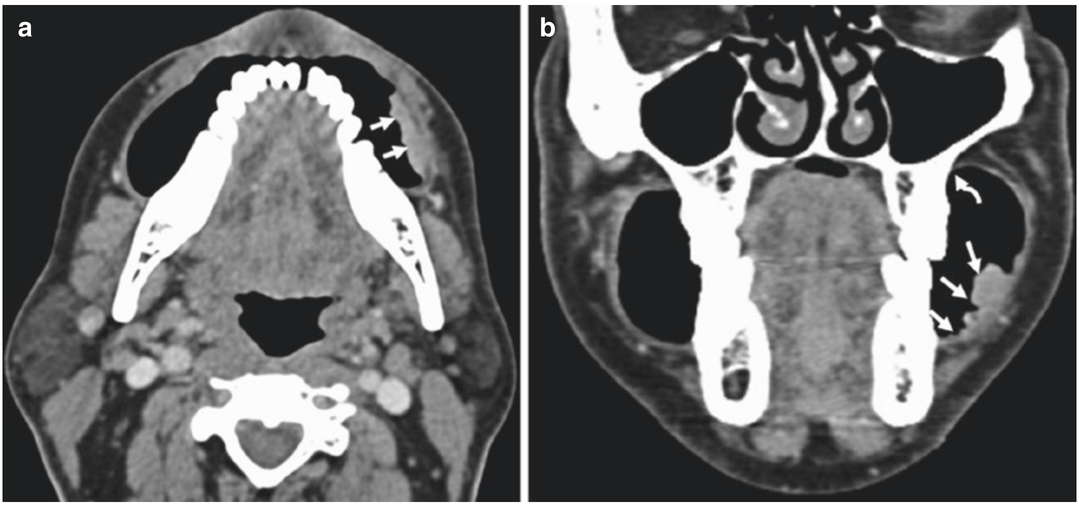

Fig. 5.14 Early lower gingivo-buccal carcinoma. (**a**) Axial and (**b**) coronal contrast-enhanced CT images showing enhancing proliferative lesion (short arrows) confined to left buccal mucosa near the lower gingivo-buccal sulcus which is well appreciated with the puffed cheek technique. The upper gingivo-buccal sulcus (curved arrow) is spared. There is no extension of tumor into the subcutaneous tissue or skin

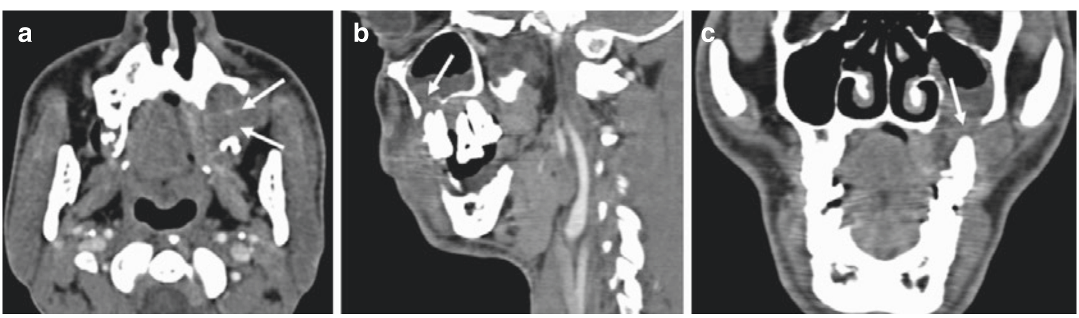

Fig. 5.15 (**a**) Axial, (**b**) sagittal, and (**c**) coronal contrast-enhanced CT images showing upper alveolar carcinoma (arrows) eroding floor of maxilla with extension into the maxillary sinus

mandible (Fig. 5.16a, b), while in the edentulous mandible, spread occurs through the occlusal ridge [66]. Lateral or inferior spread into the skin influences resection and reconstruction and is usually assessed clinically. Linear reticulations in the dermis and subcutaneous fat seen on CT adjacent to the tumor need to be recorded, but Spector et al. reported that this was often due to peritu-

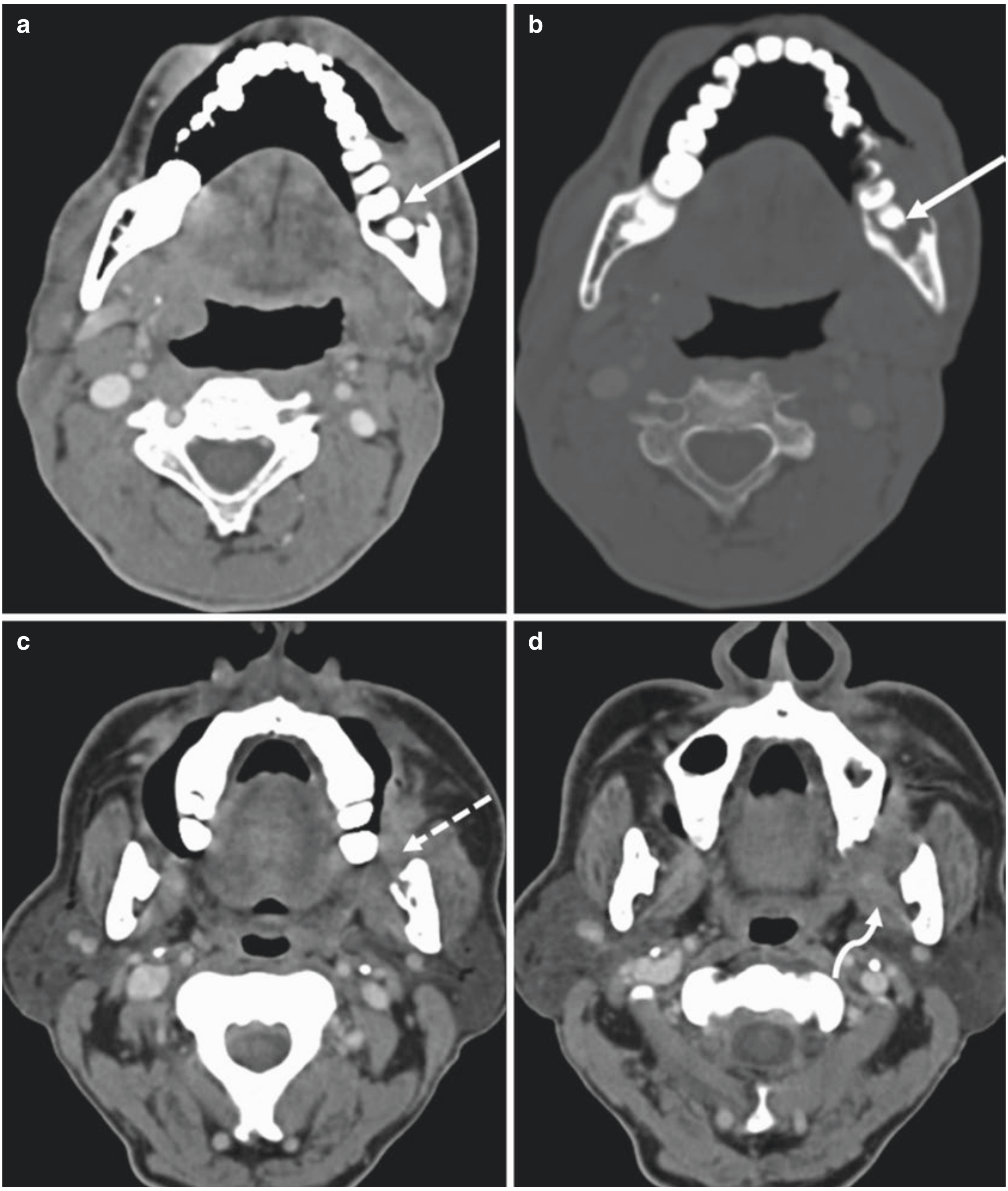

Fig. 5.16 Contrast-enhanced axial CT images in (**a**) soft tissue window and (**b**) bone window showing carcinoma of left buccal mucosa invading the mandible at the point of abutment, i.e., junction of the body and ramus (straight arrows). (**c**) and (**d**) Contrast-enhanced axial CT images of left retromolar trigone (RMT) carcinoma (dashed arrow) showing loss of fat planes with medial pterygoid (curved arrow) suggestive of extension into masticator space

moral inflammation in 11/12 cases in their series [67].

RMT SCC can spread anteriorly and laterally into the buccal mucosa and body of mandible, anteriorly and medially into the base tongue or FOM, posteriorly into the mandibular vertical ramus and muscles of masticator space (Fig. 5.16c, d), posteriorly and medially into the tonsil, and superiorly into the nasopharyngeal wall and pterygopalatine fossa.

Invasion of the skin, cortical bone, and maxillary sinus constitute T4a disease. Although considered moderately advanced, this is resectable if no other comorbidities are present. However posterior spread to invade the masticator space, pterygoid plates, carotid vessels, or skull base is classified as T4b and is considered a very advanced disease. No uniform criteria for resectability of T4b disease exist, but spread of disease to the carotid vessels, pterygopalatine fossa, (Fig. 5.17) and skull base is considered unresectable.

Perineural spread from gingival, buccal, and RMT SCC can reach the mandibular nerve in the masticator space and spread intracranial through

Fig. 5.17 Advanced carcinoma of buccal mucosa. Axial contrast-enhanced CT image shows enhancing solid tumor in right pterygopalatine fossa (arrow), suggestive of unresectable T4b disease

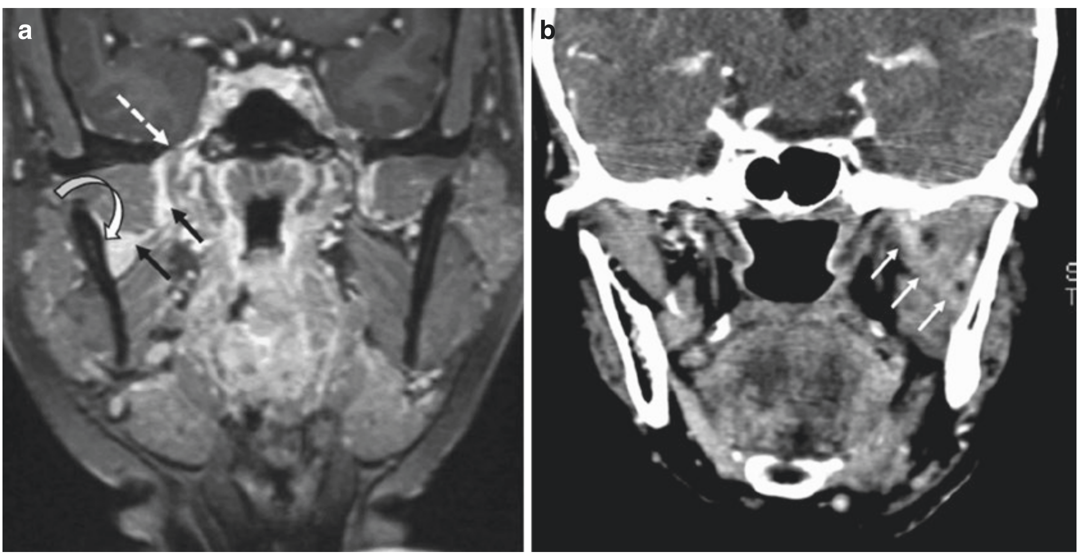

Fig. 5.18 (**a**) Coronal post-contrast MR image showing enhancement of mandibular nerve (black arrows) along its course from mandibular foramen (curved arrow) to the foramen ovale (dashed arrow) suggestive of perineural spread. (**b**) Coronal contrast-enhanced CT image in another patient with carcinoma left buccal mucosa showing thickening and enhancement of left mandibular nerve (straight white arrows) indicating perineural spread

the foramen ovale. This is best demonstrated on coronal fat-suppressed contrast-enhanced MRI sequences and is seen as increased enhancement around the mandibular foramen or foramen ovale and along the nerve (Fig. 5.18). CT depicts more advanced cases as foramen widening or erosion with loss of normal fat density [39–41]. Nerve invasion was found to be the sole adverse factor in advanced OCSCC from gingival, buccal, and RMT regions to predict local control [68]. The accuracy of imaging to detect perineural spread approaches 70% [39].

Nodal metastases from the above subsites are to ipsilateral level I and II regions and in more advanced cases to contralateral level I and II. Necrosis is the most reliable criterion for metastatic nodes and is best seen on contrast-enhanced images (Fig. 5.13). For non-necrotic nodes, size criteria have also been defined although false negatives and false positives are 15–20%, based on size alone [69].

Prognostic markers: In gingival, buccal, and RMT SCC, the posterior *soft tissue extent*, *bone erosion*, *and nodal metastases* are factors that influence prognosis and therapy [69–71]. The extent of posterior soft tissue spread influences resection as some cases of masticator space involvement although labeled T4b could be offered definitive treatment with radical surgery and appropriate reconstruction. Liao et al. described surgical outcomes of buccal, gingival, and RMT cancers that extended to the masticator space [67, 72]. On CT or MR imaging, T4b disease that extended to a level below a line of demarcation passing through the mandibular notch (between condyloid and coronoid processes shown in Fig. 5.3) had a favorable outcome similar to T4a disease (Fig. 5.19) [72].

The presence or absence of bone erosion and its extent influence decision between segmental mandibulectomy and marginal mandibulectomy. Segmental mandibulectomy is performed when there is significant cortical erosion and invasion of the marrow and of the inferior alveolar canal. It is also offered in edentulous and irradiated mandibles or when a large soft tissue component of OCSCC abuts a significant height of the mandible even without eroding it [5, 73]. Marginal mandibulectomy retains mandibular continuity preserving cosmesis and function. It can be offered only when there is minimal erosion of the alveolar margin or when a small soft tissue component abuts the alveolar crest of the mandible but does not erode it, in order to achieve oncologically safe resection margins [5, 65, 73]. An at least 1.0 cm height of the shaft of the mandible needs to be preserved to prevent fracture. Imaging can provide information on the height and length of erosion, helping plan surgery (Fig. 5.20).

Fig. 5.19 Contrast-enhanced axial CT image in a patient with advanced carcinoma of right buccal mucosa (arrows) involving the right buccal space and retromolar trigone with invasion into low masticator space below mandibular notch. The normal buccal space (*) and masseter (M) are seen on the left side

***Hard Palate*:** *Hard palate* SCC can spread to the nasal cavity and maxillary sinus by destroying the medial wall of the sinus. Spread to soft plate and nasopharynx can occur. The prognostic markers are *perineural spread and bone erosion*. Nodal metastases are infrequently seen with hard palate SCC. Perineural spread through the greater palatine canal to the pterygopalatine fossa is frequent and contraindicates surgery. Contrast-enhanced MRI using T1W fat-suppressed coronal sequence best demonstrates perineural spread

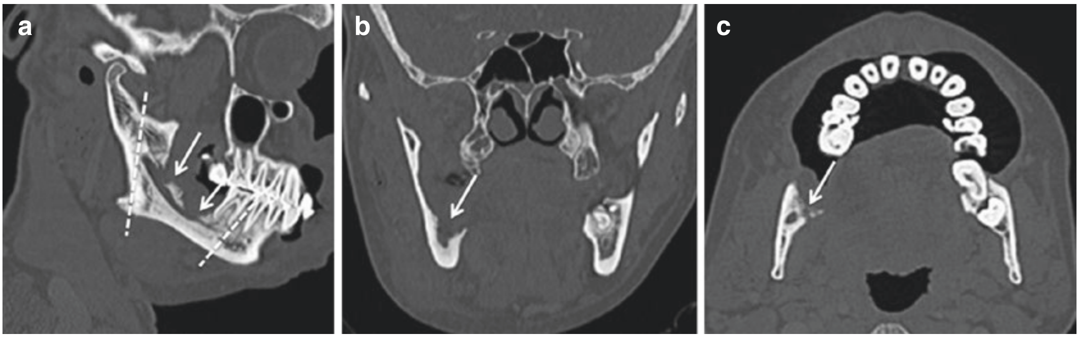

Fig. 5.20 16-row MDCT, bone algorithm images showing height and length of mandibular erosion. (**a**) Oblique sagittal reformation. (**b**) Coronal reformation. (**c**) Axial image. Arrow in (**a**) shows inferior alveolar canal invasion, which is well seen in the oblique sagittal plane. Dotted lines show planned incision lines for segmental mandibulectomy. Arrows in (**b**) and (**c**) show loss of cortical continuity (erosion). Height (depth) of erosion is measured on the coronal reformat

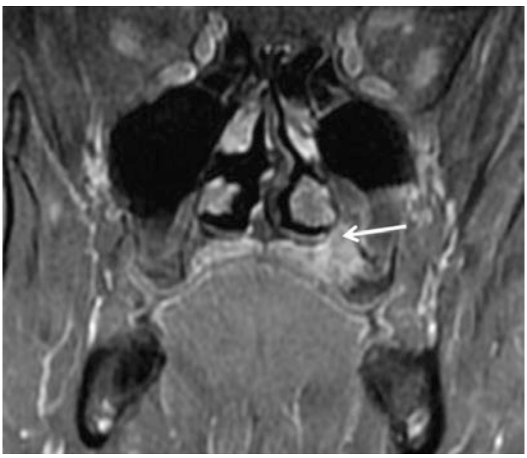

Fig. 5.21 Coronal post-contrast MR image showing carcinoma of hard palate extending into greater palatine canal suggesting perineural spread (arrow)

(Fig. 5.21). MRI is the most accurate method for marrow invasion. However MDCT may be useful for studying cortical bone erosion.

Conclusion

Imaging has an established role in the management of OCSCC. The primary role in the pretreatment setting is accurate staging that helps choose appropriate therapy. Imaging helps decide resectability, plan surgical resection of bone and soft tissue, as well as subsequent reconstruction that is essential for preserving form and function. Imaging features can also indicate prognosis. Detection is aided in those cancers where clinical examination is restricted. In treated cases, imaging can help assess response to treatment, detect recurrence suspected clinically, and distinguish it from post-therapy changes.

References

1. Sankaranarayanan R, Masuyer E, Swaminathan R, Ferlay J, Whelan S. Head and neck cancer: a global perspective on epidemiology and prognosis. Anticancer Res. 1998;18:4779–86.
2. Ow TJ, Myers JN. Current management of advanced resectable oral cavity squamous cell carcinoma. Clin Exp Otorhinolaryngol. 2011;4:1–10.
3. Arya S, Rane P, Deshmukh A. Oral cavity squamous cell carcinoma: role of pretreatment imaging and its influence on management. Clin Radiol. 2014;69:916–30.
4. Glastonbury CM, Mukherji SK, O'Sullivan B, Lydiatt WM. Setting the stage for 2018: how the changes in the American Joint Committee on Cancer/Union for International Cancer Control Cancer Staging Manual Eighth Edition Impact Radiologists. AJNR Am J Neuroradiol. 2017;38:2231–7.
5. Genden EM, Ferlito A, Silver CE, Takes RP, Suárez C, Owen RP, et al. Contemporary management of cancer of the oral cavity. Eur Arch Otorhinolaryngol. 2010;267:1001–17.
6. Forastiere AA, Goepfert H, Maor M, Pajak TF, Weber R, Morrison W, et al. Concurrent chemotherapy and radiotherapy for organ preservation in advanced laryngeal cancer. N Engl J Med. 2003;349:2091–8.
7. Huang SH, Hwang D, Lockwood G, Goldstein DP, O'Sullivan B. Predictive value of tumor thickness for cervical lymph-node involvement in squamous

cell carcinoma of the oral cavity: a meta-analysis of reported studies. Cancer. 2009;115:1489–97.
8. D'Cruz AK, Vaish R, Kapre N, Dandekar M, Gupta S, Hawaldar R, et al. Elective versus therapeutic neck dissection in node-negative oral cancer. N Engl J Med. 2015;373:521–9.
9. Arya S, Chaukar D, Pai P. Imaging in oral cancers. Indian J Radiol Imaging. 2012;22:195–208.
10. Arya S, Rane P, Sable N, Juvekar S, Bal M, Chaukar D. Retromolar trigone squamous cell cancers: a reappraisal of 16 section MDCT for assessing mandibular invasion. Clin Radiol. 2013;68:e680e8.
11. Arya S, Rane P, D'Cruz A. Infratemporal fossa, masticator space and parapharyngeal space: can the radiologist and surgeon speak the same language? Otorhinolaryngol Clin. 2012;4:125–35.
12. Kodama M, Khanal A, Habu M, Iwanaga K, Yoshioka I, Tanaka T, et al. Ultrasonography for intraoperative determination of tumor thickness and resection margin in tongue carcinomas. J Oral Maxillofac Surg. 2010;68:1746–52.
13. Natori T, Koga M, Anegawa E, Nakashima Y, Tetsuka M, Yoh J, et al. Usefulness of intra-oral ultrasonography to predict neck metastasis in patients with tongue carcinoma. Oral Dis. 2008;14:591–9.
14. Joshi SK, Kamalapur MG, Joshi AS, Hallikeri K. Ultrasonographic evaluation of carcinoma of buccal mucosa: ultrasound technique and evaluation of neoplastic conditions. J Evid Based Med Healthc. 2016;3:1649–55.
15. Weissman JL, Carrau RL. "Puffed-cheek" CT improves evaluation of the oral cavity. AJNR Am J Neuroradiol. 2001;22:741–4.
16. Sigal R, Zagdanski AM, Schwaab G, Bosq J, Auperin A, Laplanche A, et al. CT and MR imaging of squamous cell carcinoma of the tongue and floor of the mouth. Radiographics. 1996;16:787–810.
17. Dammann F, Horger M, Mueller-Berg M, Schlemmer H, Claussen CD, Hoffman J, et al. Rational diagnosis of squamous cell carcinoma of the head and neck region: comparative evaluation of CT, MRI, and 18FDG PET. AJR Am J Roentgenol. 2005;184:1326–31.
18. Kimura Y, Sumi M, Sumi T, Ariji Y, Ariji E, Nakamura T. Deep extension from carcinoma arising from the gingiva: CT and MR imaging features. AJNR Am J Neuroradiol. 2002;23:468–72.
19. Yen TC, Chang JT, Ng SH, Chang YC, Chan SC, Wang HM, et al. Staging of untreated squamous cell carcinoma of buccal mucosa with 18F-FDG PET: comparison with head and neck CT/MRI and histopathology. J Nucl Med. 2005;46:775–81.
20. Ng SH, Yen TC, Liao CT, Chang JT, Chan SC, Ko SF, et al. 18F-FDGPET and CT/MRI in oral cavity squamous cell carcinoma: a prospective study of 124patients with histologic correlation. J Nucl Med. 2005;46:1136–43.
21. Lane AP, Buckmire RA, Mukherji SK, Pillsbury HC 3rd, Meredith SD. Use of computed tomography in the assessment of mandibular invasion in carcinoma of the retromolar trigone. Otolaryngol Head Neck Surg. 2000;122:673–7.
22. Genden EM, Ferlito A, Shaha AR, Rinaldo A. Management of cancer of the retromolar trigone. Oral Oncol. 2003;39:633e7.
23. van den Brekel MW, Runne RW, Smeele LE, Tiwari RM, Snow GB, Castelijns JA. Assessment of tumour invasion into the mandible: the value of different imaging techniques. Eur Radiol. 1998;8:1552–7.
24. Brown JS, Griffith JF, Phelps PD, Browne RM. A comparison of different imaging modalities and direct inspection after periosteal stripping in predicting the invasion of the mandible by oral squamous cell carcinoma. Br J Oral Maxillofac Surg. 1994;32:347–59.
25. Mukherji SK, Isaacs DL, Creager A, Shockley W, Weissler M, Armao D. CT detection of mandibular invasion by squamous cell carcinoma of the oral cavity. AJR Am J Roentgenol. 2001;177:237–43.
26. Imaizumi A, Yoshino N, Yamada I, Nagumo K, Amagasa T, Omura K, et al. A potential pitfall of MR imaging for assessing mandibular invasion of squamous cell carcinoma in the oral cavity. AJNR Am J Neuroradiol. 2006;27:114–22.
27. Rao LP, Das SR, Mathews A, Naik BR, Chacko E, Pandey M. Mandibular invasion in oral squamous cell carcinoma: investigation by clinical examination and orthopantomogram. Int J Oral Maxillofac Surg. 2004;33:454–7.
28. Curran AJ, Toner M, Quinn A, Wilson G, Timon C. Mandibular invasion diagnosed by SPECT. Clin Otolaryngol Allied Sci. 1996;21:542–5.
29. Weisman RA, Kimmelman CP. Bone scanning in the assessment of mandibular invasion by oral cavity carcinomas. Laryngoscope. 1982;92:1–4.
30. Vidiri A, Guerrisi A, Pellini R, Manciocco V, Covello R, Mattioni O, et al. Multi-detector row computed tomography (MDCT) and magnetic resonance imaging (MRI) in the evaluation of the mandibular invasion by squamous cell carcinomas (SCC) of the oral cavity. Correlation with pathological data. J Exp Clin Cancer Res. 2010;29:73.
31. Handschel J, Naujoks C, Depprich RA, Kübler NR, Kröpil P, Kuhlemann J, et al. CT-scan is a valuable tool to detect mandibular involvement in oral cancer patients. Oral Oncol. 2012;48:361–6.
32. Goerres GW, Schmid DT, Schuknecht B, Eyrich GK. Bone invasion in patients with oral cavity cancer: comparison of conventional CT with PET/CT and SPECT/CT. Radiology. 2005;237:281–7.
33. Brockenbrough JM, Petruzzelli GJ, Lomasney L. DentaScan as an accurate method of predicting mandibular invasion in patients with squamous cell carcinoma of the oral cavity. Arch Otolaryngol Head Neck Surg. 2003;129:113–7.
34. Bolzoni A, Cappiello J, Piazza C, Peretti G, Maroldi R, Farina D, et al. Diagnostic accuracy of magnetic resonance imaging in the assessment of mandibular involvement in oral-oropharyngeal squamous cell carcinoma: a prospective study. Arch Otolaryngol Head Neck Surg. 2004;130:837–43.

35. Hendrikx AW, Maal T, Dieleman F, Van Cann EM, Merkx MA. Cone-beam CT in the assessment of mandibular invasion by oral squamous cell carcinoma: results of the preliminary study. Int J Oral Maxillofac Surg. 2010;39:436–9.
36. Dreiseidler T, Alarabi N, Ritter L, Rothamel D, Scheer M, Zöller JE, et al. A comparison of multislice computerized tomography, cone-beam computerized tomography, and single photon emission computerized tomography for the assessment of bone invasion by oral malignancies. Oral Surg Oral Med Oral Pathol Oral Radiol Endod. 2011;112:367–74.
37. De Vos W, Casselman J, Swennen GR. Cone-beam computerized tomography (CBCT) imaging of the oral and maxillofacial region: a systematic review of the literature. Int J Oral Maxillofac Surg. 2009;38:609e25.
38. Huang SH, Chien CY, Lin WC, Fang FM, Wang PW, Lui CC, et al. A comparative study of fused FDG PET/MRI, PET/CT, MRI, and CT imaging for assessing surrounding tissue invasion of advanced buccal squamous cell carcinoma. Clin Nucl Med. 2011;36:518–25.
39. Ginsberg LE. Perineural tumor spread associated with head and neck malignancies. In: Som PM, Curtin HD, editors. Head and neck imaging. 5th ed. St Louis, MO: Elsevier Mosby; 2011. p. 1021–39.
40. Nemzek WR, Hecht S, Gandour-Edwards R, Donald P, McKennan K. Perineural spread of head and neck tumors: how accurate is MR imaging? AJNR Am J Neuroradiol. 1998;19:701e6.
41. Ong CK, Chong VF. Imaging of perineural spread in head and neck tumours. Cancer Imaging. 2010;10 Spec no A:S92–8.
42. de Bondt RB, Nelemans PJ, Hofman PA, Casselman JW, Kremer B, van Engelshoven JM, et al. Detection of lymph node metastases in head and neck cancer: a meta-analysis comparing US, USgFNAC, CT and MR imaging. Eur J Radiol. 2007;64:266–72.
43. Takes RP, Righi P, Meeuwis CA, Manni JJ, Knegt P, Marres HA, et al. The value of ultrasound with ultrasound-guided fine-needle aspiration biopsy compared to computed tomography in the detection of regional metastases in the clinically negative neck. Int J Radiat Oncol Biol Phys. 1998;40:1027–32.
44. Moritz JD, Ludwig A, Oestmann JW. Contrast-enhanced color Doppler sonography for evaluation of enlarged cervical lymph nodes in head and neck tumors. AJR Am J Roentgenol. 2000;174:1279–84.
45. Wu LM, Xu JR, Liu MJ, Zhang XF, Hua J, Zheng J, et al. Value of magnetic resonance imaging for nodal staging in patients with head and neck squamous cell carcinoma: a meta-analysis. Acad Radiol. 2012;19:331–40.
46. Sumi M, Sakihama N, Sumi T, Morikawa M, Uetani M, Kabasawa H, et al. Discrimination of metastatic cervical lymph nodes with diffusion-weighted MR imaging in patients with head and neck cancer. AJNR Am J Neuroradiol. 2003;24:1627–34.
47. de Bondt RB, Hoeberigs MC, Nelemans PJ, Deserno WM, Peutz-Kootstra C, Kremer B, et al. Diagnostic accuracy and additional value of diffusion-weighted imaging for discrimination of malignant cervical lymph nodes in head and neck squamous cell carcinoma. Neuroradiology. 2009;51:183–92.
48. Vandecaveye V, De Keyzer F, Vander Poorten V, Dirix P, Verbeken E, Nuyts S, et al. Head and neck squamous cell carcinoma: value of diffusion-weighted MR imaging for nodal staging. Radiology. 2009;251:134–46.
49. Perrone A, Guerrisi P, Izzo L, D'Angeli I, Sassi S, Mele LL, et al. Diffusion-weighted MRI in cervical lymph nodes: differentiation between benign and malignant lesions. Eur J Radiol. 2011;77:281–6.
50. Fischbein NJ, Noworolski SM, Henry RG, Kaplan MJ, Dillon WP, Nelson SJ. Assessment of metastatic cervical adenopathy using dynamic contrast-enhanced MR imaging. AJNR Am J Neuroradiol. 2003;24:301–11.
51. Lim HK, Lee JH, Baek HJ, Kim N, Lee H, Park JW, et al. Is diffusion-weighted MRI useful for differentiation of small non-necrotic cervical lymph nodes in patients with head and neck malignancies? Korean J Radiol. 2014;15:810–6.
52. Kyzas PA, Evangelou E, Denaxa-Kyza D, Ioannidis JP. 18F-fluorodeoxyglucose positron emission tomography to evaluate cervical node metastases in patients with head and neck squamous cell carcinoma: a meta-analysis. J Natl Cancer Inst. 2008;100:712e20.
53. Liao LJ, Lo WC, Hsu WL, Wang CT, Lai MS. Detection of cervical lymph node metastasis in head and neck cancer patients with clinically N0 neck-meta-analysis comparing different imaging modalities. BMC Cancer. 2012;12:236.
54. Govers TM, Hannink G, Merkx MA, Takes RP, Rovers MM. Sentinel node biopsy for squamous cell carcinoma of the oral cavity and oropharynx: a diagnostic meta-analysis. Oral Oncol. 2013;49:726e32.
55. Chaturvedi P, Datta S, Arya S, Rangarajan V, Kane SV, Nair D, et al. Prospective study of ultrasound-guided fine-needle aspiration cytology and sentinel node biopsy in the staging of clinically negative T1 and T2 oral cancer. Head Neck. 2015;37:1504–8.
56. Schöder H, Carlson DL, Kraus DH, Stambuk HE, Gönen M, Erdi YE, et al. 18F-FDG PET/CT for detecting nodal metastases inpatients with oral cancer staged N0 by clinical examination and CT/MRI. J Nucl Med. 2006;47:755–62.
57. Iyer NG, Clark JR, Singham S, Zhu J. Role of pretreatment 18FDG-PET/CT in surgical decision-making for head and neck cancers. Head Neck. 2010;32:1202–8.
58. Richard C, Prevot N, Timoshenko AP, Dumollard JM, Dubois F, Martin C, et al. Preoperative combined 18-fluorodeoxyglucose positron emission tomography and computed tomography imaging in head and neck cancer: does it really improve initial N staging? Acta Otolaryngol. 2010;130:1421–4.
59. Kane SV, Gupta M, Kakade AC, D'Cruz A. Depth of invasion is the most significant histological predictor of subclinical cervical lymph node metastasis in early squamous carcinomas of the oral cavity. Eur J Surg Oncol. 2006;32:795–803.

60. Lam P, Au-Yeung KM, Cheng PW, Wei WI, Yuen AP, Trendell-Smith N, et al. Correlating MRI and histologic tumor thickness in the assessment of oral tongue cancer. AJR Am J Roentgenol. 2004;182:803–8.
61. Okura M, Iida S, Aikawa T, Adachi T, Yoshimura N, Yamada T, et al. Tumor thickness and paralingual distance of coronal MR imaging predicts cervical node metastases in oral tongue carcinoma. AJNR Am J Neuroradiol. 2008;29:45–50.
62. Yasumoto M, Shibuya H, Takeda M, Korenaga T. Squamous cell carcinoma of the oral cavity: MR findings and value of T1-versus T2-weighted fast spin-echo images. AJR Am J Roentgenol. 1995;164:981–7.
63. Arakawa A, Tsuruta J, Nishimura R, Sakamoto Y, Korogi Y, Baba Y, et al. MR imaging of lingual carcinoma: comparison with surgical staging. Radiat Med. 1996;14:25–9.
64. King AD, Tse GM, Yuen EH, To EW, Vlantis AC, Zee B, et al. Comparison of CT and MR imaging for the detection of extranodal neoplastic spread in metastatic neck nodes. Eur J Radiol. 2004;52:264–70.
65. Misra S, Chaturvedi A, Misra NC. Management of gingivo-buccal complex cancer. Ann R Coll Surg Engl. 2008;90:546–53.
66. Brown JS, Lowe D, Kalavrezos N, D'Souza J, Magennis P, Woolgar J. Patterns of invasion and routes of tumor entry into the mandible by oral squamous cell carcinoma. Head Neck. 2002;24:370–83.
67. Spector ME, Gallagher KK, McHugh JB, Mukherji SK. Correlation of radiographic and pathologic findings of dermal lymphatic invasion in head and neck squamous cell carcinoma. AJNR Am J Neuroradiol. 2012;33:462–4.
68. Liao CT, Ng SH, Chang JT, Wang HM, Hsueh C, Lee LY, et al. T4b oral cavity cancer below the mandibular notch is resectable with a favorable outcome. Oral Oncol. 2007;43:570–9.
69. Som PM, Brandwein-Gensler MS. Lymph nodes of the neck. Som PM, Curtin HD, Head & neck imaging. 2. 5th ed. St Louis, MO Elsevier Mosby; 2011 2287–2383.
70. Walvekar RR, Chaukar DA, Deshpande MS, Pai PS, Chaturvedi P, Kakade AC, et al. Prognostic factors for loco-regional failure in early stage (I and II)squamous cell carcinoma of the gingivobuccal complex. Eur Arch Otorhinolaryngol. 2010;267: 1135–40.
71. Walvekar RR, Chaukar DA, Deshpande MS, Pai PS, Chaturvedi P, Kakade A, et al. Squamous cell carcinoma of the gingiva-buccal complex: predictors of loco-regional failure in stage III-IV cancers. Oral Oncol. 2009;45:135–40.
72. Liao CT, Chang JT, Wang HM, Ng SH, Hsueh C, Lee LY, et al. Surgical outcome of T4a and resected T4b oral cavity cancer. Cancer. 2006;107:337–44.
73. Ayad T, Guertin L, Soulières D, Belair M, Temam S, Nguyen-Tân PF. Controversies in the management of retromolar trigone carcinoma. Head Neck. 2009;31:398e405.

6 Biopsy and Oral Squamous Cell Carcinoma Histopathology

Dimitrios A. Andreadis, Achilleia-Maria Pavlou, and Prashanth Panta

Abstract

Oral cancer is a fairly common disease, which is unfortunately often diagnosed when it has reached an advanced stage. Early diagnosis is crucial for better prognosis and survival. In addition to better survival figures, early diagnosis also provides sufferers with a better quality of life. Biopsy is widely accepted as the "gold standard" diagnostic method for lesions raising suspicion of malignancy. There are several types of biopsy including incisional biopsy, excisional biopsy, fine needle aspiration, punch biopsy, and brush biopsy, each with specific indications, special methodology, advantages, and disadvantages. The use of biopsy and analyzing the results under the microscope is the gold standard for confirming a diagnosis of oral squamous cell carcinoma diagnosis. Biopsy is indicated in mucosal lesions (especially ulcers), and it is of critical importance to reveal oral dysplasia, to confirm the clinical suspicion for an early invasive cancer, or to establish the grade of differentiation of oral squamous cell carcinoma for accurate therapeutic procedure and in the determination of prognosis.

D. A. Andreadis, DDS, PhD (✉)
A.-M. Pavlou, DDS, MSc
Department of Oral Medicine/Pathology,
School of Dentistry, Aristotle University of Thessaloniki,
Thessaloniki, Greece
e-mail: dandrea@dent.auth.gr

P. Panta, MDS
Department of Oral Medicine and Radiology,
MNR Dental College and Hospital,
Sangareddy, Telangana, India

6.1 Biopsy

6.1.1 Introduction

In 2012 there were 300,373 new cases of oral cancer worldwide as well as 145,353 deaths associated with this type of cancer. Tobacco and alcohol consumption constitute the main risk factors for oral cancer together with HPV infections, principally HPV-16 [1–3]. Oral cancer is initially often asymptomatic resulting in a delayed diagnosis. Early oral cancer diagnosis is crucial for a good prognosis, with patient survival being approximately 60–80% after early prognosis compared with 30–40% for late diagnosis and an advanced stage. An early diagnosis can also eliminate the need for extensive surgery and contributes to a better quality of life for patients [4–6]. Biopsy with a histological examination of the specimen is considered to be the "gold standard" diagnostic method for suspicious oral lesions. Its high reliability and its long history, more than 150 years, underpin this characterization [6–8].

P. Panta (ed.), *Oral Cancer Detection*, https://doi.org/10.1007/978-3-319-61255-3_6

6.1.2 Terminology

In this investigative method, a small amount of tissue is taken from a living organism to be microscopically examined. The term biopsy consists of two parts; the first is “bios” which means life, and the second is “opsis” which means sight [9–11].

6.1.3 Indications

- Lesions which present neoplastic or premalignant characteristics or lesions whose dimensions increase [9]
- Lesions which are characterized by few or no signs and symptoms that could lead to diagnosis [12]
- Persistent lesions without response to treatment [13]
- Persistent ulcerations present for more than 10–14 days after removal of any possible causative agent [13]
- Indicative diagnosis of some systemic diseases such as Sjögren’s Syndrome [10]
- Persistent vesicular or bullous lesions present for more than 7–15 days [9]
- Confirmation of an apparent clinical diagnosis [12]
- Intraosseous lesions undetectable by radiography [14]
- Diagnosis of granulomatous diseases [15]
- In patients who are particularly anxious about possible cancer diagnosis [12]

6.1.4 Contraindications

- In patients treated with:
- Anticoagulants
- Corticosteroids
- In immunocompromised patients [9].
- In vascular lesions incisional biopsies are contraindicated [15].
- In patients suffering from blood disorders [13].
- In pigmented lesions raising suspicion of melanoma [13].
- In lesions that are either very deep or difficult for the surgeon to access and if the biopsy procedure could harm the surrounding tissues [10].

6.1.5 Advantages

- It is a small, uncomplicated, and cheap procedure and well tolerated by patients [16].
- Few instruments and materials are required for a biopsy [14].
- Biopsy is a short and easy procedure [12].
- On many occasions a definitive diagnosis is reached through biopsy [9].

6.1.6 Disadvantages

- It is an invasive procedure [9].
- The pathologist’s findings by diagnosis of dysplasias (mild and moderate), early-stage carcinomas in situ, and squamous cell carcinomas are quite diverse [17].
- Overuse of this method could deter the patient from visiting the dentist in the future [18].
- Experience is crucial for the proper biopsy of soft tissues, while in some bone biopsies, a specialist is needed (lack of experience or when a sample from an anatomically critical area is required) [19].
- The histological findings may not be indicative of diagnosis if histological examination is conducted for a nonrepresentative tissue specimen or if the sample is inappropriately handled [20].

6.1.7 Instruments and Materials Necessary for a Biopsy (Fig. 6.1) [9, 13, 21–24]

- Local anesthetics
- Syringe and needle
- Scalpel with a No.15 blade
- Tissue forceps
- Needle holder
- Sutures
- Scissors
- Gauzes
- Hemostatic agents
- Electrocautery
- A screw-top vial which contains fixative (10% formalin, whose volume is 10 times the volume of the specimen)

Fig. 6.1 Necessary instruments for biopsy

- Disinfectants (for disinfection of the tissue over the investigated area in fine needle aspiration)
- 22, 23, 25, or 27 gauge needle (for fine needle aspiration)
- A single use, sterile, plastic 10-ml syringe (for fine needle aspiration)
- Biopsy punch (for punch biopsy)
- A specially designed brush (for brush biopsy)

6.1.8 Types of Biopsy

- Incisional biopsy
- Excisional biopsy
- Fine needle aspiration
- Punch biopsy
- Brush biopsy and exfoliative cytology

6.1.8.1 Incisional Biopsy

In incisional biopsy, a portion of the lesion is taken along with a small portion of normal adjacent tissue in order to help the pathologist in recognizing the borders of the tumor (Fig. 6.2). In this type of biopsy, a scalpel is often employed although punch, aspiration, and needle techniques are also used. Sufficient size and depth are crucial for an incisional biopsy to ensure obtaining tissue specimen from one or multiple sites (Fig. 6.3) of the tumor margins. Surface specimens are frequently nonrepresentative of a lesion and include mainly necrotic tissue or crust [14, 25–27].

Indications of incisional biopsy include large lesions, whose diameter is larger than 1–2 cm, as well as lesions which are associated with increased risk of malignancy, whose diagnosis and treatment planning require a biopsy. The treatment of the lesion usually requires a second procedure. It is still controversial as to whether incisional biopsy can lead to dissemination of cancer cells especially in cases of melanoma. Incisional biopsy in lesions whose parts present different histological features could lead to unnecessarily mild or more aggressive treatment [27–31].

The method includes administration of topical anesthetic through injection around the lesion in order to avoid distortion of the tissue and removal of a wedge-shaped portion of the

Fig. 6.2 Tissue incisional biopsy from ulcerative lesion suspected for oral squamous cell carcinoma

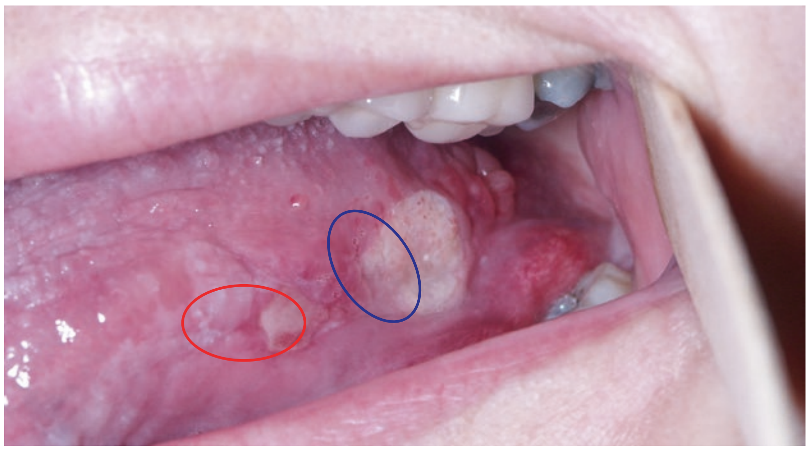

Fig. 6.3 Tissue multiple incisional biopsies from lesions suspected for leukoplakia-dysplasia (red) and malignancy (blue)

lesion (preferably at the periphery of the lesion rather than its central area, where necrotic areas are possible, with inclusion of background normal tissue), which is transferred immediately into a screw-top vial that contains fixative, followed by suturing of the open wound. In cases of tissue specimen taken from the palate or the gingiva, healing takes place via secondary intention. It is necessary to avoid harming major vessels and nerves during biopsy, and parallel incisions to the common position of smaller structures are crucial for their protection [1, 15, 21, 24–26].

Toluidine blue, a dye by which pathological areas are stained blue, can be helpful for assessing the best location from which a biopsy specimen should be taken. Specimens taken from different areas of extensive lesions, or lesions with various characteristics, could contribute to the reliability of the biopsy outcome [9, 16, 32].

6.1.8.2 Excisional Biopsy

In excisional biopsy, the entire lesion is removed together with a part of normal tissue from its periphery (Fig. 6.4). Indications of this biopsy type include lesions whose diameter is smaller than 1 cm and some larger lesions whose removal does not require an extensive surgical procedure but also include areas with possible preoral malignancy (Fig. 6.5). Excisional biopsy is often preferred as it leads to diagnosis without a waste of time, and there is no need for a second procedure [12, 16, 21, 26].

The method includes the following: local anesthetic is administered around the lesion at a distance of 2–4 mm from it, the lesion is then stabilized through a suture or forceps (gentle manipulation of the sample is crucial in order to avoid tissue artifacts), two elliptical incisions are made around the lesion in normal tissue at a distance of 2–3 mm from the lesion and the specimen is removed and transferred immediately in a screw-top vial containing fixative, and finally the wound is sutured. Malignant lesions may not be completely treated by excisional biopsy, while benign lesions may be overtreated. An excisional or incisional biopsy in cases of vascular tumors could cause a severe hemorrhage [13, 16, 18, 21, 24, 26, 27].

6.1.8.3 Fine Needle Aspiration

Fine needle biopsy indications include lesions located deep in the tissues and lesions which are difficult to access [18, 26]. In this technique a 22, 23, 25, or 27 gauge needle is used in combination with a single use, sterile, plastic 10-ml syringe; more specifically the method includes disinfection of the tissue over the investigated lesion, palpation, and lesion stabilization; the needle then reaches the lesion through the skin and suction follows. Subsequently, the needle is moved quickly back and forward to obtain specimens from various areas and then is removed and separated from the syringe, which is filled with air. Finally, the needle is attached again to the syringe and the specimen ejected onto a microscopic slide, followed by fixation and staining [4, 22]. In comparison to other biopsy types, more experience is needed [18]. Also it is possible that the sample tissue may not be representative of the investigated lesion [16].

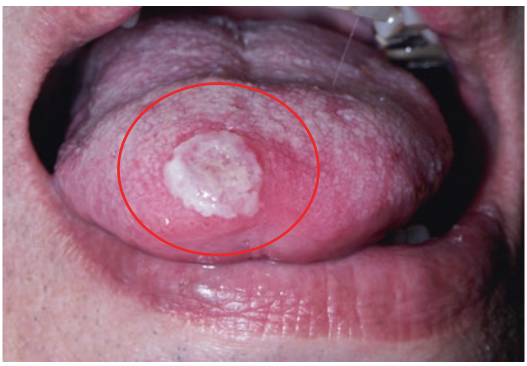

Fig. 6.4 Tissue excisional biopsy from lesion suspected for oral squamous cell carcinoma

6.1.8.4 Punch Biopsy

In this type of biopsy, a small portion of tissue is obtained using an instrument similar to a forceps. It consists of a cylindrical blade connected to a plastic grip. Various diameters ranging from 2 to 10 mm are available [15]. The method involves local anesthesia (around the biopsy area to prevent distortion of the specimen); the punch is rotated into the tissue and the specimen is obtained. Then it remains for 1 min on a piece of paper to avoid a change of its shape before being immediately transferred to a screw-top vial containing fixative. The wound is finally sutured [32]. This type of

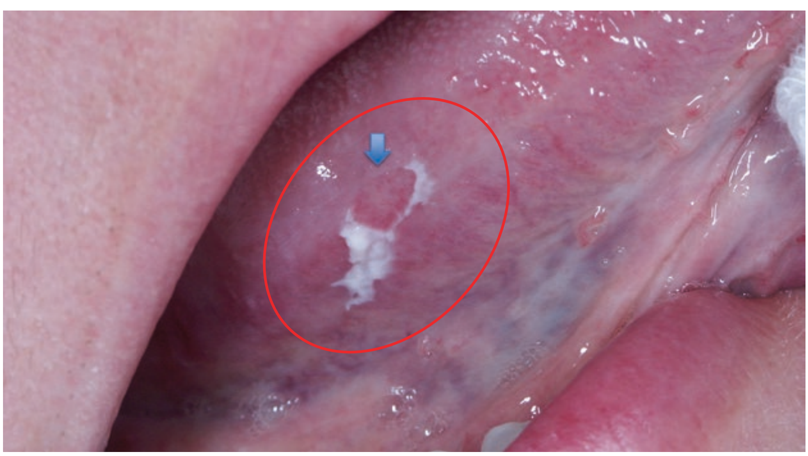

Fig. 6.5 Tissue excisional biopsy from lesion suspected for leukoplakia-dysplasia and possible malignant nest (arrow)

biopsy offers a controlled incision, a sufficient specimen is taken, and scalpel which could cause some disturbance to the patient is avoided, and it is also possible that no suturing of the wound is sometimes needed [9]. Several tissue specimens from different sites can also be taken in the same session [10].

A specific instrument is needed for this biopsy type, which is also associated with the risk of damage to the tissue. It is crucial that the laboratory knows how to deal with the specimens obtained from the punch biopsy, while the punches with larger diameters could contribute to the prevention of clinical and laboratorial problems [15].

6.1.8.5 Brush Biopsy and Conventional Exfoliative Cytology

In 1999 the computerized analysis of brush biopsies (OralCDx®, CDx Laboratories, Suffern, NY) was presented to assess lesions of the oral mucosa which seem clinically benign and, for which, in other circumstances, no conventional biopsy would have taken place. It detects atypical cells in samples that were obtained with brush biopsies from potentially malignant lesions [33].

The method involves taking the specimen consisting of epithelial cells by using a specially designed brush, followed by specimen fixation, staining, and microscopically examination, which is mediated by computer [23].

As local anesthesia is not necessary, brush biopsy can be used in cases with local anesthetic allergy [8]. This type of biopsy is well tolerated, painless, and not invasive [14]. It can also be used in numerous or large lesions and in cases in which the patient is not willing to undergo a conventional biopsy [31].

Various studies have been conducted in order to evaluate the sensitivity and specificity of brush biopsy, with the sensitivity varying from 43.5 to 92.3% and specificity varying from 32 to 94.3% [33–37]. In a study by Delavarian et al. in 2010, conventional biopsy was compared with a combination of brush biopsy and liquid-based cytology, in which a cell suspension was taken by inserting the brush with the sample into liquid. The sensitivity of this liquid-based brush biopsy was found to be 88.8%, and the specificity was 100% [38, 39]. In cases where the result indicates a pathologic situation, a conventional biopsy is necessary to confirm the diagnosis [39]. A mild hemorrhage caused by the brushing is expected, as basal cells are required for the test. A false negative result is possible in cases with intense keratinization or deep lesions, as no adequate specimen from these lesions can be obtained [40].

Exfoliative cytology is a painless, noninvasive biopsy method where a smear is taken from the surface of the suspected lesion unto a microscopic slide to examine cellular dysplastic findings under bright field microscope after staining. In a typical exfoliative cytology test, result is reported as negative, atypical (uncertain diagnostic significance) and positive. It is a feasible chairside method for mass screening and for initial judgement (decision making) before a painful biopsy is taken. The technique of conventional exfoliative cytology is slowly changing into computerized cytomorphometry, through DNA index measurement, micronucleus analysis and assessment of nucleolar organizer regions. An addition of molecular methods like immunohistochemistry, and high throughput methods like real time PCR and microarrays can significantly improve the efficiency and revolutionize the technique. Lin et al have devised a oral cancer risk index through measurement of DNA index (DI) in exfoliative brush biopsy for risk stratification of oral leukoplakia [41]. In the most most recent ADA report (2017), it was confirmed that cytology testing can be chosen as a adjuvant in case a clinician is unable to take a biopsy [42, 43].

Exfoliative cytology has a high potential for upgradation and developments in technique can be highly rewarding in terms of ease of judgment in favor of biopsy, that is to filter patients who may not be recommended for a biopsy (negative test result). The technique of conventional exfoliative cytology is evolving into oral rinse based biopsy which has also shown superior result due to the potential for capture of whole oral exfoliated epithelial cells [41].

6.2 Oral Dysplasia and Oral Squamous Cell Carcinoma under the Microscope

The use of biopsy and analyzing the results under the microscope is the gold standard for confirming an oral squamous cell carcinoma diagnosis.

Biopsy is indicated in mucosal lesions (especially ulcers), which are suspected of being neoplastic and persist over 2 weeks without resolution after the elimination of possible local traumatic factors. During incisional biopsy (excisional biopsy is suggested only for minor <1 cm, superficial lesions suspected of being cancerous) an important intact part of the lesion is retrieved with adequate depth and with the avoidance of necrotic/ulcerative areas. Biopsy of a peripheral part of the tumor is optional in order to detect the cellular tissue-invasive behavior and a representative sample for histological grading, something valuable for prognostic purposes [44, 45].

6.2.1 Oral Dysplasia

By definition, dysplasia precedes OSCC, and OSCC always arises from the covering oral mucosal epithelium with dysplastic features. Hence, dysplasia can be considered as the first histological stage (change) with an increased risk of progression to malignant transformation. Oral dysplasia is found in some of potentially malignant oral disorders such as leukoplakia and (mainly) erythroplakia, as well as submucous fibrosis, oral lichen planus, actinic keratosis, etc. (as analytically described in introduction chapter of this book). Common cellular and architectural changes that constitute dysplasia include abnormal variation in nuclear size/shape, cell size/shape, increased nuclear-cytoplasmic ratio, atypical mitotic figures, increased number/size of nucleoli, nuclear hyperchromatism, irregular stratification of epithelium, loss of basal cell's polarization, drop-shaped rete ridges, frequent and abnormally superficial mitotic figures, premature keratinization in single cells, keratin pearls within rete ridges, and loss of epithelial cohesion. Oral epithelial dysplasia is subdivided into three grades depending on the width of affected epithelium: mild dysplasia refers to changes in basal-parabasal layers, moderate dysplasia corresponds to changes from basal layer to middle layers, and severe dysplasia is dysplasia spanning from basal layer to upper layers. Interestingly, a subset of dysplasias with HPV infection reveals epithelial karyorrhexis and apoptosis [45–50].

The abovementioned microscopic features (not in the single epithelial hyperplasia) can be suggestive of mild, moderate, and severe dysplasia:

Hyperplasia: Increased number of spinous epithelial cell layers with normal maturation leading to orthokeratosis/parakeratosis, without cellular/architecture dysplastic alterations (atypia) (Figs. 6.6, 6.7, and 6.8).

Mild dysplasia: Dysplastic changes are minimal and limited to basal/parabasal layers (lower third of the epithelium) accompanied by occa-

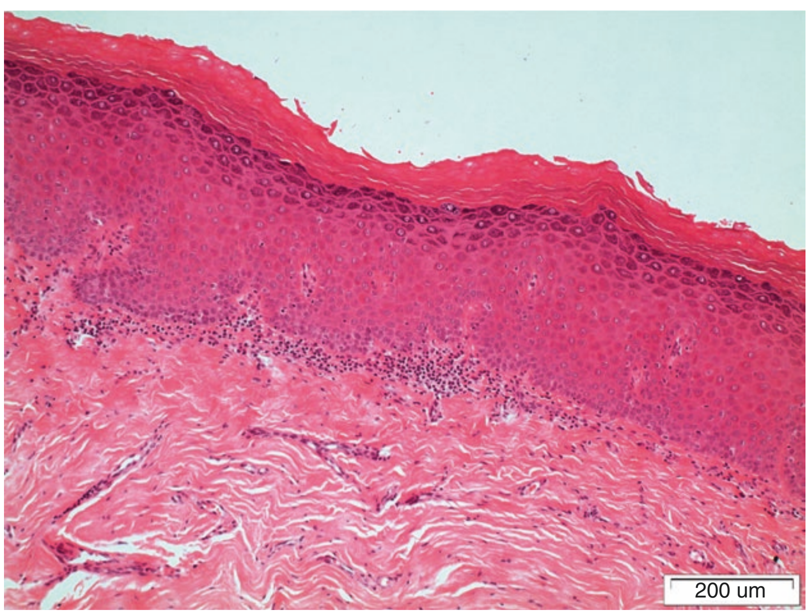

Fig. 6.6 Oral hyperkeratosis: hyperkeratotic epithelium with acanthosis without atypia due to trauma (×100)

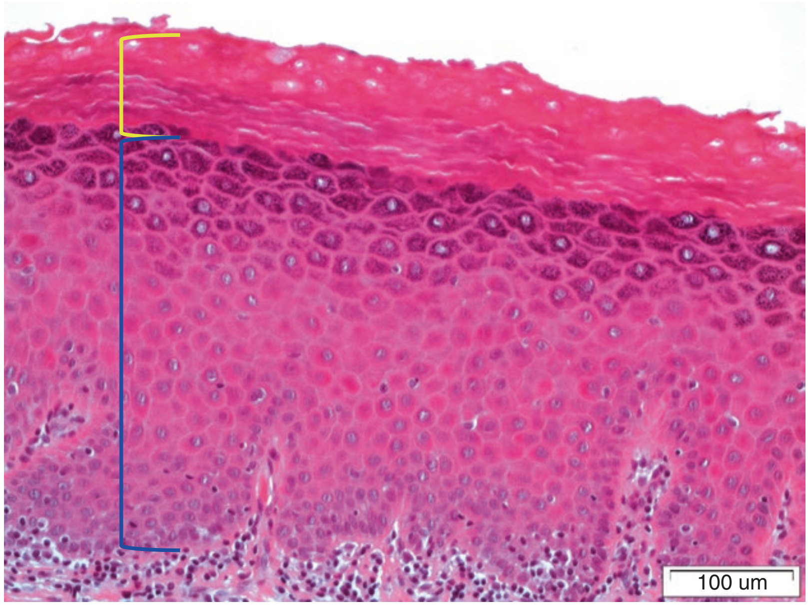

Fig. 6.7 Oral hyperkeratosis: excessive production of keratin layer (yellow bracket) and increase of spinous epithelial cell layers (stratum spinosum) with normal architecture (blue bracket) (×200)

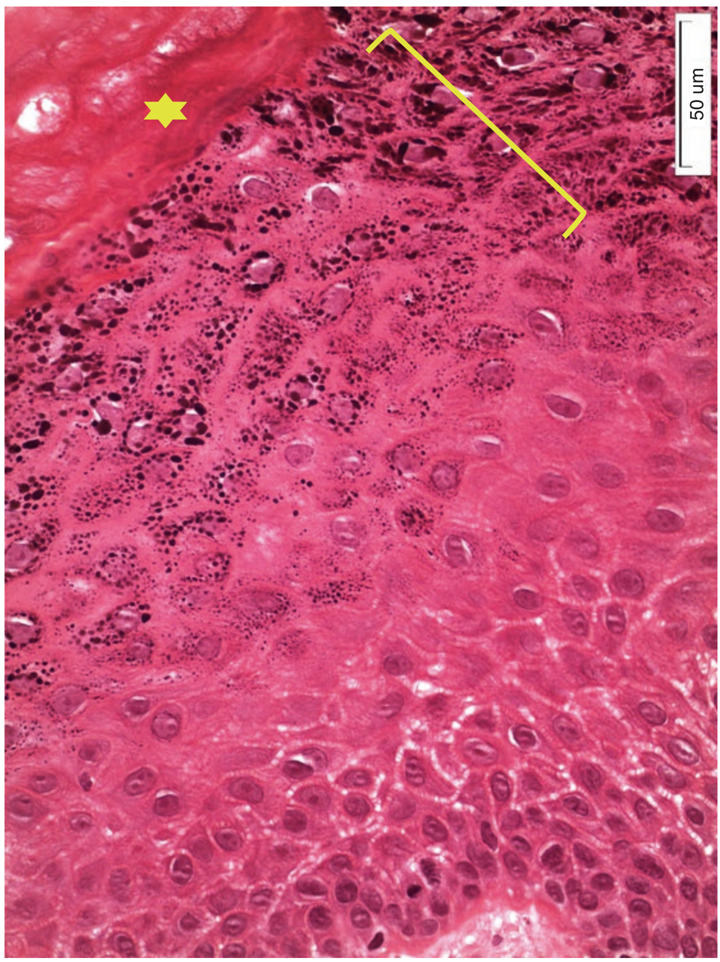

Fig. 6.8 Oral hyperkeratosis: strong presence of granular cell layer (stratum granulosum) (bracket) below keratin layer (star) (×400)

sional lymphocytes of the underlying stromal tissue (Figs. 6.9a and b).

Moderate dysplasia: The alteration of the epithelial architecture and dyskeratosis (Fig. 6.10**)** is extended from the lower third to the middle part of the oral epithelium including the spinous layer. Drop-shaped rete ridges are present and mild atypical cellular features are present. When marked cellular atypia is noted, the lesion should be categorized as severe dysplasia even though the upper third of epithelium is not involved. Moderate lymphocytic infiltration is present (Figs. 6.11 and 6.12).

Severe dysplasia and carcinoma in situ (CIS): The exact point at which dysplasia transforms into malignancy in this stage is still unclear. Architectural and cellular changes (marked cellular atypia) are observed throughout the upper third, including the total thickness of the epithelium, which may be present as keratinized or non-keratinized and hyperplastic or atrophic. The lymphocytic infiltration is moderate to marked, and, interestingly, squamous metaplasia and dysplasia may be present in salivary gland ducts of the stroma subjacent to the epithelium [44–48].

However, even in this stage of severe dysplasia/CIS, the basement membrane is intact. Additionally, keratin pearl formation is extremely unusual in CIS and, if present, is possibly an indication for invasive OSCC of adjacent area. Subsequent careful examination of the epithelial-lamina propria zone is needed to avoid microinvasion misinterpretation and is also required in cases of incisional biopsies leading to the diagnosis of severe dysplasia/CIS; an excisional surgical procedure of the lesion is critical to exclude other areas of invasion **(**Figs. 6.13, 6.14, 6.15 and 6.16**)** [49].

Differential diagnosis of oral dysplasia should include reactive atypia in cases of epithelium adjacent to ulcers (traumatic, aphthous-like, viral, etc.) and in cases of fungal infection of leukoplakia and lichenoid dysplasia, an almost meaningless term referring to dysplastic lesions with a lichenoid pattern of inflammatory infiltration (Fig. 6.17) [45, 51].

6.2.2 Oral Squamous Cell Carcinoma

6.2.2.1 Pattern of Invasion

OSCC invasion may be limited to the lamina propria (superficial invasion or microinvasion, depth 1–2 mm from basal membrane) or extends deeply into subepithelial connective tissue and submucosal tissue, which encloses muscle, bone, and fat. The appearance of the invasive islands and the cords of malignant cells is variable, as is the depth of invasion. For example, invasion may consist of the extension of the epithelium into the deeper surrounding tissues and/or individual squamous cells and cords/sheets/islands located at deeper sites of subepithelial tissues, without any continuity with

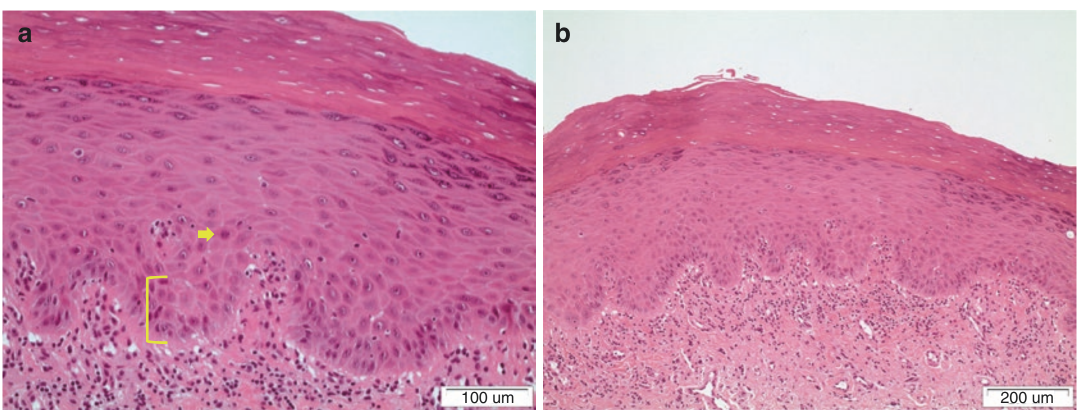

Fig. 6.9 (**a**, **b**) Mild dysplasia: mild disturbance of polarity of cells limited to basal and parabasal cell layers (bracket) with hyperchromatic nuclei (arrow) and acanthosis as well (×200 and ×100)

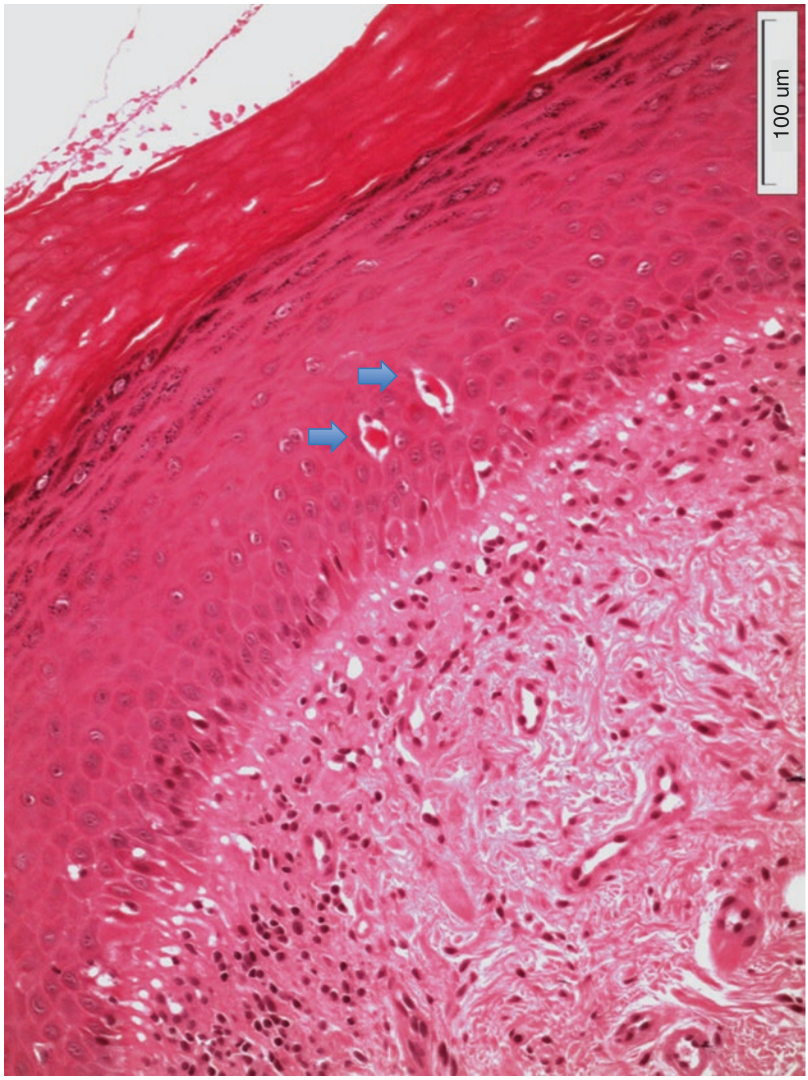

Fig. 6.10 Dyskeratosis: production of keratin in unexpected deeper layers of epithelium (arrows) (×100)

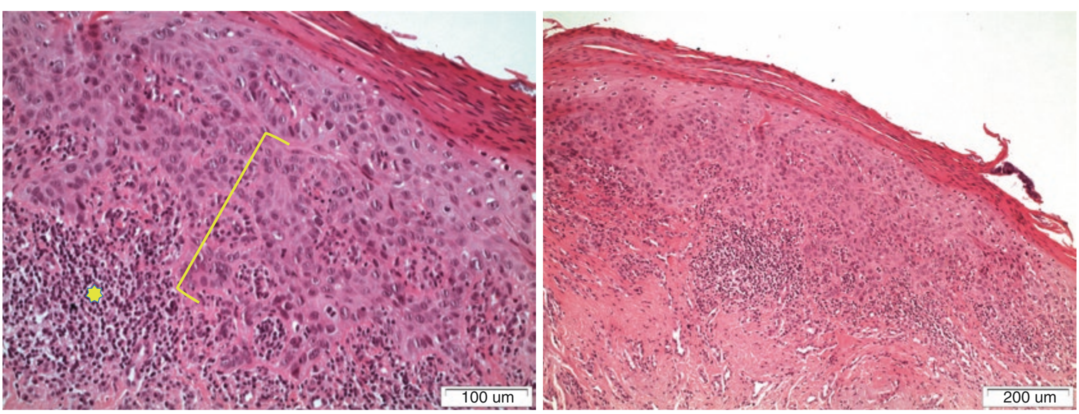

Fig. 6.11 Moderate dysplasia: elongated, drop-shaped rete processes. Loss of normal epithelial maturation and architecture with irregular stratification. Nuclear and cellular pleomorphism, increased number of mitoses, and loss of cellular polarization are presented extending to the 2/3 of the total epithelium (bracket). Moderate dysplasia may be accompanied by lymphocytic infiltration (arrow) (×200 and ×100)

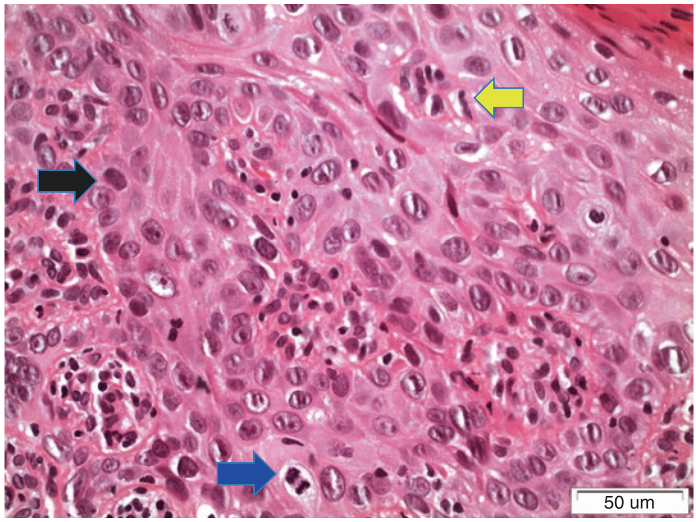

Fig. 6.12 Moderate dysplasia: loss of normal epithelial architecture and cellular polarization is presented extending to the 2/3 of the total epithelium. Nuclear and cellular pleomorphism, abnormal nuclear enlargement (black arrow), and increased number of mitoses (example of normal mitosis, blue arrow) even atypical mitoses (yellow arrow) can also be observed (×400)

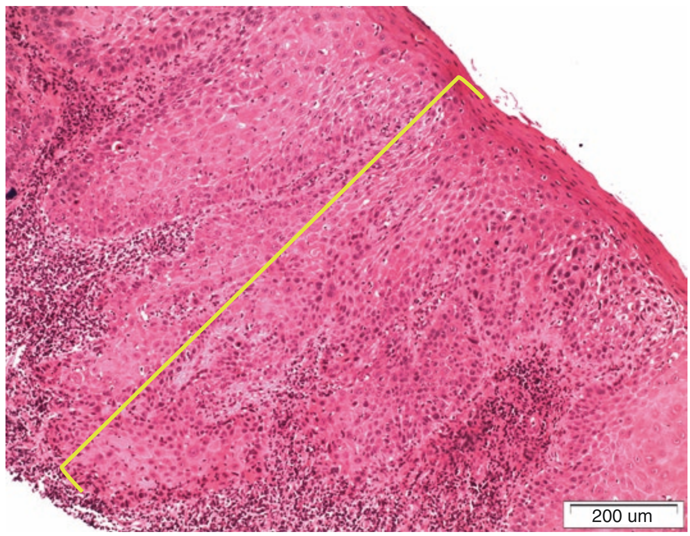

Fig. 6.13 Severe dysplasia: elongated, drop-shaped rete ridges with intense dysplasia extending to the total thickness of epithelium (bracket). Occasionally, areas of invasive oral squamous cell carcinoma may be present in adjacent tissues. The total excision of the lesion in normal tissue boundaries is critical in severe dysplasia (×100)

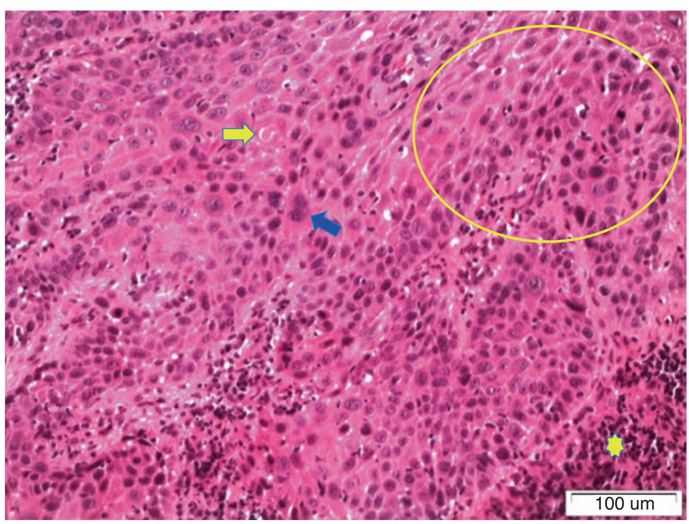

Fig. 6.14 Severe dysplasia: excessive nuclear and cellular polymorphism, altered nuclear enlargement, dyskeratosis (yellow arrow), abnormal epithelial stratification (circle), and cytological atypia (blue arrow). Lymphocytic infiltration is also present under the basement membrane (star) (×200)

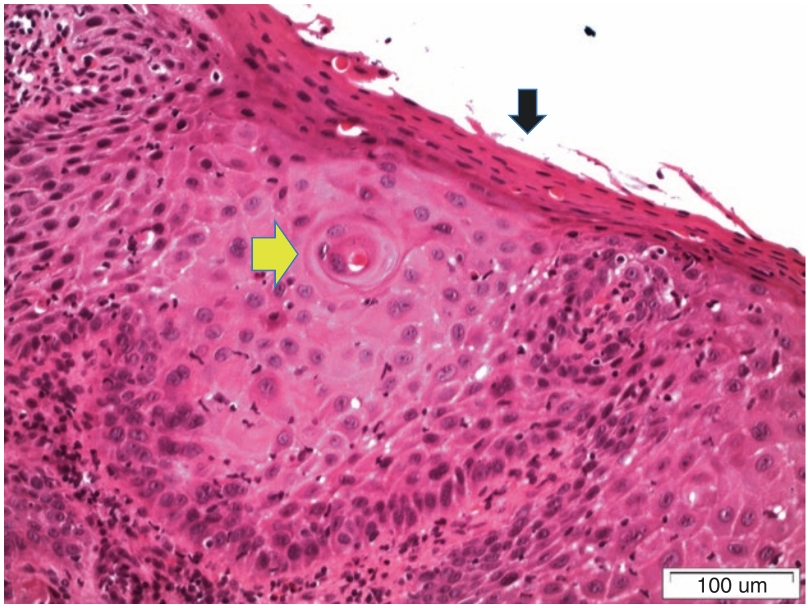

Fig. 6.15 Severe dysplasia: pearl-like abnormal production of keratin into deeper layers (yellow arrow) of atrophic parakeratinized (black arrow) epithelium (×400)

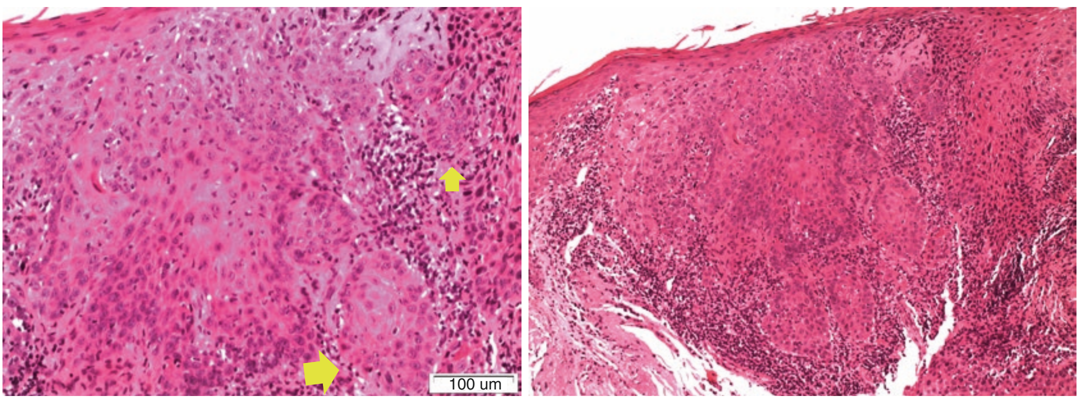

Fig. 6.16 Severe dysplasia and microinvasion: areas of invasive oral squamous cell carcinoma may be present in adjacent tissues of severe dysplasia. Nests of neoplastic cells penetrate basal membrane invading lamina propria (arrows) (×200 and ×100)

the superficial epithelium invading and destroying normal tissues. The thickness of OSCC at initial diagnosis is correlated with the prognosis being less favorable when >5 mm, and, obviously, when the neoplastic cells are close to the periphery of the excised tumor, the prognosis is even less optimistic [47, 48].

The early stages of invasion are critical in terms of diagnosis and prognosis. Epithelial cells penetrating the basal membrane of dysplastic epithelium with an unclear basal cell layer and expanding into the surrounding stroma (lamina propria) as small projections or islands constitute an early invasion (Fig. 6.18). Some authors have described specific patterns of invasion. For example, the tumor may contain cells which retain cohesion and form broad bands, columns, and bulbous formations presenting an asymmetrical but rather more expansive than infiltrative pattern at periphery. The criterion of peripheral penetration is critical. Indeed, tumor cell islands or sheets that are not rounded, but sharp edged, thin

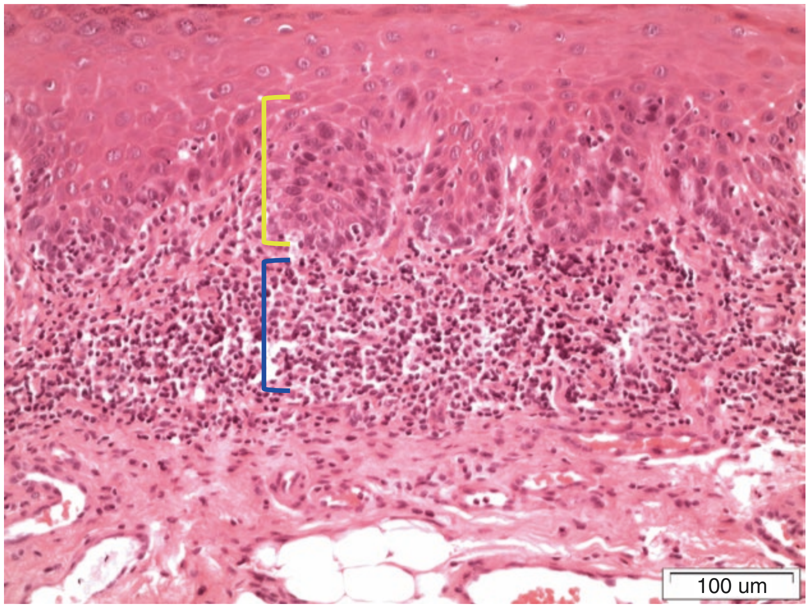

Fig. 6.17 "Lichenoid" dysplasia: drop-shaped rete ridges with mild to moderate epithelial dysplasia (yellow bracket) accompanied by subjacent intense lichenoid-like inflammatory infiltration (blue bracket) (×200)

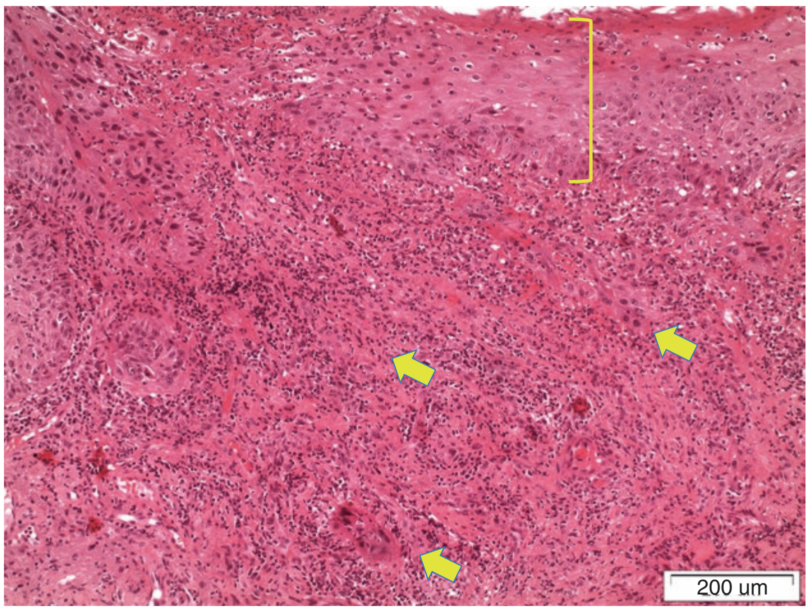

Fig. 6.18 From severe dysplasia (bracket) to early invasive OSCC (arrows): with unclear grade of differentiation (×100)

centrifugal projections, composed of dissociated, more or less differentiated epithelial cells indicate an infiltrative tendency for peripheral penetration and an overall aggressive biological behavior [44–46].

In addition, these neoplastic cells not only have the capacity to invade blood and lymphatic vessels but they can also induce the formation of new vessels (neoangiogenesis) as a progressive metastatic process. OSCC is characterized by lymph node invasion, starting as neoplastic cell emboli in lymphatic vessels and progressing to the dissemination of malignant cells into the lymph nodal medullary sinuses. In cases of neoplastic cell survival, a metastatic nest is created leading to node capsule invasion and to extracapsular spread of the tumor. In addition, invasion into the peri (into neural sheath) and endoneural (into the main nerve) is critical to the process of OSCC metastasis in aggressive cases. Finally, OSCC may form metastases to the bones in cases of adjacency (gingiva, alveolar bone in edentulous patients, spreading through the inferior alveolar nerve). Malignant structures at the periphery may erode bones with an interposed zone of connective tissue and osteoclasts, or, in contrast, malignant cells in islands or cords may infiltrate the cortex of the bone. The preexistence of a resorbed alveolar ridge and the increased function of proteases, cytokines, and growth factors secreted from malignant cells are prerequisites for this process [48, 50–54].

A very common feature under the microscope is a strong lymphocytic inflammatory infiltration occasionally presented as "lichenoid" and necrotic areas of variable size as well as a dense stromal fibrosis termed "desmoplasia" [44]. Tumor nests consist of neoplastic cells with abundant eosinophilic cytoplasm featuring large hyperchromatic nuclei and varying cellular and nuclear pleomorphism. In an attempt to mimic the normal epithelial function-differentiation, islets of neoplastic cells form keratin in a co-centric pattern called keratin pearl, and single neoplastic cells may show keratinization. The histological grading is settled by making a comparison between the alterations to the affected cells and their parent epithelial tissue. A variant of OSCC, with significantly better prognosis, is verrucous SCC. Microscopically, it is characterized by excessive epithelial hyperplasia with elongated rete but intact basal lamina, papillary surface, and increased keratin formation, without atypia, rare mitoses, and underlying strong inflammatory infiltration. Due to the extensive overgrowth pattern of verrucous SCC development, biopsy of large part or from multiple sites of the tumor is essential to exclude microinvasive or invasive form of OSCC (approximately 20%) [44, 45, 55].

6.2.2.2 Histological Grading

The histopathologic grade is based on the degree of differentiation of the neoplastic tissue and the resemblance of the neoplastic cells and their structures to normal epithelium in terms of keratinization, intercellular cohesion, cellular/nuclear polymorphism, and mitotic activity. The histological grade is an indication of the biological behavior of a tumor.

The histological grading of oral squamous cell carcinoma is divided into well differentiated or low grade (pG1) (Figs. 6.19 and 6.20), moderately differentiated (pG2) (Figs. 6.21a, b and 6.22), or

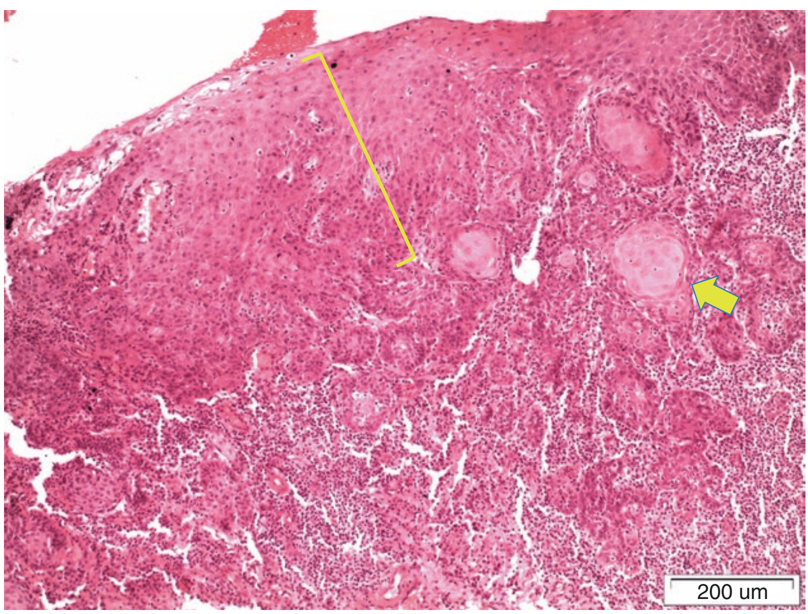

Fig. 6.19 From severe dysplasia (bracket) to well differentiated invasive OSCC: with islands of neoplastic cells under keratinization (arrow) (×100)

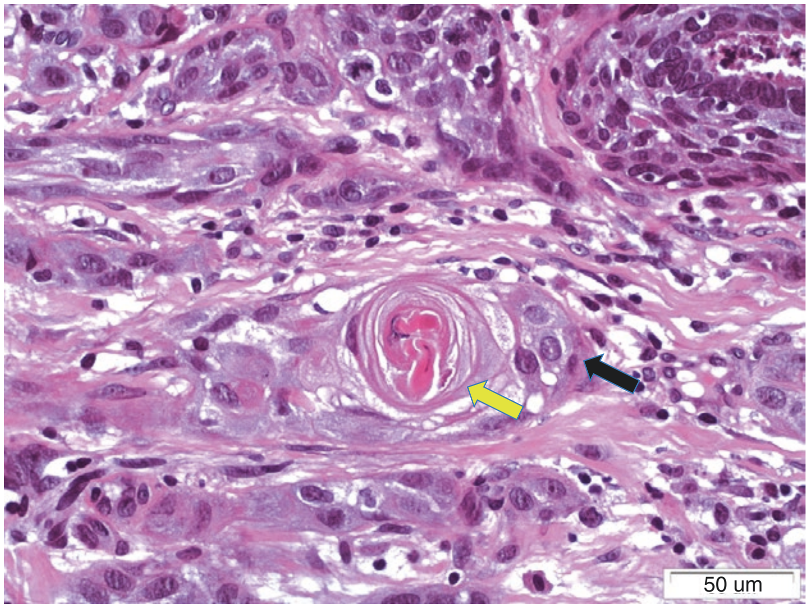

Fig. 6.20 Pearl of keratin (yellow arrow) formed by surrounding neoplastic cells (black arrow) in well-differentiated OSCC (×400)

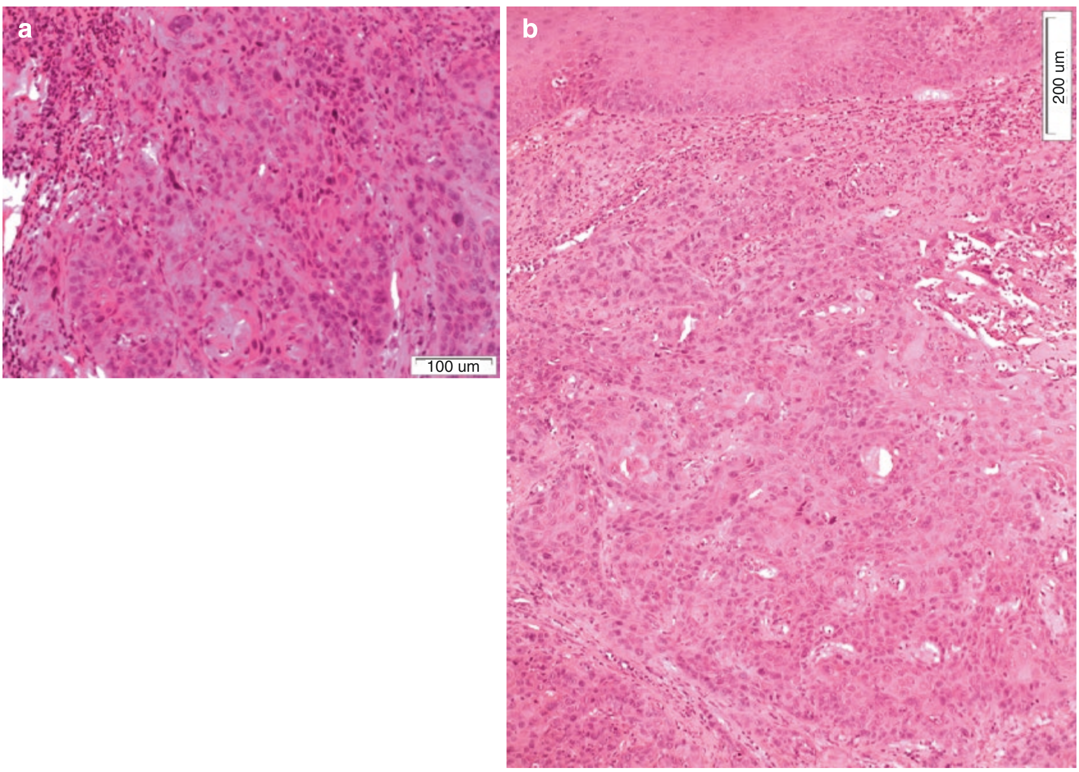

Fig. 6.21 (**a**, **b**) Moderately differentiated OSCC with aggressive sheets of neoplastic cells showing pleomorphism increased mitotic activity and atypia, without keratin formation (×100 and ×200)

poorly differentiated or high grade (pG3) (Figs. 6.23a, b and 6.24) depending on the maturity of the neoplastic cells and their morphologic resemblance compared to normal epithelium including keratinization, cellular/nuclear pleomorphism, and mitotic activity as well as intercellular connec-

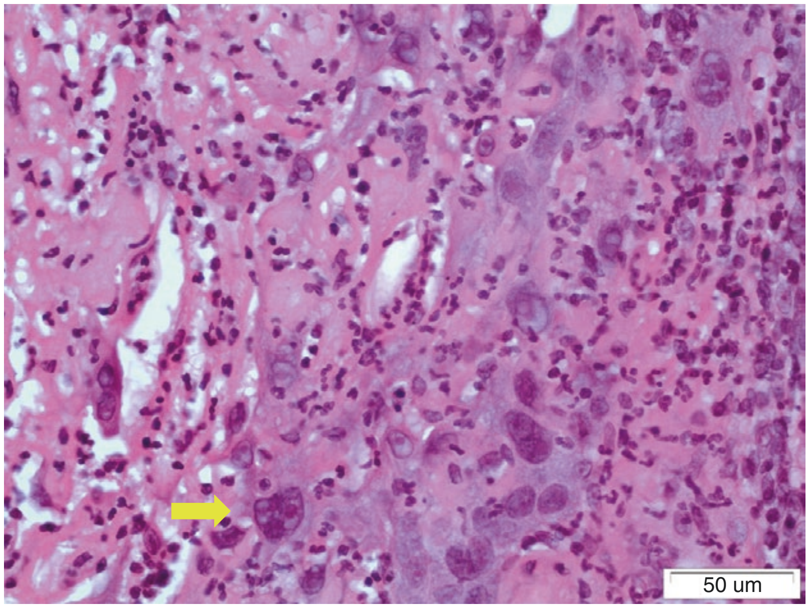

Fig. 6.22 Moderately differentiated OSCC with marked cellular pleomorphism, atypia, abnormal mitoses, and multinucleated neoplastic cells (arrow) (×400)

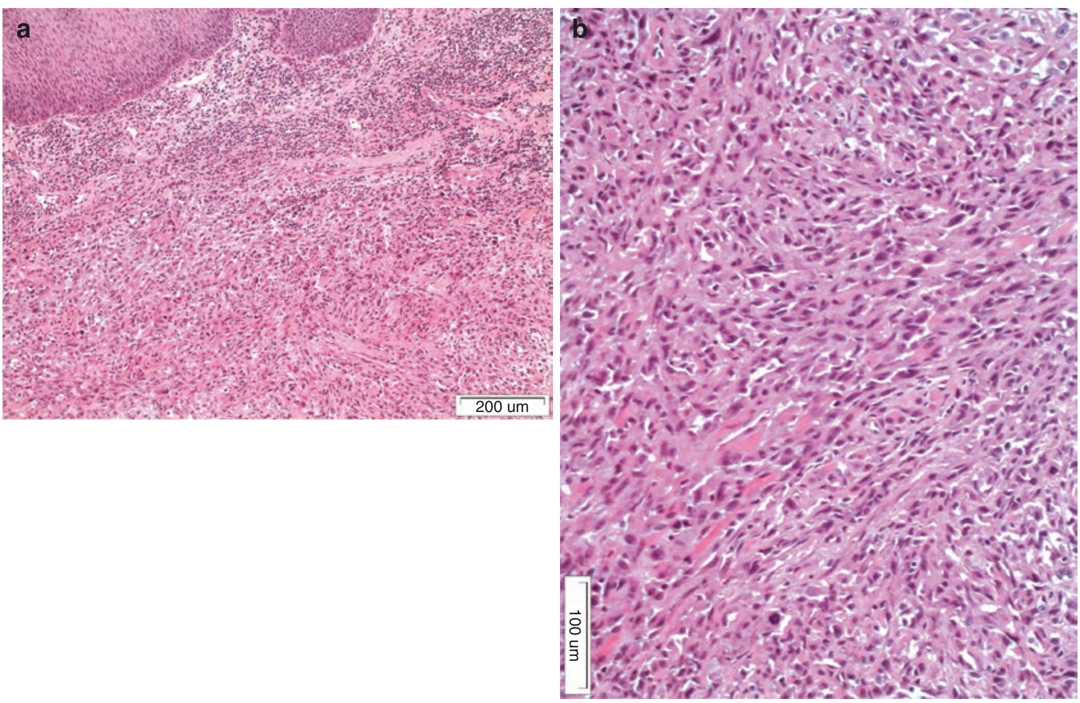

Fig. 6.23 (**a**, **b**) Poorly differentiated OSCC with aggressive sheets of spindle-like cells, with marked cellular and nuclear pleomorphism, without keratinization (×100 and ×200)

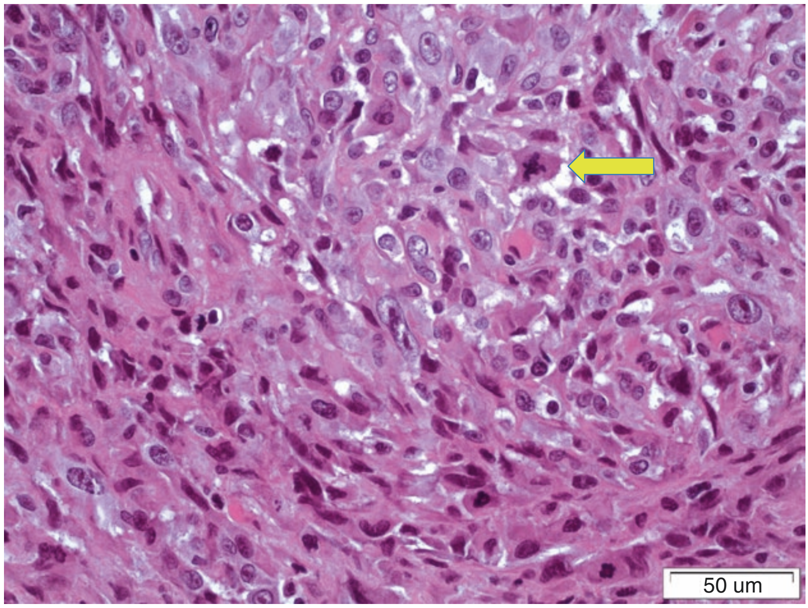

Fig. 6.24 Marked cellular and nuclear pleomorphism, spindle-like neoplastic cells, with atypical, bizarre mitoses (yellow arrow) in poorly differentiated OSCC (×400)

tions. Well-differentiated OSCC (most of the oral SCC are keratinized) closely resembles normal epithelial morphology, with tendency of malignant cells toward "normality" (low mitotic activity, minor cellular/nuclear pleomorphism, keratin production pearls) with subsequent slow growth and low metastatic capacity. On the other hand, the higher and marked cellular/nuclear pleomorphism, limited or absent keratin formation, and unclear intercellular connections indicate immature often basaloid-in-phenotype neoplastic cells, difficult to evaluate in origin, with potential to form rapidly expanding tumors, and high metastatic potential consisting of poorly differentiated high-grade OSCC. Moderately differentiated OSCC comprise a tumor with intermediate features between the two grades of differentiation described above. Overall the grading of OSCC represents the picture of the tumor from biopsy sample and depends on the area of the tumor and pathologist's criteria [44–48].

6.2.2.3 Correlation between Microscopy and Prognosis

Beyond clinical parameters (TNM T-stage, N-Nodal status, M-Metastasis), some histological features are pointers in prognosis. These microscopic features include the grade of differentiation which has to be considered together with the pattern of invasion, tumor thickness (lower than 4 mm generally indicates favorable prognosis, as opposed to greater than 9 mm), degree of keratinization, mitotic rate (Ki67 is used as a proliferative marker: the lower its expression, the better the prognosis of tumor), neoplastic cells-immune inflammatory response interface, pattern and level of invasion especially in the tumor periphery (including the thickness of clear normal tissue around excised tumor margins), invasion of nerves or bone, and extracapsular spread in nodal metastasis. Concerning the pattern of invasion, the existence of irregular cords and separated islands of cancer cells in deeper tissues indicates a less favorable prognosis [44, 45, 48, 53].

Conclusion

The current gold standard for diagnosis of oral dysplasia and oral squamous cell carcinoma remains to be clinical and histological examination. Through biopsy the grade of dysplasia in oral potentially malignant disorders, or grade of differentiation and pattern of invasion in oral squamous cell carcinomas can be objectively estimated, being the critical determinants of treatment plan and prognosis. During the biopsy procedure the incision of adequate representative areas is critical for accurate diagnosis. Biopsy methodologies like brush biopsy and exfoliative cytology have a special role in early detection and can be applicable in mass screening of oral cancer, where tissue biopsy cannot be conducted. In the context of suspicious oral lesions, selection of appropriate biopsy site remains as a challenging area and with the advent of technology, selection of biopsy site can become more objective and standardized.

References

1. Globocan 2012. Estimated cancer incidence, mortality and prevalence worldwide in 2012. Lyon: International Agency for Research on Cancer. World Health Organization. Available at http://globocan.iarc.fr/Pages/fact_sheets_population.aspx
2. Jemal A, Bray F, Center MM, Ferlay J, Ward E, Forman D. Global cancer statistics. CA Cancer J Clin. 2011;61:69–90.
3. Machiels JP, Lambrecht M, Hanin FX, Duprez T, Gregoire V, Schmitz S, et al. Advances in the management of squamous cell carcinoma of the head and neck. F1000Prime Rep. 2014;6:44.
4. Bagan J, Sarrion G, Jimenez Y. Oral cancer: clinical features. Oral Oncol. 2010;46:414–7.
5. Liu J, Duan Y. Saliva: a potential media for disease diagnostics and monitoring. Oral Oncol. 2012;48:569–77.
6. Messadi DV. Diagnostic aids for detection of oral precancerous conditions. Int J Oral Sci. 2013;5:59–65.
7. Melrose RJ, Handlers JP, Kerpel S, Summerlin DJ, Tomich CJ, American Academy of Oral and Maxillofacial Pathology. The use of biopsy in dental practice. The position of the American Academy of oral and maxillofacial pathology. Gen Dent. 2007;55:457–61. quiz 462–3,488
8. Ye X, Zhang J, Tan Y, Chen G, Zhou G. Meta-analysis of two computer-assisted screening methods for diagnosing oral precancer and cancer. Oral Oncol. 2015;51:966–75.
9. Scully C. Oral and maxillofacial medicine: The basis of diagnosis and treatment. London: Churchill Livingstone Elsevier; 2013.
10. Mota-Ramírez A, Silvestre FJ, Simó JM. Oral biopsy in dental practice. Med Oral Patol Oral Cir Bucal. 2007;12:E504–10.
11. Oxford Dictionaries (available at http://www.oxforddictionaries.com/definition/english/biopsy?q=Biopsy).
12. Mitchell DF, Standish SM, Fast TB. Oral diagnosis/oral medicine. Philadelphia: Lea &Febiger; 1971.
13. Laskaris G. Clinical stomatology diagnosis-treatment. Athens: Medical Publications Litsas; 2012.
14. Kerr DA, Ash MM, Millard HD. Oral diagnosis. St. Louis, MO: Mosby; 1978.
15. Oliver RJ, Sloan P, Pemberton MN. Oral biopsies: methods and applications. Br Dent J. 2004;196:329–33.
16. Angelopoulos AP, Spyropoulos ND. Oral diagnosis. Athens: Medical publications Litsas; 1988.
17. Patton LL, Epstein JB, Kerr AR. Adjunctive techniques for oral cancer examination and lesion diagnosis: a systematic review of the literature. J Am Dent Assoc. 2008;139:896–905.
18. Cohen L. Oral diagnosis and treatment planning. Springfield: American Lecture Series; 1973.
19. Sailer HF, Pajarola GF. Color atlas of dental medicine: oral surgery for the general dentist. Leipzig: Thieme; 1999.
20. Logan RM, Goss AN. Biopsy of the oral mucosa and use of histopathology services. Aust Dent J. 2010;55:9–13.
21. Birnbaum W, Dunne SM. Oral diagnosis: the clinicians guide. Oxford: Wright Reed Educational and Professional Publishing Ltd; 2000.
22. Myers EN, Ferris RL. Salivary gland disorders. Berlin: Springer; 2007.
23. Fedele S. Diagnostic aids in the screening of oral cancer. Head Neck Oncol. 2009;1:5.
24. Avon SL, Klieb HB. Oral soft-tissue biopsy: an overview. J Can Dent Assoc 2012;78:c75.
25. Thawley SE, Panje WR. Comprehensive management of head and neck tumors. Philadelphia, PA: W.B. Saunders Company; 1987.
26. Wood NK, Goaz PW. Differential diagnosis of oral lesions. St. Louis, MO: C.V. Mosby Company; 1980.
27. SeoaneLestón J, Diz Dios P. Diagnostic clinical aids in oral cancer. Oral Oncol. 2010;46:418–22.
28. Kusukawa J, Suefuji Y, Ryu F, Noguchi R, Iwamoto O, Kameyama T. Dissemination of cancer cells into circulation occurs by incisional biopsy of oral squamous cell carcinoma. J Oral Pathol Med. 2000;29:303–7.
29. Ramani P, Thomas G, Ahmed S. Use of Rt-PCR in detecting disseminated cancer cells after incisional biopsy among oral squamous cell carcinoma patients. J Cancer Res Ther. 2005;1:92–7.
30. Bong JL, Herd RM, Hunter JA. Incisional biopsy and melanoma prognosis. J Am Acad Dermatol. 2002;46:690–4.
31. Mehrotra R. The role of cytology in oral lesions: a review of recent improvements. Diagn Cytopathol. 2012;40:73–83.
32. Poh CF, Ng S, Berean KW, Williams PM, Rosin MP, Zhang L. Biopsy and histopathologic diagnosis of oral premalignant and malignant lesions. J Can Dent Assoc. 2008;74:283–8.
33. Poate TW, Buchanan JA, Hodgson TA, Speight PM, Barrett AW, Moles DR, et al. An audit of the efficacy of the oral brush biopsy technique in a specialist oral medicine unit. Oral Oncol. 2004;40:829–34.

34. Scheifele C, Schmidt-Westhausen AM, Dietrich T, Reichart PA. The sensitivity and specificity of the OralCDx technique: evaluation of 103 cases. Oral Oncol. 2004;40:824–8.
35. Seijas-Naya F, García-Carnicero T, Gándara-Vila P, Couso-Folgueiras E, Pérez-Sayáns M, Gándara-Vila R, et al. Applications of OralCDx® methodology in the diagnosis of oral leukoplakia. Med Oral Patol Oral Cir Bucal. 2012;17:e5–9.
36. Reddy SG, Kanala S, Chigurupati A, Kumar SR, Poosarla CS, Reddy BV. The sensitivity and specificity of computerized brush biopsy and scalpel biopsy in diagnosing oral premalignant lesions: a comparative study. J Oral Maxillofac Pathol. 2012;16:349–53.
37. Casparis S, Borm JM, Tomic MA, Burkhardt A, Locher MC. Transepithelial brush biopsy – oral CDx® -a noninvasive method for the early detection of precancerous and cancerous lesions. J Clin Diagn Res. 2014;8:222–6.
38. Davey E, Barratt A, Irwig L, Chan SF, Macaskill P, Mannes P, et al. Effect of study design and quality on unsatisfactory rates, cytology classifications, and accuracy in liquid-based versus conventional cervical cytology: a systematic review. Lancet. 2006;367:122–32.
39. Lingen MW, Kalmar JR, Karrison T, Speight PM. Critical evaluation of diagnostic aids for the detection of oral cancer. Oral Oncol. 2008;44:10–22.
40. Stefanac SJ, Nesbit SP. Treatment planning in dentistry. St. Louis, MO: Mosby Elsevier; 2007.
41. Liu Y, Li J, Liu X, Liu X, Khawar W, Zhang X, et al. Quantitative risk stratification of oral leukoplakia with exfoliative cytology. PLoS One. 2015;10:e0126760.
42. Warnakulasuriya S, Tilakaratna WM: Oral medicine & pathology: a guide to diagnosis and management. New Delhi: Jaypee Brothers Medical Publishers, 1st edition 2013.
43. Lingen MW, Tampi MP, Urquhart O, Abt E, Agrawal N, Chaturvedi AK, et al. Adjuncts for the evaluation of potentially malignant disorders in the oral cavity: diagnostic test accuracy systematic review and meta-analysis-a report of the American Dental Association. J Am Dent Assoc. 2017;148:797–813.e52.
44. Lingen MW, Abt E, Agrawal N, Chaturvedi AK, Cohen E, D'Souza G, et al. Evidence-based clinical practice guideline for the evaluation of potentially malignant disorders in the oral cavity: a report of the American Dental Association. J Am Dent Assoc. 2017;148:712–727.e10.
45. Warnakulasuriya S, Reibel J, Bouquot J, Dabelsteen E. Oral epithelial dysplasia classification systems: predictive value, utility, weaknesses and scope for improvement. J Oral Pathol Med. 2008;37:127–33.
46. Thompson L, Wenig B. Head and neck diagnostic pathology. Amirsys Inc. 2011:80–91.
47. Neville D, Bouqouot A. Oral and maxillofacial pathology, 3rd edition. Saunders Elsevier. 2009:418–20.
48. Cardesa A, Slootweg PG. Pathology of head and neck. Springer-Verlag. 2006:1–29.
49. Adel K. El-Naggar, John K.C. Chan, Jennifer R. Grandis, Takashi Takata, Pieter J. Slootweg. WHO classification of head and neck tumours. 4th ed.; 9th; Lyon: International Agency for Research on Cancer, 2017.
50. Woo SB, Cashman EC, Lerman MA. Human papillomavirus-associated oral intraepithelial neoplasia. Mod Pathol. 2013;26:1288–97.
51. Roh J, Muelleman T, Tawfik O, Thomas SM. Perineural growth in head and neck squamous cell carcinoma: a review. Oral Oncol. 2015;51:16–23.
52. Inglehart RC, Scanlon CS, D'Silva NJ. Reviewing and reconsidering invasion assays in head and neck cancer. Oral Oncol. 2014;50:1137–43.
53. Leemans CR, Braakhuis BJM, Brakehoff RH. The molecular biology of head and neck cancer. Nat Rev Cancer. 2011;11:9–22.
54. Sciubba JJ, Helman JI. Current management strategies for verrucous hyperkeratosis and verrucous carcinoma. Oral Maxillofac Surg Clin North Am. 2013;25:77–82.
55. Woolgar JA, Triantafyllou A. Pitfalls and procedures in the histopathological diagnosis of oral and oropharyngeal squamous cell carcinoma and a review of the role of pathology in prognosis. Oral Oncol. 2009;45:361–85.

7 Oral Cancer Screening: Application of Vital Stains as Adjuncts to Clinical Examination

Prashanth Panta, Laurie J. Rich, and Mukund Seshadri

Abstract

An essential first line of investigation in oral oncology is clinical examination of high-risk oral sites. Given the elevated DNA content in cancers, vital dyes such as toluidine blue, methylene blue, Lugol's iodine, and rose bengal, which have an inherent chemical capacity to bind to DNA, have been studied for their clinical utility in screening malignant changes in the oral cavity. In this chapter, we cover the basics of clinical examination and review the literature on the use of vital stains as adjunct diagnostic aids in patients with clinically suspicious oral lesions such as leukoplakia and erythroplakia. The goal of this chapter is to provide the reader with an overview of the vital stains available on the market and their potential for clinical application. A discussion of their strengths, limitations, and the rationale for development of new screening methods, has also been provided.

P. Panta, MDS (✉)
Department of Oral Medicine and Radiology, MNR Dental College and Hospital, Sangareddy, Telangana, India
e-mail: maithreya.prashanth@gmail.com

L. J. Rich, PhD · M. Seshadri, DDS, PhD
Department of Oral Oncology, Roswell Park Comprehensive Cancer Center, Buffalo, New York, USA
e-mail: laurie.rich@roswellpark.org; Mukund.Seshadri@roswellpark.org

7.1 Introduction

Oral cancer is rampant in South-Central Asia accounting to 48.7% of total cases in 2012 [1]. India contributed to one-third of the global oral cancer burden (270,000 incident cases and 145,000 deaths) in 2009 [2, 3]. The morbidity and mortality associated with this disease presents a significant burden on health care. Histologically, over 90% of these cancers are oral squamous cell carcinomas (OSCC) and are associated with tobacco and betel nut use. Most oral cancer patients are diagnosed with advanced stage disease (stages III–IV) limiting their treatment options. Standard of care typically involves wide local excision and radical neck dissection.

Detection of oral cancer at an early stage (stage I or II) has a significant impact on the prognosis and overall survival of patients. For example, the 5-year survival rate for patients with OSCC of mobile tongue is 80% at stage I (local disease) and drops to 15% at stage IV [3]. Despite occurring in an easily accessible site, patients often present with advanced tumors at initial diagnosis. A majority of oral cancers present initially as oral potentially malignant disorders (OPMDs), and it is best to identify such precursor lesions to halt progression into invasive oral cancer. Although OPMDs have characteristic clinical presentation, some precancerous changes cannot be readily detected by visual examination under white light illumination. When a dentist or oral surgeon identifies a suspicious lesion, it is

P. Panta (ed.), *Oral Cancer Detection*, https://doi.org/10.1007/978-3-319-61255-3_7

Fig. 7.1 A tobacco chewer and smoker for nearly 15 years showing diverse mucosal changes. In such relatively larger lesions, especially involving the tongue, a decision on representative biopsy location is critical

critical to perform a biopsy for histological examination. However, the lesion in question may often appear benign with no color change, making it difficult to rationalize a biopsy. To overcome this difficulty, adjunct techniques such as vital staining methods have been used as screening tools to assist in the selection of a suitable representative biopsy site (Fig. 7.1). In this chapter, we will broadly discuss the clinical utility of these vital staining methods as adjuncts to conventional examination in the context of oral cancer screening and evaluation.

Oral cancer screening and prevention programs are frequently conducted for the following reasons: (a) oral cancer is a common health-care burden; (b) early detection results in significant reduction in morbidity and mortality [4]; (c) treatment is well defined for each stage (I, II, III, or IV), and therefore, a precise treatment plan can be implemented; and (d) incisional biopsy is invasive and can potentially seed tumor cells into deeper tissue, increasing chance of metastasis [5]. Additionally, performing a biopsy of the normal mucosa is unethical. While biopsy is the current gold standard for diagnostic evaluation of OPMDs, development of cheap and effective screening strategies and diagnostic approaches can reduce the need for invasive biopsies of suspicious lesions and have a significant clinical impact, especially for high-risk patients.

7.2 Evaluation Criteria for Screening or Diagnostic Tests

A good screening technique should identify disease at the asymptomatic stage. An ideal screening tool should be noninvasive, cost effective, easy to conduct, acceptable to the patient, and must have high sensitivity and specificity. Established examples of good cancer screening methods include the “Pap smear” for cervical cancer and mammography for breast cancer. In the United Kingdom, 22 criteria set by the National Screening Committee have to be met before a screening tool is introduced for clinical use [6]. Each diagnostic approach has a certain sensitivity and specificity, and the efficacy of any method is interpreted using these parameters. For example, conventional oral examination for melanoma has a very high sensitivity and specificity, due to the characteristic color change (Fig. 7.2a). On the contrary, many oral cancerous

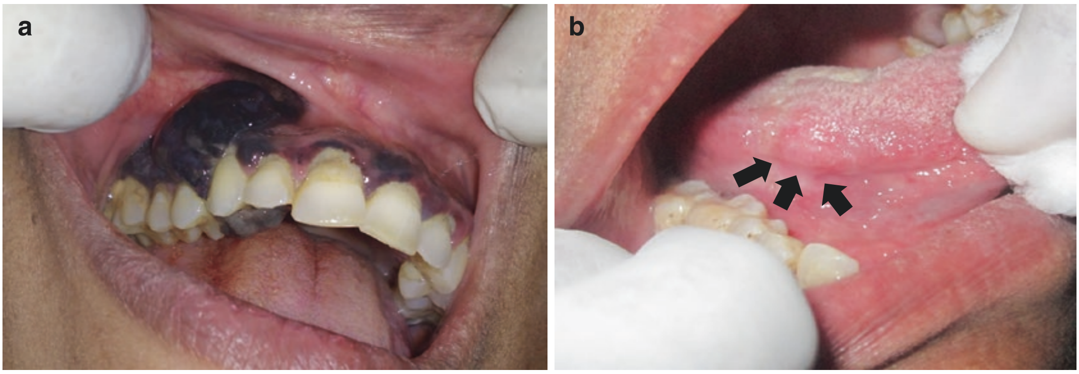

Fig. 7.2 Malignant melanoma is a rare oral cancer with typically black color change (**a**), unlike conventional oral cancer which does not show such classic color pattern (**b**)

Table 7.1 Evaluation of diagnostic power of a screening test

Total observations = 60	Test result	
	Positive	Negative
Disease = 30	A = 26 (true positive)	B = 4 (false negative)
No disease =30 i.e., controls	C = 5 (false positive)	D = 25 (true negative)

Sensitivity: The true positive rate i.e., A/A + B = 26/30 = 0.86 or 86%.
Specificity: The true negative rate i.e., D/C + D = 25/30 = 0.83 or 83%.
Positive predictive value: A/A + C = 26/31 = 0.83.
Negative predictive value: D/B + D = 25/29 = 0.86.

lesions appear benign and escape detection by clinicians by "conventional oral examination" (Fig. 7.2b).

Sensitivity is defined as the probability of a positive test result when disease is present. Specificity is defined as the probability that a result will be negative when disease is absent. Diagnostic sensitivity and specificity may be expressed in various terms, which include true positive, true negative, false positive, and false negative (Table 7.1). When a diagnostic test identifies a patient with a disease correctly, the test result is *true positive*. When a test implies that a patient is positive in the absence of disease, the test result is *false positive*. When a test result implies that a patient does not have disease in the true absence of disease, the test result is *true negative*. A test result is *false negative* when the test implies there is no disease in a patient despite the presence of disease. False positive and false negatives are dangerous and make a diagnostic test less dependable and potentially unsuitable. If a particular test yields a false positive result, it may lead to clinical misdiagnosis and unnecessary treatment that result in negative physical and psychological consequences to the patient. Alternatively, a false negative test result can lead to undertreatment. Positive predictive value is the probability that disease is present when a test is positive, while negative predictive value is the "probability that disease is absent when test is negative" [7]. Screening studies or oral cancer screening methods should always be evaluated based on their sensitivity, specificity, and predictive values. Although there is no defined value for an ideal screening test, it is desirable to have both high specificity (few false positives) and high sensitivity (few false negatives) [7].

In medicine, the test with the highest sensitivity and specificity is often considered as the choice of investigation, a "gold standard." In the assessment of any diagnostic test, ideally a gold standard should be used for comparative purposes. It is also noteworthy that in many research papers on oral cancer adjuvant screening methods, the test method was compared to conventional oral examination (not a gold standard), instead of surgical biopsy (histological findings) [8]. It is also important to include both normal and abnormal subjects to understand the results of any diagnostic test. Studies conducted on diagnostic accuracy show receiver operating characteristic (ROC) curves plotted between true

Table 7.2 Simple accuracy classification for different oral cancer methods

Accuracy range	Oral cancer diagnostic method	Comments
1	Biopsy	Gold standard reference test
AUC < 1.0	Cytology	As per existing data it is hard to say which method is superior over other methods and each method if used correctly may support an experienced and skilled clinician
	Light based methods	
	Vital stains	
	Mouth self examination	
	Conventional oral examination	

positive rate (sensitivity) and false positive rate (1-specificity). The area under the ROC curve gives the accuracy of any diagnostic test [9] with a larger area under the curve indicating greater accuracy. Although studies report on sensitivity and specificity of diagnostic methods, predictive values are often not mentioned in oral cancer literature limiting the determination of accuracy [8] (Table 7.2).

7.3 Clinical Examination of Oral Cavity

7.3.1 Relevant Anatomy

The oral cavity is oval shaped and separated into the oral vestibule and oral cavity proper. It is bound by the lips anteriorly, the cheeks laterally, the floor of the mouth inferiorly, and the oropharynx posteriorly with the palate forming the roof. The bony base of the oral cavity is represented by the maxillary and mandibular bones. The oral cavity also includes the lips, gingivae, retromolar trigone, teeth, hard palate, cheek mucosa, mobile tongue, and floor of the mouth. The oropharynx begins superiorly at the junction between the hard and soft palate and inferiorly behind the circumvallate papillae of the tongue. Cancer, limited to the regions of mouth anterior to the oropharynx, is referred to as "oral cancer." Cancer occurring below this region is referred to as "oropharyngeal cancer."

7.3.2 Conventional Oral Examination

Conventional oral examination (COE) is a standard procedure and a traditional method of oral cancer screening. Most oral precancerous lesions can at least be suspected on thorough oral examination, and frank lesions (Fig. 7.3) or warning signs (Table 7.3) in particular can be directly identified by clinical examination. The COE is conducted under proper lighting using a halogen white light illumination source. Examination instruments include mouth mirror, tongue depressor for examination of posterior oral cavity, gauze squares to inspect the lateral borders of the tongue, and examination gloves for palpation. A good knowledge of high-risk oral sites is critical for effective screening. The identification of precursor lesions by a clinician can significantly reduce future oral cancer burden. A thorough screening should include a methodic intraoral examination of high-risk oral sites and the head and neck lymph nodes. Special care and attention should be given to the tongue and floor of the mouth as a delay in diagnosis at these locations increases mortality and morbidity [1]. Epidemiologic data strongly suggests that certain oral sites are at increased risk for malignant transformation [3]. Clinicians should therefore inspect and thoroughly screen these high-risk sites which include the tongue, buccal mucosa, floor of the mouth and gingivae, and also poorly accessible sites like the vestibule [3]. Visual examination, according to the "International Agency for Research on Cancer (IARC) and World Health Organization (WHO)," can minimize a significant proportion of oral cancer-related deaths [4].

A clinician may also notice a palpable, nontender, lymph node during neck examination on the same side of a suspicious lesion. An association of a solitary lesion, i.e., nonhealing ulcer and cervical lymphadenopathy (anterior cervical chain), should raise serious suspicion of malignancy. If a lymph node is positive, an incisional biopsy or brush biopsy is recommended. If the lesion appears benign, it is a challenging decision to determine whether or not to perform biopsy and is dependent entirely on the clinician's expertise. A good diagnostic algorithm can

Fig. 7.3 A frank lesion of carcinoma (which includes relatively large proliferative lesions (**a**), grossly destructive lesions (**b**), and classic non-healing ulcers with raised borders (**c**)) requires no further investigations, except biopsy to initiate a treatment plan

Table 7.3 Common warning signs of oral cancer

1. Non healing oral ulcer (most common presentation)
2. Persisting red/white lesions
3. A nodular thickening
4. Obstructive feeling or lump in mouth.
5. Increasing trismus or decrease in tongue mobility
6. Poor fit of dentures
7. Increasing tooth mobility or pain
8. Voice changes
9. Loss of weight/loss of appetite

minimize the rate of morbidity and mortality associated with oral cancer. Generally oral cancer patients are diagnosed at either stage III or stage IV, and immediate referral for biopsy at initial suspicion can reduce mortality significantly. The presence of neck masses (enlarged lymph nodes in anterior cervical chain) is not an uncommon finding in patients (30%) with oral cancer, and are frequently enlarged in patients with advanced oral malignancies [10]. Lymphadenopathy secondary to infection is mobile and tender, whereas a metastatic lymph node is asymptomatic and fixed to the underlying structures giving a solid feel on palpation.

All oral cancers are preceded by visible changes on the oral mucous membrane and hence represent preventable clinical scenarios. Lesions may range from homogenously white areas as in leukoplakia, to deep red areas as in erythroplakia, or show mixed (red-white) appearance as in speckled leukoplakia. Inflammatory, habit-related disorders such as lichen planus present as white lesions in striated pattern, and oral submucous fibrosis presents with a blanched appearance. Potentially malignant lesions occurring on lateral tongue have a high malignant potential [10, 11], and carcinomas at this location are likely to be associated with poor outcomes. Carcinoma involving buccal mucosa can present as a benign red-white lesion or ulcers, carcinoma involving the tongue may present as an indurated ulcer or nodule, and maxillary and mandibular vestibular lesions are often present as a fissure. The presence of a nonhealing ulcer for more than 3 weeks is suggestive of either OSCC or lesions similar in nature, such as eosinophilic granuloma and tuberculous ulcer (Fig. 7.4). If trauma is suspected, the traumatic insult should be eliminated, and a follow-up examination of the patient performed after approximately 3 weeks (Fig. 7.5).

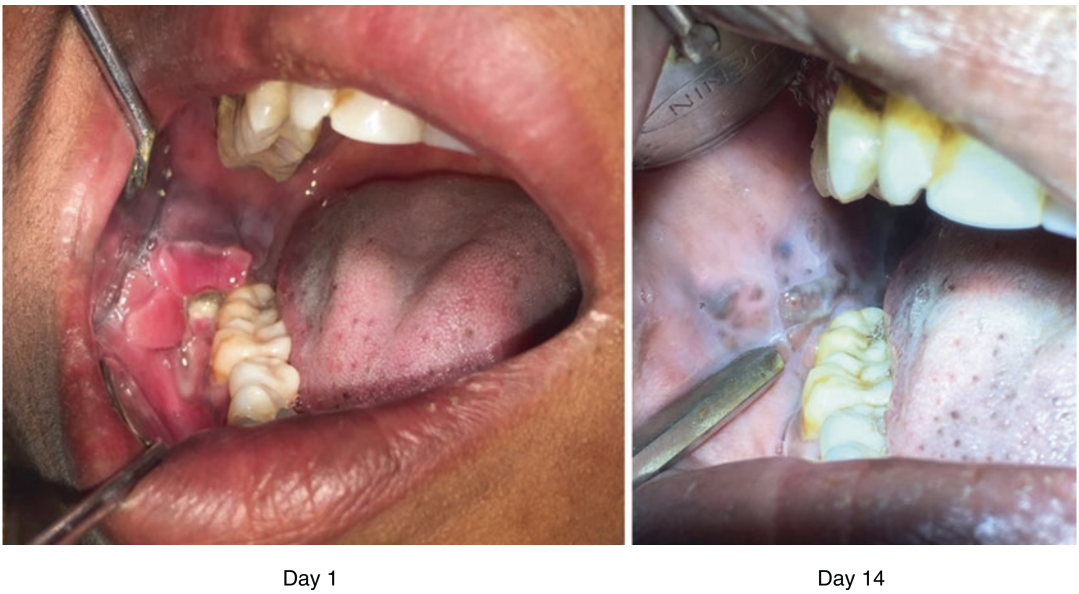

Fig. 7.4 A fibro-proliferative lesion mimicking carcinoma showed complete regression in 14 days following removal of third molar

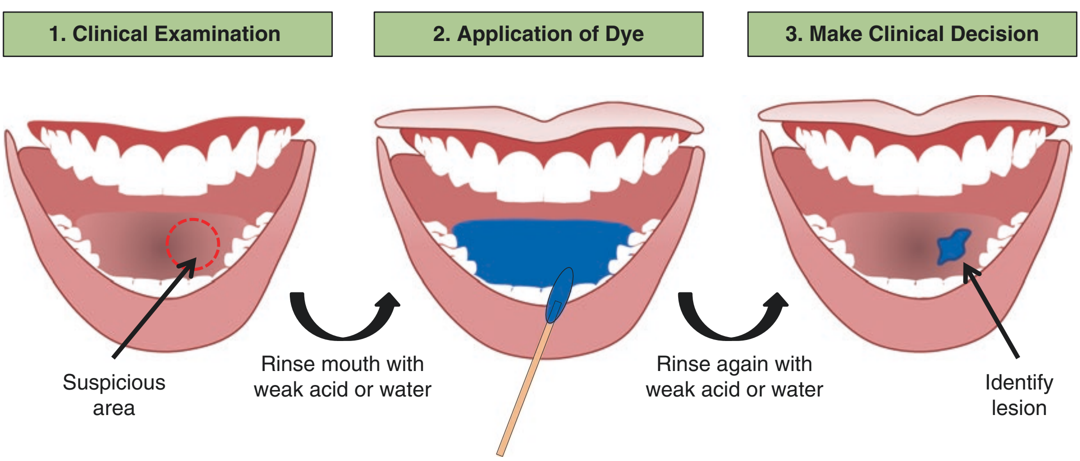

Fig. 7.5 Vital staining for detection of oral lesions

The presence of ulceration, nodularity, induration, and fixation are suggestive clinical parameters and direct indicators of OSCC. With oral malignant melanoma (MM), the diagnosis is relatively easy, as color change is a direct indicator of this disease (Fig. 7.2a). However, a tumor like MM is rare in the clinical setting, and on most occasions "oral cancer" refers to the more common squamous cell carcinoma (Fig. 7.1b).

The history and frequency of adverse habits such as smoking and betel nut use should be noted in clinical history for correlation with clinical findings (Fig. 7.5). A diagnosis is often based on duration of growth, rapidity of progression, associated pain or loss of sensation, difficulty in swallowing, speech or function, and weight loss (Table 7.3).

The strongest evidence for COE comes from a long-term, cluster randomized control trial (RCT) conducted by the Trivandrum Oral Cancer Screening Study Group in Kerala, India. The research team divided the entire patient cohort of 130,000 individuals into control and screening groups. The investigators published their results at 3-, 6-, and 9-year intervals [12–14]. No difference in 3-year survival was observed between the two groups. However, 9 years later, the authors reported that male patients with habits showed significant increase in survival rate. The authors concluded that visual screening can reduce mortality of at least 37,000 oral cancer-related deaths. It should be noted that the study by the Kerala group had some weaknesses in methodology and risk of bias was high [15]. At the 15-year follow-up, there was a sustained reduction (24%) in mortality in individuals who adhered to repeated screening rounds further supporting the role of oral screening [16]. Nevertheless, additional RCTs are warranted to further support the results of this study. According to a meta-analysis of five studies, the sensitivity and specificity of screening in the detection of oral cancer were 0.85 and 0.97, respectively [17]. While this result is satisfactory, early lesions may present with subtle features which could escape detection by visual examination white light illumination (Fig. 7.2b). Adjuvant methods are therefore needed to improve our ability to detect and diagnose oral cancers at an early stage.

7.3.3 Low Cost, Digital Camera Technology Supplements COE

Making use of good cameras for capturing images of suspected oral lesions is undoubtedly a useful and beneficial strategy for clinicians. Clinical photographs create strong impact in diagnosis and improve understanding of challenging cases. A suspicious case can be followed over time to record the changes for further evaluation. Digital photographs can also be used as efficient tools for patient education and chairside discussion to improve awareness on oral cancer. The transfer of digital photographs from remote sites to trained clinicians and dentists can also allow for distant diagnosis of patients where oral health specialists are inaccessible.

7.3.4 Mouth Self-Examination

Some data is also available on mouth self-examination (MSE) as a tool for oral cancer screening. In this method, the target population is supplied with a brochure demonstrating suitable figures showing the appearance of potentially malignant lesions and oral cancer. MSE is a feasible test which improves oral cancer awareness and was identified as an effective tool for early detection of cancer in high-risk populations [18, 19]. The sensitivity of MSE was low (18%), but specificity was 99.9%. In MSE, the detection rate of red and ulcerative lesions was high whereas white lesions often escaped detection [19]. Additionally, MSE may also reduce patient delay in seeking treatment.

7.4 Vital Stains: Dyes Reveal Oral Cancer

In vivo staining is an easy to use, inexpensive screening method for oral cancer commonly practiced in community programs for mass screening. It is a method of staining viable cells and tissues. There are two types of vital staining, intravital staining, which refers to staining of tissues in the body (in vivo), and supravital staining, which is conducted outside the body and involves staining of detached cells on a glass slide (ex vivo). Currently, four vital stains for in vivo application are described in the oral cancer literature. These include toluidine blue, methylene blue, Lugol's iodine, and rose bengal.

7.4.1 Toluidine Blue

Toluidine blue (TB) is also referred to as "tolonium chloride" and is one of the oldest oral cancer screening methods. This blue, cationic metachromatic stain has an affinity for nucleic acids. It therefore highlights abnormal malignant areas of the oral mucosa. TB is a member of the thiazine family and is soluble in water or alcohol. The clinical application of TB in neoplasia was first attempted by Richart in 1963 in cervical carcinoma, but is now routinely practiced for identification of suspicious and occult oral lesions [20, 21]. Although not approved by the FDA for cancer screening, TB staining frequently used in many parts of the world especially for clinically challenging lesions to rule out dysplasia [22]. TB staining has been shown to exhibit good sensitivity and specificity yielding an 86% accuracy when compared to histology [23]. Several studies recommend TB as a useful adjuvant method to clinical examination [4, 24, 25], and combining TB with conventional examination can reduce false negatives (underdiagnosis) [26].

7.4.1.1 Working Principle

TB selectively stains acidic cellular and tissue components to sulfates, carboxylates, and phosphate groups [21]. As nucleic acids are rich in phosphates, TB naturally stains cells rich in DNA and RNA such as cancerous and dysplastic cells. DNA, RNA, and glycosaminoglycans (GAG) are negatively charged polyanions. TB contains several electronegative groups allowing it to intercalate and interact via electrostatic interactions with these macromolecules [27, 28]. The preferential affinity of TB for DNA is superior to other phenol-thiazinium azure based stains [28]. In calf thymus DNA, TB has been shown to bind to negatively charged phosphate groups on DNA at high concentrations [29]. Proteins, being the most abundant macromolecules in cell cytoplasm or tissue, do not stain with TB, giving more contrast due to limited background staining [21]. Logically, the degree of dye intercalation depends on the amount of DNA present, which is related to the number of cells and average size of nuclei located in the epithelium. Tumor tissues are often more acidic than normal tissue due to an accumulation of lactic acid caused by a shift toward anaerobic metabolism also known as the Warburg effect [21, 30]. As TB is an acidophilic dye, it may also stain the acidic environment of tumor tissues.

TB has been shown to reveal high-risk premalignant lesions that exhibit loss of heterozygosity (LOH) at multiple loci [31]. A sixfold increase in cancer risk was associated with areas positive for TB indicating its role in detection of high-risk oral lesions; retention occurred in 12 of the 15 lesions that progressed to cancer [31]. An important feature of TB is its property of "metachromasia," its ability to color tissue in a shade different from the color of the stain itself. The dye absorbs light at multiple wavelengths depending on its concentration and aggregation caused by Vander Waals forces that induce polymerization [21]. In the monomeric form, TB is orthochromatic and in polymeric form is metachromatic. Staining of frozen sections has shown that the dark blue uptake of stain is significantly related to nuclear uptake and pale blue uptake is not associated with any nuclear uptake [32].

7.4.1.2 Method of Application

Step 1: Conduct clinical examination of suspicious oral lesion.

Step 2: Rinse mouth with water, followed by rinsing with 1% acetic acid for 20 seconds to remove debris.

Step 3: Apply 5-10 cm^3 of 1% (w/v) TB solution. It contains 86 ml distilled water, 4.19 ml absolute alcohol, 10 ml of 1% acetic acid, and 1 g toluidine blue powder [25]. If the lesion is not clinically visible, the patient is asked to gargle the solution for 1 min before expectoration, or the TB can be applied using a cotton swab if the lesion is small in size or clearly visible.

Step 4: Rinse again with 1% acetic acid to remove excess stain, followed by a final water rinse of the mouth.

Step 5: Based on dye retention, select biopsy site with dark blue staining (TB positive area) and do punch biopsy. Interpretation is done under well-illuminated conditions. Besides color, the location, size, and shape are key features that should be documented.

"Dark blue staining" is considered as "positive". Lesions that exhibit dark blue color or striped staining are considered positive uptake, and lightly or faintly stained areas are not given weightage. TB is a useful method to check the extent of a dysplastic lesion. However, false positives do occur mainly with respect to keratotic lesions, erosions, and ulcer edges. To reduce false positives (i.e., overdiagnosis), patients with suspected inflammatory lesions can be recalled after a 10–14-day waiting period [26]. The false negative (underdiagnosis) impression can also occur; however, the percentage is quite low for invasive lesions. TB is of value following radiation therapy as unnecessary biopsies can be avoided in patients given the poor healing ability of mucosa exposed to radiation. It should be used only as an adjunct method and is not recommended as a diagnostic tool.

TB is especially important in screening high-risk populations mainly in patients with carcinoma in situ (sensitivity rate of 96.7%) and high-grade dysplasia. It is better than conventional oral screening. The overall sensitivity and specificity values range from above 90 to 100% and 73.3% to 92.9%, respectively [7, 33]. Despite the abundant literature, a recent systematic review showed that only 14 out of 77 publications evaluated the importance of TB as compared to COE. Standardization of TB application, the development of proper guidelines for shade matching, and criteria for interpretation can improve our understanding of the true efficacy of this staining method. Other oral cancer methods (ViziLite Plus) are also based on the clinical application of TB, and a deeper understanding is necessary. A TB mouth rinse was also introduced under the name "OraScan" which has more potential for oral cancer identification [34]. This ready to use kit demonstrated sensitivity of 79.5% and specificity of 64% for epithelial dysplasia. Five cases were identified solely by this kit [34]. According to randomized control trials, TB identified more oral submucous fibrosis and leukoplakia [24, 35]. The overall sensitivity of TB ranges from 70 to 100%, but has less specificity due to risk of false positives. TB however was shown toxic to fibroblasts and on swallowing as per material data safety data sheet [36].

TB stain is frequently used to rule out dysplasia in suspected oral lesions. Although not absolutely reliable, it is highlighted as a potential method to detect widespread dysplastic changes. While the effectiveness of TB is not fully proven, studies have shown an added benefit over conventional oral examination [4, 24, 25, 31, 33, 35]. The lack of sufficient RCT evidence is an important limitation, and long-term prospective data can further improve our understanding.

7.4.2 Methylene Blue

Methylene blue (MB) is a phenothiazinium dye with chemical structure and properties similar to TB [36]. MB has previously been used to detect gastric, prostrate, and bladder cancers, Barrett's esophagus, intestinal metaplasia, dysplasia or carcinoma [37]. Recent RCTs suggest its use in parotid surgery for localization of tumor, preservation of facial nerve, and complete removal of glandular tissue in parotid malignancies [38]. In the last few years, MB has emerged as a new tool for mass screening for oral cancer. Solutions of 1% MB were used as a vital stain which showed remarkable accuracy (90%) [36, 39]. Considering the low toxicity and lower price, it is an excellent substitute to TB for screening in high-risk population [40]. As such, evidence also suggests that MB is an effective method for oral cancer screening. The 90% sensitivity of MB is certainly comparable to the results obtained in TB staining.

The MB stain has two solutions, (a) a dye solution consisting of 1% methylene blue, 1%

malachite, 0.5% eosin, glycerol, and dimethyl sulfoxide and (b) pre- and post-rinse solution that contains 1% lactic acid and purified water. The application of MB is as follows [36]:

7.4.2.1 Working Principle

The acidophilic nature of malignant tissues, resulting from their abnormally high levels of nucleic acids and altered metabolism, results in the differential uptake of MB, similar to TB. Spectroscopic data revealed strong binding of MB with the DNA double helix. In early experiments, the main mechanism was identified as minor groove binding with DNA [41]. Recent data suggest strong binding in intercalative mode and weak binding in electrostatic mode as the most important binding mechanisms [42, 43]. Differential binding mechanisms may also occur at the AT and GC sequences based on varying ionic strengths of MB [42]. Investigators observing interactions between MB and calf thymus DNA have noticed similar results with binding modes being dependent on molar concentration (gamma = [DNA/MB]). At low gamma, MB cations were bound at the phosphate location, and at high gamma intercalation binding was noticed in the space between two adjacent DNA base pairs [43]. These studies have established the fact that MB shows proportionate binding to DNA molecules, which accounts for an increase in intensity of stain with increase in the amount of chromatin material in OPMDs and transformed lesions.

7.4.2.2 Method of Application

Step 1: Rinse mouth with 1% lactic acid for 30 s to remove food debris and excess saliva.

Step 2: The suspected lesion (target area) is gently dried with gauze and air sprayed to ensure that lesion is saliva free.

Step 3: 5–10 ml of dye was either directly applied to lesion with cotton bud or kept for 30 s.

Step 4: Rinse again with 1% lactic acid for 30 s to wash out the excess dye.

Step 5: The pattern of dye retention is assessed based on intensity of stain retention on the lesion. The overall sensitivity of deep blue MB stain and histology was high for potentially malignant and cancerous lesions, with a high sensitivity and specificity. False positive rates are related to the retention of stain in inflamed and traumatic areas. Other factors can be irregular, papillary surfaces of lesions, which may cause the mechanical retention of dye, retention of dye material in papillae of the tongue or minor salivary gland ducts over the mucosa.

There are only few studies to date on established use of MB method in detection of oral precancerous/cancerous lesions with positive results [36, 39, 44, 45]. In a study conducted on 100 patients (50 cancerous, 50 precancerous), 88 out of 100 pathologically proven precancerous or cancerous lesions showed positive staining with localized and deep blue stain. There was high sensitivity (90%) and a negligible false negative rate [39]. Based on existing literature, MB dye may be useful for diagnostic screening. However, prospective studies are recommended to establish accuracy of MB to confirm its efficiency in differentiating benign and malignant oral conditions and in the characterization of LOH in the regions showing high uptake. This stain is recommended for mass screening [44]. Double vital staining with MB and Lugol's iodine has also been reported [45].

7.4.3 Lugol's Iodine

Many papers were published on the superior efficacy of Lugol's iodine solution. It is a cheap, easy to use stain proved useful in the determination of margin status [46]. In some studies the simultaneous use of TB and Lugol's iodine has also been explored and showed promise [47, 48]. Literature on application of Lugol's iodine in suspected esophageal lesions is extensive, but its use in oral cancer and its potential precursors has only been attempted recently [49].

7.4.3.1 Principle

The uptake of Lugol's iodine is dependent on the amount of glycogen in tissue. Iodine is by nature glycophilic, forming triiodide molecules in the glycogen spiral. The oral mucosa is made of 15–20 layers of cells forming the stratified squamous epithelium and the cells in upper and middle layers containing glycogen in the cytoplasm. Under normal circumstances, the oral mucosa, which is rich in glycogen reserves, shows heavier uptake of iodine, leading to chocolate brown color. However, in oral cancer, there is comparatively less glycogen in local tissue; hence there is "lighter stain" or "no uptake" [49, 50]. Due to changes in proliferation and differentiation in oral cancer, there is a shift in glycogen metabolism which reduces the overall glycogen concentration in tissue [50]. The reduced glycogen concentration in transformed tissue is thought to be due to the Warburg effect [49]. Areas of dysplasia and cancer therefore do not take up any stain or appear as pale areas, due to reduced glycogen reserve. In a study, the PAS (glycogen stain in microscopy) reaction was limited or not found in unstained areas [50].

7.4.3.2 Application

Lugol's iodine is made up of iodine 2 g and potassium iodide 4 g in 100 cm^3 of distilled water. Typically 10–20 ml of Lugol's iodine at 1.5% (w/v) is considered safe [49].

Step 1: Suspected lesions are irrigated with saline, 20 mL carbocisteine (125 mg/5 mL).

Step 2: A cotton swab is used to apply Lugol's iodine for 30 s.

Step 3: Tumor is irrigated with 0.9% saline followed by interpretation. Photographs can support interpretation.

Step 4: Lesion is biopsied to include the area of unstained mucosa or least uptake.

Brown stain is considered a negative result and lesions without retention are considered positive [48]. Sometimes, surface mucous can impair uptake and interpretation, and application of 1.25% carbocisteine solution before use of Lugol's iodine improves uptake. If local irritation occurs with Lugol's iodine, sodium thiosulfate may be useful. Combined use of Lugol's iodine and MB has also been shown to be superior for esophageal squamous cell carcinoma [45]. The accuracy of double staining was superior to Lugol's staining in isolation [45]. Lugol's solution is especially important as margin status is critical, and dysplasia at this location can limit locoregional spread, recurrence, and poor survival status. This stain can also be used for screening margin dysplasia. Some amount of expertise is also needed while interpreting Lugol's iodine staining result. Certain locations in the mouth such as alveolar gingiva or hard palate have strong keratinization and lack glycogen and therefore may not localize the stain.

The overall diagnostic accuracy of Lugol's iodine with TB is 90% [48]. This combination led to easy delineation of inflammatory lesion. In one study, the efficacy of TB and Lugol's iodine was comparable. Intense toxic reaction, esophagitis, and gastric injury have been noted on some occasions, but in general it is considered safe and reliable [51, 52]. As higher concentrations pose some risk, the concentration was lowered from 3–5% to 1.5% recently [52]. Based on limited evidence, Lugol's iodine has potential for OSCC detection and margin demarcation; however randomized controlled are needed trials [46]. A well-designed trial on the efficacy of Lugol's iodine for head and neck cancer surgery is currently underway and should provide useful results [49].

7.4.4 Rose Bengal

Rose bengal (RB) is a derivative of fluorescein. It is commonly used in the diagnosis of ocular diseases to delineate corneal and conjunctival neoplasm. First results of RB in premalignant lesions and OSCC were identified in 1992 [8, 53]. Even graded shade guides were prepared and color measurements were standardized by spectrophotometry to measure positive reaction to RB stain [54]. A shade guide was also used in a pilot study [53] which was further refined in the second level of investigation [54]. The sensitivity and specificity to detect dysplasia and OSCC were 93.9% and 73.7%, respectively. False positives were attributed to inflammation [54].

7.4.4.1 Principle and Procedure

Step 1: Rinsing mouth with distilled water.

Step 2: Application of RB with cotton swab or applicator tip for 2 min.

Step 3: Removal of excess RB with distilled water.

Step 4: Evaluation of staining intensity.

Table 7.4 If used by experienced and skilled clinicians, vital staining may be useful as an adjuvant method for clinical examination for the following applications

1.	Selection of biopsy site in suspicious oral lesions
2.	Follow up of oral potential malignant disorders Eg: High risk leukoplakia, erythroplakia or oral sub-mucous fibrosis
3.	Detection of margin status before surgical excision
4.	Examination of recurrence following radiotherapy or chemotherapy

Step 5: Incisional biopsy of the area showing highest uptake.

The mucous layer may block RB uptake, and late reaction may also be noted which can result in false negatives. Grade of dysplasia and intensity of RB staining were directly proportional with an accuracy of 90%; thus RB acts as a suitable screening tool for OPMDs [55].

As with other vital stains, RB stain can also be used in early diagnosis of OSCC. For mass screening, vital stains (dyes) may help to identify abnormal mucosa tissue giving clinicians improved decision-making ability (Table 7.4) [4]. To avoid false positives, patients can be recalled after 10–14 days. Since mild to severe dysplasia is asymptomatic and largely subclinical, patients may not understand the seriousness to return to clinics. To enhance the quality of interpretation, a standardized shade guide can be used for each stain. Patients with positive reaction to any of the aforementioned stains after careful interpretation can be referred to oral surgeons for further exploration or biopsy. Vital staining can be used for choice of biopsy site, in the follow-up of premalignant lesions, and for demarcation of surgical margins during excision of oral cancer or potential lesions. A pathology report based on biopsy will always remain the gold standard for accurate diagnosis of any lesion before a treatment modality is applied.

Conclusion

Early detection of the neoplastic process is the best method to improve survival rate in patients with oral cancer. COE is the most basic method for screening patients with OPMDs and oral cancer, and on many occasions, performing a biopsy at this stage can prevent associated high morbidity and mortality. Followed by conventional oral screening, vital staining methods are easy to use, but not conclusive, as they have demonstrated a wide range of diagnostic accuracies in different studies. Making use of graded shade guides and spectroscopy assisted color measurement can improve overall diagnostic power of stain results. As such, the use of adjunct aids including vital staining dyes may be better suited for use by experienced clinicians in specialty care settings for evaluating high-risk patients rather than routine use in primary care settings.

Acknowledgments Support from R01CA204636, R01DE024595, and P30CA06156 is gratefully acknowledged.

References

1. Shield KD, Ferlay J, Jemal A, Sankaranarayanan R, Chaturvedi AK, Bray F, et al. The global incidence of lip, oral cavity, and pharyngeal cancers by subsite in 2012. CA Cancer J Clin. 2017;67:51–64.
2. Subramanian S, Sankaranarayanan R, Bapat B, Somanathan T, Thomas G, Mathew B, et al. Cost-effectiveness of oral cancer screening: results from a cluster randomized controlled trial in India. Bull World Health Organ. 2009;87:200–6.
3. Warnakulasuriya S. Global epidemiology of oral and oropharyngeal cancer. Oral Oncol. 2009;45:309–16.
4. Fedele S. Diagnostic aids in the screening of oral cancer. Head Neck Oncol. 2009;1:5.
5. Kusukawa J, Suefuji Y, Ryu F, Noguchi R, Iwamoto O, Kameyama T. Dissemination of cancer cells into circulation occurs by incisional biopsy of oral squamous cell carcinoma. J Oral Pathol Med. 2000;29:303.
6. Lingen MW, Kalmar JR, Karrison T, Speight PM. Critical evaluation of diagnostic aids for the detection of oral cancer. Oral Oncol. 2008;44:10–22.
7. Lingen MW, Tampi MP, Urquhart O, Abt E, Agrawal N, Chaturvedi AK, et al. Adjuncts for the evaluation of potentially malignant disorders in the oral cavity: Diagnostic test accuracy systematic review and meta-analysis-a report of the American Dental Association. J Am Dent Assoc. 2017;148:797–813.e52.
8. Omar E. Current concepts and future of noninvasive procedures for diagnosing oral squamous cell carcinoma-a systematic review. Head Face Med. 2015;11:6.
9. Akobeng AK. Understanding diagnostic tests 3: receiver operating characteristic curves. Acta Paediatr. 2007;96:644–7.

10. Scully C, Porter S. Oral cancer. West J Med. 2001;174:348–51.
11. Farah CS, Woo SB, Zain RB, Sklavounou A, McCullough MJ, Lingen M. Oral cancer and oral potentially malignant disorders. Int J Dent. 2014;2014:853479.
12. Sankaranarayanan R, Mathew B, Jacob BJ, Thomas G, Somanathan T, Pisani P, et al. Early findings from a community-based, cluster-randomized, controlled oral cancer screening trial in Kerala, India. The Trivandrum Oral Cancer Screening Study Group. Cancer. 2000;88:664–73.
13. Ramadas K, Sankaranarayanan R, Jacob BJ, Thomas G, Somanathan T, Mahé C, et al. Interim results from a cluster randomized controlled oral cancer screening trial in Kerala, India. Oral Oncol. 2003;39:580–8.
14. Sankaranarayanan R, Ramadas K, Thomas G, Muwonge R, Thara S, Mathew B, et al. Trivandrum oral Cancer screening study group. Effect of screening on oral cancer mortality in Kerala, India: a cluster-randomised controlled trial. Lancet. 2005;365:1927–33.
15. Brocklehurst P, Kujan O, Glenny AM, Oliver R, Sloan P, Ogden G, et al. Screening programmes for the early detection and prevention of oral cancer. Cochrane Database Syst Rev. 2010; (11):CD004150.
16. Sankaranarayanan R, Ramadas K, Thara S, Muwonge R, Thomas G, Anju G, et al. Long term effect of visual screening on oral cancer incidence and mortality in a randomized trial in Kerala, India. Oral Oncol. 2013;49:314–21.
17. Downer MC, Moles DR, Palmer S, Speight PM. A systematic review of test performance in screening for oral cancer and precancer. Oral Oncol. 2004;40:264–73.
18. Mathew B, Sankaranarayanan R, Wesley R, Nair MK. Evaluation of mouth self-examination in the control of oral cancer. Br J Cancer. 1995;71:397–9.
19. Elango KJ, Anand krishnan N, Suresh A, Iyer SK, Ramaiyer SK, Kuriakose MA. Mouth self-examination to improve oral cancer awareness and early detection in a high-risk population. Oral Oncol. 2011;47:620–4.
20. Richart RM. A clinical staining test for the in vivo delineation of dysplasia and carcinoma in situ. Am J Obstet Gynecol. 1963;86:703–12.
21. Sridharan G, Shankar AA. Toluidine blue: a review of its chemistry and clinical utility. J Oral Maxillofac Pathol. 2012;16:251–5.
22. Allegra E, Lombardo N, Puzzo L, Garozzo A. The usefulness of toluidine staining as a diagnostic tool for precancerous and cancerous oropharyngeal and oral cavity lesions. Acta Otorhinolaryngol Ital. 2009;29:187–90.
23. Pallagatti S, Sheikh S, Aggarwal A, Gupta D, Singh R, Handa R, et al. Toluidine blue staining as an adjunctive tool for early diagnosis of dysplastic changes in the oral mucosa. J Clin Exp Dent. 2013;5:e187–e191.
24. Richards D. Does toluidine blue detect more oral cancer? Evid Based Dent. 2010;11:104–5.
25. Singh D, Shukla RK. Utility of toluidine blue test in accessing and detecting intra-oral malignancies. Indian J Otolaryngol Head Neck Surg. 2015;67:47–50.
26. Mashberg A. Reevaluation of toluidine blue application as a diagnostic adjunct in the detection of asymptomatic oral squamous carcinoma: a continuing prospective study of oral cancer III. Cancer. 1980;46:758–63.
27. Ilanchelian M, Ramaraj R. Binding interactions of Toluidine Blue O with Escherichia coli DNA: formation of bridged structure. J Fluoresc. 2011;21:1439–53.
28. Paul P, Suresh Kumar G. Spectroscopic studies on the binding interaction of phenothiazinium dyes toluidine blue O, azure A and azure B to DNA. Spectrochim Acta A Mol Biomol Spectrosc. 2013;107:303–10.
29. Chi Z, Liu R, Sun Y, Wang M, Zhang P, Gao C. Investigation on the toxic interaction of toluidine blue with calf thymus DNA. J Hazard Mater. 2010;175:274–8.
30. Koppenol WH, Bounds PL, Dang CV. Otto Warburg's contributions to current concepts of cancer metabolism. Nat Rev Cancer. 2011;11:325–37.
31. Zhang L, Williams M, Poh CF, Laronde D, Epstein JB, Durham S, et al. Toluidine blue staining identifies high-risk primary oral premalignant lesions with poor outcome. Cancer Res. 2005;65:8017–21.
32. Gandolfo S, Pentenero M, Broccoletti R, Pagano M, Carrozzo M, Scully C. Toluidine blue uptake in potentially malignant oral lesions in vivo: clinical and histological assessment. Oral Oncol. 2006;42:89–95.
33. Patton LL, Epstein JB, Kerr AR. Adjunctive techniques for oral cancer examination and lesion diagnosis: a systematic review of the literature. J Am Dent Assoc. 2008;139:896–905. quiz 993-4
34. Warnakulasuriya KA, Johnson NW. Sensitivity and specificity of OraScan (R) toluidine blue mouth rinse in the detection of oral cancer and precancer. J Oral Pathol Med. 1996;25:97–103.
35. Su WW, Yen AM, Chiu SY, Chen TH. A community-based RCT for oral cancer screening with toluidine blue. J Dent Res. 2010;89:933–7.
36. Lejoy A, Arpita R, Krishna B, Venkatesh N. Methylene blue as a diagnostic aid in the early detection of potentially malignant and malignant lesions of oral mucosa. Ethiop J Health Sci. 2016;26:201–8.
37. Canto MI, Setrakian S, Willis J, Chak A, Petras R, Powe NR, et al. Methylene blue-directed biopsies improve detection of intestinal metaplasia and dysplasia in Barrett's esophagus. Gastrointest Endosc. 2000;51:560–8.
38. Vaiman M, Jabarin B, Abuita R. Methylene blue staining in the parotid surgery: randomized trial, 144 patients. Am J Otolaryngol. 2016;37:22–6.
39. Riaz A, Shreedhar B, Kamboj M, Natarajan S. Methylene blue as an early diagnostic marker for oral precancer and cancer. Spring. 2013;2:95.
40. Chen YW, Lin JS, Fong JH, Wang IK, Chou SJ, Wu CH, et al. Use of methylene blue as a diagnostic aid

in early detection of oral cancer and precancerous lesions. Br J Oral Maxillofac Surg. 2007;45:590–1.
41. Rohs R, Sklenar H. Methylene blue binding to DNA with alternating AT base sequence: minor groove binding is favored over intercalation. J Biomol Struct Dyn. 2004;21:699–711.
42. Nogueira JJ, González L. Molecular dynamics simulations of binding modes between methylene blue and DNA with alternating GC and AT sequences. Biochemistry. 2014;53:2391–412.
43. Tong C, Hu Z, Wu J. Interaction between methylene blue and calf thymus deoxyribonucleic acid by spectroscopic technologies. J Fluoresc. 2010;20:261–7.
44. Chen YW, Lin JS, Wu CH, Lui MT, Kao SY, Fong Y. Application of in vivo stain of methylene blue as a diagnostic aid in the early detection and screening of oral squamous cell carcinoma and precancer lesions. J Chin Med Assoc. 2007;70:497–503.
45. Peng G, Long Q, Wu Y, Zhao J, Chen L, Li X. Evaluation of double vital staining with lugol's iodine and methylene blue in diagnosing superficial esophageal lesions. Scand J Gastroenterol. 2011;46:406–13.
46. Petruzzi M, Lucchese A, Baldoni E, Grassi FR, Serpico R. Use of Lugol's iodine in oral cancer diagnosis: an overview. Oral Oncol. 2010;46:811–3.
47. Epstein JB, Scully C, Spinelli J. Toluidine blue and Lugol's iodine application in the assessment of oral malignant disease and lesions at risk of malignancy. J Oral Pathol Med. 1992;21:160–3.
48. Nagaraju K, Prasad S, Ashok L. Diagnostic efficiency of toluidine blue with Lugol's iodine in oral premalignant and malignant lesions. Indian J Dent Res. 2010;21:218–23.
49. McCaul JA, Cymerman JA, Hislop S, McConkey C, McMahon J, Mehanna H, et al. LIHNCS - Lugol's iodine in head and neck cancer surgery: a multicentre, randomised controlled trial assessing the effectiveness of Lugol's iodine to assist excision of moderate dysplasia, severe dysplasia and carcinoma in situ at mucosal resection margins of oral and oropharyngeal squamous cell carcinoma: study protocol for a randomised controlled trial. Trials. 2013;14:310.
50. Ohta K, Ogawa I, Ono S, Taki M, Mizuta K, Miyauchi M, et al. Histopathological evaluation including cytokeratin 13 and Ki-67 in the border between Lugol-stained and -unstained areas. Oncol Rep. 2010;24:9–14.
51. Park JM, Seok Lee I, Young Kang J, Nyol Paik C, Kyung Cho Y, Woo Kim S, et al. Acute esophageal and gastric injury: complication of Lugol's solution. Scand J Gastroenterol. 2007;42:135–7.
52. Sreedharan A, Rembacken BJ, Rotimi O. Acute toxic gastric mucosal damage induced by Lugol's iodine spray during chromoendoscopy. Gut. 2005;54:886–7.
53. Chen HZ. Rose bengal staining for clinical detection of oral premalignant lesions and carcinomas. Zhonghua Kou Qiang Yi Xue ZaZhi. 1992;27:44–7.
54. Du GF, Li CZ, Chen HZ, Chen XM, Xiao Q, Cao ZG, et al. Rose Bengal staining in detection of oral precancerous and malignant lesions with colorimetric evaluation: a pilot study. Int J Cancer. 2007;120:1958–63.
55. Mittal N, Palaskar S, Shankari M. Rose Bengal staining–diagnostic aid for potentially malignant and malignant disorders: a pilot study. Indian J Dent Res. 2012;23:561–4.

8 Optical Techniques: Investigations in Oral Cancers

Piyush Kumar and C. Murali Krishna

Abstract

The routine oral cancer screening involves a clinical oral examination followed by biopsy. The biopsied sample is subjected to histopathology, the gold standard. As this procedure is prone to subjective errors, requires experienced pathologists and is time consuming, it is pertinent to explore newer diagnostic adjuncts/methods. The changes in the biochemical properties of an organ/tissue are also known to be reflected in the optical properties which can be conveniently exploited through optical techniques. Optical techniques are shown to be rapid, objective, and noninvasive and are sensitive to tissue biochemistry. Since biochemical changes often precede visible morphological alterations, these techniques can serve as potential screening/diagnostic tools. This chapter highlights the advancements of optical/spectroscopic techniques, such as fluorescence spectroscopy, elastic scattering spectroscopy, diffuse reflectance spectroscopy, optical coherence tomography, Fourier-transform infrared spectroscopy, and Raman spectroscopy, in the field of oral cancer diagnostics/screening. The chapter begins with discussion on scope of optical techniques and basic principles of these techniques, followed by a brief discussion of multivariate statistical tools which play a major role in data analysis. The last section provides an overview on explorations of optical techniques in oral cancer screening/diagnosis.

The routine oral cancer screening involves a clinical oral examination followed by biopsy. The biopsied sample is subjected to histopathology, the gold standard. As this procedure is shown to be prone to subjective errors, requires experienced pathologists and is time consuming, it is pertinent to explore newer diagnostic adjuncts/methods. The changes in the biochemical properties of an organ/tissue are also known to be reflected in the optical properties which can be conveniently exploited through optical techniques. Optical techniques are shown to be rapid, objective, and noninvasive and are sensitive to tissue biochemistry. Since biochemical changes often precede visible morphological alterations, these techniques

P. Kumar, PhD
Chilakapati Laboratory, Advanced Center for Treatment, Research and Education in Cancer (ACTREC), Tata Memorial Centre, Kharghar, Maharashtra, India

Homi Bhabha National Institute, Mumbai, Maharashtra, India

Amity Institute of Biotechnology, Amity University Mumbai, Panvel, Navi Mumbai, Maharashtra, India

C. Murali Krishna, PhD (✉)
Chilakapati Laboratory, Advanced Center for Treatment, Research and Education in Cancer (ACTREC), Tata Memorial Centre, Kharghar, Maharashtra, India

Homi Bhabha National Institute, Mumbai, Maharashtra, India
e-mail: mchilakapati@actrec.gov.in

P. Panta (ed.), *Oral Cancer Detection*, https://doi.org/10.1007/978-3-319-61255-3_8

can serve as potential screening/diagnostic tools. This chapter highlights the advancements of optical/spectroscopic techniques, such as fluorescence spectroscopy, elastic scattering spectroscopy, diffuse reflectance spectroscopy, optical coherence tomography, Fourier-transform infrared spectroscopy, and Raman spectroscopy, in the field of oral cancer diagnostics/screening. The chapter begins with discussion on scope of optical techniques and basic principles of these techniques, followed by a brief discussion of multivariate statistical tools which play a major role in data analysis. The last section provides an overview on explorations of optical techniques in oral cancer screening/diagnosis.

8.1 Conventional Diagnosis Vis-à-Vis Optical Techniques

Early detection of cancers is the most crucial aspect of cancer management as it can significantly improve prognosis [1, 2]. The conventional screening procedures involve a clinical oral examination (COE) of the oral cavity followed by biopsy of suspected sites. The biopsied specimen is subjected to histopathology where tissue sections are stained using hematoxylin and eosin dyes and evaluated by trained pathologists. Histopathology, the horseback for confirmatory diagnosis, is the gold standard and has been irreplaceable in clinics though several new methods have been explored [3, 4]. However, existing methodologies are shown to have several limitations in terms of scope and applications.

(a) COE demands experienced medical practitioners. Clinical risk stratification often lacks accuracy and reproducibility. Studies have shown that conventional visual screening was effective mainly in the high-risk groups, i.e., tobacco/alcohol habitués [2]. Thus, better tools are needed for screening the general population.
(b) Histopathology is prone to subjectivity, is time consuming, and, most importantly, is invasive, which makes it inconvenient as a screening methodology of choice. Additionally, it has practical limitations in the hugely populated nations such as India where oral cancers are almost epidemic.
(c) It is often difficult to recognize subtle clinical changes which are indicative of early neoplastic transformation in precancers. This can also lead to the dilemma of *when and where to biopsy*. Thus, histological risk stratification requires highly trained pathologists and clinicians.
(d) Reliable biomarkers with good sensitivity/specificity in for oral cancers are still under exploration. Moreover, the storage and transportation conditions can influence results. Other methodologies based on vital dyes, transcriptomics still need the scrutiny over large clinical samples as studies have revealed reduced accuracy and increased false-positive findings in low-risk populations [3].

8.2 Optical Techniques: Basic Principles

Rapid, objective, and noninvasive technologies which are sensitive to tissue biochemistry could be more effective for early diagnosis and screening, as biochemical changes often precede visible morphological alterations. These changes in biochemical properties are also reflected in the optical properties. The electromagnetic spectrum provides an array to explore potential tools to probe and exploit the optical changes in biological systems. Often, such optical techniques utilize ultraviolet (UV), visible, near-infrared (NIR), and infrared (IR) regions to measure absorption, scattering, and/or fluorescence in biological samples. Thus optical techniques are being widely explored, and as will be discussed, have shown great promise in discrimination of diseased and healthy tissues and organs. Multimodal methodologies involving two or more techniques to gain additional and complementary information simultaneously are also being explored. The Jablonski diagram (Fig. 8.1), first proposed by Professor Alexander Jablonski in 1935, summarizes some optical phenomena in response to interaction of light and matter, in terms of energy exchange.

Typically, optical techniques employ a source of excitation (often lasers). Detectors are used to

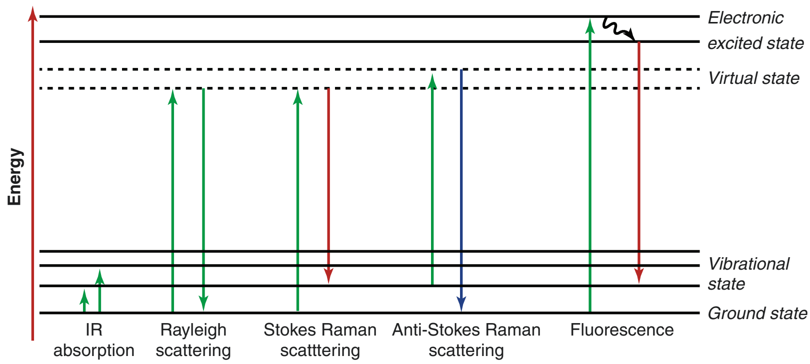

Fig. 8.1 Jablonski diagram depicting photophysical phenomena of IR, Rayleigh and Raman scattering, and fluorescence

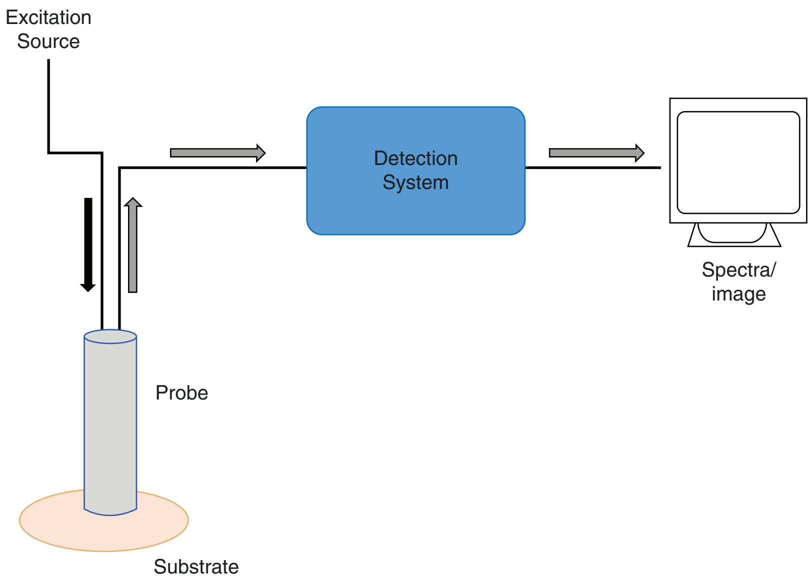

Fig. 8.2 Typical layout of an optical technique. Appropriate modifications, involving a combination of lenses, filters, and/or mirrors, can be used to design a given spectroscopic technique

record the output signals. The detection system mostly consists of a charge-coupled device (CCD) in modern instruments. Nowadays, fiber-optic probes are used for transmission of light from excitation source to samples as well as collection of signals to detectors. The probes usually contain a combination of optical elements (lenses, filters, and mirrors) to facilitate collection of desired signals. A schematic for a typical optical technique is shown in Fig. 8.2.

8.2.1 Fluorescence Spectroscopy

Sir David Brewster reported several observations related to fluorescence, a term which was coined by Sir George Gabriel Stokes in the 1840s [5]. Explained as Stoke's law, fluorescence is often characterized by the wavelength of the emitted light, longer than that used for excitation [6]. Fluorescence spectroscopy can exploit endogenous fluorophores present in the tissues (autofluorescence) or exogenous fluorophores (light-sensitive chemicals/photosensitizers) which can be introduced in the biological system to induce fluorescence (induced fluorescence). Typically, this technique involves irradiation of organs/tissues at some specific wavelength (mostly near-ultraviolet or visible) to excite fluorophores. The selection of wavelength depends on the fluorophore being targeted. The fluorescent emission is represented as an emission spectrum (fluorescence emission intensity vs. wavelength) Fig. 8.3.

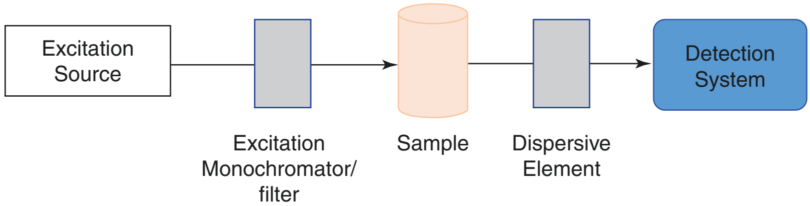

Fig. 8.3 Schematics for fluorescence spectroscopy

Induced fluorescence: Photosensitizers or precursors to photosensitizers are introduced in subjects, which leads to a differential accumulation of fluorophores in healthy and tumor tissues. Some examples of such photosensitizers include hematoporphyrin derivative (HpD), meso-tetra-(hydroxyphenyl)-chlorin (MTHPC), benzoporphyrin derivative (BPD), and phthalocyanine [7]. The most commonly used fluorophore in oral cancers is 5-aminolaevulinic acid (ALA) which is a precursor of protoporphyrin IX (PpIX), a fluorescent photosensitizer. ALA can be applied topically to the oral mucosa/facial skin [8]. Subsequent irradiation of the ALA-applied area with visible light, to excite the main absorption peak of PpIX (405 nm), leads to red fluorescence emission at 635 nm [8]. Nonphotosensitizers such as Nile blue derivatives and caretenoporphyrins have also been explored as exogenous fluorophores [9].

Autofluorescence: Few biomolecules, such as amino acids (tyrosine and tryptophan), proteins (collagen), coenzymes (FAD, NAD), vitamins, and porphyrins, can fluoresce and thus contribute to autofluorescence when excited with suitable wavelengths. For the endogenous fluorophores, excitation maxima often lie in the 250–450 nm range (spanning the UV/visible spectral range), whereas their emission maxima fall in the 280–700 nm range (spanning the UV/visible/NIR spectral range) [10]. Various pathological changes can alter endogenous fluorophore distribution. The changes may be in the structure (e.g., hyperkeratosis, hyperchromatin, and increased cellular/nuclear pleomorphism) and metabolism (e.g., flavin adenine dinucleotide (FAD) [11] and nicotinamide adenine dinucleotide (NAD) concentration) in the epithelium and subepithelial stroma (e.g., composition of collagen matrix and elastin) [3, 12]. Many studies have explored utility of fluorescence spectroscopy in oral cancers [3, 12–14] and have been described in detail in Sects. 8.4.1–8.4.3. Fluorescence-based commercial diagnostic systems such as VELscope® are also available [15, 16].

8.2.2 Elastic Scattering Spectroscopy (ESS)

The process of scattering may be classified as elastic and inelastic scattering. When photons interact with matter, the energy of the scattered photons may remain same or undergo a change. The former process is known as elastic while the latter is referred to inelastic scattering. Elastic scattering is also called Rayleigh scattering. Inelastic scattering is discussed in Sect. 8.2.6. ESS is wavelength-dependent phenomenon and provides information about the structural and morphological changes. Being sensitive to size and shape of dense subcellular organelles like nucleus, nucleolus, chromatin content, and nuclear-cytoplasmic ratio, ESS is an attractive technique as it provides information about the subcellular morphology as well as the chromophore content [17]. ESS is distinguished from a similar technique, diffuse reflectance spectroscopy (described in Sect. 8.2.3), wherein the source-detector separation is very small in comparison to the scattering mean free path of ESS [17]. In ESS, the tissue is subjected to short pulses of white light, while the elastically scattered light is analyzed to gain information Fig. 8.4.

8.2.3 Diffuse Reflectance Spectroscopy (DRS)

DRS measures tissue scattering/absorption properties to provide information like nuclear size, distribution, collagen content, and the oxy/deoxy status of hemoglobin, utilizing UV-visible-NIR

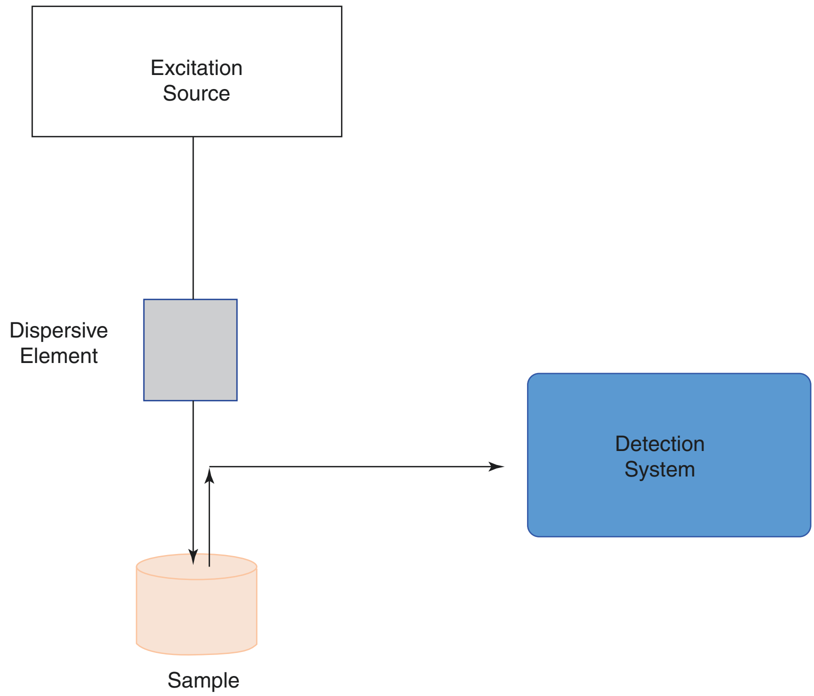

Fig. 8.4 Schematic for elastic scattering spectroscopy

excitation (300–800 nm). DR is generated from single and multiple backscattering of the excitation light and is sensitive to the absorption and scattering properties of epithelial tissues. The relationship between reflectance, absorbance, and light scattering is given by the Kubelka-Munk equation [18]. A simplified form of the equation is as follows:

$$f_{(R)} = \frac{(1-R)^2}{2R} = \frac{K}{S}$$

(R = absolute reflectance; K = molar absorbance coefficient; S = scattering coefficient of the specimen)

In biological samples, hemoglobin (both oxygenated, HbO_2, and deoxygenated, Hb), in blood vessels/stroma, are dominant absorbers, while light scattering is caused mainly by cell nuclei and other organelles in epithelium and stroma, collagen, and cross-links in stroma. During neoplastic transformation, stromal layer absorption increases due to angiogenesis, while scattering in stroma decreases due to degradation of extracellular matrix. On the contrary, epithelial scattering increases due to hyperplasia, increase in nuclear size and DNA content. DRS is useful because of attributes such as cost-effectiveness, rapidity, and high sensitivity. A novel DRS (light distribution modulated DRS) method utilizes a few diffuse reflectances measured at one source-detector separation by using a liquid crystal (LC) cell whose scattering property can be modulated by the bias voltage. The LC cell is placed between the light source and the sample, and the spatial distribution of light can be varied as the scattering property of the LC cell to induce intensity variation of the collected diffuse reflectance [19] Fig. 8.5.

8.2.4 Optical Coherence Tomography (OCT)

OCT imaging in biomedical field was originally introduced in 1991 for noninvasive imaging of retina [20]. In the last two decades, OCT underwent rapid and dramatic developments with major applications in ophthalmology [21, 22], oncology [23–25], cardiology [26], and developmental biology [27]. OCT has been used ex vivo for 2D imaging as well as 3D en face imaging [28, 29]. OCT images can also be used to obtain functional information to detect the presence of embedded blood vessels. Such

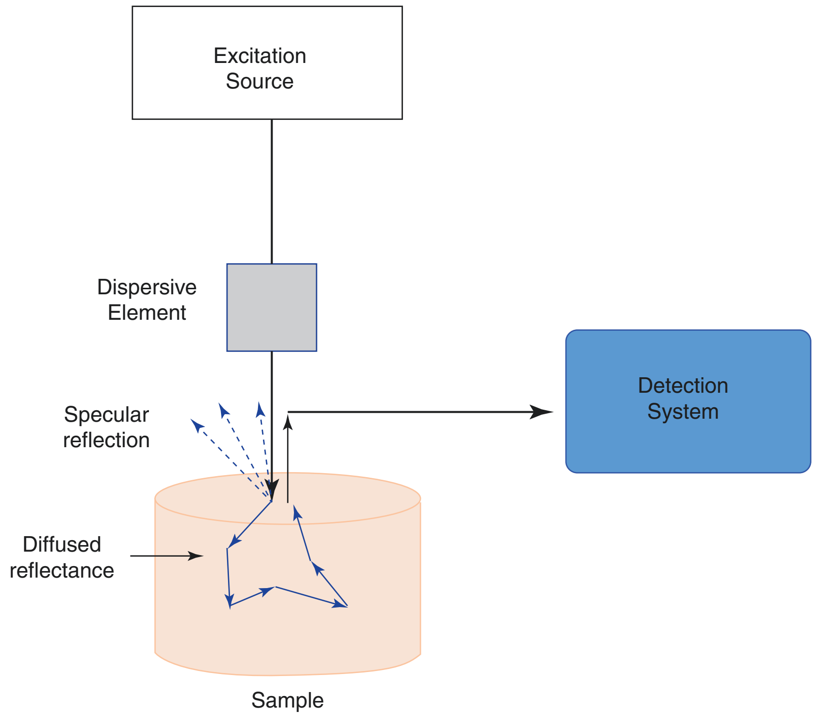

Fig. 8.5 Schematic for diffuse reflectance spectroscopy (the thickness of arrows indicating reflection is not to scale)

measures can preclude bleeding or stroke-related complications during surgery [30]. OCT uses low-coherence interferometry to produce two-dimensional images of optical backscattering from internal tissue microstructures analogous to ultrasonic pulse-echo imaging [20]. One can term OCT as an optical analog of ultrasound imaging wherein backscattered intensity of light is measured instead of sound. OCT enables in vivo, noninvasive imaging of the macroscopic characteristics of epithelial and subepithelial structures Fig. 8.6.

8.2.5 Fourier-Transform Infrared (FTIR) Spectroscopy

Vibrational spectroscopic techniques such as FTIR and Raman spectroscopy (RS) are relatively simple, nondestructive to the tissue and require a very small amount of sample with minimum sample preparation. In addition, these techniques also provide molecular-level information allowing investigation of functional groups, bonding types, and molecular conformations. Spectral bands in vibrational spectra are molecule specific and provide direct information about the biochemical composition, leading to a "molecular fingerprint." As biochemical composition is affected during pathogenesis, spectral features are altered, which can be exploited for disease detection. The bands are relatively narrow, easy to resolve, and sensitive to molecular structure, conformation, and environment. Both RS and FTIR exploit changes in vibrational modes of biological tissues/organs with respect to the changing tissue biochemistry in response to pathological changes. However, while FTIR is based on the principle of absorption, RS is based on inelastic scattering. RS is described in Sect. 8.2.6. Raman and FTIR are complementary techniques.

An infrared spectrum represents a fingerprint of a sample with absorption peaks corresponding to the frequencies of vibrations between the bonds of the atoms that make up the material being probed and can provide rapid information. The energy of the absorbed infrared radiation by

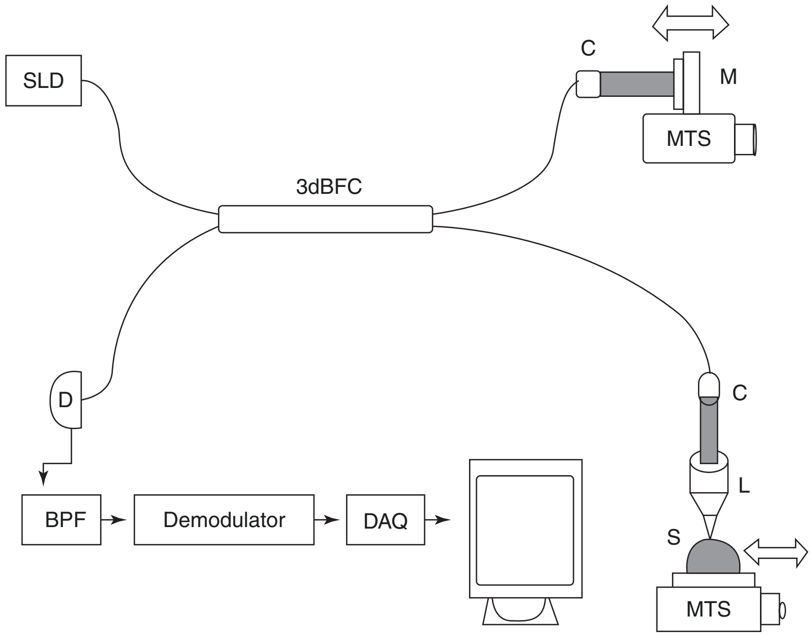

Fig. 8.6 Schematic of OCT system; *BPF* bandpass filter, *C* collimator, *D* photodetector, *FC* fiber coupler, *L* lens, *M* mirror, *MTS* motorized translation stage, *S* sample, *SLD* superluminescent diode

a molecule is equal to the difference between two energy levels of the molecule's vibration. Thus, the absorption occurs on the basis of transition between the energy levels of molecular vibration, leading to a vibrational spectrum of a molecule. The advent of Fourier-transform spectrometers, around 1970, revolutionized the field of FTIR spectroscopy, permitting simultaneous measurement of spectra in the entire wavenumber region with higher accuracy and resolution Fig. 8.7.

8.2.6 Raman Spectroscopy (RS)

RS, based on the principle of inelastic or Raman scattering, was experimentally verified by Nobel Laureate Sir C. V. Raman [31]. Depending on changes in energy or frequency, the scattered light may be classified as inelastic (change in energy) and elastic (no change in energy). Inelastic scattering constitutes Raman scattering, further classified as anti-Stokes (the scattered photon gains energy) or Stokes (the scattered photon loses energy). As mentioned in Sect. 8.2.3, RS is a vibrational spectroscopic technique which can detect biochemical perturbations in an organ or tissue. Further, due to negligible interference of water, a major constituent of living cells and organs, Raman can serve as a promising tool for in vivo biomedical investigations.

Since RS is a weak phenomenon, its applications were initially very much limited in biological systems. The development of powerful lasers, Rayleigh rejection filters, and better detection systems such as CCDs gave an impetus to biological applications of RS. Many portable/transportable instruments are now available at reduced costs. A schematic for RS is shown in Fig. 8.8. Typical pictorial presentations of Raman spectral acquisition from an ex vivo tissue and an anesthetized animal are shown in Fig. 8.9.

8.2.6.1 Raman Spectroscopy: Adaptations for Enhancement of Raman Signal

RS being an inherently weak process, several modifications/adaptions are made to the conventional Raman methodology to enhance the

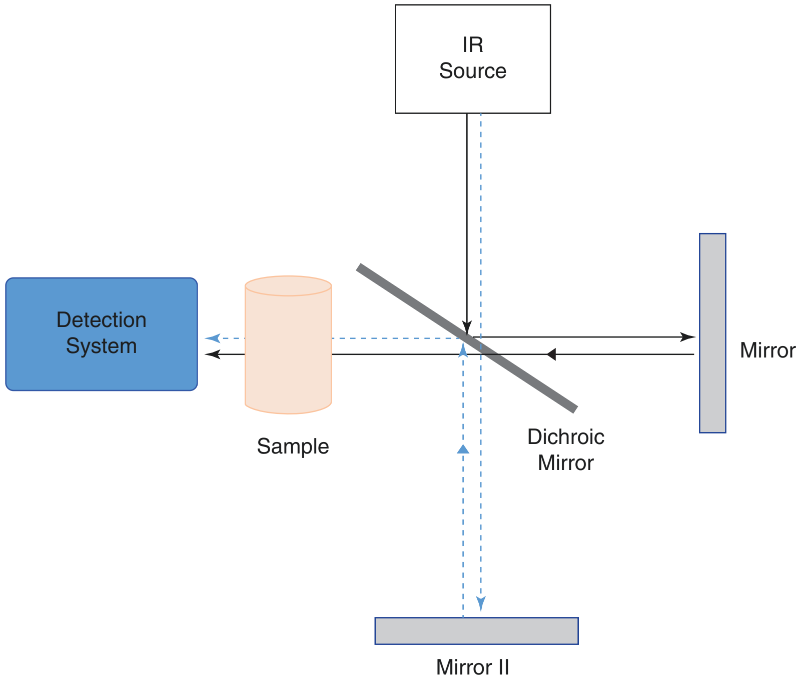

Fig. 8.7 Schematics for FTIR spectroscopy

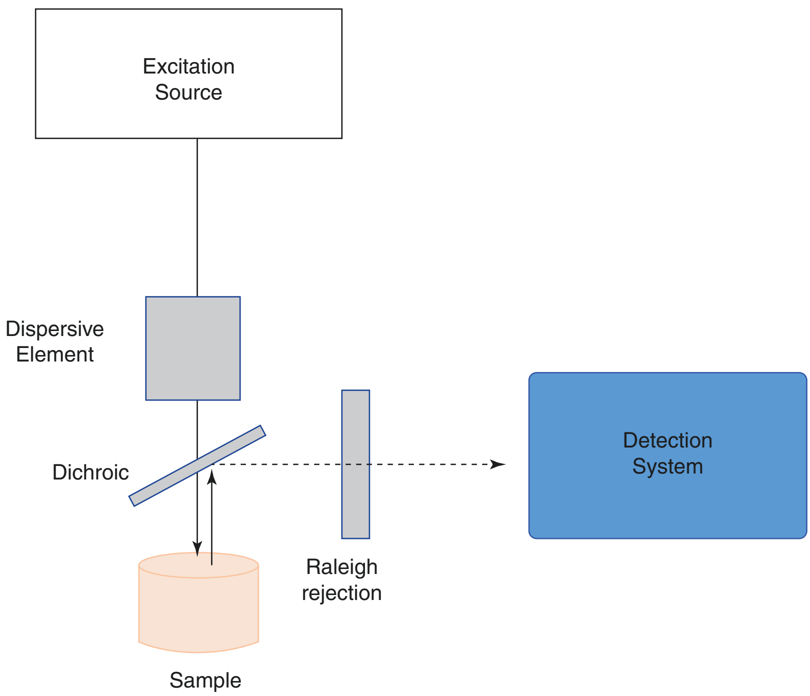

Fig. 8.8 Schematic of Raman spectrometer

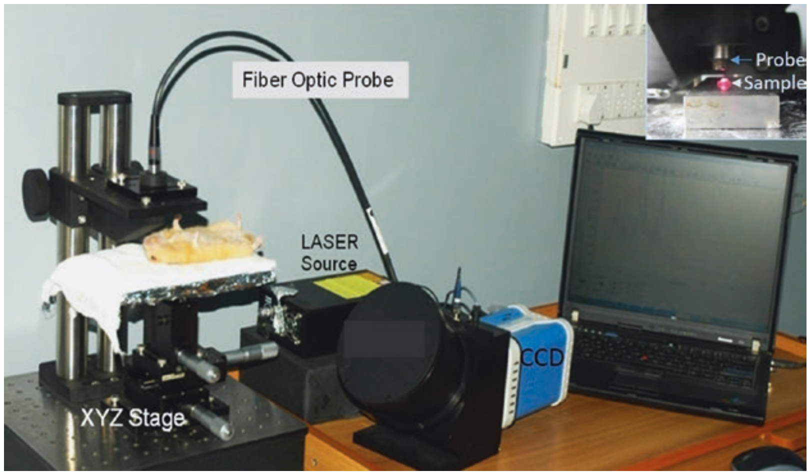

Fig. 8.9 In vivo Raman spectra being acquired from an anesthetized animal. The inset shows acquisition of Raman spectra from an ex vivo tissue with 785 nm laser

overall efficiency and the range of applications. Some adaptions include surface-enhanced Raman spectroscopy (SERS) [32, 33], resonance Raman spectroscopy (RRS), coherent anti-Stokes Raman spectroscopy (CARS) [34, 35], stimulated Raman spectroscopy (SRS) [36–38], drop-coating deposition Raman (DCDR) spectroscopy [39–41], spatially offset Raman spectroscopy (SORS) [42], and surface-enhanced spatially offset Raman spectroscopy (SESORS) [43, 44].

8.3 Optical Techniques: Role of Multivariate Analysis

Information derived from various optical techniques are in the form of spectra or images which may need further preprocessing and analysis using various univariate and multivariate analysis tools to bring out an objective discrimination among the classes/groups of samples explored. Preprocessing is needed to get rid of spectral contamination from optical components and background noise. The preprocessing steps vary across the techniques.

Spectroscopic techniques in conjunction with proper chemometric tools can distinguish subtle but significant changes in the complex biological environment. However, it is important to know the limits and assumptions employed in each method for a reliable and reproducible diagnosis. Both univariate and multivariate analyses can be carried out for spectroscopic data. However, in view of levels of complexity in living organisms, multivariate analysis may be a suitable approach. Multivariate analysis can be unsupervised or supervised. In case of unsupervised methods, no prior information is given and the method tries to establish relationships or trends in classification de novo. Principal component analysis (PCA) is a commonly employed unsupervised method [45, 46]. In the absence of preliminary information, unsupervised methods provide a first-hand estimate about the nature of data and trends in classification. In the supervised methods, spectral groups are trained for classification on the basis of first-hand information. These models can be evaluated with an independent data set. The following table highlights the salient features of some commonly employed methods of analysis Table 8.1.

Table 8.1 Summary of some commonly employed analysis methods

Statistical tool	Salient features
Univariate analysis	Corresponding *p* values are measure of significance. Prone to false positive unless corrected significance limit is used
Cluster analysis	Classification scheme to divide data in clusters. Hierarchical clustering provides relationships between clusters
Principal component analysis (PCA)	Provides an overview for large data sets. Identify outliers, clusters, and trends in dataset
Partial least squares regression	To predict a set of dependent variables from a (very) large set of independent variables
Bayes classifier	Ideal classification but a large training set is needed
Linear discriminant analysis (LDA)	Discrimination method related to multiple linear regressions. Number of variables must be smaller than number of observations
Neural networks	High flexibility in modeling nonlinear data but prone to overfitting
Support vector machines	High flexibility in modeling nonlinearities. Careful model selection reduces possibility of overfitting

8.4 Optical Techniques: Applications in Oral Cancers

Classification between tumor and normal conditions has been demonstrated in many cancers. But, for better prognosis, an ideal cancer detection should be in an early phase when clinically palpable changes are not apparent. The exploration of various optical techniques in oral cancers has been mentioned in this section.

8.4.1 Animal Model-Based Studies

Owing to ethical and practical considerations, many exploratory and feasibility studies are often carried out on animal models. Palate cancer in animal model was one of the first cancers to be (DMBA) induced [47]; cancer in hamster buccal pouch (HBP) is a widely used model for experimental oral carcinogenesis [48, 49]. The Syrian golden HBP has been widely used on account of its anatomical and physiological features which resemble the human oral mucosa [50]. One pouch under the cheek muscles on each side of the mouth opens into the anterior part of the oral cavity and is associated with small salivary glands that produce both serous and mucous secretions. The pouches extend backwards along the oral cavity, but not as far as the pharynx. Histologically, the buccal cavity is lined with squamous epithelium. The hamster model reflects many aspects of human oral cancer development [48, 51–54]. Repeated application of carcinogen results into tumors through four histologically recognizable stages: hyperplasia, papilloma, carcinoma in situ, and squamous cell carcinoma (SCC). Changes in oncogenic expressions of p53 and/or ras, expression of proliferation markers, early expression of c-glutamyltranspeptidase, and downregulation of keratin 76 expression are in concordance with human buccal mucosa [54–59]. The exploration of oral carcinogenesis in animal models employing optical techniques is described below.

Fluorescence spectroscopy: Initial studies using 300 nm excitation on hamster buccal pouch (HBP) tissues showed discrimination of healthy, premalignant, and tumor tissues [60, 61]. Findings have shown concordance with intermediate stages available in literature: normal tissues, hyperplasia, dysplasia and early cancers, and invasive cancers using 320 nm excitation [62]. Fluorescence lifetime imaging (FLIM) of HBP tissues has shown the in vivo diagnostic potential [63]. A handheld device, capable of continuous lifetime imaging at multiple emission bands simultaneously, has been also developed [64].

DRS: HBP model was utilized for DRS studies with encouraging results in the 500–800 nm spectral range [65]. SVM-based algorithms have suggested significant decrease in the absorption and reduced scattering coefficient at 460 nm in neoplastic tissues, compared to normal tissues. This study demonstrated 90% classification accuracy [66].

OCT: OCT studies have also employed HBP model [67–71]. The earliest studies were carried out by Wilder Smith et al. [71] and Mathney et al.

[67] who demonstrated feasibility of detecting malignancy in HBP model using OCT. 3D OCT has also been reported [72]. In another study, OCT was carried out on carcinogen (DMBA) treated and normal HBP tissues [73]. Tissues corresponding to early and late stages of DMBA-induced carcinogenesis were investigated. OCT images showed well-distinguished layers of epithelial and subepithelial layers in most controls and early week DMBA-treated tissues. Two control tissues also showed disrupted epithelial architecture. These observations were later on confirmed by RS and were attributed to repeated injuries incurred by regular pulling out of buccal pouches [74]. Another recent multimodal study has used combined FLIM and OCT features to obtain an accuracy of 87.4%, which was statistically higher than accuracy based on only FLIM (83.2%) or OCT (81.0%) features. Further, the complementary information provided by FLIM and OCT features resulted in high sensitivity and specificity for the combined FLIM and OCT features for discriminating benign (88.2% sens., 92.0% spec.), precancerous (81.5% sens., 96.0% spec.), and cancerous (90.1% sens., 92.0% spec.) classes [75].

RS: Rodents have been commonly employed in oral cancer research [76]. The earliest applications of Raman spectroscopy in animal model date back to late 1980s, which was a study on diabetic cataract model [77–80]. Further, studies on mineralizations were carried out in rat models (1995) [81, 82]. Schut et al. used a protocol involving application of carcinogen 4-nitroquinoline 1-oxide to develop palate cancers in rats. They obtained specificity as well as sensitivity of 100% for detecting high-grade dysplasia/carcinoma in situ [47]. The next major study in experimental oral carcinogenesis was carried out in HBP model by Oliveira et al. [83]. Employing 1064 nm for excitation, this FT Raman study, employing PCA, could differentiate tumors and healthy tissues. Another ex vivo study on DMBA-treated HBP tissues for 0, 2, 4, 8, and 12 weeks demonstrated feasibility of classifying changes based on duration of DMBA application [84]. The spectra reported for normal buccal pouch and tumors in these studies were found to have features similar to those reported later on in human studies [85–89]. Ex vivo as well as in vivo week-wise monitoring of sequential progression of oral carcinogenesis has been carried out with RS over the 14-week period of carcinogenesis in HBP model. While efficiency of classification increases up to 70% by 8 weeks, it plateaus between 8 and 11 weeks due to accumulation of dysplastic changes over the buccal mucosa. From week 12 onwards, classification increases up to 100% by 14 weeks [90]. Misclassifications observed in such studies were majorly due to heterogeneity in the carcinogen-treated tissues as several stages of cancers may be observed in the mucosa. A small number of misclassifications could also be attributed to development of abnormal pathologies in the control tissues, ascribed to repeated mechanical injuries incurred during the experiment [74]. RS has also been carried out to study antitumor activities of nanoencapsulated drugs such as silibinin [91] and hesperetin [92] in HBP models.

8.4.2 Ex Vivo Studies

Optical techniques have explored ex vivo samples, majorly tissue biopsies as a proof of concept. Major achievements in ex vivo studies are mentioned below.

Fluorescence spectroscopy: Study using ALA-induced fluorescence suggests that oral dysplastic lesions have more red fluorescence in comparison to benign lesions. Enhanced intensity of PpIX in the cancerous tissues can be primarily attributed to plasma lipoproteins, low pH in tissues, and increased vasculature [93–95]. Tissue autofluorescence has been explored in the screening and diagnosis of precancers and early cancers such as lung, cervix, skin, and oral cavity [12]. One of the earliest explorations of autofluorescence was in 1924 in malignant tumors, observed by Policard as red fluorescence from hematoporphyrin in rat sarcomas using ultraviolet radiation [96]. In vivo and ex vivo explorations of autofluorescence spectroscopy for oral cancer diagnosis have shown encouraging results [60, 61, 97–102]. About 635 nm has also been used to characterize variation in porphyrin excitation between normal volunteers and oral cancer subjects [100]. Several wavelengths including 350, 380, and 400 nm have been explored to identify the optimal excitation for detection of oral neoplasia [97]. Autofluorescence spectroscopy can also differentiate potentially malignant conditions such as oral submucous fibrosis (OSMF), leukoplakia, erythroplakia, and lichen planus from normal tissues [102, 103]. Autofluorescence spectroscopy could provide good diagnostic efficiency to discriminate between different grades of oral cancers by analyzing porphyrin emission peaks [104]. Fluorescence studies on early perturbations in oral cavity owing to tobacco/areca nut habit indicate a variation in collagen and flavin levels (areca nut habitues) and hemoglobin and porphyrin levels (tobacco habitues) with respect to non-habitues [105, 106]. Various experimental parameters such as area of exposure, source stability, and angular/distance dependence of a fiber probe from the specimen surface have been reported [107].

ESS: Feasibility of identifying metastasis in cervical nodes of oral cancer subjects [108] has been explored on 130 lymph nodes from 13 subjects who underwent neck dissection. The nodes (formalin fixed, bivalve) were subjected to ESS and processed for histopathology yielding a sensitivity of 98% and a specificity of 68%. Bony resection margins from formalin-fixed samples assessed by ESS and correlated with the histopathological diagnosis (21 subjects) yielded a sensitivity of 87% and a specificity of 80% using linear discriminant analysis (LDA) [109]. Thus ESS can identify tumors in resection margins.

DRS: DRS has been explored to identify malignant changes in oral epithelium. Bimodal autofluorescence and DR spectra have shown classification of normal, benign, premalignant, and malignant lesions [110]. Spectral ratio 540/575 of oxygenated hemoglobin bands [111] could be used to distinguish normal oral mucosal areas from hyperplastic and dysplastic ones [112]. Reflectance spectral intensity from malignant lesions is observed to be higher than that from normal mucosa [113]. Tungsten-halogen lamp is often employed as an excitation source on biopsy specimens (tongue, buccal mucosa, and alveolus) to measure diffusely reflected light. Advancements such as multispectral imaging camera system that records diffuse reflectance (DR) images of the oral lesion at 545 and 575 nm with white light illumination can scan entire oral lesions [41]. Portable low-cost DRS devices have been developed [114]. Significant changes in the DR ratio have been observed according to the stage of oral malignancy. Ex vivo measurements with a minimum time lag is supposed to circumvent tissue degradation and signal loss. The potential of DRS has also been explored for tongue cancer detection [115].

OCT: OCT images from cancerous tissues and comparison with histopathology images suggest that epithelium, basement membrane, lamina propria, microanatomical histological structures, and pathological processes are clearly identified [116]. Correct identification of the keratin cell layer and its structural changes is reported in 87% of a cohort of 78 cancer subjects. The accuracy for the epithelial layer and basement membranes was 93.5% and 94%, respectively. Microanatomical structures could be identified with accuracy of 64% for blood vessels, 58% for salivary gland ducts, and 89% for rete pegs [117].

FTIR: Initial studies employing FTIR suggested malignant and healthy tissues can be differentiated majorly on basis of 1745 cm^{-1} band, which was present in normal tissues but absent/weak in malignant ones [118]. Raman spectroscopic and FTIR measurements were in agreement with each other [118]. FTIR spectral differences have been studied across a range of samples such as oral SCC and normal gingival epithelium (NGE) or normal subgingival tissue (NST) [119]. FTIR spectroscopy of paraffin-embedded tissue sections for leukoplakia and SCC has shown 81.3% sensitivity and 95.7% specificity [120].

RS: One of the first studies on human oral cancer biopsies was reported in 2001. The study analyzed 140 spectra from 49 biopsies acquired using 785 nm excitation and SpeXTriax 320 spectrometer. PCA-based multivariate analysis showed sensitivity and specificity of 85% and

90%, respectively [121]. A successive study by the same group in 2004 demonstrated the suitability of formalin-fixed tissues for Raman spectroscopy [122]. Classification of normal, cancerous, precancerous, and inflammatory conditions was reported, with lipid-rich features in normal conditions and predominant protein features in the pathological conditions, including tumors [123]. Confocal Raman microspectroscopy of 66 human oral mucosa tissues (43 normal and 23 malignant) has also been used where PCA along with calculation of areas under bands 1004, 1156, 1360, 1587, and 1660 cm^{-1} was used as a classification method [124]. Employing NIR excitation, RS of normal epithelium and different grades of oral cancer has shown changes in the relative intensities of bands at 1656, 1440, and 1450 cm^{-1} [125]. Raman imaging of oral tissue sections has also been explored. In a study on ten normal and ten tumor tissue sections, Raman maps of normal sections could resolve epithelium layers. Inflammatory, tumor, and stromal regions could be identified. Epithelium and stromal regions of normal cells and cellular components of normal and tumor sections could be distinguished, employing PCA [126]. In another study, Raman imaging of 11 oral SCC and 14 healthy tissues from 10 oral cancer subjects was followed by 127 pseudo-color images, correlated with histopathology of same sections [127] to build LDA model. There were 88 oral SCC and 632 healthy tissue spectra further evaluated to distinguish SCC spectra from the spectra of adipose tissue, nerve, muscle, gland, CT, and squamous epithelium in 100%, 100%, 97%, 94%, 93%, and 75% cases, respectively.

Besides tissues sections, minimally invasive ex vivo samples such as body fluids (blood, serum, urine) and exfoliated cells have also been explored through optical techniques. The ease and low cost of collection, along with transportability of such samples to a centralized facility, makes it a viable screening approach. Further, low-risk and minimal/noninvasive methodology leads to better compliance by cancer subjects/risk-prone individuals. Most studies on minimally invasive samples have been carried out using FTIR and RS; there are some fluorescence-based studies as well. However, sample preparation such as drying, involved in FTIR, can lead to artifacts, especially for cytological samples. Prospects of biofluid vibrational spectroscopy have been recently reviewed by Baker et al. [128].

Fluorescence spectroscopy of plasma was carried out in 2003 using 405 and 420 nm excitation. A classification of 93.7% was obtained for cancerous and normal samples, while a classification of 91.8% was obtained across normal, early stage of oral malignancy, advanced oral malignancy, and liver diseases [129]. Urine samples were explored by fluorescence spectroscopy to obtain 94.1% classification. The study suggested that fluorophores NADH and flavins can serve as potential urine biomarkers to diagnose oral cancers [130].

RS has been explored in samples such as serum, urine, and exfoliated cells. Harris et al. (2009) explored potential of a peripheral blood sample in diagnosis of head and neck cancer. Twenty subjects each of head and neck cancers and respiratory diseases were employed [131]. LDA yielded an accuracy of 65% while genetic evolutionary algorithm led to accuracy of 83%. SERS-based specific identification of nasopharyngeal cancers is also reported [132]. Diagnosis of oral cancers using both resonance and conventional RS with an efficiency of 78% and 70%, respectively, has been shown between normal and oral cancer groups [133, 134]. These studies were followed up with a large cohort of 328 subjects belonging to healthy controls, premalignant, disease controls, and oral cancer groups. Sensitivity and specificity rates of 64 and 80%, respectively, were obtained which are comparable to standard screening approaches [135]. Recurrence in oral cancers was also identified by serum RS employing 22 oral cancer subjects [with recurrence ($n = 10$) and no-recurrence ($n = 12$)] before and after surgery [136]. PC-LDA could not classify before-surgery samples, while a classification efficiency of ~78% was obtained in after-surgery samples. Urine was explored for oral cancer diagnosis by Elumalai et al. PC-LDA findings yielded sensitivity and specificity of 98.6% and 87.1%, respectively, to discriminate healthy and cancer subjects [137]. RS of exfoliated cells from 15 healthy volunteers (HV), 15 healthy tobacco users (HT), and 20 cancer subjects with 20 contralateral or disease control (DC) and 20 tumor (T) sites of same oral cancer subjects demonstrated increase in severity of pathology from HV to T, higher DNA, and changes in secondary structure of proteins. The findings were relatable with cytopathological observations [138].

8.4.3 In Vivo Studies

Spectroscopic technique-based tissue diagnosis has shown potential in cancer detection, but the fact remains that tissue-based approaches are inherently invasive. The utility of optical techniques lies in a label-free and noninvasive approach which can facilitate in vivo spectral acquisition in clinics. In vivo applications have greatly benefitted from development of fiber-optic probes which have enabled packaging of optical component in small probes and eased spectral acquisition from the organs.

Fluorescence spectroscopy: In vivo autofluorescence spectra from oral mucosa have explored various wavelengths for excitation (337, 365, 410, and 635 nm) on healthy volunteers as well as cancers subjects. The ratio of red region (635 nm) to blue region (455–490 nm) intensities, ascribed to NADH and porphyrin levels, is greater in abnormal areas. The best discrimination was achieved by excitation at 410 nm [98]. Fluorescence studies on early perturbations in oral cavity owing to tobacco/areca nut habit suggest variations in collagen and flavin levels (areca nut habitués) and hemoglobin and porphyrin levels (tobacco habitués) with respect to non-habitués [105, 106]. In vivo preliminary studies on buccal mucosa of normal, premalignant, and malignant human volunteers have shown good discrimination between healthy and diseased conditions [107]. A recent study employed VELscope device on 2404 subjects who were examined using white light as well as VELscope to identify 357 subjects with lesions, out of which 192 (54%) were positive for fluorescence emission [16].

ESS: Diagnosis of premalignant and malignant oral lesions has also been investigated along with a corresponding histopathological analysis [139] on 25 oral sites from 25 subjects with oral leukoplakia. LDA yielded sensitivity of 72% and specificity of 75%. These results suggest that ESS may be able to identify dysplasia in oral tissues.

DRS: Under in vivo conditions spectra have been acquired from the buccal mucosa of healthy controls and precancerous and cancerous subjects using a fiber-optic probe-coupled system in the 400–700 nm regions and compared against the gold standard histopathology. DR spectra of healthy and pathological conditions show a significant dip around 545 and 575 nm, assigned to oxygenated hemoglobin [112, 140]. The ratio (545/575) increases significantly with the severity in pathology, i.e., from healthy to cancerous lesions through hyperplasic, dysplastic stages. Sensitivities and specificities ranging from 95 to 100% have been observed for different groups. Additionally, methemoglobin and melanin absorption by tissues can also be exploited alongside, and enhancements can be achieved using Monte Carlo method and inverse algorithms to simulate the tissue diffuse reflectance of normal and oral cancer tissues [141]. A trimodal study involving fluorescence, DRS, and light scattering spectroscopy on 91 sites from 15 subjects with varying degrees of malignancy (normal, dysplastic, and cancerous sites) and 8 healthy volunteers has shown a sensitivity and specificity of 96% and 96%, respectively, in distinguishing abnormal and normal tissues. In addition, dysplastic regions could be distinguished from cancerous tissue with a sensitivity of 64% and a specificity of 90% [101].

OCT: Epithelial thickness within the oral cavity has been employed as a parameter to detect oral cancers at different stages [142]. OCT imaging of normal and precancerous oral mucosae has demonstrated demarcation of epithelium (EP) and lamina propria (LP) layers to determine the EP thickness and estimate the range of dysplastic cell distribution with sensitivity and specificity up to 82 and 90%, respectively [143]. OCT imaging and perspectives have been recently reviewed by Rao et al. [144] and Reddy et al. [145]. A recent report on biopsy guidance using wide-field OCT has catered to two conditions: first, automated segmentation of wide-field OCT images and, second, registering imaging location with markers placed on tissues [146].

RS: Several reports have enriched the field of in vivo RS. Raman studies were undertaken for intraoperative tumor margin assessment in nine breast cancer subjects undergoing partial mastectomy in 2006 [147]. Interestingly, one spectrum from a margin was correlated as cancerous, though no lesion was apparently visible. Postoperative pathology of the margin suggested it to be positive for cancer, and thus a second operation for excision was carried out. The first report of in vivo RS on human oral cavity by Guze et al. (2009) identified site-wise variations in the human oral cavity. Reproducibility of Raman spectra from normal oral mucosa among anatomic oral sites (buccal mucosa, tongue, floor of mouth, lip, and hard palate) on 51 subjects (25 Caucasian and 26 Asian) across races and gender was explored. Analysis of high-wavenumber region (2800–3100 cm^{-1}) indicated spectra were not influenced by subject ethnicity, and different oral cavity sites could be discriminated based on degree of keratinization [148]. In vivo RS of different anatomical regions (inner lip, attached gingiva, floor, dorsal tongue, ventral tongue, hard palate, soft palate, and buccal) in the oral cavity in the fingerprint region (800–1800 cm^{-1}) has also been investigated. These sites can be grouped together based on anatomical and spectral similarity to develop diagnostic algorithms [149]. The first in vivo spectral acquisition from oral cancer subjects in clinically implementable time was reported by Singh et al. [87, 150]. Subsequent studies showed objective discrimination of the premalignant conditions from normal and tumor conditions [86] as well as malignancy-associated changes (MAC) or cancer field effects (CFE) in oral cancer subjects [85]. It has also been shown that age-related physiological changes have no bearing on the classification between healthy and tobacco-related pathological changes [89]. Spectral differences in different oral cavity subsites suggested classification of the subsites into four major anatomical clusters: (a) outer lip and lip vermillion, (b) buccal mucosa, (c) hard palate, and (d) dorsal, lateral, and ventral tongue and soft palate [151, 152]. In another recent report on subsite classification, anatomical differences between buccal mucosa, tongue, and lip as subsites and their possible influence on healthy vs pathological classification were investigated on 85 oral cancer and 72 healthy subjects. Buccal mucosa and tongue were spectrally distinct, while lip misclassified with both. The pooled subsites model with 98% specificity and 100% sensitivity may be useful for preliminary screening applications in oral cancers [153].

Conclusion

Optical techniques hold great potential as adjuncts to the conventional diagnostics and are better suited for screening purposes. Major advantages of optical techniques are being rapid and nondestructive and requirement of minimal sample preparation, which enhances their utility as clinical tools. As these techniques exploit biochemical perturbations in tissues/organs, such techniques can also help in better understanding of the disease conditions. However, each optical technique has advantages as well as limitations. Fluorescence spectroscopy requires very simple and inexpensive instrumentation, but only limited biomolecules are also fluorophores. There are insufficient in vivo reports on ESS and OCT (and FTIR) in case of human subjects, though ex vivo and animal studies have shown potential of these techniques. Vibrational techniques such as FTIR and RS are sensitive and can yield information about total biomolecules present in a biological system but require sophisticated instrumentation. FTIR is further affected by the presence of water, and thus the in vivo application is severely limited. Raman scattering is a weak phenomenon and thus better excitation and detection sources are required. Recent adaptations of conventional RS have shown signal enhancement and improved scope of in vivo applications. But, many of them are yet to be explored in vivo.

While all the techniques mentioned in the chapter (and several others which could not be addressed) have been employed in oral cancer explorations, majority of the in vivo studies have utilized fluorescence or RS, indicating their potential in in vivo diagnostics and screening. Many groups have explored multimodal applications of the above techniques where in more than one technique is simultaneously used for spectral/image acquisition, and better sensitivity and specificity have been observed for the multimodal apparatus. Further advancements in the field and large-scale community-based screening programs may help translation of these tools to clinics.

References

1. Mehrotra R, Gupta DK. Exciting new advances in oral cancer diagnosis: avenues to early detection. Head Neck Oncol. 2011;3:33.
2. Sankaranarayanan R, Ramadas K, Thomas G, Muwonge R, Thara S, Mathew B, Rajan B, Trivandrum oral cancer screening study G. Effect of screening on oral cancer mortality in Kerala, India: a cluster-randomised controlled trial. Lancet. 2005;365:1927–33.
3. Lingen MW, Kalmar JR, Karrison T, Speight PM. Critical evaluation of diagnostic aids for the detection of oral cancer. Oral Oncol. 2008;44:10–22.
4. Fedele S. Diagnostic aids in the screening of oral cancer. Head Neck Oncol. 2009;1:5.
5. Masters BR. The development of fluorescence microscopy. In: eLS. Chichester: Wiley; 2010.
6. Stokes GG. On the change of refrangibility of light. In: Philosophical transactions of the royal society of London; 1852. p. 463–562.
7. Wagnieres GA, Star WM, Wilson BC. In vivo fluorescence spectroscopy and imaging for oncological applications. Photochem Photobiol. 1998;68:603–32.
8. Pottier R. In vitro and in vivo fluorescence monitoring of photosensitizers. J Photochem Photobiol B. 1990;6:103–9.
9. Nilsson H, Johansson J, Svanberg K, Svanberg S, Jori G, Reddi E, et al. Laser-induced fluorescence in malignant and normal tissue in mice injected with two different carotenoporphyrins. Br J Cancer. 1994;70:873.
10. Ramanujam N. Fluorescence spectroscopy in vivo. In: Encyclopedia of analytical chemistry. Chichester: Wiley; 2000.
11. Neves V, Heister E, Costa S, Tilmaciu C, Flahaut E, Soula B, et al. Design of double-walled carbon nanotubes for biomedical applications. Nanotechnology. 2012;23:365102.
12. De Veld D, Witjes M, Sterenborg H, Roodenburg J. The status of in vivo autofluorescence spectroscopy and imaging for oral oncology. Oral Oncol. 2005;41:117–31.
13. Inaguma M, Hashimoto K. Porphyrin-like fluorescence in oral cancer: in vivo fluorescence spectral characterization of lesions by use of a near-ultraviolet excited autofluorescence diagnosis system and separation of fluorescent extracts by capillary electrophoresis. Cancer. 1999;86:2201–11.
14. Patton L, Epstein J, Kerr A. Adjunctive techniques for oral cancer examination and lesion diagnosis: a systematic review of the literature. J Am Dent Assoc. 2008;139:896–905.
15. Kois JC, Truelove E. Detecting oral cancer: a new technique and case reports. Dent Today. 2006;25:94, 96-97.
16. Laronde DM, Williams PM, Hislop TG, Poh C, Ng S, Bajdik C, Zhang L, MacAulay C, Rosin MP. Influence of fluorescence on screening decisions for oral mucosal lesions in community dental practices. J Oral Pathol Med. 2014;43:7–13.
17. A'Amar O, Liou L, Rodriguez-Diaz E, De las Morenas A, Bigio I. Comparison of elastic scattering spectroscopy with histology in ex vivo prostate glands: potential application for optically guided biopsy and directed treatment. Lasers Med Sci. 2013;28:1323–9.
18. Kubelka P. New contributions to the optics of intensely light-scattering materials. Part II: nonhomogeneous layers*. J Opt Soc Am. 1954;44:330–5.
19. Huang P-Y, Chien C-Y, Sheu C-R, Chen Y-W, Tseng S-H. Light distribution modulated diffuse reflectance spectroscopy. Biomed Opt Express. 2016;7:2118–29.
20. Huang D, Swanson EA, Lin CP, Schuman JS, Stinson WG, Chang W, et al. Optical coherence tomography. Science. 1991;254:1178–81.
21. Drexler W, Morgner U, Ghanta RK, Kärtner FX, Schuman JS, Fujimoto JG. Ultrahigh-resolution ophthalmic optical coherence tomography. Nature Med. 2001;7:502–7.
22. An L, Wang RK. In vivo volumetric imaging of vascular perfusion within human retina and choroids with optical micro-angiography. Opt Express. 2008;16:11438–52.
23. Boppart SA, Luo W, Marks DL, Singletary KW. Optical coherence tomography: feasibility for basic research and image-guided surgery of breast cancer. Breast Cancer Res Treat. 2004;84:85–97.
24. Vakoc BJ, Fukumura D, Jain RK, Bouma BE. Cancer imaging by optical coherence tomography: preclinical progress and clinical potential. Nat Rev Cancer. 2012;12:363–8.
25. Wessels R, De Bruin D, Faber D, Van Leeuwen T, Van Beurden M, Ruers T. Optical biopsy of epithelial cancers by optical coherence tomography (OCT). Lasers Med Sci. 2014;29:1297–305.

26. Bezerra HG, Costa MA, Guagliumi G, Rollins AM, Simon DI. Intracoronary optical coherence tomography: a comprehensive review clinical and research applications. JACC Cardiovasc Interv. 2009;2:1035–46.
27. Larina IV, Ivers S, Syed S, Dickinson ME, Larin KV. Hemodynamic measurements from individual blood cells in early mammalian embryos with Doppler swept source OCT. Opt Lett. 2009;34:986–8.
28. Böhringer H, Boller D, Leppert J, Knopp U, Lankenau E, Reusche E, et al. Time-domain and spectral-domain optical coherence tomography in the analysis of brain tumor tissue. Lasers Surg Med. 2006;38:588–97.
29. Assayag O, Grieve K, Devaux B, Harms F, Pallud J, Chretien F, et al. Imaging of non-tumorous and tumorous human brain tissues with full-field optical coherence tomography. Neuro Image Clin. 2013;2:549–57.
30. Kut C, Chaichana KL, Xi J, Raza SM, Ye X, McVeigh ER, et al. Detection of human brain cancer infiltration ex vivo and in vivo using quantitative optical coherence tomography. Sci Transl Med. 2015;7:292ra100.
31. Raman CV, Krishnan KS. A new type of secondary radiation. Nature. 1928;121:501–2.
32. Kneipp K, Kneipp H, Itzkan I, Dasari RR, Feld MS. Surface-enhanced Raman scattering and biophysics. J Phys Condens Matter. 2002;14:R597.
33. Xie W, Schlücker S. Medical applications of surface-enhanced Raman scattering. Phys Chem Chem Phys. 2013;15:5329–44.
34. Tolles WM, Nibler J, McDonald J, Harvey A. A review of the theory and application of coherent anti-stokes Raman spectroscopy (CARS). Appl Spectrosc. 1977;31:253–71.
35. Kudelski A. Analytical applications of Raman spectroscopy. Talanta. 2008;76:1–8.
36. White JC. Stimulated raman scattering. In: Tunable lasers. Berlin: Springer; 1987. p. 115–207.
37. Yakovlev VV, Petrov GI, Zhang HF, Noojin GD, Denton ML, Thomas RJ, et al. Stimulated Raman scattering: old physics, new applications. J Mod Opt. 2009;56:1970–3.
38. Eesley GL. Coherent raman spectroscopy. New York: Elsevier; 2013.
39. Dingari NC, Horowitz GL, Kang JW, Dasari RR, Barman I. Raman spectroscopy provides a powerful diagnostic tool for accurate determination of albumin glycation. PLoS One. 2012;7:e32406.
40. Barman I, Dingari NC, Kang JW, Horowitz GL, Dasari RR, Feld MS. Raman spectroscopy-based sensitive and specific detection of glycated hemoglobin. Anal Chem. 2012;84:2474–82.
41. Filik J, Stone N. Drop coating deposition Raman spectroscopy of protein mixtures. Analyst. 2007;132:544–50.
42. Matousek P, Clark I, Draper E, Morris M, Goodship A, Everall N, et al. Subsurface probing in diffusely scattering media using spatially offset Raman spectroscopy. Appl Spectrosc. 2005;59:393–400.
43. Stone N, Kerssens M, Lloyd GR, Faulds K, Graham D, Matousek P. Surface enhanced spatially offset Raman spectroscopic (SESORS) imaging–the next dimension. Chem Sci. 2011;2:776–80.
44. Sharma B, Ma K, Glucksberg MR, Van Duyne RP. Seeing through bone with surface-enhanced spatially offset Raman spectroscopy. J Am Chem Soc. 2013;135:17290–3.
45. Abdi H, Williams LJ. Principal component analysis. Wiley Interdiscip Rev Comput Stat. 2010;2:433–59.
46. Varmuza K, Filzmoser P. Introduction to multivariate statistical analysis in chemometrics. Boca Raton: CRC press; 2009.
47. Bakker Schut TC, Witjes MJ, Sterenborg HJ, Speelman OC, Roodenburg JL, Marple ET, et al. In vivo detection of dysplastic tissue by Raman spectroscopy. Anal Chem. 2000;72:6010–8.
48. Gimenez-Conti IB, Slaga TJ. The hamster cheek pouch carcinogenesis model. J Cell Biochem. 1993;53:83–90.
49. Salley JJ. Experimental carcinogenesis in the cheek pouch of the Syrian hamster. J Dent Res. 1954;33:253–62.
50. Keyes PH, Dale PP. A preliminary survey of the pouches and dentition of the Syrian hamster. J Dent Res. 1944;23:427–38.
51. Shklar G. Experimental oral pathology in the Syrian hamster. Prog Exp Tumor Res. 1972;16:518–38.
52. Balasenthil S, Saroja M, Ramachandran C, Nagini S. Of humans and hamsters: comparative analysis of lipid peroxidation, glutathione, and glutathione-dependent enzymes during oral carcinogenesis. Br J Oral Maxillofac Surg. 2000;38:267–70.
53. Nagini S, Letchoumy PV, Thangavelu A, Ramachandran C. Of humans and hamsters: a comparative evaluation of carcinogen activation, DNA damage, cell proliferation, apoptosis, invasion, and angiogenesis in oral cancer patients and hamster buccal pouch carcinomas. Oral Oncol. 2009;45:e31–7.
54. Ambatipudi S, Bhosale PG, Heath E, Pandey M, Kumar G, Kane S, et al. Downregulation of keratin 76 expression during oral carcinogenesis of human, hamster and mouse. PLoS One. 2013;8:e70688.
55. Suda D, Schwartz J, Shklar G. GGT reduction in beta carotene-inhibition of hamster buccal pouch carcinogenesis. Eur J Cancer Clin Oncol. 1987;23:43–6.
56. Solt DB. Localization of gamma-glutamyl transpeptidase in hamster buccal pouch epithelium treated with 7, 12-dimethylbenz [a] anthracene. J Nat Cancer Inst. 1981;67:193–200.
57. Gimenez-Conti IB, Bianchi AB, Stockman SL, Conti CJ, Slaga TJ. Activating mutation of the ha-ras gene in chemically induced tumors of the hamster cheek pouch. Mol Carcinog. 1992;5:259–63.
58. Gimenez-Conti IB, LaBate M, Liu F, Osterndorff E. p53 alterations in chemically induced hamster cheek-pouch lesions. Mol Carcinog. 1996;16:197–202.
59. Husain Z, Fei Y, Roy S, Solt DB, Polverini PJ, Biswas DK. Sequential expression and cooperative interaction of c-ha-ras and c-erbB genes in in vivo chemical carcinogenesis. Proc Nat Acad Sci. 1989;86:1264–8.

60. Chen CT, Chiang HK, Chow SN, Wang CY, Lee YS, Tsai JC, et al. Autofluorescence in normal and malignant human oral tissues and in DMBA-induced hamster buccal pouch carcinogenesis. J Oral Pathol Med. 1998;27:470–4.
61. Wang CY, Tsai T, Chen HC, Chang SC, Chen CT, Chiang CP. Autofluorescence spectroscopy for in vivo diagnosis of DMBA-induced hamster buccal pouch pre-cancers and cancers. J Oral Pathol Med. 2003;32:18–24.
62. Wang C-Y, Chen C-T, Chiang C-P, Young S-T, Chow S-N, Chiang HK. Partial least-squares discriminant analysis on autofluorescence spectra of oral carcinogenesis. Appl Spectrosc. 1998;52:1190–6.
63. Sun Y, Phipps J, Elson DS, Stoy H, Tinling S, Meier J, et al. Fluorescence lifetime imaging microscopy: in vivo application to diagnosis of oral carcinoma. Opt Lett. 2009;34:2081–3.
64. Cheng S, Cuenca RM, Liu B, Malik BH, Jabbour JM, Maitland KC, et al. Handheld multispectral fluorescence lifetime imaging system for in vivo applications. Biomed Opti Express. 2014;5:921–31.
65. Chen Y-W, Liaw Y-K, Hung H-R, Chung P-C, Tseng S-H Differentiating early oral cancer from normal oral tissue using diffuse reflectance spectroscopy. In: Asia communications and photonics conference, 2013. Optical Society of America. p. AF4I. 3.
66. Skala MC, Palmer GM, Vrotsos KM, Gendron-Fitzpatrick A, Ramanujam N. Comparison of a physical model and principal component analysis for the diagnosis of epithelial neoplasias in vivo using diffuse reflectance spectroscopy. Opt Express. 2007;15:7863–75.
67. Matheny ES, Hanna NM, Jung WG, Chen Z, Wilder-Smith P, Mina-Araghi R, et al. Optical coherence tomography of malignancy in hamster cheek pouches. J Biomed Opt. 2004;9:978–81.
68. Hanna NM, Waite W, Taylor K, Jung WG, Mukai D, Matheny E, et al. Feasibility of three-dimensional optical coherence tomography and optical Doppler tomography of malignancy in hamster cheek pouches. Photomed Laser Surg. 2006;24:402–9.
69. Graf RN, Robles FE, Chen X, Wax A. Detecting precancerous lesions in the hamster cheek pouch using spectroscopic white-light optical coherence tomography to assess nuclear morphology via spectral oscillations. J Biomed Opt. 2009;14:064030.
70. Pande P, Shrestha S, Park J, Serafino MJ, Gimenez-Conti I, Brandon J, Cheng Y-S, Applegate BE, Jo JA. Automated classification of optical coherence tomography images for the diagnosis of oral malignancy in the hamster cheek pouch. J Biomed Opt. 2014;19:086022.
71. Wilder-Smith P, Jung W-G, Brenner M, Osann K, Beydoun H, Messadi D, Chen Z. In vivo optical coherence tomography for the diagnosis of oral malignancy. Lasers Surg Med. 2004;35: 269–75.
72. Jung W, Zhang J, Chung J, Wilder-Smith P, Brenner M, Nelson JS, Chen Z. Advances in oral cancer detection using optical coherence tomography. IEEE J Sel Top Quantum Electron. 2005;11:811–7.
73. Kumar P, Krishna CM, Sahoo NK, Rao KD. Multimodal spectroscopic applications in cancer diagnosis: combined Raman spectroscopy and optical coherence tomography. Asian J Phys. 2015;24:00.
74. Kumar P. Raman spectroscopy in experimental oral carcinogenesis: investigation of abnormal changes in control tissues. J Raman Spectrosc. 2016;47: 1318–26.
75. Pande P, Shrestha S, Park J, Gimenez-Conti I, Brandon J, Applegate BE, et al. Automated analysis of multimodal fluorescence lifetime imaging and optical coherence tomography data for the diagnosis of oral cancer in the hamster cheek pouch model. Biomed Opt Express. 2016;7:2000–15.
76. Mognetti B, Di Carlo F, Berta GN. Animal models in oral cancer research. Oral Oncol. 2006;42:448–60.
77. Mizuno A, Nozawa H, Yaginuma T, Matsuzaki H, Ozaki Y, Iriyama K. Effect of aldose reductase inhibitor on experimental diabetic cataract monitored by laser Raman spectroscopy. Exp Eye Res. 1987;45:185–6.
78. Mizuno A, Toshima S, Mori Y. Confirmation of lens hydration by Raman spectroscopy. Exp Eye Res. 1990;50:647–9.
79. Nozawa H, Yaginuma T, Mizuno A. Raman spectroscopic study of the effect of aldose reductase inhibitor on experimental diabetic cataract. Nippon Ganka Gakkai Zasshi. 1988;92:194–201.
80. Mizuno A, Kanematsu EH, Suzuki H, Ihara N. Laser Raman spectroscopic study of hereditary cataractous lenses in ICR/f-strain rat. Jpn J Ophthalmol. 1988;32:281–7.
81. Wang C, Wang Y, Huffman NT, Cui C, Yao X, Midura S, et al. Confocal laser Raman microspectroscopy of biomineralization foci in UMR 106 osteoblastic cultures reveals temporally synchronized protein changes preceding and accompanying mineral crystal deposition. J Biol Chem. 2009;284:7100–13.
82. Ohsaki K, Shibata A, Yamashita S, Oe M, Wang KQ, Cui PC, et al. Demonstrations of de-and remineralization mechanism as revealed in synthetic auditory ossicle (Apaceram) of rats by laser-Raman spectrometry. Cell Mol Biol (Noisy-le-Grand). 1995;41:1155–67.
83. Oliveira AP, Bitar RA, Silveira L, Zangaro RA, Martin AA. Near-infrared Raman spectroscopy for oral carcinoma diagnosis. Photomed Laser Surg. 2006;24:348–53.
84. Ghanate AD, Kumar G, Talathi S, Maru GB, Krishna CM Raman spectroscopic detection of early stages in DMBA-induced tumor evolution in hamster buccal pouch model: an exploratory study. In: Photonics 2010: Tenth International Conference on Fiber Optics and Photonics; 817303 (2011), Proceedings Volume 8173. International Conference on Fiber Optics and Photonics, 2010, Guwahati, India. p. 817303–817307.

85. Singh SP, Sahu A, Deshmukh A, Chaturvedi P, Krishna CM. In vivo Raman spectroscopy of oral buccal mucosa: a study on malignancy associated changes (MAC)/cancer field effects (CFE). Analyst. 2013;138:4175–82.
86. Singh SP, Deshmukh A, Chaturvedi P, Murali Krishna C. In vivo Raman spectroscopic identification of premalignant lesions in oral buccal mucosa. J Biomed Opt. 2012;17:105002.
87. Singh SP, Deshmukh A, Chaturvedi P, Krishna CM. Raman spectroscopy in head and neck cancers: toward oncological applications. J Cancer Res Ther. 2012;8:S126–32.
88. Deshmukh A, Singh SP, Chaturvedi P, Krishna CM. Raman spectroscopy of normal oral buccal mucosa tissues: study on intact and incised biopsies. J Biomed Opt. 2011;16:127004.
89. Sahu A, Deshmukh A, Ghanate AD, Singh SP, Chaturvedi P, Krishna CM. Raman spectroscopy of oral buccal mucosa: a study on age-related physiological changes and tobacco-related pathological changes. Technol Cancer Res Treat. 2012;11:529–41.
90. Kumar P, Bhattacharjee T, Ingle A, Maru G, Krishna CM. Raman spectroscopy of experimental oral carcinogenesis: study on sequential cancer progression in hamster buccal pouch model. Technol Cancer Res Treat. 2016;15:NP60–72.
91. Gohulkumar M, Kumar P, Murali Krishna C, Krishnakumar N. Evaluation of Raman spectroscopy for prediction of antitumor response to silibinin and its nanoparticulates in DMBA-induced oral carcinogenesis. J Raman Spectrosc. 2016; 47:375–383.
92. Gurushankar K, Gohulkumar M, Kumar P, Krishna CM, Krishnakumar N. Raman spectroscopy detects biomolecular changes associated with nanoencapsulated hesperetin treatment in experimental oral carcinogenesis. Laser Phys Lett. 2016; 13:035901.
93. Sharwani A, Jerjes W, Salih V, MacRobert A, El-Maaytah M, Khalil H, et al. Fluorescence spectroscopy combined with 5-aminolevulinic acid-induced protoporphyrin IX fluorescence in detecting oral premalignancy. J Photochem Photobiol B. 2006;83:27–33.
94. Betz CS, Stepp H, Janda P, Arbogast S, Grevers G, Baumgartner R, et al. A comparative study of normal inspection, autofluorescence and 5-ALA-induced PPIX fluorescence for oral cancer diagnosis. Int J Cancer. 2002;97:245–52.
95. Leunig A, Betz CS, Mehlmann M, Stepp H, Arbogast S, Grevers G, et al. Detection of squamous cell carcinoma of the oral cavity by imaging 5-aminolevulinic acid-induced protoporphyrin IX fluorescence. Laryngoscope. 2000;110:78–83.
96. Policard A. Etude sur les aspects offerts par des tumeurs experimentales examinees a la lumiere de Wood. CR Soc Biol. 1924;91:1423–4.
97. Heintzelman DL, Utzinger U, Fuchs H, Zuluaga A, Gossage K, Gillenwater AM, et al. Optimal excitation wavelengths for in vivo detection of oral neoplasia using fluorescence spectroscopy. Photochem Photobiol. 2000;72(1):103–13.
98. Gillenwater A, Jacob R, Ganeshappa R, Kemp B, El-Naggar AK, Palmer JL, et al. Noninvasive diagnosis of oral neoplasia based on fluorescence spectroscopy and native tissue autofluorescence. Arch Otolaryngol Head Neck Surg. 1998;124:1251–8.
99. Braichotte DR, Wagnieres GA, Bays R, Monnier P, van den Bergh HE. Clinical pharmacokinetic studies of photofrin by fluorescence spectroscopy in the oral cavity, the esophagus, and the bronchi. Cancer-Philadelphia. 1995;75:2768.
100. Ebenezar J, Ganesan S, Aruna P, Muralinaidu R, Renganathan K, Saraswathy TR. Noninvasive fluorescence excitation spectroscopy for the diagnosis of oral neoplasia in vivo. J Biomed Opt. 2012;17:97007–1.
101. Müller MG, Valdez TA, Georgakoudi I, Backman V, Fuentes C, Kabani S, et al. Spectroscopic detection and evaluation of morphologic and biochemical changes in early human oral carcinoma. Cancer. 2003;97:1681–92.
102. Venugopal C, Nazeer SS, Balan A, Jayasree R. Autofluorescence spectroscopy augmented by multivariate analysis as a potential noninvasive tool for early diagnosis of oral cavity disorders. Photomed Laser Surg. 2013;31:605–12.
103. Haris PS, Balan A, Jayasree RS, Gupta AK. Autofluorescence spectroscopy for the in vivo evaluation of oral submucous fibrosis. Photomed Laser Surg. 2009;27:757–61.
104. Jayanthi J, Mallia RJ, Shiny ST, Baiju KV, Mathews A, Kumar R, et al. Discriminant analysis of autofluorescence spectra for classification of oral lesions in vivo. Lasers Surg Med. 2009;41:345–52.
105. Shaiju SN, Ariya S, Asish R, Haris PS, Anita B, Kumar GA, Jayasree RS. Habits with killer instincts: in vivo analysis on the severity of oral mucosal alterations using autofluorescence spectroscopy. J Biomed Opt. 2011;16:087006.
106. Nazeer SS, Asish R, Venugopal C, Anita B, Gupta AK, Jayasree RS. Noninvasive assessment of the risk of tobacco abuse in oral mucosa using fluorescence spectroscopy: a clinical approach. J Biomed Opt. 2014;19:057013..
107. Unnikrishnan V, Nayak R, Bernard R, Priya KJ, Patil A, Ebenezer J, et al. Parameter optimization of a laser-induced fluorescence system for in vivo screening of oral cancer. J Laser Appl. 2011;23:032004.
108. Jerjes W, Swinson B, Pickard D, Thomas G, Hopper C. Detection of cervical intranodal metastasis in oral cancer using elastic scattering spectroscopy. Oral Oncol. 2004;40:673–8.
109. Jerjes W, Swinson B, Johnson K, Thomas G, Hopper C. Assessment of bony resection margins in oral cancer using elastic scattering spectroscopy: a study on archival material. Arch Oral Biol. 2005;50:361–6.
110. De Veld DC, Skurichina M, Witjes MJ, Duin RP, Sterenborg HJ, Roodenburg JL. Autofluorescence

and diffuse reflectance spectroscopy for oral oncology. Lasers Surg Med. 2005;36:356–64.
111. Subhash N, Mallia J, Thomas SS, Mathews A, Sebastian P, Madhavan J. Oral cancer detection using diffuse reflectance spectral ratio R540/ R575 of oxygenated hemoglobin bands. J Biomed Opt. 2006;11:014018.
112. Jayanthi J, Nisha G, Manju S, Philip E, Jeemon P, Baiju K, et al. Diffuse reflectance spectroscopy: diagnostic accuracy of a non-invasive screening technique for early detection of malignant changes in the oral cavity. BMJ Open. 2011;1:e000071.
113. Mallia R, Thomas SS, Mathews A, Kumar R, Sebastian P, Madhavan J, et al. Oxygenated hemoglobin diffuse reflectance ratio for in vivo detection of oral pre-cancer. J Biomed Opt. 2008;13:041306.
114. Yu B, Shah A, Nagarajan VK, Ferris DG. Diffuse reflectance spectroscopy of epithelial tissue with a smart fiber-optic probe. Biomed Opt Express. 2014;5:675–89.
115. Mallia RJ, Narayanan S, Madhavan J, Sebastian P, Kumar R, Mathews A, et al. Diffuse reflection spectroscopy: an alternative to autofluorescence spectroscopy in tongue cancer detection. Appl Spectrosc. 2010;64:409–18.
116. Jerjes W, Upile T, Betz CS, Abbas S, Sandison A, Hopper C. Detection of oral pathologies using optical coherence tomography. Eur Oncol. 2008;4:57–9.
117. Hamdoon Z, Jerjes W, Al-Delayme R, McKenzie G, Jay A, Hopper C. Structural validation of oral mucosal tissue using optical coherence tomography. Head Neck Oncol. 2012;4:1.
118. Wu JG, Xu YZ, Sun CW, Soloway RD, Xu DF, Wu QG, et al. Distinguishing malignant from normal oral tissues using FTIR fiber-optic techniques. Biopolymers. 2001;62:185–92.
119. Fukuyama Y, Yoshida S, Yanagisawa S, Shimizu M. A study on the differences between oral squamous cell carcinomas and normal oral mucosas measured by Fourier transform infrared spectroscopy. Biospectroscopy. 1999;5:117–26.
120. Banerjee S, Pal M, Chakrabarty J, Petibois C, Paul RR, Giri A, et al. Fourier-transform-infrared-spectroscopy based spectral-biomarker selection towards optimum diagnostic differentiation of oral leukoplakia and cancer. Anal Bioanal Chem. 2015;407:7935–43.
121. Venkatakrishna K, Kurien J, Pai KM, Valiathan M, Kumar NN, Murali Krishna C, et al. Optical pathology of oral tissue: a Raman spectroscopy diagnostic method. Current Sci. 2001;80:665–9.
122. Krishna CM, Sockalingum G, Kurien J, Rao L, Venteo L, Pluot M, et al. Micro-Raman spectroscopy for optical pathology of oral squamous cell carcinoma. Appl Spectrosc. 2004;58:1128–35.
123. Malini R, Venkatakrishna K, Kurien J, Pai KM, Rao L, Kartha VB, et al. Discrimination of normal, inflammatory, premalignant, and malignant oral tissue: a Raman spectroscopy study. Biopolymers. 2006;81(3):179–93.
124. Hu Y, Jiang T, Zhao Z. Discrimination of squamous cell carcinoma of the oral cavity using Raman spectroscopy and chemometric analysis. In: ICINIS'08 First International Conference on. Intelligent networks and intelligent systems, 2008. IEEE; 2008. p. 633–6.
125. Sunder N, Rao N, Kartha V, Ullas G, Kurien J. Laser raman spectroscopy: a novel diagnostic tool for oral cancer. J Orofac Sci. 2011;3:15.
126. Behl I, Kukreja L, Deshmukh A, Singh SP, Mamgain H, Hole AR et al. Raman mapping of oral buccal mucosa: a spectral histopathology approach. J Biomed Opt. 2014;19:126005.
127. Cals FL, Bakker Schut TC, Hardillo JA, Baatenburg de Jong RJ, Koljenovic S, Puppels GJ. Investigation of the potential of Raman spectroscopy for oral cancer detection in surgical margins. Lab Investig. 2015;95:1186–96.
128. Baker MJ, Hussain SR, Lovergne L, Untereiner V, Hughes C, Lukaszewski RA, et al. Developing and understanding biofluid vibrational spectroscopy: a critical review. Chem Soc Rev. 2016;45:1803–18.
129. Madhuri S, Vengadesan N, Aruna P, Koteeswaran D, Venkatesan P, Ganesan S. Native fluorescence spectroscopy of blood plasma in the characterization of oral malignancy. Photochem Photobiol. 2003;78:197–204.
130. Rajasekaran R, Aruna PR, Koteeswaran D, Padmanabhan L, Muthuvelu K, Rai RR, et al. Characterization and diagnosis of cancer by native fluorescence spectroscopy of human urine. Photochem Photobiol. 2013;89:483–91.
131. Harris AT, Lungari A, Needham CJ, Smith SL, Lones MA, Fisher SE, et al. Potential for Raman spectroscopy to provide cancer screening using a peripheral blood sample. Head Neck Oncol. 2009;1:1–8.
132. Feng S, Chen R, Lin J, Pan J, Chen G, Li Y, et al. Nasopharyngeal cancer detection based on blood plasma surface-enhanced Raman spectroscopy and multivariate analysis. Biosens Bioelectron. 2010;25:2414–9.
133. Sahu A, Sawant S, Mamgain H, Krishna CM. Raman spectroscopy of serum: an exploratory study for detection of oral cancers. Analyst. 2013;138:4161–74.
134. Sahu A, Sawant S, Talathi-Desai S, Murali Krishna C. Raman spectroscopy of serum: a study on oral cancers. Biomed Spectrosc Imaging. 2015;4(2): 171–87.
135. Sahu AK, Dhoot S, Singh A, Sawant SS, Nandakumar N, Talathi-Desai S et al. Oral cancer screening: serum Raman spectroscopic approach. J Biomed Opt. 2015;20:115006.
136. Sahu A, Nandakumar N, Sawant S, Krishna CM. Recurrence prediction in oral cancers: a serum Raman spectroscopy study. Analyst. 2015;140:2294–301.
137. Elumalai B, Prakasarao A, Ganesan B, Dornadula K, Ganesan S. Raman spectroscopic characterization of urine of normal and oral cancer subjects. J Raman Spectrosc. 2015;46:84–93.

138. Sahu A, Tawde S, Pai V, Gera P, Chaturvedi P, Nair S, et al. Raman spectroscopy and cytopathology of oral exfoliated cells for oral cancer diagnosis. Anal Methods. 2015;7:7548–59.
139. Sharwani A, Jerjes W, Salih V, Swinson B, Bigio I, El-Maaytah M, et al. Assessment of oral premalignancy using elastic scattering spectroscopy. Oral Oncol. 2006;42:343–9.
140. Stephen MM, Jayanthi JL, Unni NG, Kolady PE, Beena VT, Jeemon P, et al. Diagnostic accuracy of diffuse reflectance imaging for early detection of premalignant and malignant changes in the oral cavity: a feasibility study. BMC Cancer. 2013;13:1.
141. Einstein G, Udayakumar K, Aruna PR, Koteeswaran D, Ganesan S. Diffuse reflectance spectroscopy for monitoring physiological and morphological changes in oral cancer. Optik-Int J Light Electron Opt. 2016;127:1479–85.
142. Prestin S, Rothschild SI, Betz CS, Kraft M. Measurement of epithelial thickness within the oral cavity using optical coherence tomography. Head Neck. 2012;34:1777–81.
143. Lee CK, Chi TT, Wu CT, Tsai MT, Chiang CP, Yang CC. Diagnosis of oral precancer with optical coherence tomography. Biomed Opt Express. 2012;3:1632–46.
144. Divakar Rao K, Sahoo N, Krishna CM. Perspectives of optical coherence tomography imaging and Raman spectroscopy in cancer diagnosis. Biomed Spectrosc Imaging. 2015;4:35–55.
145. Reddy RS, Praveen KNS. Optical coherence tomography in oral cancer: a transpiring domain. J Cancer Res Ther. 2017;13:883–888.
146. Lee AM, Goldan R, Pahlevaninezhad H, Hohert G, Liu K, MacAulay CE, et al. Towards biopsy guidance of oral lesions with wide-field OCT imaging. In: Biomedical optics 2016, Fort lauderdale, Florida, 2016/04/25 2016. OSA Technical Digest (online). Opt Soc Am. p. JM4A.4.
147. Haka AS, Volynskaya Z, Gardecki JA, Nazemi J, Lyons J, Hicks D et al. In vivo margin assessment during partial mastectomy breast surgery using raman spectroscopy. Cancer Res. 2006;66:3317–22.
148. Guze K, Short M, Sonis S, Karimbux N, Chan J, Zeng H. Parameters defining the potential applicability of Raman spectroscopy as a diagnostic tool for oral disease. J Biomed Opt. 2009;14: 014016-014016-014019.
149. Bergholt MS, Zheng W, Huang Z. Characterizing variability in in vivo Raman spectroscopic properties of different anatomical sites of normal tissue in the oral cavity. J Raman Spectrosc. 2012;43: 255–62.
150. Singh S, Deshmukh A, Chaturvedi P, Krishna CM. In vivo Raman spectroscopy for oral cancers diagnosis. In: SPIE BiOS, 2012. International society for optics and photonics. p. 82190K–82190K–82196.
151. Krishna H, Majumder SK, Chaturvedi P, Gupta PK. Anatomical variability of in vivo Raman spectra of normal oral cavity and its effect on oral tissue classification. Biomed Spectrosc Imaging. 2013;2:199–217.
152. Krishna H, Majumder SK, Chaturvedi P, Sidramesh M, Gupta PK. In vivo Raman spectroscopy for detection of oral neoplasia: a pilot clinical study. J Biophotonics. 2014;7:690–702.
153. Sahu A, Deshmukh A, Hole AR, Chaturvedi P, Krishna CM. In vivo subsite classification and diagnosis of oral cancers using Raman spectroscopy. J Innov Opt Health Sci. 2016;09:1650017.

Optical Imaging in Oral Oncology

9

Prashanth Panta, Laurie J. Rich, and Mukund Seshadri

Abstract

There has been widespread interest in the application of simple light-based methods and optical imaging as adjunctive tools in oral oncology. These optical imaging techniques exploit differences in properties such as absorption, reflectance, and light scattering between normal and transformed epithelium. Optical imaging methods can also utilize tissue autofluorescence arising from endogenous chromatophores to detect malignant tissue. For example, early oral malignancy is often associated with a loss of fluorescence or fluorescence visualization loss (FVL) which may be used to aid in tissue selection for biopsy. The autofluorescence-based Visual Enhanced Lightscope (VELscope®), chemiluminescence-based ViziLite® system, the Identafi® system that uses multispectral fluorescence and reflectance, and narrow band imaging (NBI) instruments are among the optical imaging-based diagnostic platforms that are currently available for clinical use. In addition, photoacoustic imaging (PAI) is an advanced hybrid imaging method that allows for deep tissue imaging and is actively being evaluated for diagnostic applications in oncology. In this chapter, we will review the basics of these optical imaging methods and summarize preclinical and clinical evidence on their performance in oral oncology. The goal of this chapter is to provide the reader with an overview of these methods and their potential clinical applications.

9.1 Introduction to Light-Based Methods

Reliable identification of oral cancer and precancer cannot be based on visual examination alone since the human eye is not optimized to detect disease based on tissue contrast [1]. However, spectral differences between normal and diseased tissue can be visualized through the use of optical imaging methods that can improve our visual perception. These optical methods can exploit differences in optical properties of tissues such as fluorescence, reflectance, and chemiluminescence.

P. Panta, MDS (✉)
Department of Oral Medicine and Radiology, MNR Dental College and Hospital, Sangareddy, Telangana, India
e-mail: maithreya.prashanth@gmail.com

L. J. Rich, PhD · M. Seshadri, DDS, PhD
Department of Oral Oncology, Roswell Park Comprehensive Cancer Center, Buffalo, NY, USA
e-mail: laurie.rich@roswellpark.org; Mukund.Seshadri@roswellpark.org

P. Panta (ed.), *Oral Cancer Detection*, https://doi.org/10.1007/978-3-319-61255-3_9

9.2 Tissue Fluorescence or Autofluorescence

Cells and tissues in the body contain molecules which have the ability to "fluoresce" (i.e., glow) when excited by light of specific wavelength. When a tissue is illuminated with light of short wavelength (for example, blue light), cells become excited and emit light that is of a longer wavelength (low energy). Importantly, while normal cells emit green light, abnormal cells do not emit light. Exposure to blue light spectra (400–460 nm) may maximize a differential profile in areas undergoing neoplastic change [2]. This fluorescent signal arises from naturally occurring compounds in tissues called chromatophores or fluorophores. Fluorophores are molecules that absorb light at one wavelength and emit light at longer wavelength [3]. The main fluorophores capable of fluorescence in the 400–460 nm range are nicotinamide adenine dinucleotide (NADH) and flavin adenine dinucleotide (FAD), cellular coenzymes, collagen, and elastin in connective tissue. Hemoglobin (in blood) also absorbs light and results in loss of fluorescence in regions with high concentration. Other endogenous fluorophores include structural proteins and amino acids. Each fluorophore has a unique excitation spectrum, allowing for multispectral assessment of specific fluorophores. For example, increased metabolism typically observed in cancer changes FAD levels [4]. Scattering is another mechanism of fluorescent visualization that is influenced by tissue keratinization status, epithelial thickening of oral mucosa, and by nuclear scatter at the cellular level. The degree of keratinization varies from individual to individual and is also site-specific. For example, the tongue and buccal and alveolar mucosa are covered by keratinized epithelium, while the floor of mouth is nonkeratinized. A greater nuclear scatter can result from the high nuclear-to-cytoplasmic ratio in dysplastic tissues. This is especially true for amelanotic epithelial tumors like OSCC [5]. The scatter cross section (μm^2) in dysplastic nuclei (80 μm^2) is approximately four times greater than a normal cell (20 μm^2) at the same wavelength [5, 6]. At the fundamental level, fluorescence visualization is dependent on the absorption of light by certain absorbers, and emission of fluorescent light by naturally occurring tissue fluorophores, in addition to scattering caused by thick keratin blanket covering tissues [3] (Table 9.1).

Table 9.1 Mechanisms behind loss of fluorescence

Mechanism	Reasons	
Increased absorption	Absorption of light by hemoglobin and other absorbers.	
Decreased emission	By chomatophores: NADH, FAD, collagen, elastin etc.	
Increased scatter	Cell level	Cellular nuclei contribute to scatter
	Tissue level	Keratin, thick epithelium, and stromal collagen contribute to scatter

Malignant transformation results in cellular changes such as increased nuclear-to-cytoplasmic ratio, nuclear clumping, pleomorphism and changes in epithelium, and alterations in stromal architecture. The breakdown of collagen in the extracellular matrix and break in basement membrane also contribute to the loss of tissue fluorescence [7]. Studies have shown significant changes in stromal biology during the evolution of oral precancer [8]. The volume fraction of collagen fibers in supporting stroma decreases with the progression of disease [5]. In tissue stroma, collagen fibers are the main light scatterers. Collagen by nature has high refractive index, and hence scattering of light in the stroma is higher than the scattering in the epithelium. The hallmark autofluorescence and reflectance signals in oral malignancy are primarily due to changes in the underlying connective tissue. During malignant progression, several enzymes (proteases, etc.) mediate the invasion of tumor into connective tissue, destroying collagenous stromal architecture. As a result, the collagen fibers are broken down, and their arrangement becomes disorganized and more detached with a tendency to aggregate [5]. The gap created between collagen fibers due to this breakdown adds to contrast and represents a constant intensity region. This arrangement of collagen fibers can be validated using confocal microscopy. The identification of subtle changes

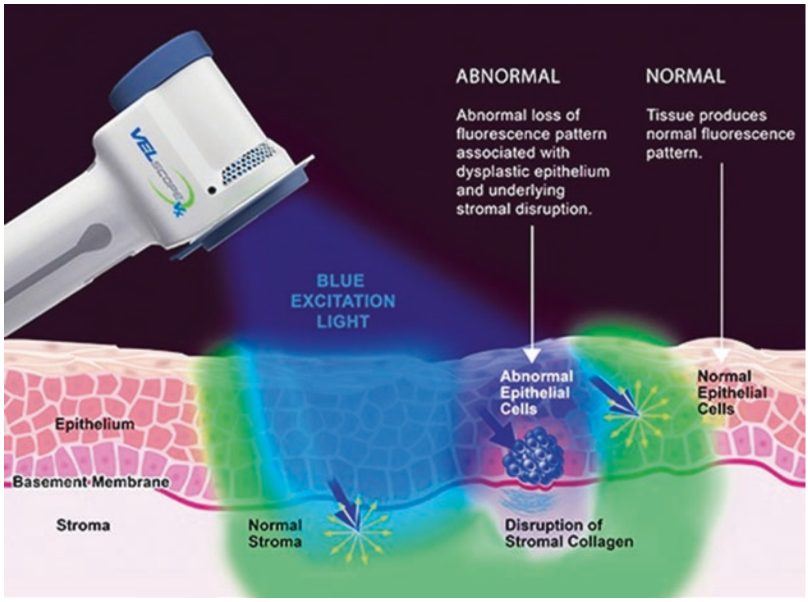

Fig. 9.1 Appearance of normal and abnormal mucosa under VELscope® tissue fluorescence imaging (courtesy of LED Dental, Inc.)

in connective tissue is therefore possible with autofluorescence-based optical methods and scattering-based methods such as optical coherence tomography. Loss of fluorescence or fluorescence visualization loss (FVL) was also used in the detection and mapping of field changes in oral malignant and potentially malignant disorders [9]. FVL was noticed in all 20 tumors and was extending far away (25 mm) from the clinically visible lesion (subclinical extension). In the study, 32 of 36 (~89%) FVL-guided biopsies showed histological change ranging from low-grade dysplasia to squamous cell carcinoma [9]. All 36 biopsies showed either histological change and/or genetic alteration. The FVL-guided margin biopsies in oral tumors with low-grade dysplasia or no dysplasia revealed loss of heterozygosity at 3p and/or 9p, a molecular change associated with high recurrence [9].

VELscope® (Visual Enhanced Light scope) is now a widely used handheld optical device for oral cancer screening that uses autofluorescence technology. It is an approved visual enhancement system compatible for use as an adjuvant tool for oral assessment in combination with routine oral examination. The VELscope® device utilizes blue light excitation between 400 and 460 nm to visualize the abnormality of the oral cavity by the property of direct tissue autofluorescence. The normal oral mucous membrane demonstrates a pale green fluorescence on absorption of blue light emitted by the device (Fig. 9.1). Abnormal tissue (i.e., tissue with dysplasia or malignancy) presents as a dark region due to loss of autofluorescence, a property natural to healthy tissues. Fluorescence visualization loss (FVL) is the hallmark of neoplastic process. The VELscope® device exploits this biological characteristic to distinguish healthy tissues or benign lesions from dysplastic tissue. In inflammatory lesions, this device shows false positives mainly due to the elevated blood flow and concentration of hemoglobin, which is a natural chromatophore that absorbs light resulting in FVL [10].

It takes ~2 min for complete visualization and is hence an easy-to-use clinical device. Newer generation devices also possess an imaging adapter compatible with a mobile device for case documentation. The device now has a single-use lens cap to prevent cross contamination between patients. Lesions that are positive on VELscope® examination are suggested to be observed for 2 weeks for resolution, or else biopsy is recommended [11].

9.3 Chemiluminescence

The technique of chemiluminescence was first applied in the detection of cervical dysplasia. ViziLite® is the popular device that employs the principle of chemiluminescence developed by Zila Pharmaceuticals (Phoenix, AZ). In 2001, it received FDA clearance. This technology is utilized in gynecology, where it was termed as "speculoscopy" and is followed by thorough cervical examination [12]. Commercial chemiluminescence devices are either peroxyoxalate or luminol based systems. Three commercially available devices operate with the working principle of chemiluminescence for detection of oral cancer. They include ViziLite®, ViziLite Plus®, and Microlux/DL™. In the oral cancer setting, chemiluminescence was shown to be superior to tolonium chloride [13]. The specificity of ViziLite® was poor, but accuracy was 80%. They (ViziLite® and ViziLite Plus®) were able to improve brightness, sharpness, texture, and size of the lesion [14, 15]. This technique is entirely based on reflectance of oral tissue as a result of the increased nuclear-cytoplasmic ratio.

The examination is done in a dim lighted room to facilitate lesion recognition. It is best to photograph the observations made by ViziLite® for documentation purposes. The ViziLite® kit has (a) 1.1% acetic acid rinse; (b) capsule which contains sodium benzoate, propylene glycol, and alcohol base; and (c) retractor. Once activated, the glass vial containing hydrogen peroxide breaks and reacts with acetylsalicylic acid (aspirin). The energy liberated in this reaction is absorbed by a fluorescent dye to convert it into white light. In the chemiluminescence system, a light of specific wavelength is emitted from a reaction between hydrogen peroxide and acetylsalicylic acid inside a light stick [16]. The reaction produces blue light at the desired wavelength for exposure of oral tissues. It involves the use of an oral rinse of acetic acid (1%) for 1 minute followed by examination of oral mucosa under diffuse chemiluminescent low-energy blue/white light at a wavelength of 490–510 nm. The chemiluminescence test has an acetic acid prerinse step to remove debris and glycoprotein coat that limits passage of light through tissue. Acetic acid desiccates the tissue, coagulates, and precipitates proteins on the epithelial surface. The majority of potentially malignant disorders (75%) were aceto-white. The theory behind this observation is that acetic acid removes glycoprotein and slightly desiccates the oral mucosa. Hence, the normal mucosa will appear blue, while the abnormal mucosa will reflect light due to high nuclear-cytoplasmic ratio. Furthermore, abnormal mucosa appears more aceto-white and brighter, with sharper and more distinct margins. In a typical exam, the occurrence of acetowhite staining is considered as "positive," and the absence of acetowhitening is considered as "negative."

Recently, the ViziLite® system was modified to include toluidine blue (ViziLite Plus®-toluidine blue system). The major disadvantage with ViziLite® kit is that it is a single-use product. The ViziLite Plus® kit consists of swab components with 1% acetic acid rinse, toluidine blue, and a decolorizer [12]. The toluidine blue in ViziLite Plus® improves the visualization by chemiluminescence. In a large patient cohort, leukoplakias were more significantly aceto-white than erythroplakia [17]. In a study comparing efficacy of chemiluminescent light, toluidine blue and exfoliative cytology, the chemiluminescent test was shown to generate reliable results [18]. Several studies have shown high sensitivity with ViziLite Plus®, although low specificity was the main limitation [15–18]. Identification and delineation of dysplasia is challenging, but potentially malignant lesions can be easily identified. In summary, the ViziLite Plus® chemiluminescence system can be used as a supplementary investigation following routine oral examination to improve identification of oral abnormalities [17].

Microlux/DL™ is a battery-operated device with comparable efficacy to ViziLite® and ViziLite Plus® [19]. Microlux/DL™ was shown to enhance clinical visibility, but could not uncover clinically invisible lesions. The overall sensitivity and specificity were 77.8% and 70.7%, respectively [19]. Adding toluidine blue did not increase the efficacy of Microlux/DL™ [20]. Further studies are needed on the efficacy of Microlux/DL™.

9.4 Multispectral Fluorescence-Reflectance Imaging

Identafi® 3000 is the most recent of commercially available optical devices for detection of oral cancer. The system utilizes multispectral fluorescence and reflection technology to enhance visualization of mucosal abnormalities. This small, cordless, handheld device, similar to a dental airotor, offers a three-wavelength optical illumination and visualization system. Identafi® 3000 uses white, violet, and green-amber wavelengths of light which excite the oral tissues. Reusable eye wear is available which enhances contrast and visual effect and allows transmission of reflected light. In the first stage, concentrated white light is used for a thorough oral examination. The clinician then switches to violet to make second observation. Violet light (405 nm) excites oral tissues that exhibit intrinsic fluorescence. Suspected lesions do not exhibit fluorescence and therefore appear dark. There is sufficient evidence that violet light can differentiate normal and cancerous tissue with high sensitivity and specificity [8, 21]. When an abnormality is suspected, the clinician switches to green-amber light (540–575 nm), which enhances the tissue's reflectance to allow the clinician to directly observe the tissue vascularity [22], which can be used to make a tentative diagnosis. In the normal mucosa, the vasculature is clearly defined, while malignant or OPMDs exhibit dilated and diffuse vascular architecture that is more diffuse. This multispectral light system gives more visual information to the clinician, supporting decision-making on suitable management [23].

Identafi® 3000 has been shown to exhibit high sensitivity (82%) and specificity (87%) in differentiating neoplastic from nonneoplastic tissue [24]. The degree of vascularity observed using the system has been shown to correlate with expression of CD34 in histological sections [22]. Overall, 66% agreement was observed between clinical and histological grade [22]. The increase in vascularity was not limited to carcinomas, but even simple leukoplakias, hyperkeratotic lesions and lichen planus have demonstrated increased vascularity. Patients with severe clinical (green-amber light visualization) and histological grade of vascularity may be kept for future follow-up, but this consideration needs validation.

9.5 Narrow Band Imaging

Generally, endoscope-connected narrow band imaging (NBI) systems are useful in the visualization of the posterior oral cavity (oropharynx) not accessible during routine oral examination. In the past, it was applied mainly to the larynx, esophagus, stomach, and colon. The extensive work of Yang et al. [25–29] has provided foundational evidence on the use of NBI in oral malignant lesions and potentially malignant disorders and has shown specific in vivo application [30, 31]. NBI has been used in the identification of high-grade dysplasia/carcinoma in oral erythroplakia [31]. Ottaviani et al., have shown that NBI can also be used tumor angiogenesis [32]. In a more recent meta-analysis by Zhou et al. on head and neck cancer which included 6187 lesions, the overall area under the summary receiver operating characteristic (SROC) curve was 96.94% and for oral and oropharyngeal cancers (1071 lesions), the area under the SROC curve was 94.53% [33].

9.5.1 Principle

Endoscope-guided NBI enhances the visualization of oral tissue through the magnification of mucosal texture and vascularity. As a result, NBI provides more information than broadband white light images. In NBI, white light is filtered to produce two narrow bands (~30 nm) of blue and green light (Fig. 9.2a) [34]. The blue band (415 nm) corresponds to the Soret absorption peak of hemoglobin, and the green band (540 nm) supports the visualization of underlying vasculature [34, 35] (Fig. 9.2b). Imaging at the blue wavelength reveals superficial, fine vasculature, while the green wavelength light reveals deeper vessels with large diameter (Fig. 9.2c). In normal tissues, the capillaries in connective tissue below the epithelium are visible because many regions of the oral mucosa are free of appendages, except for the minor salivary glands. Capillaries in the floor of mouth, lip, and buccal mucosa are more

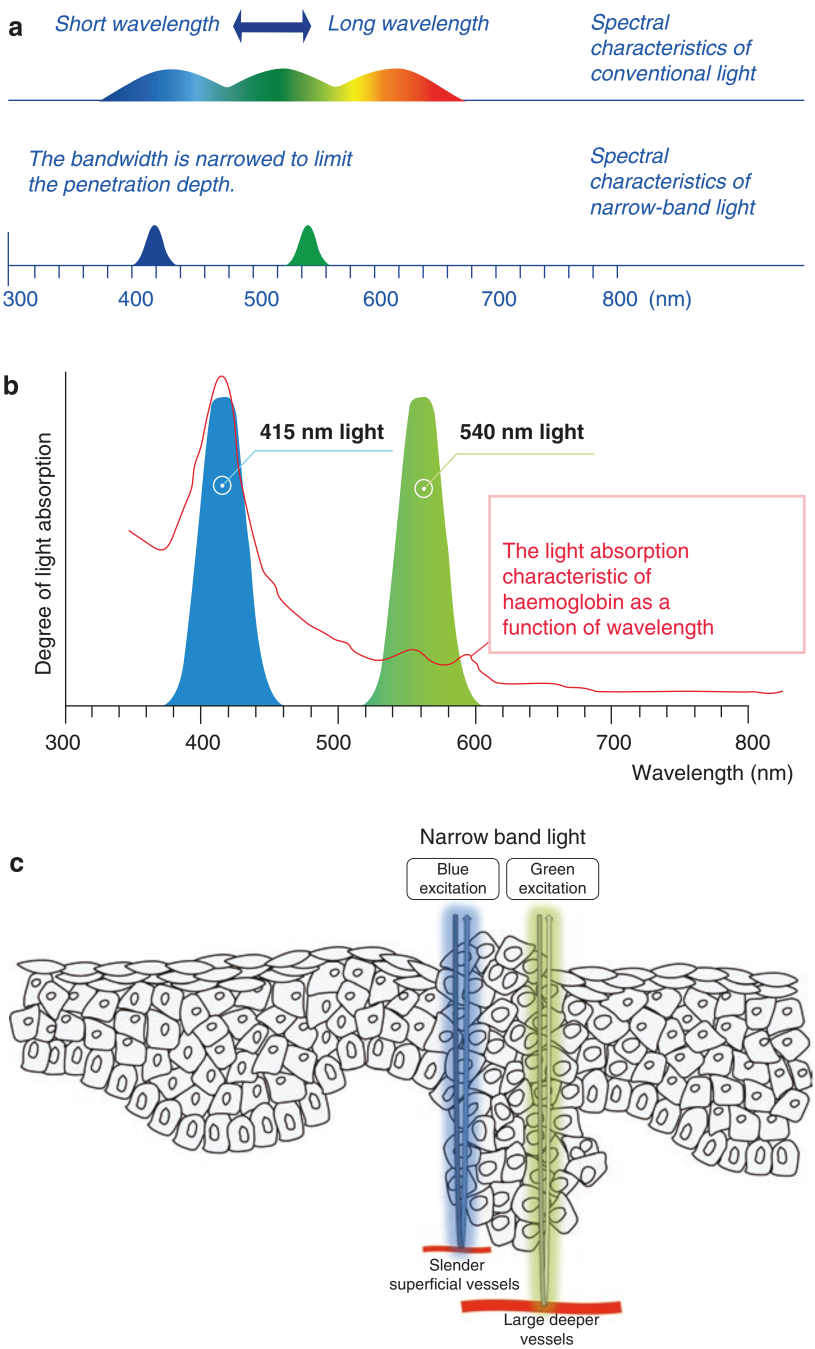

Fig. 9.2 Panel (**a**): Spectral characteristics of conventional white light, and narrow band light is blue-green spectrum; Panel (**b**): the absorptive characteristics of hemoglobin which falls within the blue and green spectrum; Panel (**c**): Illumination of visible light in narrow wavelength band (centered on blue and green spectrum). The absorption and reflectance gives a neat picture of the underlying vasculature as it contains hemoglobin, the major endogenous chromatophores. The distribution of slender peripheral vessels and larger deep submucosal veins is distinctive. (**a** and **b** courtesy of Olympus)

prominent than capillaries at other locations like the ventral tongue [36]. The rete pegs and connective tissue papilla are closely connected and intact, forming uniform loops. In cancer, when the association between rete pegs and underlying connective tissue is lost, the homogenous arrangement of microvasculature in tissue is disrupted. In advanced cancers, the high growth rate of capillaries may be also visualized as discolored areas or spotting of tissue. Based on the pattern of tumor growth (inward or outward), this architecture and organization of vessels is disturbed leading to an irregular pattern. At the tissue level, three phenomena occur in and around transformed tissue which are detectable by NBI: (i) vascularization due to tumor angiogenesis, (ii) vascular destruction due to uncontrolled proliferation, and (iii) displacement of existing vasculature leading to irregular vessel pattern or discolored appearance of cancer tissue [36]. NBI is based on the intrapapillary capillary loops (IPCL), and microvascular morphology detected by narrow band imaging (NBI) can assist in diagnosis. Normal mucosa shows regular looping in uniform pattern (Type I), nonneoplastic lesions show mild change in morphology (Type II, Type III), and neoplastic lesions show irregular pattern with several loop shapes (Type III, Type IV) [37] (Table 9.2). In NBI, the severity of OSCC as measured by tumor size, nodal status, TNM stage, lymphovascular or perineural invasion, depth of tumor infiltration, and

Table 9.2 Comparison of IPCL patterns in suspicious oral lesions

Type I	Regular brown dots	• Normal mucosa • Homogenous Leukoplakia • Squamous hyperplasia	Low risk IPCL pattern
Type II	Dilation and crossing		
Type III	Elongated and meandering	• High-grade dysplasia • Carcinoma in situ • Carcinoma in leukoplakia • Carcinoma in erythroplakia • Carcinoma in non-healing ulcers	High risk IPCL pattern
Type IV	Destruction and angiogenesis		

IPCL patterns advance with increasing severity of pathology; the destructive pattern is associated with the most advanced carcinomas (classification of Takano et al. [37] and IPCL correlation adapted from Yang et al. [25–29, 31, 38])

tumor differentiation was associated with specific morphological patterns in intrapapillary microvasculature, with PCL destruction from tumor angiogenesis being associated with more advanced disease stage [38]. Takano et al. have demonstrated the value of NBI as a potential tool for the detection of early cancer, and microvascular organization is a dependable biomarker of oral cancer [37]. A narrow band image of high-grade dysplasia and oral cancer shows increased number of tortuous, dilated, twisted, elongated, and corkscrew vessel morphology (Fig. 9.3) [31]. Elongated, twisted, and destructive pattern are indicators of dysplasia, carcinoma in situ, and invasive carcinoma arising in 'erythroplakia' [31].

NBI is a safe, noninvasive endoscopic imaging method for detailed viewing of oral cancer, oral leukoplakia, and erythroplakia [29, 36, 37]. NBI has also been used in the identification of squamous cell carcinoma arising in nonhealing ulcers [36]. Furthermore, NBI is capable of evaluating microvascular organization and provides clear images for simplified clinical decision-making. Understanding the intrapapillary capillary loops (IPCL) during oral carcinogenesis could potentially enhance the clinical utility of NBI [37, 38]. Changes in IPCL have been previously correlated with invasion depth of esophageal SCC and histological atypia [39]. IPCL patterns have also been correlated with increased severity in leukoplakia [29]. Additionally, IPCL was the only independent factor associated with the occurrence of squamous cell carcinoma in oral chronic nonhealing ulcers [36]. Some individuals with early cancer also presented with brown coloration on NBI [36, 37]. Future studies should continue to focus on the identification and characterization of specific microvascular patterns relating to different stages in the evolution of cancer and molecular parameters [34]. A multispectral digital microscope was recently developed which creates images in narrow band, fluorescence, and orthogonal polarized reflectance mode [35]. NBI has also been applied in robotic-guided surgical procedures in HNSCC for identification of margin dysplasia to obtain safe surgical margins in anatomically challenging areas to minimize morbidity and functional preservation of normal tissue.

Fig. 9.3 Suspicious oral lesions under NBI light showing different IPCL vessel patterns. (**a**) Dilatation, meandering of capillaries (intramucosal cancer); (**b**) dilatation, meandering, calibre change, nonuniformity of intrapapillary capillary loop (intramucosal cancer); (**c**) uniform small dots in submucosally (carcinoma in situ); (**d**) thin capillaries uniformly distributed between white spotted lesion (inflammatory pathology-hyperplastic candidiasis); (e) inflammatory base with uniformly distributed capillaries in submucosal plane; (**f**) hyperkeratotic lesion ("umbrella effect") without surrounding mucosal changes (homogenous leukoplakia) (courtesy of Rakesh Srivastava, India)

9.6 Quest for Deep Tissue Imaging

Light-based systems exploit tissue features like epithelial thickness, blood vessel pattern (vascularity), and cellular features like nuclear-cytoplasmic ratio to generate structural and functional information on these tissues. Alterations of these tissue characteristics can therefore be exploited to differentiate normal tissues from those that have undergone or are undergoing malignant transformation [23].

There is some contradicting evidence on the role of light-based detection methods for oral cancer screening [40]. The scope of optical tools in diagnosis has increased due to their ease of use, short image acquisition times, and lower cost compared to traditional radiologic techniques such as PET or CT. Furthermore, these noninvasive optical imaging methods are patient-friendly (less intimidating or claustrophobic) and offer the ability to provide structural and functional information in real time. Moreover, optical imaging can be repeated frequently without risk of exposure to ionizing radiation or radioactive tracers [23]. However, depth of penetration is a limitation for most optical methods (in the order of millimeters) that contributes to inadequate visualization of subsurface layers in tomographic sections. Increased scattering of light with increasing depth is the primary limitation of traditional ballistic optical imaging methods which restricts imaging depths to a few millimeters. In this regard, photoacoustic imaging (PAI) is a hybrid optical and ultrasound imaging method that exploits optical properties of tissue to provide molecular information of tissue at imaging depths typically associated with ultrasound. The following section describes the potential of this emerging advanced optical imaging method since it is currently not readily available for clinical application but has strong potential as a chairside tool in the near future. However, it is important to remember that all optical techniques are ultimately intended to serve as adjuvant aids that compliment clinical assessment.

9.7 Photoacoustic Imaging

PAI is a hybrid imaging technique that combines optics and ultrasound (US) and is based on the photoacoustic effect [41]. The photoacoustic effect was first explored by Alexander Graham Bell [42] and is a phenomenon wherein light is absorbed by photoabsorbers within a medium resulting in a localized thermoelastic expansion, producing pressure waves that can be acoustically detected [42]. It took 100 years to evolve as a biomedical imaging technique (1981) based on fundamental work by Dr. Theodore Bowen [43–45]. However, it was not until the 1990s that PAI was developed for imaging in tissues, pioneered by Dr. Robert Kruger [46, 47]. Similar to conventional optical techniques, PAI can detect endogenous chromophores through multispectral excitation and detection of the unique absorption profile of each chromophore [48]. In this manner, PAI can provide important molecular information of tissue at clinically relevant imaging depths (on the order of several centimeters).

9.7.1 Principle

PAI can be considered an ultrasound-based imaging method with light-generated contrast. The generation of PA signal relies on three steps (Fig. 9.4): (1) deposition of electromagnetic energy (EM) into the tissue being imaged, (2) absorption of the EM energy by photoabsorbers within tissue, and (3) thermal expansion of optical species in tissue to release pressure waves detectable by US [48, 49]. Whereas traditional optical imaging techniques are limited to 2–3 mm due to relatively high scattering of light in tissue, tissues show low acoustic scattering (1/1000 times less than optical scattering) allowing for significantly improved imaging depths in the order of centimeters [48].

Contrast in PAI is influenced by the optical absorption coefficient and concentration of photoabsorbers in each tissue type [50, 51]. PAI works optimally on tissues with high optical coefficients like blood vessels which contain high levels of hemoglobin [52]. PAI can also be performed at longer infrared wavelengths as it is not as rapidly absorbed by tissue and can therefore penetrate deep in tissue [50]. The main optical absorbers and generators of photoacoustic signal in tissue are hemoglobin, melanin, lipids, and water [53]. In vivo photoacoustic signal that returns from these endogenous species in tissue can be used to obtain structural and functional information including vascular hemodynamics, hemoglobin concentration, oxygen saturation, and tissue composition of photoabsorbers [53]. Image reconstruction allows for the localization of photoabsorbers within tissue through time and amplitude-based detection of PA signal. In the majority of commercially available PAI systems, the light source and ultrasonic detector are incorporated together into a single transducer for more efficient work flow. The two most common PAI systems utilize either a ring/bowl array where piezoelectric elements are positioned around the tissue being imaged or a linear array where piezoelectric elements line the face of the image probe [48, 49]. In the first design, generated PA signal is detected at multiple positions around the tissue and then back-projected to determine the original

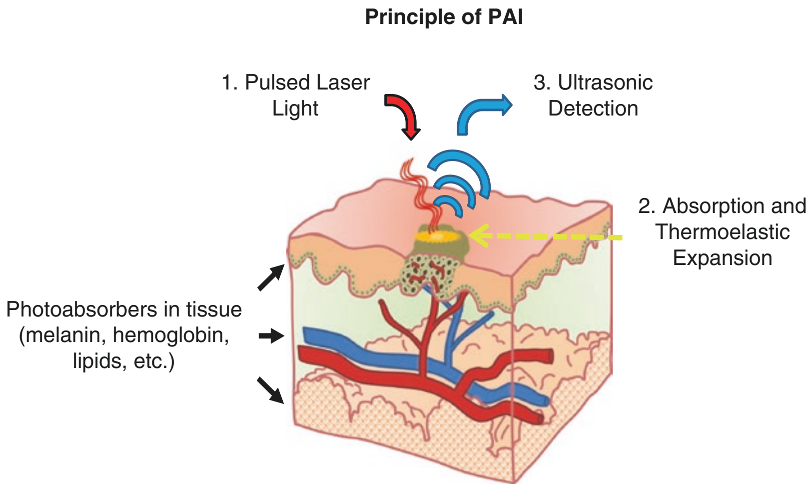

Fig. 9.4 Principles of PA signal generation. Light is pulsed into tissue (1) where it is absorbed by photoabsorbers (2), resulting in pressure waves that can be detected by ultrasound (3)

source of the PA signal, similar to reconstruction methods used for x-ray computed tomography [51]. The second design functions similar to standard ultrasound where the generated PA signal is detected by individual elements along the axis of the probe corresponding to a specific image segment [54]. In this method, the light pulse is synchronized with the image acquisition time to allow for accurate spatial localization of the photoabsorber. Photoabsorber depth is then estimated by measuring the time of PA signal arrival. While tomographic techniques can provide greater sensitivity and resolution compared to that of linear array techniques, linear array techniques readily allow for simultaneous PAI and US enabling structural, functional, and molecular imaging of tissue [55–58].

9.7.2 Contrast Agents in PAI

9.7.2.1 Endogenous Contrast Mechanisms

In oral cancer, angiogenesis and hypoxia are a fundamental process, and their grade increases with severity of malignancy [59, 60]. Consequently, PA-based assessment of tissue hemoglobin and oxygenation could assist in the diagnosis and staging of oral lesions. Early work by Oraevsky and colleagues highlighted the potential of PAI for detecting DMBA-induced oral lesions in the hamster buccal pouch carcinoma model [61, 62]. In the same model, Fatakdawala et al. evaluated the ability of PAI to detect both precancerous and cancerous lesions within the oral cavity [63]. PAI detected high vascular density in oral lesions compared to normal oral mucosa associated with increased angiogenesis. Furthermore, they were able to detect increased accumulation of mucin, a key component of mucus, in precancerous lesions. In ex vivo thyroid tissue specimens, Dogra et al. found that malignant samples had significantly higher deoxyhemoglobin levels than both benign and normal thyroid tissue samples, indicating that the oxygenation status of suspicious lesions can also be used to identify malignant tissues [64]. A recent study evaluating the ability of PAI to differentiate malignant and benign thyroid nodules in vivo found that malignant lesions had higher PA signals at 760, 850, 930, and 950 nm wavelengths [65]. Multiple studies in preclinical models of oral and head and neck cancers have also highlighted the potential of PAI for tumor oxygenation kinetics and response to chemotherapy and radiation [66, 67]. These studies have demonstrated that PAI can be effectively utilized for frequent and repeated assessment of tumor oxygenation before, during, and after radiation therapy (RT) [67]. Recent work has also revealed the potential of PAI based biomarkers of oxygenation as early indicators of therapeutic efficacy [67, 68].

9.7.2.2 Exogenous Contrast Agents

While the ability of PAI to detect endogenous chromophores is a major strength of the technique, exogenous contrast agents can also be utilized to enhance contrast and signal-to-noise (SNR) in PAI [69–71]. Several classes of agents ranging from near-infrared optical dyes such as indocyanine green (ICG), metal or semiconducting nanoparticles such as gold or silver nanorods, and organic nanostructures such as chimeric polypeptide nanoparticles have been studied for their utility as contrast agents for PAI [70]. These agents can be administered as neat solutions without targeting moieties to measure vascular parameters, or with targeting ligands to visualize molecular processes.

Recently, nanostructures prepared from gold and silver have been used as exogenous contrast agents for PAI [72]. The advantage of gold nanoparticles is their strong optical absorption due to their high cross section tuned to the optical window (~730 nm). This minimizes PA signal from endogenous absorption while maximizing imaging depth [41]. These metallic nanoparticles have a fivefold to ninefold higher optical absorption due to surface plasmon resonance (SPR), the property by which incident light excites the outer electrons in metals producing oscillations of conducting electrons [73]. SPR structures used for PAI include gold nanoclusters, gold nanospheres, gold nanorods, gold nanoshells, gold cages, and silver nanoplates [72]. Injection and accumulation of these agents in tumors produces increased PA signal associated with tumor angiogenesis and vascular perfusion [73]. Consequently, these agents have been used for selective identification of tumors from non-tumor tissue [74] and to assess temporal and spatial changes in PA signal corresponding to areas of high vascular perfusion [75]. In head and neck tumor models, PAI has been shown to detect differential uptake of EGFR and human epidermal growth factor receptor 2 (HER2) targeted gold nanorods, highlighting the potential of PAI for molecular profiling of tumors and treatment planning of OSCC patients [76]. In addition to standard PEGylated metallic nanoparticles, silica coated hybrid particles show stable and improved PAI signal [77, 78]. A threefold enhancement in PA signal was seen in silica-coated gold rods [78]. However, biodegradable nanoparticles are preferable as metallic particles pose risk of toxicity due to accumulation.

PAI studies have also utilized NIR absorbing dyes (methylene blue, indocyanine green) to enhance PAI contrast as they are inexpensive, widely available, and approved for clinical use (Figs. 9.5 and 9.6) [76]. Their structure is typically comprised of a series of conjugated double bonds in ring system which lowers the energy necessary for excitation [77]. The two US Food

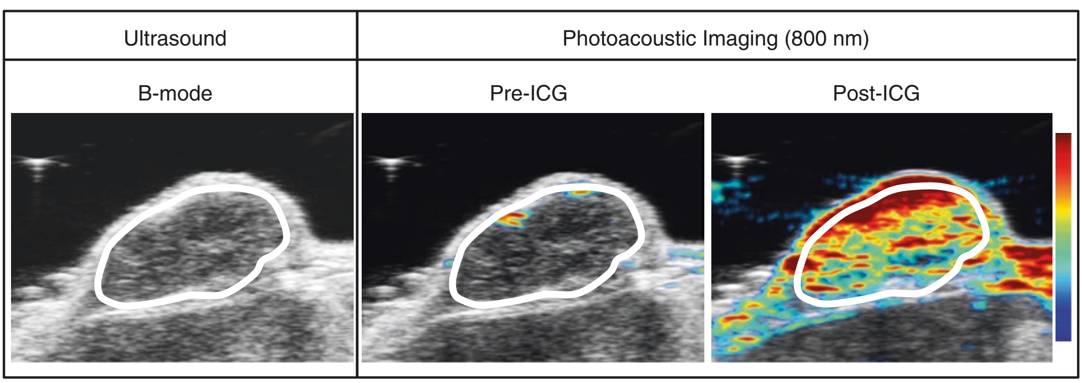

Fig. 9.5 Enhancement of photoacoustic imaging signal using an exogenous dye. (Left) B-mode ultrasound image shows presence of subcutaneous patient derived head and neck tumor xenograft (white outline) grown in a severe combined immunodeficient mouse. (Right) Photoacoustic signal intensity maps (800 nm) acquired before and immediately following injection of 2 mM indocyanine green (ICG) dye (200 μl). Following injection, vascularized areas show a noticeable increase in photoacoustic signal (areas of red)

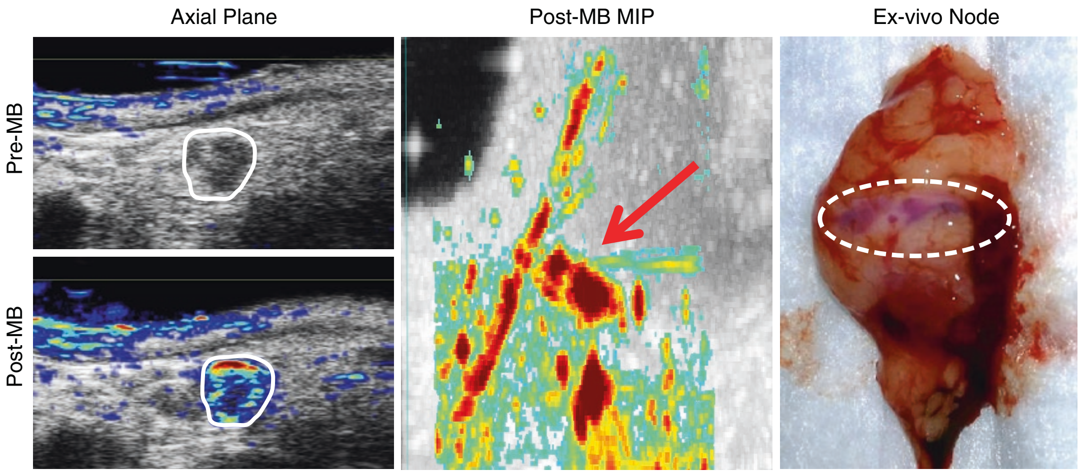

Fig. 9.6 Photoacoustic lymphangiography of a draining lymph node in a New Zealand white rabbit. (Left) Photoacoustic signal intensity maps (680 nm) of the parotid lymph nodes before and immediately following injection of 1% methylene blue (MB) dye in the rabbit ear. (Middle) Maximum intensity projection (MIP) showing the draining lymph vessel tract and accumulated dye in the parotid lymph node (red arrow). (Right) Ex vivo white light image of the rabbit parotid gland removed following imaging shows dye accumulating in the node (white circle)

and Drug Administration-approved dyes, indocyanine green (ICG) and methylene blue, can also serve as effective contrast agents for PAI of tumors and tumor-draining lymph nodes (Fig. 9.6). Studies have demonstrated the potential of PA-guided tumor lymphangiography for mapping of sentinel lymph nodes [79, 80]. Porphyrins are also organic compounds that are highly tunable and have intense absorptive properties allowing for PAI [81]. Using porphyrin nanoparticles, Muhanna and colleagues used PAI prior to photothermal therapy to measure the drug uptake levels in the VX2 carcinoma model of invasive OSCC, showing that PAI can be used to guide cancer therapies to improve treatment efficacy [82]. Targeting moieties have also been added to optical dyes to increase their tumor specificity and to identify molecular processes. Using a novel caspase-9 near-infrared PAI probe, Yang et al. were able to detect increased contrast uptake in tumors 24 h after treatment with cisplatin [83].

Luke et al. used PAI to detect metastatic cervical lymph nodes in mice bearing FaDu tumors of the tongue, by measuring the uptake of EGFR-targeted molecularly activated plasmonic nanosensors following peritumoral injection [84]. Importantly, their method provided a sensitivity and specificity of 100% and 87.5% compared to 50% and 87% of current PET methods. The ability of PAI to detect metastatic lesions was also assessed using a VX2 carcinoma large animal model of invasive OSCC, where dual PA and fluorescent nanoparticles were injected into the peritumoral space and used to guide surgical resection of tumor-draining lymph nodes [85]. Luke et al. also showed that it was possible to detect metastatic nodes without the need for exogenous contrast as metastatic lymph nodes had significantly lower %sO_2 levels than healthy nodes, although their sensitivity and specificity was reduced to 71% and 83%, respectively [86]. This is a considerable advantage over conventional lymphangiography methods as it would not require the administration of exogenous agents for the detection of sentinel lymph nodes.

In summary, PAI has the potential to become a simple dental chairside or bedside imaging tool for the diagnosis and staging of oral cancer. The development of compact PAI systems with co-registered US could facilitate widespread clinical utilization of this promising imaging modality. Enhancing PAI signal using exogenous agents can significantly improve PAIs' ability to detect and characterize oral lesions and could have a role for treatment planning and therapeutic response monitoring.

Conclusion

Optical imaging methods can probe the tissue architectural, cellular, biochemical, and metabolic landscape in oral cancer. Given their ease of use, a number of optical imaging methods have been studied for clinical applications in oral oncology. Tissue architectural changes in precancerous and cancerous tissues affect their optical properties and can be visualized using autofluorescence, chemiluminescence, multispectral fluorescence, and narrow band imaging methods. Optical and optoacoustic imaging methods using exogenously administered optical contrast agents for cancer diagnosis have also shown promise. Combined or multimodal application of these optical techniques can improve their diagnostic utility. However, the optical imaging methods can only serve as adjuvant tools. The findings from using these aids should always be interpreted in the context of clinical examination and are often useful when performed by skilled and experienced clinicians. Future developments in hardware and improved algorithms could improve their overall diagnostic power and enable creation of cheap, easy-to-use, and reliable tools for in vivo visualization of oral cancer and precancer.

Acknowledgments Support from R01CA204636, R01DE024595, S10OD010393-01, and P30CA06156 is gratefully acknowledged.

References

1. Utzinger U, Bueeler M, Oh S, Heintzelman DL, Svistun ES, Abd-El-Barr M, et al. Optimal visual perception and detection of oral cavity neoplasia. IEEE Trans Biomed Eng. 2003;50:396–9.
2. Lane PM, Gilhuly T, Whitehead P, Zeng H, Poh CF, Ng S, et al. Simple device for the direct visualization of oral-cavity tissue fluorescence. J Biomed Opt. 2006;11:024006.
3. Laronde DM, Williams PM, Hislop TG, Poh C, Ng S, Bajdik C, et al. Influence of fluorescence on screening decisions for oral mucosal lesions in community dental practices. J OralPathol Med. 2014;43: 7–13.
4. Skala MC, Riching KM, Gendron-Fitzpatrick A, Eickhoff J, Eliceiri KW, White JG, et al. In vivo multiphoton microscopy of NADH and FAD redox states, fluorescence lifetimes, and cellular morphology in precancerous epithelia. Proc Natl Acad Sci U S A. 2007;104:19494–9. Epub 2007 Nov 27
5. Arifler D, Pavlova I, Gillenwater A, Richards-Kortum R. Light scattering from collagen Fiber networks: micro-optical properties of normal and neoplastic Stroma. Biophys J. 2007;92:3260–74.
6. Pavlova I, Weber CR, Schwarz RA, Williams MD, Gillenwater AM, Richards-Kortum R. Fluorescence spectroscopy of oral tissue: Monte Carlo modeling with site-specific tissue properties. J Biomed Opt. 2009;14:014009.
7. Pavlova I, Williams M, El-Naggar A, Richards-Kortum R, Gillenwater A. Understanding the biological basis of autofluorescence imaging for oral cancer detection: high-resolution fluorescence microscopy in viable tissue. Clin Cancer Res. 2008;14:2396–404.
8. Lane P, Lam S, Follen M, MacAulay C. Oral fluorescence imaging using 405-nm excitation, aiding the discrimination of cancers and precancers by identifying changes in collagen and elastic breakdown and neovascularization in the underlying stroma. Gend Med. 2012; 9: S78–82.e1–8.
9. Poh CF, Zhang L, Anderson DW, Durham JS, Williams PM, Priddy RW, et al. Fluorescence visualization detection of field alterations in tumor margins of oral cancer patients. Clin Cancer Res. 2006;12:6716.
10. Shin D, Vigneswaran N, Gillenwater A, Richards-Kortum R. Advances in fluorescence imaging techniques to detect oral cancer and its precursors. Future Oncol. 2010;6:1143–54.
11. Kois JC, Truelove E. Detecting oral cancer: a new technique and case reports. Dent Today. 2006;25: 96–7.
12. Shashidara R, Sreeshyla HS, Sudheendra US. Chemiluminescence: A diagnostic adjunct in oral precancer and cancer: a review. J Cancer Res Ther. 2014;10:487–91.
13. Ram S, Siar CH. Chemiluminescence as a diagnostic aid in the detection of oral cancer and potentially malignant epithelial lesions. Int J OralMaxillofac Surg. 2005;34:521–7.
14. Mojsa I, Kaczmarzyk T, Zaleska M, Stypulkowska J, Zapala-Pospiech A, Sadecki D. Value of the ViziLite plus system as a diagnostic aid in the early detection of oral cancer/premalignant epithelial lesions. JCraniofac Surg. 2012;23:e162–4.
15. Awan KH, Morgan PR, Warnakulasuriya S. Utility of chemiluminescence (ViziLite™) in the detection of oral potentially malignant disorders and benign keratoses. J Oral Pathol Med. 2011;40:541–4.
16. Nagi R, Reddy-Kantharaj YB, Rakesh N, Janardhan-Reddy S. Sahu S. Efficacy of light based detection systems for early detection of oral cancer and oral

potentially malignant disorders: systematic review. Med Oral Patol Oral Cir Bucal. 2016;21:e447–55.
17. Kerr AR, Sirois DA, Epstein JB. Clinical evaluation of chemiluminescent lighting: an adjunct for oral mucosal examinations. J Clin Dent. 2006;17:59–63.
18. Rajmohan M, Rao UK, Joshua E, Rajasekaran ST, Kannan R. Assessment of oral mucosa in normal, precancer and cancer using chemiluminescent illumination, toluidine blue supravital staining and oral exfoliative cytology. J Oral Maxillofac Pathol. 2012;16:325–9.
19. McIntosh L, McCullough MJ, Farah CS. The assessment of diffused light illumination and acetic acid rinse (Microlux/DL) in the visualisation of oral mucosal lesions. Oral Oncol. 2009;45:e227–31.
20. Ibrahim SS, Al-Attas SA, Darwish ZE, Amer HA, Hassan MH. Effectiveness of the Microlux/DL™ chemiluminescence device in screening of potentially malignant and malignant oral lesions. Asian Pac J Cancer Prev. 2014;15:6081–6.
21. Roblyer D, Kurachi C, Stepanek V, Williams MD, El-Naggar AK, Lee JJ, et al. Objective detection and delineation of oral neoplasia using autofluorescence imaging. Cancer Prev Res (Phila). 2009;2:423–31.
22. Messadi DV, Younai FS, Liu HH, Guo G, Wang CY. The clinical effectiveness of reflectance optical spectroscopy for the in vivo diagnosis of oral lesions. Int J Oral Sci. 2014;6:162–7.
23. Wilder-Smith P, Holtzman J, Epsteinz J, Le A. Optical diagnostics in the oral cavity: an overview. Oral Dis. 2010;16:717–28.
24. Schwarz RA, Gao W, Weber CR, Kurachi C, Lee JJ, El-Naggar AK, et al. Noninvasive evaluation of oral lesions using depth-sensitive optical spectroscopy. Cancer. 2009;115:1669–79.
25. Yang SW, Lee YS, Chang LC, Chien HP, Chen TA. Clinical appraisal of endoscopy with narrow-band imaging system in the evaluation and management of homogeneous oral leukoplakia. ORL J OtorhinolaryngolRelat Spec. 2012;74:102–9.
26. Yang SW, Lee YS, Chang LC, Hwang CC, Chen TA. Diagnostic significance of narrow-band imaging for detecting high-grade dysplasia, carcinoma in situ, and carcinoma in oral leukoplakia. Laryngoscope. 2012;122:2754–61.
27. Yang SW, Lee YS, Chang LC, Hwang CC, Chen TA. Use of endoscopy with narrow-band imaging system in detecting squamous cell carcinoma in oral chronic non-healing ulcers. Clin Oral Investig. 2014;18:949–59.
28. Yang SW, Lee YS, Chang LC, Chien HP, Chen TA. Light sources used in evaluating oral leukoplakia: broadband white light versus narrowband imaging. Int J Oral Maxillofac Surg. 2013;42:693–701.
29. Yang SW, Lee YS, Chang LC, Hwang CC, Luo CM, Chen TA. Use of endoscopy with narrow-band imaging system in evaluating oral leukoplakia. Head Neck. 2012;34:1015–22.
30. Green B, Cobb AR, Brennan PA, Hopper C. Optical diagnostic techniques for use in lesions of the head and neck: review of the latest developments. Br J Oral Maxillofac Surg. 2014;52:675–80.
31. Yang SW, Lee YS, Chang LC, Hwang CC, Luo CM, Chen TA. Clinical characteristics of narrow-band imaging of oral erythroplakia and its correlation with pathology. BMC Cancer. 2015;15:406.
32. Ottaviani G, Gobbo M, Rupel K, D'Ambros M, Perinetti G, Di Lenarda R, et al. The diagnostic performance parameters of narrow band imaging: a preclinical and clinical study. Oral Oncol. 2016;60:130–6.
33. Zhou H, Zhang J, Guo L, Nie J, Zhu C, Ma X. The value of narrow band imaging in diagnosis of head and neck cancer: a meta-analysis. Sci Rep. 2018;8:515.
34. Vu A, Farah CS. Narrow band imaging: clinical applications in oral and oropharyngeal cancer. Oral Dis. 2016;22:383–90.
35. Roblyer D, Richards-Kortum R, Sokolov K, El-Naggar AK, Williams MD, Kurachi C, et al. Multispectral optical imaging device for in vivo detection of oral neoplasia. J Biomed Opt. 2008;13:024019.
36. Shibahara T, Yamamoto N, Yakushiji T, Nomura T, Sekine R, Muramatsu K. Narrow-band imaging system with magnifying endoscopy for early oral cancer. Bull Tokyo Dent Coll. 2014;55:87–94.
37. Takano JH, Yakushiji T, Kamiyama I, Nomura T, Katakura A, Takano N, et al. Detecting early oral cancer: narrow band imaging system observation of the oral mucosa microvasculature. Int J OralMaxillofac Surg. 2010;39:208–13.
38. Yang SW, Lee YS, Chang LC, Hsieh TY, Chen TA. Implications of morphologic patterns of intraepithelial microvasculature observed by narrow-band imaging system in cases of oral squamous cell carcinoma. Oral Oncol. 2013;49:86–92.
39. Sato H, Inoue H, Ikeda H, Sato C, Onimaru M, Hayee B, et al. Utility of intrapapillary capillary loops seen on magnifying narrow-band imaging in estimating invasive depth of esophageal squamous cell carcinoma. Endoscopy. 2015;47:122–8.
40. Lingen MW, Tampi MP, Urquhart O, Abt E, Agrawal N, Chaturvedi AK, et al. Adjuncts for the evaluation of potentially malignant disorders in the oral cavity: Diagnostic test accuracy systematic review and meta-analysis-a report of the American Dental Association. J Am Dent Assoc. 2017;148:797–813.e52.
41. Wang LV, Hu S. Photoacoustic tomography: in vivo imaging from organelles to organs. Science. 2012;335:1458–62.
42. Bell AG. On the production and reproduction of sound by light. Am J Sci. 1880;118:305–24.
43. Bowen T, Nasoni RL, Pifer AE, Sembroski GH. Some experimental results on the thermoacoustic imaging of tissue equivalent phantom materials. Ultrasonics Symposium. 1981:823–7.
44. Bowen T. Radiation-induced thermoacoustic soft tissue imaging. Ultrasonics Symposium. 1981:817–22.
45. Bowen T, Nasoni RL, Pifer AE. Thermoacoustic imaging induced by deeply penetrating radiation. Acoustical Imaging. 1984;13:409–27.

46. Kruger RA. Photoacoustic ultrasound. Med Phys. 1994;21:127–31.
47. Kruger RA, Liu P, Appledorn CR. Photoacoustic ultrasound (PAUS)—reconstruction tomography. Med Phys. 1995;22:1605–9.
48. Xu M, Wang LV. Photoacoustic imaging in biomedicine. Rev Sci Instrum. 2006;77:041101.
49. Valluru KS, Chinni B K, RaoN A, BhattS, Dogra, V S. Basics and clinical applications of photoacoustic imaging. Ultrasound Clinics 2009; 4 , 403–429.
50. Zhou Y, Wang D, Zhang Y, Chitgupi U, Geng J, Wang Y, et al. A phosphorus phthalocyanine formulation with intense absorbance at 1000 nm for deep optical imaging. Theranostics. 2016;6:688–97.
51. Li C, Wang LV. Photoacoustic tomography and sensing in biomedicine. Phys Med Biol. 2009;54:R59–97.
52. KolkmanR G, Hondebrink E, Steenbergen W, Mul F. In vivo photoacoustic imaging of blood vessels using an extreme-narrow aperture sensor. IEEE J Selected Topics Quantum Electronics. 2003;9:343–6.
53. Laufer J, Delpy D, Elwell C, Beard P. Quantitative spatially resolved measurement of tissue chromophore concentrations using photoacoustic spectroscopy: application to the measurement of blood oxygenation and haemoglobin concentration. Phys Med Biol. 2007;52:141–68.
54. Needles A, Heinmiller A, Sun J, Theodoropoulos C, Bates D, Hirson D, et al. Development and initial application of a fully integrated photoacoustic micro-ultrasound system. IEEE Trans Ultrason Ferroelectr Freq Control. 2013;60:888–97.
55. Beard P. Biomedical photoacoustic imaging. Interface Focus. 2011;1:602–31.
56. Lakshman M, Needles A. Screening and quantification of the tumor microenvironment with micro-ultrasound and photoacoustic imaging. Nat Methods. 2015;2015:12.
57. Liu Q. Role of optical spectroscopy using endogenous contrasts in clinical cancer diagnosis. World J Clin Oncol. 2011;2:50–63.
58. Yao DK, Maslov K, Shung KK, Zhou Q, Wang LV. In vivo label-free photoacoustic microscopy of cell nuclei by excitation of DNA and RNA. Opt Lett. 2010;35:4139–41.
59. Smith B D, Smith GL, Carter, D, Sasaki C T, Haffty B G. Prognostic significance of vascular endothelial growth factor protein levels in oral and oropharyngeal squamous cell carcinoma. J Clin Oncol 2000; 18: 2046–2052.
60. Brennan PA, Mackenzie N, Quintero M. Hypoxia-inducible factor 1α in oral cancer. J Oral Pathol Med. 2005;34:385–9.
61. Oraevsky AA, Karabutov AA, Savateeva EV, Bell BA, Motamedi M, Thomsen SL, et al. Optoacoustic imaging of oral cancer: Feasibility studies in hamster model of squamous cell carcinoma. In BiOS'99 International Biomedical Optics Symposium; 1999. International Society for Optics and Photonics, pp. 385–396.
62. Savateeva EV, Karabutov AA, Motamedi M, Bell BA, Johnigan RM, Oraevsky AA. Noninvasive detection and staging of oral cancer in vivo with confocal opto-acoustic tomography. In BiOS 2000 the international symposium on biomedical optics; 2000. International Society for Optics and Photonics. pp. 55-66.
63. Fatakdawala H, Poti S, Zhou F, Sun Y, Bec J, Liu J, et al. Multimodal in vivo imaging of oral cancer using fluorescence lifetime, photoacoustic and ultrasound techniques. Biomed Opt Express. 2013;4:1724–41.
64. Dogra VS, Chinni BK, Valluru KS, Moalem J, Giampoli EJ, Evans K, et al. Preliminary results of ex vivo multispectral photoacoustic imaging in the management of thyroid cancer. Am J Roentgenol. 2014;202:W552–8.
65. Kima J, Kimb MH, Job K, Hab J, Kima Y, Limb DJ et al. Photoacoustic analysis of thyroid cancer in vivo: a pilot study. In Proc. of SPIE Vol 2017, March. (Vol. 10064, pp. 1006408–1).
66. Rich LJ, Seshadri M. Photoacoustic imaging of vascular hemodynamics: validation with blood oxygenation level–dependent MR imaging. Radiology. 2015;275:110–8.
67. Rich LJ, Seshadri M. Photoacoustic monitoring of tumor and normal tissue response to radiation. Sci Rep. 2016;6:21237.
68. Mallidi S, Watanabe K, Timerman D, Schoenfeld D, Hasan T. Prediction of tumor recurrence and therapy monitoring using ultrasound-guided photoacoustic imaging. Theranostics. 2015;5:289–301.
69. Luke GP, Yeager D, Emelianov SY. Biomedical applications of photoacoustic imaging with exogenous contrast agents. Ann Biomed Eng. 2012;40:422–37.
70. Weber J, Beard PC, Bohndiek SE. Contrast agents for molecular photoacoustic imaging. Nat Methods. 2016;13:639–50.
71. Emelianov SY, Li PC, O'Donnell M. Photoacoustics for molecular imaging and therapy. Phys Today. 2009;62:34–9.
72. Li W, Chen X. Gold nanoparticles for photoacoustic imaging. Nanomedicine (Lond). 2015;10:299–320.
73. Pan D, Kim B, Wang LV, Lanza GM. A brief account of nanoparticle contrast agents for photoacoustic imaging. Wiley Interdiscip Rev Nanomed Nanobiotechnol. 2013;5:517–43.
74. Mallidi S, Larson T, Tam J, Joshi PP, Karpiouk A, Sokolov K, Emelianov S. Multiwavelength photoacoustic imaging and plasmon resonance coupling of gold nanoparticles for selective detection of cancer. Nano Lett. 2009;9:2825–31.
75. Nie L, Chen M, Sun X, Rong P, Zheng N, Chen X. Palladium nanosheets as highly stable and effective contrast agents for in vivo photoacoustic molecular imaging. Nanoscale. 2014;6:1271–6.
76. Li PC, Wang CR, Shieh DB, Wei CW, Liao CK, Poe C, et al. In vivo photoacoustic molecular imaging with simultaneous multiple selective targeting using antibody-conjugated gold nanorods. Opt Express. 2008;16:18605–15.
77. Chen YS, Frey W, Kim S, Homan K, Kruizinga P, Sokolov K, et al. Enhanced thermal stability of silica-coated gold nanorods for photoacoustic

imaging and image-guided therapy. Opt Express. 2010;18:8867–78.

78. Chen YS, Frey W, Kim S, Kruizinga P, Homan K, Emelianov S. Silica-coated gold nanorods as photoacoustic signal nanoamplifiers. Nano Lett. 2011;11:348–54.
79. Garcia-Uribe A, Erpelding TN, Krumholz A, Ke H, Maslov K, Appleton C, et al. Dual-modality photoacoustic and ultrasound imaging system for noninvasive sentinel lymph node detection in patients with breast cancer. Sci Rep. 2015;5:15748.
80. Stoffels I, Morscher S, Helfrich I, Hillen U, Leyh J, Burton NC, et al. Metastatic status of sentinel lymph nodes in melanoma determined noninvasively with multispectral optoacoustic imaging. Sci Transl Med. 2015;7:317ra199.
81. Huynh E, Lovell J, Helfield BL, Jeon M, Kim C, Goertz DE, et al. Porphyrin shell microbubbles with intrinsic ultrasound and photoacoustic properties. J Am Chem Soc. 2012;134:16464–7.
82. Muhanna N, Jin CS, Huynh E, Chan H, Qiu Y, Jiang W, et al. Phototheranostic porphyrin nanoparticles enable visualization and targeted treatment of head and neck cancer in clinically relevant models. Theranostics. 2015;5:1428–43.
83. Yang Q, Cui H, Cai S, Yang X, Forrest ML. In vivo photoacoustic imaging of chemotherapy-induced apoptosis in squamous cell carcinoma using a near-infrared caspase-9 probe. J Biomed Opt. 2011;16:116026.
84. Luke GP, Myers JN, Emelianov SY, Sokolov KV. Sentinel lymph node biopsy revisited: ultrasound-guided photoacoustic detection of micrometastases using molecularly targeted plasmonic nanosensors. Cancer Res. 2014;74:5397–408.
85. Shakiba M, Ng KK, Huynh E, Chan H, Charron DM, Chen J, et al. Stable J-aggregation enabled dual photoacoustic and fluorescence nanoparticles for intraoperative cancer imaging. Nanoscale. 2016;8:12618.
86. Luke GP, Emelianov SY. Label-free detection of lymph node metastases with US-guided functional photoacoustic imaging. Radiology. 2015;277:435–42.

10 Colposcopy: A Direct Oral Microscopy for Oral Cancer and Precancer

Silvano Costa and Prashanth Panta

Abstract

Colposcope is a diagnostic tool frequently used in the practice of gynecology. Colposcopic examination is a painless procedure that is less time consuming and requires no anesthesia. The studies of this decade and a few from the previous one have shed light on the use of colposcopy in oral potentially malignant disorders and oral cancers. Cervical colposcopy is also associated with a few adverse outcomes which are not known to occur in oral colposcopy (direct oral microscopy) and the procedure does not vary much when applied to the oral mucosa. The colposcopic impression is mainly based on changes in the characteristics such as blood vessel caliber and pattern, spacing between capillaries, margins, color, and contour; however, for oral esions, the most important changes of value are the changes in vascular pattern. Direct oral miscroscopy is especially important in the selection of biopsy site. In this chapter a colposcopist and a stomatologist worked at the intersection to offer a basic knowledge of colposcopy practice in the arena it is routinely used, with a summary of the studies on oral oncology.

10.1 Introduction

Colposcopy is a diagnostic procedure developed in 1925 by H. Hinselmann, Director of the Gynecological Clinic of the University of Hamburg, Germany, for examining the uterine cervix and vagina in vivo, using a binocular magnification system with various magnification lenses and a light source. The word "colposcope" is derived from the ancient Greek word *colpos* which means "vagina." This procedure, conceived for the early detection of the pathological conditions of the cervix, is considered worldwide the most studied method for detection of early cervical neoplasia [1, 2].

The aim of colposcopy is to detect preneoplastic and neoplastic changes by analyzing the characteristics of the abnormal tissues such as (a) color, (b) morphology, (c) size, and (d) topography [3–5]. Comparison of these characteristics with established disease patterns allows the clinician to detect lesions and identify abnormal areas which may require a biopsy. Colposcopy is therefore an irreplaceable guidance exploration for pathology of the epithelium, be it cervical mucosa or oral mucosa. In the most recent times, colposcopy has been applied for oral cancers and oral

S. Costa, MD
Gynaecology Unit, MF Toniolo Hospital, via Toscana, Bologna, Italy

P. Panta, MDS (✉)
Department of Oral Medicine and Radiology, MNR Dental College and Hospital, Sangareddy, Telangana, India
e-mail: maithreya.prashanth@gmail.com

P. Panta (ed.), *Oral Cancer Detection*, https://doi.org/10.1007/978-3-319-61255-3_10

potentially malignant disoders (OPMDs) by many authors. In this chapter we sequentially discuss on colposcopy system, tissue basis of cervical colposcopy, and its potential applications in oral oncology.

10.1.1 The Colposcope

The colposcope is basically a magnifying system with a powerful light source and consists of three main parts (Fig. 10.1).

10.1.1.1 Binocular Magnification System

The colposcope consists of a binocular microscope with different magnifications ranging from 5× to 40×. The lowest magnifications give a view of the whole cervix and vagina and allow the localization of the areas of interest. 6× to 12× times are the magnifications most frequently used for starting the procedure. Magnifications higher than 20× reduce the field of view and the depth of focus and are usually required to assess the microscopic details, particularly the vessels' size and shape. The objective lenses affect the focal length (distance between the lenses and the tissue surface); the most favorable focal distance is 300 mm. This consents an optimal working distance and maneuvering of the instruments without interfering with vision. A green filter, which absorbs certain wavelengths, enhances the finer details of the vascular pattern of the target epithelium.

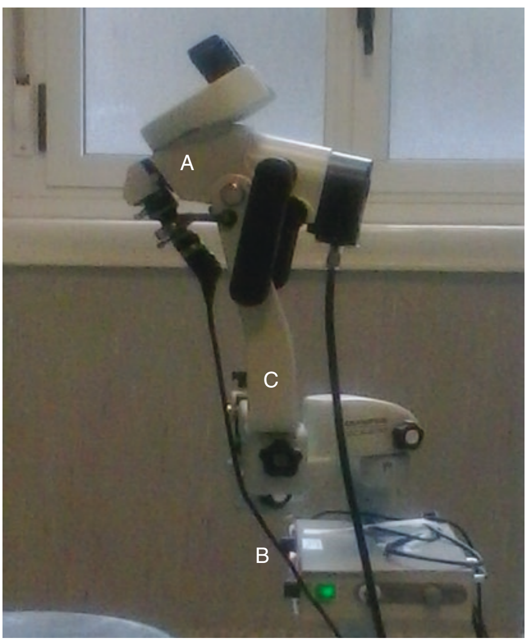

Fig. 10.1 The colposcope consists of a binocular microscope with different magnifications ranging from 5× to 40×. (**a**). Cold light sources such as fiber optic lighting or LED offer brighten illumination and clearness of the images that are essential for taking photographs or videos (**b**). The optical system is mounted on a mobile support that allows displacement of the microscope in the vertical and horizontal directions in order to facilitate visual inspection (**c**)

10.1.1.2 Light Source

Cold light sources such as fiber optic lighting or LED (light-emitting diode) offer brighter illumination and clearness of the images that are essential for taking photographs or videos.

10.1.1.3 Articulated and Movable Support

The optical system is mounted on a mobile support that allows displacement of the microscope in the vertical and horizontal directions in order to facilitate visual inspection.

10.1.2 Histological Basis of Cervical Colposcopy

As mentioned before, the instrument was developed for detecting cervical diseases; therefore, it is essential to briefly mention about the epithelium lining of the cervix. Three different epithelia are present in the uterine cervix [6–8]:

Squamous epithelium: Original squamous epithelium originates from the vaginal plate of the urogenital sinus, derived from Wolffian ducts, and starts at the Hart's line between the labia minora and the vaginal introitus which marks vulvar vestibule. It is characterized by several layers of squamous, glycogenated cells. The vaginal plate migrates upward to cover the uterine cervix and meets the columnar Müllerian epithelium which coats the endocervical canal. Under the squamous epithelium, there is a basal, flat capillary network with very thin vertical terminal vessels, usually ending in a small ring.

Columnar epithelium: The columnar epithelium, originated from the Müllerian ducts, is characterized by a single layer of tall mucus-secreting cells which lines the endocervix. They are arranged in folding clefts with typical grape-like stromal villi, giving a papillary appearance. The papillae, characterized by stromal tissue with a capillary vascular axis and lined by columnar cells, often cover part of the ectocervix. The place where the two epithelia meet is named squamous-columnar junction (SCJ). The SCJ seat changes during the life of a woman: during childhood, it is located into the endocervix, and after hormonal crisis, it usually moves outside of the external os (EO), while in postmenopausal women, there is a retraction of the glandular mucosa in the endocervical canal.

Metaplastic squamous epithelium. At the SCJ, there is a continuous realignment process corresponding to the progression of squamous epithelium and the regression of glandular elements. The papillary glandular epithelium is replaced by cells transformed from columnar to squamous epithelium. This process is known as "metaplasia" and leads to the formation of a new squamous epithelium analogous to the original. The progression from glandular to squamous epithelium starts from subcylindrical immature cells or reserve cells located beneath the columnar cells. These cells, round or cuboidal with a large dense nucleus, are converted into squamous cells. As metaplasia progresses, the reserve cells proliferate and gain more cytoplasm, the nuclei decrease in size, and cell layers increase. Maturation and gradual differentiation lead to the development of a newly formed squamous epithelium, analogous to the original one [4, 5, 7].

10.1.2.1 The Transformation Zone

The area where columnar epithelium is replaced by a new squamous epithelium is named "transformation zone" (TZ). This zone is of particular interest to the colposcopist, because this is the area where neoplasia can develop. In fact the TZ may be normal (NTZ) when there are no features of atypical transformation or abnormal (ATZ) when there is an evidence of dysplastic changes. Actually during the early stages of metaplasia, the epithelium still immature and undifferentiated may be particularly sensitive to mutagenic factors such as the integration of the DNA of human papillomavirus (HPV) and overexpression of viral oncogenes which alter the genomic structure leading to clonal expansion of undifferentiated cells with abnormalities and an increased risk of neoplastic transformation (Fig. 10.2). Abnormal cells show changes in shape and size of the cytoplasm, increased nuclear volume with hyperchromasia and irregular thickening of the nuclear membrane associated with an alteration of the distribution of chromatin. It will therefore be a squamous epithelium with dysplastic cytohistological structure.

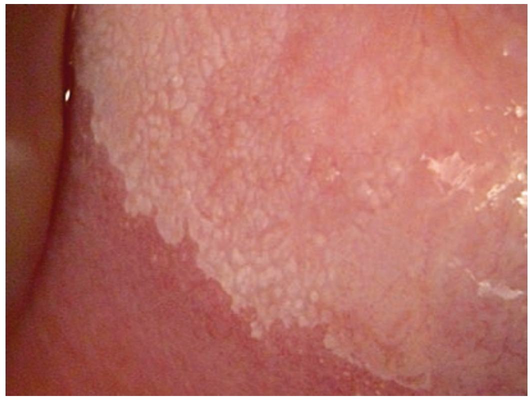

Fig. 10.2 This acetowhite lesion has peripheral flat, irregular, scalloped margins. This is a biopsy proven grade 1 cervical intraepithelial neoplasia and can serve as a model to understand early color changes in oral cancer

10.1.3 Tissue Basis of Colposcopy

Colposcopy uses an external light source to illuminate the surface of the cervix which reflects the incident white light. The surface color depends on characteristics of the epithelium and underlying superficial capillaries. Beneath the squamous epithelium, there are two different vascular networks: basal capillaries and terminal vessels; these end in a small loop just beneath the basal membrane. The multilayered thick normal epithelium acts as a barrier, absorbing and reflecting part of the incident light while the remaining is reflected by the stromal vessels; therefore the colposcopic effect is a pink coloration. On the other hand, the glandular epithelium is formed by a single layer of columnar cells, and the incident light is totally reflected by the superficial vessels bestowing a red coloration [7–10].

In the vagina, there is no transformation zone, except in a few women with congenital vaginal adenosis; the normal vaginal epithelium is squamous, quite similar to the epithelium lining the oral cavity, and the colposcopic appearance is analogous to that observed in the native squamous epithelium of the cervix.

10.1.4 Steps of Colposcopic Examination

The first step of colposcopy is a direct inspection, to assess the shape and size of the cervix. It is advisable to wet the epithelium with normal saline solution which makes transparent the surface, and the squamous epithelium is seen as a translucent smooth epithelium with a pink color. In case of eversion on the ectocervix of glandular epithelium, a dark red area is observed with a villous, papillary appearance, in contrast to the smooth pink surface of the squamous epithelium.

During this phase, it is important to observe the vessel network using a green filter to enhance the contrast of the blood capillaries. Using a high magnification (20×), two types of vessels are visible: (a) reticular network or (b) hairpin-shaped capillaries. While the former have a horizontal direction, the latter ascend vertically from the reticular pattern and appear as small loops on the epithelial surface. Intercapillary distance in normal epithelium is $\leq 350\ \mu$, while a distance $>350\ \mu$ may indicate new angiogenesis in the dysplastic areas [7].

The second step is the application of 5% acetic acid solution. Within 30–60 s, a contrast between normal epithelium, which remains unaltered, and abnormal epithelium, which becomes white, is seen. It is important to note the intensity, the duration, and the time of disappearance of the acetic reaction because it is related to the severity of the lesion. The effect is transient and is lost in 20 s to 2 min, depending on the number of cells, the amount of cytoplasm, and the nuclear density. The acetic acid application produces a reversible agglutination of nuclear proteins, cytokeratin skeleton, and cytoplasmic dehydration. As in the dysplastic cells, there is a high protein concentration, the light is not reflected by the vascular stroma but by the epithelial surface, and a white reaction in dysplastic areas appears (Fig. 10.3).

The third step is painting the epithelial surface with Lugol's iodine solution. The normal tissue appears dark mahogany brown, indicating that glycogen is present in the superficial layers of normal squamous cells, while absent staining indicates a non-glycogenated state, typical of the abnormal epithelium which, in turn, appears yellow pale, mustard, or nonstained. Because glandular columnar cells containing mucin and the normal metaplastic epithelium also lacks of glycogen, the iodine application should be used to confirm the findings that result from acetic acid application.

10.1.5 Abnormal Colposcopic Patterns

The colposcopic diagnosis of cervical neoplasia is based on the recognition of five main aspects of the acetowhite reaction: (*a*) *color intensity*, *(b) margins*, *(c) surface*, *(d) vascular features*, of the white areas, and *(e) color change after Lugol application:*

1. *Color intensity*: The appearance of well-defined, white opaque, and dense areas is the most significant and frequent colposcopic feature indicating cervical intraepithelial neoplasia. The degree of uptake of acetic solution correlates with the degree of the lesion. High-

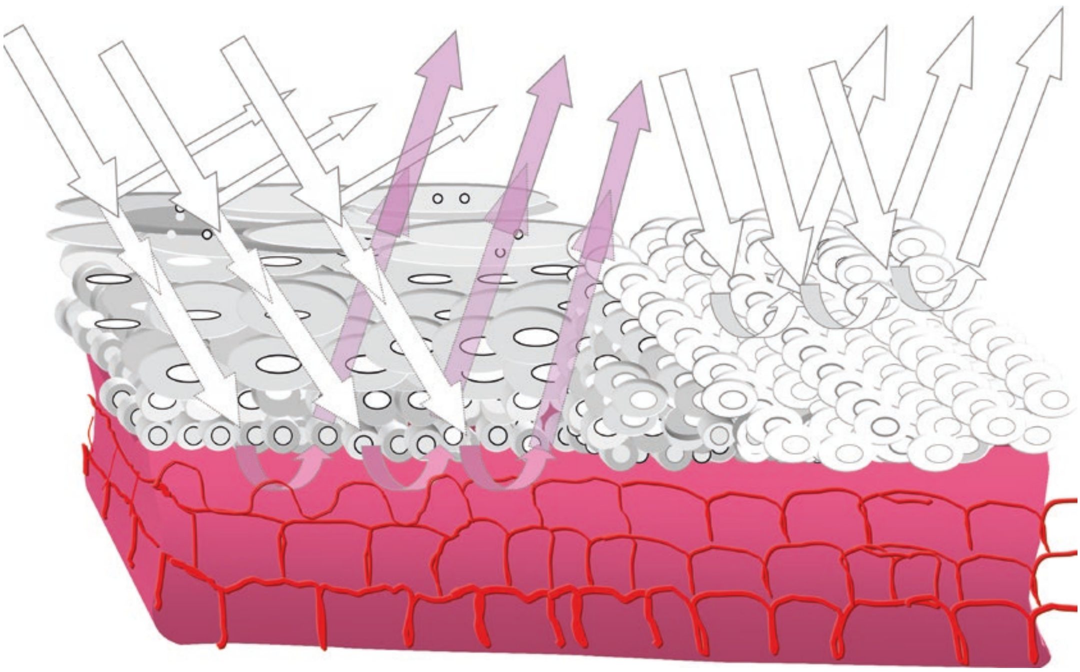

Fig. 10.3 The surface color depends on characteristics of the epithelium and underlying superficial capillaries. Beneath the squamous epithelium, there are networks of fine capillaries; the multilayered thick squamous epithelium acts as a barrier, absorbing and reflecting part of the incident light, while the remaining is reflected by the stromal vessels; therefore the colposcopic effect is a pink coloration (left side). The acetic acid application produces a reversible agglutination of nuclear proteins, cytokeratin skeleton and cytoplasmic dehydration. As in the dysplastic cells, there is a high protein concentration, the light is not reflected by the vascular stroma but by the epithelial surface, and a white reaction in dysplastic areas appears (right side)

grade dysplastic areas turn dense white, dull, or oyster gray rapidly, indicating a thickened epithelium and a marked increase of nuclear activity. On the other hand, mild dysplastic zones have a thin, pale, scalloped, or @feathered withe aspect. Not all severe preinvasive lesions exhibit abnormal vessels due to the thickness of the epithelium which doesn't permit the observation of the underlying vascular network.

2. *Margins:* The line of demarcation between normal and abnormal epithelium is sharp and well defined. High-grade lesions have distinct, well-demarcated margins frequently showing raised and rolled borders.
3. *Surface:* The surface of preinvasive lesions is less velvety and smooth of normal squamous epithelium; irregular, uneven, or nodular roughness areas are usually seen on the superficial epithelial layers, related to irregular cell proliferation.
4. *Vascular features:* Not all severe preinvasive lesions exhibit abnormal vessels because of the thick epithelium. When observed, abnormal vascular network shows the characteristic patterns of (a) punctation, (b) mosaicism, and (c) atypical vessels.
   (a) Punctation: The stromal terminating vessels, compressed by blocks of undifferentiated cells, appear as red points or dots, irregular in shape and size, in a dense acetowhite areas, making what are described in colposcopy as punctuate areas or punctation. As the grade of dysplasia increases, the caliber of the vessels increases as well as the intercapillary distance, and the pattern appears coarse (Fig. 10.4).
   (b) Mosaic: In this feature the atypical vessels, running parallel to the surface, encircle the blocks of pathological epithelium

and appear as a cobblestone or mosaic pattern; the capillaries have an irregular branching, caliber, and course. Coarse punctation and mosaics are seen in severe dysplastic areas and sometimes may occur together (Fig. 10.5).

(c) Atypical vessels: Atypical vessels display irregular and abrupt changes in direction, appearing and disappearing suddenly with bizarre patterns such as corkscrew, tadpole, hairpin, or comma form. This feature is frequently observed in microinvasive or invasive disease and will be described in detail.

Fig. 10.4 This vascular feature represents often a neovascularization due to angiogenic factors in case of early invasion

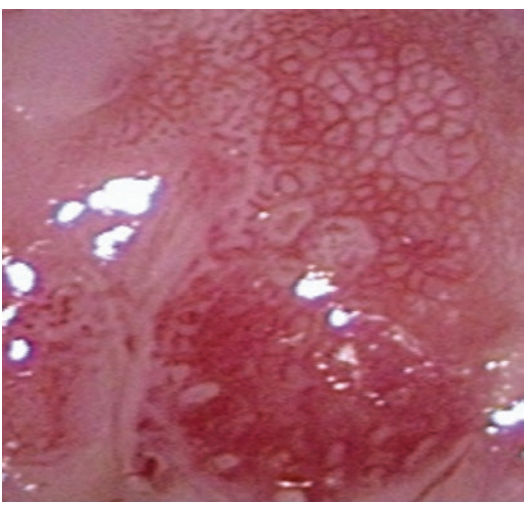

Fig. 10.5 A high-grade (grade 3) cervical intraepithelial neoplasia showing mosaic pattern

5. *Color change after Lugol application:* After examining the cervix with 5% acetic acid, Lugol's solution is applied to the epithelial surface. The principle of iodine staining, also named Schiller's test, is that mature squamous epithelium is glycogenated, whereas intraepithelial and invasive cancer contains little or no glycogen. Thus neoplastic epithelium does not stain dark brown but appears yellow pale or yellow mustard or nonstained.

10.1.6 Colposcopy of Microinvasive and Invasive Carcinoma

As the tumor invasion advances, infiltrating fingerlike projections or confluent growth pattern invades the connective tissue with diffuse stromal reaction, lymphocytic infiltration, edema, and necrosis; these tissue modifications decrease the acetowhite reaction determining a grayish-white or yellow-hued color suggesting a tissue degeneration and a deeper invasion. Exophytic nodular pattern or bleeding ulcerations as well as atypical vessels are the most specific and frequent features; vessels are two to ten times wider than normal and irregular in shape and course (Fig. 10.6).

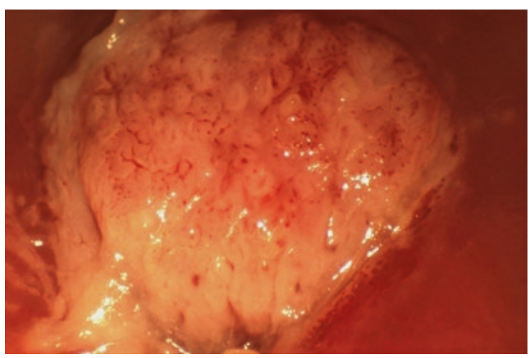

Fig. 10.6 Microinvasive lesions present elevated and sharply demarcated margins and capillaries 2 to 10 times wider than normal with irregularity in shape and course may be revealed (from S. Costa, K Syrjanen. Gestione delle Pazienti con Pap test anormale, Athena Ed., Modena, 2005. Courtesy of Editor)

Vascular changes occur due to angiogenetic processes with engorged, thin-walled capillaries with sudden changes in caliber, appearing and disappearing abruptly bizarre patterns such as "corkscrew, tadpole, or comma" form; irregular and increased intercapillary distance >350 μ are the hallmark of invasion [11].

Colposcopy is a critical step in detecting abnormal changes in color and morphology of cervical mucosa. Comparison of these features with established patterns of disease allows classification of observed lesions and identifying abnormal areas that warrant biopsy [12–14].

10.2 Emergence of Direct-Oral Microscopy

Oral squamous cell carcinoma (OSCC) accounts to more than 90% of all oral cancers [15]. In a recent report based on 2012 data, it was shown that south central Asia contributed to 48.7% of world oral cancer burden [16]. About two- third of these patients already have an advanced disease at the time of diagnosis; and for this reason, diagnostic aids have been developed. There are numerous methods developed to facilitate identification of early oral cancers, which include conventional examination of high-risk sites, vital staining including toluidine blue, exfoliative cytology, and other light-based detection strategies like white light florescence imaging, optical coherence tomography, photoacoustic imaging etc. All these methods have an essential limitation, the high risk of false positives and false negatives. Moreover, in a recent meta-analysis report on some of the early detection strategies none, atleast in the present condition , could be considered as having true potential for early screening [17, 18]. In a randomized controlled trial by Fedele et al., screening using visual examination of the oral mucosa under normal light was effective in reducing mortality [19]. Visual examination under white light is a potential method. Although colposcopy or direct oral microscopy is a light-based detection system that uses simple white light its results are superior to conventional oral examination because of the additional maginification system and the green filter accesory. Changes in surface pattern, color tone, opacity, and clarity of demarcation are more easily seen with microscopy when compared to routine clinical examination. The green filter can further aid in the potential visualization and delineation of signature capillary patterns similar to narrow band imaging.

Although colposcopy represents a technique primarily used in the examination of cervix and the tissues of the vagina, many recent studies have shed light on its use in oral oncology (Table 10.1). The intraoral application of colposcopy was initiated as early as 1989 when L'Estrange P et al. used "contact microcolpohysteroscope" for examining the surface topography of the hard and soft tissues of the oral cavity [20]. They recommended for the first time that colposcopy can become a promising and a noninvasive method for oral lesions and have mentioned a few modifications for its oral use. The first comprehensive clinical study on the oral application was conducted in 2000 by Gynther et al. [21]. Gynther et al. studied 35 patients with various OPMDs and suspected oral lesions. Different grading and scoring systems have been devised for colposcopic examination. One of the most frequently used criteria is the Reid's index (87% accuracy) [22, 23] (Table 10.2). Reid's index is a scoring system helpful in predicting the severity of premalignant cervical lesions. This same criterion may also be applied for direct oral microscopy. The staining procedure in direct oral microscopy remains the same as in cervical colposcopy.

Although cervical colposcopy is a routinely performed and appears as a relatively noninvasive procedure, it is associated with a few long-term adverse outcomes. They include adverse obstetric outcomes, persisting anxiety, increased rates of sexual dysfunction, and reduced quality of life [24]. Direct oral microscopy on the other hand is not associated with any disturbing outcomes.

Table 10.1 Summary of studies on direct oral microscopy in oral oncology

Investigator	Year	Main findings
Hans Hinselmann	1925	Colposcope introduced
L'Estrange et al.	1989	Intraoral applications of contact microcolpohysteroscopy were discussed [20]
Gynther et al.	2000	Direct oral microscopy (DOM) guided biopsies identified advanced histological signs [21]. Two biopsies were taken from each of the 35 patients, 1 through clinical examination and the second through DOM. According to colposcopic criteria, 29 patients (83%) showed changes in vascular pattern on DOM. In 14 patients (40%), biopsy sites identified by DOM showed more advanced histologic signs than those selected by routine clinical examination. Four patients (11%) had advanced histologic signs in biopsy samples, as identified during routine clinical examination. In 17 patients (49%), they found no differences between the biopsy specimens
Shetty et al.	2011	In 26 patients (52%), the biopsy specimens selected through DOM appeared to be more representative of histologic findings than those selected with routine clinical examination. Thirty-nine patients (78%) showed changes in the vascular picture on DOM. Twenty of these had punctation vessels, 7 had mosaic vessels, and 12 had atypical vessels [34]
Drogoszewska et al.	2013	Reported a standard picture of healthy oral mucosae by DOM [35]. Network capillaries were noticed in 36.7% patients and hairpin capillaries in 63.3% patients. Healthy oral mucosae presented in pale-rosy (26.7%) to rosy (73.3%) coloration. DOM revealed subclinical lesions in 9 patients, who showed subepithelial punctation and mosaic capillaries. In 6 of those cases, signs of dysplasia were detected; and in all 9 except for a change in vascular pattern, all other parameters were as per established standard
	2014	DOM picture of 30 erosive OLP (a OPMD) was described [25]. Biopsies obtained through DOM revealed dysplasia in 16 patients (53.3%), and biopsies through clinical examination revealed dysplasia in 3 cases (10%)
Nayyar et al.	2014	Study was conducted on a large sample of 180 patients (100 leukoplakia and 80 carcinoma-buccal mucosa) to assess Colposcopic examination in selection of biopsy site [26]. The sensitivity and specificity in selection of biopsy site by colposcopic examination was found to be higher for leukoplakia than for carcinoma-buccal mucosa [26]. DOM may be more reliable for selection of biopsy site in larger, suspicious oral lesions like leukoplakia and for carcinomas clinical examination was found as appropriate
Chomik et al.	2015	DOM was examined in the context of margin-status around invasive oral squamous cell carcinoma. Biopsies from areas indicated by DOM revealed dysplasia in 86.7% patients and, biopsies from areas indicated by clinical examination revealed dysplasia in 40% patients, pointing at the possible application of DOM in mucosal margin estimation [27]
Ujwala et al.	2016	Reported a sensitivity of 71%, specificity of 91% and a positive predictive value of 91% for the colposcopic screening test compared to histology. There work included a wide spectrum of OPMDs covering oral submucous fibrosis, leukoplakia, lichen planus, and suspected malignancies [28]

10.2.1 Direct Oral Microscopy-Guided Biopsies

The biopsy site chosen during routine clinical examination is a function of the clinician's experience, and as of now there is no standard method for selecting it. In a preliminary study [21] conducted on 35 patients with leukoplakia, oral lichenoid lesions, and suspected malignancy, 29 patients (83%) showed changes in the vascular picture direct oral microscopy (DOM) DOM-guided biopsies identified advanced histological signs in 14 patients (40%), and clinical examination revealed advanced histologic signs in the biopsy samples in only four patients (11%). There were significant differences between both methods DOM of OPMDs seems to have significant impact in selecting more representative sites

Table 10.2 A schematic diagram showing the parameters that influence the overall score on modified Reid's colposcopic index

Colposcopic sign	Zero point	One point	Two points
Margin	Flat margins, indistinct borders, geographic or scalloped margins, satellite lesions	Sharp non-elevated borders, straight margins	Prominent straight, rolled margins, internal borders between areas of different whitening
Color	Transparent acetowhite, pale acetowhite, snow white	Shiny white, opaque white	Gray white, oyster gray
Surface	Flat, smooth	Wrinkled	Rough, jagged, nodular
Vessels	Fine caliber, regular distribution, tiny capillaries loop, ill-defined areas with fine punctation or mosaic	Absence of superficial vessel	Irregular-coarse punctation or mosaic Compressed or dilated vessels, abrupt changes in direction Bizarre, irregular caliber
Iodine staining	Uniform uptaking with mahogany color	Partial or irregular uptaking	Yellow-mustard
Total score		Interpretation	
0–2		Normal or CIN1	
3–5		CIN1 or CIN2	
6–8		CIN2 or CIN3	
9–10		CIN3-invasion	

A low score implies less serious disease, and a high score indicates a high-grade lesion or early invasive carcinoma

for biopsy than routine clinical examination. In another study in 2014 DOM was used by Drogoszewska et al. to describe the in vivo picture of erosive oral lichen planus (OLP), another potential OPMD. The unique signature in terms of pattern, density of subepithelial blood vessels, surface texture, color, transparency, and borders of the lesions was taken into consideration [25]. The biopsies obtained using DOM revealed dysplasia in 16 patients (53.3%), and the biopsies obtained through conventional oral examination revealed dysplasia in only three cases (10%). DOM is superior to routine clinical examination, at least with regard to erosive OLP [25]. Using DOM directed biopsies, it is possible to sample with high degree of accuracy the most advanced histopathological changes.

A study was conducted by Nayyar et al. on 180 patients (100 leukoplakia and 80 carcinoma of buccal mucosa) to assess the role of DOM in the selection of biopsy site [26]. The sensitivity and specificity for the selection of biopsy site by DOM were found to be higher for leukoplakia than for carcinoma buccal mucosa [26]. For carcinoma cases, clinical examination was found to be more appropriate. We can understand by the results of their study that for selecting biopsy site in frank carcinomas, the clinician can rely on COE, but for selection of biopsy site in larger, suspicious oral lesions like leukoplakia, DOM may be of value. The altered vascular patterns are used for selecting more representative sites for biopsy of suspected oral cancer [21, 25, 26].

In 2015, Chomik et al. [27] have researched the subject of DOM in the context of margin status around invasive oral squamous cell carcinoma. Biopsies from areas indicated by DOM revealed dysplasia in 86.7% patients, and biopsies from areas indicated by clinical examination revealed dysplasia in 40% patients, pointing at the possible application in study of margin status [27].

In 2016, Ujwala et al. [28] conducted a study on 90 subjects composed 30 cases of oral submucous fibrosis, 20 cases each of hyperkeratotic lesions including homogeneous and nonhomogeneous leukoplakias and 20 oral lichen planus and 20 cases of histopathologically proven oral squamous cell carcinoma. As compared to histological diagnosis, colposcopic screening test has shown a sensitivity of 71% , specificity of 91% and positive predictive value of 91% [28]. Another advantage of direct-oral-microscopy is that the extent of the lesions can be visualized providing additional clarity of the overall lesion size and to improve decision making on the most representative biopsy site.

10.2.2 Tumor Angiogenesis: A Basis for Direct Oral Microscopy

The capillary changes in neovascularization process that occurs during repair and regeneration is different from tumor angiogenesis seen in cancer, which is more chaotic. Tumor angiogenesis is a process of formation of new microvessels from the preexisting vasculature in response to angiogenic-vascular growth factors which are produced in response to tumor associated hypoxia. Tumors cannot grow more than 1–2 mm^3 in volume, unless they synthesize this network of new vessels [29]. Vascular endothelial growth factor (VEGF), fibroblast growth factor (FGF), and transforming growth factor alpha (TGF-α) are responsible for the new capillaries. The mean vessel density (MVD) which is responsible for the various patterns at the fundamental-tissue level differs little between normal mucosa and dysplasia, but swiftly increases with increasing tumor size and stage of invasion [29–31]. Mast cells are also known to promote angiogenesis [32], and the degree of angiogenesis (scored through Immuno-Histo-Chemistry) can be considered as a definitive indicator of evolution of SCC from epithelial dysplasia [31–33]. Direct optical visualization of these vascular patterns would therefore be helpful in the early detection. As explained in the previous sections, Moreover in the technique of DOM the visualization of subepithelial mucosal vessels is facilitated by the application of a green filter to the light source which enhances the contrast between vessels and surrounding tissues.

There is a strong relation between tumor progression and vascularity. The transition from normal to dysplastic and neoplastic tissue in the oral mucosa is accompanied by quantitative or qualitative changes in the vascularity of the tissue; and the most frequent antibodies used are aganist von Willebrand Factor (vWF) and CD31, or alpha v beta 3 integrin (markers of neo-angiogenesis) [33]. Pazouki et al. concluded that an analysis of microvascular volume is more informative than microvascular density [33].

Shetty et al. [34] conducted a study (n=50 lesions) on the relevance of tumor angiogenesis patterns as a diagnostic and prognostic indicator in OPMD and cancer. For selecting biopsy sites in the oral cavity, they used established colposcopic criteria for vascular features. In 26 patients (52%), the biopsy specimens selected with direct oral microscopy appeared to be more representative of histologic findings than those selected with routine clinical examination. Thirty-nine of the patients (78%) showed changes in the vascular picture. Twenty of them had punctation vessels, 7 had mosaic vessels, and 12 had atypical vessels.

In a recent study by Ottaviani et al. [35] 50 mice were included that were treated with a chemical carcinogen to induce both dysplastic and neoplastic oral lesions, along with a clinical sample of 91 patients with suspicious premalignant and malignant oral lesions. The images of experimental animals and lesions in patients were imaged using both white light (using digital camera) and Narrow Band Imaging prior to biopsy and two raters examined and classified the lesions, which were later compared to histological diagnosis. In this investigation narrow band imaging was found to be a more accurate method. In this context we emphasize that the basic format of both narrow band imaging and colposcopy which uses the green filter is nearly same, and even the colposcopic criteria for malignancy overlap very closely with the NBI criteria for malignant (Type III-IV IPCL pattern) and both are fundamentally depend on the derailed vessel patterns [35]. The additional feature of DOM is the use of criteria for contour and surface which are particularly important in the context of OPMDs since they are often diffuse and wide lesions, which cause confusion about the approprite biopsy site. In normal tissues the blood vessels are more defined and regular and in the malignant tissues they are chaotic.

10.2.3 A Summary of Standard Direct Oral Microscopy Findings - In Health and Malignancy

The standard DOM picture of healthy oral mucosa comes from the study conducted by Drogoszewska et al. [36]. They found network capillaries in 36.7% patients and hairpin capillaries in 63.3%

patients. Healthy oral mucosae presented a range of colors from pale rosy (26.7%) to rosy (73.3%) by DOM. Also subclinical lesions were revealed in nine patients; they mainly showed subepithelial punctation and mosaic capillaries. In six of those cases, signs of dysplasia were detected. In all nine patients, except for a change in vascular pattern, all other parameters were not any different from the established standard.

Healthy oral mucosae are pink (pale rosy to rosy), moist, glossy and smooth with non-folded surface and demonstrates fine and regularly -red subepithelial vessels. It mainly shows two types of capillaries: hairpin and network capillaries. Subepithelial blood vessels are more clearly visible in the buccal mucosa region. When the mucosa is thin, blood vessels can be seen through the epithelium even without the aid of a green filter. In dysplasia and carcinoma in situ, punctation and mosaic vessels are common. Punctation and mosaic vessels are usually seen in sharply demarcated areas. When the pattern is difficult to describe, the term "atypical vessels" is used. Capillary punctation, mosaic, or atypical patterns are encountered in oral malignant lesions. Therefore, the presence of one of these patterns indicates the need for biopsy and further histopathologic examination. The characteristic vascular patterns in healthy oral mucosa, dysplasia, and advanced carcinoma have shown concordance with the colposcopic criteria for cervical mucosa and the gold standard histology.

Conclusion

Colposcopy or 'direct oral microscopy' is among the few techniques that evolved for gynecologic pathology but is slowly gaining importance for oral applications. The main goal of direct oral microscopy is to aid in the early identification of malignant areas within widely extented OPMDs, in the selection of representative biopsy sites and in the determination of margin status. Direct oral microscopy has also identified subclinical lesions which showed no visible color change and later proved to be dysplastic. Colposcopy, besided narrow band imaging is one among the few techniques capable to identify deviations in vascular patteri, which must be biopsied and scrutinized histologically. The results of direct oral microscopy are chiefly based on vascular pattern and to a lesser degree on tissue change, which are clearly visible on routineoral examination, unlike cervical mucosa which is less accesible than oral mucosa. A close relation exists between vascularity and tumor progression and therefore the underlying vascular patterns can indicate early changes in oral cancer. We suggest investigators to conduct further studies and broaden the scope of this area. Direct oral microscopy has the potential of becoming a chairside method in the diagnosis of oral cancer and digital applications and automated image analysis can lead to promising results.

References

1. Stafl A. Colposcopy in diagnosis of cervical neoplasia. Am J Obstet Gynecol. 1973;115:286.
2. Mestwerd G, Wespi HJ. Atlas der Kolposkopie. Stuttgart: Verlag Ed.; 1976.
3. Coppleson M. Gynecologic oncology. London: Churchill Livingstone Ed; 1992.
4. Anderson M, Jordan J, Morse A, Sharp F. A text and atlas of integrated colposcopy. Chapman & Hall Ed., Londona, 1992.
5. Burghardt E, Pickel H, Girardi H. Colposcopy and cervical pathology. Stuttgart: Thieme Verlag Ed; 1998.
6. Eifel PJ, Levengack C. Cancer of the female lower genital tract. Hamilton, London: BC Decker Ed; 2001.
7. Apgar BS, Brotzman GL, Spitzer M. Colposcopy. Philadelphia: Principle and practice. Saunders W.B. Ed; 2002.
8. Bagghish MS. Colposcopy of the cervix, vagina and vulva. Philadelphia: Mosby Ed; 2003.
9. Sellors W, Sankaranarayanan R. Colposcopy and treatment of cervical intraepithelial neoplasia. Lyon: IARC Ed; 2003.
10. Bosze P, Luesley DM. Course book on colposcopy. In: Primed, vol. X. Budapest: Press Ed; 2003.
11. Orlandi C, Costa S, Terzano P. Presurgical assessment and therapy of microinvasive carcinoma of the cervix. Gynecol Oncol. 1995;59:255–60.
12. Bucchi, P. Cristiani, S. Costa, P. Schincaglia, P. Garutti, P. Sassoli de Bianchi et al., Rationale and development of an on-line quality assurance programme for colposcopy in a population-based cervical screening setting in Italy. BMC Health Serv Res, 2013; 13: p. 237.

13. Cristiani P, Costa S, Schincaglia P, Garutti P, Sassoli de Bianchi P, Naldoni C, et al. An online quality assurance program for colposcopy in a population-based cervical screening setting in Italy: results on colposcopic impression. J Low Genit Tract Dis. 2014;18:309–13.
14. Sideri M, Garutti P, Costa S, Cristiani P, Schincaglia P, Sassoli de Bianchi P, et al. Accuracy of colposcopically directed biopsy: results from an on-line quality assurance programme for colposcopy in a population-based cervical screening setting in Italy. Biomed Res Int. 2015;2015:1.
15. Panta P, Venna VR. Salivary RNA signatures in oral Cancer detection. Anal Cell Pathol (Amst). 2014;2014:450629.
16. Parkin DM, Bray F, Ferlay J, Pisani P. Global cancer statistics, 2002. CA Cancer J Clin. 2005;55:74–108.
17. Singh A, Carroll DJ, Mehrotra R. Pitfalls and Limitations of Oral Cytopathology. In: Mehrotra R, editor. Oral cytology: a concise guide. New York: Springer; 2013. p. 147–56.
18. Lingen MW, Kalmar JR, Karrison TC, Speight PM. Critical evaluation of diagnostic aids for the detection of oral cancer. Oral Oncol. 2007;44:10–22.
19. Fedele S. Diagnostic aids in the screening of oral cancer. Head Neck Oncol. 2009;1:5–15.
20. L'Estrange P, Bevenius J, Williams L. Intraoral application of microcolpohysteroscopy. A new technique for clinical examination of oral tissues at high magnification. Oral Surg Oral Med Oral Pathol 1989;67:282–5.
21. Gynther GW, Rozell B, Heimdahl A. Direct oral microscopy and its value in diagnosing mucosal lesions. a pilot study Oral Surg Oral Med Oral Pathol Oral Radiol Endod. 2000;90:164–70.
22. Ferris DG, Greenberg MD. Reid's Colposcopic index. J Fam Pract. 1994;39:65–70.
23. Boonlikit S. Correlation between Reid's colposcopic index and histologic results from colposcopically directed biopsy in differentiating high-grade from low-grade squamous intraepithelial lesion at Rajavithi hospital. J Med Assoc Thail. 2011;94:S59–65.
24. Flanagan SM, Wilson S, Luesley D, Damery SL, Greenfield SM. Adverse outcomes after colposcopy. BMC Womens Health. 2011;11:2.
25. Drogoszewska B, Chomik P, Polcyn A, Michcik A. Clinical diagnosis of oral erosive lichen planus by direct oral microscopy. Postepy dermatol alergol. 2014;31:222–8.
26. Nayyar AS, Khan M, Bafna UD, Siddique A, Gayitri HC. Colposcopy: gynecological vision in viewing oral lesions. Indian J Pathol Microbiol. 2014;57:223–30.
27. Chomik P, Michcik A, Michajłowski I, Starzyńska A. Application of direct oral microscopy in evaluating mucosal margins around invasive oral squamous cell carcinoma. Postepy Dermatol Alergol. 2015;32:349–57.
28. Ujwala N, Singh NA, Milind N, Prafulla P, Vidhya P, Bhushan B, et al. Colposcopy in pre-malignant lesions and oral squamous cell carcinoma: Linking threads of clinical, histopathological and colposcopic inferences. J Cancer Res Ther. 2016;12: 295–301.
29. Astekar M, Joshi A, Ramesh G, Metgud R. Expression of vascular endothelial growth factor and microvessel density in oral tumorigenesis. J Oral Maxillofac Pathol. 2012;16:22–6.
30. Li C, Shintani S, Terakado N, Klosek SK, Ishikawa T, Nakashiro K, et al. Microvessel density and expression of vascular endothelial growth factor, basic fibroblast growth factor, and platelet-derived endothelial growth factor in oral squamous cell carcinomas. Int J Oral Maxillofac Surg. 2005;34:559–65.
31. Johnstone S, Logan RM. The role of vascular endothelial growth factor (VEGF) in oral dysplasia and oral squamous cell carcinoma. Oral Oncol. 2006;42:337–42.
32. Mohtasham N, Babakoohi S, Salehinejad J, Montaser-Kouhsari L, Shakeri MT, Shojaee S, et al. Mast cell density and angiogenesis in oral dysplastic epithelium and low- and high-grade oral squamous cell carcinoma. Acta Odontol Scand. 2010;68:300–4.
33. Pazouki S, Chisholm DM, Adi MM, Carmichael G, Farquharson M, Ogden GR, et al. The association between tumour progression and vascularity in the oral mucosa. J Pathol. 1997;183:39–43.
34. Shetty DC, Ahuja P, Rathore AS, Ahuja US, Kumar K, Ahuja A, et al. Relevance of tumor angiogenesis patterns as a diagnostic value and prognostic indicator in oral pre-cancer and cancer. Vasc Health Risk Manag. 2011;7:41–7.
35. Ottaviani G, Gobbo M, Rupel K, D'Ambros M, Perinetti G, Di Lenarda R, et al. The diagnostic performance parameters of Narrow Band Imaging: A preclinical and clinical study. Oral Oncol. 2016;60:130–6.
36. Drogoszewska B, Chomik P, Michcik A, Polcyn A. A standard picture of healthy oral mucosae by direct oral microscopy. Postepy Dermatol Alergol. 2013;30:159–64.

Optical Coherence Tomography: Emerging In Vivo Optical Biopsy Technique for Oral Cancers

11

Optical Coherence Tomography: Emerging In Vivo Optical Biopsy Technique for Oral Cancers

Prashanth Panta, Chih-Wei Lu, Piyush Kumar, Tuan-Shu Ho, Sheng-Lung Huang, Pawan Kumar, C. Murali Krishna, K. Divakar Rao, and Renu John

Abstract

Oral cancers are a major health burden, and patients suffer from low survival rate owing to their late detection. Optical techniques are rapid, objective, and noninvasive methods with the potential to serve as adjunct screening/diagnostic tools, especially for cancers. This chapter highlights the advancements in oral cancer exploration using optical coherence tomography (OCT) with a discussion on basic principles of OCT, followed by a detailed description of oral cancer studies, subgrouped into animal studies, and ex vivo and in vivo human studies. We have included full-field OCT system-derived in vivo oral mucosa images in a healthy volunteer at different subsites showing standard microanatomy at various depths and also narrated some strategies to improve OCT results by multimodal approaches as well as through contrast enhancement for improved visualization.

11.1 Introduction

Optical coherence tomography (OCT) is a widely explored imaging modality that can provide high-resolution, cross-sectional tomographic images of the ultrastructure of biological samples. OCT applications were reported in the early 1990s for noninvasive imaging of the retina [1, 2], and owing to its numerous advantages, it has been explored in a range of biomedical applications

P. Panta, MDS (✉)
Department of Oral Medicine and Radiology, MNR Dental College and Hospital, Sangareddy, Telangana, India
e-mail: maithreya.prashanth@gmail.com

C.-W. Lu, PhD
Apollo Medical Optics, Ltd. (AMO), Taipei, Taiwan
e-mail: cwlu@mdamo.com

P. Kumar, PhD
Amity Institute of Biotechnology, Amity University Mumbai, Navi Mumbai, Maharashtra, India

T.-S. Ho, PhD · S.-L. Huang, PhD
Apollo Medical Optics, Ltd. (AMO), Taipei, Taiwan

Graduate Institute of Photonics and Optoelectronics, National Taiwan University, Taipei, Taiwan

P. Kumar · R. John, PhD
Department of Biomedical Engineering, Indian Institute of Technology, Hyderabad, Telangana, India
e-mail: renujohn@iith.ac.in

C. Murali Krishna, PhD
Chilakapati Laboratory, Advanced Centre for Treatment Research and Education in Cancer (ACTREC), Tata Memorial Centre (TMC), Mumbai, Maharashtra, India

Homi Bhabha National Institute, Anushakti Nagar, Mumbai, India

K. Divakar Rao, PhD
Photonics and Nanotechnology Section, Bhabha Atomic Research Centre Facility, Visakhapatnam, India

P. Panta (ed.), *Oral Cancer Detection*, https://doi.org/10.1007/978-3-319-61255-3_11

including ophthalmology [3, 4], oncology [5–7], cardiology [8], and developmental biology [9]. OCT became a tool of choice for cancer researchers due to the feasibility of noninvasive high-resolution functional imaging and tumor margin assessment and has been extensively explored in skin cancers [10–12], laryngeal cancers [13], esophageal cancers [14–17], cervical cancers [18], bladder cancers [19], and oral cancers [20–22]. Oral cancers have become a global burden, especially in the developing nations of Southeast Asia [23]. Despite advancements in treatment approaches, the survival rate is dismal particularly due to late detection, often at stages III–IV at time of diagnosis. Optical techniques, like OCT, have thus become an important tool to serve as a powerful diagnostic adjunct to clinical examination. In this chapter we will summarize the developments in the field of OCT and discuss its applications for oral cancers.

11.1.1 Basis for OCT

While histology utilizes thin tissue sections (~5 μm) stained to highlight salient features, OCT generates cross-sectional images (similar to microtome sectioning) from light backscattered through tissues, typically without the need for any staining methods. OCT can be understood as an optical analog of ultrasound imaging which measures backscattered intensity of light instead of sound. It is noteworthy that histology and OCT images correspond well and thus can be used for appropriate clinical correlation. Cancer progression disrupts tissue architectural arrangement leading to a change in the intensity of backscattered light. OCT images can thus be used for noninvasive, real-time imaging to obtain cross-sectional as well as three-dimensional images.

11.2 Instrumentation

11.2.1 Working Principle

OCT is an interferometry-based imaging technique that uses near-infrared (NIR) light to map the depth-wise reflections from tissue to form cross-sectional images of morphological features at the scale of a micrometer. Huang et al. used OCT to obtain two-dimensional images based on the optical scattering of microstructures within the retina. Since then, several adaptations of OCT have been developed. A typical setup for OCT would consist of a low-coherence light source, a lateral-scanning mechanism, and an optical interferometer (Fig. 11.1). The Michelson interferometer splits the light into sample arm and reference arm and recombines the backscattering signal

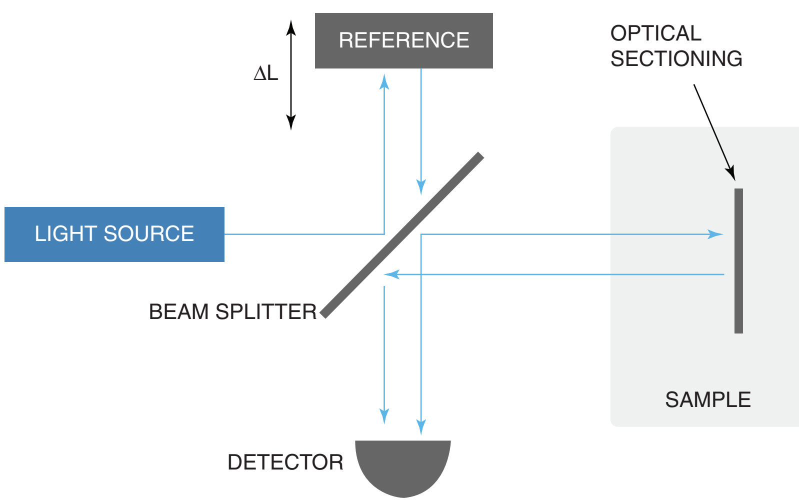

Fig. 11.1 Schematic showing optical sectioning of sample (ΔL, change of optical path length)

with the reflected reference light to a photodetector. OCT originated from optical coherence-domain reflectometry and rapidly gained value for biological applications [24, 25]. The spatial resolution of modern OCT systems is ~1–15 μm, and the imaging depth in scattering tissues is around 1–3 mm [26, 27]. Axial resolution of 10 μm is commonly employed, whereas ultrahigh axial resolution of ~1 μm has been achieved with a photonic crystal fiber [28]. Usually light source includes a low-coherence length source that can be generated by a superluminescent diode or an ultrafast (titanium-sapphire) laser (Fig. 11.2a–c). Incident signal is passed through a fiber coupler which is split into a sample arm and reference arm of the interferometer. Light reflected from sample is collected by sample arm fiber, and light reflected by reference mirror is collected by reference arm fiber. Reflected light from both arms is once again passed through the coupler and split into two parts where it is redirected toward the detector to form an interference pattern. The interference pattern is visible only when the optical path difference between the two arms is less

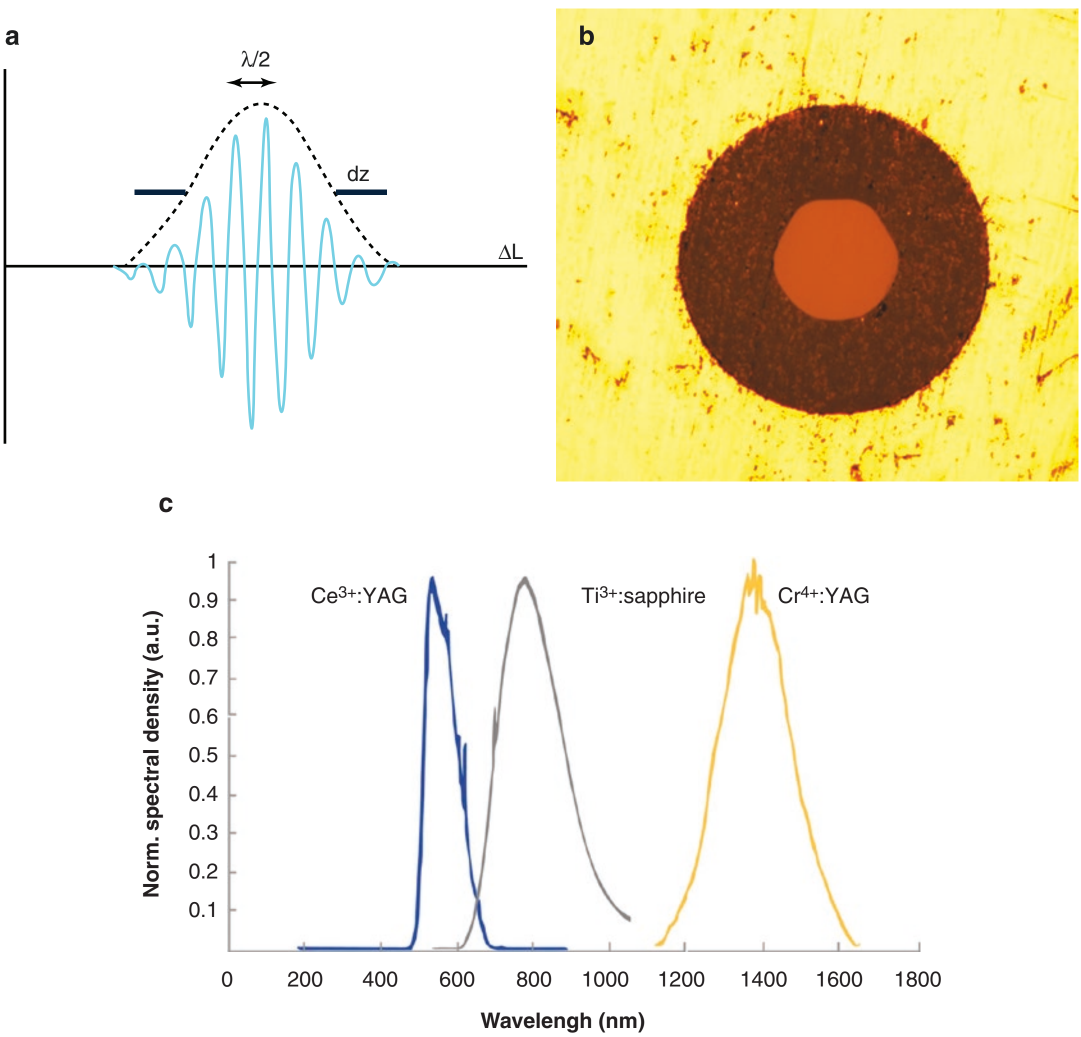

Fig. 11.2 Panel (**a**) shows the low-coherence length in OCT imaging characteristic of shorter center wavelength and broader bandwidth (λ, center wavelength of light source; dz, coherence length; ΔL, change of optical path length); panel (**b**) shows the crystalline fiber core cross section; and panel (**c**) compares spectral densities of different crystal-based light sources

than the coherence length of the light source. Since coherence length is inversely proportional to the optical bandwidth of the light source, OCT integrated with broadband low-coherence light source is able to discriminate closely adjacent signals and produces high-resolution image. In the recent times, imaging is being performed using a scanned optical beam from surgical microscopes, through user-friendly handheld probes and minimally invasive needle-biopsy probes.

11.2.2 Adaptation of OCT

Depending on the signal detection mechanism and data processing algorithms, OCT is classified as either time domain OCT (TD-OCT) or Fourier domain OCT (FD-OCT). FD-OCT can be further categorized into spectral domain OCT (SD-OCT) and swept-source OCT (SS-OCT). Other improvements on OCT include polarization-sensitive OCT, which detects changes in the polarization state of reflected light [29].

TD-OCT was the first generation of OCT, where the reference mirror is mounted on a moving stage and the depth profile is recorded by shifting the mirror linearly. As mechanical movement is involved in TD-OCT, it is restricted to a slow imaging speed, thereby limiting its biomedical application. In SD-OCT, the reference arm does not move, and depth-resolved structural information is extracted by capturing the interference spectrum in a spectrometer. In the case of SS-OCT, depth information of the sample is extracted by sweeping the individual wavelength spectrum emitted from a broadband source. Consequently, SS-OCT is also called optical frequency-domain imaging (OFDI). An advantage of the FD-OCT methods is higher signal to noise ratio and faster acquisition speed in comparison to TD-OCT. Furthermore, with SS-OCT, higher image acquisition rate and longer depth of imaging are achieved in comparison to SD-OCT. OCT techniques can also be combined with optical coherence microscopy (OCM) for confocal imaging. OCT combined with optical Doppler tomography (ODT) has been used for early diagnosis as well as evaluation of chemotherapy-induced oral mucositis and is capable of providing information about functional activity in tissue such as tissue blood flow. PS-OCT measures reflected both light intensity and the polarization state of the light signal coming from the sample. As such, PS-OCT can provide higher contrast between normal tissue and diseased tissue.

11.3 Biological Applications: OCT in Oral Cancers

OCT can be used both as an ex vivo and in vivo diagnostic tool and provides information on architectural changes or disorganized orientation and can discern epithelial pathology in oral tissues. Gross histological features suggestive of oral squamous cell carcinoma (OSCC) that can be detected with OCT include enlarged nuclei, increased nuclear-cytoplasmic ratio, altered rete peg organization, and discontinuity in basement membrane, which are common cellular and tissue alterations. The last two decades have witnessed OCT taking a major stride in oral cancer detections, leading to advancement in the field of novel diagnostic tools. In this chapter, we systematically discuss the topic by broadly classifying oral cancer studies into animal studies, ex vivo studies on human tissues, and in vivo clinical studies (Table 11.1).

11.3.1 Animal Studies

There are several exploratory OCT studies which have employed animal models of oral cancers [30–35]. A commonly used animal model is the hamster buccal pouch (HBP) model, already elaborated in the Chapter titled “Optical techniques: Investigations in Oral Cancers” in this book and also in these references [36, 37]. Briefly, HBP model forms tumors in 14 weeks, progressing through stages like hyperplasia,

Table 11.1 Summary of landmark studies on optical coherence tomography application for oral cancers, oral potentially malignant conditions, and healthy oral mucosa

Author	Year	Study type	Findings
Feldchetein et al	1998	First in vivo study	In vivo OCT imaging differentiates keratinized and nonkeratinized mucosa with high resolution [48]
Petra Wilder-Smith et al.	2004	Hamster pouch	Epithelial and subepithelial changes were recorded in hamster pouch model ($n = 32$). Agreement of OCT diagnosis and histopathology was 80% [34]
Matheny et al.	2004	Hamster pouch	OCT and optical Doppler tomography (ODT) combination detected vascular changes in hamster cheek pouch ($n = 22$). Good resolution was obtained to depth of 1–3 mm [30]
Petra Wilder-Smith et al.	2005	Hamster pouch	Specific application of OCT and ODT in hamster pouch ($n = 120$) and also in vivo multi-wavelength multiphoton (MPM) and second harmonic-generated (SHG) fluorescence as promising noninvasive modalities [21]
Hanna et al.	2006	Hamster pouch	OCT offered exceptional cheek pouch depth (1–3 mm), and 3D construction was possible for visualizing extent and tumor margins [31]
Ridgway et al.	2006	In vivo	OCT images of normal oral cavity ($n = 41$ patients) and pathological changes (leukoplakia, invasive cancer, etc.) were obtained [50]
Tsai et al.	2008	Ex vivo (SS-OCT)	First use of swept-source OCT for ex vivo oral lesion delineation, particular value in the determination of margins [39]
	2009	In vivo	Differentiating oral lesions based on carcinogenic stage of lesion using a SS-OCT system was possible because well-differentiated SCC had higher tissue absorption and decay constants [22]
Petra Wilder-Smith et al.	2009	In vivo	OCT showed excellent in vivo capability (i.e., histopathology agreement) in oral malignancy/premalignancy diagnosis ($n = 50$ lesions) [21]
Kim et al.	2009	First contrast enhancement attempt in hamster model	Contrast enhancement in OCT using surface plasmon resonant gold nanoparticles via microneedle and ultrasound-assisted delivery [82]
Park et al.	2010	Hamster pouch	Dual modality of OCT and FLIM for derivation of structural and functional information was attempted [70]
Jerjies et al.	2010	Ex- vivo	SS-OCT successfully identified malignant changes in suspicious oral lesions ($n = 34$) through analysis of four variables [40]
Ahn et al.	2011	Hamster pouch	3D-OCT and polarimetry were combined, which helped in the identification of oral cancer field cancerization areas and lesion margins ($n = 9$) [69]
Hamdoon et al.	2012	Ex vivo	OCT capable to identify difference between normal and diseased oral mucosa through evaluation of five microanatomical structures ($n = 78$ suspected oral lesions) [41]
	2013	Ex vivo	Wide spectrum of oral pathologies were studied ($n = 125$ lesions), which included 43 microinvasive carcinoma; accuracy was 82%, and kappa for intraobserver agreement was 0.72 for "need for biopsy" [43]
Pande et al.	2014	Hamster pouch	Automated classification of optical coherence tomography images for diagnosis of oral cancer in hamster cheek pouch [33]
Choi et al.	2014	In vivo	Devoted three-dimensional vascular perfusion maps were reconstructed using novel vessel extraction algorithms [56]
Lee et al.	2015	Instrument design	Constructed a wide-field polarization-sensitive swept-source OCT for in vivo oral application [47]
Yoon et al.	2015	Instrument design	Constructed in vivo wide-field reflectance imaging and polarization-sensitive OCT to procure both morphological and fluorescence information [46]

(continued)

Table 11.1 (continued)

Author	Year	Study type	Findings
Hamdoon et al.	2016	In vivo	OCT assessment of surgical margins (n = 112 margins in 28 (T1-T2 N0 M0) OSCC cases). Positive margins showed elevated epithelial thickness [44]
Pande et al.	2016	Hamster pouch	Automated classification of fluorescence lifetime imaging (FLIM) and combined OCT data for diagnosis of oral cancer in hamster pouch, with comparatively high sensitivity and specificity [71]
Lee et al.	2016	In vivo	Biopsy guidance of oral lesions using wide-field OCT and automated segregation of images [55]
Tsai et al.	2017	In vivo	High-resolution images of oral mucosa microcirculation were obtained [57]. "Microcirculation" may evolve as a novel OCT signature with high potential for oral cancer detection
Wei et al.	2017	In vivo	Three-dimensional images of microcirculation and quantitative metrics of capillary loop density were possible [58]

dysplasia, to squamous cell carcinoma (SCC), on application of carcinogens such as 7,12-dimethylbenzanthracene (DMBA). The earliest reported studies are by Matheny et al. [30] and Wilder-Smith et al. [34] who carried out feasibility studies and demonstrated OCT-based malignancy detection in the HBP model. While Matheny et al. employed 22 animals, and carried out both in vivo and ex vivo studies, and obtained good resolution to a depth of 1–3 mm, Wilder-Smith et al., from the same laboratory, performed in vivo studies on 36 animals and imaged epithelial and subepithelial changes. Their findings suggested that epithelial and subepithelial structures could be clearly distinguished, and corresponding histopathological analysis of the tissues suggested 80% concordance. The same group carried out further studies using 3D OCT image constructs and compared these with the gold standard histopathological images—both conventional and 3D images. The extent and localization of tumor margins were visualized to confirm dysplastic and malignant changes [31]. HBP tissues were assessed using parallel frequency-domain optical coherence tomography (FDOCT) and a thermal light source by Graf et al. [38] who in another study also assessed nuclear morphology via spectral oscillations while investigating HBP precancerous lesions [32]. Pande et al. attempted to develop automated algorithms to quantify malignancy-specific structural features of the oral epithelium by processing OCT data from HBP tissues. Statistical classification model based on this algorithm yielded sensitivity and specificity of 90.2% and 76.3%, respectively [5]. In another study, OCT was carried out on carcinogen-treated and normal HBP tissues [24]. Tissues corresponding to early and late stages of carcinogen-induced carcinogenesis were investigated. OCT images showed well-distinguished layers of epithelial and subepithelial layers in most controls and early week DMBA-treated tissues. Two control tissues also showed disrupted epithelial architecture. These observations were also confirmed by Raman spectroscopy and was attributed to repeated injuries incurred by regular pulling out of buccal pouches [37]. Several multimodal applications of OCT in conjunction with other optical techniques have been employed in pursuit of better sensitivity and specificity to distinguish cancerous and healthy conditions. Such studies are described in the section on "Multimodal Applications."

11.3.2 Ex Vivo Studies

OCT of ex vivo cancerous and oral potentially malignant conditions has been explored and compared with histopathology in several studies. A report on ex vivo imaging of an oral cancer sample with an SS-OCT system (axial resolution: 8 μm) suggested distinction of abnormal regions from normal regions [40]. In 2010, Jerjes et al. in a study on 34 oral lesions in 27 subjects, two clinicians blinded to histological diagnosis correctly segregated cases where biopsy was actually necessary; but the basement membrane was recognized only in 15 lesions [39]. Keratin cell layer identification and structural alterations in the layers have been shown in 87% of the cases in a cohort of 78 cancer subjects. Epithelial layer and basement membranes could be distinguished with an accuracy of 93.5% and 94%, respectively. An accuracy of 64% for blood vessels, 58% for salivary gland ducts, and 89% for rete pegs was also observed [41].

Ex vivo analysis of fibro-epithelial polyps, mild dysplasia, and moderate/severe dysplasia suggested epithelial differentiation as a function of depth and optical scattering from the cell nuclei. Mucosal layers in OCT images of oral dysplasia were not clear because of the higher density of abnormal cell nuclei, which impede light penetration. 3D-OCT datasets from same samples showed classification of biopsy samples into normal/mild and moderate/severe groups [42]. A major prospective study involving 125 suspicious lesions (125 subjects) utilized 2 independent team of readers to assess OCT images, which showed a sensitivity of 85%, specificity of 78%, and accuracy of 82%. Kappa coefficient of interobserver agreement was 0.72 on "the need for biopsy" [43]. Hamdoon et al. have also shown valuable application of OCT in the assessment of resection margins [44]. Their study on 112 margins (28 subjects) revealed 22 tumor-associated margins and 90 tumor-free margins. OCT accuracies for two independent expert readers were 88% and 84%, with an interobserver agreement as "very good" for superior, inferior, and medial margins and "good" for lateral surgical margin [44]. Birefringence can also be a potential parameter to distinguish healthy and cancerous tissues. A recent study involving eight oral mandibular tissues exploited in spectral domain polarization-sensitive optical coherence tomography (SD-PSOCT) suggested that monitoring of tissue birefringence along with backscattered intensity allows discrimination to differentiate between normal and cancerous lesions [45]. In relation to PSOCT, two previous studies had indicated that healthy buccal mucosa has higher birefringence compared to normal tongue tissue [46] and submucosal fibrosis has higher birefringence compared to adjoining normal mucosa [47]. PSOCT can pave way for distinguishing abnormal sites, based on collagen distribution.

11.3.3 In Vivo Clinical Studies

One of the earliest in vivo OCT studies imaged oral hard and soft tissues [48]. Several regions of the oral mucosa, including the masticatory mucosa (hard palate, gingival mucosa), the lining mucosa (soft palate, alveolar, buccal mucosa), the specialized mucosa (dorsum of the tongue), as well as the tooth structure, were imaged. The various types of keratinized and nonkeratinized mucosa could be distinguished with high accuracy [48]. Normal as well as abnormal gingiva and buccal mucosa classification was shown in 2005 [49]. In an attempt to explore further regions adjacent to oral mucosa, the mucosa of oropharynx was imaged ($n = 41$) during operative endoscopy. OCT imaging, in conjunction with endoscopic photography for gross and histologic image correlation, provided important microanatomical information for normal and pathological sites, with distinct zones of "normal, altered, and ablated tissue microstructures" for each pathology studied [50].

In order to discriminate successive cancer stages, several indicators may be needed to achieve good specificity. Swept-source OCT (SS-OCT) system data often uses three primary indicators—standard deviation (SD) and exponential decay constant (α) of an A-mode-scan spatial-frequency spectrum and the epithelium thickness—to distinguish normal and pathological tissues. Usually, in abnormal mucosa, the SD increases, α becomes smaller, and the epithelium becomes thicker. Studies have been carried out to evaluate the accuracy of these indicators. It is shown that SD and α are good diagnostic indicators for moderate dysplasia and squamous cell carcinoma (SCC), while epithelial thickness can discriminate epithelia hyperplasia and moderate dysplasia [51]. The field of diagnostic OCT experienced a surge in the number of studies undertaken after these initial reports. Some of these studies include differentiating oral lesions at different stages of carcinogenesis [22], oral dysplasia and malignancy (n = 50) [21], labial gland imaging using handheld SS-OCT system for healthy volunteers (n = 5) in both two and three dimensions [52], and lesions of upper aerodigestive tract (n = 52, 100 lesions) [53].

As mentioned previously, information about various parameters/indicators representing normal/healthy tissues can be of great importance while analyzing abnormal tissues. Normal values of oral epithelial thickness can thus be one such reference value. This was attempted on a large sample size of 143 healthy subjects, and epithelial thickness was measured at seven different locations. Buccal mucosa (294 μm) and the hard palate (239 μm) showed highest thickness, whereas the floor of the mouth (99 μm) showed the thinnest epithelium [20].

While OCT is a potential tool for oral cancer diagnosis, better results can also be achieved by improvements in methods of image analysis. Many research groups have tried to achieve this through innovative approaches. A procedure for analyzing OCT images involved plotting of the boundary between the layers of epithelium (EP) and lamina propria (LP) to determine the EP thickness and estimate distribution of dysplastic cells, based on standard deviation (SD) mapping. Laterally average range of 70% SD in the EP was shown to be a reasonable threshold for differentiating moderately dysplastic lesions (n = 44) from mild dysplastic ones (n = 39), with sensitivity and specificity of 82% and 90%, respectively [54].

Like other optical techniques, the field of OCT is continually evolving, and advancements are being made by several groups to improve instrumentation, image acquisition, and processing. For better in vivo results, an imaging device must be able to access lesions located anywhere in the oral cavity and should have a sufficient field of view (FOV) to scan extensively wide like leukoplakia lesions. Lee et al. in 2015 reported a handheld OCT device with a large FOV that enabled rapid volumetric imaging in a single acquisition. The use of fast rotary pullback catheters (RPC) facilitated easy placement of probe on lesions. Thus, this system could scan suspicious lesion in most of the regions of oral cavity in a clinically implementable time. With this system, 176 in vivo OCT volumes (51 subjects) were scanned for a range of lesions from scars to dysplasia and SCC, as well as contralateral sites. Birefringence may always give additional insights which can be further explored [47]. Wide-field imaging has also been explored to address issues such as automated segmentation of images [55].

In the recent times, OCT has evolved as an angiography tool for evaluation of oral mucosa microcirculation [56–58]. In a report by Maslennikova et al. who followed radiation therapy patients, for oropharyngeal and nasopharyngeal carcinoma, a dose-dependent microvascular reaction to radiation injury was shown, even before the early clinical signs of mucositis [59]. Microcirculation can be a potential biomarker, as angiogenesis is an important feature of advanced oral cancers and may be used for evaluation of oral cancer recurrence in patients following radiotherapy/chemotherapy.

11.4 Quest for Improved Oral Cancer Diagnosis

A major limitation associated with OCT is morphologically and optically similar scattering properties of different pathological tissues; it is sometimes difficult to optically detect early-stage cancers simply on the basis of conventional OCT imaging [60, 61]. While several improvements in the conventional OCT mechanism are regularly reported, other approaches are also being explored for improved diagnosis. We have discussed two such approaches in this chapter. The first approach involves multimodal applications where OCT in combination with other optical techniques is exploited to yield comparatively improved results than when the techniques are used individually. Another approach involves contrast enhancement mechanisms coupled with OCT.

11.4.1 Multimodal Applications

Individual optical modalities are typically sensitive to a small aspect of abnormal and pathological changes. Two or more imaging modalities when combined can simultaneously probe several tissue characteristics to elucidate pathological changes and provide better sensitivity and specificity, compared to a single modality. Multimodal systems have combined OCT with several modalities, including multiphoton microscopy [62], fluorescence spectroscopy [63], fluorescence lifetime imaging (FLIM) [64], multiphoton tomography [65], and Raman spectroscopy (RS) [66, 67]. Out of these modalities, some of them have been explored in oral cancers as well. However, the disparate optical requirements, different optical sources, and wavelengths sometimes limit their widespread clinical applications. Moreover, such multimodal approaches would be more useful if the light sources and detection elements can be coupled in a single instrument which will also help achieve image registration and correlation.

OCT and Polarimetry: Both ex vivo and in vivo imaging, using HBP model (n = 9), to assess the efficacy of combined polarimetry [68] and OCT, have revealed information on epithelial and subepithelial changes during carcinogenesis [69]. The polarimetry technique identified up to five times increased retardance in sites with SCC and up to three times increased retardance in dysplastic sites, when compared with normal tissues.

FLIM and OCT: Co-registered OCT/FLIM images from multiple 2 × 2 mm^2 regions of HBP tissues have been shown. While the OCT images have shown thickening of epithelial layer, and loss of layered structure, the FLIM images suggested higher nicotinamide adenine dinucleotide and reduced collagen emission within the cancerous regions [64, 70]. A recent study combining FLIM and OCT obtained an accuracy of 87.4%, better than accuracy based on only FLIM (83.2%) or OCT (81.0%). The complementary information provided by combined FLIM-OCT features showed high sensitivity and specificity for discriminating benign (88.2% and 92.0%), precancerous (81.5% and 96.0%), and cancerous (90.1% and 92.0%) stages [71].

RS and OCT: RS-OCT images compensate for limitations of both the techniques. Microstructural and biochemical features of dental caries analyzed using RS and OCT were reported in 2005 [66]. Dual-modal device capable of sequential RS-OCT image acquisition along a common optical axis that could utilize NIR to acquire data through common sampling optics [67] and integrated common clinical probe [72] is reported. Cancerous and normal HBP tissues probed by both OCT and RS have been investigated [24]. In a combined Raman and OCT study on HBP tissues, OCT images have shown well-distinguished layers of epithelial and subepithelial layers in most controls and early week DMBA-treated tissues; however, some control tissues corresponding to higher duration of carcinogen application showed disrupted epithelial architecture. Representative OCT images of HBP tissues, healthy and carcinogen treated for 9 and 13 weeks, are shown in Fig. 11.3. These observa-

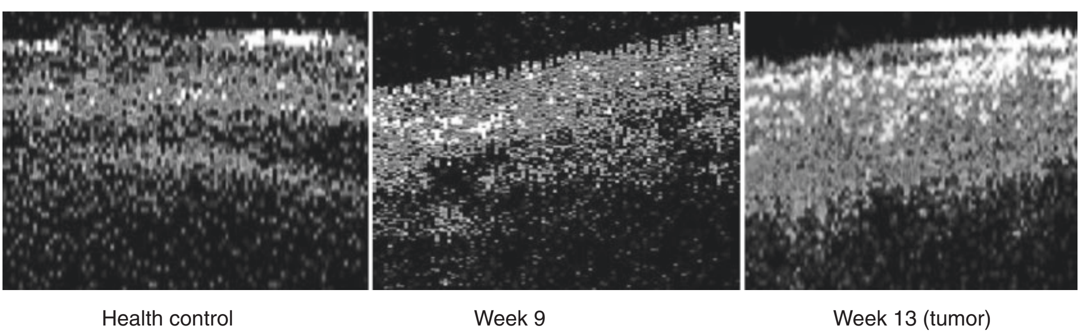

Fig. 11.3 OCT images of healthy control showing layered structures, and DMBA-treated tissues after 9 and 13 weeks showing disrupted architecture of epithelium. Week 13 tissues showing complete disruption of epithelium

tions, also confirmed by RS, were attributed to repeated injuries incurred during regular pulling out of buccal pouches for carcinogen application and regular observations [37]. Thus, combined application of RS and OCT provided an unbiased confirmation of the findings.

RCM and OCT: Reflectance confocal microscopy (RCM) is another emerging noninvasive imaging technique that enables an en face tissue visualization at the cellular level with good lateral and axial dimensions [46, 73]. Multimodal endoscopic systems that combine wide-field reflectance and fluorescence imaging with PS-OCT have been explored for human oral cavity. Wide-field reflectance/fluorescence imaging provided information of tissue surface based on reflectance and fluorescence, while PS-OCT provided information about subsurface structures and birefringence. Wide-field imaging with adjustable depth of focus (DOF) was used for high-sensitivity guided imaging [46].

RCM systems usually adapt optics with high focusing power for high lateral resolution, but the axial resolution is typically more than three times worse than the lateral resolution [73] due to anisotropic light propagation.

A full-field optical coherence tomography (FF-OCT) system can be considered as a light microscope with the axial resolution assisted by the coherence gating effect of OCT (Fig. 11.4). Compared to SD-OCT used in ophthalmic application, FF-OCT is a TD-OCT technique using a camera as detector to increase the scanning speed of traditional TD-OCT system (Fig. 11.5). A FF-OCT images all the lateral pixels simultaneously and performs axial scanning and dynamic focusing at the same time. By using high focusing power optics, lateral resolution similar to RCM can be achieved; accompanied with a broadband light source and corresponding narrow coherent gate, a FF-OCT system can achieve cellular resolution in all three dimensions (Fig. 11.4). FF-OCT can provide 3D in vivo image of oral tissue with 1 μm resolution and several hundred microns penetration depth. In the cross-sectional view of FF-OCT image, the boundary of epithelial and lamina propria layer can be distinguished which is an important information for oral cancer detection in the early stage. For reference purpose we have obtained in vivo OCT images in a healthy volunteer to show the lip, tongue, and skin microanatomy and tissue architecture at different depths, at nearly cellular resolution (refer to Figs. 11.6, 11.7, and 11.8). In the stratified squamous epithelial layer, the squamous cells are more keratinized with thinner thickness and irregular shape which can be observed in the OCT cross-sectional and en face images. The taste buds of tongue mucosa can be detected between the boundary of epithelial and lamina propria layer (Fig. 11.7). In the lamina propria layer, the features of elastic and collagen fiber which are parallel to the epithelium can be observed in the OCT cross-sectional image. The FF-OCT images correspond well with histology as RCM does, but the thickness of cell and tissue layer can be better distinguished with cross-sectional view of OCT images.

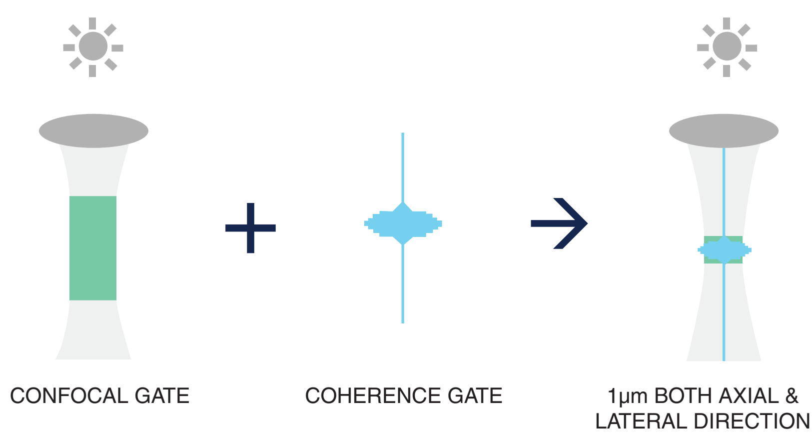

Fig. 11.4 Through confocal and coherence gating, excellent axial and lateral resolution can be achieved

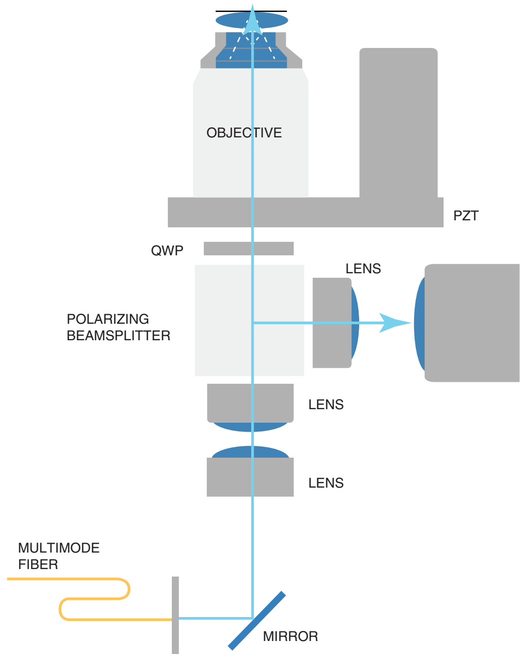

Fig. 11.5 Dissection of (Mirau-based) full-field OCT imaging system (PZT, piezoelectric transducer; QWP, quarter wave plate)

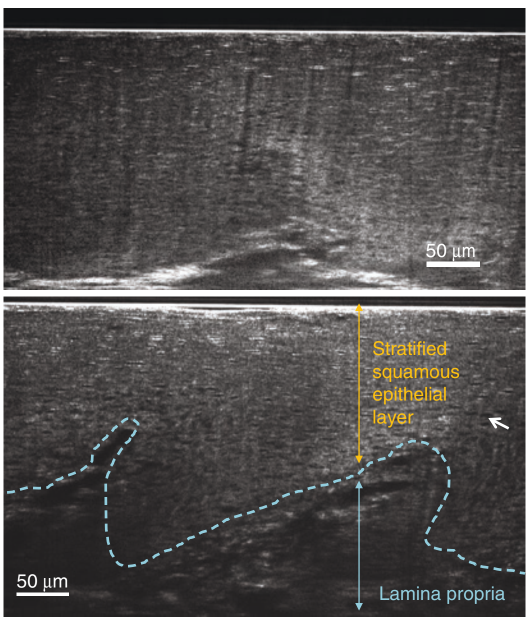

Fig. 11.6 The 3D cross section of in vivo OCT images (natural logarithmic gray level, 32 bit filtered by ImageJ) is of the lip taken in a healthy volunteer (41-year-old male). The dotted blue line indicates the epidermis-dermis junction, and the orange line indicates the thickness of the stratified squamous epithelium. The white arrow (showing the dark hole) indicates the nucleus of stratum spinosum. The incident power unto the sample and CCD exposure time are 4.5 mW and 2.7 milliseconds. The 3D cross-sectional images at different depths, 7 µm (panel **a**), 38 µm (panel **b**), 105 µm (panel **c**), 203 µm (panel **d**), 292 µm (panel **e**), are shown along with the oblique sections (panel **f**)

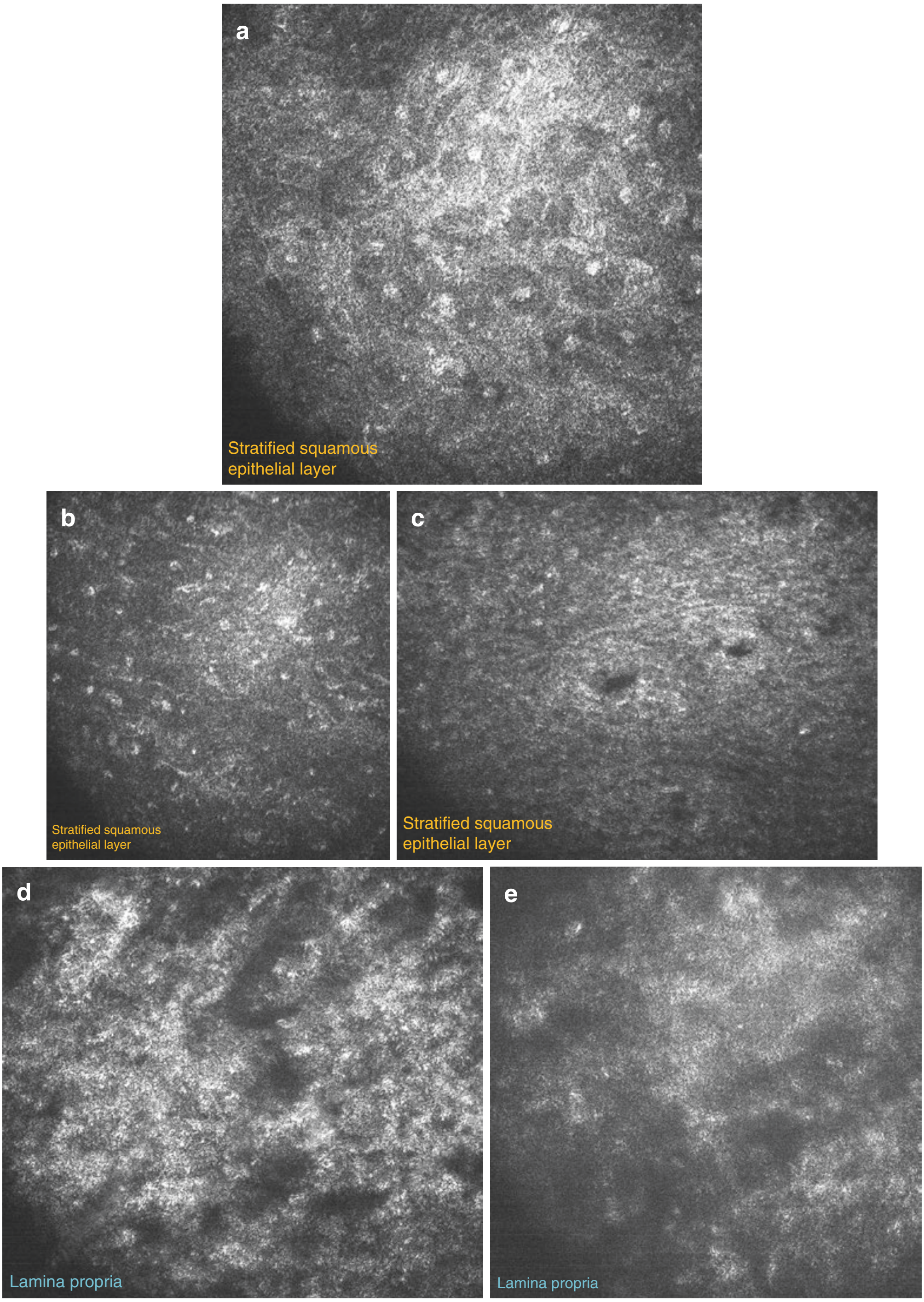

Fig. 11.6 (continued)

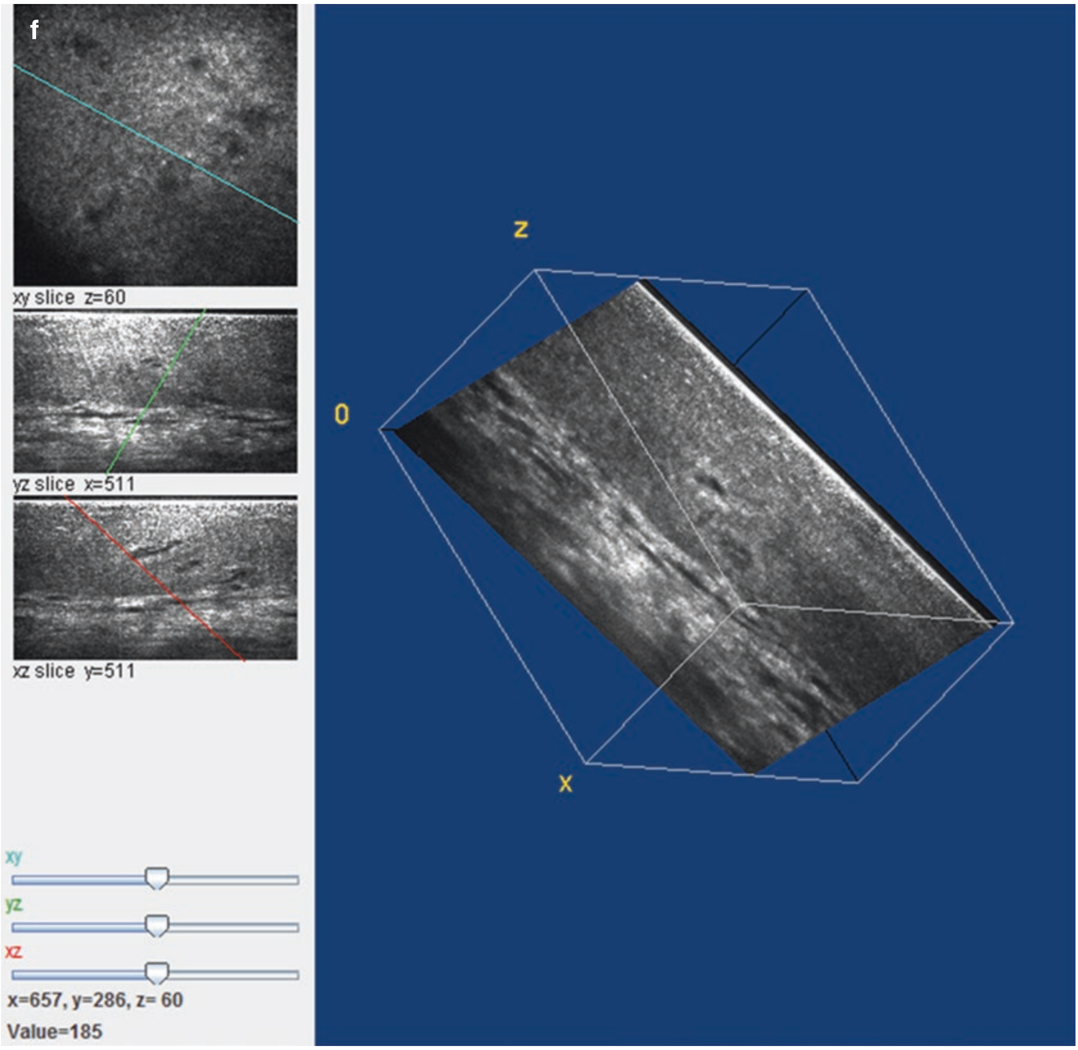

Fig. 11.6 (continued)

In view of complexity of biological phenomena, a single technique may not be sufficient to probe tissue characteristics, especially in case of cancers. Multimodal optical techniques can thus provide additional and complementary information from the same tissue and helps in better understanding of the biological complexity. A simple example can be of scars that leads to thickening due to fibrosis and alteration in the layered structure. OCT images alone can misinterpret them as cancerous, whereas fluorescence spectroscopy would suggest presence of collagen (healthy), rather than changes in NADH/FAD (indicator of possible cancerous changes). Multimodal application can thus be instrumental in preventing misdiagnosis.

11.4.2 Contrast Improvement

Although there is more progress in developing contrast agents to enhance OCT images in vivo, several contrast agents [74, 75] have been explored to overcome limitations. Contrast-enhancing mechanisms coupled with OCT will be useful. Spectroscopic OCT (SOCT) [76], pump and probe techniques [77], engineered microspheres [61], microbubbles [75], and nanocages or nanoparticles [78] are some of the reported methods.

SOCT utilizes the relative spectral difference between source and backscattered signals to measure absorption and scattering. However, SCOT can identify only those features with absorption scattering less than the source bandwidth. OCT contrast enhancement can also be achieved by exploiting nonlinear processes such as coherent anti-Stokes Raman scattering (CARS) and second harmonic generation. Research group led by Prof. Stephen Boppart has been working in this field using broadband illumination for imaging purposes, as well as molecular level contrast enhancement [60]. Pump and probe-based contrast enhancement for OCT imaging relies on transient absorptions in a sample that can be induced by an external pump

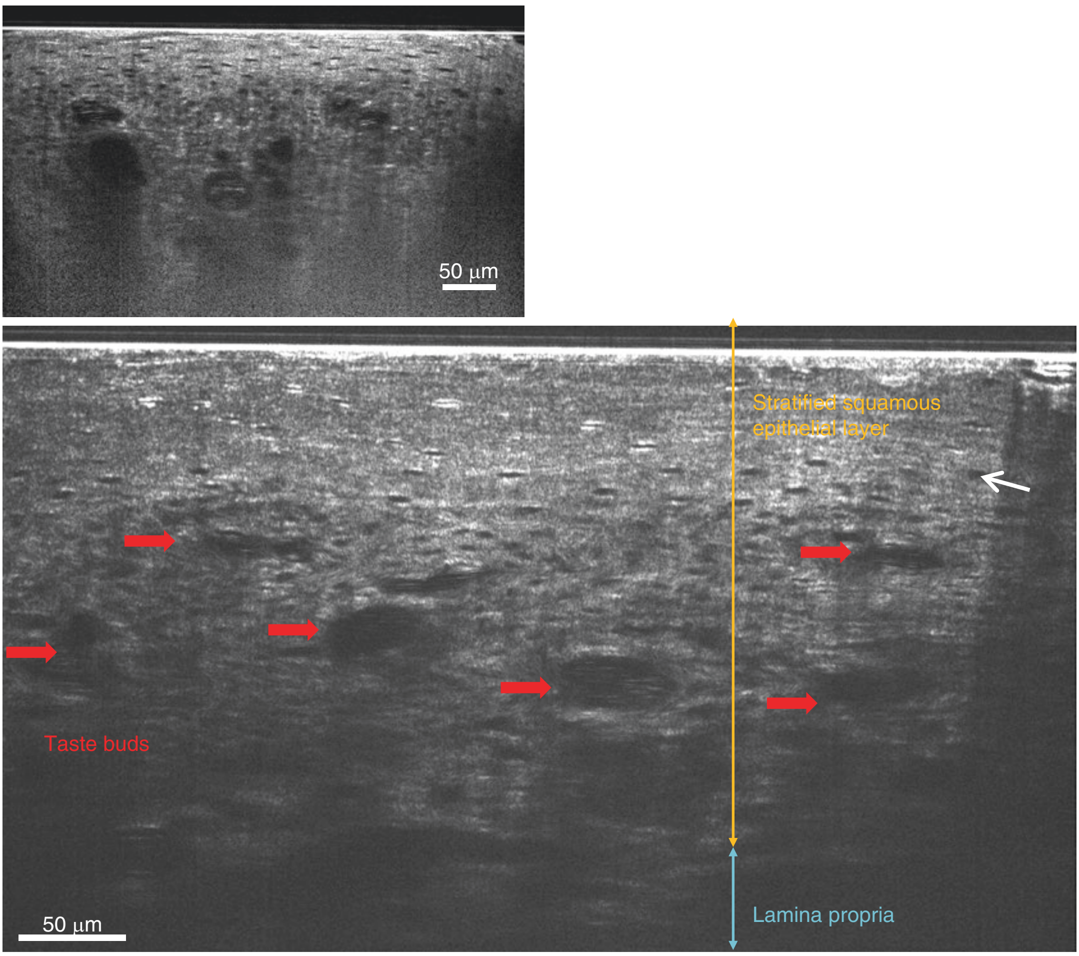

Fig. 11.7 The 3D cross section of in vivo OCT images are (natural logarithmic gray level, 32 bit depth filtered by ImageJ) of oral tongue taken in a healthy volunteer (41-year-old male). The dotted blue line indicates the epidermis-dermis junction, and the orange line indicates the thickness of the stratified squamous epithelium, and the red arrows are pointing the taste buds. The white arrow (showing the dark hole) indicates the nucleus of stratum spinosum. The incident power unto the sample and CCD exposure time are 4.5 mW and 2.7 ms. The cross-sectional images are shown at different depths: 40 µm (panel **a**), 64 µm (panel **b**), 113 µm (panel **c**), 181 µm (panel **d**) which are shown along with the oblique sections (panel **e**)

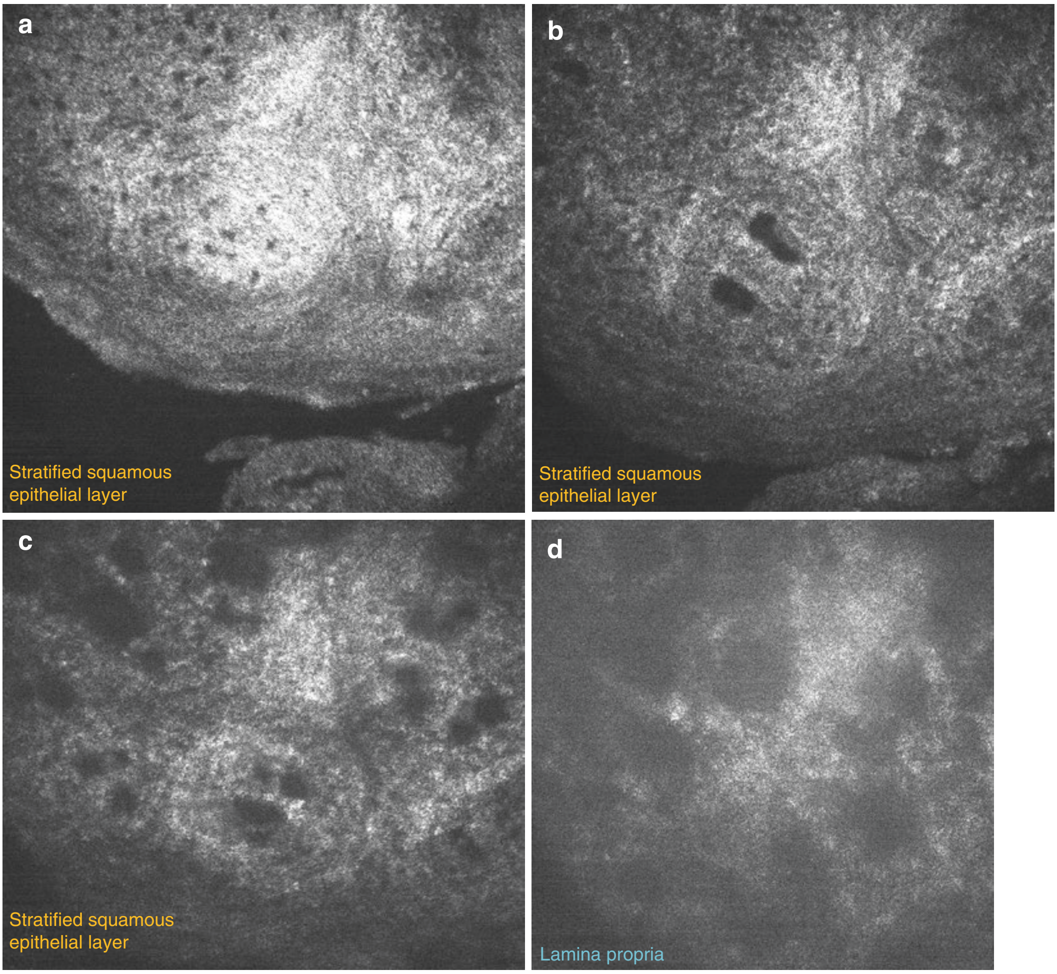

Fig. 11.7 (continued)

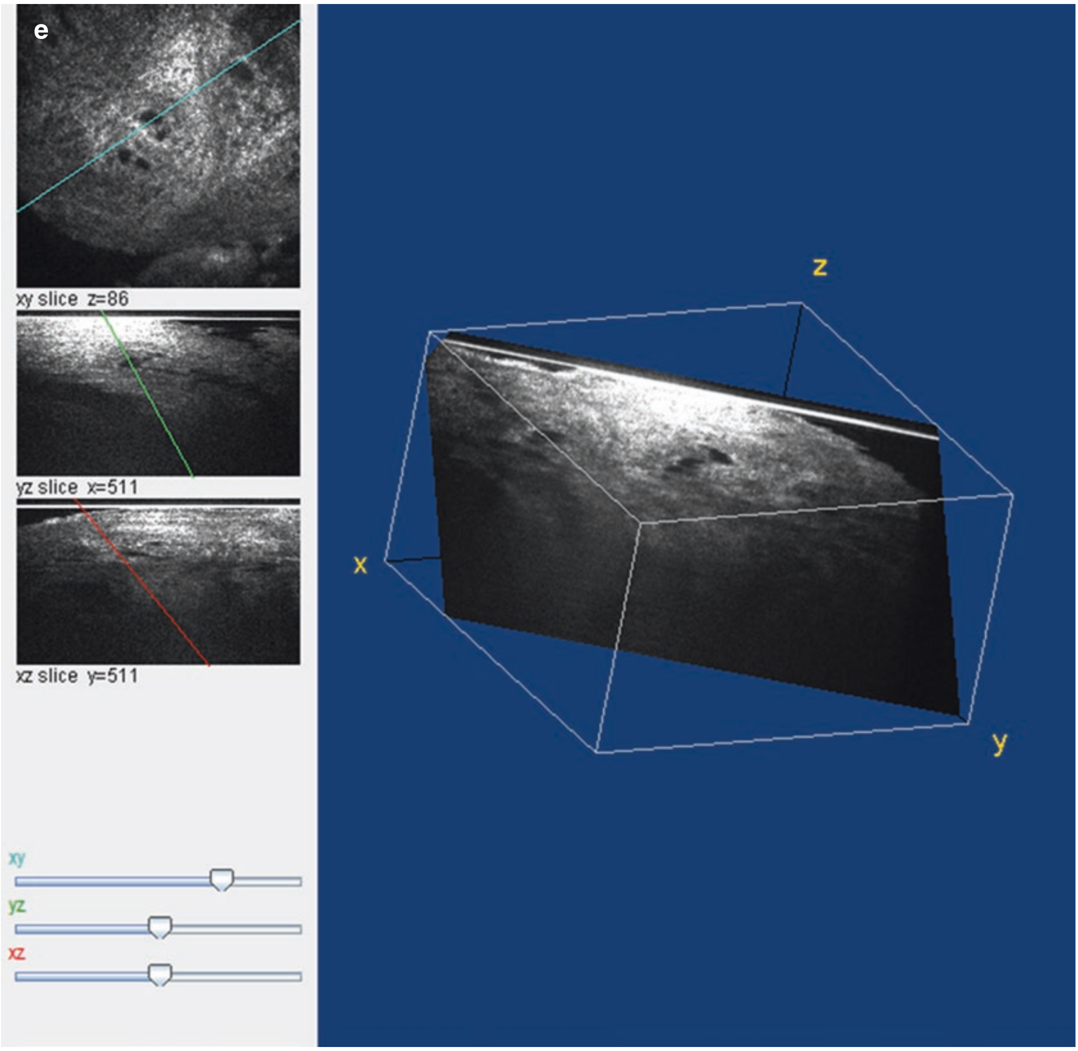

Fig. 11.7 (continued)

beam. However, this method requires introduction of different contrast agents, depending on the excitation source and the transient spectra of the molecules being investigated [76]. An alternative contrast enhancement method is using exogenous contrast agents like engineered microspheres that can change the absorption and scattering properties. These microspheres change the absorption and scattering characteristics in selected regions and can be targeted to structures like cellular receptors [61]. Most of these methods that are currently being used for contrast enhancement need a contrast agent. Moreover, further biomedical explorations are required to assess their success. Therefore, more studies and new techniques could help eliminate this limitation.

Nanoparticles (NPs), such as nanospheres, nanocages, nanoshells, and nanorods, have been explored to overcome OCT limitations by enhancing the contrast [78–80] but with limited in vivo success till date. Gold nanoparticles (Au NPs) are promising contrast agents as they are biocompatible, easy to synthesize, and can be specifically targeted through functional moieties. Moreover, optical resonance properties of Au

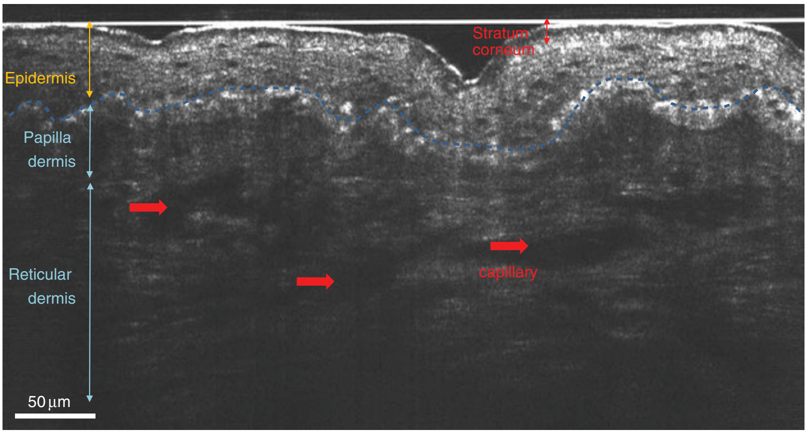

Fig. 11.8 In vivo OCT image of the skin from a healthy volunteer (age 41-year-old male). The dotted blue line indicates the epidermis-dermis junction, and the orange line indicates the thickness of the epidermis. The blue lines indicate the thicknesses of the papilla and reticular dermis. The red line indicates the thickness of the stratum corneum. Melanin can be observed on the epidermis-dermis junction which show white spot feature. The keratinocytes can be observed in the epidermis layer. In the dermis layer, the patterns of papilla and reticular dermis can be distinguished, and capillary can be seen in this layer too. The incident power unto the sample and CCD exposure time are 4.5 mW and 2.7 ms

NPs can be controlled by modifying their shapes and sizes [81]. One potential method is the topical application of gold nanoparticles on the epithelial surface. Moreover, topical application as compared to systemic administration can reduce toxicity burden, often associated with metallic nanoparticles. The stratum corneum, which is the uppermost layer of the oral epithelium is thick and can act as a biological barrier to the delivery of NPs. Kim et al. overcame this barrier in HBP model using microneedles assisted by ultrasound forces [82]. Recently developments have shown encouraging results with severalfold enhancements and increased depth of penetration. These studies have shown picomolar level sensitivity useful in in vivo imaging [83]. This approach still suffers from potential limitations including toxicity and poor in vivo delivery and distribution.

Conclusion

OCT can be used to obtain functional optical biopsies. OCT imaging combined with quantification of physiological functional parameters such as perfusion/oxygenation and cellular organization and improvements in signal analysis can allow achievement of goal. For better in vivo results, an imaging device must be able to access lesions located anywhere in the oral cavity where lesions may be actually located and should have a sufficient field of view (FOV) to quickly scan extensive lesions in a clinically feasible timing. Recent advancements in the field of OCT-based biomedical diagnosis suggest OCT can be an effective tool in oral cancer diagnosis. Limitations in OCT images can be overcome through multimodal application with other optical techniques like white-light fluorescence and photo-acoustic imaging as well as through contrast improvement. Availability of handheld OCT probe can serve as a real-time chairside diagnostic tool. Though it is extremely difficult to reach the accuracy of conventional histopathology, with the rapid advancement in biomedical engineering and computation, in the nearest future OCT can become a useful adjunct to chairside clinical examination, to screen suspected oral lesions, particularly to rule out oral cancers. Overall, OCT has a strong potential to be a noninvasive imaging technique and clinically useful diagnostic adjunct.

Acknowledgment We thank Yunglin David Ma and Allen Lin from Apollo Medical Optics, Ltd. for their cooperation.

References

1. Huang D, Swanson E, Lin C, Schuman J, Stinson W, Chang W, Hee M, Flotte T, Gregory K, Puliafito CA, et al. Optical coherence tomography. Science. 1991;254:1178–81.
2. Fujimoto JG. Optical coherence tomography for ultrahigh resolution *in vivo* imaging. Nat Biotechnol. 2003;21:1361–7.
3. Drexler W, Morgner U, Ghanta RK, Kärtner FX, Schuman JS, Fujimoto JG. Ultrahigh-resolution ophthalmic optical coherence tomography. Nat Med. 2001;7:502–7.
4. An L, Wang RK. In vivo volumetric imaging of vascular perfusion within human retina and choroids with optical micro-angiography. Opt Express. 2008;16:11438–52.
5. Boppart SA, Luo W, Marks DL, Singletary KW. Optical coherence tomography: feasibility for basic research and image-guided surgery of breast cancer. Breast Cancer Res Treat. 2004;84:85–97.
6. Vakoc BJ, Fukumura D, Jain RK, Bouma BE. Cancer imaging by optical coherence tomography: preclinical progress and clinical potential. Nat Rev Cancer. 2012;12:363–8.
7. Wessels R, De Bruin D, Faber D, Van Leeuwen T, Van Beurden M, Ruers T. Optical biopsy of epithelial cancers by optical coherence tomography (OCT). Lasers Med Sci. 2014;29:1297–305.
8. Bezerra HG, Costa MA, Guagliumi G, Rollins AM, Simon DI. Intracoronary optical coherence tomography: a comprehensive review: clinical and research applications. J Am Coll Cardiol Intv. 2009;2:1035–46.
9. Larina IV, Ivers S, Syed S, Dickinson ME, Larin KV. Hemodynamic measurements from individual blood cells in early mammalian embryos with Doppler swept source OCT. Opt Lett. 2009;34:986–8.
10. Olmedo JM, Warschaw KE, Schmitt JM, Swanson DL. Optical coherence tomography for the characterization of basal cell carcinoma in vivo: a pilot study. J Am Acad Dermatol. 2006;55:408–12.
11. Mogensen M, Joergensen TM, Nürnberg BM, Morsy HA, Thomsen JB, Thrane L et al. Assessment of optical coherence tomography imaging in the diagnosis of non-melanoma skin cancer and benign lesions versus normal skin: observer-blinded evaluation by dermatologists and pathologists. Dermatol Surg. 2009;35:965-72.
12. Jørgensen TM, Tycho A, Mogensen M, Bjerring P, Jemec GB. Machine-learning classification of non-melanoma skin cancers from image features obtained by optical coherence tomography. Skin Res Technol. 2008;14:364–9.
13. Wong BJ, Jackson RP, Guo S, Ridgway JM, Mahmood U, Su J, Shibuya TY, Crumley RL, Gu M, Armstrong WB. In vivo optical coherence tomography of the human larynx: normative and benign pathology in 82 patients. Laryngoscope. 2005;115:1904–11.
14. Çilesiz I, Fockens P, Kerindongo R, Faber D, Tytgat G, ten Kate F, van Leeuwen T. Comparative optical coherence tomography imaging of human esophagus: how accurate is localization of the muscularis mucosae? Gastrointest Endosc. 2002;56:852–7.
15. Cobb MJ, Hwang JH, Upton MP, Chen Y, Oelschlager BK, Wood DE, Kimmey MB, Li X. Imaging of subsquamous Barrett's epithelium with ultrahigh-resolution optical coherence tomography: a histologic correlation study. Gastrointest Endosc. 2010;71:223–30.
16. Pitris C, Jesser C, Boppart SA, Stamper D, Brezinski ME, Fujimoto JG. Feasibility of optical coherence tomography for high-resolution imaging of human gastrointestinal tract malignancies. J Gastroenterol. 2000;35:87–92.
17. Poneros JM, Brand S, Bouma BE, Tearney GJ, Compton CC, Nishioka NS. Diagnosis of specialized intestinal metaplasia by optical coherence tomography. Gastroenterology. 2001;120:7–12.
18. Escobar P, Belinson J, White A, Shakhova N, Feldchtein F, Kareta M, et al. Diagnostic efficacy of optical coherence tomography in the management of preinvasive and invasive cancer of uterine cervix and vulva. Int J Gynecol Cancer. 2004;14:470–4.
19. Tearney G, Brezinski M, Southern J, Bouma B, Boppart S, Fujimoto J. Optical biopsy in human urologic tissue using optical coherence tomography. J Urol. 1997;157:1915–9.
20. Prestin S, Rothschild SI, Betz CS, Kraft M. Measurement of epithelial thickness within the oral cavity using optical coherence tomography. Head Neck. 2012;34:1777–81.
21. Wilder-Smith P, Lee K, Guo S, Zhang J, Osann K, Chen Z, Messadi D. In vivo diagnosis of oral dysplasia and malignancy using optical coherence tomography: preliminary studies in 50 patients. Lasers Surg Med. 2009;41:353–7.
22. Tsai M-T, Lee C-K, Lee H-C, Chen H-M, Chiang C-P, Wang Y-M, Yang C-C. Differentiating oral lesions in different carcinogenesis stages with optical coherence tomography. J Biomed Opt. 2009;14:044027–8.
23. Ferlay J, Soerjomataram I, Dikshit R, Eser S, Mathers C, Rebelo M, Parkin DM, Forman D, Bray F. Cancer incidence and mortality worldwide: sources, methods and major patterns in GLOBOCAN 2012. Int J Cancer. 2015;136:E359–86.
24. Kumar P, Krishna CM, Sahoo NK, Rao KD. Multimodal spectroscopic applications in cancer diagnosis: combined Raman spectroscopy and optical coherence tomography. Asian J Phys. 2015;7
25. Takada K, Yokohama I, Chida K, Noda J. New measurement system for fault location in optical waveguide devices based on an interferometric technique. Appl Opt. 1987;26:1603–6.

26. Fujimoto JG, Pitris C, Boppart SA, Brezinski ME. Optical coherence tomography: an emerging technology for biomedical imaging and optical biopsy. Neoplasia. 2000;2:9–25.
27. Zysk AM, Nguyen FT, Oldenburg AL, Marks DL, Boppart SA. Optical coherence tomography: a review of clinical development from bench to bedside. J Biomed Opt. 2007;12:051403–21.
28. Wang Y, Zhao Y, Nelson J, Chen Z, Windeler RS. Ultrahigh-resolution optical coherence tomography by broadband continuum generation from a photonic crystal fiber. Opt Lett. 2003;28:182–4.
29. De Boer JF, Milner TE. Review of polarization sensitive optical coherence tomography and stokes vector determination. J Biomed Opt. 2002;7:359–71.
30. Matheny ES, Hanna NM, Jung WG, Chen Z, Wilder-Smith P, Mina-Araghi R, Brenner M. Optical coherence tomography of malignancy in hamster cheek pouches. J Biomed Opt. 2004;9:978–81.
31. Hanna NM, Waite W, Taylor K, Jung WG, Mukai D, Matheny E, et al. Feasibility of three-dimensional optical coherence tomography and optical Doppler tomography of malignancy in hamster cheek pouches. Photomed Laser Surg. 2006;24:402–9.
32. Graf RN, Robles FE, Chen X, Wax A. Detecting precancerous lesions in the hamster cheek pouch using spectroscopic white-light optical coherence tomography to assess nuclear morphology via spectral oscillations. J Biomed Opt. 2009;14:064030–8.
33. Pande P, Shrestha S, Park J, Serafino MJ, Gimenez-Conti I, Brandon J, Cheng Y-S, Applegate BE, Jo JA. Automated classification of optical coherence tomography images for the diagnosis of oral malignancy in the hamster cheek pouch. J Biomed Opt. 2014;19:086022.
34. Wilder-Smith P, Jung W-G, Brenner M, Osann K, Beydoun H, Messadi D, Chen Z. In vivo optical coherence tomography for the diagnosis of oral malignancy. Lasers Surg Med. 2004;35:269–75.
35. Jung W, Zhang J, Chung J, Wilder-Smith P, Brenner M, Nelson JS, Chen Z. Advances in oral cancer detection using optical coherence tomography. IEEE J Sel Top Quantum Electron. 2005;11:811–7.
36. Kumar P, Bhattacharjee T, Ingle A, Maru G, Krishna CM. Raman spectroscopy of experimental oral carcinogenesis: study on sequential cancer progression in hamster buccal pouch model. Technol Cancer Res Treat. 2016;15:NP60–72.
37. Kumar P, Bhattacharjee T, Pandey M, Hole AR, Ingle A, Murali Krishna C. Raman spectroscopy in experimental oral carcinogenesis: investigation of abnormal changes in control tissues. J Raman Spectrosc. 2016;47:1318.
38. Graf R, Brown W, Wax A. Parallel frequency-domain optical coherence tomography scatter-mode imaging of the hamster cheek pouch using a thermal light source. Opt Lett. 2008;33:1285–7.
39. Tsai MT, Lee HC, Lu CW, Wang YM, Lee CK, Yang CC et al. Delineation of an oral cancer lesion with swept-source optical coherence tomography. J Biomed Opt. 2008;13:044012.
40. Jerjes W, Upile T, Conn B, Hamdoon Z, Betz CS, McKenzie G, Radhi H, et al. In vitro examination of suspicious oral lesions using optical coherence tomography. Br J Oral Maxillofac Surg. 2010;48:18–25.
41. Hamdoon Z, Jerjes W, Al-Delayme R, McKenzie G, Jay A, Hopper C. Structural validation of oral mucosal tissue using optical coherence tomography. Head Neck Oncol. 2012;4:29.
42. Adegun OK, Tomlins PH, Hagi-Pavli E, Mckenzie G, Piper K, Bader DL, et al. Quantitative analysis of optical coherence tomography and histopathology images of normal and dysplastic oral mucosal tissues. Lasers Med Sci. 2012;27:795–804.
43. Hamdoon Z, Jerjes W, Upile T, McKenzie G, Jay A, Hopper C. Optical coherence tomography in the assessment of suspicious oral lesions: an immediate ex vivo study. Photodiagn Photodyn Ther. 2013;10:17–27.
44. Hamdoon Z, Jerjes W, McKenzie G, Jay A, Hopper C. Optical coherence tomography in the assessment of oral squamous cell carcinoma resection margins. Photodiagn Photodyn Ther. 2016;13:211–7.
45. Sharma P, Verma Y, Sahu K, Kumar S, Varma AV, Kumawat J, et al. Human ex-vivo oral tissue imaging using spectral domain polarization sensitive optical coherence tomography. Lasers Med Sci. 2017;32:143–50.
46. Yoon Y, Jang WH, Xiao P, Kim B, Wang T, Li Q, et al. In vivo wide-field reflectance/fluorescence imaging and polarization-sensitive optical coherence tomography of human oral cavity with a forward-viewing probe. Biomed Opt Express. 2015;6:524–35.
47. Lee AMD, Cahill L, Liu K, MacAulay C, Poh C, Lane P. Wide-field in vivo oral OCT imaging. Biomed Opt Express. 2015;6:2664–74.
48. Feldchtein FI, Gelikonov GV, Gelikonov VM, Iksanov RR, Kuranov RV, Sergeev AM, Gladkova ND, Ourutina MN, Warren JA, Reitze DH. In vivo OCT imaging of hard and soft tissue of the oral cavity. Opt Express. 1998;3:239–50.
49. C. Shu-Fan, L. Chih-Wei, T. Meng-Tsan, W. Yih-Ming, C.C. Yang, C. Chun-Ping, Oral Cancer Diagnosis with Optical Coherence Tomography, 2005 IEEE Engineering in Medicine and Biology 27th Annual Conference, 2005, pp. 7227–7229.
50. Ridgway JM, Armstrong WB, Guo S, et al. In vivo optical coherence tomography of the human oral cavity and oropharynx. Arch Otolaryngol Head Neck Surg. 2006;132:1074–81.
51. Tsai M-T, Lee H-C, Lee C-K, Yu C-H, Chen H-M, Chiang C-P, Chang C-C, Wang Y-M, Yang CC. Effective indicators for diagnosis of oral cancer using optical coherence tomography. Opt Express. 2008;16:15847–62.
52. Ozawa N, Sumi Y, Shimozato K, Chong C, Kurabayashi T. *In vivo* imaging of human labial glands using advanced optical coherence tomography.

Oral Surg Oral Med Oral Pathol Oral Radio Endod. 2009;108:425–9.
53. Volgger V, Stepp H, Ihrler S, Kraft M, Leunig A, Patel PM, Susarla M, Jackson K, Betz CS. Evaluation of optical coherence tomography to discriminate lesions of the upper aerodigestive tract. Head Neck. 2013;35:1558–66.
54. Lee CK, Chi TT, Wu CT, Tsai MT, Chiang CP, Yang CC. Diagnosis of oral precancer with optical coherence tomography. Biomed Opt Express. 2012;3:1632–46.
55. A.M. Lee, R. Goldan, H. Pahlevaninezhad, G. Hohert, K. Liu, C.E. MacAulay, et al, Towards biopsy guidance of oral lesions with wide-field OCT imaging, Biomedical Optics 2016, Optical Society of America, Fort Lauderdale, Florida, 2016, pp. JM4A4.
56. Choi WJ, Wang RK. *In vivo* imaging of functional microvasculature within tissue beds of oral and nasal cavities by swept-source optical coherence tomography with a forward/side-viewing probe. Biomed Opt Express. 2014;5:2620–34.
57. Tsai MT, Chen Y, Lee CY, Huang BH, Trung NH, Lee YJ, et al. Noninvasive structural and microvascular anatomy of oral mucosae using handheld optical coherence tomography. Biomed Opt Express. 2017;8:5001–12.
58. Wei W, Choi WJ, Wang RK. Microvascular imaging and monitoring of human oral cavity lesions in vivo by swept-source OCT-based angiography. Lasers Med Sci. 2018;33:123–34.
59. Maslennikova AV, Sirotkina MA, Moiseev AA, Finagina ES, Ksenofontov SY, Gelikonov GV, et al. In-vivo longitudinal imaging of microvascular changes in irradiated oral mucosa of radiotherapy cancer patients using optical coherence tomography. Sci Rep. 2017;7:16505.
60. Vinegoni C, Bredfeldt JS, Marks DL, Boppart SA. Nonlinear optical contrast enhancement for optical coherence tomography. Opt Express. 2004;12:331–41.
61. Lee TM, Oldenburg AL, Sitafalwalla S, Marks DL, Luo W, Toublan FJ-J, et al. Engineered microsphere contrast agents for optical coherence tomography. Opt Lett. 2003;28:1546–8.
62. Vinegoni C, Ralston T, Tan W, Luo W, Marks DL, Boppart SA, et al. Integrated structural and functional optical imaging combining spectral-domain optical coherence and multiphoton microscopy. Appl Phys Lett. 2006;88:053901.
63. Barton JK, Guzman F, Tumlinson A. Dual modality instrument for simultaneous optical coherence tomography imaging and fluorescence spectroscopy. J Biomed Opt. 2004;9:618–23.
64. Jo JA, Applegate BE, Park J, Shrestha S, Pande P, Gimenez-Conti IB, Brandon JL. *In Vivo* simultaneous morphological and biochemical optical imaging of oral epithelial Cancer. IEEE Trans Biomed Eng. 2010;57:2596–9.
65. König K, Speicher M, Bückle R, Reckfort J, McKenzie G, Welzel J, et al. Clinical optical coherence tomography combined with multiphoton tomography of patients with skin diseases. J Biophotonics. 2009;2:389–97.
66. Ko AC, Choo-Smith LP, Hewko M, Leonardi L, Sowa MG, Dong CC et al. Ex vivo detection and characterization of early dental caries by optical coherence tomography and Raman spectroscopy. J Biomed Opt. 2005;10:031118.
67. Patil CA, Bosschaart N, Keller MD, van Leeuwen TG, Mahadevan-Jansen A. Combined Raman spectroscopy and optical coherence tomography device for tissue characterization. Opt Lett. 2008;33:1135–7.
68. Bickel WS, Davidson J, Huffman D, Kilkson R. Application of polarization effects in light scattering: a new biophysical tool. Proc Natl Acad Sci USA. 1976;73:486–90.
69. Ahn Y-C, Chung J, Wilder-Smith P, Chen Z. Multimodality approach to optical early detection and mapping of oral neoplasia. J Biomed Opt. 2011;16:076007.
70. Park J, Jo JA, Shrestha S, Pande P, Wan Q, Applegate BE. A dual-modality optical coherence tomography and fluorescence lifetime imaging microscopy system for simultaneous morphological and biochemical tissue characterization. Biomed Opt Express. 2010;1:186–200.
71. Pande P, Shrestha S, Park J, Gimenez-Conti I, Brandon J, Applegate BE, et al. Automated analysis of multimodal fluorescence lifetime imaging and optical coherence tomography data for the diagnosis of oral cancer in the hamster cheek pouch model. Biomed Opt Express. 2016;7:2000–15.
72. C.A. Patil, H. Krishnamoorthi, D.L. Ellis, T.G. van Leeuwen, A. Mahadevan-Jansen. A clinical probe for combined Raman spectroscopy-optical coherence tomography (RS-OCT) of the skin cancers, 2010, pp. 75480L.
73. García-Hernández A, Roldán-Marín R, Iglesias-Garcia P, Malvehy J. *In Vivo* noninvasive imaging of healthy lower lip mucosa: a correlation study between high-definition optical coherence tomography, reflectance confocal microscopy, and histology. Dermatol Res Pract. 2013;2013:205256.
74. Boppart SA, Oldenburg AL, Xu C, Marks DL. Optical probes and techniques for molecular contrast enhancement in coherence imaging. J Biomed Opt. 2005;10:041208–14.
75. Barton JK, Hoying JB, Sullivan CJ. Use of microbubbles as an optical coherence tomography contrast agent. Acad Radiol. 2002;9:S52–5.
76. Morgner U, Drexler W, Kärtner F, Li X, Pitris C, Ippen E, et al. Spectroscopic optical coherence tomography. Opt Lett. 2000;25:111–3.
77. Rao KD, Choma MA, Yazdanfar S, Rollins AM, Izatt JA. Molecular contrast in optical coherence tomography by use of a pump–probe technique. Opt Lett. 2003;28:340–2.
78. Cang H, Sun T, Li Z-Y, Chen J, Wiley BJ, Xia Y, et al. Gold nanocages as contrast agents for spec-

troscopic optical coherence tomography. Opt Lett. 2005;30:3048–50.

79. Oldenburg AL, Hansen MN, Zweifel DA, Wei A, Boppart SA. Plasmon-resonant gold nanorods as low backscattering albedo contrast agents for optical coherence tomography. Opt Express. 2006;14:6724–38.
80. Agrawal A, Huang S, Wei Haw Lin A, Lee M-H, Barton JK, Drezek RA, Pfefer TJ. Quantitative evaluation of optical coherence tomography signal enhancement with gold nanoshells. J Biomed Opt. 2006;11:041121–8.
81. Wilson R. The use of gold nanoparticles in diagnostics and detection. Chem Soc Rev. 2008;37:2028–45.
82. Kim CS, Wilder-Smith P, Ahn Y-C, Liaw L-HL, Chen Z, Kwon YJ. Enhanced detection of early-stage oral cancer *in vivo* by optical coherence tomography using multimodal delivery of gold nanoparticles. J Biomed Opt. 2009;14:034008.
83. Liba O, SoRelle ED, Sen D, de la Zerda A. Contrast-enhanced optical coherence tomography with picomolar sensitivity for functional in vivo imaging. Sci Rep. 2016;6:23337.

12 Bioimpedance in Oral Cancer

Gargi S. Sarode, Sachin C. Sarode, and Prashanth Panta

Abstract

Bioimpedance is described as the response of living organisms to an external current. It is an amount of obstruction to the flow of the external current through the tissues. Bioimpedance is a noninvasive method for evaluating the structure of a living organism. A bioimpedance signal can be used for describing the tissues. Bioimpedance of a tissue differs with different applied frequencies. It is an established technique in detection of breast cancer, cervical cancer, prostate cancer, and other cancers. There are evidences that significant differences exist between bioimpedance of normal and malignant tissue. With this view in mind, a comprehensive description of the technique is hereby given to deliberate the role of bioimpedance with a special emphasis on oral cancer. We have also discussed the studies carried out on oral potentially malignant disorders (OPMDs) and oral squamous cell carcinoma (OSCC) and realized the necessity for more studies especially on OPMDs and OSCC together.

G. S. Sarode, MDS, PhD (✉)
S. C. Sarode, PhD
Department of Oral Pathology and Microbiology, Dr. D. Y. Patil Dental College and Hospital, Pune, Maharashtra, India

P. Panta, MDS
Department of Oral Medicine and Radiology, MNR Dental College and Hospital, Sangareddy, Telangana, India
e-mail: maithreya.prashanth@gmail.com

12.1 Introduction

Impedance, by definition, is the effective resistance of an electric circuit or component to alternating current (AC), arising from the combined effects of ohmic resistance and reactance, or it is considered as a complex ratio of the voltage to the current in an AC circuit. It is the extent of the opposition that a circuit offers to a current when a voltage is applied. The word, *impedance*, was coined by Oliver Heaviside in 1886 [1]. Arthur Kennelly was the first to characterize impedance with complex numericals in 1893 [2]. Impedance encompasses the notion of resistance to AC circuits and retains both magnitude and phase, whereas resistance only has magnitude. The impedance caused by inductance and capacitance collectively denotes reactance and forms the imaginary part of impedance, while resistance forms the real part.

12.2 Bioimpedance

Bioimpedance is about the electrical properties of a tissue or a biomaterial. It simply means to what degree the tissue is a suitable conductor. It is the amount of how well the tissue opposes electric current course. It is the response of a living tissue to an externally applied electric current. It is an amount of the opposition to the course of current passing, as contrast to electrical conductivity. Thus, it is defined as the measurement of the impedance signal, which is

P. Panta (ed.), *Oral Cancer Detection*, https://doi.org/10.1007/978-3-319-61255-3_12

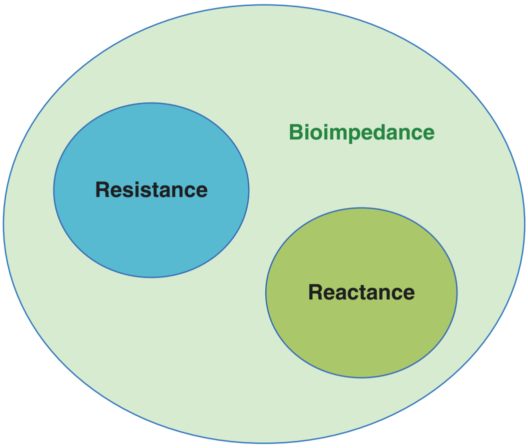

Fig. 12.1 Correlation between bioimpedance, resistance, and reactance

obtained by injecting a low-level sinusoidal current into the tissue and measuring the voltage drop generated by the tissue impedance. In short, it is the summation of tissue resistance and reactance (Fig. 12.1).

Electrical properties of a cell depend upon intracellular composition [3]. The conductivity and permittivity are frequency dependent [4], and if there is an alteration in bioimpedance, it is due to the augmented water and salt content, distorted membrane permeability, packing concentration, and positioning of cells [5].

Thus the bioelectrical properties of cells convey information about the cellular morphology and physiology [6]. Various parameters can be measured using this technique and can be used to detect pathologies [7]. Cellular bioimpedance depends upon its physiology and chemical constituents [8–10] and physiochemical alterations of the tissues [11].

12.3 Electrical Properties of Human Tissues

Human tissues are groups of cells with resistive cellular fluids. The electrical parameters of tissues diverge considerably depending on their make-ups. The cellular membrane composed of a reedy bilayered lipids with permeable ion channels is both capacitive and resistive. As bioimpedance of the tissues contains both resistance and capacitance (the electrostatic storage of charge induced by voltage), it is complex and can be explained as $Z = R + jX$, where Z is the impedance, R is the resistance, and X is the reactance [12].

Resistance is the opposition of a conductor to the AC. As the electric current trips within the body, resistance is consistent with that in non-biological conductors [13, 14]. Reactance is created by the surplus opposition to the current from the capacitance effect of the cell membranes, tissue interfaces, and structural characters [15]. Reactance signifies the cells' capacity to store energy and this energy is stored in the cell membrane. Thus, reactance indicates the total intact cell membranes in the human body. The reactance aids in calculating the metabolically active proportion of the body.

Capacitance is a parameter, which resists a voltage change and helps to store energy. On the other hand, permittivity reveals the capability of charges in the material to travel as a reaction to an electric field. Phase angle indicates condition and integrity of the cells. It is expressed in degrees and changes as a response to changes in the current frequency [16]. The correlation between the phase angle and cellular condition is increasing and almost linear. Phase angle gives an indication of cell lipid status and is consistent with intact, healthy cell membranes and body cell mass.

The frequency applied modifies the electric properties of cells and is presented in the form of α-, β-, and γ-dispersion [17–19]. The α-dispersion (low frequencies, i.e., 10 Hz–10 kHz) depends on the ionic environment. The β-dispersion describes structure relaxation (10 kHz–10 MHz). The γ-dispersion is linked with tissue water molecules, but at high frequencies (Fig. 12.2) [18]. The bioimpedance also fluctuates with temperature and time [19] and is anisotropic [19, 20].

12.4 Measurement of Bioimpedance

Bioimpedance is determined by applying a trivial electric current to the tissue with two electrodes and picking up the subsequent small voltage with

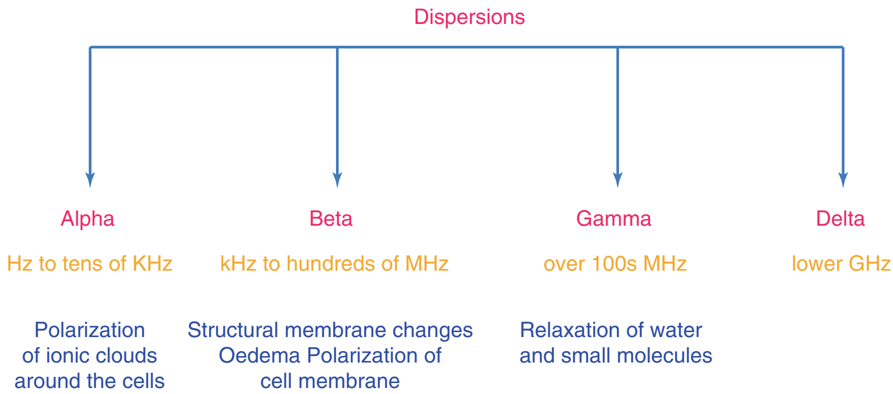

Fig. 12.2 Types of dispersions and their significance

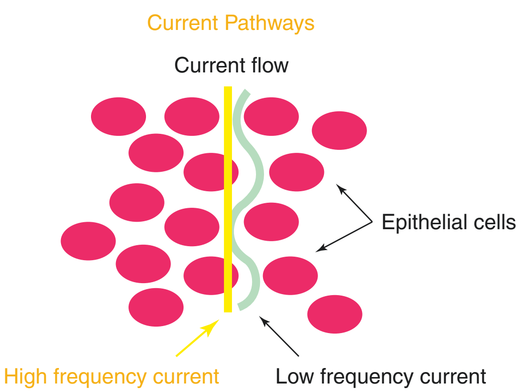

Fig. 12.3 High- and low-frequency current pathways through the epithelium

an additional set of electrodes. The lower the voltage, the lower will be the bioimpedance. The cellular membranes are thin but possess a high resistivity, and they perform electrically as tiny capacitors [21]. Bioimpedance can thus be expended to gauge the volumes, shapes, or tissue electrical properties and can be used to characterize the state of a tissue or organs and get diagnostic images (Fig. 12.3).

It is also considered a safe method as the current frequency used is not enough to excite electrically impulsive cells. There are no reported cases of untoward incidents provoked by bioimpedance after several trials. The magnitude of the applied current is below the perception threshold. But, there are no established safety protocols for devices using bioelectrical impedance. Thus, methodical formal safety standards are required to be set [22].

12.5 Bioimpedance Measurement Devices

Electrical properties of tissues have been recognized since 1872. They were also further discussed using a broader range of frequencies on various tissues. Thomasset piloted the research work with bioimpedance as an index of total body water. Hoffer et al. and Nyboer are the first to introduce the technique using four surface electrodes. By the 1970s, the foundation of the technique was established. Several single-frequency analyzers then were made commercially available. By the 1990s, the numerous multifrequency analyzers were readily available to use. The use of bioimpedance has increased as the device is portable and safer; the technique is simpler, noninvasive, real time, and economical [23].

Devices for measurement of bioimpedance are classified as point bioimpedance measurement devices and spectrum bioimpedance measurement devices [24–26].

There are also bioimpedance imaging systems available, which are classified into transverse [27–31] and planar bioimpedance imaging systems. Following this, a CMOS microelectrode array was devised by Chai et al. [32] and a 2D imaging system by Ching et al. [33]. Also, Rodriguez et al. [34] have introduced an implantable bioimpedance sensor ASIC.

We have used a precision impedance analyzer, AD5934 from Analog Devices, USA, to measure the bioimpedance of oral potentially malignant disorders (OPMDs) and oral squamous cell carcinoma (OSCC) for their reliable detection.

12.6 Bioimpedance in Various Malignancies

- The use of bioimpedance in cancer detection is well known since 1926 on breast cancer [25].
- In 1988, Surowiec et al. [35] disclosed that the dielectric coefficients and the conductivity of lesional tissues varied among different samples.
- In 1990, Morimoto et al. [36] revealed that there were significant differences in the impedance values of breast cancers and benign tumors.
- Morimoto et al. [37] in 1993 showed significant differences between various tissues and tumors, thus proposing its feasible implications in diagnosis.
- In 1994, Joines et al. [38] demonstrated that at all the frequencies, both the parameters, conductivity and relative permittivity, were higher in malignancies than in the normal tissues of the same type.
- In 1996, Jossinet et al. [39] found that the lowest dispersions were gathered from adipose tissue, carcinoma, and fibroadenoma of the excised specimens [40]. Jossinet and Schmitt [41] attempted to describe a novel set of eight factors which can differentiate cancerous tissue from the other tissues.
- Then Emtestam et al. [42] in 1998 disclosed statistically significant changes in various indices in basal cell carcinoma (BCC).
- In 1999, Chauveau et al. [43] have also explored that cancer cells can be distinguished from normal and those with fibrocystic changes.
- Subsequently, in 1999, an impedance imaging system for detection of breast cancer known as TransScan TS2000 was approved by the American Food and Drug Administration as an aid to mammography.
- In 1999, Lee et al. [44] used bioimpedance for occult prostate cancer.
- Afterwards, Brown et al. [8] in 2000 concluded that bioimpedance can be utilized to differentiate normal from precancerous cervical tissues.
- Malich et al. [45] in 2002 reviewed the differentiation of sonographically equivocal lesions using bioimpedance.
- Subsequent to this, Glickman et al. [46] in 2003 considered the technique as a noninvasive one for differentiation of benign from malignant skin lesions. Beetner et al. [47] in 2003 concluded that bioimpedance can provide a quick noninvasive differentiation of BCC from other lesions. Later on, Hope et al. [48] in 2003 suggested several benefits of the technique like easy on patients, economical, and useful in diagnosis.
- Afterward, Ohmine et al. [49] in 2004 used local percutaneous measurement of bioimpedance for diagnosis.
- Aberg et al. [50] in 2004 concluded that the technique has 96% sensitivity and 86% specificity; Aberg et al. [51] in 2005 attained distinction between nevi and BCC and nevi and melanomas.
- Abdul et al. [52] in 2005 proved bioimpedance as an assuring cervical screening tool.
- Gupta et al. [53] in 2008 concluded that phase angle can be used as an independent prognostic marker. Halter et al. [54] in 2008 concluded that conductivity and permittivity were higher in normal than in prostrate malignant tissue.
- Ching et al. [55] in 2010 conducted a maiden study on the use of bioimpedance in the screening of OSCC of the tongue and found a significant difference at 50 kHz between cancerous and surrounding normal tissue which

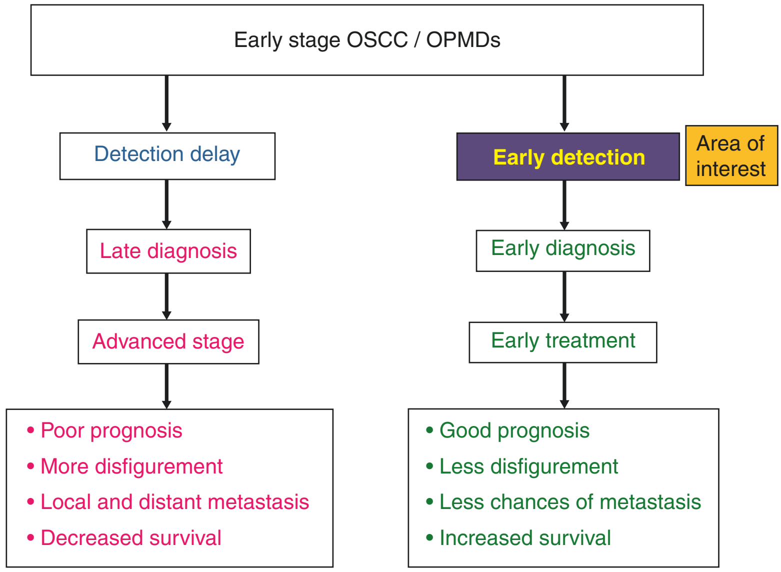

Fig. 12.4 Need for early detection of oral squamous cell carcinoma using bioimpedance

was extended by Sun et al. [56] in 2010 (Fig. 12.4).

- Arias et al. [57] in 2010 used the electric cell-substrate impedance sensing (ECIS) system to analyze the behavior of OSCC cells and concluded that the method is real time.
- Yang et al. [58] in 2011 proved the method as a rapid, label-free and noninvasive to detect oral cancer.

"OSCC has been studied from various standpoints from clinic-pathological to molecular-genetic aspects, but the electromagnetic context is relatively underexplored. And one of interesting concepts of this area is bioimpedance." So far, only a few studies have been carried out in the context of OSCC. Moreover, no study has been carried on OSCC of any other oral tissue except for the tongue. For such reasons, we have studied various electrical properties in different OPMDs and OSCC.

12.7 Study of Electrical Properties in OSCC and OPMDs

We used precision impedance analyzer AD5934, Analog Devices, USA, for the measurement of bioimpedance in OSCC of various oral tissues and oral potentially malignant disorders. Fifty patients with clinical and histopathological diagnosis of OSCC, oral leukoplakia, and OSMF each and 22 of oral erythroplakia were included. Age- and sex-matched healthy individuals without deleterious habits or any clinically evident oral lesions or systemic diseases were selected as controls, while subjects with pacemakers were excluded from the study.

The impedance analyzer used in this study was precision impedance analyzer AD5934 from Analog Devices, USA. Measurements were taken by a disposable probe with four 1 mm diameter silver electrodes (2 mm between electrode centers) fixed in square configuration on a wooden spatula (5 mm width × 3 mm thick × 100 mm long) (Fig. 12.5) [59].

12.7.1 Procedure

The relevant history of each patient was recorded with comprehensive history of present illness, predisposing factors, duration of lesion, and responses to the past treatment. The oral cavity was examined thoroughly to determine location and clinical presentation. Four electrical properties were measured for each patient: impedance (Z), phase angle

(θ), real part of impedance (R), and imaginary part of impedance (X). At every position, measurements were made at six different frequencies, 20 Hz, 50 kHz, 1.3 MHz, 2.5 MHz, 3.7 MHz, and 5 MHz, with the applied voltage of 200 mV (Fig. 12.6).

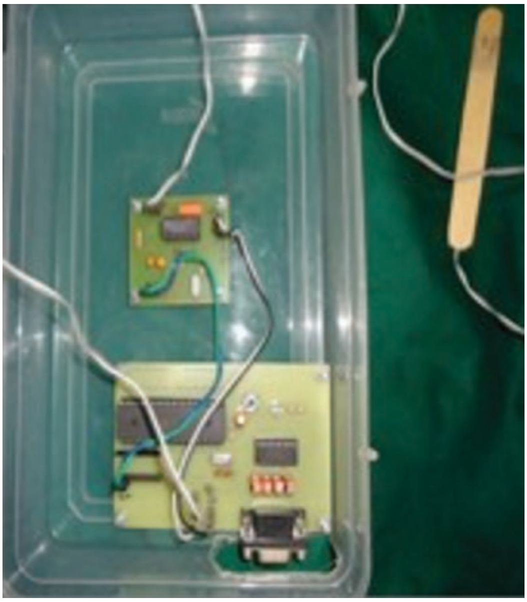

Fig. 12.5 AD5934 impedance analyzer: hardware

Fig. 12.6 Placement of probe with four silver electrodes on lesional tissue

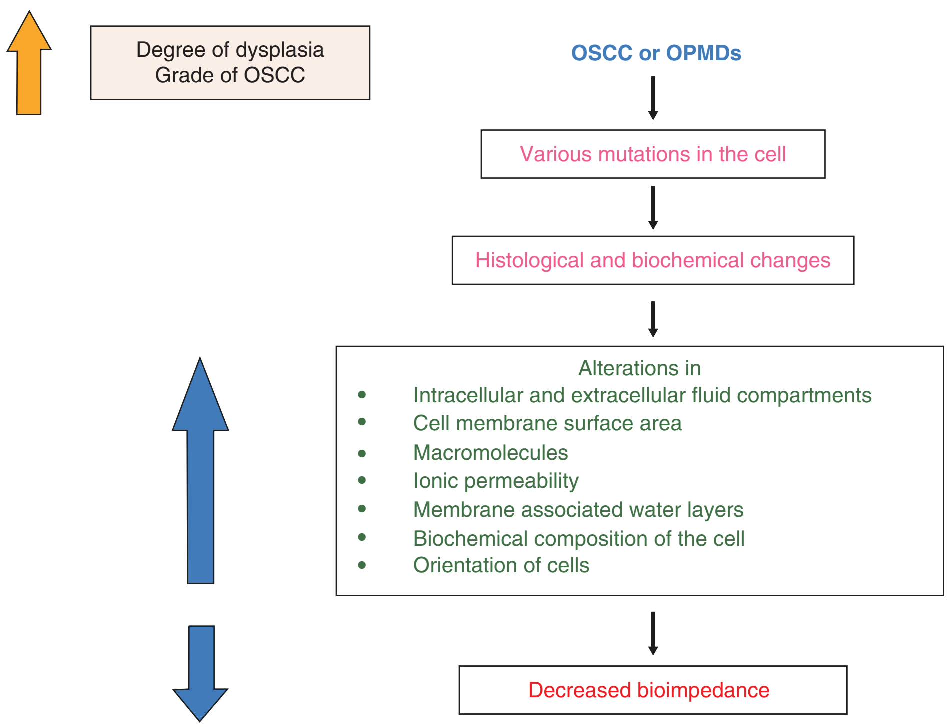

Fig. 12.7 Statement of problem

12.8 Results and Observations

12.8.1 Oral Squamous Cell Carcinoma

12.8.1.1 Bioimpedance in Oral Squamous Cell Carcinoma [59]

Four electrical parameters (Z, θ, R, and X) were assessed in the α- and β-dispersion regions (20 Hz–5 MHz) to examine if significant difference in values obtained in the oral mucosa of patients and healthy subjects existed. Our findings disclosed that specific frequencies (α- and β-dispersion regions) are useful in distinguishing the OSCC from normal tissue.

Only the electrical property measurement at 20 Hz and 50 kHz could significantly distinguish the affected tissue from normal tissue. The capacitive cell membranes have a high impedivity at low frequencies. And in a structured compact tissue like epithelium, current can only follow the narrow extracellular path. This leads to a high electrical resistance. But in pathologies, the pathway is relatively wider and thus offers lesser resistance. Moreover, reduced cell volume removes the complex pathways through the epithelium. This results in reduction of low-frequency impedivity [48].

In the present study, impedance values decreased from 4493 ± 216.9 Ω to 28.85 ± 3.481 Ω for OSCC patients and from 15,490 ± 287.2 Ω to 30.13 ± 2.601 Ω for controls as the frequency increased from 20 Hz to 5 MHz. At 20 Hz, the bioimpedance for OSCC patients ranged from 4236.5 Ω to 5159.1 Ω with a mean of 4493 ± 216.9 Ω, whereas for controls the impedance values ranged from 14,939.1 Ω to 15,926.9 Ω with a mean of 15,490 ± 287.2 Ω. At 50 KHz the bioimpedance for OSCC patients ranged from 309.1 Ω to 414.1 Ω with a mean of 370.0 ± 26.45 Ω, whereas for controls the impedance values ranged from 830.3 Ω to 800.4 Ω with a mean of 817.1 ± 7.227 Ω. Statistically significant difference was noted between the study and control group at 20 Hz and 50 KHz with a p value <0.0001. Similar results were obtained by Ching et al. [55] and Sun et al. [56] in their studies on tongue tissue. Results of the study conducted by Ching et al. showed that Z of CTT ($Z = 4318$ Ω at 20 Hz and 372 Ω at 50 kHz) was significantly smaller than that of the surrounding NTT ($Z = 12{,}772$ Ω at 20 Hz and 783 Ω at 50 kHz). Results of the study by Sun et al. showed that Z of CTT ($Z = 4356$ Ω at 20 Hz and 381 Ω at 50 kHz) was significantly smaller than that of the surrounding NTT ($Z = 13{,}295$ Ω at 20 Hz and 764.8 Ω at 50 kHz) as well as that in healthy subjects ($Z = 14{,}459$ Ω at 20 Hz and 816.9 Ω at 50 kHz) (Graph 12.1). Inter-patient variability stemmed from a number of patient-dependent conditions that occur during data acquisition including different electrode and tissue contact impedances associated with fluid content of the saliva, slight variations in pressure applied between the probe and tissue, and inherent patient-to-patient tissue variation. A malignant tissue is expected to have more conductivity than adjacent tissue, since cancerous tissue has more cellular water and salt content, altered membrane permeability, packing density and orientation of cells, and hence higher conductivity. Conductivity is inversely proportional to resistance and thus impedance, and hence cancerous tissue shows lower levels of impedance as compared to normal tissues (Fig. 12.7). Our results are also in accordance with the in vivo study by Wang et al. [60] on prostate cancer.

For clinico-pathological correlation, the 50 OSCC patients were divided into four groups according to TNM staging into stages I–IV and into 3 groups according to histopathological grade into well, moderate, and poorly differentiated.

Six cases were in stage I, 3 cases in stage II, 17 cases in stage III, and 24 cases in stage IV. Moreover, 16 of the cases were found to be well differentiated, 8 cases were moderately differentiated, and 6 cases were poorly differentiated (Graph 12.2) [59].

Bioimpedance values of the three groups classified according to TNM stage and histopathological grades were compared at frequencies of 20 Hz, 50 KHz, 1.3 MHz, 2.5 MHz, 3.7 MHz, and 5 MHz. Bioimpedance values decreased from stage I to stage IV. Statistically significant differences in values of bioimpedance were

Graph 12.1 Comparison of bioimpedance in OSCC at various frequencies

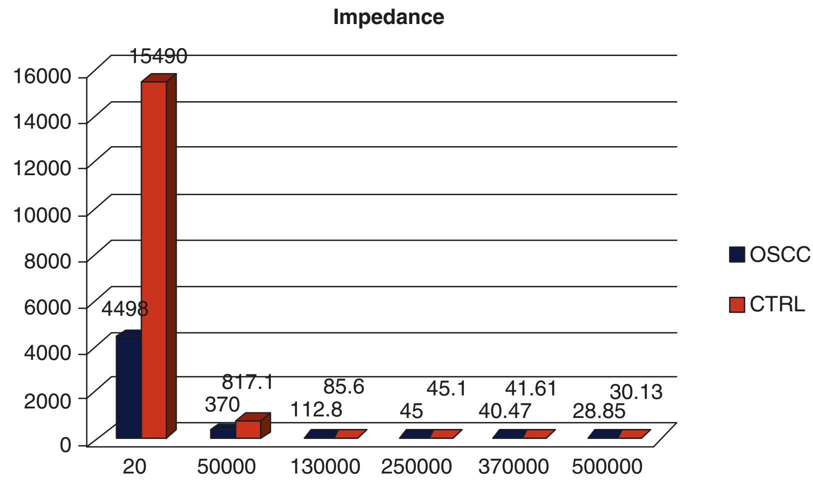

Graph 12.2 Comparison of bioimpedance in various histopathological grades at 20 Hz

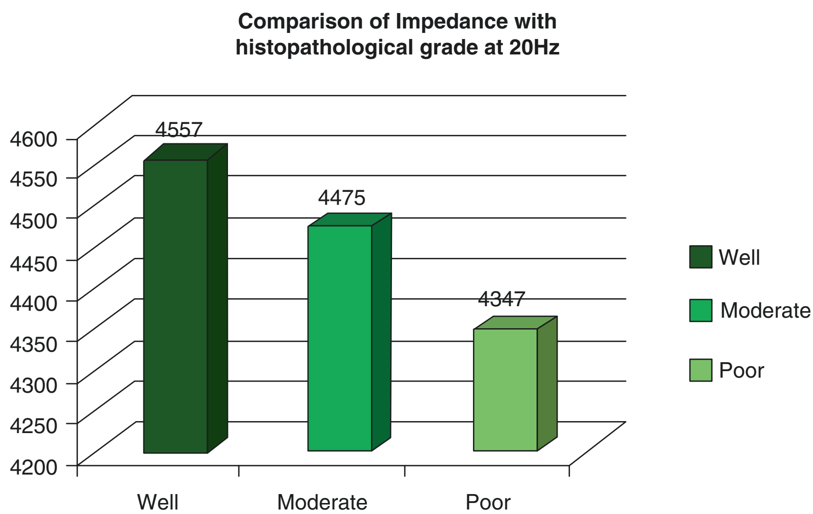

observed between stage I (4881 ± 262.5 Ω) and stage IV (4500 ± 181.6 Ω) at frequency of 20 Hz (*p* value 0.0060) and also between stage I (4881 ± 262.5 Ω) and stage III (4376 ± 121.3 Ω) at frequency of 20 Hz (*p* value 0.0005). However, no statistically significant difference was noted in the other parameters like phase angle and real and imaginary parts of impedance between the three stages (Graph 12.3) [59].

Furthermore, bioimpedance values dropped as the histological grade advanced from well differentiated to poorly differentiated. Statistically significant differences in values of bioimpedance were also observed between the grades well (4557 ± 260.8 Ω) and poor (4347 ± 76.12 Ω) only at 20 Hz (*p* value = 0.0004). Moreover, no statistically significant difference was noted in the other parameters of phase angle and real and imaginary parts of impedance between the three grades. To the best of our knowledge, reports on the bioimpedance values in relation to different stages and grades of OSCC is not available in the current literature.

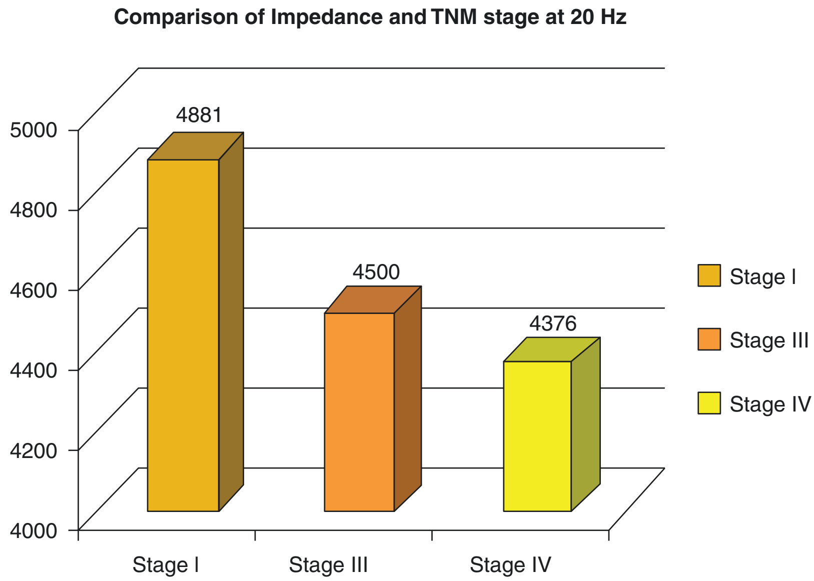

Graph 12.3 Comparison of bioimpedance in various TNM stages at 20 Hz

12.8.1.2 Phase Angle in Oral Squamous Cell Carcinoma

Phase angle in the present study decreased from −21.81$^{\theta}$ ± 2.092$^{\theta}$ to −99.25$^{\theta}$ ± 38.57$^{\theta}$ for the study group and from −14.56$^{\theta}$ ± 0.6917$^{\theta}$ to −111.9$^{\theta}$ ± 5.806$^{\theta}$ for the control group as the measurement frequency increased from 20 Hz to 5 MHz. At 20 KHz, the phase angle of OSCC patients ranged from −17.9$^{\theta}$ to −25.2$^{\theta}$ with a mean of −21.81$^{\theta}$ ± 2.092$^{\theta}$, whereas for controls the phase angle ranged from −13.2$^{\theta}$ to −15.8$^{\theta}$ with a mean of −14.56$^{\theta}$ ± 0.6917$^{\theta}$. At 50 KHz, the phase angle of OSCC patients ranged from −29.7$^{\theta}$ to −42.0$^{\theta}$ with a mean of −37.24$^{\theta}$ ± 2.614$^{\theta}$, whereas for controls the phase angle ranged from −47.6$^{\theta}$ to −53.4$^{\theta}$ with a mean of −50.35$^{\theta}$ ± 1.787$^{\theta}$. Statistically significant difference was noted between the study and control group at 20 Hz and 50 KHz with a p value <0.0001 (Graph 12.4).

These findings are consistent with those of Ching et al. [57] which showed that the phase angle of CTT (θ = −22.74 at 20 Hz and −37.97 at 50 kHz) was significantly larger than that of the surrounding NTT (θ = −13.40 at 20 Hz and −49.78 at 50 kHz).

Results of the study by Sun et al. [58] showed that the phase angle of CTT (θ = −21.10$^{\theta}$ at 20 Hz and −37.5$^{\theta}$ at 50 kHz) was significantly larger than that of the surrounding NTT (θ = −14.3$^{\theta}$ at 20 Hz and −49.6$^{\theta}$ at 50 kHz) as well as that of healthy subjects (θ = −14.7$^{\theta}$ at 20 Hz and −50.1$^{\theta}$ at 50 kHz).

12.8.1.3 Real Part of Impedance in Oral Squamous Cell Carcinoma

In the present study, real part of impedance decreased from 4198 ± 162.6 Ω to −8.617 ± 0.3957 Ω for the study group and from 14,000 ± 348.7 Ω to −12.26 ± 1.478 Ω for the control group as the measurement frequency amplified from 20 Hz to 5 MHz. At 20 KHz, the real part of impedance of OSCC patients ranged from 3948.8 Ω to 4495.8 Ω with a mean of 4198 ± 162.6 Ω, whereas for controls the values for real part of impedance ranged from 13,336.4 to 14,998.6 Ω with a mean of 14,000 ± 348.7 Ω. At 50 KHz, the real part of impedance of OSCC patients ranged from 309.3 Ω to 321.4 Ω with a mean of 315.0 ± 3.666 Ω, whereas for controls the values for real part of impedance ranged from 519.7 Ω to 530.1 Ω with a mean of 523.7 ± 3.072 Ω. Statistically significant difference was noted between the study and control group at 20 Hz and 50 KHz with a p value <0.0001 (Graph 12.5).

These findings were in accordance with the results of the study by Ching et al. [55] which

Graph 12.4 Comparison of phase angles in OSCC at various frequencies

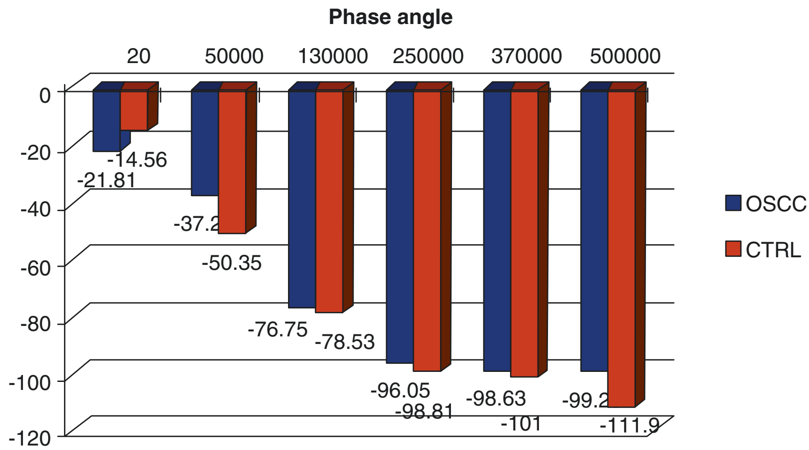

Graph 12.5 Comparison of real part of impedance in OSCC at various frequencies

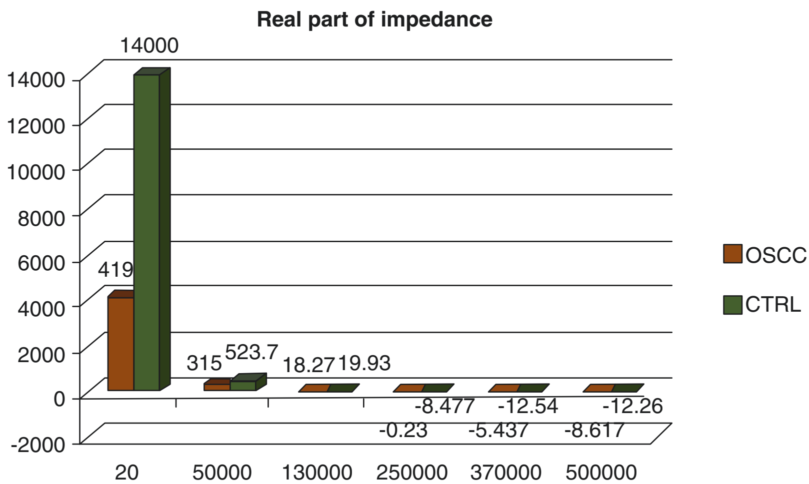

showed that real part of impedance of CTT (R = 4050 Ω at 20 Hz and 290 Ω at 50 kHz) was significantly smaller than that of the surrounding NTT (R = 12,432 Ω at 20 Hz and 501 Ω at 50 kHz). Similarly, results of the study by Sun et al. [56] showed that real part of impedance of CTT (R = 4115.2 Ω at 20 Hz and 312.4 Ω at 50 kHz) was significantly smaller than that of the surrounding NTT (R = 12,911 Ω at 20 Hz and 486.7 Ω at 50 kHz) as well as that of healthy subjects (R = 13,946 Ω at 20 Hz and 523.8 Ω at 50 kHz).

12.8.1.4 Imaginary Part of Impedance in Oral Squamous Cell Carcinoma

Imaginary part of impedance decreased from −1375 ± 34.76 Ω to −22.65 ± 1.98 Ω for the study group and from −3552 ± 211.2 Ω to −23.95 ± 2.957 Ω for the control group as the measurement frequency increased from 20 Hz to 5 MHz in the present study. At 20 KHz, the imaginary part of impedance of OSCC patients ranged from −1423.3 Ω to −1299.3 Ω with a mean of −1375 ± 34.76 Ω, whereas for controls the values of imaginary part of impedance ranged from −3981.4 Ω to −3100.8 Ω with a mean of −3552 ± 211.2 Ω. At 50 KHz, the imaginary part of impedance of OSCC patients ranged from −190.1 Ω to −180.9 Ω with a mean of −185.3 ± 2.877 Ω, whereas for controls the values for imaginary part of impedance ranged from −629.1 Ω to −610.6 Ω with a mean of −620.8 ± 3.530 Ω. Statistically significant difference was noted between the study and control group at 20 Hz and 50 KHz with a p value <0.0001 (Graph 12.6).

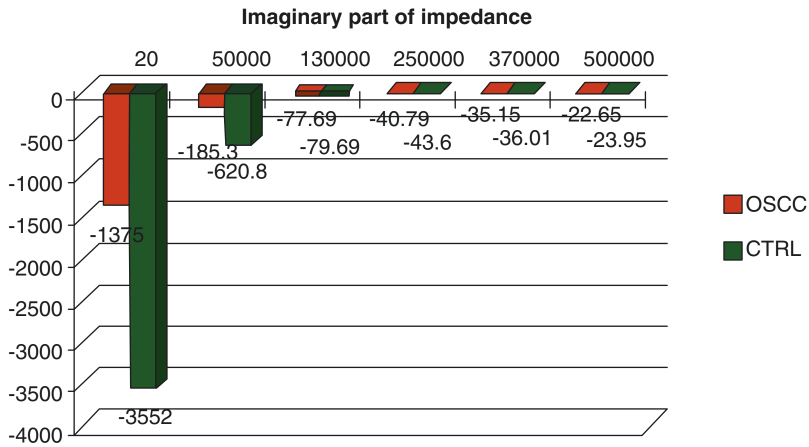

Graph 12.6 Comparison of imaginary part of impedance in OSCC at various frequencies

These results were consistent with those of Ching et al. [55], which showed that the imaginary part of impedance of CTT ($X = -1440.95$ at 20 Hz and −228.91 at 50 kHz) was significantly smaller than that of the surrounding NTT ($X = -2918.89$ at 20 Hz and −599.18 at 50 kHz).

Also, results of the study by Sun et al. [56] were in accordance with our findings. Their results showed that the imaginary part of impedance of CTT was significantly smaller than that of the surrounding NTT as well as that of healthy subjects. Thus, in the present study, both 20 Hz and 50 kHz frequencies were found to be useful to distinguish cancerous tissue from normal tissue on the basis of measurement of four electrical properties (Z, θ, R, and X). Therefore, both 20 Hz and 50 kHz were recommended as the best frequencies for separating cancerous tissue from normal tissue.

12.8.2 Oral Potentially Malignant Disorders

12.8.2.1 Bioimpedance in Oral Potentially Malignant Disorders [61]

In the present study, at 20 Hz the mean impedance for the leukoplakia, erythroplakia, and OSMF patients was 12,292 ± 675.5Ω, 13,100 ± 1145 Ω, and 977.7 ± 138.3 Ω, respectively. All the values are less than in control subjects which is in accordance with the results by Balasubramani et al. [62] who found that premalignant cervical tissue had much smaller bioimpedance than normal. At 50 kHz, the mean impedance for the leukoplakia, erythroplakia, and OSMF patients was 727.6 ± 63.64 Ω, 780.1 ± 46.49, and 896 ± 41.19, respectively. We found that there was statistical significant difference between bioimpedance values of leukoplakia tissue with no dysplasia and severe dysplasia, mild and severe dysplasia, and moderate and severe dysplasia. There were also significant statistical differences between stages I, III, and IV of leukoplakia at 20 Hz. In erythroplakia, we also found statistically significant differences between bioimpedance values of different histopathological grades like moderate, severe, and intraepithelial carcinoma. We also found statistically significant differences between different histopathological grades at 20 Hz but no difference in various clinical stages of OSMF.

12.8.2.2 Phase Angle in Oral Potentially Malignant Disorders

In the present study, at 20 Hz the mean phase angle for the leukoplakia, erythroplakia, and OSMF patients was $-14.31 \pm 1.112^{\theta}$, $-14.35 \pm 1.170^{\theta}$, and $-20.28 \pm 2.233^{\theta}$, respectively. At 50 kHz, the mean impedance for the leukoplakia, erythroplakia, and OSMF patients was −55.80 ± 2.152$^{\theta}$, −55.16 ± 1.740$^{\theta}$, and −57.90 ± 2.898$^{\theta}$, respectively.

12.8.2.3 Real Part of Impedance in Oral Potentially Malignant Disorders

In the present study, at 20 Hz the mean real part of impedance for the leukoplakia, erythroplakia, and OSMF patients was 12,385 ± 400.3 Ω, 12,396 ± 424.3 Ω, and 13,488 ± 347.5 Ω, respectively. At 50 kHz, the mean real part of impedance for leukoplakia, erythroplakia, and OSMF patients was 12,385 ± 400.3 Ω, 12,396 ± 424.3 Ω, and 13,488 ± 347.5 Ω, respectively.

12.8.2.4 Imaginary Part of Impedance in Oral Potentially Malignant Disorders

In the present study, at 20 Hz the mean imaginary part of impedance for the leukoplakia, erythroplakia, and OSMF patients was −2574 ± 194.5 Ω, −2561 ± 211.2 Ω, and −2388 ± 248.6 Ω, respectively. At 50 kHz, the mean imaginary part of impedance for leukoplakia, erythroplakia, and OSMF patients was −476.4 ± 64.14 Ω, −474 ± 63.20 Ω, and −430.2 ± 58.66 Ω, respectively.

12.9 Comparison of All the Parameters Between Different Groups

It was found that the bioimpedance of OSCC group is smaller as compared to other study groups as well as control group at all the frequencies except 1.3 MHz. It was found that there is a statistical difference among the phase angles of different study groups along with the controls at all frequencies except at 5 MHz. It was also found that there is a statistical difference among the real part of impedance of different study groups along with the controls at all frequencies. There is a statistical difference among the imaginary part of impedance of different study groups along with the controls at all frequencies.

12.9.1 Bioimpedance of Patients from All the Study Groups and Controls Measured at Different Frequencies

After application of ANOVA, it was found that the bioimpedance of OSCC group is smaller as compared to other study groups as well as control group at all the frequencies except 1.3 MHz, which shows statistical significance (Graph 12.7).

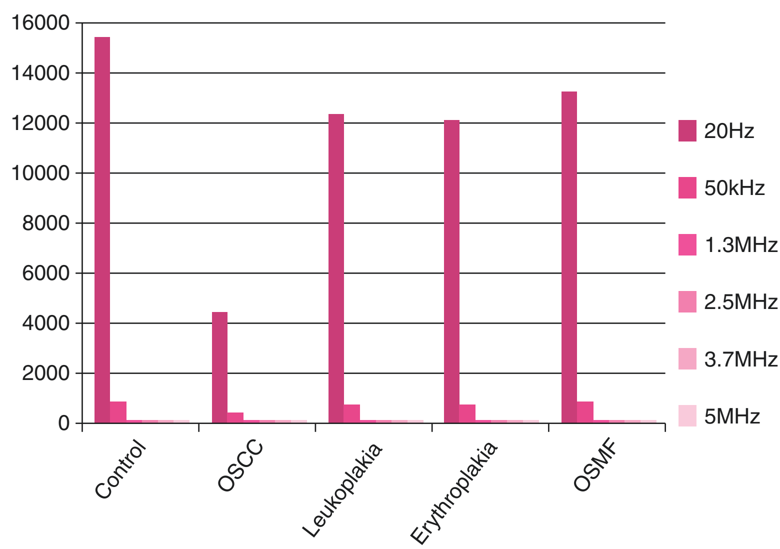

Graph 12.7 Comparison of bioimpedance between different study groups

12.9.2 Phase Angle of Patients from All the Study Groups and Controls Measured at Different Frequencies

It was found that there is a statistical difference among the phase angles of different study groups along with the controls at all frequencies except at 5 MHz (Graph 12.8).

12.9.3 Real Part of Impedance of Patients from All the Study Groups and Controls Measured at Different Frequencies

After application of ANOVA, it was found that there is a statistical difference among the real part of impedance of different study groups along with the controls at all frequencies (Graph 12.9).

Graph 12.8 Comparison of phase angles between different study groups

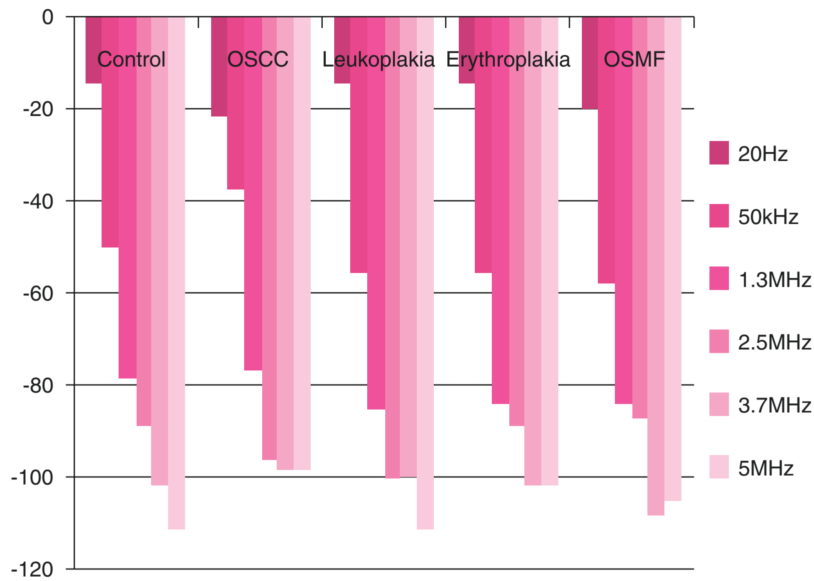

Graph 12.9 Comparison of real part of impedance between different study groups

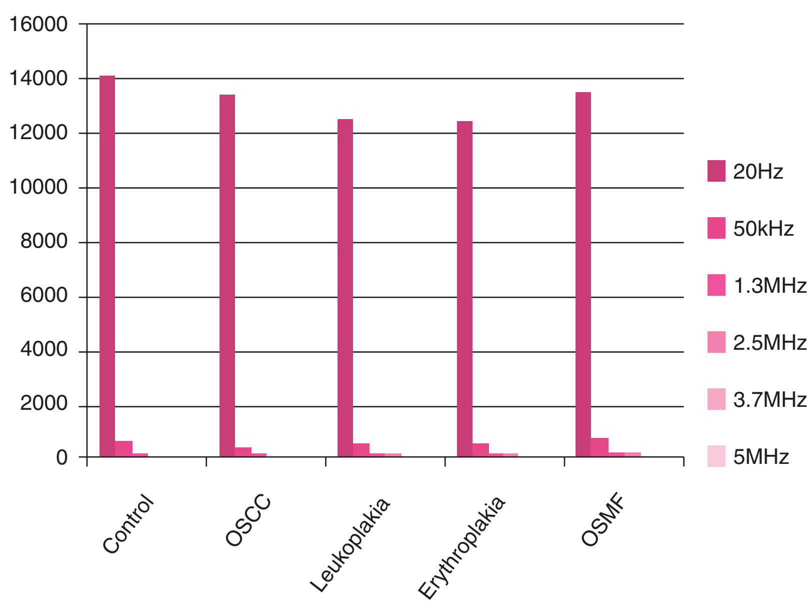

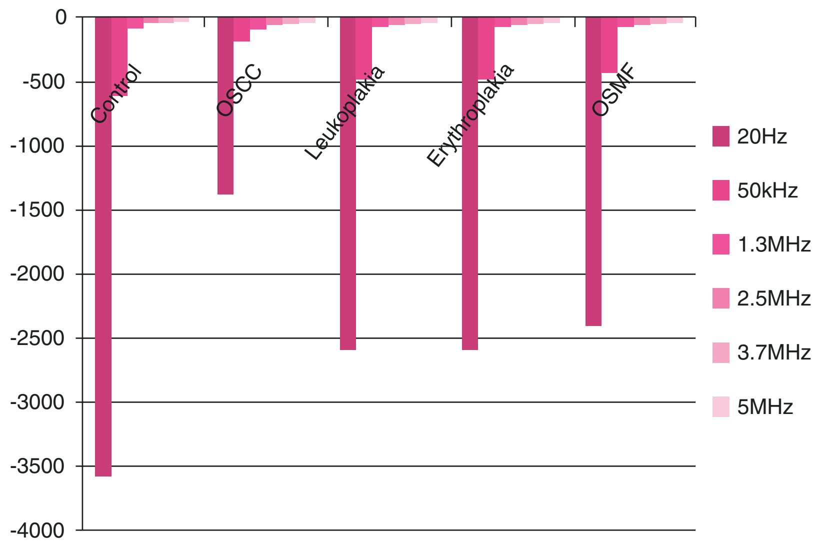

Graph 12.10 Comparison of imaginary part of impedance between different study groups

12.9.4 Imaginary Part of Impedance of Patients from All the Study Groups and Controls Measured at Different Frequencies

After application of ANOVA, it was found that there is a statistical difference among the imaginary part of impedance of different study groups along with the controls at all frequencies (Graph 12.10).

12.10 Future Directions

Bioimpedance is a proven technique used in detection of various cancers. The published literature illustrates the role of that bioimpedance in early oral cancer detection [59–61]. We believe that the comparison of bioimpedance in OPMDs and oral cancer will rationalize the role of bioimpedance in early detection of cancer. We also suggest more studies on bioimpedance levels of body fluids like saliva in OPMDs and OSCC. For definite understanding of its usefulness as an early detection marker, studies with large sample sizes are desirable [63].

In India and Southeast Asia, it has been observed that OSCC are commonly preceded by an OPMD. Hence during screening programs, bioimpedance can be utilized as a diagnostic adjunct to the classical visual screening. However a large number of multicentric studies with extensive data collection are needed to thoroughly validate the technique.

References

1. Heaviside O. The Electrician: AMS Bookstore; 23 July 1886., reprinted as Electrical Papers, p 64. p. 212. isbn:ISBN 0-8218-3465-7.
2. Kennelly AE. Impedance. Trans Am Inst Electr Eng. 1893;10:172–232.
3. Weaver JC. Electroporation: a general phenomenon for manipulating cells and tissues. J Cell Biochem. 1993;51:426–35.
4. Bayford RH. Bioimpedance tomography (electrical impedance tomography). Annu Rev Biomed Eng. 2006;8:63–91.
5. Scholz B, Anderson R. On electrical impedance scanning—principles and simulations. Electromedica. 2000;68:35–44.
6. Davey CL, Markx GH, Kell DB. On the dielectric method of monitoring cellular viability. Pure Appl Chem. 1993;65:1921–6.
7. Abdul S, Brown BH, Milnes P, Tidy JA. A clinical study of the use of impedance spectroscopy in the detection of cervical intraepithelial neoplasia (CIN). Gynecol Oncol. 2005;99:S64–6.
8. Brown BH, Tidy JA, Boston K, Blackett AD, Smallwood RH, Sharp F. Relation between tissue structure and imposed electrical current flow in cervical neoplasia. Lancet. 2000;355:892–5.

9. Bera TK, Nagaraju J. Electrical impedance spectroscopic study of broiler chicken tissues suitable for the development of practical phantoms in multifrequency EIT. J Electr Bioimpedance. 2011;2:48–63.
10. Bauchot AD, Harker FR, Arnold WM. The use of electrical impedance spectroscopy to assess the physiological condition of kiwifruit. Postharvest Biol Technol. 2000;18:9–18.
11. Abdul S, Brown BH, Milnes P, Tidy JA. The use of electrical impedance spectroscopy in the detection of cervical intraepithelial neoplasia. Int J Gynecol Cancer. 2006;16:1823–32.
12. Zou Y, Gou Z. A review of electrical impedance techniques for breast cancer detection. Med Eng Phys. 2003;25:79–90.
13. Kay CF, Bothwell PT, Foltz EL. Electrical resistivity of living body tissues at low frequencies. J Physiol. 1954;13:131–6.
14. Nyboer J. Electrical impedance plethysmography. Hoboken/Springfield, IL: Blackwell/Charles C. Thomas; 1959. p. xvii+243. 60s
15. Baker LE. Principles of the impedance technique. IEEE Eng Med Biol Mag. 1989;3:11–5.
16. Baumgartner RN, Chumlea WC, Roche AF. Bioelectric impedance phase angle and body composition. Am J Clin Nutr. 1988;48:16–23.
17. Pethig R. Dielectric properties of body tissues. Clin Phys Physiol Meas. 1987;8:A5–A12.
18. Blad B, Baldetorp B. Impedance spectra of tumor tissue in comparison with normal tissue: a possible clinical application for electrical impedance tomography. Physiol Meas. 1996;17:A105–A15.
19. Rabbat A. Tissue resistivity. In: Webster JG, editor. Electrical impedance tomography. Bristol and New York: IOP Publishing; 1990. p. 8–20.
20. Schwan HP. The practical success of impedance techniques from an historical perspective. Ann N Y Acad Sci. 1999;873:1–12.
21. Grimnes S, Martinsen O. Bioimpedance and bioelectricity basics. 2nd ed: Academic Press. Department of physics. The Faculty of Mathematics and Natural Sciences Site ; 2008.www.mn.uio.no
22. Institute of Medicine (US) Committee on Military Nutrition Research. Carlson-Newberry SJ, Costello RB, editors. Emerging technologies for nutrition research: potential for assessing military performance capability. Washington, DC: National Academies Press (US); 1997.
23. Chumlea WC, Guo SS. Bioelectrical impedance: a history, research issues, and recent consensus. In: Institute of Medicine (US) Committee on Military Nutrition Research, Carlson-Newberry SJ, Costello RB, editors. . Washington, DC: National Academies Press (US); 1997.
24. Castelló J, García-Gil R, Espí JM. A PC-based low cost impedance and gain-phase analyzer. Measurement. 2008;41:631–6.
25. Yang Y, Wang J. A design of bioimpedance spectrometer for early detection of pressure ulcere. In: Engineering in Medicine and Biology Society, IEEE-EMBS 2005. 27th Annual International Conference of the IEEE; 2005. p. 6602–4.
26. Yang Y, Wang J, Yu G, Niu F, He P. Design and preliminary evaluation of a portable device for the measurement of bioimpedance spectroscopy. Physiol Meas. 2006;27:1293.
27. Seoane F, Bragós R, Lindecrantz K. Current source for multifrequency broadband electrical bioimpedance spectroscopy systems. A novel approach. In: Engineering in Medicine and Biology Society, 2006. EMBS'06. 28th Annual International Conference of the IEEE; 2006. p. 5121–5.
28. Zlochiver S, Arad M, Radai MM, Barak-Shinar D, Krief H, Engelman T, Abboud S. A portable bioimpedance system for monitoring lung resistivity. Med Eng Phys. 2007;29:93–100.
29. Rangraz P, Sheikhani A, Hemmati N. Design and simulation of a current source for electrical impedance tomography. In: Proceedings of the 24th IASTED international conference on Biomedical engineering: ACTA Press. p. 396–400.
30. Dickin F, Wang M. Electrical resistance tomography for process applications. Meas Sci Technol. 1996;7:247.
31. Sun T, Tsuda S, Zauner KP, Morgan H. On-chip electrical impedance tomography for imaging biological cells. Biosens Bioelectron. 2010;25:1109–15.
32. Chai KT, Hammond PA, Cumming DRS. Modification of a CMOS microelectrode array for a bioimpedance imaging system. Sens Actuators B Chem. 2005;111:305–9.
33. Ching CTS, Chen JH. A non-invasive, bioimpedance-based 2-dimensional imaging system for detection and localization of pathological epithelial tissues. Sens Actuators B Chem. 2015;206:319–26.
34. Rodriguez S, Ollmar S, Waqar M, Rusu AA. Batteryless sensor ASIC for implantable bioimpedance applications. IEEE Trans Biomed. 2015;10:533–44.
35. Surowiec A, Stanislaw SS, Barr JR, Swarup A. Dielectric properties of breast carcinoma and the surrounding tissues. IEEE Trans Biomed Eng. 1988;35:257–63.
36. Morimoto T, Kinouchi Y, Iritani T, Kimura S, Konishi Y, Mitsuyama N, et al. Measurement of the electrical bioimpedance of breast tumors. Eur Surg Res. 1990;22:86–92.
37. Morimoto T, Kimura S, Konishi Y, Komaki K, Uyama T, Monden Y, et al. A study of the electrical bio-impedance of tumors. J Investig Surg. 1993;6:25–32.
38. Joines WT, Zhang Y, Li C, Jirtle RL. The measured electrical properties of normal and malignant human tissues from 50 to 900 MHz. Med Phys. 1994;21:547–50.
39. Jossinet J. Variability of impedivity in normal and pathological breast tissue. Med Biol Eng Comput. 1996;34:346–50.
40. Jossinet J. The impedivity of freshly excised human breast tissue. Physiol Meas. 1998;19:61–75.

41. Jossinet J, Schmitt M. A review of parameters for the bioelectrical characterization of breast tissue. Ann N Y Acad Sci. 1999;873:30–41.
42. Emtestam L, Nicander I, Stenström M, Ollmar S. Electrical impedance of nodular basal cell carcinoma: a pilot study. Dermatology. 1998;197:313–6.
43. Chauveau N, Hamzaoui L, Rochaix P, Rigaud B, Voigt JJ, Morucci JP. Ex vivo discrimination between normal and pathological tissues in human breast surgical biopsies using bioimpedance spectroscopy. Ann N Y Acad Sci. 1999;873:42–50.
44. Lee BR, Roberts WW, Smith DG, Ko HW, Epstein JI, Lecksell K. Bioimpedance: novel use of a minimally invasive technique for cancer localization in the intact prostate. Prostate. 1999;39:213–8.
45. Malich A, Boehm T, Facius M, Freesmeyer M, Azhari T, Werner B. Electrical impedance scanning of lymph nodes: initial clinical and technical findings. Clin Radiol. 2002;57:579–86.
46. Glickman YA, Filo O, David M, Yayon A, Topaz M, Zamir B, et al. Electrical impedance scanning: a new approach to skin cancer diagnosis. Skin Res Technol. 2003;9:262–8.
47. Beetner DG, Kapoor S, Manjunath S, Zhou X, Stoecker WV. Differentiation among basal cell carcinoma, benign lesions, and normal skin using electric impedance. IEEE Trans Biomed Eng. 2003;50:1020–5.
48. Hope TA, Iles SE. Technology review: the use of electrical impedance scanning in the detection of breast cancer. Breast Cancer Res. 2004;6:69–74.
49. Ohmine Y, Morimoto T, Kinouchi Y, Iritani T, Takeuchi M, Haku M, et al. Basic study of new diagnostic modality according to non-invasive measurement of the electrical conductivity of tissues. J Med Investig. 2004;51:218–25.
50. Aberg P, Nicander I, Hansson J, Geladi P, Holmgren U, Ollmar S. Skin cancer identification using multifrequency electrical impedance-a potential screening tool. IEEE Trans Biomed Eng. 2004;51:2097–102.
51. Aberg P, Geladi P, Nicander I, Hansson J, Holmgren U, Ollmar S. Non-invasive and microinvasive electrical impedance spectra of skin cancer—a comparison between two techniques. Skin Res Technol. 2005;11:281–6.
52. Abdul S, Brown BH, Milnes P, Tidy JA. A clinical study of the use of impedance spectroscopy in the detection of cervical intraepithelial neoplasia (CIN). Gynecol Oncol. 2005;99:64–6.
53. Gupta D, Lammersfeld CA, Vashi PG, King J, Dahlk LK, Grutsch JF, et al. Bioelectrical impedance phase angle as a prognostic indicator in breast cancer. BMC Cancer. 2008;8:249.
54. Halter RJ, Schned A, Heaney J, Hartov A, Schutz S, Paulsen KD. Electrical impedance spectroscopy of benign and malignant prostatic tissues. J Urol. 2008;179:1580–6.
55. Ching CT, Sun TP, Huang SH, Hsiao CS, Chang CH, Huang SY. A preliminary study of the use of bioimpedance in the screening of squamous tongue cancer. Int J Nanomedicine. 2010;7:213–20.
56. Sun TP, Ching CT, Cheng CS, Huang SH, Chen YJ, Hsiao CS, et al. The use of bioimpedance in the detection/screening of tongue cancer. Cancer Epidemiol. 2010;34:207–11.
57. Arias LR, Perry CA, Yang L. Real-time electrical impedance detection of cellular activities of oral cancer cells. Biosens Bioelectron. 2010;25:2225–31.
58. Yang L, Arias LR, Lane TS, Yancey MD, Mamouni J. Real-time electrical impedance-based measurement to distinguish oral cancer cells and noncancer oral epithelial cells. Anal Bioanal Chem. 2011;399: 1823–33.
59. Sarode GS, Sarode GS, Kulkarni M, Karmarkar S, Patil S, Augustine D. Bioimpedance Assessment of oral squamous cell carcinoma with clinic-pathologic correlation. J Contemp Dent Pract. 2015;16:715–22.
60. Wang Y, Borsic A, Heaney J, Seigne J, Schned A, Baker M, et al. Transrectal electrical impedance tomography of the prostate: spatially coregistered pathological findings for prostate cancer detection. Med Phys. 2013;40:063102.
61. Sarode GS, Sarode SC. 370P Determination of bioimpedance in oral potentially malignant disorders. Ann Oncol. 2016;27(suppl_9). mdw587.012
62. Balasubramani L, Brown BH, Healey J, Tidy JA. The detection of cervical intraepithelial neoplasia by electrical impedance spectroscopy: the effects of acetic acid and tissue homogeneity. Gynecol Oncol. 2009;115:267–71.
63. Sarode GS, Sarode SC, Kulkarni M, Karmarkar S, Patil S. Role of bioimpedance in cancer detection: a brief review. Int J Dent Sci Res. 2016;3:15–21.

13

Sensitive Crystallization Patterns in Oral Cancer

Sachin C. Sarode, Gargi S. Sarode, and Prashanth Panta

Abstract

Pfeiffer, a German scientist in 1938, first developed the crystallization test, which baffled many researchers ever since. Later on, cupric chloride crystallization test was widely used in the literature to investigate its efficacy in detection of various malignancies. Studies on oral cancer also proved its effectiveness for early detection. The crystallization appearance called "transverse form" is regarded as a hallmark pattern in malignancies. It is postulated that increased concentration of polyamines and diamines in blood of cancer patients as well as altered protein structure is responsible for formation of this peculiar, signature pattern. However, in normal healthy patients, the cupric chloride crystallization pattern is characterized by an eccentrically placed center of gravity and radiating crystals without any disturbances. In this chapter, we have reviewed the crystallization test with emphasis on potential mechanisms, crystallization test procedure and methodology, image interpretation, crystal patterns, and all studies conducted on oral cancer. The qualities of reliability, simplicity, cost-effective, and noninvasive nature of crystallization test make it an efficient tool for sensitive detection of oral cancer.

S. C. Sarode, PhD (✉) · G. S. Sarode, PhD
Department of Oral Pathology and Microbiology,
Dr. D. Y. Patil Dental College and Hospital,
Pune, Maharashtra, India

P. Panta, MDS
Department of Oral Medicine and Radiology,
MNR Dental College and Hospital,
Sangareddy, Telangana, India
e-mail: maithreya.prashanth@gmail.com

13.1 Introduction

Pfeiffer originally introduced the biocrystallization method in 1931, which was later termed "sensitive crystallization" and "copper chloride crystallization" [1]. This method involves crystallization of salt solution by evaporation of water under controlled atmospheric conditions. Differential pattern formation by virtue of interaction of biological material with molecular forces during crystallization is the basis of biocrystallization test [2]. It was used in agricultural research concerning crop quality, in addition to chemical analyses of vitamins, proteins, etc. [3]. A most common application is investigation of effects of different farming systems and fertilization practices on the morphological alterations found in the crystal structures [3–5]. It has also been applied as a bioassay in the field of homeopathy [6]. In the context of human diseases, crystallization method has been applied for renal diseases like pyelonephritis [7–9] and pulmonary conditions of the upper respiratory tract [10]. The application of sensitive crystallization processes in the early detection of malignancies is the most

P. Panta (ed.), *Oral Cancer Detection*, https://doi.org/10.1007/978-3-319-61255-3_13

unique application and remains as the main focus of the chapter, particularly with relevance to oral cancers.

The phenomena of crystallization have always attracted many workers over centuries. Pfeiffer (1938) first developed the crystallization test using cupric chloride solution [1]. It was based on the importance of physical and molecular forces in maintaining the integrity of the molecules and the chemicals. The typical hallmark of crystallization pattern in malignancy was shown to be “transverse form” (TF) formation [11]. Gruner (1940) [12] concluded that the different crystallization patterns in health and disease are due to the pivotal role of colloidal proteins in dilute solution of blood. The specific pattern in cancer reflects the specific nature of the abnormal proteins with changes in the position of amino and sulfhydryl groups. Gulati et al. (1994) [11] and Kuczkowski et al. (1995) [13] carried out this test in head and neck malignancies and concluded that it is a simple, reliable, economical, less time-consuming, and less invasive diagnostic procedure suitable for mass screening.

13.2 Crystallization Dynamics

Crystallization is defined as formation of solid crystals precipitating from a solution, melts or more rarely deposited directly from a gas. It also involves solid-liquid separation phenomenon wherein mass transfer of a solute from the liquid occurs leading to pure solid crystals. The crystallization is carried out in a crystallizer under controlled physical and environmental conditions. Thus, crystallization is an act of precipitation, obtained through a variation of the solubility conditions of the solute in the solvent, in contrary to precipitation due to chemical reaction [14].

The events in the crystallization are divided into two major categories, *nucleation* and *crystal growth*. In *nucleation* phase, solute molecules dispersed in the solvent start to gather into clusters, on the nanometer scale, that become stable under the current operating conditions. These stable clusters are called nuclei. The clusters need to reach a critical size for complete stabilization; otherwise, they become unstable and get dissolve. Such critical size of clusters is dictated by various operating conditions like temperature, supersaturation, humidity, vibrations, etc. Subsequently, atoms arrange in a defined and periodic manner that defines the crystal structure. “Crystal structure” is a special term that refers to the relative arrangement of the atoms, not the macroscopic properties of the crystal (size and shape), although those are a result of the internal crystal structure [15].

13.3 Review of the Literature

Glauber (1648) first investigated the causes of crystallization and concluded that some occult force controls it. He extensively studied the crystallization patterns produced by organic and inorganic substances in combination with various colloidal solutions. He concluded that morphological and histological patterns of living organisms have close resemblance to complicated crystallization patterns [12].

After a long gap of nearly three centuries, Kopaczewski (1933) stated that the different patterns of crystallization are produced by organic and inorganic salts in addition to different colloidal solutions, mainly due to a variation in the rate and amplitude of molecular movements involved in the evaporation process. It was concluded that the pattern formation process is controlled by trikinetic forces consisting of (1) molecules of organic and inorganic substances, (2) molecules of colloidal substances, and (3) water molecules [12].

Pfeiffer, a German scientist (1938), first developed the crystallization test. This test was based on the importance of physical and molecular forces in maintaining the integrity of molecules and the chemicals. He used cupric chloride crystallization pattern with and without combination with body fluids from human samples and plant- and animal-derived extracts to evaluate the role of colloidal impurities over crystallization pattern. Further experiments with blood from patients affected by various diseases showed significant differences when compared with healthy blood samples [1].

Gruner (1940) suggested that no chemical changes occur during the crystallization process and stressed the physical nature of the process. He also pointed out that different crystal arrangement pattern seen with human samples and plant- and animal-derived extracts was due to the molecular forces, different rates, and amplitude of molecular movements during evaporation process. Thus, trikinetic forces control the whole process of crystallization. It was observed that the substances added to cupric chloride solution prevent the normal pattern of cupric chloride crystals and ultimately lead to the development of a characteristic signature pattern as seen in blood crystallization images. It was concluded that the different crystal patterns in health and disease are due to the pivotal role of colloidal proteins in dilute solution of blood. The specific pattern in cancer reflects on specific nature of the abnormal protein with changes in position of amino and sulfhydryl groups. He further stressed that the physical process of crystallization is delayed, retarded, or suppressed in cancer ultimately to produce an abnormal pattern [12].

Sabarth and Williams (1975) [16] observed similar blood crystallization patterns after addition of blood solution to cupric chloride (20%), magnesium sulfate (20%), and lead acetate (10%) solution, even though each of these solutions had different chemical identity. The dilution of blood and salt solution was also an important factor in the crystallization process. It was also observed that the specific crystallization patterns of cupric chloride were present only in the presence of those chemicals which supports life, such as sodium chloride, sodium carbonate, sodium bicarbonate, potassium chloride, ammonium sulfate, etc., whereas these patterns were absent with substance which are inert for life, e.g. paraldehyde, formalin, etc.

Quadeer (1980) [17] studied crystallization test on 225 healthy controls and 325 cases of histologically proven malignancies of various body regions. Positive crystallization pattern for malignancy (TF formation) was observed in 94.15% cases. It was concluded that crystallization is reliable test for detection of malignancy in cases where the lesion is inaccessible to biopsy and other procedures. The future utility of this test as a screening method for epidemiological studies was also suggested.

Shaikh et al. (1992) [18] concluded that crystallization test is of great value in detecting the malignancy of female genital tract, where the lesion is inaccessible to biopsy and other procedures. The crystallization test was carried out on 211 patients of female genital tract malignancy and 50 healthy controls. The test showed positive crystal pattern for malignancy in 200 (94.78%) malignancy cases and negative in 45 (90%) control subjects.

Later on, Gulati et al. (1994) [11] studied the crystallization test on 25 patients with head and neck carcinoma and 25 healthy individuals. The crystallization test showed positive crystal pattern for malignancy in 88% of cases of head and neck malignancy and negative in 92% healthy controls. It was found that there was no correlation between the stages of carcinoma and the number of TFs. However, maximum numbers of TFs were seen in stage II and stage IV carcinomas. It is concluded that crystallization is simple, reliable, economical, and above all useful method for a mass screening program.

Kuczkowski et al. (1995) [13] carried out crystallization test on 21 patients with head and neck neoplasms and 10 healthy control subjects. The results were positive in 71.5% of cancer patients.

13.4 Crystallization Test Procedure

13.4.1 The Procedure for Crystallization Test Is as Follows [12–14]

1. Blood sample collection: Blood sample is collected under aseptic conditions by pricking ring finger. One drop of blood is added to 1 cc of double distilled water at room temperature, which gives a final dilution of 6% hemolyzed blood.
2. 20% cupric chloride solution is prepared by adding anhydrous cupric chloride powder (20 g) to double distilled water (100 mL).

3. 0.1–0.2 cc of blood sample is added to 10 cc of 20% cupric chloride solution.
4. Pour this mixture immediately in the pre-warmed flat-bottom petri dish of 10 cm diameter.
5. Place the petri dish in biological oxygen demand (BOD) incubator (temperature, 28–32 °C, and humidity, 35–55%) in an isolated room. BOD incubator should be placed in vibration-free environment.
6. Make sure that petri dish is horizontally placed in an incubator.
7. Crystallization process takes around 18–19 h later.

13.4.2 Incubator Settings

BOD incubator is ideal for crystallization test. Incubator should be kept free of vibrational disturbance. Absolute horizontal positioning of incubator is mandatory, which can be maintained with the help of water-level test. Dust-free environment of incubator is the key for accurate results. The incubator is set at 32 °C. Humidity in the crystallization chamber is maintained within the range of 35–55% by using wet- and dry-bulb thermometer. These settings should be religiously followed in order to get valid and reproducible crystallization results [12–14].

13.4.3 Interpretation of Crystallization Test

The crystallization patterns are studied in daylight using handheld magnifying lens. Recently, we have developed a new method in which petri dish is placed on X-ray viewing machine. [19] Black cardboard sheet can be used to block the surrounding unwanted light from X-ray viewer. This method provides clearer picture of crystal orientation and also facilitates good-quality photographs [19].

The evaluation of crystallization pictures is frequently performed by means of visual evaluation. Recently, computerized image analysis has been investigated, which is still in the stage development, with high scope for accuracy and precision. As of now, visual evaluation is considered as superior in discriminating differences between crystal patterns and in identifying pictures as originating from different cultivation systems. In fact, the visual evaluation directs the future development of more productive computerized evaluation of patterns.

13.5 Crystal Patterns

The mechanisms of the crystallization process on glass plates are not yet completely comprehended. The topographical features of glass plate have been proposed as important factor affecting crystallization pattern [20]. Hence, the clean (dust-free) glass plate and the evaporation rate (depends on temperature and humidity of chamber) of the solution are important factors. It was found that the main variation step in the biocrystallization is not the sample preparation but the crystallization step itself. A key to understanding this problem was connected to the understanding of the “dewetting” phenomena [20]. The possibility of the appearance of dewetting with the falling of the height of the solution between a critical height is described for fluids by Sharma and Ruckenstein [21].

13.5.1 Crystal Patterns of Cupric Chloride Solution

The crystallization pattern of cupric chloride solution alone shows thick textured crystals with needles arranged at an arbitrary angle. The needles either show side branching in fan-shaped manner or lengthwise linear growth. Secondary and tertiary branches are also observed. Each needle with its side branching represents one single entity with independent center of gravity (Fig. 13.1). Sabarth and Williams (1975) [16] labeled such pattern as “muddle formation.”

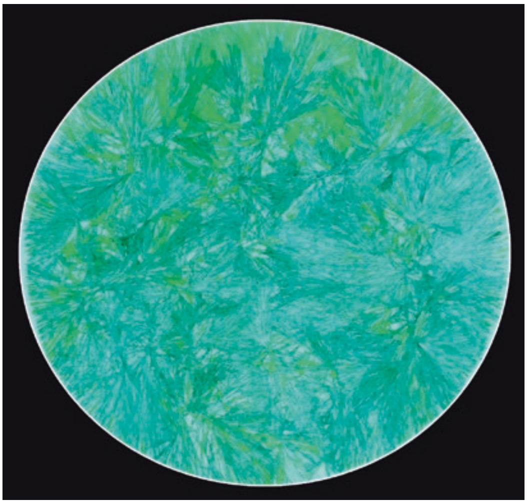

Fig. 13.1 Crystallization pattern of cupric chloride solution alone showing thick textured crystals with needles arranged at an arbitrary angle. Each needle with its side branching represents one single entity with independent center of gravity

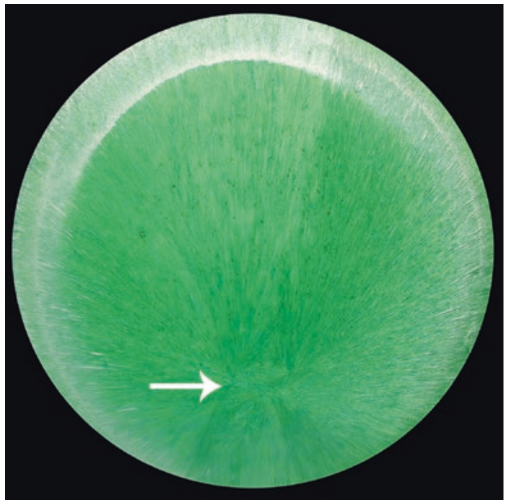

Fig. 13.2 Crystallization pattern of cupric chloride solution admixed with blood from healthy individual showing a single eccentrically situated center of gravity (white arrow) with orderly arrangement of radiating crystals emanating from the center toward the periphery

13.5.2 Crystal Patterns of Cupric Chloride Solution Admixed with Blood from Healthy Individuals

The crystallization pattern in this case shows a single eccentrically situated center of gravity (point from which crystal radiates) with an orderly arrangement of radiating crystals emanating from the center toward the periphery (Fig. 13.2). The center of gravity is always situated eccentrically in the crystallization plate dividing whole field into two zones: (1) zone of long radiation and (2) zone of short radiation. These radiating crystals fail to reach the periphery of the petri dish leaving behind the area occupied by crystals with different types of arrangement. This zone is termed as peripheral zone and has pattern similar to crystallization pattern of cupric chloride alone. Sometimes variations such as empty spaces, network of thin needles, or encrusted areas are also observed (Fig. 13.3). This particular crystallization pattern reflects on the decreasing gradient of pattern formation force of blood from center toward the periphery. Hence, it was concluded that the peripheral zone has less/no formative forces and showed different types of crystal arrangement.

In the center of gravity, instead of one single center, there might be a conglomeration of two or more centers (Fig. 13.4). The wing-like crystal formation with variable number and with or without blank spaces between them can also be seen.

13.5.3 Crystal Patterns of Cupric Chloride Solution in Malignancy

The crystallization pattern in malignancy shows single or double eccentrically situated center of gravity with orderly arrangement of radiating crystals emanating from the center toward periphery. In addition to this, sharply set off transverse crystals which are arranged almost perpendicular to the main radiating crystals are a characteristic feature in cancer patients (Fig. 13.5). Such crystals are called transverse forms (TF). TF consists

Fig. 13.3 Crystallization pattern of cupric chloride solution admixed with blood from healthy individual showing peripheral zone with crusted appearance of crystals (black arrow)

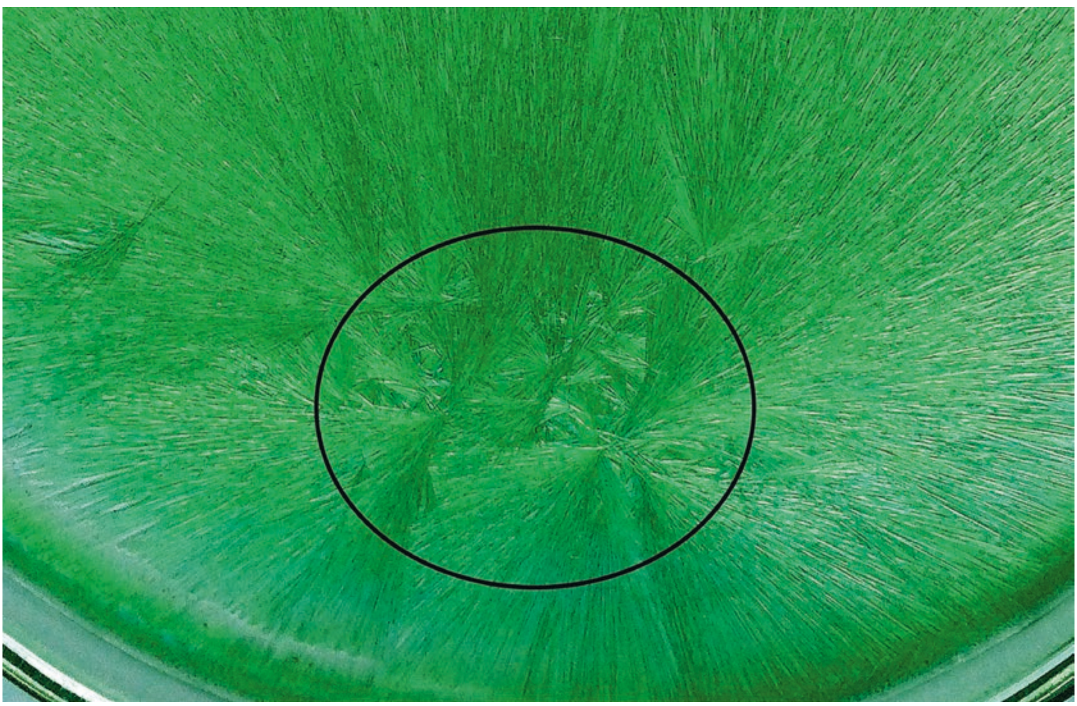

Fig. 13.4 Crystallization pattern of cupric chloride solution admixed with blood from healthy individual showing conglomeration of multiple centers of gravities (black circle)

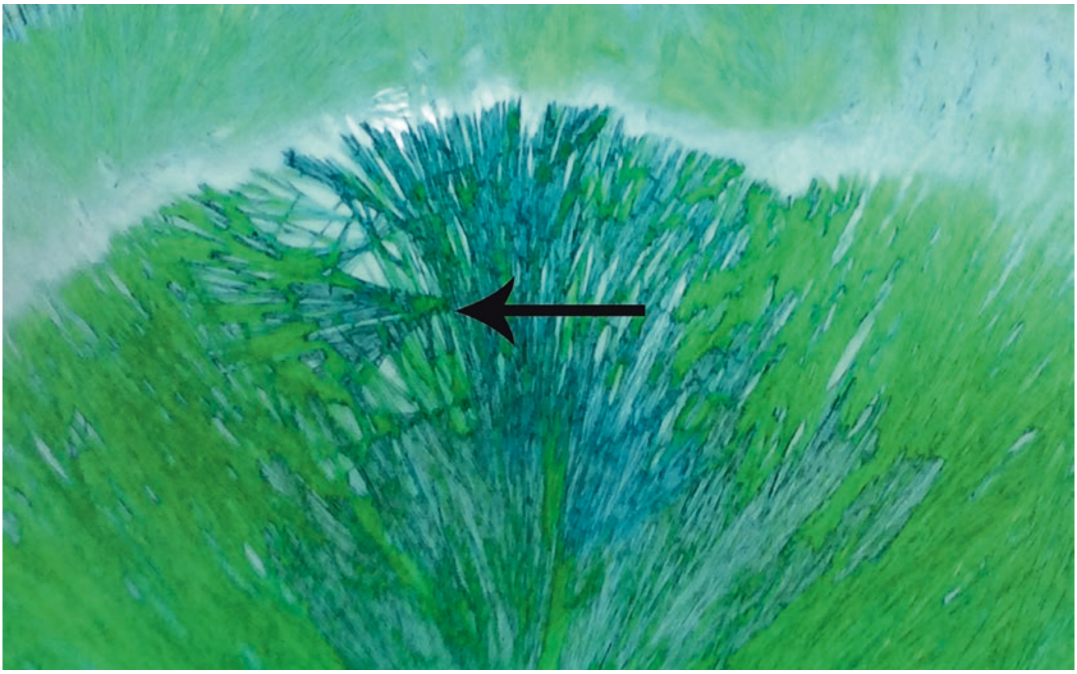

Fig. 13.5 Magnified view of transverse forms showing fan-shaped crystals perpendicular to radiating crystals. The radiating crystals fail to pierce through the transverse form

of transverse needles with wing-like formation on either or both sides. Secondary and tertiary branching formation was remarkably absent in TF. The needles of the central radiation fail to pierce through the TF. Increased number of TF reflects the advanced stage of malignancy.

The appearance of new center of nucleus ahead of growing central radiation marks the beginning of malignancy pattern. From the nuclear core point, side branches are laid down at an angle to the diagonal line of fine needles already laid down imparting stratified appearance. The side branches show less angulation and hence formed dense stratification. Secondary and/or tertiary branching from side branches is remarkably absent. The needles of the pattern are as thick or sometimes thicker than the needles of central radiation. The size of pattern is variable ranging from 2 to 30 mm.

13.6 Reason for Alterations in Cupric Chloride Crystal Pattern in Cancer

In malignancy, a number of cell products, especially the components of the cell surface and enzymes involved in the metabolism of nucleic acids, are shed into the blood circulation. Thus, blood acts as a unique medium, reflecting the various signature biochemical changes occurring in malignancy [16, 22]. Hence, blood can be used as a less invasive diagnostic tool.

The biochemical change occurring in the blood in malignancy has molecular basis at grass root level. It is well known that molecular forces govern the integrity of molecular structure. In malignancy, these biochemical changes bring about the change in the molecular forces. Similar type of molecular forces also acts to maintain the cohesion of molecules in the crystalline form, which are responsible for the peculiar pattern-forming tendency in any particular crystalline substance. It can, therefore, be anticipated that any malignancy in the body can be detected through the agency of physical forces, which maintain the integrity of molecular structure and that of chemical substances [23]. It has been observed that in malignancy, there is a high concentration of polyamines and diamines in the blood, which are the intermediate products of protein metabolism. It was found that the colloidal proteins in dilute solution of blood play a pivotal role in formation of different crystallization in health and disease [17]. Thus, it can be concluded that the proteins or degraded products of proteins, i.e., polyamines and diamines, may be responsible for particular cancer specific pattern in crystallization test, i.e., TF.

One of the most intriguing aspects of the crystallization test is that it can determine the site of illness based on the location of the altered crystal pattern on petri dish. For site determination ability of crystallization test, petri dish is divided into four quadrants formed by two perpendicular axes passing through the center of gravity. The narrow area between the point of intersection of the two imaginary axes and the edge of the glass plate corresponds to head or nervous system and organ of sense. The circulatory and respiratory system zones are present as wider area in the vicinity of horizontal axis. The other zones are shown in the figure. The areas below the center of gravity represents head zone where TFs are expected to occur in oral squamous cell carcinoma patients. It was considered by Pfeiffer in his book, *Sensitive Crystallization Process*, that the crystallization dish represents the body regions in two dimensions, which is a very controversial argument.

13.7 Crystallization Test in Oral Squamous Cell Carcinoma

In one of our previous studies out of 50 OSCC cases, 48 cases showed positive crystallization test, i.e., 96% reliability and 4% false negative [19]. Out of 30 control subjects, 29 showed negative crystallization test, i.e., 96.66% reliability. The positive and negative predictive values were found to be 97.96% and 93.55%, respectively. The application of chi-square test revealed a p value of 0.0001 which indicates that crystallization test was highly relevant for detection of OSCC [19]. Gulati et al. [11] demonstrated positive crystal pattern for malignancy in 88% of cases of head and neck malignancy and negative in 92% healthy controls. Kuczkowski et al. (1995) [13] carried out crystallization test on 21 patients with head and neck neoplasms and 10 healthy control subjects. The results were positive in 71.5% of cancer patients.

The mean TF frequency was calculated and found to be increasing from grade I (3.20 ± 15%) to grade II (653 ± 2.23%), and difference was statistically significant ($P = 0.0001$). Similarly, the mean TF frequency in clinical stage II was 5.8 ± 4.658%, whereas that in stages III and IV were 5.75 ± 2.417% and 4.90 ± 2.315%, respectively. This difference was statistically insignificant [19]. Gulati et al. [11] found no such correlation between the stages of carcinoma and the number of TFs formed. However, maximum numbers of TFs were seen in stage II and stage IV carcinomas. All the TFs obtained in the study were located above the center of gravity and horizontal axes. In contrast, as per the literature, area bellow center of gravity (also called K zone) is designated for pathologies related to head region. For more clarity on this aspect, we recommend future studies in this direction on larger sample sizes.

Recently, Rawat et al. studied crystallization pattern in oral leukoplakia [24]. Leaf-like pattern was observed in 46 cases (92%), while 4 cases (8%) exhibited star-form pattern. Transverse bar formations were absent in all the 50 cases of leukoplakia. By considering leaf-like pattern as positive crystallization test, 92% reliability and 8% false negative were obtained.

Conclusion

Based on our previous research and a few other reports, crystallization test may be considered as a promising investigation for early detection of oral cancers. However, there are many gray areas pertaining to the very nature of the crystallization test, and no data currently provides convincing evidence about the fundamental mechanisms involved in this biophysical event. The changes in the levels of key proteins and their products and several other genomic and metabolic markers seen in oral cancers blood samples may exert these subtle molecular forces, once thought as ethereal forces. Due to the occult nature of this investigation, there has been little advance in this field, but few authors are firm believers. We suggest investigators to validate the crystallization patterns on a larger number of blood samples from clinically staged oral squamous cell carcinoma across different populations, using advanced machine learning algorithms for accurate *pattern determination*. The specific challenges however include the tendency for specific patterns in different diseases and site-based patterns. In this age of technology, simultaneously screening the entire biomarker panel using "omics" technologies alongside the crystallization test can provide deeper insights.

References

1. Pfeiffer E. Kristalle. Stuttgart: Orient-Occident; 1930.
2. Kleber W, Steinike-Hartung U. EinBetragzur-Kristallization von Kupfer (II)–Chlorid–Dihydrataus Lo sungen. Zeitschr Kristallogr. 1959;111:213–34.
3. Balzer U, Balzer F. Picture-developing methods. Effect of three farming systems (bio-dynamic, bio-organic conventional) on yield and quality of beetroot (Beta vulgaris L. var. esculenta L.) in a seven year crop rotation. Acta Hortic. 1993;339:11–31.
4. Busscher N, Kahl J, Ploeger A. From needles to pattern in food quality determination. J Sci Food Agric. 2014;94(13):2578–81.
5. Busscher N, Kahl J, Doesburg P, Mergardt G, Ploeger A. Evaporation influences on the crystallization of an aqueous dihydratecupric chloride solution with additives. J Colloid Interface Sci. 2010;344(2):556–62.
6. Baumgartner S, Doesburg P, Scherr C, Andersen JO. Development of a biocrystallisation assay for examining effects of homeopathic preparations using cress seedlings. Evid Based Complement Alternat Med. 2012;2012:125945.
7. Chebotareva VD, Maĭdannik VG, Paderno VN. A crystallographic method in the diagnosis of kidney diseases. Vrach Delo. 1990;11:70–4.
8. Maĭdannik VG, Paderno VN, Pokrasen NM, Martynenko AN. Diagnostic possibilities of a crystallographic method in pyelonephritis in children. Pediatriia. 1990;5:46–51.
9. Slobodianik GI. The importance of crystallography in the diagnosis of pyelo- and glomerulonephritis in children. Lik Sprava. 2000;2:74–6.
10. Teodor IL, Chumakov FI, Moroz LA, Mikhaĭlova GE. Role of the crystallographic study in the diagnosis of various diseases of the upper respiratory tract. Vestn Otorinolaringol. 1983;5:55–8.
11. Gulati SP, Sachdeva CP, Adlakha RP. Crystallization test for detection of head and neck cancer. ORL J Otorhinolaryngol Relat Spec. 1994;56:283–6.
12. Gruner OC. Experience with the Pfeffer crystallization method for diagnosis of cancer. Can Med Assoc J. 1940;43:99–106.
13. Kuczlowski J, Zaorski P, Betlejewski A. Crystallization test in patients with head and neck neoplasms. Otolaryngol Pol. 1995;49:121–4.
14. Aizenberg J. Crystallization in patterns: a bio-inspired approach. Adv Mater. 2004;16:1295–302.
15. De Yoreo JJ, Vekilov PG. Principles of crystal nucleation and growth. Rev Mineral Geochem. 2003;54:57–93.
16. Sabarth E, Williams HN. Sensitive crystallization process as demonstration of formative forces in the blood. 2nd ed. Spring Valley: Anthroposophic; 1975.
17. Quadeer A. Crystallization test for detection of malignancy. J Anat Soc India. 1980;29:2.
18. Shaikh SI, Kawale DN, Diwan CV, Quadeer A, Kharkar AR. Crystallization test for detection of malignancy in the female genital tract. Int J Basic Med Sci. 2012;3:118–24.
19. Sarode SC, Sarode GS, Barpande S, Tupkari JV. Efficacy of crystallization test for screening of oral squamous cell carcinoma with clinico-pathological correlation. Indian J Dent Res. 2013;24:464–7.
20. Kahl J, Busscher N, Hoffmann W, Mergardt G, Clawin-Raedecker I, Ploeger A. A novel approach for differentiation of milk fractions and polyvinylpyrrolidone with different molecular weight by patterns derived from cupric chloride crystallization with additives. Anal Methods. 2014;6:3173–6.
21. Sharma A, Ruckenstein E. An analytical nonlinear theory of thin film rupture and its application to wetting films. J Colloid Interface Sci. 1986;113:456–79.
22. Burkhardt A. Advanced method in the evaluation of premalignant lesions and carcinomas of the oral mucosa. J Oral Pathol. 1985;14:751–78.
23. Savory J, Shipe JR. Serum and urine polyamines in cancer. Ann Clin Lab Sci. 1975;5:110–4.
24. Rawat G, Kureel K, Urs AB. An insight into crystallization test: A neoteric approach for screening premalignant and malignant lesions. J Can Res Ther. https://doi.org/10.4103/jcrt.JCRT_275_17.

14 Salivary Biomarkers in Oral Cancer

Prashanth Panta and David T. W. Wong

Abstract

Saliva is an easily accessible biofluid with immense diagnostic potential in oral cancer. The identification of potential saliva signatures for early, noninvasive detection of oral squamous cell carcinoma (OSCC) lead to early detection, better outcome, and survival. More than 100 biomarkers have shown differential levels in saliva of patients with OSCC. They encompass a large number of proteins which cover cell surface molecules (CD44sol, CA-125, etc.), cytoskeleton fragments (CYFRA 21-1), intracellular proteins (ZNF-510, Mac-2 binding protein), proteases (MMPs) and inflammation-associated proteins (CRP, defensin-1, IL-6, IL-8), and mRNA signatures (IL-8, IL-1B, DUSP1, OAZ1, SAT, and H3F3A) and recently some noncoding RNA (miRNA and circular RNA). Some of these salivary biomarkers (both RNA and proteins) have displayed high sensitivity and specificity and were shown to reflect the underlying molecular characteristics and severity of OSCC. The salivary-mutated and salivary-methylated DNA, HPV-DNA, telomerase level, certain oral microbiota, metabolic and oxidative stress biomarkers, and inorganic ion concentration have also shown biomarker potential. Moreover, the unstable RNA is protected in exosomes, allowing their stable detection and easy quantification. The salivary transcriptome (coding, noncoding RNAs) has also displayed performance in multiethnic cohorts of oral cancer patients. In this chapter, the potential salivary biomarker signatures, corresponding tissue and serum concentration, and their role in OSCC are discussed.

P. Panta, MDS (✉)
Department of Oral Medicine and Radiology, MNR Dental College and Hospital, Sangareddy, Telangana, India
e-mail: maithreya.prashanth@gmail.com

D. T. W. Wong, DMD, DMSc
Center for Oral/Head and Neck Oncology Research, School of Dentistry, University of California Los Angeles, Los Angeles, CA, USA

Jonsson Comprehensive Cancer Center, University of California Los Angeles, Los Angeles, CA, USA

Head and Neck Surgery/Otolaryngology, David Geffen School of Medicine, University of California Los Angeles, Los Angeles, CA, USA

School of Engineering and Applied Science, University of California Los Angeles, Los Angeles, CA, USA
e-mail: dtww@ucla.edu

14.1 Introduction

Oral cancer is the sixth most common malignancy in the world [1]. Oral squamous cell carcinoma (OSCC) accounts for ~90% of total oral cancer cases [1]. A significant portion of the global oral cancer burden occurs in the Indian subcontinent. Oral cancer progression is a multistep process

P. Panta (ed.), *Oral Cancer Detection*, https://doi.org/10.1007/978-3-319-61255-3_14

associated with preventable risk factors. The primary risk factors for OSCC include tobacco exposure, both in the form of smoking and chewable forms, areca nut use, and alcohol consumption. Additional risk factors include nutritional deficiency, trauma, and genetic predisposition. Most of the cases present at stage III or IV, ending in morbid disease with low survival, and it is therefore necessary to focus on early detection. When diagnosis is made at stage I, prognosis is good and 5-year survival reaches 80% [2, 3].

"Early detection" is therefore a key strategy to reduce the high mortality and morbidity associated with OSCC. OSCC identified in the asymptomatic stage requires minimum management. The role of post biopsy methods, using prognostic markers, in predicting risk of malignant transformation from "oral potentially malignant disorders" (OPMDs) is also of limited value, as decision is based on excised tissue specimen. Fear of pain resulting from biopsy also leads to delay, after reaching a clinical diagnosis of oral cancer [4]. It is therefore advantageous to develop methods which are painless and noninvasive for patients and safe for handling, with less committed procedures for preservation and accurate analysis.

The presence of signature biomarkers in local secretions is universal to many malignancies, and their identification has the highest potential in early detection [5]. Liquid biopsy of blood, body fluids like urine and local secretions like bronchial washings, pleural effusion, and ascetic fluid, was extensively tested as a suitable diagnostic medium for malignancies [5]. Similarly, potential biomarkers are reflected in saliva, may inform subtle tissue molecular changes, and may be useful in the detection of early OSCC cases. "Saliva based liquid biopsy" is therefore a viable alternative for diagnosis or at least as an adjuvant method for further confirmation with biopsy, supporting decision made by clinicians.

14.2 Saliva: Diagnostic Biofluid in Oral Cancer

Saliva sampling is noninvasive and less infectious (risk-free), and preservation is also easy as it shows no clotting ability, satisfying the clinical requirements of an ideal diagnostic medium [6] (Fig. 14.1).

Fig. 14.1 Saliva an ideal diagnostic bio-fluid

Saliva contains a wealth of chemical compounds (i.e., information), and a change in their concentration can reflect local and systemic disease status. Saliva is especially useful for oral diseases like OPMDs and oral cancer, because it shares direct physical contact with these lesions. As saliva bathes oral lesions, it reflects their internal molecular environment more precisely than distal body fluids like blood. Saliva samples can also be collected in patients with special needs or disabilities, in anxious individuals, in children posing challenge to blood sampling, or in patients harboring high-risk infectious and communicable disease. The chances of transmission of high-risk infectious diseases like HIV is low with saliva samples [1]. Saliva collection reduces discomfort and embarrassment to patients. Also handling saliva samples is much easier compared to blood samples which require complex preservation and handling protocols. It is possible to detect oral cancer before the physical symptoms appear (asymptomatic stage) using saliva, as it reflects the molecular changes which occur before malignant transformation of tissue. Genetic and epigenetic, cellular, and metabolic events precede gross tissue changes during the development of OSCC. Furthermore, dentists and stomatologists who identify these patients are highly receptive to the application of saliva in diag-

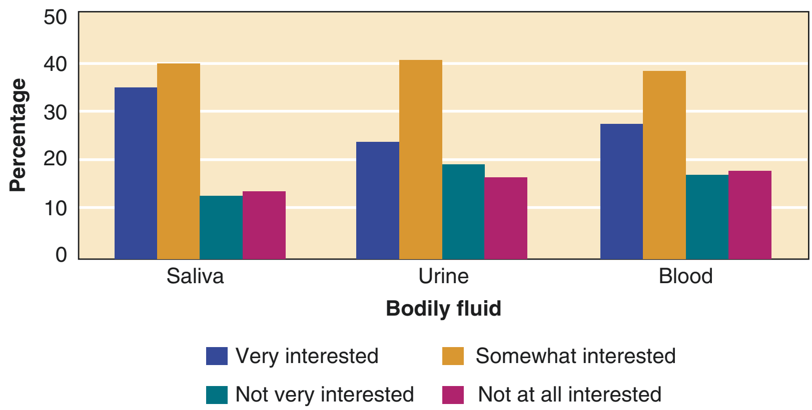

Fig. 14.2 Saliva is a more potential fluid-of-choice for patient-centered diagnostic tests. Figure shows the percentage distribution of subjects interested in donating saliva, over urine and blood for a research study. *Reprinted from J Am Dent Assoc, vol 139, Koka et al, The preferences of adult outpatients in medical or dental care settings for giving saliva, urine or blood for clinical testing, pages 735–740. Copyright (2008) with permission from Elsevier*

nostics [6, 7]. Moreover the general public will be more interested to donate saliva over other bodyfluids (Fig. 14.2)

14.2.1 Saliva: Natural Composition

Saliva is a clear, slightly acidic fluid (pH = 6.5–7) secreted by the numerous minor (~300–400) and three pairs of major salivary glands [8]. Despite being rich in water, its viscosity is five times higher than blood [8, 9]. Humans generate around 1–1.5 liters of serous and mucous saliva per day at an average flow rate of 0.5 mL/min [10]. Saliva is important for speech, mastication and digestion, and defense function. Saliva can be divided into cellular and acellular (fluid) components. The major host cells in saliva include exfoliated epithelial cells, lymphocytes, and erythrocytes, and oral microbiota mainly include bacteria. The acellular component of saliva includes water (99%), proteins (enzymes, hormones, immunoglobulins, growth factors ~0.3%), inorganic ions and enzyme cofactors (calcium, magnesium, iron, copper, zinc, or manganese ~0.2%) metabolites, RNA, and DNA [10]. Saliva proteins include enzymes involved in food digestion (α-amylase), defense proteins like lysozyme and peroxidase, secretary immunoglobulins (IgA, IgG), and highly glycosylated mucin proteins (MUC5B, MUC7, MUC19, MUC1, MUC4) that support lubrication [10–12]. The mucin proteins are the most abundant saliva proteins, and they exert the viscoelastic property to water-rich saliva [11, 12]. In the secretory process, the proteins in the salivary acini are transported from acinar endoplasmic reticulum via secretory granules to the plasma membrane, where they are released through exocytosis into gland lumen. Exocytosis is a continuous process but can accelerate with neural stimulation. Sympathetic stimulation of parotid and submandibular glands and parasympathetic stimulation of sublingual gland can increase protein release from acini [10]. The ductal cells predominantly absorb the isotonic, near plasma-concentrated saliva and modify it into a hypotonic solution (low Na^+ and Cl^-, high K^+ and $HCO3^-$). This ion exchange happens through transporters (e.g., Na/K ATPase, Na-K-Cl cotransporter). Significant ion exchange occurs in the ductal lumen, and water permeability by acinar cells is mediated by aquporin-5. A useful web resource (http://www.skb.ucla.edu/) on current knowledge base on saliva is maintained by the University of California, Los Angeles (UCLA) [13].

14.2.2 Saliva Biomarkers in Oral Cancer

A biomarker is any signature that can reflect normal biological process, pathologic process in tissue, or response to therapeutic intervention, in a quantifiable manner [1]. Saliva was used for

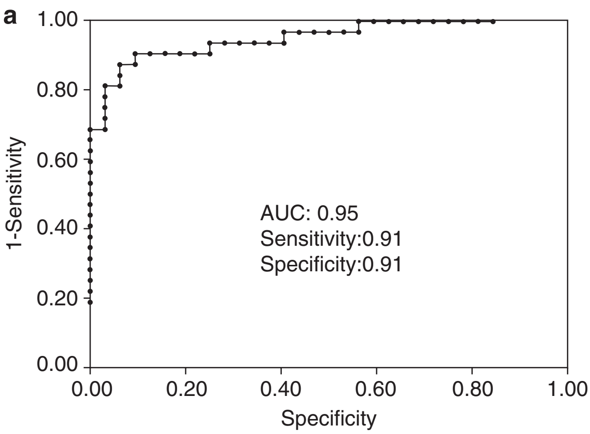

Fig. 14.3 (**a**) ROC curve analysis for the predictive power of combined salivary mRNA biomarkers (*IL1B, OAZ1, SAT*, and *IL8*). Using a cutoff probability of 50%, a sensitivity of 91% and specificity of 91% by ROC was found. The area under the ROC curve (AUC) was 0.95. *Reprinted with permission from (Li et al. Salivary transcriptome diagnostics for oral cancer detection. Clin Cancer Res. 2004; 10: 8442-50). Copyright (2004) American Association for Cancer Research*. (**b**) ROC analysis based on the validation results of these five candidate protein markers (M2BP, MRP14, CD59, catalase, and profilin). The sensitivity and specificity were 90% and 83%, respectively and area under the ROC curve (AUC) was 0.93. *Reprinted with permission from (Shen et al. Salivary Proteomics for Oral Cancer Biomarker Discovery. Clin Cancer Res. 2008; 14: 6246–6252). Copyright (2008) American Association for Cancer Research*

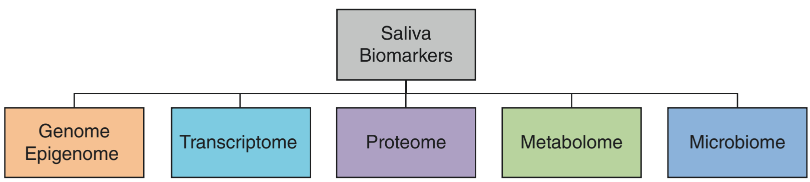

Fig. 14.4 Saliva contains a wide spectrum of biomarkers with high utility index in early detection of oral cancer

screening distant tumors for the first time in 1986 by Jenzano et al. [14]. Saliva kallikrein activity was significantly higher in patients with malignant tumors (breast and gastrointestinal cancer), remote from the oral cavity [14]. The first saliva biomarker to be discovered was the human epidermal growth factor receptor 2 (HER-2), associated with breast cancer. Unlike breast cancer, carcinogens in tobacco smoke (>5000) and chewable forms lead to gross changes in genome and aberrations in key signaling pathways. It is therefore unlikely that a single marker can serve as a reliable indicator of OSCC. Over the years several groups have published excellent results (>90% accuracy), but a perfect prediction model capable of identifying OSCC in asymptomatic patients is yet to be identified (Fig. 14.3) [1]. This accuracy (>90%) may seem encouraging but is still insufficient for routine clinical use.

The saliva biomarkers for OSCC can be broadly divided into proteomic, transcriptomic, genomic and epigenomic, metabolic, and microbiota-based biomarkers [7] (Figs. 14.4 and 14.5). A noninvasive diagnostic test can therefore be designed to detect OSCC by identifying changes in the salivary proteome, transcriptome, genome and epigenome, metabolome, or microbiome or their unique combination [7]. Despite several advantages of salivary biomarker, limitations do exist. The concentration of most analytes in saliva is significantly lower (100–1000-fold) as compared to their relative concentration in blood [10]. However, with reference to oral cancer, this may not be a serious limitation as the majority of analytes are locally released from the

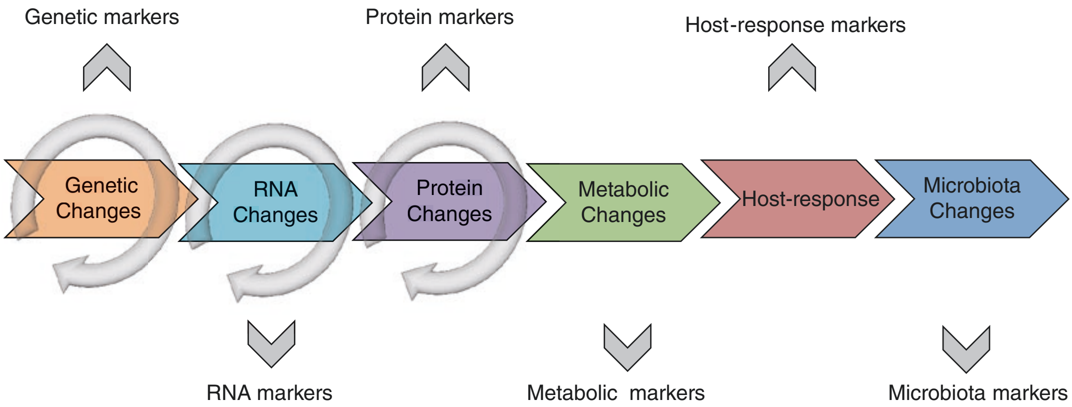

Fig. 14.5 In oral cancer, dysregulation occurs at genomic, transcriptomic, proteomic and metabolic levels producing unique biomarker signatures representing each of these subtle events. Host response and microbial colonization also change with the development of oral cancer which results in host-response related markers and microbiota based markers

tumor site. Cutoff values should be established for potential biomarkers through high-power studies applicable to unknown OSCC cases. For biomarker studies, prospective-specimen collection, retrospective-blinded-evaluation (PRoBE) design is best suited [10]. In PRoBE, samples are first collected prospectively from target population before diagnosis. Later they are examined, and individuals with known diagnosis and controls are selected randomly and tested in a blinded fashion. Strict adherence to this methodology leads to definitive Food and Drug Administration (FDA) biomarker approval [15]. Saliva biomarker test is an ideal diagnostic investigation as certain biomarkers have demonstrated highest sensitivity and specificity. The core technology for biomarker discovery is referred to as "salivaomics." As it is impossible to present an exhaustive description on all established salivary biomarkers (~100) in oral cancer [1], we have classified and relied on the most significant candidates.

14.2.2.1 Proteomic Biomarkers

A decade ago, the human saliva protein pool (proteome) was known to contain only 1166 proteins [16]. In 2013, Schulz et al. compared proteome database of plasma with saliva (International Human Plasma Proteome Project) and reported that 30% of saliva proteins arise from plasma itself [16]. Today, more than 2000 proteins are known to constitute the saliva proteome (www.hspp.ucla.edu) [8]. In a recent report by Yu et al., following careful survey of existing literature, 49 proteins were identified as potential biomarkers of OSCC [2]. The salivary proteins differentially expressed in OSCC patients include cell surface proteins (CD44sol, cancer antigen 125, carcinoembryonic antigen, carcinoma-associated antigen 50), cytoskeleton fragments (CYFRA 21-1, tissue polypeptide antigen, etc.), intracellular proteins (zinc finger protein 510 peptide, Mac-2 binding protein), proteases like matrix metalloproteinases, inflammation-related proteins (cytokines, C-reactive protein, defensin-1), etc. [17–19]. The total number of salivary proteins and total saliva protein also elevates in oral cancer patients as compared to healthy volunteers and OPMDs [20–22]. Saliva proteins can aid the early detection of OSCC.

14.2.3 Cell Surface Glycoproteins

14.2.3.1 CD44

CD44 is a ubiquitous cell surface adhesion molecule linked to cell-cell and cell-extracellular matrix interaction. Structurally it is made of 20 exons; the first and last 5 make up a constant region, and central 10 exons make up a variable region [23]. The CD44 (CD44s) has four components: an extracellular domain, a proximal domain, a transmembrane domain, and a small cytoplasmic tail [23]. The extracellular domain is positioned for its ligands, hyaluronan, collagen, fibronectin, laminin, and chondroitin sulfate, and the cytoplasmic domain links to cytoskeleton through ankyrin and ezrin-moesin-radixin (EMR) family [23, 24]. In cancer, the extracellular domain of CD44 is detached to form "CD44sol" and released into body fluids (saliva or plasma). CD44sol corresponds to its tissue level and is released from tumor cells due to proteolytic digestion via membrane type 1 matrix metalloproteinase [26, 27]. CD44 is also a good tissue biomarker candidate, showing strong expression in advanced stages of OSCC [25]. CD44 expression is particularly seen within the oral cancer stem cell compartment [25, 26]. In a meta-analysis, it also correlated with worse tumor features in head and neck cancers [25]. CD44 elevation was initially reported in oral rinse in 19/25 patients with HNSCC [27]. In serial studies by Franzmann et al., CD44sol levels and methylation status of the CD44 gene promoter were established as potential markers in oral rinse of OSCC patients [27–29]. Salivary soluble CD44 is an important protein in oral cancer, due to its local release from cancer cells [30].

14.2.3.2 Cancer Antigen 125

Cancer antigen or carbohydrate antigen 125 (CA-125) is a tumor-associated antigen. It is a mucin glycoprotein, expressed also in OSCC [31]. CA-125 is known to support tumor growth through suppression of natural killer cells, promoting metastatic invasion. This molecule has a long structure with three domains: N-terminal, tandem repeat, and C-terminal. The N-terminal and tandem repeat domains are in the extracellular position and highly glycosylated. The extracellular portion of the protein is susceptible to proteolytic digestion and is released into body fluids. In one study, mean salivary CA-125 was approximately tenfold in OSCC compared to controls [32]. CA-125 is useful and showed sufficient accuracy in the diagnosis of OSCC along with tissue polypeptide-specific antigen [32, 33].

Other cell surface glycoproteins include carcinoembryonic antigen (CEA), carcinoma-associated antigen 50, cancer antigen 19–9 (CA19–9), and epidermal growth factor receptor 2 (erbB2). In a study on benign and malignant lesions of oral cavity and salivary glands, the combined saliva levels of CEA and CA-50 were significantly higher in malignancies [34]; saliva levels were also higher than corresponding serum levels. In a clinical study, higher levels of erbB2 were detected in unstimulated saliva but not in serum from OSCC patients compared to controls and individuals with OMPD [35].

14.2.4 Cytoskeleton Fragments

Cytokeratins (CK) 8, 18, and 19 are expressed in epithelial cells and released from proliferating and apoptotic cells; both the phenomena occur in OSCC. They are cleaved by caspases, and following digestion they are released into the tumor microenvironment, circulation, and saliva [36]. Fragments of CK-8, 18, and 19 are important markers of epithelial malignancies. The cytokeratin markers in OSCC include CYFRA 21-1, tissue polypeptide antigen, and tissue polypeptide-specific antigen [30].

14.2.4.1 CYFRA 21-1

CYFRA 21-1 (human cytokeratin fragment 21–1) is the soluble fragment of cytokeratin-19, overexpressed in OSCC tissue, serum, and saliva [37–41]. Pre-operative serum levels of CYFRA 21-1 have shown potential as candidate biomarker for risk stratification in OSCC, with higher levels associated with increased tumor depth, bone and skin invasion, and distant metastasis [38]. Salivary CYFRA 21-1 levels correlate well with its parent cytokeratin-19 and also disease recurrence [39]. Salivary CYFRA 21-1 levels have been reported to be threefold higher than serum levels in patients with OSCC [40, 41].

14.2.4.2 Tissue Polypeptide-Specific Antigen

Tissue polypeptide-specific antigen (TPS) is a fragment of cytokeratin-18. TPS is an indicator of high tumor proliferative rate. Its role was identified in nasopharyngeal carcinoma and oral and head and neck squamous cell carcinoma [42]. Its serum level also correlated with therapy, being lower following therapy [42]. Patients with lower levels of TPS had longer survival following therapy, and it was shown as a good predictor of advanced disease, having both diagnostic and prognostic significance [43].

14.2.5 Intracellular Proteins

14.2.5.1 Mac-2 Binding Protein

Mac-2 binding protein is essential in the regulation of growth and motility of OSCC cells [44]. Elevated levels of the protein in tissue, sera, and saliva have been documented in several studies [30, 44, 45].

14.2.5.2 Salivary Zinc Finger Protein 510 Peptide

Zinc finger proteins are the largest family (5926 members) of transcription factors in the human genome playing versatile roles in metabolism, differentiation, and autophagy [46]. Besides DNA binding, they also interact with RNA, proteins, and lipids [46]. The zinc finger proteins hold both oncogenic and tumor suppressor functions. Salivary zinc finger protein 510 peptide (ZNF-510) is a zinc finger protein involved in transcriptional regulation, localized chiefly to the cell nucleus [46]. The 24-mer peptide of ZNF-510 was elevated in immunohistochemical analysis of tumor and saliva [47]. It was not found in the saliva of healthy controls, and its levels correlated significantly with tumor stage, i.e., $T3 + T4 > T1 + T2$ ($n = 45$) [47]. In a systematic review, it was revealed as the only peptide to increase with increasing tumor stage [48]. ZNF-510 is a powerful marker that can differentiate early and late OSCC, and more studies are required for further validation.

14.2.6 Enzymes

14.2.6.1 Matrix Metalloproteinases

Matrix metalloproteinases (MMPs) are key proteases secreted by tumor stroma, involved in the digestion of extracellular matrix, promoting the local invasion and metastasis of oral cancer [49]. Among the many enzymes in the MMP family, in a systematic review, MMP-1 and MMP-3 were identified as potential oral cancer markers [48]. Saliva concentrations of MMP-1 and MMP-3 are elevated several folds in OSCC and increase with increasing tumor grade [50]. MMP-9 can digest type IV collagen, a major basement membrane component, elastin, and fibronectin. MMP-9 was also identified in the saliva of OSCC and OPMD [51]. Matrix metalloproteinase 1 is an interstitial collagenase which was also identified as a potential biomarker (AUC = 0.871) to discriminate OSCC from healthy controls [2].

14.2.7 Inflammation-Related Proteins

14.2.7.1 Cytokines

The pro-inflammatory and pro-angiogenic cytokines IL-6, IL-8, TNF-β, and IL-1β are linked to aggressive malignant behavior in OSCC [52, 53]. They promote SCC, and higher concentrations of cytokines are related to larger tumor size and metastatic potentials. As their expression is silenced in normal tissue, monitoring their levels could be advantageous [52–54]. In a study focused on early TI/T2 OSCC, IL-8 showed elevation in saliva, whereas IL-6 showed elevation in serum [54]. The predictive power of detection increased when saliva IL-8 was used in combination with serum IL-6 (accuracy = 0.998) [54]. Their elevation is seen at both protein and mRNA level. The high expression of IL-6 and IL-8 is established in cell lines and tissue specimens and was linked to growth potential. Moreover, serum levels of these cytokines decrease after surgical treatment, chemo- or radiotherapy, reflecting their true biomarker potential [52]. IL-6 and IL-8 showed significant elevation across multiple cohorts of OSCC [30, 55]. The proteomic marker IL-8 showed highest AUC value in the discrimination between OSCC, OPMDs, and controls, and IL-8 and IL-1β, together produced improved discrimination between OSCC and controls [56].

14.2.7.2 C-Reactive Protein

Cancer-associated inflammation can elevate the levels of acute phase protein enzymes like C-reactive protein (CRP) significantly. CRP is produced and released by the hepatocytes in liver in response to inflammation and is a potential marker for activation of immune response [40, 57]. CRP is known to be regulated by the pro-inflammatory cytokines (IL-1, IL-6, and IL-8, TNFα) secreted by the neutrophils and macrophages. The production of CRP can increase to 50,000-fold in response to acute inflammation, and its assessment is a test for inflammation [57]. As chronic inflammation is associated in OPMDs and OSCC, it serves as a good biomarker. It is primarily a serum marker, and its elevation correlated with clinico-pathological features and disease-free survival in buccal cancers [57]. The ratio of C-reactive protein/albumin score was shown to have good prognostic ability in OSCC; the group with high ratio had high TNM clinical stage and low survival [58].

14.2.7.3 Defensin-1

Human neutrophil defensin proteins designated as HNP-1, HNP-2, and HNP-3 are host defense-related cytotoxic peptides primarily derived from the azurophilic granules in neutrophils [59]. Defensin-1 has been reported in saliva of OSCC patients and may represent defense response of host to OSCC tissue [59]. They originate from saliva ductal cells, oral epithelial cells, and blood cells [60]. Salivary levels of defensin-1 increase with oral inflammation and showed a strong positive correlation with CRP [61]. Saliva defensins also increase in OPMDs like leukoplakia and lichen planus [62].

Other proteomic biomarkers include S100A9 and thioredoxin (small redox proteins) [53], salivary actin and myosin [63], endothelin, and resistin [20]. Salivary amylase declined, and concentrations of albumin, lactate dehydrogenase (LDH), and IgG increase in OSCC [22]. A five-candidate proteomic panel, M2BP, myeloid-related protein 14 (MRP14), CD59 (protectin), profilin, and catalase (cell protector against oxidative stress), yielded a high accuracy (>90%) in OSCC detection [19]. Salivary antibodies to early genetic aberrations like p53 and circulatory antibodies against heat shock proteins have also been identified in OSCC and OPMDs in some studies [64, 65]. The formation of antibodies represents a “humoral immune response” to accumulated nonfunctional proteins [66].

14.2.8 Techniques Investigating Saliva Proteome

The proteome is the protein complement of the genome. It is primarily analyzed by 2D or 1D polyacrylamide gel electrophoresis (PAGE), where proteins appear as spots [58]. PAGE can separate different molecules with similar molecular weight and also isoforms of same proteins, providing a snapshot of the saliva proteome [67, 68]. The gels are stained with silver (5 ng/spot) as per protocols, visualized under the CCD camera system and imaged for optical density and calculated in parts per million [67]. Following electrophoretic separation, the most consistently upregulated bands can be excised and subjected to trypsin digestion for mass spectrometry (MS) analysis. Through MS, a range of proteins can be identified in nontraditional samples like saliva, and MS has already yielded high-quality information about the proteome component of saliva supporting the role of saliva as a diagnostic biofluid. The ionization methods, electrospray ionization (ESI) and matrix-assisted laser desorption ionization (MALDI) with mass analyzers (quadrupole/linear ion trap, time-of flight (TOF), quadrupole time-of-flight (QTOF), and Fourier transform ion cyclotron (QTOF), Orbitrap), improve sensitivity, resolution, accuracy, and efficiency of protein sequence determination [19]. Targeted MALDI-TOF MS peptide analysis can also be performed [69]. High-performance liquid chromatography (HPLC) and MS has also been conjugated. Using dendrimer-associated MS, MALDI-MS, and targeted high-performance liquid chromatography (HPLC)-ESI-MS/MS even posttranslational changes such as phosphorylation, glycosylation, acetylation, and methylation can be characterized [70]. Posttranslationally modified proteins (e.g., glycoproteins and phosphoproteins) occur routinely in oral cancer, which are also present in saliva [70]. Recently, Jiang et al. utilized MALDI-TOF-MS combined with magnetic beads and identified 50 proteins differentially expressed in early OSCC tumors ($n = 40$) [71], and each signature is represented by a protein peak showing discrimination of oral and esophageal cancer [72]. Protein microarrays are also available for the determination of more than 5000 proteins with only microliters of sample [72]. More recently another proteomic approach surface-enhanced laser desorption/ionization-time-of-flight/mass spectrometry (SELDI-TOF/MS), with precision of MALDI and high-throughput nature of protein arrays, has also been developed [73]. SELDI-TOF allows the separation of less abundant proteins, with great accuracy suitable for saliva diagnostics. Through MS abundant data is generated complicating analysis, and there is often a lack of procedure standardization between laboratories, which is perhaps the only limitation [72]. In the recent times, evolving data automation improved feasibility of MS applications. More recently, Luminex point-of-care technology and selected reaction monitoring (SRM)-based tandem mass spectrometry have been used for targeted identification of multiple proteins in oral cancer [51, 53, 74, 75]. Zymography can also be performed using SDS-PAGE for oral cancer proteolytic enzymes like MMPs [76, 77]. In this method, the gels are stained and quantified, and the corresponding protease activity could be measured based on optical density [76, 77].

14.2.8.1 RNA Signatures

RNAs are important in cell metabolism transcribed from DNA. In a recent study using massive parallel sequencing, more than 4000 coding and noncoding RNAs were characterized in the saliva of healthy individuals. Most of the annotated genes (~90%) belong to the coding family. Most of the noncoding genes belonged to the "small nucleolar RNA family" [78]. Extracellular RNA research was funded by the National Institutes of Health (NIH) Common Fund's Extracellular RNA Communication Program, a consortium devoted to define function and produce reference catalog in different body fluids, biomarkers, and development of discovery tools [79, 80]. RNA can arise from blood, salivary glands, and oral microbial flora, and many reads do not align with the human genome [78]. About 20–25% RNA reads in cell-free saliva align with human genome (eukaryotic transcriptome), and 30% RNA sequences align with the human oral microbial genome database (prokaryotic transcriptome) [78]. Microbial RNA markedly reduces the sensitivity of human RNA analysis [78]. The whole saliva transcriptome therefore includes both eukaryotic and prokaryotic transcriptome. Removal of RNA arising from microbiota increases sequencing perfection of human salivary RNA to define true molecular signatures. Centrifugation at low speed is one such step that removes microbial RNA significantly.

Human RNA molecules in saliva include coding RNAs (messenger RNAs) and noncoding RNAs (microRNA, piwi-interacting RNA (piRNA), small nucleolar RNA, and circular RNA) [81]. The saliva transcriptome is hence a complex agglomeration. The saliva cell-free RNA may exist in intact or fragmented form. Intact RNA is mostly from the apoptotic bodies released from tumors, or via actively released exosomes, or through circulation.

14.2.8.2 Messenger RNA

The role of salivary messenger RNA (mRNA) in oral cancer detection was reported by Li et al. in 2004 [82]. Their utility as circulating biomarkers has also been reported [83]. Although large inter-patient variability is known to exist for mRNA, seven transcripts have shown significance in OSCC in several reports [30, 54, 82, 84]. They include interleukin-8 (IL-8) and interleukin-1B (IL-1B), dual specificity phosphatase 1 (DUSP1), ornithine decarboxylase antizyme 1 (OAZ1), S100 calcium-binding protein P (S100P), spermidine/spermine N1-acetyltransferase 1 (SAT), and H3 histone family 3A (H3F3A). Among the seven mRNAs, IL-8 and SAT were identified as top performers, in multiple OSCC cohorts and in a large sample (n = 395 patients) [30]. PRoBE studies validated six markers repeatedly demonstrating approximately two to four fold increase (ct values), highlighting their superiority [85, 86]. The mRNAs may arise locally from tumor tissue or due to a tumor-induced response [30].

14.2.8.3 IL-8 and IL-IB

A group of investigators have successfully linked IL8 protein a candidateoral cancer marker to IL8 mRNA, through electrochemical sensors [54, 87]. This test has yielded a high sensitivity and specificity for both IL-8 and IL8- mRNA, alone and in combination.In a study by Brinkmann et al, RNAs: IL-8, IL1B were among the 4 RNA which were significantly elevated in OSCC [45]. However, in chronic periodontitis the levels of these inflammatory RNAs can be potentially affected [88, 89]

14.2.8.4 DUSP-1

Dual specificity protein phosphatase 1 plays an essential role in the activation of MAPK pathway linked to protein modification, oxidative stress, and signal transduction [90–93]. *DUSP-1* is controlled by p53, and its hypermethylation has been implicated in oral carcinogenesis [56, 94]. However, in some studies saliva DUSP-1-mRNA was nonsignificant and elevated in early OSCC [45, 96].

14.2.8.5 OAZ1

Ornithine decarboxylase antizyme 1 (OAZ1) has effect on proliferation and differentiation of oral cancer cells, through inhibition of polyamine production necessary to prevent cell proliferation [95]. Stable expression of *OAZ1* in squamous cell carcinoma cell lines induces G1 phase and increases epithelial islands. This tumor suppressor molecule participates in the repair of DNA double stranded breaks and in regulation of DNA methylation [95–97]. Salivary OAZ1-mRNA was shown to correlate with OSCC patients during remission and in oral lichen planus (OLP) patients [96].

14.2.8.6 S100P

S100P ("S" solubility, "P" placenta) is a calcium-binding protein overexpressed in a broad range of malignancies [98]. S100P protein is overexpressed in cancer and has a multifaceted role [99, 100]. It participates in the degradation of heat shock proteins (Hsp70 and Hsp90) important in oncogenesis [98], partners with a scaffolding protein IQGAP1 affecting downstream pathways for G protein-coupled receptors [99], and upregulates oncogenes cyclin D1 [100, 101]. It participates actively in the regulation of cytoskeleton and microtubule assembly through binding and activation of ezrin. S100P mRNA is seen with high expression in "anoikis"-resistant OSCC cell line than anoikis-sensitive OSCC, indicating its role in cancer cell survival and metastasis [100]. S100P was shown to be a reliable marker of OSCC, irrespective of poor oral hygiene status in periodontitis [101].

14.2.8.7 Sat 1

Spermidine/spermine N1-acetyltransferase 1 is a protein belonging to the acetyltransferase family that participates in the catabolism of polyamines [102, 103]. SAT-mRNA was among the four proteins identified in a transcriptome panel that showed elevation in late-stage OSCC, in a study by Brinkmann et al. [89]. This was also among the six mRNA (IL-1β, IL-8, OAZ1, SAT, S100P, and DUSP1) that showed elevation in the studies of Martin et al. [85, 86].

14.2.8.8 H3F3A

H3 histone, family 3A is a nuclear protein that forms the histone background responsible for the structural integrity of chromosomal nucleosome; mutations in H3F3A have been linked to some cancers [104, 105]. The H3F3A-mRNA is a cell proliferation marker [104, 106]. In the study of Gleber-Netto et al., H3F3A-mRNA combined with IL-8 protein gave high accuracy in the discrimination of OSCC and OPMD [54]. H3F3A-mRNA was validated as a potential marker in a multi-cohort study, adding strong evidence to its biomarker potential [30, 85, 89].

14.2.8.9 Noncoding RNAs

Besides the well-known messenger RNA landscape, significant changes have been reported in the noncoding RNA family. Nearly 98% of all transcriptional output in humans is noncoding RNAs (ncRNAs) [107]. The ncRNAs have two types, small noncoding RNAs (<200 bps) which include microRNAs and small nucleolar RNAs and long noncoding RNAs (>200 bps) [108]. The ncRNAs are now emerging biomarkers of OSCC. Moreover, ncRNAs are not as susceptible as mRNAs to the action of RNase. They are short sized and therefore more stable in body fluids like urine, blood cerebrospinal fluid, sweat, pleural discharge, and saliva, showing promise for a saliva test [108].

MicroRNA

Among the noncoding RNAs, microRNAs (miR) are the most important biomarkers in OSCC demonstrating highest fold change. They are 19–23 nucleotides long, single-stranded RNA molecules [1]. About 1000 miR molecules have been reported in human genome. They are important functional molecules as a single molecule can bind with more than 100 mRNAs through nonselective binding, and more than 30 mRNAs are posttranscriptionally modified by miRNAs [109].

The ultimate advantage of miRNA markers is the fold change (10–1000 times higher expression) compared to messenger RNAs [109]. In a meta-analysis, the overall diagnostic accuracy of OSCC detection through body fluid miRNA was 0.832 [110]. The main miRs that have been implicated in OSCC include miR-125a, miR-200a, miR-31, miR184, miR-27b, and miR-7 [111]. Some have shown downregulation and some have shown upregulation. For example, miR-125 and miR-200a are significantly degraded, and miR-31 is oncogenic and frequently upregulated in plasma and saliva [112, 113]. Recently miR-184 was identified as a marker of oral mucosal malignant transformation, with threefold increase observed in OSCC, and oral potential malignant disorder compared to normal subjects [114]. In a genome-wide study on salivary RNAs, miRNA-27b was identified as a valuable marker to identify OSCC [115].

The advantage of profiling miRNA in saliva over other body fluids is their overabundance. Saliva was shown to have the largest number of microRNAs, among 12 body fluids tested, exceeding plasma levels [116]. Among the abundant salivary miRNA, only few arise from plasma, and majority come from regular cell turnover and lysis in the oral cavity [116]. This highlights the local release of miRNA from tumor tissue. The important disadvantage of saliva RNA is its high susceptibility to digestion by RNase and cumbersome handling problems during analysis. Moreover, OSCC patients were also shown to possess elevated RNase activity [84].

Circular RNA

In a customized bioinformatics report, more than 400 circular RNAs (circRNAs) were isolated from cell-free saliva in healthy controls [81]. circRNAs are highly abundant in cells, greatly exceeding the concentrations of linear RNA [117]. circRNA compliments the role of microRNA [117]. Their size ranges from few hundred to thousands of nucleotides, forms a circular loop without 5′ cap or a 3′ poly A tail, and acts as microRNA sponge, competitively suppressing microRNA action, and as transcriptional regulators through interactions with RNA-binding proteins and as parent gene expression modifiers by accumulating around transcription site [117–120]. They are abundant in the nucleus, and their knockdown leads to repression of parent genes [119]. The "circRNA-miRNA" axis has a critical role in signaling pathways in cancer [117]. A CircInteractome web tool (http://circinteractome.nia.nih.gov) is available for exploring the interaction between circular RNA and their respective proteins and mRNA [121].

The half-life ($t_{1/2}$) of circRNA is 48 h, approximately four times that of mRNAs, indicating a superior stability [120]. Their overall stability, abundance, and superior $t_{1/2}$ support their role as potential biomarkers [122]. The absence of free ends adds to their resistance against the action of debranching enzymes and exonucleases. The role of CDR1as (or ciRS-7), a circular RNA acting as miRNA 7 sponge, has been implicated in tongue cancer [123]. Another circRNA, ci-mcm5 an enhancer of mcm5 expression, is also known to participate in OSCC. Higher expression of MCM5 is associated with the early stages of oral neoplasia, progression, and poor prognosis [124]. Recently a circular RNA circRNA_100290 through interaction with miR-29 family members was identified as a critical regulator of OSCC development [125]. circRNAs are a new diagnostic alphabet in the RNA biomarker family, and identifying them in saliva can be a new trend in OSCC detection. In the current literature, only little evidence is available linking circRNA and OSCC [125].

14.2.9 Techniques in Transcriptome Landscape

Transcriptome is an emerging landscape in oral cancer for noninvasive detection. Initial microarray and qRT-PCR validation studies were performed by Prof. David Wong and colleagues (University of California, Los Angeles) who identified an enormous transcriptome load in saliva [126]. Subsequently, the advent of next-generation sequencing led to a rapid expansion in the number of RNAs identified. Identification of RNA was chiefly by microarray technology and quantitative real-time PCR, but the disadvantage is the loss of biomolecules due to fragmentation. These two methods, quantitative PCR and microarray, were preliminary methods in saliva-based biomarker discovery and identification; quantitative real-time PCR (qRT-PCR) can also be used, but low amounts of RNA in saliva can hinder the performance of qRT-PCR. This can be overcome by multiplex reverse transcriptase-PCR-based pre-amplification approaches. Significant improvement was made with the advent of next-generation sequencing (NGS)-based approaches and 3-poly (A)-independent amplification technology, which offers no loss of information recovering all salivary RNA fragments [126].

14.2.9.1 Microarray Technology

Microarray is the key technique to identify expression of cancer-associated genes and RNA biomarkers from samples. These gene chips can detect specific gene expression by detecting RNA transcripts in the sample giving insight into the genes activated and inactivated. It is a genome-wide screening tool frequently applied to investigate the expression profile of a very large number of genes. Previously, Northern blotting technique was used for investigating expression of one or several genes. In OSCC and OPMDs, expression profiling of a large set of gene changes provides a “whole-genome fingerprint” [127–129]. A microarray platform (e.g., Affymetrix U133 Plus 2.0, Human Exon 1.0 ST) is a collection of several miniature spots of specific DNA sequences (oligonucleotides) located on a solid base (glass or silicon chip) [126, 130, 131]. Hybridization is the core principle behind microarray analysis. It contains thousands of probe sets and distinct oligonucleotide features representing the entire human genome [1, 126]. Each oligonucleotide sequence known as a “probe” allows hybridization of c-DNA from an unknown sample, but before this, the sequences (c-DNA or RNA) in the sample under study are fused to fluorescent dyes (e.g., cyanine 3, cyanine 5) [132]. The fluorescent labels tagged to the target sequences hybridize with probe sequences to generate a signal whose strength can be measured. This measurement is proportional to the number of photons emitted after excitation with a laser of particular wavelength [130]. A digital image is formed, and intensity values are obtained for each probe set. Microarray manufacturers provide data analysis software (e.g., MicroArray Suite) along with plate readers that help in the creation of huge raw data. Once images are made, they are corrected for background and quality, through filtration, aggregation, and normalization, followed by recognition of gene expression pattern. Any gene set is reliably “present” if $p < 0.001$ and intensity value >200 [126]. The gene chip array information can be tallied with reference gene mining tool of the respective company.

Today, several robust network clustering algorithms are available for cancer subtype discovery (e.g., acute myeloid leukemia, acute lymphoblastic leukemia) based on microarray data [131, 133]. Each cancer type has a characteristic expression profile of genes in key signaling pathways upregulated and downregulated [133]. Microarrays can be used for molecular classification of OSCC or OPMDs, apart from simple diagnosis [127, 134]. Through use of computational algorithms, it is possible to differentiate oral cancer from normal tissue [135]. In a microarray study by Li et al., it was possible to predict biomarkers of oral squamous cell carcinoma using microarray data [131]. It was calculated through bioinformatics that 78 genes showed differential expression in OSCC which were also validated through in vitro and in vivo experiments [131]. Data mining software such as DAVID bioinformatics resource can be used for enrichment analysis of differentially expressed genes to give biological meaning to large gene sets obtained through microarray data [131, 136]. Through microarrays, it is also now possible to predict cancer tissue of origin and cancer subtypes without examining histology, with much more clinical implementation in the future [137], showing good prospects for noninvasive diagnosis from biofluids. However, the key limitations of microarrays include high cost, technical errors and false readings, large tissue sampling, destructive testing, and lacking reusability [137].

14.2.9.2 Quantitative Real-Time Polymerase Chain Reaction (qRT-PCR)

The qRT-PCR is a modification, and major development of PCR technology, carried out in a thermocycler [138]. It minimizes contamination that occurs during PCR product handling [138]. It is a robust method for RNA quantification (i.e., copy number), which is a direct measure of targeted gene expression [139]. Based on the amount of RNA in the given sample, qRT-PCR allows reliable measurement of products at the end of amplification cycles [140]. The RNA in the sample should be reverse transcribed to complementary DNA (RNA to c-DNA) [126]. The c-DNA sample is mixed with sequence-specific probes intercalated to fluorescent molecules known as “reporters.” The fluorophore-labeled sequence gets hybridized to the complementary sequence. The qRT-PCR thermal cycler can illuminate each sample with a light of specific wavelength, and sensors detect the fluorescence emitted by the excited fluorophore; measurements are made through accumulation of fluorescence emitted by the labeled fluorescent probes following release of the quencher [138]. qRT-PCR can also be used in cases where partial fragmentation of target RNA is suspected and where threshold values (Ct values) can be used [139]. In such cases there is loss of amplifiable templates in RNA population; extensive RNA degradation leads to loss of amplicons and increase in Ct value [139]. Quantification of gene expression is primarily by two methods: relative quantification and absolute quantification [141, 142]. Absolute quantification gives the exact number of DNA molecules, and relative quantification determines fold changes in the expression of a specific gene. This method can also be used to quantify any RNA type (mRNA, miRNA, etc.) in the saliva sample, to further validate DNA microarray results.

Hybridization platforms like microarrays and probe (or tag)-based methods provide heavy data connected to the overall expression of a large set of genes (thousands) involved in key signaling events in any disease process.

14.2.9.3 Next-Generation Sequencing

Although hybridization-based microarrays give broad knowledge base, they have inherent problems. The main limitation of microarray profiling for salivary RNA signatures is the presence of cross hybridization noise and dependence on gene annotation [143]. Next-generation sequencing (NGS) methods such as RNA sequencing (RNA-seq) or massively parallel DNA sequencing (c-DNA sequencing at massive scale) have shown unprecedented detail of the human saliva transcriptome [81, 144, 145]. The major advantage of RNA-seq includes its high sensitivity to the identification of genes/exons and splice isoforms, RNA editing, and fusion transcripts in a single experiment [15, 146]. RNA-seq can provide characterization of RNA beyond the inputs provided by microarrays and probe-based PCR examinations [146].

RNA-seq was successfully applied to study RNA signatures in saliva of cancer subjects [146]. The major limitation of RNA-seq for body fluids includes low inputs of RNA, vulnerability to isolation techniques, and the complexity of preparing libraries [147].

In the recent times, NGS revealed its extraordinary ability in the characterization of ncRNA species (miRNAs, piRNAs, and circRNAs) in human saliva. RNA sequencing (RNA-seq) offers single nucleotide information and is highly sensitive and accurate in transcript detection, capable of detecting novel RNA species and transcript isoforms. RNA-seq is a dynamic technology, and a large number of new bioinformatic tools are emerging for analysis of RNA-seq data, ranging from rapid short-read aligners to detailed examination of RNA expression patterns. Owing to improvements in these techniques, the catalog of human genes (both coding and noncoding RNA genes) has been greatly expanded in the last 10 years. The basic steps in RNA-seq analysis include saliva collection and RNA extraction through various methods (e.g., TRIzol method) followed by quantification, c-DNA library construction, and sequencing [148]. Among the RNA-seq library preparation methods, New England Biolabs (NEB)Next library preparation method resulted in the highest number of genes and even small RNAs, with a low total RNA input of 100 ng [149–151]. The HiSeq 2500 from Illumina® is one NGS platform for RNA sequencing. NGS companies are constantly improving their platforms and sequencing abilities. The current application of RNA-seq is mainly based on c-DNA synthesis. The conversion of RNA to c-DNA by reverse transcriptase itself can be a source of error sequences, due to template switching and spurious second-strand synthesis [152]. The amplification RNA is essential for subsequent sequencing and comparison to reference genome or to transcriptome [15]. Initially, amplification methods resulted in some discrepancies and errors. The ideal amplification must maintain a zero error or keep the error as low as possible [152]. The preservation of the original sample is another important aspect. Sequencing samples with low RNA amounts are more challenging as the error rate is higher.

In the recent past, another NGS method, "direct RNA sequencing" (DRS), has been reported, which does not involve c-DNA conversion [152]. DRS is based on the presence of natural poly (A) tails, and in their absence, an additional in vitro step of polyadenylation induction is performed. This method gives information of poly $(A)^+$RNA in the unknown sample. Through this method gene expression pattern can be profiled, and polyadenylation sites can be quantified in a genome-wide manner [152]. DRS is universal in application to decode all RNA*s* without c-DNA conversion.

14.2.10 DNA Signatures

Cell-free tumor DNA (ct-DNA) can be directly investigated in saliva samples. ct-DNA is released from cells undergoing apoptosis or necrosis during OSCC development and progression. Therefore ct-DNA analysis can provide insight into the basic mutation profile of tumors. Saliva samples produce sufficient quantity and quality of DNA [8]. Although the quantity of DNA obtained from blood is tenfold due to the enormous number of white blood cells, salivary ct-DNA is also of sufficient quantity (~24 μg) suitable for analysis [8]. In OSCC, tumor DNA is preferentially enriched in saliva as compared to plasma [153]. As distance between the tumor site and saliva decreases, the chance of finding its ct-DNA biomarkers in saliva increases and plasma decreases [153]. Saliva therefore shows highest sensitivity for detection of ct-DNA for oral cavity cancers [153]. As little as 5 ng/ml is considered optimum for genotyping [8]. The exfoliated epithelial cells from oral tumors within saliva also can provide sufficient genetic material for analysis [84]. The strategies for detecting salivary ct-DNA include NGS, PCR-based (qRT-PCR), and PCR enhancement techniques (clamped-based PCR technique, etc.); MS; beads, emulsion, amplification, and magnetics (BEAMing); or nanoparticle-based techniques [15].

14.2.10.1 Mitochondrial DNA

Mitochondrial dysfunction is an important finding in oral cancer cells [154]. Alterations in mt-DNA content occurs in advanced head and neck squamous cell carcinoma, independent of age and smoking habit, and is potentially detectable in saliva [156–164]. The salivary levels of mt-DNA also decreased following treatment with primary surgical resection and radiotherapy [156]. The main alterations in mitochondrial genome include mutations and copy number changes. Mitochondrial mutations occur in coding (cytochrome c oxidase genes) and noncoding regions, and sometimes mutations occur only in a subset of mitochondrial DNA (mt-DNA) copies, out of the 10^3–10^4 copies in each cell, a condition called heteroplasmy [155–157]. Displacement loop (D-loop) is the hot spot for mutations in the mitochondrial genome, with strong biomarker potential [158–160]. The presence of D-loop mutations potentially alters respiratory chain and bioenergetics. Mutated mitochondrial DNA (mt-DNA) is 19–220 times more abundant than mutated p53 DNA and is readily accessible from bodily fluid like saliva [161].

Mitochondrial DNA copy number is high in tobacco-betel quid chewers with OSCC [162]. Due to the high copy number change, they can be assessed in body fluids and are therefore well suited to serve as potent salivary marker of OSCC [163]. Testing for salivary mt-DNA could be used for early detection of OSCC and for treatment monitoring [161, 163]. Microarray platforms (Human MitoChip) were designed for detecting mutations in mitochondrial genome in body fluid samples [165]. Recently, a novel method "MitoRS" was reported for amplification of entire mitochondrial genome in a single reaction with a starting material of 5 ng [166].

14.2.10.2 Nuclear DNA: Mutation and Methylation

P53 mutations were identified in several studies using saliva samples [106, 167]. The first report of saliva as a diagnostic medium for oral squamous cell carcinoma was published by Liao et al. and was based on (C-deletions) in exon4, condon63 of p53, in 5/8 patients [106]. In a recent study on saliva of 20 OSCC samples, C-deletion was identified in 100% cases [167].

Hypermethylation of gene promoters is an important molecular mechanism for gene silencing and is therefore an important biomarker of oral cancer. DNA methylation status of tumor suppressor genes (P16, death-associated protein kinase (DAPK), methylguanine-DNA methyltransferase (MGMT)) also correlated with smoking history, and oral rinse showed good correlation [168–170]. An exfoliative brush can be used to brush the oral cavity or just the suspected lesions, and then rinsing and gargling can provide a more informative sample [168]. Based on the concordance of results between oral rinse with and without brush, it was identified that oral rinse itself without brush is sufficient [168]. The tumors with more epigenetic burden reflect their methylation in oral rinse, due to significant shedding of cells from widely methylated epithelial fields [168]. Saliva methylation status perfectly reflects tissue methylation status [169]. Aberration in methylation pattern of one of three genes, p16 (CDKN2A), O6-methylguanine-DNA methyltransferase (MGMT), and death-associated protein kinase (DAPK), was identified in saliva of 17/30 patients with HNSCC [170]. In a study by Righina et al., methylation in either of the six genes (p16, MGMT, DAPK, TIMP3, ECAD, RASSF1) was identified in 75% OSCC samples [169]. In 22 patients followed after treatment, there was abnormal methylation in saliva of 5 patients few months after treatment, which correlated with early recurrence on FDG-PET [169]. Methylation pattern of cancer-related genes in saliva can be efficient biomarkers for oral cancer. High-quality DNA can be obtained from saliva, and following this a methyl PCR can be run on samples. Methylated DNA is suitable biomarker for early detection of OSCC and may help in the assessment of relapse [169].

14.2.10.3 Detecting Methylation

Since methylation of DNA causes gene silencing (lack of transcription) a protein is not formed. ELISA and electrophoresis are therefore unsuitable methods. As methylation is a general phenomenon in OSCC involving a large set of genes, a panel of tumor suppressors can be selected for screening saliva samples. Since more genes are involved, initially it is important to depend on genome-wide approaches following which quantitative methylation-specific PCR or pyrosequencing methods can be employed. In fact, methylation enrichment pyrosequencing, a combination of methyl-specific PCR and pyrosequencing, was first described on saliva and tissue samples of OSCC [171]. Several newly available methylation arrays can screen methylation at a large number of CpG islands on several hundred genes [171]. Classifiers can be used to construct the smallest possible panel of genes for clinical application. MethyLight can be used with multiplexed PCR for clinical use to screen methylation at multiple regions [172]. Single methylation events can be investigated directly by a methylation-specific PCR. Study results may vary widely, when two different CpG islands on the same gene are screened [173]. It is important to select the most sensitive CpGs for analysis. The genes selected should also be of highest relevance to OSCC, such as P16.

For examination of DNA mutation or methylation pattern, saliva can be collected in vials or as saline mouthwash or via sponge kits [174]. A saliva sample is superior and presents more DNA for analysis than a mouthwash or saliva collected through sponge kits [174]. However, it should be noted that all saliva methods produce sufficient DNA for analysis.

14.2.10.4 Telomerase

Telomere attrition and telomerase activation are detected in 85–90% malignancies, including OSCC [175, 176]. Telomerase is a ribonucleoprotein that is frequently upregulated in oral malignant cells. It is a marker of 'cell escape from senescence', an important step in cancer progression. Telomerase is not active in normal tissues, and highly up-regulated in HNSCC tissue [175, 176]. As a result, detectable telomerase activity is identified in a considerable fraction (32%) of oral rinse samples of HNSCC cases [177]. The telomerase repeat amplification assay (TRAP assay) is a key investigation in the estimation of telomerase activity in body fluids like oral rinse [72, 178]. Sensitive fluorescent and electrochemical strategies for telomerase activity detection using exonuclease III-aided target recycling and T7 exonuclease-assisted target recycling amplification is reported with limited telomerase positive cancer cells, which can beobtained through saliva [179–181].

14.2.10.5 Viral DNA

Oral infection with HPV confers a 50-fold risk of developing HPV-positive OSCC. The genomic sequence of human papillomavirus (HPV-16 and 18) can be recovered in saliva and oral epithelial scrapings of OSCC and OPMDs, due to their high prevalence in corresponding tissues [153, 182, 183]. A conventional PCR assay is sufficient. Recently, a Hybrid capture 2 test for use in low resource countries, GP5+/6+-Based Luminex Assay based on microsphere suspension technology or cartridge-based Xpect PCR amplification assay capable to detect 14 types of HPV in less than 1 hour can be used to screen for genomic DNA (E6, E7) of high risk HPV [182–186]. Screening for HPV is a reliable method to document the additional risk of OSCC development within OPMDs? This is also necessary for couples to screen their unaffected partners for emerging HPV associated OSCC/HNSCC! The presence of HPV is not diagnostic of OSCC or HNSCC, but, indicates a possible additional risk.

14.2.10.6 The Metabolic Profile

Metabolites are small compounds formed in the various metabolic processes. Saliva metabolites are unique fingerprints and can reflect physiologic and pathologic states [187]. In saliva, nearly 853 metabolites were identified (http://www.salivametabolome.ca/statistics) [187]. Saliva metabolic markers emerged useful in many conditions (pancreatic cancer, Sjogren's syndrome, periodontitis), and recent evidence document its usefulness in oral cancer [16]. In oral cancer, as a result of genetic changes, significant changes also occur in critical metabolic pathways like glycolysis, tricarboxylic acid cycle, pentose phosphate cycle, polyamine synthesis, urea metabolism, etc. [188, 189]. The metabolism in oral cancer is therefore different from metabolism in healthy normal tissue. Metabolic profile of saliva has showed excellent precision and accuracy in OSCC detection; 17 metabolites showed significant changes in saliva and tissue of OSCC patients [188].

Oral cancer tumor tissue revealed more glucose consumption and lactate accumulation (Warburg effect), glutamine consumption and glutamine to lactate conversion, and changes in several metabolites. Both tissue and saliva revealed significant changes in levels of spermidine, kynurenine, S-adenosylmethionine, methionine, choline, betaine, pipecolate, etc. [188, 189]. However, glycolysis remains a chief source of energy in OSCC [190]. The metabolite combination of choline, betaine, pipecolic acid, and l-carnitine yielded a very high accuracy (0.997) in saliva of stage I–II OSCC cases [191]. Amino acids, L-leucine and L-phenylalanine, have a promising role in diagnosis of early- and late-stage OSCC cases, respectively [192]. Their combination has also yielded superior accuracy. The methyl donor, S-adenosylmethionine (S-Adm), which adds methyl groups to a range of biomolecules (phospholipids, proteins, ribosomal RNA, and DNA) formed from methionine also shows elevation in tissue and saliva [188]. This partly explains the hypermethylation noticed in OSCC [193]. In oral cancer, there is upregulation in polyamine synthesis which correlates with increase in proliferation rate [194]. The enzyme necessary for polyamine synthesis is ornithine decarboxylase [194]. Metabolic polyamines include putrescine, cadaverine, spermidine, and spermine which play roles in ion channel modulation, ribosomal functions, and programmed cell death in cancer. Polyamines are important salivary biomarkers of oral cancer. The metabolic profile is primarily investigated using capillary electrophoresis and time-of-flight mass spectrometer [189].

14.2.10.7 Oxidative Stress-Related Biomarkers

The various free radicals and oxidants cause damage to cell and cell organelle membranes and DNA. Free radical damage can occur through lipid peroxidation, DNA damage, protein damage, and enzyme activity alteration and can also induce cytokine signaling [195]. Oxidative stress is when the balance between free radicals and antioxidant mechanisms is lost and is common to OSCC. Reactive oxygen species can form from endogenous metabolic pathways (e.g., electron transport chain) or due to exogenous sources like tobacco. Oxidative biomarkers in saliva are mainly related to smoking-related malignancies like oral cancer or lung cancer. Tobacco in smoke and chewable form contains several oxidizing agents and carcinogens leading to oxidative stress-related biomarkers in the saliva of OSCC and OPMDs. Free radicals such as reactive oxygen and nitrogen species formed in response to tobacco make up the main pillars in pathogenesis of oral cancer. They involve at various stages of cancer development including promotion, initiation, and termination. Even saliva has been implicated to play some part in the genesis of oral cancer [196]. In the presence of cigarette smoke, saliva loses it protective antioxidant capacity and becomes highly deleterious [196]. In this way saliva catalyzes oral carcinogenesis, favoring its evolution. Saliva antioxidant compounds are therefore linked intimately to oral cancer, and saliva oxidative radicals definitely reflect stage of oral cancer and early detection [196]. Saliva carbonyls are significantly elevated in saliva of OSCC patients, due to the direct action of free radicals on saliva proteins, an indicator of oxidative damage to proteins [197]. Carbonylation of proteins is irreversible damage and an indicator of oxidative damage to proteins. Substantial carbonylation (256%) was present in saliva patients with OSCC [197]. Salivary malondialdehyde (MDA), a principal product of lipid peroxidation, was also used to measure oxidation and antioxidant imbalance, but wide variation between healthy controls was noticed. Salivary MDA, however, arises from systemic source and food material and can change with smoking and drug history [198]. The saliva level of malondialdehyde showed statistically significant elevation in oral precancer and cancer groups as compared to controls [199, 200]. MDA is also highly toxic and may induce oral carcinogenesis [200]. Although individual oxidation markers can be used, total antioxidant capacity (AOC) defined as moles of oxidant neutralized by a liter of solution can be a more convenient biomarker for examining the antioxidant potential of saliva [201]. Saliva total antioxidant capacity is a reduced in OPMDs like leukoplakia, oral lichen planus, erythroplakia, and oral cancer, and a low AOC may indicate cancer inception [201]. In oral cancer and OPMDs, markers of lipid damage (MDA, 8-hydroxy-2-deoxyguanosine (8-OHdG)) and protein carbonyls are increased, and antioxidant vitamins (vitamins A, C, E), retinol, carotenes, and total antioxidant capacity are reduced [198, 202].

14.2.10.8 Oral Microbiota

Through NGS, as many as 10,000 microbial florae were identified in healthy oral cavity, as opposed to 700 bacterial species mentioned in Human Oral Microbiome Database (http://www.homd.org/), a database of NIH [10, 16]. Healthy oral cavity shows abundance of bacterial species in the *phyla Firmicutes* (e.g., *Streptococcus*), *Proteobacteria*, *Bacteroidetes*, *Actinobacteria*, and *Fusobacteria*, with small individual variation. The most common bacterial genes include *Streptococcus* and less occasionally the genus *Prevotella*, *Veillonella*, *Neisseria*, and *Haemophilus* [203]; different oral locations also show some variation. The microbiota dynamics can also change with the intake of certain drugs or with deleterious habits like smoking and alcoholism or in the presence of certain diseases [10].

Shifting microbiome is an important finding in oral cancer. This change can be perceived in two distinct ways: as an effect of local cancer microenvironment and as a cause of the disease itself or due to associated oral habits like smoking. The pathogen, i.e., microbial saliva marker linked to OSCC, should always be associated with the disease and should diminish in a patient responding to treatment reflecting true disease status [10]. Mager et al. report emphasized that oral cancer causes significant changes compared to smoking or periodontitis, so changes in microbiome may be due to a direct effect of the cancer environment [204]. In OSCC, changes were noticed in microorganisms in 6–8 phyla, majority belonging to *Firmicutes* and *Bacteroidetes* [205–207]. Three oral florae, *Capnocytophaga gingivalis*, *Prevotella melaninogenica*, and *Streptococcus mitis*, could differentiate OSCC and healthy controls with a sensitivity and specificity of 80% [10, 204]. Certain microbiota were also linked with Fanconi's anemia (FA), a model of oral cancer risk, where patients have developed OSCC following hematopoietic stem cell transplantation. Many microbiota can be easily cultured using saliva samples and probed to provide information about OPMDs and their progression to cancer, differentiation of cancer subtypes, and potential recurrence [208, 209]. Technologies of value in the investigation of oral microbiota include human oral microbe identification microarrays (HOMIM) which are 16 s rRNA based, restriction fragment length polymorphism (T-RFLP) analysis, and deep sequencing. These technologies can be useful even for uncultivatable strains [10, 207, 210].

14.2.10.9 Inorganic Components and Immunoglobulins

Saliva mineral composition and immunoglobulin concentrations also change in OSCC patients [211–217]. In OSCC, high levels of calcium (Ca), inorganic phosphate (P), magnesium (Mg), and sodium (Na) and low levels of potassium (K) were reported [22, 211]. The change in ionic composition can be linked to oral dehydration, which may be linked more to alcoholism than OSCC [212, 213]. Mineral biomarkers were also linked to cancer in certain oral sub-sites [212]. The secretary IgA which maintains mucosal immunity is decreased in patients with oral cancer [22, 214]. The basis for this decline may be due to inhibition of steps in the formation of Ig antibody (extracellular hydrolysis of polymeric immunoglobulin receptor PIgR) by the tumor tissue [214, 215]. The levels of sialic acid were also increased in smokers and in patients with OPMDs and OSCC [21, 216–218]. Their levels were also higher in OSCC than OPMDs [219]. It is difficult to draw conclusions on mineral composition and saliva antibodies (secretory IgA, IgG) from low-power studies. Moreover, these biomolecules enter saliva primarily through the salivary glands. The mineral composition in saliva is primarily influenced by hydration status and oral habits (smokers and smokeless tobacco, alcoholism), as a result may be reliable but not highly representative biomarkers [22, 216, 217].

14.2.11 Mechanisms of Biomarker Entry into Saliva

Saliva biomarkers (metabolites, proteins, RNA, DNA) move into saliva in a defined manner.

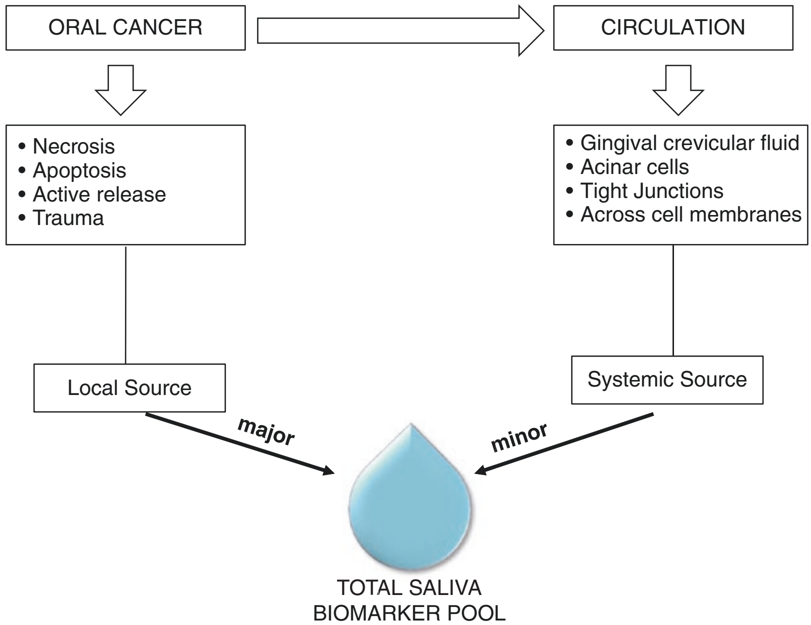

Fig. 14.6 Source of salivary biomarkers and their release mechanisms. Local mechanisms are the main source of salivary biomarkers in OSCC

Proteins, RNA, and DNA biomarkers in the saliva are formed from salivary glands, exfoliated oral mucosal cells, oral microbiota and HPV, circulation through passive diffusion, active transport and ultrafiltration, food particles, and most importantly tumor tissue. These biomolecules enter saliva either locally (major mechanism) from the oral lesion itself (OSCC or OPMD) or secreted in response to the oral tumor through the circulation (minor mechanism) (Fig. 14.6). From the bloodstream, they can enter through the cells or between the cells [10]. The passage between cells is referred to as "transcellular entry," which occurs through passive intracellular diffusion or active transport. The passage of chemical compounds can also occur via "paracellular entry" via extracellular ultrafiltration [10]. Due to these mechanisms, certain biomarkers can en route from blood and reflect in saliva, supporting "saliva" as a "mirror of blood biochemistry." This is of particular significance as some salivary biomarkers like CRP and IL-6 elevate primarily in the systemic circulation. This limits the identification of circulatory biomarkers that increase in response to OSCC. The most important source for salivary OSCC biomarkers is through local release mechanisms via extracellular vesicles from the tumor tissue site.

14.2.11.1 Extracellular Vesicles: Potential Local Source of Biomarkers

Cancer cells often shed several vesicles around 30 nm from the cell surface into extracellular matrix and to the exterior environment (Fig. 14.7) [220]. The vesicles are bound by phospholipid bilayer and contain a range of substances including proteins involved in metal transport, proliferation, etc., RNA, and DNA. These extracellular vesicles (EVs) gained attention only recently, when speculated for hidden mechanisms protecting salivary RNA. EVs are broadly divided into exosomes, microvesicles, or apoptotic bodies (Fig. 14.8). The EVs attach to cells to deliver key molecules through endocytosis or directly release their constituents into cell cytoplasm. In this way, they mediate complex functions like cellular communication, propagation of oncogenesis, and also in establishment of premetastatic niche [221, 222]. So they can be the perfect targets to grasp the molecular and biomarker landscape of oral malignant and premalignant tissue.

Their size and morphology can be validated using atomic force or transmission electron microscope (Fig. 14.7). EVs have an elastic membrane and exhibit different shapes. Under low-atomic force mode, their structure is simple,

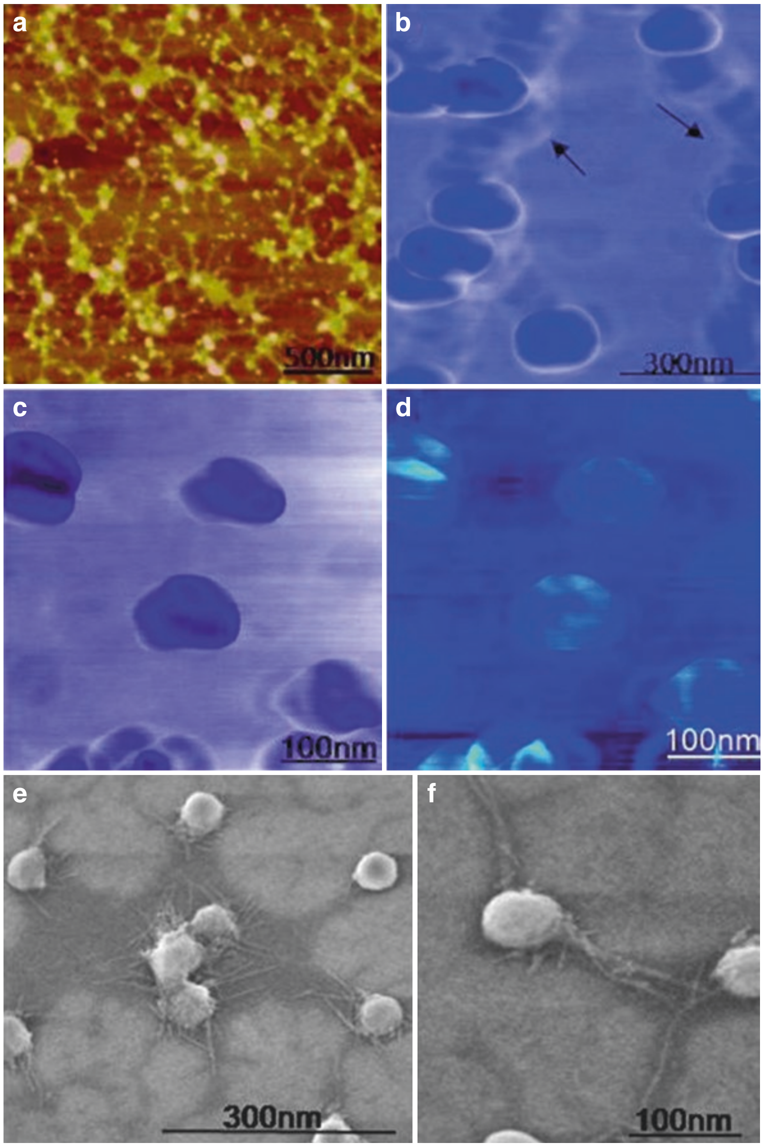

Fig 14.7 Ultrastructure of individual saliva exosomes observed under Tapping mode, AM-Atomic force microscope (AFM) and microscopy (FESEM). (**a**) Tapping mode topographic AFM image showing round morphology of isolated exosomes. (**b**) AM-AFM phase image of aggregated exosomes. Interconnections (arrows) lacking characteristic phase shift, probably indicate some extra-vesicular protein content. (**c**) At higher forces under AM-AFM (~2 nN) representative single exosome phase images reveal trilobed sub-structure within the centre of the vesicles. The contrast in images may be attributed to variable constitutive elements (lipid, protein, RNA ratio). (**d**) Corresponding height images show a central depression of the vesicles. (**e**) FESEM exosome image showing multiple exosomes and (**f**) single isolated vesicles as round bulging structures without a central depression and well resolved intervesicular connections. *Reprinted with permission from (Sharma et al, Structural-mechanical characterization of nanoparticle exosomes in human saliva, using correlative AFM, FESEM, and force spectroscopy. ACS Nano. 2010; 4: 1921-6). Copyright (2010) American Chemical Society*

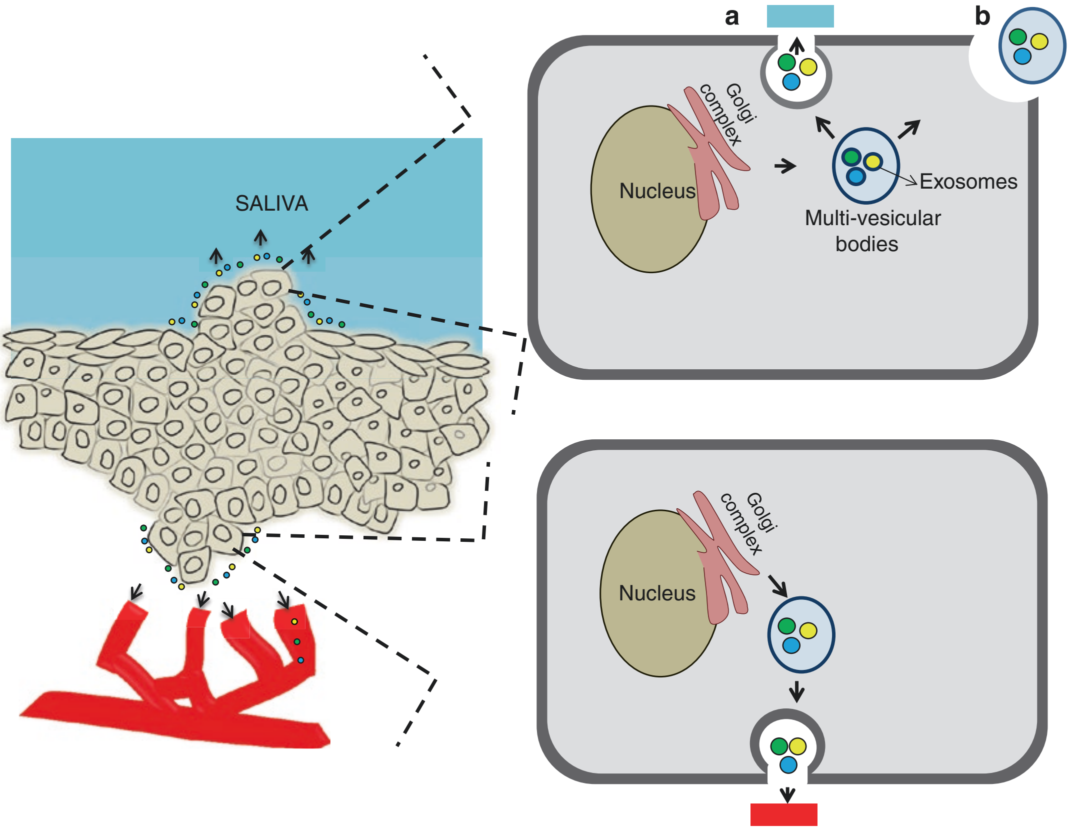

Fig 14.8 Exosome released from oral cancer cell into saliva and circulation. The exosomes are contained within the multi-vesicular bodies and are produced from the golgi complex. They are released into the saliva through membrane fusion (**a**) or via membrane rupture (**b**). The deeply placed tumor cells close to the blood vessels release exosomes and biomarkers frequently into the circulation. Local release of exosomes and biomarkers into saliva is a more common mechanism in oral squamous cell carcinoma

presenting as round (50–70 nm) and homogenous structures [223]. At slightly higher atomic force, they present with channel like elongations, and at much higher forces (>5nN), they rupture, breaking into small fragments, releasing their contents [223]. Even the antigenic surface of EVs has been characterized using gold nanoparticles [223]. EVs can be separated using ultracentrifugation and can be tracked using nanoparticle or through immunodetection against membrane proteins [220]. The approaches for extracellular vesicular structures include density gradient centrifugation and differential centrifugation chromatography, gel filtration, and immunocapture [224]. A modified chromatography column with a filter system has recently been used in the characterization of saliva proteomics through exosome capture [224].

14.2.12 Saliva Collection and Handling

14.2.12.1 Standardization

The optimal timing for saliva collection is 12 h fasting after dinner between 8 AM and 10 AM [67, 225]. The secretion of saliva is controlled by the sympathetic and parasympathetic systems and varies during the day due to a circadian rhythm [10]. Saliva secretion is dependent on many stimuli including age, sex, diet, oral habits, health and disease status, and medication [10]. This is the reason saliva sampling must be standardized. To reduce the chance of degradation of saliva markers, the time gap between collection and analysis needs to be minimized (time delay<5 min). The participants must avoid smoking, aggressive mouth movements like eating and chewing, and oral hygiene procedures 30–90 min before collection [30]. Also before saliva collection, deionized water can be used to rinse the mouth to clean the oral cavity thoroughly to get rid of food debris.

14.2.12.2 Basic Saliva Collection Protocol

There are two types of saliva: gland-specific and whole saliva. Gland-specific saliva can be collected into Lashley cup or Carlson-Crittenden collector but is not so relevant for OSCC biomarkers and more appropriate for analyzing biomarker alterations in salivary gland disorders [10]. For OSCC, whole saliva is the preferred option. Whole saliva (WS) is a mixture of secretions from all the salivary glands (submandibular, parotid and sublingual, and minor glands). Collection of whole saliva can be spitting, suctioning, and draining or drool methods [10]. Whole saliva can be (a) stimulated or (b) unstimulated. Stimulation brings more saliva due to reflex activity, from chewing a paraffin block or gum base or using 2% citric acid [67]. However, for saliva sampling in OSCC frequently stimulated, whole saliva (WS) is appropriate for analysis and paraffin stimulation resulted in least variability [67]. Stimulation can be used in patients who find it difficult to produce enough saliva. The unstimulated saliva is a collection method without exogenous facilitation. Even 5 minutes of unstimulated saliva collection will yield approximately 5 ml of saliva, sufficient for any analysis [126].

Usually the first few drops are discarded to reduce the chance of contamination. For saliva collection, the participant is asked to tilt the head slightly forward and let the saliva to be collected in the floor of the mouth before collection into precooled collection device. Depending on the type of salivary analyte (DNA/RNA/protein), one can choose the appropriate saliva collection devices (saliva collection aid, Salimetrics oral swab (Salimetrics®); Oragene DNA, Oragene RNA (DNA Genotek®)) [10].

14.2.12.3 Saliva Sample Handling

- Current saliva handling protocol includes a mandatory centrifugation step, followed by freezing at minus 80 °C or dry ice for transportation [6]. Whole saliva contains many epithelial cells, microbes, and food debris which needs to be centrifuged (2600 *g* for 15 min) and removed [126]. The supernatant (acellular phase) is suitable for analysis. A protease inhibitor (e.g., trifluoroacetic acid) or RNase inhibitor can be added, and sample can be stored in minus 80 °C for further analysis [126]. Suitable protocols have also been established for stable preservation up to 2 weeks for saliva proteomics [8, 19]. Between the two temperatures minus 80 °C and minus 20 °C, minus 80 °C was shown to generate more stable results [226]. The addition of stabilizing agent and snap freezing reduces the chances of RNA degradation [126]. For optimal proteomic analysis, the samples can be fast frozen in liquid nitrogen, but multiple freeze cycles should always be avoided. The stabilization of transcriptome and proteome is a critical challenge due to the action of nucleases and proteases. Recently, a novel collector system (RNAPro•SAL) for making accurate measurements of proteins and nucleic acids was developed with performance comparable to UCLA standard clinical collection procedure [6, 224].

14.2.13 Selection of Appropriate Controls

The selection of correct controls is important for accurate test result in biomarker studies. In the control group, individuals without any disease and with matching age, sex, and demographic characteristics (same cohort) can be used for comparison as all these factors influence saliva secretion. The weakness of many studies arises in the improper identification of controls and careful exclusion. In a recent systematic review, it was shown that only 12 of 28 studies mentioned caution of oral conditions before sample collection, pointing at a basic flaw in overall methodology [227]. The elevation of cytokines and several mRNAs is common to inflammatory oral diseases like chronic periodontitis or lichen planus, and it is important to exclude such patients for biomarker studies in oral cancer [228, 229]. Also in oral bleeding, the concentration of certain biomarkers can elevate significantly due to local release, leading to biased results. Hence it is essential to exclude patients with gingivitis or periodontitis which are often associated with oral bleeding. To avoid false positives, careful exclusion of patients with local inflammatory and bleeding diseases like gingivitis and periodontitis is necessary for accurate biomarker study [228]. It is excellent if we identify a biomarker which is not confounded by common oral conditions or other possibly coexisting diseases in the general population. We must identify a biomarker unique to OSCC and highly representative.

Conclusion

Oral cancer is an aggressive disease in which changes in saliva precede phenotypic tissue changes that manifest clinically. Hence we must design and optimize methods based on salivary changes (subtle event), rather than relying on gross clinical patterns or tissue changes, which occur at a comparatively later stage. *'Non-invasiveness'* is the holy grail in diagnostics, and is ideally achievable through saliva sampling. The main challenges in the realization of routine saliva testing for oral cancer include the identification of a *'perfect biomarker'* or a *'perfect prediction model* 'with 100 percent accuracy, on a portable hand-held platform. There is still missing evidence to strongly support the use of saliva based diagnosis at the asymptomatic or sub-clinical stage (<T1 stage) of OSCC, which recommends intense research focus. Through high throughput experiments on large number of patient derived saliva samples, from multi-ethnic and multi-cohort studies, rigorous biomarker profiling and validation is possible, for the conclusive identification of a universal biomarker or biomarker panel significantly affected in initial malignancies.

Disclosures David Wong is the co-founder of the RNAmeTRIX Inc., a molecular diagnostic company. He holds equity in RNAmeTRIX and serves as a company director and scientific advisor. The University of California also holds equity in RNAmeTRIX. Intellectual property that David Wong invented and which was patented by the University of California has been licensed to RNAmeTRIX. Additionally, he is a consultant to GlaxoSmithKline, Wrigley, EZlife Bio Inc, and Colgate-Palmolive Company.

Acknowledgment Support from the Ronnie James DioStand Up and Shout Cancer Research Fund.

References

1. Panta P, Venna VR. Salivary RNA signatures in oral cancer detection. Anal Cell Pathol (Amst). 2014;2014:450629.
2. Yu JS, Chen YT, Chiang WF, Hsiao YC, Chu LJ, See LC, et al. Saliva protein biomarkers to detectoral squamous cell carcinoma in a high-risk population in Taiwan. Proc Natl Acad Sci U S A. 2016;113:11549–54.
3. Wong DT. Towards a simple, saliva-based test for the detection of oral cancer 'oral fluid (saliva), which is the mirror of the body, is a perfect medium to be explored for health and disease surveillance'. Expert Rev Mol Diagn. 2006;6:267–72.
4. Martin JL, Wolanin A, Lerner I. Oral Cancer screening. Reducing fear using salivary diagnostics. Dent Today. 2016;35:14.
5. Yanning Ma, Xian Wang, and Hongchuan Jin. Methylated DNA and microRNA in body fluids as biomarkers for cancer detection. Int J Mol Sci. 2013; 14: 10307–10331.
6. Fang WE, Wong DT. Point-of-care platforms for salivary diagnostics. Chin J Dent Res. 2012;15:7–15.
7. Wong DT. Saliva omics. J Am Dent Assoc. 2012;143:19S–24S.
8. Wang X, Kaczor-Urbanowicz KE, Wong DT. Salivary biomarkers in cancer detection. Med Oncol. 2017;34:7. Epub 2016 Dec 10
9. Kazuya Iwai, Tamiko Minamisawa, Kanako Suga,YasutomoYajima, Kiyotaka Shiba. Isolation of human salivary extracellular vesicles by iodixanol density gradient ultracentrifugation and their characterizations. J Extracell Vesicles. 2016;5:30829.
10. Yoshizawa JM, Schafer CA, Schafer JJ, Farrell JJ, Paster BJ, Wong DT. Salivary biomarkers: toward future clinical and diagnostic utilities. Clin Microbiol Rev. 2013;26:781–91.

11. Frenkel ES, Ribbeck K. Salivary mucins in host defense and disease prevention. J Oral Microbiol. 2015;7:29759.
12. Aps JK, Martens LC. Review: the physiology of saliva and transfer of drugs into saliva. Forensic Sci Int. 2005;150:119–31.
13. Ai J, Smith B, Wong DT. Saliva ontology: an ontology-based framework for a Salivaomics Knowledge Base. BMC Bioinformatics. 2010;11:302.
14. Jenzano JW, Courts NF, Timko DA, Lundblad RL. Levels of glandular kallikrein in whole saliva obtained from patients with solid tumors remote from the oral cavity. J Dent Res. 1986;65:67–70.
15. Kaczor-Urbanowicz KE, Carreras-Presas CM, Kaczor T, Michael T, Wei F, Garcia-Godoy F, Wong DTW. Emerging technologies for salivaomics in cancer detection. J Cell Mol Med. 2017;21:640–7.
16. Wang A, Wang CP, Michael T, Wong DTW. Oral biofluid biomarker research: current status and emerging Frontiers. Diagnostics (Basel). 2016;6:45.
17. Nagler RM. Saliva as a tool for oral cancer diagnosis and prognosis. Oral Oncol. 2009;45:1006–10.
18. Shah FD, Begum R, Vajaria BN, Patel KR, Patel JB, Shukla SN et al. A review on salivary genomics and proteomics biomarkers in oral Cancer. Ind J Clin Biochem. 2011;26:326–334.
19. Yu-Hsiang Lee, David T. Wong. Saliva: an emerging biofluid for early detection of diseases. Am J Dent. 2009; 22: 241–248.
20. Wu CC, Chu HW, Hsu CW, Chang KP, Liu HP. Saliva proteome profiling reveals potential salivary biomarkers for detection of oral cavity squamous cell carcinoma. Proteomics. 2015;15:3394–404.
21. Dhakar N, Astekar M, Jain M, Saawarn S, Saawarn N. Total sialic acid, total protein and total sugar levels in serum and saliva of oral squamous cell carcinoma patients. A case control study Dent Res J (Isfahan). 2013;10:343–7.
22. Shpitzer T, Bahar G, Feinmesser R, Nagler RM. A comprehensive salivary analysis for oral cancer diagnosis. J Cancer Res Clin Oncol. 2007;133:613–7.
23. Naor D, Sionov RV, Ish-Shalom D. CD44: structure, function, and association with the malignant process. Adv Cancer Res. 1997;71:241–319.
24. Rudzki Z, Jothy S. CD44 and the adhesion of neoplastic cells. Mol Pathol. 1997;50:57–71.
25. Chen J, Zhou J, Lu J, Xiong H, Shi X, Gong L. Significance of CD44 expression in head and neck cancer: a systemic review and meta-analysis. BMC Cancer. 2014;14:15.
26. Trapasso S, Allegra E. Role of CD44 as a marker of cancer stem cells in head and neck cancer. Biologics. 2012;6:379–83.
27. Franzmann EJ, Reategui EP, Carraway KL, Hamilton KL, Weed DT, Goodwin WJ. Salivary soluble CD44: a potential molecular marker for head and neck cancer. Cancer Epidemiol Biomark Prev. 2005;14:735–9.
28. Franzmann EJ, Reategui EP, Pedroso F, Pernas FG, Karakullukcu BM, Carraway KL, et al. Soluble CD44 is a potential marker for the early detection of head and neck cancer. Cancer Epidemiol Biomark Prev. 2007;16:1348–55.
29. Franzmann EJ, Reategui EP, Pereira LH, Pedroso F, Joseph D, Allen GO, et al. Salivary protein and solCD44 levels as a potential screening tool for early detection of head and neck squamous cell carcinoma. Head Neck. 2012;34:687–95.
30. Elashoff D, Zhou H, Reiss J, Wang J, Henson B, Shen H, et al. Pre-validation of salivary biomarkers for oral Cancer detection. Cancer Epidemiol Biomark Prev. 2012;21:664–72.
31. Jacobs I, Bast RC Jr. The CA 125 tumour-associated antigen: a review of the literature. Hum Reprod. 1989;4:1–12.
32. Balan JJ, Rao RS, Premalatha BR, Patil S. Analysis of tumor marker CA 125 in saliva of normal and oral squamous cell carcinoma patients: a comparative study. J Contemp Dent Pract. 2012;13:671–5.
33. Geng XF, Du M, Han JX, Zhang M, Tang XF, Xing RD. Saliva CA125 and TPS levels in patients with oral squamous cell carcinoma. Int J Biol Markers. 2013;28:216–20.
34. He H, Chen G, Zhou L, Liu Y. A joint detection of CEA and CA-50 levels in saliva and serum of patients with tumors in oral region and salivary gland. J Cancer Res Clin Oncol. 2009;135:1315–21.
35. Varun C, Dineshkumar T, Jayant VS, Rameshkumar A, Rajkumar K, Rajashree P, et al. Salivary Her2/neu levels in differentiation of oral premalignant disorders and oral squamous cell carcinomas. Asian Pac J Cancer Prev. 2015;16:5773–7.
36. Barak V, Goike H, Panaretakis KW, Einarsson R. Clinical utility of cytokeratins as tumor markers. Clin Biochem. 2004;37:529–40.
37. Zhong LP, Zhu HG, Zhang CP, Chen WT, Zhang ZY. Detection of serum Cyfra 21-1 in patients with primary oral squamous cell carcinoma. Int J Oral Maxillofac Surg. 2007;36:230–4.
38. Hsu YP, Hsieh CH, Chien HT, Lai CH, Tsao CK, Liao CT, et al. Serum markers of CYFRA 21-1 and C-reactive proteins in oral squamous cell carcinoma. World J Surg Oncol. 2015;13:253.
39. Zhong LP, Zhang CP, Zheng JW, Li J, Chen WT, Zhang ZY. Increased Cyfra 21-1 concentration in saliva from primary oral squamous cell carcinoma patients. Arch Oral Biol. 2007;52:1079–87.
40. Nagler R, Bahar G, Shpitzer T, Feinmesser R. Concomitant analysis of salivary tumor markers--a new diagnostic tool for oral cancer. Clin Cancer Res. 2006;12:3979–84.
41. Rajkumar K, Ramya R, Nandhini G, Rajashree P, Ramesh Kumar A, Nirmala Anandan S. Salivary and serum level of CYFRA 21-1 in oral precancer and oral squamous cell carcinoma. Oral Dis. 2015;21:90–6.

42. Sun SS, Hsieh JF, Tsai SC, Ho YJ, Kao CH. Tissue polypeptide specific antigen (TPS) as a tumor marker in nasopharyngeal carcinoma. Anticancer Res. 2000;20:4661–3.
43. Barak V, Meirovitz A, Leibovici V, Rachmut J, Peretz T, Eliashar R, Gross M. The diagnostic and prognostic value of tumor markers (CEA, SCC, CYFRA 21-1, TPS) in head and neck Cancer patients. Anticancer Res. 2015;35:5519–24.
44. Weng LP, Wu CC, Hsu BL, Chi LM, Liang Y, Tseng CP, et al. Secretome-based identification of mac-2 binding protein as a potential oral cancer marker involved in cell growth and motility. J Proteome Res. 2008;7:3765–75.
45. Brinkmann O, Kastratovic DA, Dimitrijevic MV, Konstantinovic VS, Jelovac DB, Antic J, et al. Oral squamous cell carcinoma detection by salivary biomarkers in a Serbian population. Oral Oncol. 2011;47:51–5.
46. Jen J, Wang YC. Zinc finger proteins in cancer progression. J Biomed Sci. 2016;23:53.
47. Jou YJ, Lin CD, Lai CH, Tang CH, Huang SH, Tsai MH, et al. Salivary zinc finger protein 510 peptide as a novel biomarker for detection of oral squamous cell carcinoma in early stages. Clin Chim Acta. 2011;412:1357–65.
48. Gualtero DF, Suarez Castillo A. Biomarkers in saliva for the detection of oral squamous cell carcinoma and their potential use for early diagnosis: a systematic review. Acta Odontol Scand. 2016;74:170–7.
49. Thomas GT, Lewis MP, Speight PM. Matrix metalloproteinases and oral cancer. Oral Oncol. 1999;35:227–33.
50. Stott-Miller M, Houck JR, Lohavanichbutr P, Mendéz E, Upton MP, Futran ND, et al. Tumor and salivary matrix metalloproteinase levels are strong diagnostic markers of oral squamous cell carcinoma. Cancer Epidemiol Biomark Prev. 2011;20:2628–36.
51. Venugopal A, Uma Maheswari TN. Expression of matrix metalloproteinase-9 in oral potentially malignant disorders: a systematic review. J Oral Maxillofac Pathol. 2016;20:474–9.
52. Russo N, Bellile E, Murdoch-Kinch CA, Liu M, Eisbruch A, Wolf GT, et al. Cytokines in saliva increase in head and neck cancer patients after treatment. Oral Surg Oral Med Oral Pathol Oral Radiol. 2016;122:483–490.e1.
53. Arellano-Garcia ME, Hu S, Wang J, Henson B, Zhou H, Chia D, et al. Multiplexed immunobead-based assay for detection of oral cancer protein biomarkers in saliva. Oral Dis. 2008;14:705–12.
54. St John MA, Li Y, Zhou X, Denny P, Ho CM, Montemagno C, et al. Interleukin 6 and interleukin 8 as potential biomarkers for oral cavity and oropharyngeal squamous cell carcinoma. Arch Otolaryngol Head Neck Surg. 2004;130:929–35.
55. ÉvaCsősz PL, Kalló G, Márkus B, Emri M, Szabó A, et al. Proteomics investigation of OSCC-specific salivary biomarkers in a Hungarian population highlights the importance of identification of population-tailored biomarkers. PLoS One. 2017;12:e0177282.
56. Gleber-Netto FO, Yakob M, Li F, Feng Z, Dai J, Kao HK, Chang YL, Chang KP, Wong DT. Salivary biomarkers for detection of oral squamous cell carcinoma in a Taiwanese population. Clin Cancer Res. 2016;22:3340–7.
57. Tai SF, Chien H-T, Young C-K, Tsao C-K, de Pablo A, Fan K-H, et al. Roles of preoperative C-reactive protein are more relevant in buccal cancer than other subsites. World J Surg Oncol. 2017;15:47.
58. Park H-C, Kim M-Y, Kim C-H. C-reactive protein/albumin ratio as prognostic score in oral squamous cell carcinoma. J Korean Assoc Oral Maxillofac Surg. 2016;42:243–50.
59. Mizukawa N, Sugiyama K, Fukunaga J, Ueno T, Mishima K, Takagi S, Sugahara T. Defensin-1, a peptide detected in the saliva of oral squamous cell carcinoma patients. Anticancer Res. 1998;18:4645–9.
60. Abiko Y, Nishimura M, Kaku T. Defensins in saliva and the salivary glands. Med Electron Microsc. 2003;36:247–52.
61. Mizukawa N, Sugiyama K, Ueno T, Mishima K, Takagi S, Sugahara T. Levels of human defensin-1, an antimicrobial peptide, in saliva of patients with oral inflammation. Oral Surg Oral Med Oral Pathol Oral Radiol Endod. 1999;87:539–43.
62. Mizukawa N, Sugiyama K, Ueno T, Mishima K, Takagi S, Sugahara T. Defensin-1, an antimicrobial peptide present in the saliva of patients with oral diseases. Oral Dis. 1999;5:139–42.
63. de Jong EP, Xie H, Onsongo G, Stone MD, Chen XB, Kooren JA, et al. Quantitative proteomics reveals myosin and actin as promising saliva biomarkers for distinguishing pre-malignant and malignant oral lesions. PLoS One. 2010;5:e11148.
64. Tavassoli M, Brunel N, Maher R, Johnson NW, Soussi T. p53 antibodies in the saliva of patients with squamous cell carcinoma of the oral cavity. Int J Cancer. 1998;78:390–1.
65. Castelli M, Cianfriglia F, Manieri A, Palma L, Pezzuto RW, Falasca G, et al. Anti-p53 and anti-heat shock proteins antibodies in patients with malignant or pre-malignant lesions of the oral cavity. Anticancer Res. 2001;21:753–8.
66. Ralhan R, Nath N, Agarwal S, Mathur M, Wasylyk B, Shukla NK. Circulating p53 antibodies as early markers of oral cancer: correlation with p53 alterations. ClinCancer Res. 1998;4:2147–52.
67. Jasim H, Olausson P, Hedenberg-Magnusson B, Ernberg M, Ghafouri B. The proteomic profile of whole and glandular saliva in healthy pain-free subjects. Sci Rep. 2016;6:39073.
68. Walz A, Stühler K, Wattenberg A, Hawranke E, Meyer HE, Schmalz G, et al. Proteome analysis of glandular parotid and submandibular-sublingual saliva in comparison to whole human saliva by two-dimensional gel electrophoresis. Proteomics. 2006;6:1631–9.

69. Szanto I, Mark L, Bona A, Maasz G, Sandor B, Gelencser G, et al. High-throughput screening of saliva for early detection of oral cancer: a pilot study. Technol Cancer Res Treat. 2012;11:181–8.
70. Majem B, Rigau M, Reventós J, Wong DT. Non-coding RNAs in saliva: emerging biomarkers for molecular diagnostics. Int J Mol Sci. 2015;16:8676–98.
71. Jiang WP, Wang Z, Xu LX, Peng X, Chen F. Diagnostic model of saliva peptide finger print analysis of oral squamous cell carcinoma patients using weak cation exchange magnetic beads. Biosci Rep. 2015; 35.pii: e00211.
72. Alicia D. Powers, Sean P. Palecek. Protein analytical assays for diagnosing, monitoring, and choosing treatment for cancer patients. J Healthc Eng. 2012;3:503–34.
73. Ardito F, Perrone D, Cocchi R, Lo Russo L, DE Lillo A, Gianna tempo G, et al. Novel possibilities in the study of the salivary proteomic profile using SELDI-TOF/MS technology. Oncol Lett. 2016;11:1967–72.
74. Kawahara R, Bollinger JG, Rivera C, Ribeiro ACP, Brandão TB, Leme AFP, et al. A targeted proteomic strategy for the measurement of oral cancer candidate biomarkers in human saliva. Proteomics. 2016;16:159–73.
75. Aziz S, Ahmed SS, Ali A, Khan FA, Zulfiqar G, Iqbal J, et al. Salivary immunosuppressive cytokines IL-10 and IL-13 are significantly elevated in oral squamous cell carcinoma patients. Cancer Investig. 2015;33:318–28.
76. Vandooren J, Geurts N, Martens E, Van den Steen PE, Opdenakker G. Zymography methods for visualizing hydrolytic enzymes. Nat Methods. 2013;10:211–20.
77. Singh RD, Haridas N, Patel JB, Shah FD, Shukla SN, Shah PM, Patel PS. Matrix Metalloproteinases and their inhibitors: correlation with invasion and metastasis in oral Cancer. Indian J Clin Biochem. 2010;25:250–9.
78. Spielmann N, Ilsley D, Gu J, Lea K, Brockman J, Heater S, et al. The human salivary RNA transcriptome revealed by massively parallel sequencing. Clin Chem. 2012;58:1314–21.
79. Ainsztein AM, Brooks PJ, Dugan VG, Ganguly A, Guo M, Howcroft TK, et al. The NIH extracellular RNA communication consortium. J Extracell Vesicles. 2015;4:27493.
80. Laurent LC, Abdel-Mageed AB, Adelson PD, Arango J, Balaj L, Breakefield X, et al. Meeting report: discussions and preliminary findings on extracellular RNA measurement methods from laboratories in the NIH extracellular RNA communication consortium. J Extracell Vesicles. 2015;4:26533.
81. Bahn JH, Zhang Q, Li F, Chan TM, Lin X, Kim Y, et al. The landscape of microRNA, Piwi-interacting RNA, and circular RNA in human saliva. Clin Chem. 2015;61:221–30.
82. Li Y, St John MA, Zhou X, Kim Y, Sinha U, Jordan RC, et al. Salivary transcriptome diagnostics for oral cancer detection. Clin Cancer Res. 2004;10:8442–50.
83. Li Y, Elashoff D, Oh M, Sinha U, St John MA, Zhou X, Abemayor E, Wong DT. Serum circulating human mRNA profiling and its utility for oral cancer detection. J Clin Oncol.2006; 24:1754–1760.
84. Adami GR, Adami AJ. Looking in the mouth for noninvasive gene expression-based methods to detect oral, oropharyngeal, and systemic cancer. ISRN Oncol 2012;2012:931301.
85. Martin JL, Gottehrer N, Zalesin H, Hoff PT, Shaw M, Clarkson JH, et al. Evaluation of salivary transcriptome markers for the early detection of oral squamous cell cancer in a prospective blinded trial. Compend Contin Educ Dent. 2015;36:365–73.
86. Martin JL. Validation of reference genes for oral Cancer detection panels in a prospective blinded cohort. PLoS One. 2016;11:e0158462.
87. Modi WS, Dean M, Seuanez HN, Mukaida N, Matsushima K, O'Brien SJ. Monocyte-derived neutrophil chemotactic factor (MDNCF/IL-8) resides in a gene cluster along with several other members of the platelet factor 4 gene superfamily. Hum Genet. 1990;84:185–7.
88. Yumoto H, Nakae H, Fujinaka K, Ebisu S, Matsuo T. Interleukin-6 (IL-6) and IL-8 are induced in human oral epithelial cells in response to exposure to period ontopathic Eikenella corrodens. Infect Immun. 1999;67:384–94.
89. Yamazaki K, Nakajima T, Gemmell E, Polak B, Seymour GJ, Hara K. IL-4- and IL-6-producing cells in human periodontal disease tissue. J Oral Pathol Med. 1994;23:347–53.
90. Keyse SM, Emslie EA. Oxidative stress and heat shock induce a human gene encoding a protein-tyrosine phosphatase. Nature. 1992;359:644–7.
91. Martell KJ, Kwak S, Hakes DJ, Dixon JE, Trent JM. Chromosomal localization of four human VH1-like protein-tyrosine phosphatases. Genomics. 1994;22:462–4.
92. Tanoue T, Yamamoto T, Maeda R, Nishida E. A Novel MAPK phosphatase MKP-7 acts preferentially on JNK/SAPK and p38 alpha and beta MAPKs. J Biol Chem. 200; 276: 26629–39.
93. Slack DN, Seternes OM, Gabrielsen M, Keyse SM. Distinct binding determinants for ERK2/p38alpha and JNK map kinases mediate catalytic activation and substrate selectivity of map kinase phosphatase-1. J Biol Chem. 2001;276:16491–500.
94. Khor GH, Froemming GR, Zain RB, Abraham MT, Omar E, Tan SK, et al. DNA methylation profiling revealed promoter Hypermethylation-induced silencing of p16, DDAH2 and DUSP1 in primary oral squamous cell carcinoma. Int J Med Sci. 2013;10:1727–39.
95. Wang X, Jiang L. Effects of ornithine decarboxylase antizyme 1 on the proliferation and differentiation of human oral cancer cells. Int J Mol Med. 2014;34:1606–12.
96. Cheng YS, Jordan L, Rees T, Chen HS, Oxford L, Brinkmann O, Wong D. Levels of potential oral cancer salivary mRNA biomarkers in oral cancer

patients in remission and oral lichen planus patients. ClinOral Investig. 2014;18:985–93.
97. Tsuji T, Katsurano M, Ibaragi S, Shima K, Sasaki A, Hu GF. Ornithine decarboxylase antizyme upregulates DNA-dependent protein kinase and enhances the nonhomologous end-joining repair of DNA double-strand breaks in human oral cancer cells. Biochemistry. 2007;46:8920–32.
98. Prica F, Radon T, Cheng Y, Crnogorac-Jurcevic T. The life and works of S100P - from conception to cancer. Am J Cancer Res. 2016;6:562–76.
99. Heil A, Nazmi AR, Koltzscher M, Poeter M, Austermann J, Assard N, et al. S100P is a novel interaction partner and regulator of IQGAP1. J Biol Chem. 2011;286:7227–38.
100. Kupferman ME, Patel V, Sriuranpong V, Amornphimoltham P, Jasser SA, Mandal M, et al. Molecular analysis of anoikis resistance in oral cavity squamous cell carcinoma. Oral Oncol. 2007;43:440–54.
101. Cheng YL, Jordan L, Chen HS, Kang D, Oxford L, Plemons J, et al. Chronic periodontitis can affect the levels of potential oral cancer salivary mRNA biomarkers. J Periodontal Res. 2017;52:428–37.
102. Xiao L, Celano P, Mank AR, Griffin C, Jabs EW, Hawkins AL, et al. Structure of the human spermidine/spermine N1-acetyltransferase gene (exon/intron gene organization and localization to Xp22.1). Biochem Biophys Res Commun. 1992;187:1493–502.
103. Coleman CS, Pegg AE. Polyamine analogues inhibit the ubiquitination of spermidine/spermine N1-acetyltransferase and prevent its targeting to the proteasome for degradation. Biochem J. 2001;358:137–45.
104. Zhang Y, Reinberg D. Transcription regulation by histone methylation: interplay between different covalent modifications of the core histone tails. Genes Dev. 2001;15:2343–60.
105. Yuen BTK, Knoepfler PS. Histone H3.3 mutations: a variant path to cancer. Cancer Cell. 2013;24: 567–74.
106. Liao PH, Chang YC, Huang MF, Tai KW, Chou MY. Mutation of p53 gene codon 63 in saliva as a molecular marker for oral squamous cell carcinoma. Oral Oncol. 2000;36:272–6.
107. Mattick JS. Non-coding RNAs: the architects of eukaryotic complexity. EMBO Rep. 2001;2:986–91.
108. Wong DT. Salivary extracellular noncoding RNA: emerging biomarkers for molecular diagnostics. Clin Ther. 2015;37:540–51.
109. Felekkis K, Touvana E. ChStefanou, and C deltas microRNAs: a newly described class of encoded molecules that play a role in health and disease. Hippokratia. 2010;14:236–40.
110. Tian X, Chen Z, Shi S, Wang X, Wang W, Li N, Wang J. Clinical diagnostic implications of body fluid MiRNA in oral squamous cell carcinoma: a meta-analysis. Medicine (Baltimore). 2015;94:e1324.
111. Park NJ, Zhou H, Elashoff D, Henson BS, Kastratovic DA, Abemayor E, Wong DT. Salivary microRNA: discovery, characterization, and clinical utility for oral cancer detection. Clin Cancer Res. 2009;15:5473–7.
112. Liu CJ, Lin SC, Yang CC, Cheng HW, Chang KW. Exploiting salivary miR-31 as a clinical biomarker of oral squamous cell carcinoma. Head Neck. 2012;34:219–24.
113. Liu CJ, Kao SY, Tu HF, Tsai MM, Chang KW, Lin SC. Increase of microRNA miR-31 level in plasma could be a potential marker of oral cancer. Oral Dis. 2010;16:360.
114. Zahran F, Ghalwash D, Shaker O, Al-Johani K, Scully C. Salivary microRNAs in oral cancer. Oral Dis. 2015;21:739–47.
115. Momen-Heravi F, Trachtenberg AJ, Kuo WP, Cheng YS. Genomewide study of salivary MicroRNAs for detection of oral Cancer. J Dent Res. 2014;93:86S–93S.
116. Jessica A. Weber, David H. Baxter, Shile Zhang, David Y. Huang, Kuo How Huang, Ming Jen Lee, et al. The MicroRNA spectrum in 12 body fluids. Clin Chem. 2010; 56: 1733–1741.
117. Qu S, Zhong Y, Shang R, Zhang X, Song W, Kjems J, Li H. The emerging landscape of circular RNA in life processes. RNA Biol. 2016 Aug;11:1–8.
118. Qu S, Yang X, Li X, Wang J, Gao Y, Shang R. Circular RNA: a new star of noncoding RNAs. Cancer Lett. 2015;365:141–8.
119. Zhang Y, Zhang XO, Chen T, Xiang JF, Yin QF, Xing YH, Zhu S, Yang L, Chen LL. Circular intronic long noncoding RNAs. Mol Cell. 2013;51:792–806.
120. Meng S, Zhou H, Feng Z, Zihao X, Tang Y, Li P, Minghua W. CircRNA: functions and properties of a novel potential biomarker for cancer. Mol Cancer. 2017;16:94.
121. Dudekula DB, Panda AC, Grammatikakis I, De S, Abdelmohsen K, Gorospe M. CircInteractome: A web tool for exploring circular RNAs and their interacting proteins and microRNAs. 2016; 13:34–42.
122. Wang F. Adil J Nazarali, Shaoping Ji. Circular RNAs as potential biomarkers for cancer diagnosis and therapy Am J Cancer Res. 2016;6:1167–76.
123. Jingqiu Li, Jie Yang, Ping Zhou, Yanping Le, Chengwei Zhou, Shaomin Wang, et al. Circular 44RNAs in cancer: novel insights into origins, properties, functions and implications. Am J Cancer Res. 2015; 5: 472–480.
124. Yu SY, Wang YP, Chang JY, Shen WR, Chen HM, Chiang CP. Increased expression of 44MCM5 is significantly associated with aggressive progression and poor prognosis of oral squamous cell carcinoma. J Oral Pathol Med. 2014;43:344–9.
125. Chen L, Zhang S, Wu J, Cui J, Zhong L, Zeng L, Ge S. circRNA_100290 plays a role in oral cancer by functioning as a sponge of the miR-29 family. Oncogene. 2017;36:4551–61.
126. Palanisamy V, Wong DT. Transcriptomic analyses of saliva. Methods Mol Biol. 2010;666:43–51.
127. Yoshizawa JM, Wong DTW. Salivary MicroRNAs and oral Cancer detection. Methods Mol Biol. 2013;936:313–24.

128. Abdulmajeed AA, Farah CS. Gene expression profiling for the purposes of biomarker discovery in oral potentially malignant lesions: a systematic review. Clin Med Insights Oncol. 2013;7:279–90.
129. Méndez E, Cheng C, Farwell DG, Ricks S, Agoff SN, Futran ND, et al. Transcriptional expression profiles of oral squamous cell carcinomas. Cancer. 2002;95:1482–94.
130. Maskos U, Southern EM. Oligonucleotide hybridizations on glass supports: a novel linker for oligonucleotide synthesis and hybridization properties of oligonucleotides synthesised in situ. Nucleic Acids Res. 1992;20:1679–84.
131. Li G, Li X, Yang M, Lvzi X, Deng S, Ran L. Prediction of biomarkers of oral squamous cell carcinoma using microarray technology. Sci Rep. 2017;7:42105.
132. Shalon D, Smith SJ, Brown PO. A DNA microarray system for analyzing complex DNA samples using two-color fluorescent probe hybridization. Genome Res. 1996;6:639–45.
133. Wu MY, Dai DQ, Zhang XF, Zhu Y. Cancer subtype discovery and biomarker identification via a new robust network clustering algorithm. PLoS One. 2013;8:e66256.
134. Golub TR, Slonim DK, Tamayo P, Huard C, Gaasenbeek M, Mesirov JP, et al. Molecular classification of cancer: class discovery and class prediction by gene expression monitoring. Science. 1999;286:531–7.
135. Kuo WP, Hasina R, Ohno-Machado L, Lingen MW. Classification and identification of genes associated with oral cancer based on gene expression profiles. A preliminary study. N Y State Dent J. 2003;69: 23–6.
136. Huang da W, Sherman BT, Lempicki RA. Systematic and integrative analysis of large gene lists using DAVID bioinformatics resources. Nat Protoc. 2009;4: 44–57.
137. Ramaswamy S, Tamayo P, Rifkin R, Mukherjee S, Yeang CH, Angelo M, et al. Multiclass cancer diagnosis using tumor gene expression signatures. Proc Natl Acad Sci U S A.
138. Heid CA, Stevens J, Livak KJ, Williams PM. Real time quantitative PCR. Genome Res. 1996;6:986–94.
139. Antonov J, Goldstein DR, Oberli A, Baltzer A, Pirotta M, Fleischmann A, et al. Reliable gene expression measurements from degraded RNA by quantitative real-time PCR depend on short amplicons and a proper normalization. Lab Investig. 2005;85:1040–50.
140. Wong ML, Medrano JF. Real-time PCR for mRNA quantitation. BioTechniques. 2005;39:75–85.
141. Livak KJ, Schmittgen TD. Analysis of relative gene expression data using real-time quantitative PCR and the 2(−Delta Delta C(T)) method. Methods. 2001;25:402–8.
142. Dhanasekaran S, Doherty TM, Kenneth J; TB Trials Study Group. Comparison of different standards for real-time PCR-based absolute quantification. J Immunol Methods. 2010;354:34–39.
143. Lin X, Lo H-C, Wong DTW, Xiao X. Noncoding RNAs in human saliva as potential disease biomarkers. Front Genet. 2015;6:175.
144. Bonne NJ, Wong DT. Salivarybiomarkerdevelop ment using genomic, proteomic and metabolomic approaches. Genome Med. 2012;4:82.
145. Shendure J. The beginning of the end for microarrays? Nat Methods. 2008;5:585.
146. Costa V, Aprile M, Esposito R, Ciccodicola A. RNA-Seq and human complex diseases: recent accomplishments and future perspectives. Eur J Hum Genet. 2013;21:134–42.
147. Danielson KM, Rubio R, Abderazzaq F, Das S, Wang YE. High throughput sequencing of extracellular RNA from human plasma. PLoS One. 2017;12:e0164644.
148. Majem B, Li F, Sun J, Wong DT. RNA sequencing analysis of salivary extracellular RNA. Methods Mol Biol. 2017;1537:17–36.
149. Steven R. Head, H. Kiyomi Komori, Sarah A. LaMere, Thomas Whisenant, Filip Van Nieuwerburgh, Daniel R. Salomon. Library construction for next-generation sequencing: Overviews and challenges. Biotechniques. 2014; 56: 61–passim.
150. Podnar J, Deiderick H, Huerta G, Hunicke-Smith S. Next-generation sequencing RNA-Seq library construction. Curr Protoc Mol Biol. 2014;106: 4.21.1–19.
151. Shore S, Henderson JM, Lebedev A, Salcedo MP, Zon G, McCaffrey AP, et al. Small RNA library preparation method for next-generation sequencing using chemical modifications to prevent adapter dimer formation. PLoS One. 2016;11:e0167009.
152. Ozsolak F, Milos PM. RNA sequencing: advances, challenges and opportunities. Nat Rev Genet. 2011;12:87–98.
153. Yuxuan Wang, Simeon Springer, Carolyn L. Mulvey, Natalie Silliman, Joy Schaefer, Mark Sausen, et al. Detection of somatic mutations and HPV in the saliva and plasma of patients with head and neck squamous cell carcinomas. Sci Transl Med. 2015; 7: 293ra104.
154. Chattopadhyay E, De Sarkar N, Singh R, Ray A, Roy R, Paul RR, et al. Genome-wide mitochondrial DNA sequence variations and lower expression of OXPHOS genes predict mitochondrial dysfunction in oral cancer tissue. Tumour Biol. 2016;37:11861–71.
155. Dasgupta S, Koch R, Westra WH, Califano JA, Ha PK, Sidransky D, et al. Mitochondrial DNA mutation in normal margins and tumors of recurrent head and neck squamous cell carcinoma patients. Cancer Prev Res (Phila). 2010;3:1205–11.
156. Jiang WW, Rosenbaum E, Mambo E, Zahurak M, Masayesva B, Carvalho AL, et al. Decreased mitochondrial DNA content in posttreatment salivary rinses from head and neck cancer patients. Clin Cancer Res. 2006;12:1564–9.
157. Hu L. XinyueYao, and Yi Shen. Altered mitochondrial DNA copy number contributes to human cancer

risk: evidence from an updated meta-analysis Sci Rep. 2016;6:35859.
158. Lin JC, Wang CC, Jiang RS, Wang WY, Liu SA. Impact of somatic mutations in the D-loop of mitochondrial DNA on the survival of oral squamous cell carcinoma patients. PLoS One. 2015;10:e0124322.
159. Mondal R, Ghosh SK. Accumulation of mutations over the complete mitochondrial genome in tobacco-related oral cancer from Northeast India. Mitochondrial DNA. 2013;24:432–9.
160. Lièvre A, Blons H, Houllier AM, Laccourreye O, Brasnu D, Beaune P, et al. Clinicopathological significance of mitochondrial D-loop mutations in head and neck carcinoma. Br J Cancer. 2006;94:692–7.
161. Fliss MS, Usadel H, Caballero OL, Wu L, Buta MR, Eleff SM, et al. Facile detection of mitochondrial DNA mutations in tumors and bodily fluids. Science. 2000;287:2017–9.
162. Mondal R, Ghosh SK, Choudhury JH, Seram A, Sinha K, Hussain M, et al. Mitochondrial DNA copy number and risk of oral Cancer: a report from Northeast India. PLoS One. 2013;8:e57771.
163. Chatterjee A, Dasgupta S, Sidransky D. Mitochondrial subversion in Cancer. CancerPrev Res (Phila). 2011;4:638–54.
164. Jiang WW, Masayesva B, Zahurak M, Carvalho AL, Rosenbaum E, Mambo E, et al. Increased mitochondrial DNA content in saliva associated with head and neck cancer. Clin Cancer Res. 2005;11: 2486–91.
165. Maitra A, Cohen Y, Gillespie SE, Mambo E, Fukushima N, Hoque MO, et al. The human MitoChip: a high-throughput sequencing microarray for mitochondrial mutation detection. Genome Res. 2004;14:812–9.
166. Marquis J, Lefebvre G, Kourmpetis YAI, Kassam M, Ronga F, De Marchi U, et al. MitoRS, a method for high throughput, sensitive, and accurate detection of mitochondrial DNA heteroplasmy. BMC Genomics. 2017;18:326.
167. Sukhija H, Krishnan R, Balachander N, Raghavendhar K, Ramadoss R, Sen S. C-deletion in exon 4 codon 63 of p53 gene as a molecular marker for oral squamous cell carcinoma: a preliminary study. Contemp Clin Dent. 2015;6:S227–34.
168. Sun W, Zaboli D, Liu Y, Arnaoutakis D, Khan T, Wang H, et al. Comparison of promoter Hypermethylation pattern in salivary rinses collected with and without an exfoliating brush from patients with HNSCC. PLoS One. 2012;7:e33642.
169. Righini CA, de Fraipont F, Timsit JF, Faure C, Brambilla E, Reyt E, et al. Tumor-specific methylation in saliva: a promising biomarker for early detection of head and neck cancer recurrence. Clin Cancer Res. 2007;13:1179–85.
170. Rosas SL, Koch W, da Costa Carvalho MG, Wu L, Califano J, Westra W, et al. Promoter hypermethylation patterns of p16, O6-methylguanine-DNA-methyltransferase, and death-associated protein kinase in tumors and saliva of head and neck cancer patients. Cancer Res. 2001;61:939–42.
171. Shaw RJ, Akufo-Tetteh EK, Risk JM, Field JK, Liloglou T. Methylation enrichment pyrosequencing: combining the specificity of MSP with validation by pyrosequencing. Nucleic Acids Res. 2006;34:e78.
172. Viet CT, Jordan RC, Schmidt BL. DNA promoter hypermethylation in saliva for the early diagnosis of oral cancer. J Calif Dent Assoc. 2007; 35: 844–9.
173. Dmitry A Ovchinnikov, Matthew A Cooper, Pratibala Pandit, William B Coman, Justin J Cooper-White, Patricia Keith, et al. Tumor-suppressor gene promoter hypermethylation in saliva of head and neck cancer patients. Transl Oncol. 2012; 5: 321–326.
174. Matthews AM, Kaur H, Dodd M, D'Souza J, Liloglou T, Shaw RJ, et al. Saliva collection methods for DNA biomarker analysis in oral cancer patients. Br J Oral Maxillofac Surg. 2013;51:394–8.
175. Boscolo-Rizzo P, Da Mosto MC, Rampazzo E, Giunco S, Del Mistro A, Menegaldo A, et al. Telomeres and telomerase in head and neck squamous cell carcinoma: from pathogenesis to clinical implications. Cancer Metastasis Rev. 2016;35:457–74.
176. Cunci L, Vargas MM, Cunci R, Gomez-Moreno R, Perez I, Baerga-Ortiz A, et al. Real-time detection of telomerase activity in Cancer cells using a label-free electrochemical Impedimetric biosensing microchip. RSC Adv. 2014;4:52357–65.
177. Califano J, Ahrendt SA, Meininger G, Westra WH, Koch WM, Sidransky D. Detection of telomerase activity in oral rinses from head and neck squamous cell carcinoma patients. Cancer Res. 1996;56:5720–2.
178. Hess JL, Highsmith WE Jr. Telomerase detection in body fluids. Clin Chem. 2002;48:18–24.
179. Zuo X, Xia F, Patterson A, Soh HT, Xiao Y, Plaxco KW. Two-step, PCR-free telomerase detection by using exonuclease III-aided target recycling. Chembiochem. 2011;12:2745–7.
180. Wang HB, Wu S, Chu X, Yu RQ. A sensitive fluorescence strategy for telomerase detection in cancer cells based on T7 exonuclease-assisted target recycling amplification. ChemCommun (Camb). 2012;48:5916–8.
181. Liu X, Li W, Hou T, Dong S, Yu G, Li F. Homogeneous electrochemical strategy for human telomerase activity assay at single-cell level based on T7 exonuclease-aided target recycling amplification. Anal Chem. 2015;87:4030–6.
182. Chaudhary AK, Pandya S, Mehrotra R, Bharti AC, Singh M, Singh M. Comparative study between the hybrid capture II test and PCR based assay for the detection of human papillomavirus DNA in oral submucous fibrosis and oral squamous cell carcinoma. Virol J. 2010;7:253.
183. Gichki AS, Buajeeb W, Doungudomdacha S, Khovidhunkit SO. Detection of human papillomavirus in normal oral cavity in a group of Pakistani

subjects using real-time PCR. Asian Pac J Cancer Prev. 2012;13:2299–304.

184. Tsiodras S, Georgoulakis J, Chranioti A, Voulgaris Z, Psyrri A, Tsivilika A, et al. Hybrid capture vs. PCR screening of cervical human papilloma virus infections. Cytological and histological associations in 1270 women. BMC Cancer. 2010;10:53.
185. Lin CY, Li L. Comparison of DNA testing strategies in monitoring human papillomavirus infection prevalence through simulation. BMC Infect Dis. 2016;16:642.
186. Geraets DT, Cuschieri K, de Koning MNC, van Doorn LJ, Snijders PJF, Meijer CJLM, et al. Clinical evaluation of a GP5+/6+-based Luminex assay having full high-risk human papillomavirus genotyping capability and an internal control. J Clin Microbiol. 2014;52:3996–4002.
187. David J. Beale, Oliver A. H. Jones, Avinash V. Karpe, Saravanan Dayalan, Ding Yuan Oh, Konstantinos A. Kouremenos, et al. A review of analytical techniques and their application in disease diagnosis in Breathomics and Salivaomics research. Int J Mol Sci 2017; 18: 24.
188. Ishikawa S, Sugimoto M, Kitabatake K, Sugano A, Nakamura M, Kaneko M, et al. Identification of salivary metabolomic biomarkers for oral cancer screening. Sci Rep. 2016;6:31520.
189. Ogawa T, Washio J, Takahashi T, Echigo S, Takahashi N. Glucose and glutamine metabolism in oral squamous cell carcinoma: insight from a quantitative metabolomic approach. Oral Surg Oral Med OralPathol Oral Radiol. 2014;118:218–25.
190. Sandulache VC, Ow TJ, Pickering CR, Frederick MJ, Zhou G, Fokt I, et al. Glucose, not glutamine, is the dominant energy source required for proliferation and survival of head and neck squamous carcinoma cells. Cancer. 2011;117:2926–38.
191. Wang Q, Gao P, Wang X, Duan Y. Investigation and identification of potential biomarkers in human saliva for the early diagnosis of oral squamous cell carcinoma. ClinChim Acta. 2014;427:79–85.
192. Wang Q, Gao P, Cheng F, Wang X, Duan Y. Measurement of salivary metabolite biomarkers for early monitoring of oral cancer with ultra performance liquid chromatography-mass spectrometry. Talanta. 2014;119:299–305.
193. Chiang PK, Gordon RK, Tal J, Zeng GC, Doctor BP, Pardhasaradhi K, McCann PP. S-Adenosylmethionine and methylation. FASEB J. 1996;10:471–80.
194. Iwata S, Sato Y, Asada M, Takagi M, Tsujimoto A, Inaba T, et al. Anti-tumor activity of antizyme which targets the ornithine decarboxylase (ODC) required for cell growth and transformation. Oncogene. 1999;18:165–72.
195. Katakwar P, Metgud R, Naik S, Mittal R. Oxidative stress marker in oral cancer: a review. J Cancer Res Ther. 2016;12:438–46.
196. Reznick AZ, Hershkovich O, Nagler RM. Saliva--a pivotal player in the pathogenesis of oropharyngeal cancer. Br J Cancer. 2004;91:111–8.
197. Shpitzer T, Hamzany Y, Bahar G, Feinmesser R, Savulescu D, Borovoi I, et al. Salivary analysis of oral cancer biomarkers. Br J Cancer. 2009;101:1194–8.
198. Khoubnasabjafari M, Ansarin K, Jouyban A. Salivary malondialdehyde as an oxidative stress biomarker in oral and systemic diseases. J Dent Res Dent Clin Dent Prospects. 2016 Spring;10:71–4.
199. Chole RH, Patil RN, Basak A, Palandurkar K, Bhowate R. Estimation of serum malondialdehyde in oral cancer and precancer and its association with healthy individuals, gender, alcohol, and tobaccoabuse. J Cancer Res Ther. 2010;6:487–91.
200. Shetty SR, Babu S, Kumari S, Shetty P, Hegde S, Castelino R. Status of salivary lipid peroxidation in oral cancer and precancer. Indian J Med Paediatr Oncol. 2014;35:156–8.
201. Peluso I, Raguzzini A. Salivary and urinary Total antioxidant capacity as biomarkers of oxidative stress in humans. Patholog Res Int. 2016;2016:5480267.
202. Kaur J, Politis C, Jacobs R. Salivary 8-hydroxy-2-deoxyguanosine, malondialdehyde, vitamin C, and vitamin E in oral pre-cancer and cancer: diagnostic value and free radical mechanism of action. Clin Oral Investig. 2016;20:315–9.
203. Zhang Y, Sun J, Lin CC, Abemayor E, Wang MB, Wong DT. The emerging landscape of salivary diagnostics. Oral Health Dent Manag. 2014;13:200–10.
204. Mager DL, Haffajee AD, Devlin PM, Norris CM, Posner MR, Goodson JM. The salivary microbiota as a diagnostic indicator of oral cancer: a descriptive, non-randomized study of cancer-free and oral squamous cell carcinoma subjects. J Transl Med. 2005;3:27.
205. Pushalkar S, Mane SP, Ji X, Li Y, Evans C, Crasta OR, et al. Microbial diversity in saliva of oral squamous cell carcinoma. FEMS Immunol Med Microbiol. 2011;61:269–77.
206. Pushalkar S, Ji X, Li Y, Estilo C, Yegnanarayana R, Singh B, et al. Comparison of oral microbiota in tumor and non-tumor tissues of patients with oral squamous cell carcinoma. BMC Microbiol. 2012;12:144.
207. Guerrero-Preston R, Godoy-Vitorino F, Jedlicka A, Rodríguez-Hilario A, González H, Bondy J, et al. 16S rRNA amplicon sequencing identifies microbiota associated with oral cancer, human papilloma virus infection and surgical treatment. Oncotarget. 2016;7:51320–34.
208. Hu X, Zhang Q, Hua H, Chen F. Changes in the salivary microbiota of oral leukoplakia and oral cancer. Oral Oncol. 2016;56:e6–8.
209. Schmidt BL, Kuczynski J, Bhattacharya A, Huey B, Corby PM, Queiroz EL, et al. Changes in abundance of oral microbiota associated with oral cancer. PLoS One. 2014;9:e98741.
210. Hooper SJ, Crean SJ, Fardy MJ, Lewis MA, Spratt DA, Wade WG, et al. A molecular analysis of the bacteria present within oral squamous cell carcinoma. J Med Microbiol. 2007;56:1651–9.

211. Błoniarz J, Rahnama M, Zareba S. Influence of carcinogenesis in the oral cavity on the level of some bioelements in the saliva. Rocz PanstwZakl Hig. 2003;54:295–300.
212. Dziewulska A, Janiszewska-Olszowska J, Bachanek T, Grocholewicz K. Salivary mineral composition in patients with oral cancer. Magnes Res. 2013;26: 120–4.
213. Fuchs PN, Rogić D, Vidović-Juras D, Susić M, Milenović A, Brailo V, et al. Salivary analytes in patients with oral squamous cell carcinoma. Coll Antropol. 2011;35:359–62.
214. Zhang S, Zhang X, Yin K, Li T, BaoY, Chen Z. Variation and significance of secretory immunoglobulin A, interleukin 6 and dendritic cells in oral cancer. Oncol Lett. 2017; 13:2297–2303.
215. Johansen FE, Braathen R, Brandtzaeg P. Role of J chain in secretory immunoglobulin formation. Scand J Immunol. 2000;52:240–8.
216. Farhad Mollashahi L, Honarmand M, Nakhaee A, Mollashahi G. Salivary Sialic acid levels in smokeless tobacco users. Int J High Risk Behav Addict. 2016;5:e27969.
217. Kurtul N, Gökpınar E. Salivary lipid peroxidation and total sialic acid levels in smokers and smokeless tobacco users as Maraş powder. Mediat Inflamm 2012;2012:619293.
218. Vajaria BN, Patel KR, Begum R, Shah FD, Patel JB, Shukla SN, et al. Evaluation of serum and salivary total sialic acid and α-l-fucosidase in patients with oral precancerous conditions and oral cancer. Oral Surg Oral Med Oral Pathol Oral Radiol. 2013;115:764–71.
219. Chaudhari V, Pradeep GL, Prakash N, Mahajan AM. Estimation of salivary sialic acid in oral premalignancy and oral squamous cell carcinoma. Contemp Clin Dent. 2016;7:451–6.
220. Winck FV, Prado Ribeiro AC, Ramos Domingues R, Ling LY, Riaño-Pachón DM, Rivera C, et al. Insights into immune responses in oral cancer through proteomic analysis of saliva and salivary extracellular vesicles. Sci Rep. 2015;5:16305.
221. Al-Nedawi K, Meehan B, Micallef J, Lhotak V, May L, Guha A, et al. Intercellular transfer of the oncogenic receptor EGFRvIII by microvesicles derived from tumour cells. Nat Cell Biol. 2008;10:619–24.
222. Palanisamy V, Sharma S, Deshpande A, Zhou H, Gimzewski J, Wong DT. Nanostructural and transcriptomic analyses of human saliva derived exosomes. PLoS One. 2010;5:e8577.
223. Sharma S, Rasool HI, Palanisamy V, Mathisen C, Schmidt M, Wong DT, et al. Structural- mechanical characterization of nanoparticles-Exosomes in human saliva, using correlative AFM, FESEM and force spectroscopy. ACS Nano. 2010;4:1921–6.
224. Sun Y, Xia Z, Shang Z, Sun K, Niu X, Qian L, et al. Facile preparation of salivary extracellular vesicles for cancer proteomics. Sci Rep. 2016;6:24669.
225. Chiang SH, Thomas GA, Liao W, Grogan T, Buck RL, Fuentes L, et al. RNAPro•SAL: a device for rapid and standardized collection of saliva RNA and proteins. Biotechniques. 2015; 58: 69–76.
226. Al-Tarawneh SK, Border MB, Dibble CF, Bencharit S. Defining salivary biomarkers using mass spectrometry-based proteomics: a systematic review. OMICS. 2011;15:353–61.
227. Stuani VT, Rubira CM, Sant'Ana AC, Santos PS. Salivary biomarkers as tools for oral squamous cell carcinoma diagnosis: a systematic review. Head Neck. 2017;39:797–811.
228. Lu R, Zhang J, Sun W, Du G, Zhou G. Inflammation-related cytokines in oral lichen planus: an overview. J Oral Pathol Med. 2015;44:1–14.
229. Lisa Cheng YS, Jordan L, Gorugantula LM, Schneiderman E, Chen HS, Rees T. Salivary interleukin-6 and -8 in patients with oral cancer and patients with chronic oral inflammatory diseases. J Periodontol. 2014;85:956–65.

15 Saliva-Based Point-of-Care in Oral Cancer Detection: Current Trend and Future Opportunities

Prashanth Panta and David T. W. Wong

Abstract

Development of point-of-care (POC) for saliva-based, noninvasive detection of OSCC is an active area of research. Portable and easy-to-use biomedical devices and advanced electrochemical platforms (*OFNASET)* or simple paper-strip chromatography (e.g., *OncAlert*®), based on a single or a panel of salivary biomarkers, are already available for clinical use. In this chapter, the emerging core technologies and approaches assisting early POC detection are discussed. Knowledge from closely related fields like nanotechnology is also summarized to provide insight on possible future approaches that can be tailored for oral cancer detection. POC for oral cancer can be designed to work on a potential biomarker candidate (validated in multi-cohort and multiethnic studies) among the wide range of 100 signature analytes from proteins to RNA, cytomorphometry of exfoliated cells in saliva (analogous to circulating tumor cells in plasma), or through high-throughput screening of salivary exosomes for potential signatures. Surface-enhanced Raman scattering (SERS) was also used as a saliva assay previously, and such attempts will evolve significantly if saliva samples are mucin-free. ELISA is a common method for low-cost protein detection, with great POC potential. Its performance can be optimized through bead and nanoparticle technology. Sophisticated Luminex multi-analyte profiling (xMAP) technology and metal-linked immunosorbent assay (MeLISA), based on ELISA and biocatalytic ability of enzymes, were already reported with high sensitivity and specificity, which can be extrapolated to saliva samples. Some technologies have also assisted detection of mutations, such as "electric field-induced release and measurement" (EFIRM) recently deployed for identification of EGFR mutations through saliva samples. In this chapter, we have narrated the current trend and future opportunities for POC development in saliva-based oral cancer detection.

P. Panta, MDS (✉)
Department of Oral Medicine and Radiology, MNR Dental College and Hospital, Sangareddy, Telangana, India
e-mail: maithreya.prashanth@gmail.com

D. T. W. Wong, DMD, DMSc
Center for Oral/Head and Neck Oncology Research, School of Dentistry, University of California Los Angeles, Los Angeles, CA, USA

Jonsson Comprehensive Cancer Center, University of California Los Angeles, Los Angeles, CA, USA

Head and Neck Surgery/Otolaryngology, David Geffen School of Medicine, University of California Los Angeles, Los Angeles, CA, USA

School of Engineering and Applied Science, University of California Los Angeles, Los Angeles, CA, USA
e-mail: dtww@ucla.edu

P. Panta (ed.), *Oral Cancer Detection*, https://doi.org/10.1007/978-3-319-61255-3_15

15.1 Point-of-Care

Early findings in saliva diagnostics have initiated a series of research grants by the National Institute of Dental and Craniofacial Research (NIDCR) and the UCLA Collaborative Oral Fluid Diagnostic Research Center aiming to develop saliva-based point-of-care platforms [1, 2]. The program "Development and Validation Technologies for Saliva Based Diagnostics" funded by NIDCR involved seven research teams in different disease domains, one dedicated entirely to oral cancer led by Prof. David Wong (UCLA) [3].

Today, several point-of-care (POC) platforms for saliva based detection of HIV, hepatitis C (oraquick ADVANCE®, oraquick®-OraSure technologies) and HPVvirus (OraRisk®- Oral DNA labs), steroids like cortisol (sailometrics®), alpha-amylase (Nipro), and alcohol and drugs (Oral-Eze®- quest diagnostics) are already available [4]. The possibility of POC for OSCC detection was identified very early in research and devices based on electrochemical sensors (OFNASET®) and also comparatively simple kits based on lateral chromatography came into being. POC systems are often integrated systems incorporating technology on a small structure (miniaturization). The terms 'lab-on-chip' or more recently 'lab-on-paper' applies to such a technology. The principal technologies used in POC saliva testing include microfluidics, Immunoassays, Micromechanical and Electrochemical sensors, and nanotechnology based methods; the POC system can be dominant with one technology or may be integrated.

The POC platforms for saliva should work on small volumes with very low analyte concentration. Simplified saliva collection, detection, user interface and data presentation are essential for designing POCs for oral cancer. The preliminary step however is to collect saliva from patients which is a critical step. These platforms must provide biomarker information and diagnosis at home or chairside or bedside. With such tools, 'mass screening' can be conducted, leading to early oral cancer detection and control of mortality and morbidity at nation scale [5].

15.2 Emerging Core Platforms in Point-of-Care

Advancements in microfluidics, immunoassays, micromechanical and electrochemical detection, and bead- and nanoparticle-based technology benefit fabrication of POC diagnostics. The developments in microfluidics and plumbing have led to improved efficiency in transfer of saliva sample and economical automation for analysis of cellular features. The second advance is the development of electronic transducers, which can be combined onto microfluidics. The most recent advance is the use of nanoparticles in the detection of oral cancer, as they can increase the signal to noise ratio. In the electrochemical systems, the sensitivity can be highly challenged by the high molecular weight mucins which compete with the surface of the transducers. The technologies should often be perfectly integrated with each other to produce a fully functional POC device like OFNASET. The performance of POC is usually tested by serial dilutions of biomarker of interest to the desired serum or saliva concentrations in OSCC patients and validated on patient samples. Although some POCs were not directly tested in saliva of OSCC patients, data about performance of these platforms is obtained from centrifuged culture media where cell lines were grown, which is actually representative of saliva [6, 7].

15.2.1 Microfluidics

Microfluidics is handling fluids at micro- or nanoliter scale. Microfluidics fabricated through injection micromolding plastics creates a fine nozzle diameter at micron scale (~ 1/4 thickness of human hair), taking the advantage of the principle of capillarity, simplifying the fluid components in POC. The advent of i-STAT system revolutionized microfluidics into credit card-shaped chips (lab-on-chip) for detection. They can be instrumented or un-instrumented. The instrumented device has a disposable cassette housing a circuit, reaction chambers, interconnecting channels, necessary reagents, and analyzer. The main advantage of microfluidics is the use of less sample, less time, automation, low reagent expenditure, and excellent flow control. Apart from achievement of strict laminar flow, parallel processing of multiple solutions can be attempted [8]. Initially, microfluidic devices were made of plastics, elastomers, but today paper microfluidics are emerging platforms. Microfluidics have reached multistep, complex laboratory techniques like PCR and electrophoresis. A microfluidic PCR platform can have two configurations: a stationary and flow through. For OSCC diagnosis, integrated electrophoresis-based microfluidic platforms hold more promise than PCR-based platforms, as protein biomarker estimation is more important than genetic screening. Protein biomarker screening can also be conducted on microfluidics with many parallel lanes or channels.

Microfluidics are two-decade-old and ventured in cancer detection in distinct ways including exosome separation and mutation analysis, cancer cytology (i.e., isolation of circulating tumor cells, characterization of tumor cells, and study of tumor migration and metastatic process), and for high-throughput molecular profiling of body fluid (e.g., protein quantification) with nanoparticle technology [9, 10]. The most potential application of microfluidic assembly in OSCC however is the molecular examination of OSCC cells from scrapings of suspected oral lesions and through saliva.

- Microfluidics can also be used in the separation of microvesicles (exosomes), through a functionalized surface [11]. The exosomes rich in RNA and other biomarkers indicate the biochemical status of tumors and are highly informative [11]. Microfluidic platforms were also used in genetic analysis to detect *JAK2-V617F* oncogenic mutations in myeloproliferative neoplasms via patient whole blood, with high accuracy and time efficiency (<1 h) [12]. This system can be extrapolated to detection of mutation in saliva. The functions performed by Wang et al. are genomic DNA isolation, nucleic acid amplification, and visual detection of identified mutations [12].
- "Nano-biochips" and "cytology on chip" are also available for oral cancer detection. This advanced detection format integrates simple microfluidic assembly with immunohistochemistry and fluorescence microscopy imaging for sensing atypical cellular and cell surface features with simple liquid biopsy, oral cytology, or oral rinse. Liquid biopsy is superior to conventional cytology in terms of blood and sample adequacy for studying cell morphology [13–15]. McDevitt et al. (Rice University, Houston, TX) reported a novel cytology-sensor-chip for oral cancer [16, 17]. It detects premalignant and malignant cells based on nuclear-cytoplasmic (N/C) ratio and through the quantification of oral cancer biomarker epidermal growth factor receptor (EGFR). The cytology suspension is channeled via a pressure-driven microfluidic flow to the sensor. Here, cells larger than the defined pore size of the filtering membrane are retained. The cells captured are stained by fluorescent dyes and immuno-reagents against cytoplasm (staining with phalloidin – red color) and nucleus (4′-6-diamidino-2-phenylindole: DAPI blue) and surface marker EGFR in green (Alexa Fluor®488). The stained cells are visualized under 3D fluorescent microscope, and an automated image analysis is conducted through an open-source software, aiming to assess the OSCC signatures related to cellular morphology and surface biomarker expression. This study was conducted on 52 OSCC and healthy samples and yielded a good test result showing steady increase in nuclear size, nuclear-cytoplasmic ratio, and the intensity of emission of EGFR from normal (6.5 arbitrary units) to premalignancy (9.5 arbitrary units) to OSCC (11.8 arbitrary units) showing highest [16]. The N/C ratio and nuclear area showed best performance (AUC = 0.93) and EGFR an AUC of 0.83 [16]. Their combined panel showed much superior discrimination (AUC = 0.94) of OSCC [16]. In initial cell-based sensor studies carried out by McDevitt et al., EGFR expression analysis was identified as a potential change in oral cancer cell lines [17]; later the same group incorpo-

rated cytomorphometric parameters into the detection panel [16, 18]. Moreover, EGFR-based assays consume little time and are highly productive as this surface marker shows strong expression in early and aggressive cancer phenotypes [16–18]. According to a recent, large population-based exhaustive cytology analysis by the same group, the signature cytological parameters in OSCC detection were cell circularity, nuclear area, cell area, and nuclear-cytoplasmic ratio, and important biomarkers were EGFR and Ki-67 [19].

Several nanostructured microfluidic platforms using glutathione gold nanoparticles are emerging for the simultaneous ultrasensitive detection of several cancer biomarker proteins including IL-6 and IL-8 from the attempts of Rusling et al. [6]. The "lab-on-chip" format is slowly being replaced by "lab on paper or lab on stamp" which consists of chromatographic paper, wax, and filter [20]. Paper-based microfluidics are low-cost, lightweight, and disposable technology and the future of microfluidics [21].

15.2.2 Immunodetection

15.2.2.1 Enzyme-Linked Immunosorbent Assay (ELISA)

ELISA is common in the laboratory setting for the detection of proteins without much cost, suitable for low-resource and developing countries [22]. In a regular lab-based ELISA, several time-consuming steps (~6 h) are involved including a final stage spectrometry detection of compounds based on color intensity [23]. The limit of detection (LOD) of ELISA is in the range of 1picomolar (1 pg/ml) [24]. The adaptation of the same method in POC would be running an unknown sample on a special surface functionalized with antibodies, later acted by antibodies linked to enzymes emitting a signal of measurable intensity. ELISA-based POC is somewhat challenging due to the efforts required to minimize the larger number of steps involved. Paper-based ELISA was reported for α-fetoprotein, cancer antigen 125, and carcinoembryonic antigen, potential saliva markers in OSCC [25, 26]. A sophisticated Luminex multi-analyte profiling (xMAP) technology (Luminex Corp., USA) combining bead technology (50–100; 5.6 micron polystyrene beads) and flow cytometry is being used for monoplexed or multiplexed detection (500 analytes) of proteins, nucleic acid biomarkers, virus, and microbiota. In principle, it is similar to ELISA, but in performance, it is sensitive to much lower concentrations of analyte, in the range of few pg/ml with around 25–50 μl sample volume [27–30]. The antibodies are immobilized onto the beads, but unlike ELISA, nonspecific binding is greatly minimized [27, 30]. ELISA assay can also be converted into a Luminex xMAP platform [30]. With metal-linked immunosorbent assay (MeLISA), based on a combination of ELISA, antibody-antigen reaction, and biocatalytic ability of enzymes, the sensitivity and specificity of detecting PSA in serum reached 100% [31]. The performance of ELISA can be optimized using bead and nanoparticle technology [23, 30]. The complementation of nanoparticles with ELISA can minimize the problem connected to analysis instrumentation, making feasibility of image analysis with Android-based digital cameras [23]. It is difficult to multiplex ELISA [32].

15.2.2.2 Lateral Chromatography (LF) Test

An example of a simple LF test is the home pregnancy detection strip. The lateral flow test, also referred to as immune-chromatographic flow test, is a simple and inexpensive technique that can be built on a porous paper like material, nitrocellulose. There are few test lines for multiplexed detection and a control line as reference, and on the test line, antibodies are immobilized against a known target molecule. The sample is mixed with buffer and applied to one end of the test line, where sample is sucked through capillary action. The test result can be reported using the naked eye, and flow of specimen is not assisted by any micro motor or pumps. Gold or carbon nanoparticles can be used as reporters for visible detection [33]. The important difference between ELISA and LF is the lack of signal amplification in LF, leading to low sensitivity and specificity. A LT test that operates on the detection of salivary CD44sol is available (OncAlert® – Vigilant Biosciences). A lateral flow immunoassay test has also been used for detecting exosomes, based on nanoparticle detection probes, by capturing antibodies immobilized on nitrocellulose base [35]. Through this approach, exosomes in human plasma have been detected by the naked eye, at concentrations of 5 µg [35].

15.2.3 MEMS-/NEMS-Based Electrochemical Detection

Microelectromechanical system (MEMS) or nanoelectromechanical systems (NEMS) are integrated systems that have a central microprocessor and components connected to microsensors. To develop a POC based on this technology, a team of clinicians and nano-mechanical engineers is required. The oral fluid nano-sensor test (OFNASET) is an ideal example of oral cancer screening tool that is a MEMS-based electrochemical system, without ELISA, PCR, pumps, or valves. The visionary investment of NIDCR has initiated saliva microfluidics, and "OFNASET" is one product that emerged through this project. OFNASET is a handheld probe, an integrated system with cutting-edge technology enabling the rapid detection of proteins and mRNA, for early disease detection including oral cancer [4, 36]. The LOD for RNA is 1 fM/mland; for protein it is 1 pg/mL with multiplexed detection in less than 20 min, with 90% accuracy (http://hspp.dent.ucla.edu/OFNASET.htm). Under multiplexing model, the LOD of IL8-mRNA reaches 3.9 fM and IL-8 protein 7.4 pg/ml (Fig. 15.1) [37]. This platform developed by UCLA is a fully functional electrochemical platform that allows sample collection, processing, and multiplexed determination of proteomic, transcriptomic, and genomic biomarkers including telomerase [38]. It is capable of measuring up to eight biomarkers and was introduced in a cohort of Indian patients with accuracy comparable to traditional laboratory methods (ELISA and PCR) [38].

In 2009, an electrochemical detection technique termed 'electric field-induced release and measurement' (EFIRM) was deployed [2, 37]. It uses an array of probes and read out enzymes to capture saliva biomarkers [37]. EFIRM was first applied in oral cancer detection, by the collaborative efforts of UCLA schools of dentistry and engineering [37]. EFIRM has also shown much promise in other cancer models like lung malignancy with an, extremely high accuracy (AUC=1),

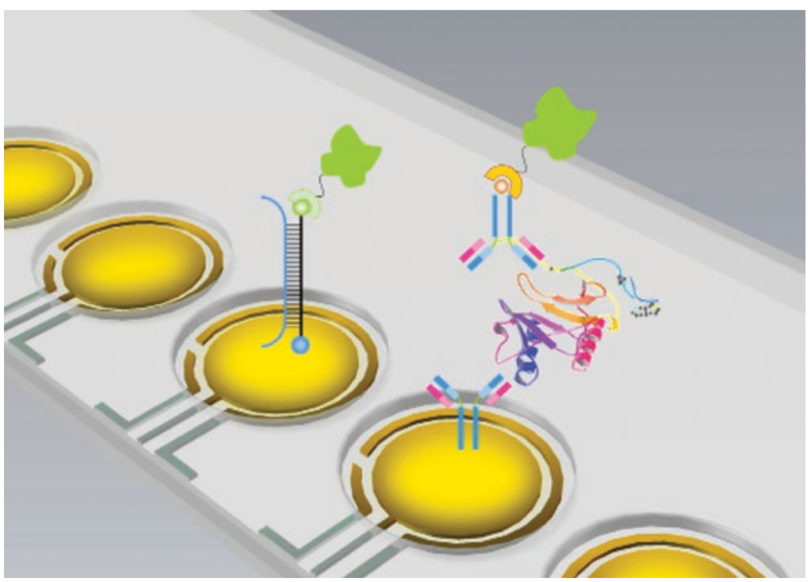

Fig. 15.1 Schematic of an electro-chemical sensor strategy for multiple salivary biomarker detection reported in 2009. An array of electrodes with both mRNA (left) and protein (right) detection are shown. *Reprinted with permission from (Wei et al. Electrochemical Sensor for Multiplex Biomarkers Detection. Clin Cancer Res. 2009; 15: 4446–4452. Copyright (2009) American Association for Cancer Research*

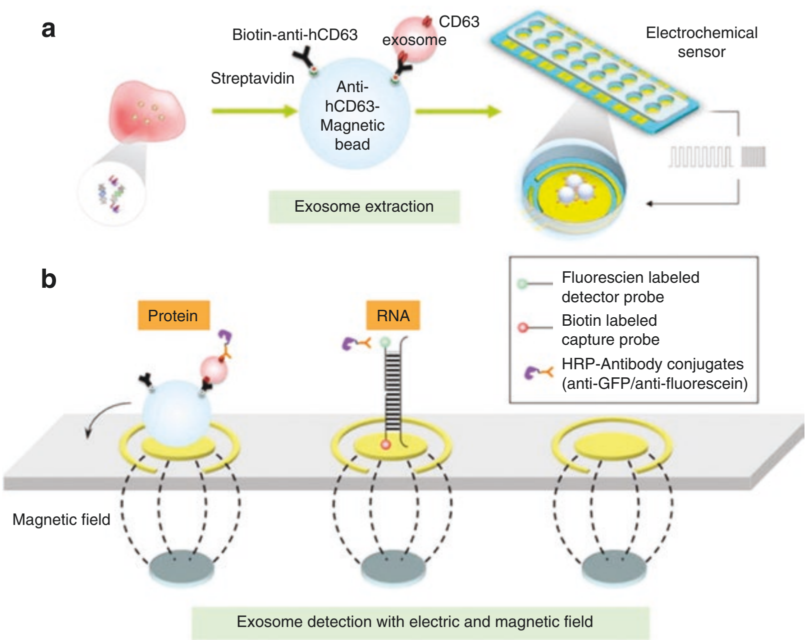

Fig. 15.2 Schematic of the electric field-induced release and measurement (EFIRM) system for detection of exosomal biomarker. (**a**) Anti-hCD63 antibodies conjugation and exosome extraction; (**b**) magnetic force assisted exosome extraction and electric field induced release. *Reprinted from Biosens Bioelectron, volume 44, Wei et al.* Detection of exosomal biomarker by electric field-induced release and measurement (EFIRM), *page 115-121, copyright (2013) with permission from Elsevier*

based on screening of EGFR mutations (Figs. 15.2 and 15.3) [39–41]. EGFR mutations are also universal to in epithelial malignancies like OSCC. EFIRM has also been applied around the same time for the identification of tumor specific exosome like microvesicles in saliva [42, 43]. They can be used to extract exosomes through magnetic particles from biofluids like saliva, to test the composition of their cargo (Fig. 15.2) [43]. EFIRM is an easy to use, real time, cost-effective platform for cancer detection [39]. This test can be carried out with a minimal sample size of <200 μL of saliva or plasma and can generate results in less than 30 min [41]. An electrochemical sensor technology using endonuclease target recycling amplification was also used to identify DNA of oral cancer overexpressed 1 (OLAOV1) in saliva of oral cancer patients (Figs. 15.3 and 15.4) [44]. Recently for detection of saliva metabolite: uric acid and lactic acid, a mouth-guard enzymatic biosensor was used with wireless electronics [2, 45, 46]. Thin-film Au/ZnO surface plasmon resonance-biosensors were used in evaluation of salivary CA-125, an important tumor antigen in OSCC, as its LOD falls around the salivary cutoff point (4U/mL) of cancer patients [47]. Electrochemical sensors enriched with nanoparticles and carbon nanotube assembly were used as ultrasensitive platforms for inflammatory markers IL-6, IL-8 [6, 7]; the single wall nanotube forests were shown to be more sensitive, but linear range was higher with the gold nanoparticle immunosensor [48]. Semiconductor based silicon nanowire field-effect transistor biosensors (SiNW-FET) were used for multiplexed detection of IL-8, and tumor necrosis factor α (TNF-α), CRP, important biomarkers in OSCC [49, 50]. The advantages beinglow LOD, and specific recognition [49, 50]. An electrochemical immunosensor was also reported for IL-6 with Carbon Nanotube Forest Electrodes and Multilabel Amplification [32]. Similar electrochemical strategies have been useful for telomerase detection, a potential marker in OSCC [51–53].

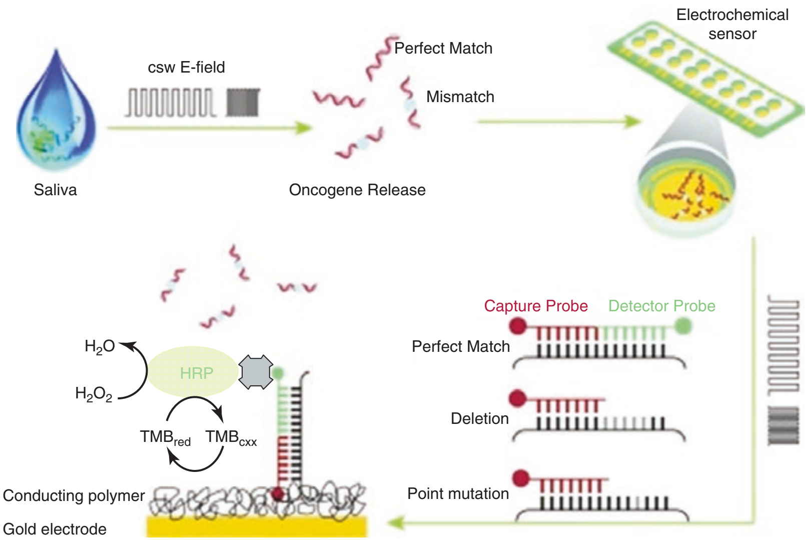

Fig. 15.3 Illustration depicting an advanced version of Electric field-induced release and measurement (EFIRM) technology for the detection of mutations (epidermal growth factor receptor) in bodily fluids like saliva. The cyclic-square wave of the electrical field (csw E-field) is applied to release and detect the mutations. *EGFR* sequences were measured on the electrochemical sensor with a capture probe pre-coated in conducting polymer. The horseradish peroxidase (HRP)-labeled reporter probe generated amperometric signals when there was a reaction with the 3, 3′, 5, 5′-tetra-methylbenzidine (TMB) substrate under a −200 mV electrical field. *Reprinted with permission from the American Thoracic Society. Copyright (2014). American Thoracic Society. Wei et al./(2014)/ Noninvasive saliva-based EGFR gene mutation detection in patients with lung cancer/Am J Respir Crit Care Med/190/1117–26*

15.2.3.1 Future Biofluid Diagnosis Powered by Nanoparticles: Basic Principles and Applications

Nanoparticles synthesized from inert metals like gold and silver, and nanotubes made from carbon, can act as powerful molecular and optical sensors in the detection of disease biomarkers. Gold nanoparticles (AuNPs) can be synthesized into various sizes (1–100 nm) and shapes [54]. Their synthesis is easy, and size depends on salt concentration, temperature, and rate at which reactants are added and has been designed into various shapes: hexagon and boot, with unique surface-enhanced Raman scattering properties [55]. Small size, variable shape, and facile surface chemistry, i.e., ability to be manipulated by any functional group (amine, thiol, cyano, carboxyl, or chloro) through electrostatic, covalent, or hydrophobic interactions, are important features of AuNPs [56]. For detection of biomarkers, the AuNPs are often conjugated with antibodies (anti-EGFR) or oligonucleotides or anti-mouse immunoglobulin antibodies [56–58]. The surface of AuNPs is negatively charged which aids in the simple mixing and conjugation through simple electrostatic interactions with positively charged moieties. They are small enough to scatter light, and particle size and the interparticle distance correlate directly to their color [55]. The ligand and carrier molecule used for conjugation depend on the type of application, whether diagnostic or therapeutic. Once the particle has the appropriate functional group on the surface, coupling agents may be utilized to covalently link bio-recognition molecules with good efficiency; coupled NPs can be stored at 4 °C [57].

Nanoparticles enrich microfluidics, immunoassays, and electrochemical platforms to POC flexibility [6, 7, 48, 59]. The extremely small size and high surface area of AuNPs enhance Raman scattering via surface-enhanced Raman scattering (SERS) and localized surface plasmon resonance (LSPR), and their suspension and aggregation can cause visible color changes that can be studied through colorimetry and fluorescence,

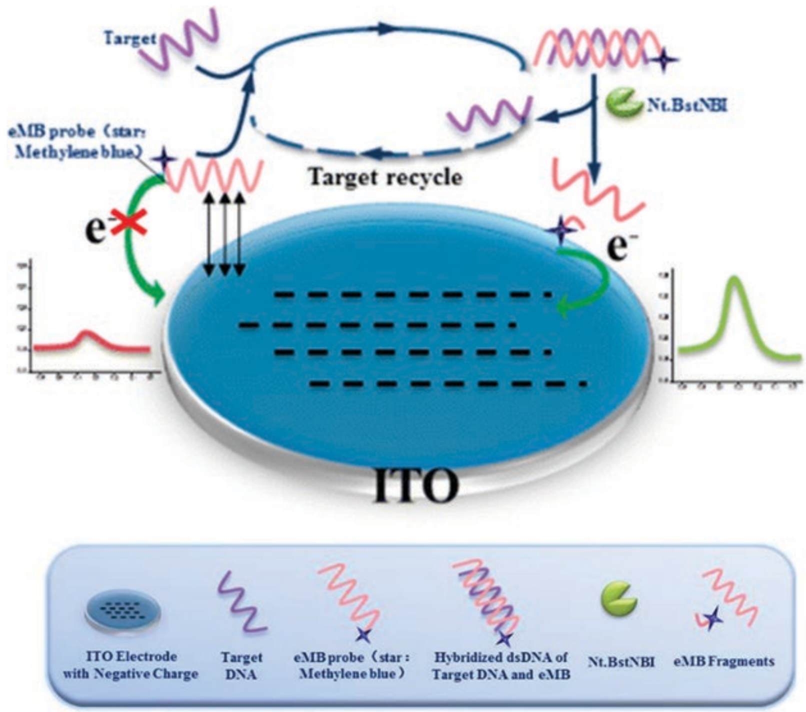

Fig. 15.4 Schematic of an ultrasensitive electro-chemical sensor for detection of salivary DNA in oral cancer (targeted for oral cancer overexpressed 1). This strategy combines signal amplification of nicking endonuclease assisted target recycling with the immobilization-free electrochemical method. *Reprinted with permission from (Tan et al. Ultraselective homogeneous electrochemical biosensor for DNA species related to oral cancer based on nicking endonuclease assisted target recycling amplification. Anal Chem. 2015; 87: 9204-8). Copyright (2015). American chemical society*

dynamic light scattering (DLS), and two-photon scattering (TPS), due to which they have emerged as unique components of detection platforms. They can help in the detection of proteins, nucleic acids (DNA, RNA), whole tumor cells, and exosomes [35]. AuNPs have broad applications in OSCC detection, primarily based on surface-enhanced Raman scattering spectra assessment, and surface plasmon resonance, a property inherent to metallic surfaces or as a direct colorimetric assay based on "nanoparticle-protein assemblies." In the literature, many studies have addressed detection of OSCC, based on nanoparticles using plasma samples; however, saliva may be a much more potential substitute. In the following section, the possible current and future role of nanoparticles in saliva-based detection of OSCC is highlighted based on available and related evidence. We foresee nanoparticles to expand saliva-based oral cancer detection!

Surface-Enhanced Raman Scattering Assays

Raman spectroscopy can differentiate healthy tissue, OPMDs, and OSCC with high accuracy [60, 61]. In an initial report by Lin et al., Raman spectra of sera from normal and cancer patients showed significant differences [62]. The changes in spectra are attributed mainly to higher concentration of proteins and DNA and lower concentration of lipids in oral cancer tissue [63–65]. Surface-enhanced Raman scattering (SERS) is a surface enhancement technique of Raman spectroscopy, an ultrasensitive analytical technique, useful in the identification of OSCC biomarkers in centrifuged serum and saliva [57, 66–68]. However, weak Raman signals are produced in this method. This limitation can be countered by the use of a laser light, tuned to plasma frequency of AuNPs, which heavily amplify the scattering cross section, leading to enhanced spectroscopic signal (i.e., high-quality spectra). SERS tags are based on plasmonically active nanoparticles whose resonance can be tuned to obtain optimal SERS signals [69]. Sharp narrow peaks are true SERS signals representative of the sample, while broad peaks represent background noise [22]. AuNPs have special importance in SERS, as they enhance Raman scattering by 14–15 orders [66, 70]. SERS can be used in two ways:

Direct labeling approach

- In the direct labeling method, the metallic nanoparticles are linked to Raman reporters which are bound to binding molecule-like antibody [71]. The solution, centrifuged serum or saliva samples suspected to contain biomarker or biomarkers, is mixed with a colloid of "SERS-optimized nanotags" and incubated, following which a drop of the incubate is transferred onto a cover slip (drop-dry approach), and a Raman spectrometer is employed for making SERS measurements, focused at several regions on the cover slip [65, 71]. Even a signal drop can be quantified using SERS. Au and Ag nanoparticles mixed with plasma of histologically proven nasopharyngeal carcinoma increased Raman signal significantly with high accuracy of detection [72, 73]. The binding of target analyte with specific binding molecule leads to characteristic Raman spectra (Fig. 15.5) [71].

Immunoassay format

- In immuno-sandwich assay, SERS principle is used to enhance the Raman signal due to antibody and biomarker (target analyte) interaction [71]. It is a slightly complex format, principal wise comparable to ELISA [71]. Nanoparticles are joined together like a film or monolayer. But once a molecule (such as biomarker) snips them apart, the signal will diminish and the signal intensity reduces. Kah et al. have used a SERS active gold nanoparticle monolayer film for simple biosensing in a saliva assay [57]. In their assay, the colloidal gold nanoparticles were prepared and conjugated to anti-epidermal growth factor, considering EGFR as a biomarker, and closely packed unto a monolayer film following which a saliva sample was used in a drop-dry approach [57]. SERS was also applied by Tianxun et al. for body fluid MMP detection [74]. Their platform has a SERS-based bimetallic-film-over-nanosphere (BMFON) substrate and gold nanoparticles, where substrate and nanoparticles bind through biotin-avidin-biotin complexation. Their binding is hindered by the MMP peptide chain. By measuring SERS spectra with BMFON, and after peptide cleavage and AuNPs binding due to protease activity, MMP signatures (MMP-2, MMP-7) can be measured as SERS peaks [74].
- Algorithms routinely employed to analyze the Raman data include: principle component analysis (PCA), discrimination function analysis (DFA), partial least squares, and more recently support vector machine (SVM) [65, 75]. To provide more accurate diagnosis from SERS spectra, advanced algorithms are required. Support vector machine algorithm proved its superiority in the discrimination of OSCC [66, 76]. The SERS as a saliva-based assay can be promising if tested on a large number of saliva samples as suggested by Kah et al. (Fig. 15.5) [57]. The large molecular size (e.g., proteins) and low concentration of certain biomarkers in saliva may pose a problem to the overall sensitivity of SERS application leading to Raman band overlap, but as most of the OSCC markers are released locally, this issue may not be that important.

Surface Plasmon Resonance Assays

Surface Plasmon resonance (SPR) is a phenomenon that occurs due to oscillation of conduction electrons, when light hits a metal surface [77, 78]. SPR is inherent to AuNPs and exhibits good sensitivity and success in diagnostics [79]. It is based on the refractive index changes associated with the binding of antigen with the bio-recognition molecules (e.g.: anti-EGFR) on the sensor surface [80]. The mass change on sensor surface due to the presence of an immune complex, results in a change in angle between incident light and reflected light, captured by

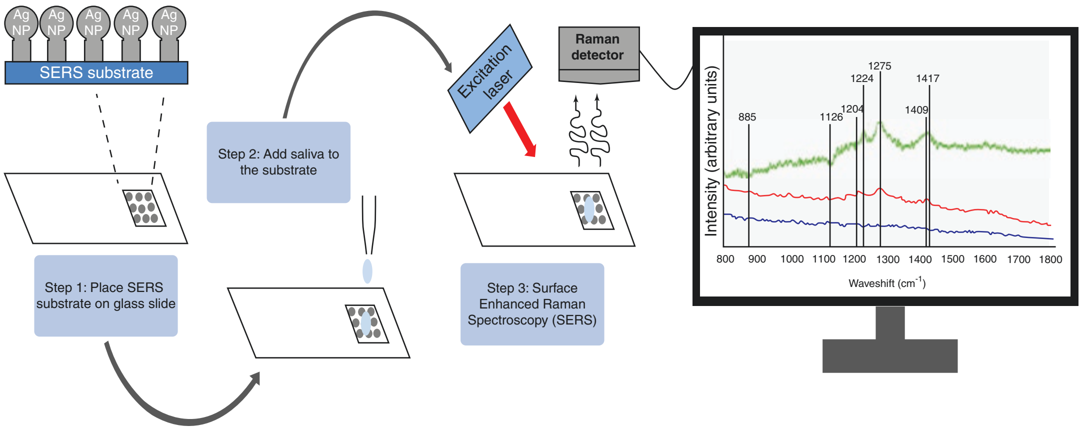

Fig. 15.5 Application of silver nanoparticle (Ag-NP) based surface-enhanced Raman spectroscopy (SERS) of saliva and desquamated oral cells in the detection of oral squamous cell carcinoma (OSCC). *Reprinted from Nanomedicine, vol 12, Connolly et al., Non-invasive and label-free detection of oral squamous cell carcinoma using saliva surface-enhanced Raman spectroscopy and multivariate analysis, Pages No. 1593-601. Copyright (2016) with permission from Elsevier*

the subtle detectors as signal(Response Units-RU) [77]. Through SPR analysis, the binding constants, kinetic analysis of binding can be studied [77]. In SPR, the binding interactions between two surfaces are measured; one immobilized on the metal surface and the other is a biomarker of interest freely available in the biofluid like saliva [81]. SPR directly detects concentration or mass, without the need for fluorescent labeling, allowing label free detection, and minimizing complexity [81].The measurements are made in a time dependent manner by a two-dimensional array of photodiodes or charge couple detectors [77].

AuNPs exert strong localized surface Plasmon resonance (LSPR), which is the oscillation of conducting electrons induced by the energy of incident light. 'AuNPs' are therefore 'SPR based biosensors'. They have been used in the detection of circulating whole tumor cells [58], proteins, DNA, and even microbiota with good success [82]. The wave length of the incident light can be tunable between 'visible light to infrared band', which is dependent on size, shape, particle distance of AuNPs, with extinction coefficient in the order 10^8–10^{11} $M^{-M}cm^{-m}$ [56]. LSPR sensing strategy is ideal to study binding mechanisms and with the use of LSPR, ultrasensitive detection can be reached with amplification methods, to single molecule sensitivity [56]. In the ovarian cancer model, ascites samples demonstrated exosomes released from ovarian cancer cells in a nanoplasmonic exosome (nPLEX) assay based on LSPR principle [83]. The nanoparticle assembly is made of nanohole layout, on a glass base with 200 nm hole at 450 nm periodicity [83]. Each array is functionalized by antibodies to exosomes with specific antigens. Exosomes are ubiquitous to all body fluids, but more abundant in saliva [84]. The sensitivity is 10^4 times higher than western blot and 10^2 than ELISA [83]. This methodology is applicable when specific saliva exosomes become characterized as biomarkers of OSCC based on the surface antigenicity.

- The role of AuNPs as SPR biosensors in living whole cells was highlighted by El-Sayed et al. [85]. They showed a superior binding affinity (600%) of anti-EGFR antibody-conjugated AuNPs with oral cancer cells compared to noncancerous cells [85]. These AuNPs can also be used for tumor cells in plasma or saliva. In whole blood of HNSCC patients, about 1–720 circulating tumor cells (CTCs) are present per ml, whereas in saliva their levels will be much elevated [58]. AuNPs targeted for OSCC detection can be conjugated to anti-EGFR antibody, chiefly expressed in OSCC. When AuNPs containing a recognizer like anti-EGFR antibody combine with EGFR-containing malignant cells, an optical signal is produced. This method may be used for exploration of exfoliated cells in saliva of OSCC subjects through SPR spectral imaging.

'LSPR peak' is also a sensitive marker for AuNP inter-particular distance. As individual particles AuNPs exhibit red color with an LSPR in the range of 520 nm, and when brought into close proximity, they change to blue due to a phenomenon is referred as 'Plasmon coupling' [85]. The spectral shift decays exponentially with interparticular distance and decay length is dependent on metal type, particle size, shape and medium dielectric constant. Due to this phenomenon, the colorimetric property of AuNPs can be harnessed to identify salivary biomarkers and specific molecular sensors can be designed. A nano-plasmonic colorimetric assay was also designed for exosomes and micro-vesicles [86].

15.3 AuNPs as Sensors in Direct Colorimetric Detection

Nanoparticles are smart sensors that enable naked eye detection of low concentration (ng-pg/ml) cancer biomarkers in body fluids [87]. This colorimetric assay is a simple method, without the use of advanced instrumentation, and wide range of applications possibly for saliva analytes. The ultra-high extinction coefficients allow detection of several molecular species including nucleic acids, proteins, saccharides, ions, organic molecules, pathogens and cells [56]. Nanoparticles have unique size dependent and distance dependent optical properties [85, 88], such that peptide, oligonucleotide functionalized AuNPs can be used for colorimetric detection [89].

The peptide functionalized AuNPs can work in two ways: the presence of protease (e.g.: MMPs) may cleave the peptide at certain locations leading to a decrease in size and net charge, leading to aggregation of NPs and a LPSR shift (color shift) (Fig. 15.6b) [89]. In the second technique, the presence of a protease breaks the peptide, setting nanoparticles free and ready to disperse, leading to a color change (Fig. 15.6a). Through color change, the presence of minuscule

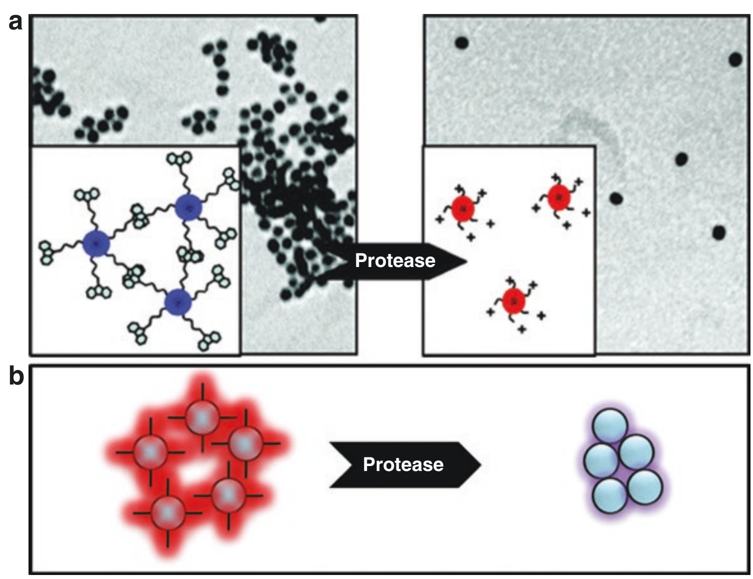

Fig. 15.6 (**a**) Schematic of "protease-triggered NP dispersion approach". TEM images of 8.5 nm gold NPs after functionalization with peptide are shown (left), followed by their dispersion through the action of a protease (right). (**b**) Schematic of "protease-triggered NP aggregation approach". *Reprinted with permission from (Laromaine et al. Protease-triggered dispersion of nanoparticle assemblies. J Am Chem Soc. 2007; 129: 4156-7). Copyright (2007). American chemical society*

amounts of key OSCC biomarkers can thus be unveiled? AuNPs in this way can be used in the visual identification of nucleic acids (Single nucleotide polymorphisms), proteins, much larger circulating tumor cells or even exosomes. The color change is a measure of concentration, and can be captured through, photometry, resonance light scattering or DLS, and interesting through visual detection! [90].

15.4 Detection of Mutations

- AuNPs can act as gene sensors, assisting visual detection of mutations [55]. AuNPs are incubated and functionalized with oligonucleotide aptamers which have the ability to detect a complimentary strand [91]. In the presence of mutation or single-nucleotide polymorphism (SNP), there will be no hybridization between the strands, and fluorescence is detected. In the presence of normal DNA, there is hybridization of complimentary strands, and fluorescence is quenched [55]. This method can identify single base-pair substitution with as low as 10 picomole DNA [92]. Recently Latorre et al. used "nanoparticle with oligonucleotide aptamer and a cholesterol tag" as gene sensors to screen point mutations in many genes including *KRAS* [91]. When the solution with specific mRNA or cDNA sequence undergoes hybridization with oligonucleotides, the nanostructure unfolds to open the hidden cholesterol group to water, causing an aggregation of nanoparticles accompanied by a visible color change [91]. Following aggregation, the red color of the colloidal nanoparticle solution turns either bluish or the sample with mutation may take up differing saturation of red [91]. Suitable target genes in OSCC can be selected which often undergo point mutations and are detectable in saliva (e.g., *TP53*), in which case the oligonucleotides may be designed for hotspots of those specific genes [92]. As numerous genes undergo mutation in OSCC and readily available in saliva, this methodology may help in early diagnosis [92]. This system can detect mutations at low nano-molar concentration of target sequence. This type of investigation is promising for oral cancer detection, as saliva bathes the oral lesions, it is preferentially enriched than plasma for DNA markers related to oral cancer. Tumor DNA in plasma is representative of subsites other than oral cavity, whereas saliva DNA is more relevant for oral cancer.

15.5 Protein Detection

- Nanoparticles were applied for the detection of protein analytes like PSA, CEA, CA 15.3, and EGFR, which are also biomarkers for OSCC [93]. Laromaine et al. for the first time, demonstrated protease-triggered nanoparticle assemblies for colorimetric detection [94], and their studies are now focused on the oral cancer model. The principle is "protein co-assembly and enzyme-triggered disassembly." The low sensitivity and specificity of nanoparticle-based colorimetric detection can be amplified through enzyme-assisted gold nanoparticle-mediated colorimetric detection [87]. They used gold particles 10 nm wide and glued them with short peptide chains that link the gold nanoparticles together to form aggregates, to form a blue solution [94]. When the solution is exposed to nACT-PSA, an enzyme related to prostate cancer, the solution turns red [94]. This color change occurs because nanoparticles disperse after the enzyme, "a protease by nature" breaks the peptides that maintain the nanoparticles together. This sets the nanoparticles free from the peptide links and they readily scatter [94]. Once the peptide bond is cleaved, at the end of the peptide, a positive charge is reached, which makes the particles to further repel. In this method, the protein itself acts as a signal amplifier reaching an LOD in the range of zeptograms/ml [93]. In another study by Maher et al., the same kit was used exploiting SERS application to identify hot spots for disease-specific

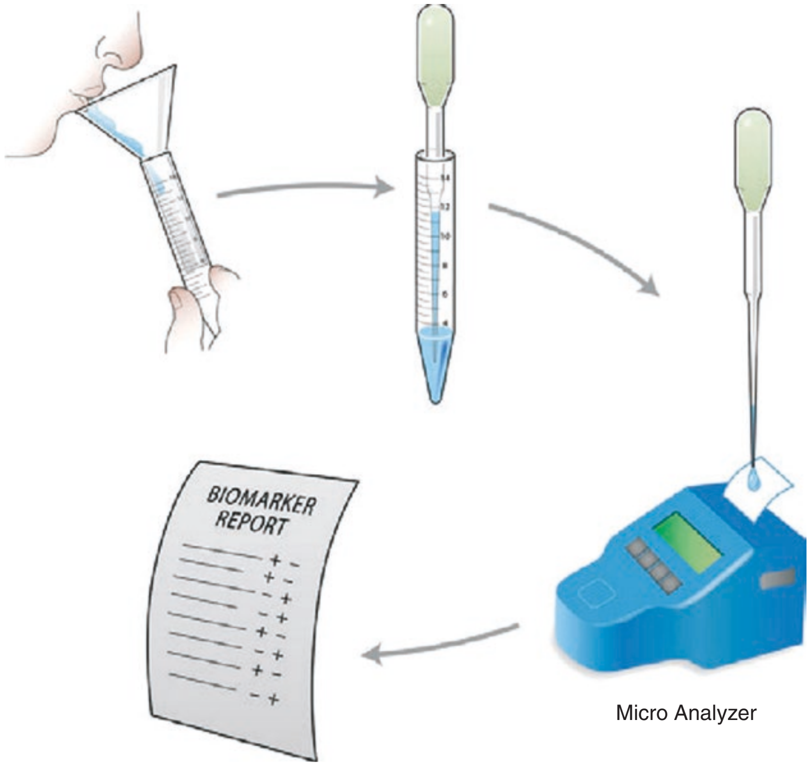

Fig. 15.7 Strategy for oral fluid sampling and analysis with a rapid point-of-care or lab-on-a-chip device for the generation of oral cancer biomarker report and diagnosis *Reprinted with permission from Ramseier et al. Periodontal disease. In: Wong DT, editor. Salivary diagnostics. Ames, Iowa, USA: Wiley-Blackwell, 2008*

enzyme detection [95]. This is a simple explanation of how nanoparticles could be harnessed in colorimetry-based cancer detection. This assay can be extrapolated to saliva samples in OSCC since several proteases (e.g., matrix metalloproteinases) are enriched in saliva at different stages of oral cancer. The prospect of this application is therefore high for oral cancer.

15.5.1 Ideal Requirements of POC

The ideal characteristics of POC according to World Health Organization (WHO) include: Affordability, sensitivity, specificity, user friendly, rapid treatment and robust use, equipment free, and delivered to those in need [96]. The POC therefore must have a simple organization with minimum reagents and less complex equipment, having low total cost per examination, portability, accurately matching the typical laboratory reference. The main requirements of an ideal POC platform are accuracy and robustness, multiplexibility, convenience, cost efficiency and portability of device and data (Fig. 15.7) [38].

15.5.1.1 Accuracy and Robustness

Accuracy is the biggest challenge to any POC platform. The low concentration of biomarkers is the main reason for low accuracy, and this recommends on increasing the concentration of target molecule using amplification methods. The signal intensity in any method is dependent on solute concentration, and good signal intensity is necessary for detection. To improve the accuracy, a nanoparticle-based platform can be used to concentrate a solute without a small region of the detector. There are two methods to improve signal: first is by increasing concentration of target biomarker of interest and second is by increasing regional concentration. Background noise (high molecular weight proteins in saliva) is always a limiting factor for accuracy and can be countered by using specific probes. Laboratory-level identification of OSCC and detection through POC are at two ends. To understand accuracy of any POC, a comparison can be made with its opposing laboratory methods, namely, ELISA (for proteins) and PCR (for nucleic acids). The achievement of accuracy comparable to traditional methods is the greatest challenge.

Robustness of a test is the quality to reproduce precise measurements repeatedly. A good POC platform must perform under variable conditions such as changing temperature and humidity [38]. Ideally, the variation should be less than 20%, for any POC platform to survive in the clinical scenario [38]. Quality control measures are essential to check robustness in performance, which can be made before and after a batch of samples are tested.

15.5.1.2 Multiplexibility

Multiplexibility is an important feature to be adapted by oral cancer POC platforms. Even in simple cancer models like ovarian cancer, not directly related to external carcinogens, multiple markers (3–5) showed an accuracy of 0.94 [37]. Oral cancer (OSCC) is a much more complex model characterized by a wider spectrum of genomic, epigenomic, transcriptomic, proteomic, and metabolic biomarkers, and the degree of molecular variability is extremely high compared to simple tumor models. So a test result based on a single biomarker naturally yields a poor result and multiplexed detection is required. The typical accuracy of oral cancer saliva biomarkers is 0.65–0.85 [38], which improves significantly with multiplexing [97–99]. Many studies concluded multiplexing as an important requirement for early detection of OSCC [99]. Their combined accuracy was higher, assisting in the discrimination of OSCC. Multiplexing can include biomarkers in different categories such as proteins and nucleic acids like RNA [97, 100, 101]. Multiplexing using two classes of biomarkers mRNA (IL8-mRNA) and proteins (IL-8) in OSCC was first reported by Wei et al. using a simple electrochemical sensor [37].

15.5.1.3 Convenience, Cost Efficiency, and Portability of Device and Data

For a highly prevalent condition like oral cancer, POC must be available with all clinicians at low cost for “mass screening.” The test kit must be easily operable with limited training and should make simple and rapid real-time measurements (<10 min). A recommendation to operate at a range of humidities (10–90%) and temperatures (4–30 °C) is suitable for the climatic conditions of different users [38]. Among the many technical tests, the lateral force-based chromatography (strip test) is most convenient owing to its simple structure and less economical burden for the clinicians [38]. The greatest challenge in building a POC platform for oral cancer is the miniaturization of technology to facilitate mass screening. New biosensor and wireless technology can greatly elevate the sensitivity of detection of oral cancer biomarkers and distance transfer of information to an Android or Apple device for easy and immediate decision making. Using oral cancer POC, dentists or physicians should perform chairside detection of OSCC saving valuable time both for the patients and clinicians, reducing diagnostic delay significantly.

OFNASET is a device satisfying these ideal requirements. If saliva-based diagnosis through POC is explored, it can potentially enhance mass screening and clinical staging, and it may be also possible to evaluate the success of treatment (prognosis) or detection of recurrence. The role of technology and the combination of both RNA and protein biomarkers into a diagnostic panel brings us close to the real-time application of saliva biomarkers for early detection of OSCC [102]. The major limitations in research on saliva biomarkers include low power studies, lack of standard sampling method, inconsistent methodology, and insufficient exploration of all potential biomarkers in a single experiment [103, 104].

Conclusion

The future for non-invasive detection of oral cancer is promising, and superior results in oral cancer detection should be possible with the advent of new technologies, and the problem of high viscosity of saliva may also be countered. Saliva shows more promise than other methods in OSCC detection, and with the simultaneous development in core technologies like micro-fluidics, immunoassays, sensor- and nano-technology, a perfect point-of-care platform can evolve for routine low cost, clinical testing.

Disclosures David Wong is a co-founder of RNAmeTRIX Inc., a molecular diagnostic company. He holds equity in RNAmeTRIX and serves as a company Director and Scientific Advisor. The University of California also holds equity in RNAmeTRIX. Intellectual property that David Wong invented and which was patented by the University of California has been licensed to RNAmeTRIX. Additionally, he is a consultant to GlaxoSmithKline, Wrigley, EZLife Bio Inc, and Colgate-Palmolive Company.

Acknowledgment Support from Ronnie James Dio Stand Up and Shout Cancer Research Fund.

References

1. Wong DT. Towards a simple, saliva-based test for the detection of oral cancer 'oral fluid (saliva), which is the mirror of the body, is a perfect medium to be explored for health and disease surveillance'. Expert Rev Mol Diagn. 2006;6:267–72.
2. Kaczor-Urbanowicz KE, Carreras-Presas CM, Kaczor T, Michael T, Wei F, Garcia-Godoy F, Wong DTW. Emerging technologies for salivaomics in cancer detection. J Cell Mol Med. 2017;21:640–7.
3. Daniel Malamud, Isaac R. Rodriguez-Chavez. Saliva as a Diagnostic fluid. Dent Clin N Am 2011; 55: 159–178.
4. Lee Y-H, Saliva DTW. An emerging biofluid for early detection of diseases. Am J Dent. 2009; 22:241–8.
5. Ziober BL, Mauk MG, Falls EM, Chen Z, Ziober AF, Bau HH. Lab-on-a-chip for oral cancer screening and diagnosis. Head Neck. 2008;30:111–21.
6. Malhotra R, Patel V, Chikkaveeraiah BV, Munge BS, Cheong SC, Zain RB, et al. Ultrasensitive detection of Cancer biomarkers in the clinic using a nanostructured microfluidic Array. Anal Chem. 2012;84:6249–55.
7. Munge BS, Coffey AL, Doucette JM, Somba BK, Malhotra R, Patel V, et al. Nanostructured immunosensor for attomolar detection of cancer biomarker interleukin-8 using massively labeled superparamagnetic particles. Angew Chem Int Ed Engl. 2011;50:7915–8.
8. Kumar S, Kumar S, Ali MA, Anand P, Agrawal VV, John R, Maji S, Malhotra BD. Microfluidic-integrated biosensors: prospects for point-of-care diagnostics. Biotechnol J. 2013;8:1267–79.
9. Zhang JZ, Nagrath S. Microfluidics and Cancer: are we there yet? Biomed Microdevices. 2013;15: 595–609.
10. Ying L, Wang Q. Microfluidic chip-based technologies: emerging platforms for cancer diagnosis. BMC Biotechnol. 2013;13:76.
11. Chen C, Skog J, Hsu CH, Lessard RT, Balaj L, Wurdinger T. Microfluidic isolation and transcriptome analysis of serum microvesicles. Lab Chip. 2010;10:505–11.
12. Wang H, Liu W, Zhang X, Xu X, Kang Z, Li S, et al. Toward point-of-care testing for JAK2 V617F mutation on a microchip. J Chromatogr A. 2015;1410:28–34.
13. Hayama FH, Motta AC, Silva Ade P, Migliari DA. Liquid-based preparations versus conventional cytology: specimen adequacy and diagnostic agreement in oral lesions. Med Oral Patol Oral Cir Bucal. 2005;10:115–22.
14. Navone R, Burlo P, Pich A, Pentenero M, Broccoletti R, Marsico A, et al. The impact of liquid-based oral cytology on the diagnosis of oral squamous dysplasia and carcinoma. Cytopathology. 2007;18: 356–60.
15. Navone R. Cytology of the oral cavity: a re-evaluation. Pathologica. 2009;101:6–8.
16. McDevitt J, Weigum SE, Floriano PN, Christodoulides N, et al. A new bio-nanochip sensor aids oral cancer detection. SPIE Newsroom. 2011;003547
17. Weigum SE, Floriano PN, Redding SW, Yeh CK, Westbrook SD, McGuff HS, et al. Nano-bio-chip sensor platform for examination of oral exfoliative cytology. Cancer Prev Res (Phila). 2010;3: 518–28.
18. Weigum SE, Floriano PN, Christodoulides N, McDevitt JT. Cell-based sensor for analysis of EGFR biomarker expression in oral cancer. Lab Chip. 2007;7:995–1003.
19. Abram TJ, Floriano PN, Christodoulides N, James R, Kerr AR, Thornhill MH, et al. 'Cytology-on-a-chip' based sensors for monitoring of potentially malignant oral lesions. Oral Oncol. 2016; 60: 103-11.
20. Whitesides GM, Wilding P. Lab on a stamp: paper-based diagnostic tools. Interview by Molly Webster and Vikram Sheel Kumar Clin Chem 2012; 58:956–8.
21. Yetisen AK, Akram MS, Lowe CR. Paper-based microfluidic point-of-care diagnostic devices. Lab Chip. 2013;13:2210–51.
22. Alicia D. Powers, Sean P. Palecek, Ph. D. Protein analytical assays for diagnosing, monitoring, and choosing treatment for cancer patients. J Healthc Eng. 2012;3:503–34.

23. Murdock RC, Shen L, Griffin DK, Kelley-Loughnane N, Papautsky I, Hagen JA. Optimization of a paper-based ELISA for a human performance biomarker. Anal Chem. 2013;85:11634–42.
24. Tan W, Sabet L, Li Y, Yu T, Klokkevold PR, Wong DT, et al. Optical protein sensor for detecting cancer markers in saliva. Biosens Bioelectron. 2008;24:266–71.
25. Sanjay ST, Dou M, Sun J, Li X. A paper/polymer hybrid microfluidic microplate for rapid quantitative detection of multiple disease biomarkers. Sci Rep. 2016;6:30474.
26. Markopoulos AK, Michailidou EZ, Tzimagiorgis G. Salivary markers for oral Cancer detection. Open Dent J. 2010;4:172–8.
27. Venugopal A, Uma Maheswari TN. Expression of matrix metalloproteinase-9 in oral potentially malignant disorders: a systematic review. J Oral Maxillofac Pathol. 2016;20:474–9.
28. Arellano-Garcia ME, Hu S, Wang J, Henson B, Zhou H, Chia D, et al. Multiplexed immunobead-based assay for detection of oral cancer protein biomarkers in saliva. Oral Dis. 2008;14:705–12.
29. Dincer C, Bruch R, Kling A, Dittrich PS, Urban GA. Multiplexed Point-of-Care Testing - xPOCT. Trends Biotechnol. 2017;35:728–42.
30. Baker HN, Murphy R, Lopez E, Garcia C. Conversion of a Capture ELISA to a Luminex xMAP Assay using a Multiplex Antibody Screening Method. J Vis Exp. 2012; (65): 4084. (refervedio).
31. Yu R-J, Ma W, Liu X-Y, Jin H-Y, Han H-X, Wang H-Y, Long Y-T, et al. Metal-linked Immunosorbent Assay (MeLISA): the enzyme-free alternative to ELISA for biomarker detection in serum. Theranostics. 2016;6:1732–9.
32. Malhotra R, Patel V, Vaqué JP, Silvio Gutkind J, Rusling JF. Ultrasensitive electrochemical Immunosensor for oral Cancer biomarker IL-6 using carbon nanotube forest electrodes and multilabel amplification. Anal Chem. 2010;82:3118–23.
33. Hart RW, Mauk MG, Liu C, Qiu X, Thompson JA, Chen D, Malamud D, Abrams WR, Bau HH. Point-of-careoral-baseddiagnostics. Oral Dis. 2011;17:745–52.
34. Herr AE, Hatch AV, Throckmorton DJ, Tran HM, Brennan JS, Giannobile WV, Singh AK. Microfluidic immunoassays as rapid saliva-based clinical diagnostics. Proc Natl Acad Sci U S A. 2007;104: 5268–73.
35. Oliveira-Rodríguez M, López-Cobo S, Reyburn HT, Costa-García A, López-Martín S, Yáñez-Mó M, et al. Development of a rapid lateral flow immunoassay test for detection of exosomes previously enriched from cell culture medium and body fluids. J Extracell Vesicles. 2016;5:31803.
36. Segal A, Wong DT. Salivary diagnostics: enhancing disease detection and making medicine better. Eur J Dent Educ. 2008;12:22–9.
37. Wei F, Patel P, Liao W, Chaudhry K, Zhang L, Arellano-Garcia M, et al. Electrochemical sensor for multiplex biomarkers detection. Clin Cancer Res. 2009;15:4446–52.
38. Fang WE, Wong DT. Point-of-care platforms for salivary diagnostics. Chin J Dent Res. 2012;15:7–15.
39. Wei F, Lin CC, Joon A, Feng Z, Troche G, Lira ME, et al. Noninvasive saliva-based EGFR gene mutation detection in patients with lung cancer. Am J Respir Crit Care Med. 2014;190:1117–26.
40. Pu D, Liang H, Wei F, Akin D, Feng Z, Yan Q, et al. Evaluation of a novel saliva-based epidermal growth factor receptor mutation detection for lung cancer: A pilot study. Thorac Cancer. 2016; 7: 428-36.
41. Aro K, Wei F, Wong DT, Michael T. Saliva liquid biopsy for point-of-care applications. Front Public Health. 2017;5:77.
42. Yang J, Wei F, Schafer C, Wong DT. Detection of tumor cell-specific mRNA and protein in exosome-like microvesicles from blood and saliva. PLoS One. 2014;9:e110641.
43. Tu M, Wei F, Yang J, Wong D. Detection of exosomal biomarker by electric field-induced release and measurement (EFIRM). J Vis Exp. 2015;95:52439.
44. Tan Y, Wei X, Zhao M, Qiu B, Guo L, Lin Z, Yang HH. Ultraselective homogeneous electrochemical biosensor for DNA species related to oral cancer based on nicking endonuclease assisted target recycling amplification. Anal Chem. 2015;87:9204–8.
45. Kim J, Imani S, de Araujo WR, Warchall J, Valdés-Ramírez G, Paixão TRLC, Mercier PP, Wang J. Wearable salivary uric acid mouthguard biosensor with integrated wireless electronics. Biosens Bioelectron. 2015;74:1061–8.
46. Kim J, Valdés-Ramírez G, Bandodkar AJ, Jia W, Martinez AG, Ramírez J et al. Non-invasive mouthguard biosensor for continuous salivary monitoring of metabolites. Analyst. 2014;139:1632–6.
47. Liang YH, Chang CC, Chen CC, Chu-Su Y, Lin CW. Development of an au/ZnO thin film surface plasmon resonance-based biosensor immunoassay for the detection of carbohydrate antigen 15-3 in human saliva. Clin Biochem. 2012;45:1689–93.
48. Munge BS, Krause CE, Malhotra R, Patel V, Silvio Gutkind J, Rusling JF. Electrochemical Immunosensors for Interleukin-6.Comparison of carbon nanotube Forest and gold nanoparticle platforms. Electrochem Commun. 2009;11:1009–12.
49. Zhang Y, Chen R, Xu L, Ning Y, Xie S, Zhang GJ. Silicon nanowire biosensor for highly sensitive and multiplexed detection of oral squamous cell carcinoma biomarkers in saliva. Anal Sci. 2015;31:73–8.
50. Kwon SM, Kang GB, Kim YT, Kim YH, Ju BK. In-situ detection of C-reactive protein using silicon nanowire field effect transistor. JNanosci Nanotechnol. 2011;11:1511–4.
51. Wang HB, Wu S, Chu X, Yu RQ. A sensitive fluorescence strategy for telomerase detection in cancer cells based on T7 exonuclease-assisted target

recycling amplification. Chem Commun (Camb). 2012;48:5916–8.
52. Liu X, Li W, Hou T, Dong S, Yu G, Li F. Homogeneous electrochemical strategy for human telomerase activity assay at single-cell level based on T7 exonuclease-aided target recycling amplification. Anal Chem. 2015;87:4030–6.
53. Hayakawa M, Kodama M, Sato S, Tomoeda-Mori K, Haraguchi K, Habu M, et al. Electrochemical telomeraseassay for screening for oral cancer. Br J Oral Maxillofac Surg. 2016; 54:301-5.
54. Cai W, Gao T, Hong H, Sun J. Applications of gold nanoparticles in cancer nanotechnology. Nanotechnol Sci Appl. 2008;1:17–32.
55. Tiwari PM, Vig K, Dennis VA, Singh SR. Functionalized gold nanoparticles and their biomedical applications. Nanomaterials (Basel). 2011;1: 31–63.
56. Huang X, O'Connor R, Kwizera EA. Gold nanoparticle based platforms for circulating Cancer marker detection. Nano. 2017;1:80–102.
57. Kah JC, Kho KW, Lee CG, James C, Sheppard R, Shen ZX et al. Early diagnosis of oral cancer based on the surface plasmon resonance of gold nanoparticles. Int J Nanomedicine 2007; 2: 785–798.
58. Wang X, Qian X, Beitler JJ, Chen ZG, Khuri FR, Lewis MM et al. Detection of circulating tumor cells in human peripheral blood using surface-enhanced Raman scattering nanoparticles. Cancer Res. 2011; 71: 1526–1532.
59. Chikkaveeraiah BV, Mani V, Patel V, Gutkind JS, Rusling JF. Microfluidic electrochemical immunoarray for ultrasensitive detection of two cancer biomarker proteins in serum. Biosens Bioelectron. 2011;26:4477–83.
60. Singh SP, Deshmukh A, Chaturvedi P, Murali KC. In vivo Raman spectroscopic identification of premalignant lesions in oral buccal mucosa. J Biomed Opt. 2012;17:105002.
61. Xue L, Li Y, Cai Q, Sun P, Luo X, Yan B. Ramanspectral characteristics of oralsquamous cell carcinoma, epithelial dysplasia and normal mucosa. Zhonghua Kou Qiang Yi Xue Za Zhi. 2015;50:18–22.
62. Li XZ, Bai J, Lin J, et al. Serum fluorescence and Raman spectra for diagnosis of cancer. Proc SPIE. 2001;4432:124–30.
63. Sahu A, Sawant S, Mamgain H, Krishna CM. Raman spectroscopy of serum: an exploratory study for detection of oral cancers. Analyst. 2013;138:4161–74.
64. Singh SP, Sahu A, Deshmukh A, Chaturvedi P, Krishna CM. In vivo Raman spectroscopy of oral buccal mucosa: a study on malignancy associated changes (MAC)/cancer field effects (CFE). Analyst. 2013;138:4175–82.
65. Tan Y, Yan B, Xue L, Li Y, Luo X, Ji P. Surface-enhanced Raman spectroscopy of blood serum based on gold nanoparticles for the diagnosis of the oralsquamous cell carcinoma. Lipids Health Dis. 2017;16:73.
66. Yan B, Li B, Wen Z, Luo X, Xue L, Li L. Label-free blood serum detection by using surface-enhanced Raman spectroscopy and support vector machine for the preoperative diagnosis of parotid gland tumors. BMC Cancer. 2015;15:650.
67. Tu Q, Chang C. Diagnostic applications of Raman spectroscopy. Nanomedicine. 2012;8:545–58.
68. Vendrell M, Maiti KK, Dhaliwal K, Chang YT. Surface-enhanced Raman scattering in cancer detection and imaging. Trends Biotechnol. 2013;31:249–57.
69. Nolan JP, Duggan E, Liu E, Condello D, Dave I, Stoner SA. Single cell analysis using surface enhanced Raman scattering (SERS) tags. Methods. 2012;57:272–9.
70. Qian X, Peng XH, Ansari DO, Yin-Goen Q, Chen GZ, Shin DM, et al. In vivo tumor targeting and spectroscopic detection with surface-enhanced Raman nanoparticle tags. Nat Biotechnol. 2008;26:83–90.
71. Owens P, Phillipson N, Perumal J, O'Connor GM, Olivo M. Sensing of p53 and EGFR biomarkers using high efficiency SERS substrates. Biosensors (Basel). 2015;5:664–77.
72. Lin D, Pan J, Huang H, Chen G, Qiu S, Shi H, et al. Label-free blood plasma test based on surface-enhanced Raman scattering for tumor stages detection in nasopharyngeal cancer. Sci Rep. 2014; 4:4751.
73. Feng S, Chen R, Lin J, Pan J, Chen G, Li Y, et al. Nasopharyngeal cancer detection based on blood plasma surface-enhanced Raman spectroscopy and multivariate analysis. Biosens Bioelectron. 2010;25:2414–9.
74. Gong T, Kong KV, Goh D, Olivo M, Yong K-T. Sensitive surface enhanced Raman scattering multiplexed detection of matrix metalloproteinase 2 and 7 cancer markers. Biomed Opt Express. 2015;6:2076–87.
75. Head SR, Kiyomi Komori H, LaMere SA, Whisenant T, Van Nieuwerburgh F, Salomon DR. Library construction for next-generation sequencing: Overviews and challenges. Biotechniques. 2014;56:61.
76. Li Y, Wen ZN, Li LJ, Li ML, Gao N, Guo YZ. Research on the Raman spectral character and diagnostic value of squamous cell carcinoma of oral mucosa. J Raman Spectrosc. 2010;41:142–7.
77. Stahelin RV. Surface plasmon resonance: a useful technique for cell biologists to characterize biomolecular interactions. Mol Biol Cell. 2013;24:883–6.
78. El-Sayed IH. Nanotechnology in head and neckcancer: the race is on. Curr Oncol Rep. 2010;12:121–8.
79. Poser E, Genovese I, Masciarelli S, Bellissimo T, Fazi F, Colotti G. Surface Plasmon resonance: a useful strategy for the identification of small molecule Argonaute 2 protein binders. Methods Mol Biol. 2017;1517:223–37.

80. Piliarik M, Vaisocherová H, Homola J. Surface plasmon resonance biosensing. Methods Mol Biol. 2009;503:65–88.
81. Drescher DG, Ramakrishnan NA, Drescher MJ. Surface Plasmon resonance (SPR) analysis of binding interactions of proteins in inner-ear sensory epithelia. Methods Mol Biol. 2009;493:323–43.
82. Dudak FC, Boyaci IH. Rapid and label-free bacteria detection by surface plasmon resonance (SPR) biosensors. Biotechnol J. 2009;4:1003–11.
83. Im H, Shao H, Park YI, Peterson VM, Castro CM, Weissleder R, et al. Label-free detection and molecular profiling of exosomes with a nano-plasmonic sensor. Nat Biotechnol. 2014;32:490.
84. Yakob M, Fuentes L, Wang MB, Abemayor E, Wong DTW. Salivary biomarkers for detection of oral squamous cell carcinoma – current state and recent advances. Curr Oral Health Rep. 2014;1:133–41.
85. El-Sayed IH, Huang X, El-Sayed MA. Surface plasmon resonance scattering and absorption of anti-EGFR antibody conjugated gold nanoparticles in cancer diagnostics: applications in oral cancer. Nano Lett. 2005;5:829–34.
86. Maiolo D, Paolini L, Di Noto G, Zendrini A, Berti D, Bergese P, et al. Colorimetric nanoplasmonic assay to determine purity and titrate extracellular vesicles. Anal Chem. 2015;87:4168–76.
87. Xie X, Xu W, Liu X. Improving colorimetric assays through protein enzyme-assisted gold nanoparticle amplification. Acc Chem Res. 2012;45:1511–20.
88. Cordeiro M, Ferreira Carlos F, Pedrosa P, Lopez A, Baptista PV. Gold Nanoparticles for Diagnostics: Advances towards Points of Care. Diagnostics (Basel).2016;6(4).pii: E43.
89. Chen P, Selegård R, Aili D, Liedberg B. Peptide functionalized gold nanoparticles for colorimetric detection of matrilysin (MMP-7) activity. Nanoscale. 2013;5:8973–6.
90. Zhang Y, McKelvie ID, Cattrall RW, Kolev SD. Colorimetric detection based on localised surface plasmon resonance of gold nanoparticles: merits, inherent shortcomings and future prospects. Talanta. 2016;152:410–22.
91. Latorre A, Posch C, Garcimartín Y, Ortiz-Urda S, Somoza Á. Single-point mutation detection in RNA extracts using gold nanoparticles modified with hydrophobic molecular beacon-like structures. Chem Commun (Camb). 2014;50:3018–20.
92. Sun L, Zhang Z, Wang S, Zhang J, Li H, Ren L, et al. Effect of pH on the interaction of gold nanoparticles with DNA and application in the detection of human p53 gene mutation. Nanoscale Res Lett. 2008;4:216–20.
93. Nam JM, Thaxton CS, Mirkin CA. Nanoparticle-based bio-bar codes for the ultrasensitive detection of proteins. Science. 2003;301:1884–6.
94. Laromaine A, Koh L, Murugesan M, Ulijn RV, Stevens MM. Protease-triggered dispersion of nanoparticle assemblies. J Am Chem Soc. 2007;129:4156–7.
95. Maher RC, Maier SA, Cohen LF, Koh L, Laromaine A, Dick JAG, Stevens MM. Exploiting SERS hot spots for disease-specific enzyme detection. J Phys Chem C. 2010;114:7231–5.
96. Andrew St. John, Christopher P Price. Existing and emerging technologies for point-of-care testing. Clin Biochem Rev. 2014;35:155–67.
97. St John MA, Li Y, Zhou X, Denny P, Ho CM, Montemagno C, et al. Interleukin 6 and interleukin 8 as potential biomarkers for oral cavity and oropharyngeal squamous cell carcinoma. Arch Otolaryngol Head Neck Surg. 2004;130:929–35.
98. de Jong EP, Xie H, Onsongo G, Stone MD, Chen XB, Kooren JA, et al. Quantitative proteomics reveals myosin and actin as promising saliva biomarkers for distinguishing pre-malignant and malignant oral lesions. PLoS One. 2010;5:e11148.
99. Li Y, St John MA, Zhou X, Kim Y, Sinha U, Jordan RC, et al. Salivary transcriptome diagnostics for oral cancer detection. Clin Cancer Res. 2004;10:8442–50.
100. Elashoff D, Zhou H, Reiss J, Wang J, Henson B, Shen H, et al. Pre-validation of salivary biomarkers for oral Cancer detection. Cancer Epidemiol Biomark Prev. 2012;21:664–72.
101. Yamazaki K, Nakajima T, Gemmell E, Polak B, Seymour GJ, Hara K. IL-4- and IL-6-producing cells in human periodontal disease tissue. J Oral Pathol Med. 1994;23:347–53.
102. Fliss MS, Usadel H, Caballero OL, Wu L, Buta MR, Eleff SM, et al. Facile detection of mitochondrial DNA mutations in tumors and bodily fluids. Science. 2000;287:2017–9.
103. Yoshizawa JM, Schafer CA, Schafer JJ, Farrell JJ, Paster BJ, Wong DT. Salivary biomarkers: toward future clinical and diagnostic utilities. Clin Microbiol Rev. 2013;26:781–91.
104. Stuani VT, Rubira CM, Sant'Ana AC, Santos PS. Salivary biomarkers as tools for oral squamous cell carcinoma diagnosis: a systematic review. Head Neck. 2017;39:797–811.